

# **Statin-associated muscle toxicity: clinical and genomic perspectives**

Thesis submitted in accordance with the requirements of the University of  
Liverpool for the degree of Doctor of Philosophy

**Richard Myles Turner**

April 2018

## Acknowledgements

First and foremost I would first like to thank my supervisors, Prof Sir Munir Pirmohamed, Prof Andrew Morris, Dr Dan Carr and Dr Neil Kitteringham for their overwhelming support, guidance and patience throughout my fellowship.

I am indebted to Dr Mark Bayliss, Ms Sarah Whalley and Dr Anahi Santoyo-Castelazo for their expertise in small molecule mass spectrometry assay development and mass spectrometry running, and to Dr Vanessa Fontana for her partnership in validating and implementing the cardiovascular analyte assay. I am most grateful to Dr Eunice Zhang for her insight into bioinformatics procedures. I would like to extend my sincere thanks to Dr Roz Jenkins for her guidance and assistance in conducting the proteomic studies. I fondly recall my trip to the University of Dundee and I am most thankful to Dr Colin Henderson for his collaboration and help in undertaking the single-dose pharmacokinetic study. I would like to acknowledge Mr Phillip Roberts for his assistance in creating the liver microsomes.

It would be remiss of me not to sincerely thank Dr Richard FitzGerald, Dr Andrea Jorgensen, Dr Peng Yin, Mrs Anita Hanson, Mr Jon Cresswell, Mrs Rachael Hornby and the rest of the PhACS team that worked tirelessly to set up and conduct the PhACS study, and were welcoming and patient with me when I began working with them.

There are many other members of the University of Liverpool Department of Molecular and Clinical Pharmacology that have made my PhD experience completely unforgettable for all of the right reasons and so I would like to take this opportunity to collectively thank them here.

Finally, I must express my profound thanks to my dear wife, Chen, for her unfailing support and encouragement throughout the fellowship and to our new son, Henry, for his lively distractions that keep life interesting!

Richard Myles Turner

**Contents**

Abstract .....	15
Publications .....	16
List of Abbreviations .....	17
Chapter 1 Introduction.....	21
1.1 Interindividual drug response variability .....	21
1.2 An introduction to Statins.....	22
1.3 Cardiovascular disease .....	26
1.4 Atherosclerosis .....	27
1.4.1 Atherosclerosis management.....	29
1.5 Indications for statin therapy.....	29
1.6 Statin efficacy.....	30
1.7 Statin-associated myotoxicity .....	32
1.7.1 The incidence of SAM and the nocebo effect .....	32
1.8 Myotoxicity pathogenesis .....	34
1.8.1 Factors associated with statin pharmacokinetics and myotoxicity.....	36
1.8.2 Statin-induced myocyte dysfunction .....	62
1.8.3 Statin-associated myotoxicity summary .....	68
1.9 P450 oxidoreductase .....	69
1.9.1 The role of POR in drug response variability .....	72
1.9.2 In vitro observations.....	72
1.9.3 Murine observations .....	72
1.9.4 Clinical observations.....	73
1.9.5 <i>POR</i> summary.....	75
1.10 Major experimental techniques used in thesis.....	75
1.10.1 Dried blood spots .....	76
1.10.2 Liquid chromatography-mass spectrometry .....	78
1.11 Thesis research aims and objectives.....	83
Chapter 2 Investigating the prevalence, predictors and prognosis of suboptimal statin use early after a non-ST elevation acute coronary syndrome.....	84
2.1 Introduction .....	84
2.2 Methods .....	88
2.2.1 Prospective study outline.....	88
2.2.2 Cohort Selection.....	90
2.2.3 Assessment of statin adherence .....	90

2.2.4	Classification of suboptimal and constant statin use .....	92
2.2.5	Outcomes .....	93
2.2.6	Covariates.....	93
2.2.7	Subgroup analyses .....	94
2.2.8	Statistical analysis.....	94
2.2.9	Sensitivity Analyses.....	97
2.3	Results .....	99
2.3.1	Factors associated with suboptimal statin occurrence .....	100
2.3.2	Risks of MACE and ACM associated with suboptimal statin use..	102
2.3.3	Sub-group analyses.....	104
2.3.4	Sensitivity Analyses.....	106
2.4	Discussion .....	109
2.4.1	Conclusion.....	114
Chapter 3	Development and validation of a novel dried murine blood spot high performance liquid chromatography tandem mass spectrometry assay for the quantification of rosuvastatin, atorvastatin and atorvastatin metabolites.	115
3.1	Introduction .....	115
3.2	Methods .....	119
3.2.1	Chemicals and reagents .....	119
3.2.2	Simvastatin hydrolysis study.....	121
3.2.3	Preparation of RVT/ATV Calibration Standards and Quality Controls.....	121
3.2.4	Comparison of extraction methods.....	123
3.2.5	Liquid Chromatography Mass Spectrometric instrumentation and operating conditions.....	124
3.2.6	Validation .....	126
3.2.7	Selectivity .....	126
3.2.8	Carryover.....	127
3.2.9	Accuracy and Precision .....	127
3.2.10	Lower Limit of Quantification .....	127
3.2.11	Matrix Effects and Extraction Recovery.....	127
3.2.12	Dilution Integrity.....	128
3.2.13	Storage and Stability.....	128
3.2.14	Atorvastatin analyte interconversion .....	130
3.2.15	DBS-specific assay assessments.....	130

3.2.16	Data Analysis .....	131
3.3	Results .....	131
3.3.1	Representative DBS appearance on FTA Elute cards .....	132
3.3.2	Extraction process development.....	134
3.3.3	RVT/ATV chromatograms and retention times .....	135
3.3.4	Calibration curves .....	137
3.3.5	Selectivity .....	139
3.3.6	Carryover.....	139
3.3.7	Accuracy and Precision .....	141
3.3.8	Matrix effects and extraction recoveries.....	142
3.3.9	Dilution integrity .....	144
3.3.10	Storage and stability .....	145
3.3.11	Internal standard solution stability.....	145
3.3.12	Working solution stability .....	146
3.3.13	Benchtop stability of analyte solutions .....	147
3.3.14	Short term (30 minute) stability in blood .....	147
3.3.15	Longer term (seven day) stability .....	150
3.3.16	Post-preparative stability .....	151
3.3.17	DBS volume and homogeneity.....	153
3.3.18	Assay validation summary .....	155
3.4	Discussion .....	157
Chapter 4 Investigating the impact of hepatic cytochrome P450		
oxidoreductase deficiency on systemic statin exposure and liver proteomics		
using the hepatic reductase null mouse model.....		
4.1	Introduction .....	162
4.2	Methods .....	163
4.2.1	Chemicals and reagents .....	163
4.2.2	Animals.....	163
4.2.3	<i>In vivo</i> PK study.....	164
4.2.4	Analysis of livers from PK study.....	166
4.2.5	Microsome studies.....	167
4.2.6	Mass spectrometric bioanalysis of statin analyte levels .....	169
4.2.7	Liver proteomics.....	170
4.2.8	Data analysis .....	174
4.3	Results .....	176

4.3.1	<i>In vivo</i> PK study.....	176
4.3.2	Microsomal incubations.....	191
4.3.3	<i>In vivo</i> PK study liver characterisation .....	195
4.3.4	Liver proteomics.....	198
4.4	Discussion .....	211
4.4.1	RVT and ATV disposition.....	212
Chapter 5 Development, validation and application of a novel plasma high performance liquid chromatography tandem mass spectrometry assay for the quantification of six analytes from atorvastatin, bisoprolol and clopidogrel ....		
5.1	Introduction .....	223
5.2	Methods .....	228
5.2.1	Chemicals and reagents .....	228
5.2.2	Preparation of stock solutions, working solutions, internal standards solution, calibration standards, and quality controls.....	228
5.2.3	LC-MS/MS conditions .....	232
5.2.4	Method Validation.....	234
5.2.5	Selectivity .....	234
5.2.6	Carryover.....	234
5.2.7	Lower limit of quantification .....	234
5.2.8	Accuracy and Precision .....	234
5.2.9	Matrix Effect and Recovery .....	235
5.2.10	Stability .....	236
5.2.11	Atorvastatin analyte interconversion .....	237
5.2.12	Dilution Integrity.....	238
5.2.13	Application to sparse pharmacokinetics study in patients.....	238
5.2.14	Data Analysis .....	239
5.3	Results .....	240
5.3.1	Optimisation of LC-MS/MS conditions.....	240
5.3.2	Optimisation of extraction procedure.....	242
5.3.3	Method validation .....	244
5.3.4	Method validation summary.....	261
5.3.5	Application to sparse pharmacokinetics study in patients.....	261
5.4	Discussion .....	263
Chapter 6 A genome-wide association study of atorvastatin and metabolite systemic exposures and their impact on clinical outcomes in secondary prevention patients .....		
		268

6.1	Introduction .....	268
6.2	Methods .....	269
6.2.1	Prospective study outline.....	269
6.2.2	Assay of ATV analyte concentrations .....	270
6.2.3	Genotyping, imputation and quality control.....	270
6.2.4	Cohort selection .....	272
6.2.5	Covariates.....	273
6.2.6	Statistical analysis .....	275
6.3	Results .....	280
6.3.1	Clinical factors associated with ATV analytes.....	282
6.3.2	Sensitivity analyses of clinical factors associated with PK endpoints 285	
6.3.3	Genome-wide association analyses of PK endpoints .....	287
6.3.4	Biologically plausible candidate signals .....	293
6.3.5	Characterisation of biologically plausible signals.....	295
6.3.6	Sensitivity analyses of genetic association with PK endpoints .....	302
6.3.7	Impact of biologically plausible SNPs on clinical adverse events.....	304
6.3.8	Sensitivity analyses with clinical endpoints .....	304
6.4	Discussion .....	308
6.4.1	Clinical factor associations with PK endpoints.....	308
6.4.2	GWAS associations.....	311
6.4.3	Study limitations.....	316
6.4.4	Conclusion.....	317
Chapter 7	Discussion .....	318
7.1	Patient identification .....	319
7.2	Statin utilisation in statin eligible patients .....	321
7.3	Novel genetic associations.....	325
7.3.1	UGT1A locus .....	325
7.3.2	CYP3A7 locus .....	327
7.4	P450 oxidoreductase .....	329
7.5	Conclusion.....	331
Chapter 8	Appendix.....	332
Chapter 9	References.....	365

## Figures

Figure 1.1 Atherosclerotic plaque development.....	28
Figure 1.2 Statin-mediated inhibition of cholesterol synthesis.....	31
Figure 1.3 Classification of statin-associated myotoxicity .....	33
Figure 1.4 A generalised overview of statin pharmacokinetics .....	37
Figure 1.5 Structure of human P450 oxidoreductase.....	70
Figure 1.6 The central role of the electron donor, P450 oxidoreductase, in physiology and pharmacology.....	71
Figure 1.7 Liquid chromatography triple quadrupole system schematic .....	79
Figure 2.1 The Brief Medication Questionnaire.....	92
Figure 2.2 A schematic of the study selection process.....	100
Figure 2.3 Cumulative survival curves.....	105
Figure 3.1 Structure and metabolism of atorvastatin analytes .....	117
Figure 3.2 Structure and metabolism of measured rosuvastatin and simvastatin analytes.....	118
Figure 3.3 Representative DBS appearance on FTA Elute cards.....	132
Figure 3.4 Representative multiple reaction monitoring chromatograms from analyte medium quality control samples .....	136
Figure 3.5 Calibration curves.....	138
Figure 3.6 Multiple reaction monitoring chromatograms of blank blood, analytes and internal standards .....	140
Figure 3.7 Relationship between DBS pipetted volume and spot area excluding halo.....	154
Figure 3.8 Relationship between DBS pipetted volume and spot area including halo.....	154
Figure 4.1 Individual subject concentration-time profiles of RVT, ATV and ATV metabolites.....	181
Figure 4.2 Composite concentration-time profiles of RVT, ATV and ATV metabolites.....	185
Figure 4.3 Sensitivity analysis composite concentration-time profiles of RVT, ATV and ATV metabolites including all concentrations up to 8 hours post dose .....	188

Figure 4.4 Sensitivity analysis individual and mean analyte systemic exposures including all concentrations up to 8 hours post dose.....	189
Figure 4.5 Proportion of RVT and ATV remaining over time in hepatic microsomes.....	192
Figure 4.6 Rates of formation of 2- and 4-OH ATV in hepatic microsomes activated with NADPH .....	193
Figure 4.7 Hepatic microsome active and control incubations .....	194
Figure 4.8 Apparent rate of formation of ATV L in hepatic microsomal incubations activated with UDPGA.....	195
Figure 4.9 Relative analyte abundance in post dose liver homogenates .....	196
Figure 4.10 Liver histological changes of the hepatic reductase null model.....	197
Figure 4.11 Differential hepatic drug-metabolising enzyme and xenotransporter protein expressions in hepatic reductase null and wild type mice .....	199
Figure 4.12 P-gp expression by western blotting .....	201
Figure 4.13 Schematics of postulated hepatocyte handling of atorvastatin and rosuvastatin in HRN mice.....	203
Figure 4.14 Main protein networks detected by IPA core analysis comparing HRN to WT liver homogenates .....	206
Figure 5.1 Chemical structures and relevant metabolism of analytes analysed .....	226
Figure 5.2 MS/MS spectra of analytes .....	241
Figure 5.3 Chromatograms of deuterated internal standards .....	242
Figure 5.4 Representative multiple reaction monitoring chromatograms .....	245
Figure 5.5 Representative calibration curves.....	246
Figure 5.6 Detection of likely 4-OH ATV L in patient samples.....	266
Figure 6.1 A schematic of the study cohort selection process .....	280
Figure 6.2 Manhattan plots of key genome-wide association analyses .....	288
Figure 6.3 Regional locus plots of biologically plausible loci .....	293
Figure 6.4 Haplotype structure of <i>UGT1A</i> SNPs associated with 2-hydroxy atorvastatin to atorvastatin ratio with $p < 5.0 \times 10^{-8}$ .....	297
Figure 6.5 The impact of the biologically-plausible identified variants by genotype on atorvastatin and hydroxylation levels illustrated by dot plots .....	299

Figure 6.6 Sensitivity genome-wide association analysis that included all patients with high ATV concentrations.....303

Figure 8.1 Additional Manhattan plots for the following dependent variables: 2-hydroxy ATV, 2-hydroxy ATV lactone, the total sum of all four ATV analytes, and the ratio of ATV lactone/ATV (Chapter 6) .....352

Figure 8.2 Regional locus plots for loci associated with atorvastatin concentration at  $p < 1.0 \times 10^{-5}$  (Chapter 6).....356

Figure 8.3 Regional locus plots for loci associated with atorvastatin lactone concentration at  $p < 1.0 \times 10^{-5}$  (Chapter 6).....359

Figure 8.4 The lack of genetic association between P450 oxidoreductase and atorvastatin concentration or hydroxylation (Chapter 6).....361

Figure 8.5 The effect of *UGT1A3* haplotypes on atorvastatin hydroxylation (Chapter 6) .....363

## Tables

Table 1.1 Pharmacokinetic properties of the different statins.....	24
Table 1.2 Clinical risk factors of statin-associated myotoxicity .....	35
Table 1.3 Genetic variants that influence statin pharmacokinetics.....	46
Table 1.4 A systematic review of pharmacogenomic studies investigating statin-associated myotoxicity .....	51
Table 2.1 Studies investigating statin non-adherence/discontinuation/persistence/switching in cardiovascular disease.	86
Table 2.2 Statin doses estimated to lead to similar reductions in low-density lipoprotein cholesterol.....	90
Table 2.3 Characteristics of suboptimal and constant statin users .....	101
Table 2.4 Adjusted factors associated with suboptimal statin occurrence.....	102
Table 2.5 Univariate Cox regression analysis results for association with time to MACE or time to ACM.....	103
Table 2.6 Multivariable adjusted Cox regression results for risk of time to MACE or ACM .....	104
Table 2.7 Factors associated with an increased risk of suboptimal statin occurrence in multivariable logistic regression using only participants with complete data available (Sensitivity Analysis A). .....	106
Table 2.8 Summary table of all analyses of the multivariable adjusted risks of MACE, or ACM, associated with suboptimal statin users compared to constant statin users.....	107
Table 2.9 Assessment of potential healthy user bias on the risk of MACE or ACM associated with suboptimal statin use using logistic regression analysis (Sensitivity Analysis F1) .....	108
Table 2.10 Assessment of potential healthy user bias on the risks of time to MACE or ACM associated with suboptimal statin with follow up censored at 11 months after Visit 2 (Sensitivity Analysis F2) .....	109
Table 3.1 Formula and purity of compounds used.....	119
Table 3.2 Stock solution solvents and concentrations.....	120
Table 3.3 Working solution concentrations.....	121
Table 3.4 Calibration standard concentrations .....	122

Table 3.5 Quality control concentrations.....	122
Table 3.6 Extraction solvents and methods investigated for RVT and ATV .....	124
Table 3.7 Mobile phase gradient used for chromatographic separation .....	125
Table 3.8 Analyte transitions and analyte-specific operating parameters .....	126
Table 3.9 STV is rapidly hydrolysed in murine blood .....	133
Table 3.10 Influence of extraction method on ionisation and extraction.....	134
Table 3.11 Optimisation of the number of extractions carried out .....	135
Table 3.12 Analyte carryover.....	139
Table 3.13 Within-run accuracy and precision.....	141
Table 3.14 Between-run accuracy and precision.....	142
Table 3.15 Matrix and extraction recovery effects from pooled blood .....	143
Table 3.16 Interindividual matrix and recovery assessment.....	144
Table 3.17 Dilution integrity .....	144
Table 3.18 Analytes in internal standard working solution .....	145
Table 3.19 Analyte solution stability stored at 4°C.....	146
Table 3.20 Six hour bench top stability of working solutions.....	147
Table 3.21 Thirty minute stability of RVT and ATV in blood in different conditions prior to pipetting onto FTA Elute cards .....	148
Table 3.22 Thirty minute stability of ATV acid metabolites in blood in different conditions prior to pipetting onto FTA Elute cards .....	148
Table 3.23 Thirty minute stability of atorvastatin lactone metabolites in blood in different conditions prior to pipetting onto FTA Elute cards.....	149
Table 3.24 Longer term DBS storage and stability .....	150
Table 3.25 Lactone to acid conversion is only a minor contributor to the decreased response of atorvastatin lactones after storage as DBS on FTA Elute cards .....	151
Table 3.26 Post-preparative sample stability.....	152
Table 3.27 Impact of DBS volume and spot homogeneity on analyte response .....	155
Table 3.28 Assay validation summary.....	156
Table 4.1 Calibration standard concentrations for microsomal incubations.....	169
Table 4.2 8% polyacrylamide gel preparation.....	174
Table 4.3 Characteristics of the individual mice used in the <i>in vivo</i> PK study...	177

Table 4.4 Results from the quality control extracts included in the analytical run of the <i>in vivo</i> PK study dried blood spot extracts .....	178
Table 4.5 Individual subject blood concentrations of RVT, ATV and ATV metabolites.....	179
Table 4.6 Summary of main analysis analyte PK parameters .....	186
Table 4.7 Sensitivity analysis of analyte PK parameters.....	187
Table 4.8 Ratios of exposure to main acid or lactone metabolite over ATV.....	190
Table 4.9 Enzyme kinetics for 2-OH and 4-OH ATV microsomal formation .....	193
Table 4.10 Top significant results from IPA® analysis.....	204
Table 4.11 Expression fold changes for identified proteins involved in lipid metabolism.....	209
Table 5.1 Compounds .....	228
Table 5.2 Stock solutions.....	229
Table 5.3 Analyte working solutions .....	229
Table 5.4 Composite internal standard daily working solution.....	230
Table 5.5 Calibration standard and quality control concentrations.....	231
Table 5.6 Eluent gradient .....	232
Table 5.7 Valco diverter valve setup.....	233
Table 5.8 Transitions and specific operating parameters for the mass spectrometer .....	233
Table 5.9 Assay extraction method development.....	243
Table 5.10 Analyte and internal standard selectivity.....	244
Table 5.11 Carryover of analytes and internal standards .....	247
Table 5.12 Within-run (intra-day) accuracy and precision .....	248
Table 5.13 Between-run (inter-day) accuracy and precision .....	249
Table 5.14 Interindividual Matrix effects and recovery assessment.....	250
Table 5.15 Haemolysis impact on accuracy and precision of joint analytes .....	251
Table 5.16 Stock solution stability at -20°C.....	253
Table 5.17 Determination of unlabelled analyte abundance in composite internal standards working solution after 20 days at 4°C .....	254
Table 5.18 Stability of working solutions stored at 4°C .....	254
Table 5.19 Four hour room temperature bench top stability of Joint analytes	255
Table 5.20 Bench top stability of ATV lactones .....	256

Table 5.21 Freeze-thaw stability .....	257
Table 5.22 Re-injection reproducibility after 24-hours in autosampler.....	258
Table 5.23 Long term stability stored at -80°C .....	259
Table 5.24 Analytical run length validation .....	260
Table 5.25 Integrity of 20-times dilution .....	260
Table 5.26 Summary of assay validation results.....	261
Table 5.27 Summary of patient one month sample characteristics and analyte concentrations .....	262
Table 5.28 Univariate regression analyses to assess the impact of sample characteristics on patient one month analyte concentrations, determined using the validated assay.....	264
Table 6.1 CYP3A inducers, inhibitors, and OATP1B1 potential inhibitors .....	274
Table 6.2 Clinical characteristics of study patients.....	281
Table 6.3 Correlation between analytes concentrations ( $r^2$ ).....	282
Table 6.4 Clinical variables associated with ATV analyte levels in multivariable linear regression.....	283
Table 6.5 Clinical variables associated with ATV analyte total or ratios in multivariable linear regression.....	284
Table 6.6 Sensitivity analysis to determine the association between specific drugs and ATV PK endpoints in multivariable linear regression .....	286
Table 6.7 Lead SNPs from ATV, ATV L and 2-OH ATV/ATV genome-wide association analyses .....	292
Table 6.8 Additional proportion of analyte level variation explained by biologically plausible identified SNPs.....	301
Table 6.9 Impact of biologically plausible identified SNPs on statin-attributable adverse events .....	305
Table 6.10 Impact of biologically plausible identified SNPs on risk of ATV intolerance .....	306
Table 6.11 Impact of biologically plausible identified SNPs on cardiovascular events and mortality .....	307
Table 8.1 Clinical factors associated with altered statin pharmacokinetics (Introduction).....	333
Table 8.2 Cassette calibration line spiking regimens (Chapter 3).....	337

Table 8.3 Cassette quality control sample spiking regimens (Chapter 3).....	337
Table 8.4 Protein expression changes in liver homogenates from hepatic reductase null compared to wild type mice determined by iTRAQ and remained statistically significant after multiple testing correction (Chapter 4) .....	338
Table 8.5 A summary of the quality control results from the 12 analytical runs carried out to determine the concentrations of cardiovascular drug analytes in patient samples from the PhACS study using the validated liquid chromatography-mass spectrometry assay (Chapter 5) .....	345
Table 8.6 A summary of the quality control extracts that passed from the 12 analytical runs carried out to determine the concentration of cardiovascular drug analytes in patient samples from the PhACS study using the validated liquid chromatography-mass spectrometry assay (Chapter 5) .....	347
Table 8.7 Univariate linear regression analysis of association between clinical variables and ATV analyte levels in PhACS patients (Chapter 6) .....	348
Table 8.8 Univariate linear regression analysis of association between clinical variables and ATV analyte total and ratios (Chapter 6) .....	350
Table 8.9 Loci with functional effects identified <i>in silico</i> and are at least suggestively associated with atorvastatin analytes .....	362
Table 8.10 Summary of results for the effect of biologically plausible identified single nucleotide polymorphisms on all atorvastatin pharmacokinetic endpoints (Chapter 6) .....	364

## Abstract

Statins are lipid-lowering agents and amongst the most commonly prescribed medications worldwide. Although generally well-tolerated, statins cause a range of adverse myotoxicity phenotypes ranging from mild myalgia to rare life-threatening rhabdomyolysis. The aetiology of statin-associated myotoxicity (SAM) is incompletely understood but clinical risk factors that increase systemic statin exposure (e.g. older age, drug interactions) have been identified. A common nonsynonymous variant (rs4149056, V174A) in the solute carrier organic anion transporter family member 1B1 (*SLCO1B1*) gene that encodes the hepatocyte-specific sinusoidal influx transporter, organic anion-transporting polypeptide 1B1 (OATP1B1), is associated with increased statin exposure and simvastatin myopathy. The aims of this thesis were to: examine whether muscular complaints impact statin use, assess if suboptimal statin use affects cardiovascular events, and investigate statin pharmacogenomics using both the hepatic reductase null (HRN) mouse model and the Pharmacogenetics of Acute Coronary Syndrome (PhACS) study, which was a UK multicentre prospective observational study of non-ST elevation ACS patients (n=1,470).

One month after hospitalisation, 15.5% (n=156) of PhACS participants discharged on high potency statin therapy (n=1,005) had switched statin, reduced their dose, discontinued, or were statin non-adherent. Suboptimal statin therapy was associated with increased risks of time to major adverse cardiovascular events (HR 2.10, 95% CI 1.25-3.53, p= 0.005) and all-cause mortality (HR 2.46, 95% CI 1.38-4.39, p=0.003), and self-reported SAM was a risk factor for suboptimal statin use (OR 4.28, 95% CI 1.30-14.08, p=0.017).

Two novel liquid chromatography-mass spectrometry assays were developed to quantify statin analytes in murine dried blood spots or human plasma. An *in vivo* study revealed that HRN mice, which lack hepatic P450 oxidoreductase (*Por*) reducing cytochrome P450 (Cyp) activity, have increased blood levels of rosuvastatin, atorvastatin (ATV) and ATV metabolites relative to wild type mice.

ATV and ATV metabolite levels were quantified in a pre-specified sub-cohort of PhACS patients on regular ATV 40mg or 80mg daily (n=590) at one month after index hospitalisation, and were associated with several clinical factors including novel interactions with furosemide, proton pump inhibitors and clopidogrel. Genome-wide association analyses identified that *SLCO1B1* rs4149056 was suggestively associated with increased ATV (p=2.21x10<sup>-6</sup>) and 2-hydroxy (2-OH) ATV (p=1.09x10<sup>-6</sup>) levels. Importantly, the uridine 5'-diphosphoglucuronosyltransferase 1A (*UGT1A*) locus was associated with increased ratios of 2-OH ATV/ATV (lead SNP, rs887829, p=7.25x10<sup>-16</sup>) and 2-OH ATV lactone (L)/ATV L (rs887829 p=3.95x10<sup>-15</sup>). A novel locus near *CYP3A7* was associated with increased hydroxylation. *SLCO1B1* rs4149056 was associated with muscular complaints (p=0.016) and suboptimal ATV use (p=0.019). There was no association between *POR* variants and ATV levels.

In conclusion, muscular complaints increase the risk of suboptimal statin use, which is associated with a poorer prognosis. *SLCO1B1* rs4149056 increases the risk of high dose ATV-associated muscular complaints and suboptimal ATV use. Further work is required to understand mechanistically the novel drug-statin interactions and *UGT1A* and *CYP3A7* loci associations identified in this thesis.

## Publications

- 1.) Turner R M, Park B K & Pirmohamed M 2015. Parsing interindividual drug variability: an emerging role for systems pharmacology. *Wiley Interdiscip Rev Syst Biol Med*, 7, 221-41.
- 2.) Turner R M, Bula M & Pirmohamed M 2017a. Chapter 36 - Personalized Medicine in Cardiovascular Disease In: Coleman W B & Tsongalis G J (eds.) *Diagnostic Molecular Pathology*. Academic Press.
- 3.) Turner R M, Yin P, Hanson A, Fitzgerald R, Morris A P, Stables R H, Jorgensen A L & Pirmohamed M 2017b. Investigating the prevalence, predictors, and prognosis of suboptimal statin use early after a non-ST elevation acute coronary syndrome. *J Clin Lipidol*, 11, 204-214.

## Abstracts

- 1.) Turner R M, Yin P, Jorgensen A L, Fitzgerald R, Morris A P, Stables R H, Hanson A & Pirmohamed M. Investigating the prevalence, predictors, and prognosis of suboptimal statin use early after a non-ST elevation acute coronary syndrome. In: *British Pharmacological Society Annual Meeting*; 15-17 December 2015; London, UK; prize-winning oral presentation.
- 2.) Turner R M, Yin P, Hanson A, Fitzgerald R, Morris A P, Stables R H, Jorgensen A L & Pirmohamed M. Is deviating from recommended high strength statin treatment after a heart attack sensible? In: *MRC Festival of Medical Research Poster Reception*; 23 June 2016; Liverpool, UK.
- 3.) Turner R M, Bayliss M, Carr D, Kitteringham N, Henderson C & Pirmohamed M. The impact of P450 oxidoreductase knock out on systemic exposure to rosuvastatin, atorvastatin and atorvastatin metabolites. In: *British Pharmacological Society Annual Meeting*; 13-15 December 2016; London, UK.

## List of Abbreviations

ABC: adenosine triphosphate-binding cassette  
*ABCB1*: adenosine triphosphate-binding cassette subfamily B member 1  
*ABCG2*: adenosine triphosphate-binding cassette subfamily G member 2  
ABS: Antley-Bixler syndrome  
ACC/AHA: the American College of Cardiology/American Heart Association  
ACEI: angiotensin converting enzyme inhibitor  
ACM: all-cause mortality  
ACS: acute coronary syndrome  
ADR: adverse drug reaction  
*Akr1a1*: aldo-keto reductase 1a1  
AKT: protein kinase B  
amu: atomic mass units  
*Aox3*: aldehyde oxidase 3  
ARB: angiotensin II receptor blocker  
ATP: adenosine triphosphate  
ATV: atorvastatin  
AUC: area under the concentration-time curve  
BCA: bicinechoninic acid  
BCRP: breast cancer resistance protein  
BMI: body mass index  
BMQ: Brief Medication Questionnaire  
BSEP: bile salt export pump  
BSP: bisoprolol  
CABG: coronary artery bypass graft surgery  
CAD: coronary artery disease  
CES: carboxylesterase  
CI: confidence interval  
CID: collision-induced dissociation  
CK: creatine kinase  
CKD: chronic kidney disease  
CL/F: apparent clearance  
CLP-CA: clopidogrel carboxylic acid  
 $C_{max}$ : peak concentration  
CNR: case notes review  
COPD: chronic obstructive pulmonary disease  
*COQ2*: para-hydroxybenzoate-polyprenyl transferase  
CoQ<sub>10</sub>: coenzyme Q<sub>10</sub>  
Cps: counts per second  
CPT: carnitine palmitoyltransferase  
CRF: case report form  
CTT: Cholesterol Treatment Trialists  
CV: coefficient of variation  
CVD: cardiovascular disease  
CVS: cardiovascular system  
CVT: cerivastatin  
Cyb5: cytochrome b<sub>5</sub>  
CYP: cytochrome P450

DALY: disability-adjusted life year  
DBS: dried blood spot  
DDI: drug-drug interaction  
DMSO: dimethyl sulfoxide  
Dpyd: dihydropyrimidine dehydrogenase  
ECG: electrocardiography  
EDTA: ethylenediaminetetraacetic acid  
EMG: electromyography  
Ephx1: epoxide hydrolase 1  
eQTL: expression quantitative trait loci  
ER: extraction recovery  
ESI: electrospray ionisation  
FAD: flavin adenine dinucleotide  
FCS: fully conditional specification  
FDR: false discovery rate  
FMN: flavin mononucleotide  
Fmo1: flavin containing monooxygenase 1  
FPP: farnesyl pyrophosphate  
FTA Elute card: Whatman FTA™ Elute Micro Card  
FVT: fluvastatin  
GGPP: geranyl-geranyl pyrophosphate  
Gst: glutathione S-transferase  
GTEx: Genotype-Tissue-Expression project  
GWAS: genome-wide association study  
HBRN: hepatic cytochrome b5a and reductase null  
HDL-C: high-density lipoprotein cholesterol  
HLA: human leukocyte antigen  
HMGCR: 3-hydroxy-3-methylglutaryl-Coenzyme A reductase  
HPLC: high performance liquid chromatography  
HR: hazards ratio  
HRN: hepatic reductase null  
IBD: identity by descent  
IPA®: Ingenuity® Pathway Analysis  
iTRAQ: Isobaric tag for relative and absolute quantitation  
K<sub>m</sub>: Michaelis-Menten constant  
L: lactone  
LC: liquid chromatography  
LCN: liver-specific *Por* null  
LD: linkage disequilibrium  
LDH: lactate dehydrogenase  
LDL-C: low-density lipoprotein cholesterol  
LiHep: lithium heparin  
LLOQ: lower limit of quantification  
LVT: lovastatin  
MACE: major adverse cardiovascular event  
MCT4: monocarboxylate transporter-4  
ME: matrix effect  
MI: myocardial infarction  
MMTS: methylmethanethiosulfate

MPB: 2-bromo-3'-methoxyacetophenone  
MS: mass spectrometry  
MRI: magnetic resonance imaging  
MRM: multiple reaction monitoring  
mRNA: messenger ribonucleic acid  
MRP: multidrug resistance-associated protein  
*m/z*: mass-to-charge  
NADPH: reduced nicotinamide adenine dinucleotide phosphate  
NC3Rs: the National Centre for the replacement, refinement and reduction of animals in research  
ND = not done  
Nfe2l2: nuclear factor erythroid 2-related factor 2  
NICE: National Institute for Health and Care Excellence  
NNT: number needed to treat  
Nr1i: nuclear receptor subfamily 1 group i  
NSTE-ACS: non-ST elevation acute coronary syndrome  
NTCP; sodium-taurocholate co-transporting polypeptide  
NYHA: New York Heart Association  
OATP: organic anion-transporting polypeptide  
OH: hydroxy  
OR: odds ratio  
PAD: peripheral artery disease  
PAGE: polyacrylamide gel electrophoresis  
PC: principal component  
PCA: principal component analysis  
PCI: percutaneous coronary intervention  
PCSK9: proprotein convertase subtilisin/kexin type 9  
PD: pharmacodynamic  
PDC: proportion of days covered  
PE: process efficiency  
P-gp: P-glycoprotein  
PhACS: Pharmacogenetics of Acute Coronary Syndrome study  
PK: pharmacokinetic  
PIT: pitavastatin  
POR: P450 oxidoreductase  
*PPARA*: peroxisome proliferator-activated receptor- $\alpha$   
PPF: proportion of prescriptions filled  
PPI: proton pump inhibitor  
PVT: pravastatin  
QALY; quality-adjusted life year  
QC: quality control  
RCT: randomized controlled trial  
ROF: reduction-of-function  
RVT: rosuvastatin  
RYR: ryanodine receptor  
SAM: statin-associated myotoxicity  
SD = standard deviation  
SDS: sodium dodecyl sulphate  
Sec-tRNA: selenocysteine-transfer ribonucleic acid

SILAC: stable isotope labelling by amino acids in cell culture  
*SLC01B1*: solute carrier organic anion transporter family member 1B1  
SNP: single nucleotide polymorphism  
SRM: single reaction monitoring  
STEMI: ST-elevation myocardial infarction  
SVT: simvastatin  
SVT-A: simvastatin  $\beta$ -hydroxy acid  
 $t_{1/2}$ : terminal elimination half-life  
TA: thymine-adenine  
TBME: *tert*-butyl methyl ether  
TCEP: tris(2-carboxyethyl)phosphine  
TEAB: triethylammonium bicarbonate buffer  
TIA: transient ischaemic attack  
 $t_{max}$ : time taken to reach maximum concentration  
Tpmt: thiopurine methyltransferase  
TOF: time-of-flight  
TST: tris-buffered saline with tween  
UDPGA: uridine 5'-diphosphoglucuronic acid  
UGT: uridine 5'-diphospho-glucuronosyltransferase  
UK: United Kingdom  
ULN: upper limit of normal  
ULOQ: upper limit of quantification  
US: United States  
V2, V3: visit 2, visit 3  
VIF: variance inflation factor  
 $V_{max}$ : maximum rate of formation  
 $V_z/F$ : volume of distribution  
WT: wild type

## Chapter 1 Introduction

### 1.1 Interindividual drug response variability

Drug treatment is the most common therapeutic intervention advocated for patients by physicians, and its prevalence is increasing. By 2020, it is forecast that global medicine use and spending on prescription medications will reach 4.5 trillion doses and \$1.4 trillion, respectively (QuintilesIMS, 2015). However, there exists notable interindividual heterogeneity in drug response, affecting both efficacy and toxicity. It has been reported that the proportion of patients who respond beneficially to the first drug offered in the treatment of a wide range of diseases is typically just 50-75% (Spear *et al.*, 2001). Approximately 6.5% of admissions to hospitals are related to adverse drug reactions (ADRs) (Pirmohamed *et al.*, 2004) and about 15% of inpatients experience an ADR (Davies *et al.*, 2009). The World Health Organisation definition of an ADR is: “a response to a drug which is noxious and unintended, and which occurs at doses normally used in man for the prophylaxis, diagnosis, or therapy of disease, or for the modification of physiological function (World Health Organisation, 1972).” Understanding and overcoming this heterogeneity in drug response would reduce patient harm, improve clinical outcomes and lead to more efficient use of limited healthcare resources.

The reasons for variability in interindividual response are manifold, incompletely understood and vary between drugs. Sources of this variability include demographic (e.g. age, sex), clinical (e.g. liver and renal impairment, adherence, heterogeneity in underlying disease mechanisms), environmental (e.g. smoking, alcohol) and genetic factors. Pharmacogenomics is the study of the genetic determinants of drug response. Pharmacogenomics aims to improve drug effectiveness and reduce ADRs through incorporating genotype information into dose and/or drug selection prescribing decisions, and is integral therefore in the drive towards Precision Medicine.

## 1.2 An introduction to Statins

Statins are a class of oral hypolipidaemic drugs and are amongst the most highly prescribed medications worldwide (Postmus *et al.*, 2012); in the United Kingdom (UK) alone ~7 million patients are estimated to take a statin (NHS Choices, 2014). The first agent, mevastatin (ML-236B), was identified from *Penicillium citrinum* (Endo *et al.*, 1976), although it was never marketed due to adverse effects. Lovastatin (LVT), isolated from *Aspergillus terreus*, was the first approved statin, receiving its marketing authorisation in 1987 (Endo, 2004). LVT also naturally occurs in certain foods including red yeast rice (Liu *et al.*, 2006) and oyster mushrooms (Gunde-Cimerman and Cimerman, 1995).

Seven statins are currently licensed: atorvastatin (ATV), fluvastatin (FVT), LVT, pravastatin (PVT), rosuvastatin (RVT), simvastatin (SVT) and pitavastatin (PIT), with the former six available in the UK. Currently in the UK, all licensed statins are available as a generic except RVT that is patented until December 2017. Statins are indicated in both the prevention and treatment of (atherosclerotic) cardiovascular disease (CVD); in the UK SVT remains the most commonly prescribed statin, followed by ATV (National Statistics, 2015). An overview of the different statins is in Table 1.1.

Statins are often crudely sub-divided into:

- those that are administered as the therapeutically inactive lactone (L) (LVT, SVT) versus those administered as active acid statin (ATV, FVT, PVT, PIT, RVT);
- those that undergo extensive metabolism by the phase I cytochrome P450 (CYP) system (ATV, FVT, LVT, SVT) versus those that undergo little metabolism and are eliminated predominantly unchanged (PIT, PVT, RVT).
- Extensively metabolised statins are further subdivided into those primarily biotransformed by CYP3A4/5 (ATV, LVT, SVT) or CYP2C9 (FVT).

Biotransformed statins are typically referred to as lipophilic, whilst the renally excreted statins are considered hydrophilic.

Notable interindividual variability in response to statin therapy exists, with patients experiencing variable cholesterol lowering efficacy, residual risk of cardiovascular events (Cannon *et al.*, 2004; Postmus *et al.*, 2012), and 45-fold variation in statin systemic exposure (DeGorter *et al.*, 2013). Some patients also experience statin ADRs including statin-associated myotoxicity (SAM), new-onset diabetes mellitus, and probably haemorrhagic stroke (Collins *et al.*, 2016). Furthermore, transient elevation of transaminases (Golomb and Evans, 2008), adverse effects on energy levels and exertional fatigue (Golomb *et al.*, 2012) and reduced exercise capacity (Lee *et al.*, 2014) have also been reported. There are case reports of statin-induced memory loss and confusion, but overall statins are currently not thought to be associated with cognitive dysfunction (Gauthier and Massicotte, 2015).

Statin myotoxicity has a heterogeneous but dose related presentation (Alfirevic *et al.*, 2014; Golomb and Evans, 2008), and therefore there is extensive interest in factors associated with increased statin exposure.

The remainder of this introduction is subdivided into the following sections:

- CVD and atherosclerosis, in order to fully appreciate the broad clinical context of statin use
- Mechanisms of statin efficacy
- Statin myotoxicity, pharmacokinetic (PK) risk factors and mechanisms of myocyte disruption
- An overview of P450 oxidoreductase (POR)
- An overview of liquid chromatography-mass spectrometry (LC-MS)
- Thesis research aims and objective

Table 1.1 Pharmacokinetic properties of the different statins

Drug property	Atorvastatin	Cerivastatin	Fluvastatin	Lovastatin	Pitavastatin	Pravastatin	Rosuvastatin	Simvastatin
Year approved	1996	1997 to 2001	1993	1987	2009	1991	2003	1991
Generic available	Yes	No	Yes	Yes	No	Yes	No	Yes
Daily dose (mg)	10-80	0.2-0.3	20-80	10-80	1-4	10-80	5-40	10-40
Equipotent dose (mg)	20	-	>>80	80	4	80	5	40
Marketed drug form	Acid	Acid	Acid	Lactone	Acid	Acid	Acid	Lactone
log P (N-octanol/water partition coefficient)	1.11 (lipophilic)	1.70 (lipophilic)	1.27 (lipophilic)	1.70 (lipophilic)	1.49 (lipophilic)	-0.84 (hydrophilic)	-0.33 (hydrophilic)	1.60 (lipophilic)
Oral absorption (%)	30	>98	98	31	80	37	50	65-85
Bioavailability (%)	14	60	29	<5	51	17	20	5
Effect of food on bioavailability	Decrease	No effect	Decrease	Increase	No effect	Decrease	No effect	No effect
Time to C <sub>max</sub> (hours)	1-2	2-3	2.5-3	2-4	1	1-1.5	3-5	1-4
Protein binding (%)	≥98	>99	98	>95	>99	~50	88	95
Volume of distribution	381 L	0.3L/Kg	25	-	148 L	0.5 L/Kg	134 L	233 L
Overall extent of metabolism	High	High	High	High	Low	Low	Low	High
CYP enzymes involved in metabolism of acid form	CYP3A4, CYP3A5, CYP2C8*	CYP2C8, CYP3A4	CYP2C9, CYP2C8*, CYP3A4*	CYP3A4,	CYP2C9, CYP2C8*	CYP2C9, CYP3A4*, CYP3A5*	CYP2C9, CYP2C19*, CYP3A4*	CYP3A4, CYP3A5, CYP2C8*
CYP enzymes involved in metabolism of lactone form	CYP3A4, CYP3A5	CYP3A4	CYP3A4	CYP3A4	CYP3A4, CYP2D6*	Not known	CYP3A4, CYP2C9*, CYP2D6*	CYP3A4, CYP3A5
UGT enzymes involved in lactonization of acid form	UGT1A1, UGT1A3, UGT2B7	UGT1A3	Not known	UGT1A1, UGT1A3	UGT1A3, UGT2B7	None identified	UGT1A1, UGT1A3	None identified
Transporters for parent statin	<u>OATP1B1</u> , <u>BCRP</u> , MRP1, 2, 4, NTCP, P-gp OATP1A2, 1B3, 2B1	OATP1B1, BCRP	OATP1B1, 1B3, 2B1, BCRP	OATP1B1, P-gp	<u>OATP1B1</u> , 1B3, BCRP, MRP2, NTCP, P-gp	<u>OATP1B1</u> , 1B3, 2B1, BSEP, BCRP, MRP2, P-gp; <u>OAT3</u> in renal elimination	<u>OATP1B1</u> , BCRP, BSEP, MRP1, 2, 4, 5, P-gp, OATP1A2, 1B3, 2B1, NTCP; OAT3 in renal elimination	<u>BCRP</u> , P-gp (SVT lactone: <u>OATP1B1</u> )

<i>Table continued</i>								
<b>Drug</b>	<b>Atorvastatin</b>	<b>Cerivastatin</b>	<b>Fluvastatin</b>	<b>Lovastatin</b>	<b>Pitavastatin</b>	<b>Pravastatin</b>	<b>Rosuvastatin</b>	<b>Simvastatin</b>
<b>Metabolites</b>	2-OH ATV, 4-OH ATV, ATV L, 2-OH ATV L, 4-OH ATV L	M-1 acid, M-23 acid, CVT L M-1 L, M-23 L	5-OH FVT, 6-OH FVT, N-deisopropyl FVT, FVT L	LVT acid, 6-OH LVT acid	PIT L	6-epi PVT, 3 $\alpha$ -OH PVT PVT L, 3 $\alpha$ -OH PVT L	N-desmethyl RVT, RVT L	SVT acid, 3',5'-dihydrodiol, 6'-exomethylene & 3-OH acid metabolites
<b>Elimination half-life (hours)</b>	14	2-3	3	2-5	12	1-3	19	2-3
<b>Faecal excretion (%)</b>	98	70	90	83	79	70	90	60
<b>Renal excretion (%)</b>	<2	30	5	10	15	20	10-28	13
<b>References</b>	(Schirris <i>et al.</i> , 2015b; Jacobsen <i>et al.</i> , 2000; Pfizer Inc, 2015; Catapano, 2010; Black <i>et al.</i> , 1998; Knauer <i>et al.</i> , 2010; Generaux <i>et al.</i> , 2011)	(Jemal <i>et al.</i> , 1999b; Schirris <i>et al.</i> , 2015b; Muck, 2000; Muck <i>et al.</i> , 2001; Generaux <i>et al.</i> , 2011)	(Catapano, 2010; Novartis, 2012; Generaux <i>et al.</i> , 2011)	(Schirris <i>et al.</i> , 2015b; Merck & Co, 2014; Neuvonen <i>et al.</i> , 2008; Catapano, 2010; Generaux <i>et al.</i> , 2011)	(Schirris <i>et al.</i> , 2015b; Fujino <i>et al.</i> , 2003; Kowa Pharmaceuticals, 2012; Catapano, 2010; Generaux <i>et al.</i> , 2011)	(Bristol-Myers Squibb Company, 2013; Hoffman <i>et al.</i> , 2014; van Haandel <i>et al.</i> , 2016; Riedmaier, 2011; Catapano, 2010; Generaux <i>et al.</i> , 2011; Hirano <i>et al.</i> , 2005)	(Schirris <i>et al.</i> , 2015b; McCormick <i>et al.</i> , 2000; Cooper <i>et al.</i> , 2002; Cooper <i>et al.</i> , 2003c; Finkelman <i>et al.</i> , 2015; AstraZeneca, 2010; Catapano, 2010; Generaux <i>et al.</i> , 2011; Knauer <i>et al.</i> , 2010; Jemnitz <i>et al.</i> , 2010)	(Alakhali <i>et al.</i> , 2013; Merck & Co, 2015; Schirris <i>et al.</i> , 2015b; Prueksaritanont <i>et al.</i> , 2003; Kitzmiller <i>et al.</i> , 2014; Catapano, 2010; Generaux <i>et al.</i> , 2011)

Abbreviations: ATV = atorvastatin; BCRP = breast cancer resistance protein; BSEP = bile salt export pump; CVT = cerivastatin; CYP = cytochrome P450; FVT = fluvastatin; L = lactone; LVT = lovastatin; M-1 = demethylation cerivastatin metabolite; M-23 = hydroxylation cerivastatin metabolite; MRP = multidrug resistance-associated protein; NTCP = sodium-taurocholate co-transporting polypeptide; OATP = organic anion-transporting polypeptide; -OH = hydroxy; P-gp = P-glycoprotein; PIT = pitavastatin; PVT = pravastatin; RVT = rosuvastatin; SVT = simvastatin; UGT = uridine 5'-diphospho-glucuronosyltransferase

\* = denotes enzymes with a minor contribution to the known statin metabolism. Underlined transporters are considered particularly important to the disposition of the statin.

### 1.3 Cardiovascular disease

CVD is the leading cause of global mortality, responsible for ~30% of all deaths worldwide (World Health Organisation, 2016). Although lower respiratory infections and diarrhoeal diseases are the top causes of death in low-income economies, CVD is the most frequent cause in all remaining low-middle to high income countries (World Health Organisation, 2016). CVD accounts for ~15 million deaths per annum (World Health Organisation, 2016) and this is projected to increase to >23.6 million by 2030 (Laslett *et al.*, 2012). Although death rates from CVD peaked in the 1970s and 1980s and have fallen since then, morbidity and healthcare expenditure associated with CVD is rising (NICE, 2016a). Disability-adjusted life years (DALYs) measure overall disease burden by integrating mortality and morbidity measures into a single metric, and CVD underlies ~10-18% of all DALYs lost (Laslett *et al.*, 2012). CVD drugs account for ~13% of global pharmaceutical spending (statista, 2016; Clinical Gene Networks, 2012), and approximately one sixth of all healthcare expenditure in the United States (US) is spent on CVD (Greenwell, 2015). Therefore, CVD is a domineering cause of death, disability and healthcare expenditure.

The cardiovascular system (CVS) consists of the heart and vasculature (arteries, arterioles, capillaries, venules, veins). Accordingly, CVD can be defined as originating from within the heart or vasculature. Primary heart diseases include arrhythmias, valvular disease and myocarditis. Vascular disease can be anatomically categorised by the type of vessel (e.g. vein versus artery) and tissue bed (e.g. coronary) affected, and functionally as vessel hardening, stenosis, obstruction, dilatation or rupture (haemorrhage) with associated sequelae. Common venous disorders include varicose veins (dilatation), superficial thrombophlebitis and deep vein thrombosis (obstructive). Arteries may become hardened by, for example, hyaline arteriosclerosis, stenosed/obstructed by atheroma, thrombus, embolism, spasm, or vasculitis, or dilated through aneurysm formation. The CVS is interconnected and therefore primary vasculature disease (e.g. coronary artery disease - CAD) can precipitate heart disease (e.g. heart failure) and vice versa (e.g. atrial fibrillation leading to

distal thromboembolism, or right-sided heart failure leading to peripheral oedema and venous ulceration).

#### **1.4 Atherosclerosis**

Whilst multiple pathologies can cause CVD, atherosclerosis underlies the majority of CVD morbidity and mortality, and frequently leads to CAD, cerebral, and peripheral artery disease (PAD). Statins are principally indicated in atherosclerotic CVD.

The term atherosclerosis is Hellenic, encompassing thickening and fat accumulation within the tunica intima layer of arteries (Rafieian-Kopaei *et al.*, 2014). Atherosclerosis is an insidious, chronic complex inflammatory disorder, a specific type of arteriosclerosis (i.e. thickening, hardening and loss of arterial wall elasticity), and characterised by formation of arterial intimal atheromatous plaques (Figure 1.1). Non-modifiable risk factors include increasing age, male sex, and genetic predisposition; established modifiable risk factors are hypertension, insulin resistance, diabetes mellitus, hyperlipidaemia, smoking, chronic inflammation (e.g. rheumatoid arthritis) and chronic kidney disease. Emerging risk factors include stress, high alcohol intake, and sleep apnoea (Rafieian-Kopaei *et al.*, 2014). Atherosclerosis progression entails formation of fatty streaks, atheroma and finally atherosclerotic plaques (Rafieian-Kopaei *et al.*, 2014). Initial endothelial 'injury' or dysfunction may initiate atherosclerosis, for example due to shear stresses, which are thought to underlie why atherosclerosis commonly occurs at arterial bifurcations. Endothelial dysfunction leads to release of pro-inflammatory cytokines, upregulation of cellular adhesion molecules and increased intimal permeability, which results in leukocyte infiltration and accumulation of low-density lipoprotein (LDL)-cholesterol (LDL-C) (Camm and Bunce, 2012; Skeoch and Bruce, 2015). The locally increased LDL-C concentration results in both spontaneous and endothelial-cell mediated LDL-C oxidation (Tavafi, 2013). Monocytes recruited from the circulation differentiate into macrophages, which phagocytose oxidised-LDL-C via scavenger receptors leading to conversion to foam cells, and

foam cell accumulation leads to arterial lipid streak appearance (Rafieian-Kopaei *et al.*, 2014). Cytokine release stimulates smooth muscle cell migration from the tunica media to the luminal side of the arterial wall, with synthesis of extracellular matrix to form the fibrous cap of an atheroma. A shoulder of peripheral macrophages and T-cell lymphocytes develops. Further progression establishes an atheromatous plaque consisting of an atheroma core of cell lesions, foam cells, cytokine-driven neovascularisation, and debris including calcium, cholesterol esters and a mass of fatty substances, covered by the fibrous cap (Rafieian-Kopaei *et al.*, 2014).

### **Figure 1.1 Atherosclerotic plaque development**

Image reproduced from (Skeoch and Bruce, 2015). Initial endothelial activation, for example due to shear stress damage, leads to endothelial release of proinflammatory cytokines and upregulation of cellular adhesion molecules, which recruits circulating immune cells. Increased endothelial permeability permits influx of both LDL-C and immune cells into the tunica intima (Skeoch and Bruce, 2015). The locally increased LDL-C concentration leads to spontaneous and endothelial-cell mediated LDL-C oxidation (Tavafi, 2013). Recruited monocytes differentiate into macrophages, which phagocytose oxidised LDL-C via scavenger receptors to form foam cells. Pro-inflammatory cytokines stimulate further immune cell recruitment, smooth muscle cell migration from the tunica media and proliferation, and neovascularisation (Skeoch and Bruce, 2015). The smooth muscle cells synthesise extracellular matrix to form the fibrous cap (Rafieian-Kopaei *et al.*, 2014). Hypoxia and oxidative stress lead to foam cell apoptosis and formation of a necrotic lipid core. Rupture of the fragile new vessels leads to intra-plaque haemorrhage, causing further inflammation and accelerating plaque growth (Skeoch and Bruce, 2015). A shoulder of peripheral macrophages and T-cell lymphocytes develops. The resulting complex atheromatous plaque consists of an atheroma core of cell lesions, foam cells, neovascularisation and debris including calcium, cholesterol esters and a mass of fatty substances, covered by the fibrous cap (Rafieian-Kopaei *et al.*, 2014). Thinning and rupture of the fibrous plaque provokes intravascular thrombosis and acute clinical ischaemic events (Skeoch and Bruce, 2015).

Fatty streaks can reversibly develop in childhood and atheromatous plaques may appear in adolescence (McGill *et al.*, 2000). The fibromuscular plaques enlarge over subsequent years, narrowing the arterial lumen. Atherosclerosis is predominantly slowly progressive, and most plaques remain asymptomatic (subclinical). However, some lead to flow-limiting lumen stenosis resulting in clinically-apparent ischaemia (e.g. angina pectoris, intermittent claudication) (Riccioni and Sblendorio, 2012). A few plaques become unstable and may rupture/fissure/erode, leading to intravascular thrombosis, downstream tissue bed necrosis (e.g. myocardial infarction (MI), stroke) and sequelae (e.g. sudden cardiac death from ischaemia-induced fatal ventricular arrhythmias). Long term atherosclerotic-mediated coronary flow insufficiency, often with myocardial infarction(s), leads to ischaemic cardiomyopathy, which is a common cause of low-output heart failure.

#### **1.4.1 Atherosclerosis management**

Management of atherosclerotic-mediated CVD encompasses both primary and secondary prevention. Primary CVD prevention aims to reduce atherosclerosis and prevent symptom onset in asymptomatic individuals; secondary prevention reduces the burden of symptomatic atherosclerotic CVD. Therapeutic strategies include conservative, medical, and interventional. A cardioprotective diet (e.g. the 'Mediterranean' diet), avoidance of excessive alcohol consumption, physical activity, weight loss and smoking cessation are recommended (NICE, 2016a). Drugs are indicated to treat risk factors and include hypolipidaemic, anti-hypertensive, hypoglycaemic and, most recently, the anti-inflammatory agent, canakinumab (Ridker *et al.*, 2017). Interventions include percutaneous angioplasty, stent insertion, and coronary artery bypass graft (CABG) surgery.

#### **1.5 Indications for statin therapy**

Within this multifaceted overarching strategy for management of atherosclerotic CVD, statins are indicated in both the primary and secondary prevention of atherosclerotic CVD. Statins are the first line hypolipidaemic drug class for managing CVD, although ezetimibe, fibrates, bile acid sequestrants, and

novel parenteral proprotein convertase subtilisin/kexin type 9 (PCSK9) inhibitors can also be considered in specific settings. Currently, the National Institute for Health and Care Excellence (NICE) in the UK recommends 20mg ATV daily as first choice statin therapy for primary CVD prevention in all patients with at least a 10% risk of developing CVD over the following 10 years, and ATV 80mg daily is first line in secondary prevention (NICE, 2016a).

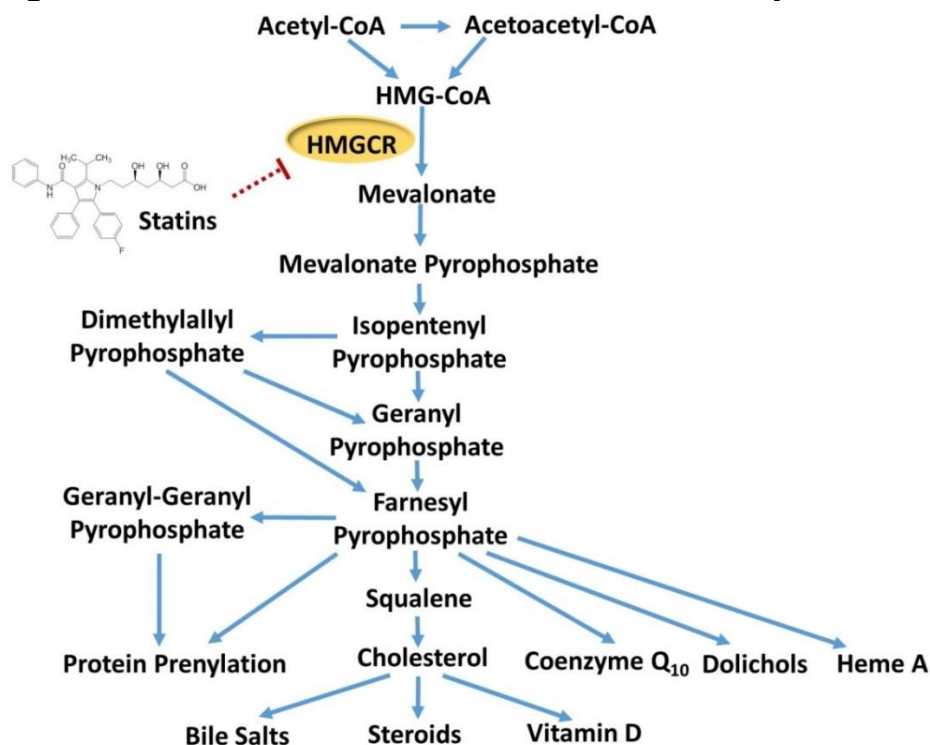
## 1.6 Statin efficacy

Multiple randomized controlled trials (RCTs) comparing statin therapy to placebo or higher intensity to lower intensity statin therapy have been conducted. The Cholesterol Treatment Trialists' (CTT) Collaboration has conducted large scale meta-analyses of statin RCTs that were scheduled to involve at least two years of statin treatment in at least 1000 patients, using individual patient data (Cholesterol Treatment Trialists Collaboration, 1995). Overall, *each* one mmol/L reduction in LDL-C with statin therapy is associated with a 22% reduction in the rate of major cardiovascular events (coronary deaths, MIs, strokes and coronary revascularisations) (Cholesterol Treatment Trialists, 2010). Lowering LDL-C by two mmol/L with statin treatment for about five years in 10,000 patients would prevent major cardiovascular events in approximately 1000 (10%) secondary prevention patients or 500 (5%) primary prevention patients (Collins *et al.*, 2016).

The principal mechanism of statin action is competitive inhibition of 3-hydroxy-3-methylglutaryl-Coenzyme A reductase (HMGCR), which is the rate limiting enzyme in *de novo* cholesterol synthesis and the first committed enzyme of the mevalonate pathway (Figure 1.2). In turn, this leads to a compensatory upregulation of hepatic LDL receptors (Goldstein and Brown, 2009). The resulting main effect is a reduction in LDL-C by ~30-63% dependent on statin and dose. Statins also reduce triglycerides (~20-40%) and raise high-density lipoprotein-cholesterol (HDL-C) (~5%) to a more modest extent (Rosenson, 2017).

Beyond lowering cholesterol, statins have been associated with a range of beneficial pleiotropic effects including anti-inflammatory, antioxidant and immunomodulatory effects, inhibition of platelet activation and increased plaque stability (Kavalipati *et al.*, 2015). For example, statins mediate a dose-dependent decrease in C-reactive protein (Cannon *et al.*, 2004). The mechanisms underlying these pleiotropic effects are incompletely understood but are thought to be related to decreases in other products of the mevalonate pathway as a result of statin-mediated HMGCR inhibition, including isoprenoid intermediates (e.g. farnesyl pyrophosphate (FPP), geranyl-geranyl pyrophosphate (GGPP)), dolichols, heme A and coenzyme Q<sub>10</sub> (CoQ<sub>10</sub>, also known as ubiquinone) (Figure 1.2) (Kavalipati *et al.*, 2015). GGPP and CoQ<sub>10</sub> are also linked to SAM (see later).

**Figure 1.2 Statin-mediated inhibition of cholesterol synthesis**



Statins competitively inhibit 3-hydroxy-3-methylglutaryl-Coenzyme A reductase (HMGCR), the first committed enzyme of the mevalonate pathway and the rate-limiting enzyme for *de novo* cholesterol synthesis. The resultant decrease in hepatic cholesterol synthesis leads to a compensatory upregulation of low-density lipoprotein-cholesterol (LDL-C) receptors on the plasma membranes of hepatocytes, which increases hepatic uptake of circulating LDL-C and so reduces plasma LDL-C. Statin-mediated inhibition of HMGCR also leads to reduced synthesis of other mevalonate metabolites including isoprenoid intermediates (e.g. farnesyl pyrophosphate (FPP), geranyl-geranyl pyrophosphate (GGPP)), dolichols, heme A and coenzyme Q<sub>10</sub>, some of which are implicated in the beneficial pleiotropic effects of statins.

## **1.7 Statin-associated myotoxicity**

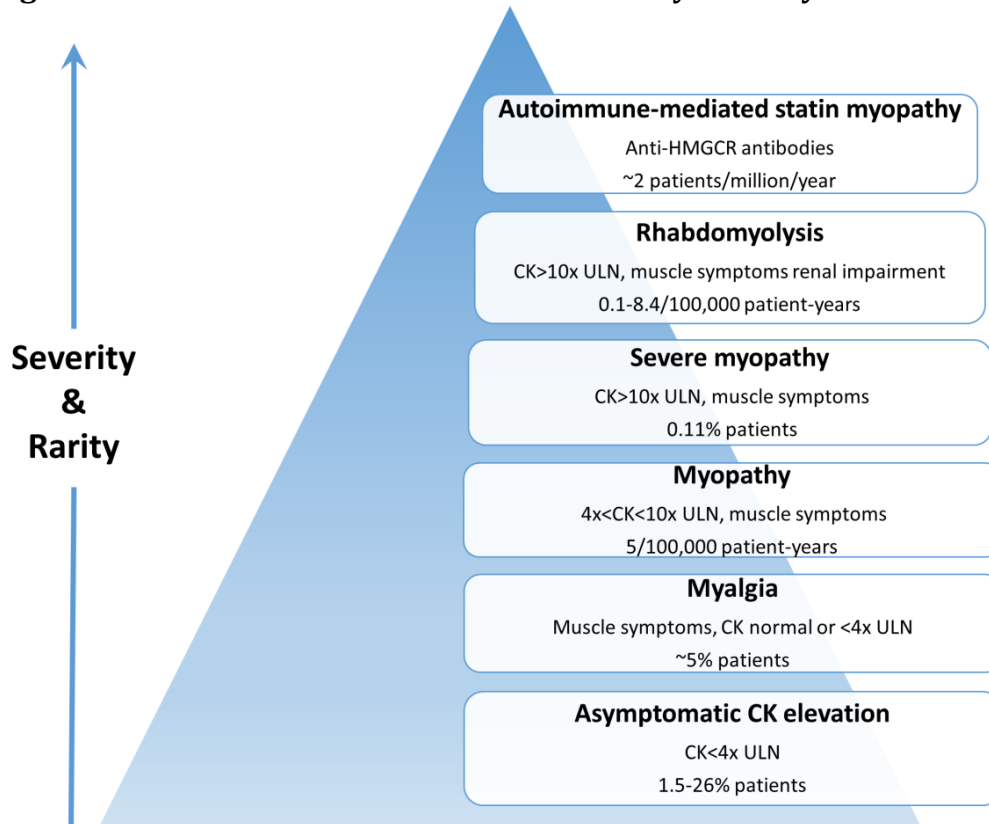
The most commonly reported statin ADR is SAM, which comprises approximately two-thirds of all statin ADRs (Raju *et al.*, 2013). SAM encompasses a spectrum of presentations (Figure 1.3) including common myalgias (aches, cramps and/or weakness) with none or minor elevations in serum creatine kinase (CK), asymptomatic minor CK elevations, symptomatic myopathies with elevated CKs of increasing severity and infrequency, rare but potentially life-threatening rhabdomyolysis, and very rare autoimmune-mediated statin myopathy that persists despite statin cessation (Alfirevic *et al.*, 2014). The most common muscular symptoms are pain, heaviness, stiffness, cramping and subjective weakness affecting the legs bilaterally (thighs, calves) or all over (Bruckert *et al.*, 2005; Elam *et al.*, 2017). Tendonitis-associated pain has also been reported (Bruckert *et al.*, 2005). SAM is most common during the first year of treatment (Hippisley-Cox and Coupland, 2010) with a median time to onset of one month (Golomb and Evans, 2008).

### **1.7.1 The incidence of SAM and the nocebo effect**

The true incidence of SAM is uncertain, occurring in 1.5-5% of participants in RCTs (relative to placebo groups) (Kashani *et al.*, 2006), compared to 10-15% in observational studies (Abd and Jacobson, 2011). This variability is likely attributable to a range of factors including different myotoxicity definitions and follow up procedures, the 'nocebo' effect, and inclusion of different patient groups. For example, both short- and long-term statin RCTs excluded individuals with impaired hepatic and renal function, at the extremes of age, those receiving concomitant interacting drugs and the long-term trials used lead-in periods to exclude patients with early-onset statin intolerance (Davidson and Robinson, 2007). This variability in reported SAM rates has also sparked disagreement and controversy over the underlying benefit-risk profile of statins, particularly in patients at the lower end of the CVD risk spectrum (Godlee, 2014). Nevertheless, there is consensus that statins definitely increase the risk of the more severe forms of myotoxicity, including severe myopathy and rhabdomyolysis (Collins *et al.*, 2016). Importantly, cerivastatin (CVT) was

voluntarily withdrawn in 2001 because of 52 cases of fatal rhabdomyolysis (Furberg and Pitt, 2001).

**Figure 1.3 Classification of statin-associated myotoxicity**



CK = creatine kinase; HMGCR = 3-hydroxy-3-methylglutaryl-Coenzyme A reductase; ULN = upper limit of normal.

Statin-associated myotoxicity (SAM) is the most common statin adverse drug reaction. SAM consists of a spectrum of adverse events ranging from asymptomatic CK rises and common myalgias through increasingly severe myopathies with rising CK levels to rhabdomyolysis that can be fatal (Alfirevic *et al.*, 2014). It has been recently recognised that statins are also associated with an autoimmune-mediated myopathy, which involves anti-HMGCR autoantibodies and is considered pathologically distinct to the other forms of SAM (Mammen, 2016). Autoimmune-mediated statin myopathy has been placed at the apex here because it is the rarest form of SAM, continues despite statin cessation, and can be severe with highly elevated CK (Hamann *et al.*, 2013).

The greater difficulty lies in correctly assigning the aetiology of the commoner milder musculoskeletal symptoms, and in particular whether they are attributable to the pharmacology of statin therapy, the nocebo effect, and/or an unrelated concomitant condition(s) (e.g. increased exercise, viral illnesses, symptomatic vitamin D deficiency, severe hypothyroidism). On the one hand, a recent six-month double-blind RCT conducted in 420 healthy volunteers administered either ATV 80mg daily or placebo found an increased rate of myalgia amongst the subjects on ATV compared to placebo (9.4% vs 4.6%,

respectively,  $p=0.05$ ) (Parker *et al.*, 2013), which suggests that myalgias may be caused by intensive ATV therapy in  $\sim 5\%$  of people. Furthermore, recent N-of-1 (single-patient) placebo-controlled trials involving patients with a prior history of SAM have reported that  $\sim 30\text{-}40\%$  still experience muscle-related events only during the statin phase and not when on placebo (Taylor *et al.*, 2015; Nissen *et al.*, 2016). On the other hand, these N-of-1 trials thus show that the majority of SAM is unlikely due to the pharmacological activity of statins. Interestingly, it was reported recently that the frequency of muscle-related adverse events in patients on ATV 10mg daily or placebo in the large double-blind ASCOT-LLA RCT ( $n=10,180$ ) was not significantly different, but became significantly more common in patients taking ATV 10mg daily (1.26% per annum) compared to placebo (1.00% per annum) in the subsequent open label non-blinded extension phase (Gupta *et al.*, 2017). The nocebo effect is in the inverse of the placebo effect and refers to adverse events, normally purely subjective, that result from expectations of harm from a drug (Tobert and Newman, 2016). These expectations can be derived from several sources, including warnings about side effects communicated by clinicians when prescribing a drug (Tobert and Newman, 2016). The contrasting results between the blinded ASCOT-LLA RCT and subsequent open label extension study demonstrate clearly that the nocebo effect contributes to reported SAM. However, it should be noted that the dose of ATV (10mg daily) in ASCOT LLA was low but SAM is dose-related (Alfirevic *et al.*, 2014), and so the magnitude of impact of the nocebo effect may decrease in patients on higher statin doses. In summary, the literature demonstrate that SAM has different aetiologies, but importantly both the milder and more severe myotoxicity forms can be due to the pharmacological activity of statin treatment. N-of-1 trials are likely to bring much needed phenotypic clarity through the identification of patients whose muscle symptoms are more or less likely to be truly statin-induced.

## 1.8 Myotoxicity pathogenesis

Several SAM risk factors have been identified (Table 1.2) and mechanisms proposed, although a unifying explanation for SAM pathogenesis remains

elusive. Two inter-dependent mechanisms are nevertheless implicated: 1.) increased statin systemic exposure due to clinical and pharmacogenomic-mediated PK alterations plausibly increasing skeletal muscle exposure and; 2.) intracellular skeletal myocyte entry with subsequent disruption of function (Moßhammer *et al.*, 2014).

**Table 1.2 Clinical risk factors of statin-associated myotoxicity**

<b>Risk factor</b>	<b>Reference</b>
<b>Demographics</b>	
Advanced age (>80 years old)	(Pasternak <i>et al.</i> , 2002; Golomb and Evans, 2008)
Female gender	(Voora <i>et al.</i> , 2009; Golomb and Evans, 2008)
Low body mass index	(Pasternak <i>et al.</i> , 2002; Davidson and Robinson, 2007)
<b>Ethnicity</b>	
Black African	(Hippisley-Cox and Coupland, 2010)
Caribbean	
<b>Co-morbidities</b>	
Chronic kidney disease (especially in diabetes)	(Pasternak <i>et al.</i> , 2002; Golomb and Evans, 2008)
Chronic liver disease	(Hippisley-Cox and Coupland, 2010; ClinRisk Ltd, 2014)
Hypothyroidism	
Type 1 diabetes	
Type 2 diabetes	
Treated hypertension (women)	(Hippisley-Cox and Coupland, 2010)
Vitamin D deficiency	(Ahmed <i>et al.</i> , 2009; Khayznikov <i>et al.</i> , 2015)
Alcohol abuse	(Pasternak <i>et al.</i> , 2002)
<b>Personal/family factors</b>	
Physical exercise	(Thompson <i>et al.</i> , 1997; Meador and Huey, 2010)
Personal or family history of muscle pain	(Bruckert <i>et al.</i> , 2005)
<b>Diet</b>	
Grapefruit juice (CYP3A4 inhibition)	(Dreier and Endres, 2004)
<b>Drugs</b>	
Higher statin dose	(Davidson and Robinson, 2007; Armitage, 2007)
Corticosteroids	(Hippisley-Cox and Coupland, 2010)
CYP3A4 inhibitors (particularly for ATV, LVT, SVT) – e.g. amiodarone, ciclosporin, clarithromycin, erythromycin, protease inhibitors (e.g. indinavir, ritonavir)	(Patel <i>et al.</i> , 2013a; Neuvonen <i>et al.</i> , 2006; Lees and Lees, 1995; Cheng <i>et al.</i> , 2002; Chanson <i>et al.</i> , 2008; Roten <i>et al.</i> , 2004; Saliba and Elias, 2005)
CYP2C9 inhibitors <sup>1</sup> (for FVT) – e.g. fluconazole	(Mirosevic Skvrce <i>et al.</i> , 2013)
OATP1B1 inhibition - e.g. gemfibrozil, ciclosporin	(Neuvonen <i>et al.</i> , 2006)

Adapted from (Alfirevic *et al.*, 2014). <sup>1</sup> = in renal transplant patients and limited to the subgroup carrying CYP2C9\*2 or \*3.

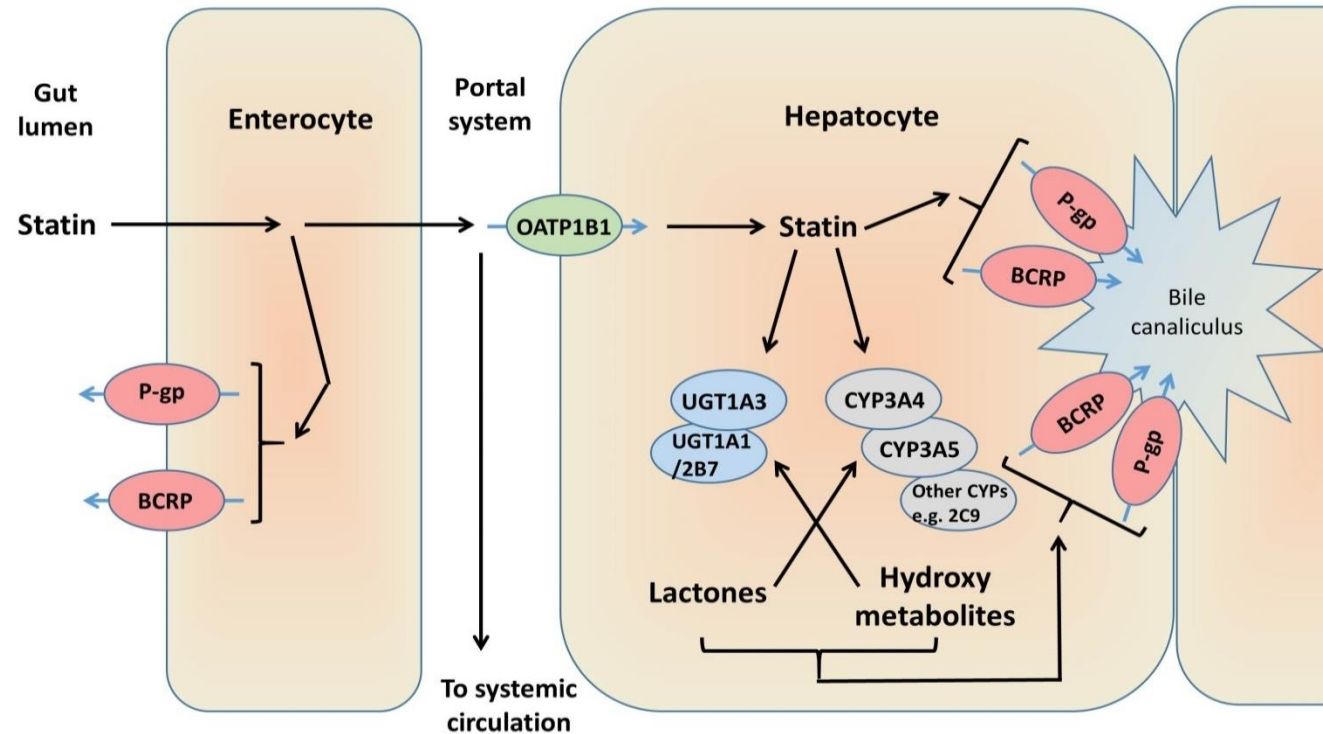
### **1.8.1 Factors associated with statin pharmacokinetics and myotoxicity**

A broad overview of the major enzymes and transporters generally involved in statin disposition is provided in Figure 1.4, which are the focus of the following sections. The absorption, distribution, metabolism and elimination (ADME) PK characteristics of the different statins are listed in Table 1.1.

Multiple clinical and pharmacogenomic factors have been associated with differential statin PK, and a subset also associated with SAM. In the following sections, the impact of clinical factors, pharmacogenomic factors and drug-drug interactions (DDIs) on statin PK and myotoxicity are sequentially reviewed.

A particular emphasis has been placed on pharmacogenomic factors here. Therefore, Table 1.3 comprehensively covers the pharmacogenomics of statin PK, and Table 1.4 summarises the results of a systematic literature review that identified 34 studies investigating the pharmacogenomics of SAM, with the first section detailing PK gene variants. Table 8.1 in the appendix tabulates clinical factors affecting statin PK.

Figure 1.4 A generalised overview of statin pharmacokinetics



This schematic provides a broad generalised overview of statin pharmacokinetics, depicting key proteins involved in the metabolism or transport of multiple (but not all) statins. All statins are orally administered, absorbed by the gut and predominantly subject to extensive first pass clearance. All statins except FVT are considered substrates for the hepatic influx transporter, organic anion-transporting polypeptide 1B1 (OATP1B1). Statin acids can undergo uridine 5'-diphosphoglucuronosyltransferase (UGT)-mediated lactonization. ATV, LVT and SVT are extensively metabolised by cytochrome P450 (CYP) 3A4/5, FVT is extensively metabolised by CYP2C9, and PIT, PVT and RVT undergo marginal CYP-mediated metabolism, mainly by CYP2C9. Both statin acids and lactones (Ls) can be CYP substrates. Ls can be hydrolysed back to their respective acid spontaneously or by plasma esterases and paraoxonases. Efflux pumps (e.g. breast cancer resistance protein (BCRP), P-glycoprotein (P-gp)) are involved in limiting gut absorption and mediating biliary excretion.

### 1.8.1.1 Clinical risk factors

Increasing dose is uniformly associated with increased statin exposure, and increasing age generally correlates with modestly greater exposure (except FVT, RVT) (Novartis, 2012; AstraZeneca, 2010) (see Table 8.1 in Appendix). Women have modestly higher exposure to most statins, except RVT for which there is no difference (Zhou *et al.*, 2013c), and modestly lower circulating ATV levels compared to men (Pfizer Inc, 2015). All statins are predominantly excreted in faeces, and therefore hepatic impairment is associated with increased exposure to most statins (except RVT) (Simonson *et al.*, 2003), and can result in several fold increased exposures (e.g. ATV, FVT) (Pfizer Inc, 2015; Novartis, 2012). On the other hand, renal impairment is only associated with increased statin exposure for statins that are at least 10% renally excreted (Table 8.1 in Appendix), with no impact on ATV or FVT PK (Pfizer Inc, 2015; Appeldingemane *et al.*, 2002). The maximum effect of renal impairment is a 3-fold increase in RVT exposure (AstraZeneca, 2010).

Importantly, increasing dose, age, female sex, low body mass index (BMI), renal impairment (especially due to diabetes) and liver disease all generally *increase* systemic statin exposure and have all been associated with SAM (Alfirevic *et al.*, 2014). For example, high statin equivalent doses increase the risk of severe myopathy ~six-fold compared to low statin doses (McClure *et al.*, 2007), confirming SAM is dose-related (Golomb and Evans, 2008).

### 1.8.1.2 Pharmacogenomic risk factors

As evidenced in Table 1.3, multiple genes alter statin PK; the main ones, *CYPs*, uridine 5'-diphospho-glucuronosyltransferases (*UGTs*), solute carrier organic anion transporter family member 1B1 (*SLCO1B1*) and the efflux transporters adenosine triphosphate (ATP)-binding cassette (*ABC*) subfamily B member 1 (*ABCB1*) and *ABCG2* are reviewed below. However, despite their impact on statin PK, only *SLCO1B1* rs4149056 has been consistently associated with myotoxicity.

### 1.8.1.2.1 CYP phase 1 hydroxylation

The human *CYP* superfamily constitutes 57 putatively functional genes and 58 pseudogenes, categorised according to their peptide sequence similarity into 18 families and 44 subfamilies (Nebert *et al.*, 1987; Zanger and Schwab, 2013). The functional genes encode CYP hemoproteins involved in several biological processes including biosynthesis of steroids, prostaglandins, bile acids and xenobiotic metabolism (Zanger and Schwab, 2013). Metabolism is responsible for the clearance of 70% of the top 200 used drugs (Wienkers and Heath, 2005), and a subset of 12 CYPs carry out 75% of these metabolic reactions (Gordon *et al.*, 2014). The majority of CYP-mediated reactions are carried out by CYP2D6, CYP3A4/5 or CYP2C9 (Canestaro *et al.*, 2014).

There is wide interindividual variability in CYP drug-metabolising activity (Zanger and Schwab, 2013). Many *CYPs* are polymorphic and metabolizer phenotype can be predicted from genotype and categorised into: extensive (normal, *\*1/\*1*), intermediate (heterozygous for a reduction-of-function (ROF) allele), poor (ROF homozygotes/compound heterozygotes) and ultra-rapid (an increased number of functioning gene copies). *CYP2D6* poor metaboliser status (e.g. homozygotes for *\*5*, *\*10*, or *\*14* haplotypes) has been associated with increased LVT (Yin *et al.*, 2004; Yin *et al.*, 2012) and SVT exposure (Choi *et al.*, 2015) (Table 1.3), although *in vitro* studies have not identified LVT/SVT to be *CYP2D6* substrates (Prueksaritanont *et al.*, 1997; Prueksaritanont *et al.*, 2003; Iyer *et al.*, 2004).

The human *CYP3A* family consists of *CYP3A4*, *3A5*, *3A7* and *3A43* within chromosome 7q22.1 (Zanger and Schwab, 2013). For the majority of individuals, *CYP3A4* is the most abundant CYP within the liver and gut. When present, *CYP3A5* may represent as much as 50% of hepatic *CYP3A* content and equal *CYP3A4* activity (Elens *et al.*, 2013b). *CYP3A7* constitutes 30-50% of total foetal liver CYP content (Shimada *et al.*, 1996), but has variably low expression

in adult livers (Zanger and Schwab, 2013). CYP3A43 is predominantly extrahepatic, metabolises endogenous compounds, and is not a major drug metabolising enzyme (DME) (Elens *et al.*, 2013b).

ATV, LVT and SVT are extensively metabolised by CYP3A4/5. CYP3A4 shows extensive interindividual variation in activity although, unlike *CYP2D6*, *CYP3A4* has no well characterised null alleles (Canestaro *et al.*, 2014). Nevertheless, a recently described novel variant, rs35599367 (\*22, 522-191C>T), within intron six of *CYP3A4* is associated with reduced *CYP3A4* hepatic mRNA and enzyme activity (Wang *et al.*, 2011). *CYP3A4\*22* leads to increased formation of non-functional CYP3A4 alternate splice variants with partial intron six retention, specifically in human liver but not small intestine (Wang and Sadee, 2016). *CYP3A4\*22* is present with a minor allele frequency (MAF) of ~5% in Europeans, but is low/rare (~1%) in African and Asian populations (Yates *et al.*, 2016). *CYP3A4\*22* is associated with reduced ATV hydroxylation (Klein *et al.*, 2012) and ethnicity-restricted increases in SVT/SVT acid concentrations (Kitzmilller *et al.*, 2014) (Table 1.3).

In addition to genetic variation, *CYP* expression is modulated by multiple factors including epigenetic influences, sex, age, disease states, inflammation, and nuclear receptor-mediated expression modulation in response to multiple endogenous and exogenous (e.g. other drugs) substances (Zanger and Schwab, 2013). Interestingly, a single nucleotide polymorphism (SNP) within peroxisome proliferator-activated receptor- $\alpha$  (*PPARA*), rs4253728, is associated with reduced human hepatic CYP3A4 protein levels (Klein *et al.*, 2012) and reduced metabolism of ATV (Klein *et al.*, 2012) and likely SVT (Tsamandouras *et al.*, 2014) (Table 1.3).

*CYP3A5\*3* is a loss of function allele defined by rs776746 (6986G>A), which introduces a cryptic mRNA splice site resulting in a non-functional truncated protein (Elens *et al.*, 2013b), and has MAFs of ~18%, 69% and 94% in African,

Asian and European populations (Yates *et al.*, 2016), indicating allele reversal. *CYP3A5\*3/\*3* has been associated with increased SVT and ATV L exposures (Shin *et al.*, 2011; Kim *et al.*, 2007).

As shown in Table 1.4, variants in *CYP2D6*, *CYP3A4*, *CYP3A5* have been differentially associated with SAM or statin tolerability in some candidate gene studies (Becker *et al.*, 2010; Frudakis *et al.*, 2007; Mulder *et al.*, 2001) but not others (Fiegenbaum *et al.*, 2005; Voora *et al.*, 2009; Zuccaro *et al.*, 2007). *PPARA* has not been specifically investigated by candidate gene studies. None of these genes were identified in SAM genome-wide association studies (GWAS) (Link *et al.*, 2008; Marciante *et al.*, 2011; Isackson *et al.*, 2011).

### 1.8.1.3 *UGT1A3* phase 2 glucuronidation

The UGT family of phase II DMEs consists of subfamilies UGT1A, UGT2A and UGT2B (Riedmaier *et al.*, 2010). UGTs catalyse glucuronidation, which transforms small lipophilic molecules into metabolites that are more hydrophilic and therefore easier to excrete. The UGT-catalysed glucuronidation reaction involves transfer of the glucuronic acid moiety of UDP-glucuronic acid to a substrate. The *UGT1A* complex locus is at chromosome 2q37.1 and consists of 13 unique alternate first exons, each with their own promoter and encoding the substrate binding site, followed by four common exons. Four of the first exons are pseudogenes; each of the remaining nine first exons can be spliced to the four common exons creating nine UGT1A protein isoforms (Gene NCBI, 2017). There is extensive linkage disequilibrium (LD) within the *UGT1A* complex locus.

Statin lactonization can occur either non-enzymatically at low intestinal pH (Kearney *et al.*, 1993), conceivably via a coenzyme A-dependent process (Li *et al.*, 2006), or via an unstable acyl glucuronide intermediate that undergoes spontaneous cyclization to the resultant L analyte (Prueksaritanont *et al.*, 2002). Depending on the statin, UGT1A3, 1A1 and UGT2B7 can be involved in acyl

glucuronidation (Schirris *et al.*, 2015b) However, UGT1A3 has been shown to consistently have the highest *in vitro* statin lactonization rate (Schirris *et al.*, 2015b). *UGT1A3\*2* consists of the minor alleles of intronic variants, rs2008584 and rs1983023, and the ancestral allele of the missense SNP, rs45449995 (p.M270V). Interestingly, *UGT1A3\*2* is associated with increased UGT1A3 hepatocyte protein expression and *\*2/\*2* volunteers have higher exposures of both ATV lactone (ATV L) and 2-hydroxy ATV lactone (2-OH ATV L) (Table 1.3) (Riedmaier *et al.*, 2010; Cho *et al.*, 2012). The common low expression *UGT1A1* promoter polymorphism, *\*28*, has seven thymine-adenine (TA) repeats instead of the wild type (WT) six TA repeats within the *UGT1A1* TATA box promoter. *UGT1A1\*28* has been associated with both *decreased* ATV L area under the concentration-time curve (AUC) (Stormo *et al.*, 2013) (Table 1.3) and *increased* lactonization (Riedmaier *et al.*, 2010); this discrepancy is likely attributable to the extensive LD within the *UGT1A* locus - for example between *UGT1A1\*28* and *UGT1A3\*2* (Riedmaier *et al.*, 2010).

*UGT1A1/1A3* variants have been sequenced for investigating their role in CVT myotoxicity, but no association was found (Marciante *et al.*, 2011) (Table 1.4). To date, they have not been included in candidate gene studies of SAM, nor identified by GWAS (Table 1.4).

#### 1.8.1.3.1 *SLC01B1* influx transporter

*SLC01B1*, located on chromosome 12p12.2, encodes the organic anion-transporting polypeptide 1B1 (OATP1B1), which is a major hepatocyte-specific sinusoidal influx xenobiotic transporter. Both *SLC01B1\*5* and *\*5* haplotypes carry the nonsynonymous SNP, rs4149056 (521T>C, p.V174A) in exon five that leads to a substitution of alanine for valine in the OATP1B1 primary polypeptide sequence, resulting in decreased intrinsic transport activity (Nies *et al.*, 2013). The MAF of rs4149056 is population-specific with average frequencies of 1%, 8% and 16% in African, Asian and European populations, respectively (Yates *et al.*, 2016). Importantly, homozygosity for the minor allele of rs4149056 has

been associated with ~1.6-3-fold increases in systemic exposures of ATV, PVT, PIT and RVT and ~3-fold increases in the major acid metabolites of LVT and SVT (Table 1.3). However, rs4149056 has not been associated with FVT or parent LVT and SVT levels (Table 1.3).

Importantly, rs4149056 was identified in a seminal GWAS in 2008 to be strongly associated with SVT myopathy (Link *et al.*, 2008). The odds ratio (OR) of myopathy in homozygous variant (CC) versus WT patients (TT) was 16.9 (95% confidence interval (CI) 4.7, 61.1), and a gene-dose trend was evident with an OR of 4.5 (95% CI: 2.6, 7.7) per C allele (Link *et al.*, 2008). This association between SVT myopathy and rs4149056 has been replicated (Link *et al.*, 2008; Brunham *et al.*, 2012; Carr *et al.*, 2013) and confirmed in a meta-analysis (Carr *et al.*, 2013). The OR for myopathy is reduced with lower SVT doses (Link *et al.*, 2008). However, rs4149056 is also associated with milder composite adverse outcomes encompassing myalgia, prescription reductions and/or minor biochemical (e.g. CK) elevations indicative of SVT intolerance (Donnelly *et al.*, 2011; Voora *et al.*, 2009; Bakar *et al.*, 2017).

Interestingly, an analysis of historical cases of CVT-related rhabdomyolysis similarly reported a gene-dose risk association with rs4149056 (OR 1.89, 9% CI 1.40, 2.56 per additional C allele) (Marciante *et al.*, 2011). However to date, *SLCO1B1* rs4149056 has not been associated with RVT (Danik *et al.*, 2013; Puccetti *et al.*, 2010) or PVT (Voora *et al.*, 2009) myotoxicity, although rare variation in *SLCO1B1* has been tentatively implicated with PVT SAM (Morimoto *et al.*, 2004). An association between rs4149056 and ATV myotoxicity has been suggested (Voora *et al.*, 2009; de Keyser *et al.*, 2014; Bakar *et al.*, 2017) or reported (Puccetti *et al.*, 2010) in some studies, but other studies found no evidence (Carr *et al.*, 2013; Brunham *et al.*, 2012; Santos *et al.*, 2012; Hubacek *et al.*, 2015). These differences may be due to the generally small ATV sample sizes used in several of the studies, and the different doses of ATV investigated. Of note, a recent candidate gene study (n=606) compared cases of intolerable

myalgia on SVT 40mg (n=107) or ATV 80mg (n=18) daily (defined as symptom occurrence within six months of initiating statin treatment, resolution on de-challenge, and symptom re-occurrence upon re-challenge, with a CK elevation <4x the upper limit of normal (ULN)) to statin tolerant controls (Bakar *et al.*, 2017). This study found the variant allele of *SLCO1B1* rs4149056 to be significantly associated with an increased risk of intolerable myalgia, and importantly the distribution of rs4149056 genotypes between the cases and controls was similar for both SVT and ATV, lending support to the suggestion that rs4149056 is relevant to ATV-induced myotoxicity at high ATV doses. However, in keeping with the other studies, the majority of cases in this study had been exposed to SVT and so the observed risk with *SLCO1B1* rs4149056 was still primarily driven by SVT. Thus, the influence of rs4149056 on the myotoxicity risk of statins other than SVT remains unclarified.

SVT acid AUC increases 221% in rs4149056 CC homozygotes compared to TT WT subjects (Pasanen *et al.*, 2006) (Table 1.3), constituting the largest increase for any statin. SVT remains the most commonly prescribed statin and so the majority of SAM cases included in studies were exposed to SVT, and SVT intrinsically appears particularly myotoxic (see below) (Skottheim *et al.*, 2008).

A second common nonsynonymous *SLCO1B1* SNP, rs2306283 (388A>G, p.N130D) in exon four, occurs with G allele frequencies of 82%, 66% and 40% in African, Asian and European populations, respectively (Yates *et al.*, 2016), indicating allele reversal. rs2306283 is associated with increased OATP1B1 protein expression and reduced ATV AUC when coexistent with WT rs4149056 (e.g. *SLCO1B1*\*14) (Nies *et al.*, 2013) (Table 1.3). However, when both minor alleles are present (*SLCO1B1*\*15), the impact of rs4149056 dominates and statin exposure is increased (Nies *et al.*, 2013). A third common nonsynonymous *SLCO1B1* SNP is rs11045819 (463C>A, p.P155T), although it appears to have no impact on statin PK (Nies *et al.*, 2013). Neither rs2306283 nor rs11045819 have been associated with SAM.

#### 1.8.1.4 ***ABCB1* and *ABCG2* efflux transporters**

*ABCB1* and *ABCG2* are both members of the superfamily of ATP-binding cassette (ABC) transporters and encode the efflux transporters P-glycoprotein (P-gp) and breast cancer resistance protein (BCRP), respectively. Both P-gp and BCRP are located in the apical (luminal) membrane of enterocytes and the canalicular membrane of hepatocytes, as well as in other locations including the blood brain barrier (Krajcsi, 2013) and placenta (Ceckova-Novotna *et al.*, 2006; Mao, 2008). They have broad substrate specificity.

*ABCB1* has three common SNPs, rs1128503 (1236T-C, synonymous), rs2032582 (missense, 2677T-G) and rs1045642 (synonymous, 3435T-C); TTT homozygotes have ~55-60% increased exposure to both ATV and SVT acid metabolite (Keskitalo *et al.*, 2008) (Table 1.3). Furthermore, the *ABCB1* T alleles have been associated with symptom-independent elevated CK levels (Ferrari *et al.*, 2014) and muscle symptoms (Fiegenbaum *et al.*, 2005; Hoenig *et al.*, 2011) in some candidate gene studies, but not with prescribing changes suggestive of statin intolerance (Becker *et al.*, 2010) (Table 1.4).

The nonsynonymous *ABCG2* SNP, rs2231142 (421C>A, p.Q141K) has MAFs of 1%, 10-29% and 9% in African, Asian and European populations, respectively (Yates *et al.*, 2016). Importantly, the minor allele homozygosity has been associated with ~2-fold increased exposures to ATV, FVT, RVT and SVT, but no difference in PIT or PVT exposures (Table 1.3). Carrying the rs2231142 variant allele has been associated with an increased risk of FVT myotoxicity in renal transplant recipients (Mirosevic Skvrce *et al.*, 2013) (Table 1.4), although replication is required.

Table 1.3 Genetic variants that influence statin pharmacokinetics

Gene	Variant	Comparison	Statin	Effect	References
SLCO1B1	rs4149056 (521T>C, p.V174A)	CC vs TT	ATV	- Increased AUC: <b>ATV</b> (2.5 fold), <b>2-OH ATV</b> (2.0 fold) - Non-significant rise in AUC: ATV L (2.0 fold), 2-OH ATV L (1.6 fold)	(Pasanen <i>et al.</i> , 2007)
			FVT	1.19 fold non-significant increase in FVT AUC	(Niemi <i>et al.</i> , 2006b)
			LVT	- 2.86 fold increased <b>LVT acid</b> AUC - LVT AUC decreased non-significantly by 16%	(Tornio <i>et al.</i> , 2015)
			PIT	- 3.08 fold increased <b>PIT</b> AUC - No significant difference in PIT L AUC	(Ieiri <i>et al.</i> , 2007)
			PVT	- 1.91 fold increased <b>PVT</b> AUC	(Niemi <i>et al.</i> , 2006b)
			RVT	- 1.62 fold increased <b>RVT</b> AUC	(Pasanen <i>et al.</i> , 2007)
			SVT	- 3.21 fold increased <b>SVT acid</b> AUC - 1.43 fold non-significant rise in SVT AUC	(Pasanen <i>et al.</i> , 2006)
	rs2306283 (388A>G, p.N130D)	Haplotype *14 (rs2306283 but not rs4149056) vs *1a GG (*1b/*1b) vs AA (*1a/*1a)	ATV	Decreased <b>ATV</b> AUC	(Nies <i>et al.</i> , 2013)
SLCO2B1	rs12422149 (935G>A, p.R312Q)	AA vs GG	SVT	79% increased apparent clearance of <b>SVT acid</b>	(Tsamandouras <i>et al.</i> , 2014)
			SLC10A1	rs2296651 (p.S267F, *2)	*2 carriers vs *1/*1
SLC22A8	rs2276299 (723T>A)	A carriers vs TT	PVT	No significant difference in renal clearance	(Nishizato <i>et al.</i> , 2003)
	rs749911923 (1166C>T, p.A389V)	CT vs CC	PVT	No significant difference in renal clearance	(Nishizato <i>et al.</i> , 2003)
ABCC2	rs113646094 (1446C>G)	GC vs CC	PVT	- Decreased PVT AUC by 68%	(Niemi <i>et al.</i> , 2006a)

<i>Table continued</i>					
Gene	Variant	Comparison	Statin	Effect	References
ABCB1	rs1128503-rs2032582-rs1045642 (1236C-T-2677G-T-3435C-T)	TTT/TTT vs CGC/CGC	ATV	- 55% increased <b>ATV</b> AUC - No significant differences for <b>ATV L</b>	(Keskitalo <i>et al.</i> , 2008)
			SVT	- 60% increased <b>SVT acid</b> AUC - No significant differences for <b>SVT</b>	(Keskitalo <i>et al.</i> , 2008)
			FVT	No significant differences	(Keskitalo <i>et al.</i> , 2009a)
			LVT	No significant differences	(Keskitalo <i>et al.</i> , 2009a)
			PVT	No significant differences	(Keskitalo <i>et al.</i> , 2009a)
			RVT	No significant differences	(Keskitalo <i>et al.</i> , 2009a)
	rs2032582-rs1045642 (2677G-T-3435C-T)	TT/TT vs GG/CC and GT/CT	ATV	- Increased elimination $t_{1/2}$ : <b>ATV, ATV L, 2-OH ATV, 2-OH ATV L</b> - No significant differences in AUC	(Lee <i>et al.</i> , 2010)
ABCB11	rs2287622 (1331T>C, p.V444A)	CC vs CT vs TT	PVT	No significant differences	(Ho <i>et al.</i> , 2007)
	rs11568364 (2029A>G, p.M677V)	GG vs GA vs GG	PVT	No significant differences	(Ho <i>et al.</i> , 2007)
ABCC2	rs717620 (-24C>T)	TT vs CT vs CC	PIT	- Decreased <b>PIT</b> AUC - <b>PIT</b> AUC decreased by 62% in TT compared to CC subjects	(Oh <i>et al.</i> , 2013)
	rs113646094 (1446C>G, p.T482=)	CG vs CC	PVT	<b>PVT</b> AUC decreased by 67%	(Niemi <i>et al.</i> , 2006a)
ABCG2	rs2231142 (421C>A, p.Q141K)	AA vs CC	ATV	- Increased AUC: <b>ATV</b> (1.7 fold), <b>ATV L</b> (1.9 fold) - Non-significant rise in AUC: 2-OH <b>ATV</b> (1.4 fold), 2-OH <b>ATV L</b> (1.5 fold), 4-OH <b>ATV L</b> (1.4 fold)	(Keskitalo <i>et al.</i> , 2009c)
			FVT	1.7 fold increased <b>FVT</b> AUC	(Keskitalo <i>et al.</i> , 2009b)
			PIT	No significant differences	(Oh <i>et al.</i> , 2013; Zhou <i>et al.</i> , 2013a)
			PVT	No significant differences	(Keskitalo <i>et al.</i> , 2009b)
			RVT	- 2.4 fold increased <b>RVT</b> AUC - 2 fold increase in <b>N-desmethyl RVT</b> plasma concentration	(Keskitalo <i>et al.</i> , 2009c; Lee <i>et al.</i> , 2013)
			SVT	- 2.1 fold increased <b>SVT</b> AUC - 1.2 non-significant rise in <b>SVT acid</b> AUC	(Keskitalo <i>et al.</i> , 2009b)

Table continued					
Gene	Variant	Comparison	Statin	Effect	References
PPARA	rs4253728 (209-1003G>A)	GA vs GG	ATV	Decreased <b>2-OH ATV</b> to ATV AUC ratio	(Klein <i>et al.</i> , 2012)
		GA/AA vs GG	SVT	24% lower apparent clearance of <b>SVT acid</b>	(Tsamandouras <i>et al.</i> , 2014)
CYP2C9	rs1799853 (p.R144C, *2)	*2/*2 vs *1/*1	FVT	No significant differences	(Kirchheiner <i>et al.</i> , 2003)
	rs1057910 (p.I359L, *3)	*3/*3 vs *1/*1	FVT	3.1-5.0 fold increase in <b>FVT AUC</b>	(Kirchheiner <i>et al.</i> , 2003)
		*3 carriers vs 1/*1	PIT	- 2.9 fold increase in <b>PIT AUC</b> - 1.7 fold increase in <b>PIT L AUC</b>	(Zhou <i>et al.</i> , 2013a)
			RVT	No significant differences in RVT or N-desmethyl RVT plasma concentrations	(Zhou <i>et al.</i> , 2013c; Lee <i>et al.</i> , 2013)
			SVT	No significant differences	(Zhou <i>et al.</i> , 2013b)
CYP2C19	- rs4244285 (p.P227=, *2) - rs4986893 (p.W212Stop gained, *3)	*2/*2, *2/*3 or *3/*3 (PMs) vs *1/*2, *1/*3 or *1/*1 (EMs)	RVT	- No significant differences in RVT, N-desmethyl RVT or RVT L pharmacokinetics	(Lee <i>et al.</i> , 2013; Finkelman <i>et al.</i> , 2015)
CYP2D6	whole gene deletion (*5)	*5/*5 vs wt/wt (*1 or *2)	LVT	- 5.1 fold increased <b>LVT AUC</b> - no significant difference in LVT acid AUC	(Yin <i>et al.</i> , 2012)
		*5/wt vs wt/wt	SVT	- <b>SVT AUC</b> decreased by 23% - no significant difference in SVT acid AUC	(Choi <i>et al.</i> , 2015)
	rs1065852 (p.S34P, *10)	*10/*10 vs wt/wt (*1 or *2)	LVT	- 2.2 fold increased <b>LVT AUC</b> - no significant difference in LVT acid AUC	(Yin <i>et al.</i> , 2012)
	rs5030865 (p.G169Stop gained, *14)	*14/*14 vs wt/wt	SVT	- 1.5 fold increased <b>SVT AUC</b> - no significant difference in SVT acid AUC	(Choi <i>et al.</i> , 2015)
	rs28371725 (*41)	*41/*41 vs wt/wt	SVT	Increased C <sub>max</sub> of both <b>SVT</b> and <b>SVT acid</b>	(Choi <i>et al.</i> , 2015)
CYP3A4	rs35599367 (*22)	*22 carriers vs *1/*1	ATV	Decreased <b>2-OH ATV</b> to ATV AUC ratio	(Klein <i>et al.</i> , 2012)
			SVT	White patients: - 14% higher <b>SVT acid</b> concentration - 20% non-significantly increased SVT concentration African American patients: - 170% higher <b>SVT</b> concentration - no significant difference in SVT acid conc	(Kitzmiller <i>et al.</i> , 2014)

<i>Table continued</i>					
Gene	Variant	Comparison	Statin	Effect	References
CYP3A5	rs776746 (*3)	*3/*3 vs *1 carriers	ATV	- 36% increased <b>ATV L AUC</b> - No significant difference in ATV AUC	(Shin <i>et al.</i> , 2011)
		*3/*3 vs *1/*3	PIT	No significant differences for PIT or PIT L	(Zhou <i>et al.</i> , 2013a)
		*3/*3 vs *1/*3	RVT	No significant differences	(Zhou <i>et al.</i> , 2013c)
		*3/*3 vs *1/*1	SVT	- 3.3 fold increased <b>SVT AUC</b> - No significant difference in SVT acid plasma levels	(Kim <i>et al.</i> , 2007; Kitzmiller <i>et al.</i> , 2014)
UGT1A1	*28	*28 vs *1/*1	ATV	- 41% reduced <b>ATV L AUC</b>	(Stormo <i>et al.</i> , 2013)
UGT1A3	*2	*2/*2 vs *1/*1	ATV	- 72% increased <b>ATV L AUC</b> - 160% increased <b>2OH ATV L AUC</b>	(Riedmaier <i>et al.</i> , 2010; Cho <i>et al.</i> , 2012)
		*1/*2 vs *1/*1		Increased <b>ATV L</b> to ATV AUC ratio	(Riedmaier <i>et al.</i> , 2010)

Unless otherwise stated, reported changes are statistically significant (statin with significant change highlighted in bold font).

AUC = area under the concentration-time curve; wt = wild type.

### 1.8.1.5 Drug-statin interactions

Drug-statin interactions are common, can lead to several fold increases in statin exposure, and are established SAM risk factors. Ciclosporin is a potent inhibitor of CYP3A4 and several transporters including OATP1B1, OATP1B3, OATP1B2, ABCG2, and P-gp (Zhang, 2010; Neuvonen *et al.*, 2006) and CYP3A4 (Amundsen *et al.*, 2012), and universally increases systemic exposure of all statins (see Appendix Table 8.1). Gemfibrozil and its glucuronide metabolite inhibit CYP2C8 and OATP1B1 and increase statin acid levels (except FVT) (Appendix Table 8.1). Ciclosporin and gemfibrozil are strongly associated with SAM, which likely involves OATP1B1 inhibition, as well as pharmacodynamic (PD) interactions (Neuvonen *et al.*, 2006). Expectedly, CYP3A4 inhibitors (e.g. itraconazole, clarithromycin, grapefruit juice), consistently increase exposure to the CYP3A4-metabolised statins (ATV, LVT, SVT) and are a significant SAM risk factor (Neuvonen *et al.*, 2006; Patel *et al.*, 2013a). Interestingly, CYP2C9 inhibitors (e.g. fluconazole) were associated with an increased risk of FVT myotoxicity in renal transplant recipients, but only in the subgroup carrying reduced function *CYP2C9\*2* or *\*3* alleles (Mirosevic Skvrce *et al.*, 2013). In recognition of the importance of statin-drug interactions, recommendations for the management of clinically significant interactions have been recently published (Wiggins *et al.*, 2016).

Table 1.4 A systematic review of pharmacogenomic studies investigating statin-associated myotoxicity

Study	Design	Genes	Variants	Statin	N	Endpoint	Result
<b>Statin Pharmacokinetics</b>							
(Bakar <i>et al.</i> , 2017)	Case-control, CG	<i>SLCO1B1</i> <i>ABCC2</i> <i>ABCG2</i> <i>CYP3A4</i> <i>COQ2</i> <i>GATM</i> <i>GPX4</i> <i>SLC16A1</i> <i>SLC16A3</i>	rs4149056 (521T>C, p.V174A)	SVT (40mg/D), ATV (80mg/D)	606	Intolerable muscle pain or weakness (initial symptoms within 6 months of starting statin therapy, resolution on de-challenge, and symptom recurrence on re-challenge) with CK <4x ULN	i) <i>SLCO1B1</i> rs4149056 CC/CT vs TT: -SVT/ATV: OR 1.66 (95% CI 1.08-2.54), p=0.014 ii) No associations detected for all other genes
(Becker <i>et al.</i> , 2010)	Cohort, CG	<i>CYP3A4</i> <i>ABCB1</i>	*1B 1236C>T, 2677G>A/T, 3435C>T	SVT, ATV	1,239	Statin dose decrease or switch to another cholesterol-lowering drug <sup>1</sup>	i) Decreased risk with <i>CYP3A4*1B</i> : -SVT/ATV: HR 0.46 (95% CI 0.24-0.90), p=0.023 -SVT only: HR 0.47 (95% CI 0.23-0.96), p=0.039 -Non-significant trend for decreased risk in patients on ATV ii) No associations detected for <i>ABCB1</i> variants
(Brunham <i>et al.</i> , 2012)	Case-control, CG	<i>SLCO1B1</i>	rs4149056 (521T>C, p.V174A)	SVT, ATV, PVT, RVT	109	Severe statin myopathy (CK>10x ULN irrespective of symptoms)	rs4149056 CC/CT vs TT: - SVT: OR 3.2 (95% CI 0.83-11.96), p=0.042 - ATV: OR 1.06 (95% CI 0.22-4.80), p=0.48 - All statins: OR 1.50 (95% CI 0.58-3.69), p=0.21

<i>Table continued</i>							
Study	Design	Genes	Variants	Statin	N	Endpoint	Result
(Carr <i>et al.</i> , 2013)	Case-control, CG	<i>SLCO1B1</i>	rs4149056 (521T>C, p.V174A)	SVT, ATV (also CVT, FVT, PVT, RVT)	448	-All myopathy (CK >4x ULN). -Severe myopathy (CK >10x ULN or rhabdomyolysis)	i) Increased risk of all myopathy per <i>SLCO1B1</i> rs4149056 C allele: - all statins: OR 2.08 (95% CI 1.35-3.23), p=0.005 - SVT: OR 2.13 (95% CI 1.29-3.54), p=0.014  ii) Increased risk of severe myopathy per <i>SLCO1B1</i> rs4149056 C allele: - all statins: OR 4.47 (95% CI 1.84-10.84), p=0.0003 - SVT: OR 4.97 (95% CI 2.16-11.43), p=0.0004  iii) rs4149056 not associated with all/severe myopathy in patients only on ATV
		<i>COQ2</i>	rs4693075 (1022C>G)				
(Danik <i>et al.</i> , 2013)	RCT, CG	<i>SLCO1B1</i>	rs4149056 (521T>C, p.V174A) rs4363657 (1331T>C)	RVT (20mg)	4,404	Myalgia, muscle weakness, stiffness, myopathy, rhabdomyolysis	No associations detected
(de Keyser <i>et al.</i> , 2014)	Cohort & a case-control, CG	<i>SLCO1B1</i>	rs4149056 (521T>C, p.V174A)	SVT, ATV	1,939  637	Statin dose decrease or switch to another cholesterol-lowering drug <sup>1</sup>	i) Discovery set: - SVT CC vs TT: HR 1.74 (95% CI 1.05-2.88), p=0.033 - ATV TC/CC vs TT only if starting dose >20mg: HR 3.26 (95% CI 1.47-7.35), p=0.004 ii) No associations detected with rs4149056 in patients on SVT or ATV in replication set iii) Meta-analysis: - SVT CC vs TT: HR 1.69 (95% 1.05-2.73) - no association detected for ATV

Table continued							
Study	Design	Genes	Variants	Statin	N	Endpoint	Result
(Donnelly <i>et al.</i> , 2011)	Cohort, CG	<i>SLCO1B1</i>	rs4149056 (521T>C, p.V174A) rs2306283 (388A>G, p.N130D)	SVT (also ATV, CVT, FVT, PVT, RVT)	2,091	Statin intolerance: a relevant prescribing change (statin discontinuation, dose reduction, switch to another statin of equivalent or lower dose) associated with either a CK measurement (both normal and CK≤3x ULN) or elevated ALT	i) Increased risk of endpoint with rs4149056 C allele: OR 2.05 (95% CI 1.02-4.09), p=0.0427 ii) Decreased risk of endpoint with rs2306283 G allele: OR 0.71 (95% CI 0.52-0.96), p=0.0257
(Elam <i>et al.</i> , 2017)	Case-control, CG	<i>SLCO1B1</i>	rs4149056 (521T>C, p.V174A)	SVT (also ATV, FVT, LVT, PVT, RVT)	19	Statin myalgia: myalgia on statin therapy, discontinuation of ≥ 1 statin due to muscle symptoms with CK ≤ 5x ULN, myalgia re-occurrence upon re-challenge with ≥ 1 statin	Variant MAF in cases to controls for: i) rs4149056: 0.33 vs 0.00, p=0.039 ii) rs12422149: 0.51 vs 0.08, p=0.01 iii) rs2819742: 1.00 vs 0.57, p=0.016
		<i>SLCO2B1</i>	rs12422149 (935G>A, p.R168Q)				
		<i>RYR2</i>	rs2819742 (A>G)				
(Ferrari <i>et al.</i> , 2014)	Case-control, CG	<i>SLCO1B1</i>	rs4149056 (521T>C, p.V174A) rs2306283 (388A>G, p.N130D)	ATV, RVT, SVT	66	CK >3x ULN (irrespective of symptoms). Myalgia with CK elevation	i) Increased risk of elevated CK: - <i>SLCO1B1</i> rs4149056 CC vs CT/TT: OR 8.5 (95% CI 1.7-42.3), p=0.001 - <i>ABCB1</i> 1236C>T TT vs CT/CC: OR 4.5 (95% CI 1.4-14.7), p=0.001 ii) Decreased risk of elevated CK in <i>SLCO1B1</i> rs2306283 GA vs AA: OR 0.25 (95% CI 0.06-0.91), p=0.022 iii) <i>ABCG2</i> 421C>A not significantly associated with elevated CK iv) No associations detected for risk of myalgia with CK elevation
		<i>ABCB1</i>	1236C>T, 3435C>T				
		<i>ABCG2</i>	rs2231142 (421C>A)				

<i>Table continued</i>							
Study	Design	Genes	Variants	Statin	N	Endpoint	Result
(Fiegenbaum <i>et al.</i> , 2005)	Cohort, CG	<i>ABCB1</i>	1236C>T, 2677G>A/T, 3435C>T	SVT (20mg/D)	116	Myalgia (muscular symptoms with no or minor associated CK elevation)	i) Increased risk of endpoint with <i>ABCB1</i> variant alleles (p<0.05)
		<i>CYP3A4</i>	*1B				ii) No associations observed for <i>CYP3A4/5</i>
		<i>CYP3A5</i>	*3				
(Frudakis <i>et al.</i> , 2007)	Case-control, CG	<i>CYP2D6</i>	*4	ATV, SVT	263	Muscle effects (myalgia, asymptomatic & symptomatic CK elevations, or rhabdomyolysis)	<i>CYP2D6</i> *4 vs WT/WT: - ATV: OR 2.5 (95% CI 1.5-4.4), p=0.001 - SVT: OR 1.7 (95% CI 0.9-3.2), p=0.067
		Multiple CGs	388 SNPs				
(Hoenig <i>et al.</i> , 2011)	Cohort, CG	<i>ABCB1</i>	3435C>T	ATV (80mg/D)	117	Muscle symptoms (myalgia, weakness +/- CK elevation)	Increased risk in patients carrying T compared to C allele (p=0.043)
(Hubacek <i>et al.</i> , 2015)	Case-control, CG	<i>SLCO1B1</i>	rs4363657 (1331T>C)	ATV, SVT (10-20mg/D)	3,294	Myalgia/myopathy based on clinical and laboratory criteria (Vrablik <i>et al.</i> , 2014)	No associations detected
(Linde <i>et al.</i> , 2010)	Cohort, CG	<i>SLCO1B1</i>	rs4149056 (521T>C, p.V174A)	ATV, SVT (also FVT, LVT, PVT, RVT)	46	Myalgia	A non-significant trend for increased risk in patients with at least one rs4149056 C allele (p=0.07)
(Link <i>et al.</i> , 2008)	Case-control, GWAS & replication	<i>SLCO1B1</i>	rs4149056 (521T>C, p.V174A)	SVT (80mg/D)	175	'Definite myopathy' (muscle symptoms with CK >10x ULN) or 'incipient' myopathy (CK both >3x ULN and 5x baseline, plus ALT>1.7x baseline with no prior isolated ALT rise)	i) Increased risk with 80mg SVT (discovery set, GWAS): - Per C allele: OR 4.5 (95% CI 2.6-7.7) - CC vs TT: OR 16.9 (95% CI 4.7-61.1), p=2*10 <sup>-9</sup>
				SVT (40mg/D)	16,664		ii) Increased risk with 40mg SVT (replication set, targeted genotyping): - Per C allele: OR 2.6 (95% CI 1.3-5.0), p=0.004

Table continued							
Study	Design	Genes	Variants	Statin	N	Endpoint	Result
(Marciante <i>et al.</i> , 2011)	Case-control, CGs sequenced & GWAS	<i>SLCO1B1</i>	Sequenced rs4149056 (521T>C, p.V174A)	CVT	917	Muscle symptoms and CK >10x ULN	i) Increased risk with <i>SLCO1B1</i> rs4149056 (521T>C) in CG analysis: -Per C allele: OR 1.89 (95% CI 1.40-2.56), p=3.62x10 <sup>-5</sup> - CC vs TT: OR 4.34 (95% CI 1.86-10.10) - No associations detected for other CGs ( <i>CYP2C8</i> , <i>UGT1A1/1A3</i> )  ii) rs4149056 not genotyped in GWAS, but a SNP in LD with it (rs4363657, r <sup>2</sup> =0.79) had similar results to rs4149056 in the CG analysis
		<i>CYP2C8</i>	Sequenced				
		<i>UGT1A1/1A3</i>	Sequenced				
		<i>RYR2</i>	rs2819742 (1559G>A)				
(Mirosevic Skvrce <i>et al.</i> , 2013)	Case-control, CGs	<i>ABCG2</i>	rs2231142 (421C>A, p.Q141K)	FVT	104	Adverse drug reactions in renal transplant recipients: -90% myotoxicity (myalgia, CK elevation, myopathy, rhabdomyolysis) -10% hepatotoxicity	i) <i>ABCG2</i> A carriage vs CC: 4.89 (95% CI 1.42-16.89) ii) No association for <i>CYP2C9</i>
		<i>CYP2C9</i>	*2, *3				
(Morimoto <i>et al.</i> , 2004)	Case report, CG	<i>SLCO1B1</i>	Sequenced rs107796321 (1628T>G, p.L543W)	PVT	2	Myopathy	In one of two patients with myopathy on PVT but not carrying rs4149056, a rare mutation (rs107796321) was identified. OATP1B1 variants with L543W have reduced PVT transport due to a decrease in V <sub>max</sub> (Furihata <i>et al.</i> , 2009).
(Mulder <i>et al.</i> , 2001)	Cohort, CG	<i>CYP2D6</i>	*3, *4, *5, *2xN	SVT (40mg/D)	88	Discontinuation due to any adverse effect <sup>1</sup>	Increased risk associated with <i>CYP2D6</i> variant alleles, compared to WT/WT patients (RR=4.7). Gene-dose trend observed
(Puccetti <i>et al.</i> , 2010)	Case-control, CG	<i>SLCO1B1</i>	rs4149056 (521T>C, p.V174A)	ATV, RVT	76	Muscular intolerance	i) <i>SLCO1B1</i> rs4149056 C minor allele: - ATV: OR 2.7 (95% CI 1.3-4.9), p<0.001 - no association with RVT
		<i>COQ2</i>	rs4693075 (1022C>G)				

Table continued							
Study	Design	Genes	Variants	Statin	N	Endpoint	Result
(Santos <i>et al.</i> , 2012)	Cohort, CG	<i>SLCO1B1</i>	rs4149056 (521T>C, p.V174A) rs2306283 (388A>G, p.N130D)	ATV	143	Myalgia (irrespective of CK) and CK > 3x ULN (irrespective of symptoms)	No associations detected
(Voora <i>et al.</i> , 2009)	RCT, CG	<i>SLCO1B1</i>	rs4149056 (521T>C, p.V174A)	ATV, SVT, PVT	452	Discontinuation from any side effect, myalgia (irrespective of CK), or CK >3x ULN (irrespective of symptoms)	i) <i>SLCO1B1</i> rs4149056 C allele: - OR 1.7 (95% CI 1.04-2.8), p=0.03. - Gene-dose trend observed. - Risk highest in patients on SVT. - A (non-significant) trend for increased risk in patients on ATV  ii) no associations observed for other CGs
		<i>CYP2D6</i>	*4, *10				
		<i>CYP2C8</i>	*3, *4				
		<i>CYP2C9</i>	*3				
(Wilke <i>et al.</i> , 2005)	Case-control, CG	<i>CYP3A4</i>	*1B	ATV	137	Myopathy (muscle symptoms and an associated elevated CK)	i) No association with <i>CYP3A4/5</i> (vs controls)  ii) In cases only, after removal of patients on gemfibrozil or niacin, <i>CYP3A5*3/*3</i> was associated with increased myopathy severity (increased CK levels) compared to <i>CYP3A5*1/*3</i> cases (p=0.010)
		<i>CYP3A5</i>	*3				
(Zuccaro <i>et al.</i> , 2007)	Case-control, CG	<i>CYP2C9</i>	*2, *3	ATV, FVT, PVT, SVT, RVT	100	Muscle symptoms +/- an associated CK elevation	No associations detected
		<i>CYP2D6</i>	*3-*6				
		<i>CYP3A5</i>	*3				
Muscle-related							
(Carr <i>et al.</i> , 2013)	Case-control, CG	<i>COQ2</i>	rs4693075 (1022C>G)	SVT, ATV (also CVT, FVT, PVT, RVT)	448	-All myopathy (CK >4x ULN). -Severe myopathy (CK >10x ULN or rhabdomyolysis)	No associations detected for <i>COQ2</i> rs4693075
		<i>SLCO1B1</i>	rs4149056 (521T>C, p.V174A)				

Table continued							
Study	Design	Genes	Variants	Statin	N	Endpoint	Result
(Dube <i>et al.</i> , 2014)	Cohort, GWAS & replication	<i>CKM</i>	rs11559024	ATV, RVT (also SVT, FVT, LVT, PVT)	3,412	Plasma CK level, irrespective of symptoms.	i) <i>CKM</i> rs11559024 and <i>LILRB5</i> rs2361797 significantly associated with CK level in discovery GWAS ( $p=3.69 \times 10^{-16}$ and $p=1.96 \times 10^{-10}$ , respectively) and replication cohort. ii) No association for these SNPs with statin myalgia case/statin-tolerant control status
		<i>LILRB5</i>	rs2361797		5,330		
(Mangravite <i>et al.</i> , 2013)	<i>In vitro</i> eQTL analysis, then CG case-control	<i>GATM</i>	rs9806699 rs1719247	SVT	292  4,121	Discovery set: 'incipient' myopathy (CK >3x ULN associated with muscle symptoms). Replication set: 'definite myopathy' (muscle symptoms with CK >10x ULN), or 'incipient' myopathy (CK >3x ULN & 5x baseline, plus ALT >1.7x baseline)	Decreased risk with <i>GATM</i> rs1719247 minor allele (in LD with top deQTL SNP, rs9806699, $r^2=0.76$ ): - Discovery set: OR 0.59 (95% CI 0.36-0.93), $p=0.024$ -Replication set: OR 0.61 (95% CI 0.42-0.88), $p=0.001$ - Meta-analysis: OR 0.60 (95% CI 0.45-0.81), $p=6.0 \times 10^{-4}$
(Marciante <i>et al.</i> , 2011)	Case-control, CGs sequenced & GWAS	<i>RYR2</i>	rs2819742 (1559G>A)	CVT	917	Muscle symptoms and CK >10x ULN	Decreased risk with <i>RYR2</i> rs2819742 (1559G>A) in GWAS: - Per A allele: OR 0.48 (95% CI 0.36-0.63), $p=1.74 \times 10^{-7}$ - AA vs GG: OR 0.24 (95% CI 0.13-0.44)
		<i>SLCO1B1</i>	Sequenced rs4149056 (521T>C, p.V174A)				
		<i>CYP2C8</i>	Sequenced				
		<i>UGT1A1/1A3</i>	Sequenced				
(Oh <i>et al.</i> , 2007)	Case-control, CG	<i>COQ2</i>	rs6535454 (G>A) rs4693075 (1022C>G)	ATV, RVT (plus others not specified)	291	Myopathy (muscle symptoms with at least one of: statin discontinuation twice, CK >3x ULN, rhabdomyolysis)	- rs6535454 AA vs GA/GG: OR 2.42 (95% CI 0.99-5.89), $p=0.047$ - rs4693075 GG vs CG/CC: OR 2.33 (95% CI 1.13-4.81), $p=0.019$ - 2-SNP haplotype recessive model: OR 2.58 (95% CI 1.26-5.28), $p=0.007$

Table continued							
Study	Design	Genes	Variants	Statin	N	Endpoint	Result
(Puccetti <i>et al.</i> , 2010)	Case-control, CG	<i>COQ2</i>	rs4693075 (1022C>G)	ATV, RVT	76	Muscular intolerance	<i>COQ2</i> rs4693075 G minor allele: - RVT: OR 2.6 (95% CI 1.7-4.4), p<0.001 - Increased risk of muscular symptoms and CK increase with ATV: OR 3.1 (95% CI 1.9-6.4), p<0.001
		<i>SLCO1B1</i>	rs4149056 (521T>C, p.V174A)				
(Ruano <i>et al.</i> , 2011)	Case-control, CG	<i>COQ2</i>	rs4693570	ATV, SVT, RVT	793	Myalgia	i) The minor variants of <i>COQ2</i> rs4693570 (p=0.000041) or <i>ATP2B1</i> rs17381194 (p=0.00079) associated with decreased risk.
		<i>ATP2B1</i>	rs17381194	(also FVT, LVT, PVT, Chinese red rice yeast)			ii) Minor variant of <i>DMPK</i> rs672348 (p=0.0016) associated with increased risk.
		<i>DMPK</i>	rs672348				
		28 CGs	Multiple SNPs				
(Vladutiu <i>et al.</i> , 2006)	Case-control, CG	<i>CPT2</i>	P50H, S113L, Q413fs, G549D, R503C, R631C	ATV, CVT, LVT, SVT	358	Pain, weakness or other muscle symptoms reported to begin with lipid-lowering therapy. Symptoms in cases commonly persist after therapy cessation	i) A fourfold increase in the number of mutant alleles (in <i>AMPD1</i> > <i>CPT2</i> / <i>PYGM</i> ) in the cases compared to the statin-tolerant controls.
		<i>PYGM</i>	R49X, G204S				
		<i>AMPD1</i>	Q12X, P48L, K287I				
(Vladutiu <i>et al.</i> , 2011)	Case-control, CG	<i>RYR1</i>	34 <i>RYR1</i> mutations or variants	Not specified	493	-Severe statin myopathy (muscle pains/weakness often with elevated CK. Symptoms commonly persist post-therapy). -Mild statin myopathy (new muscle pains that cease on statin discontinuation)	Disease causing mutations or variants in <i>RYR1</i> identified in: - 3 of 197 severe statin myopathy cases - 1 of 163 mild myopathy cases - 0 of 133 in statin-tolerant controls
		25 other muscle disease genes	71 mutations/variants				
(Zeharia <i>et al.</i> , 2008)	Case-control, CG sequenced	<i>LPIN1</i>	<i>LPIN1</i> sequenced	Not specified	20	Myopathy (muscle symptoms and elevated CK)	In 2 of 6 cases, exonic nucleotide substitutions predicted to be harmful were identified, but none were found in 14 statin-tolerant controls. One case had a GGG to GGC substitution at codon 750. The other had E769G substitution.

Table continued							
Study	Design	Genes	Variants	Statin	N	Endpoint	Result
<b>Candidate muscle-related</b>							
(Isackson <i>et al.</i> , 2011)	Pooled GWAS; fine mapping	<i>EYS</i>	rs1337512, rs9342288, rs3857532	ATV (also SVT, CVT, LVT, PVT)	399	Severe statin myopathy (muscle weakness, pain, myopathic symptoms that persist post-therapy, CK > 4x ULN)	Carrying one or more variants of <i>EYS</i> SNPs conferred increased risk (p=0.0003-0.0008). Statistically significant following Bonferroni correction for fine mapping (27 SNPs) but did not survive correction for GWAS.
<b>Immunological</b>							
(Mammen <i>et al.</i> , 2012)	Case-control, HLA typing	<i>HLA-DRB1*11</i>	-Intermediate resolution typing; -High resolution typing of <i>DR11</i>	Not specified	733	Anti-HMGCR antibodies in patients with stigmata of myopathy (muscle symptoms, elevated CK, myopathic EMG results, muscle oedema on MRI and/or myopathic features on muscle biopsy).	i) <i>HLA-DR11</i> serotype recognises <i>HLA-DRB1*11</i>  ii) <i>HLA-DR11</i> ; <i>DQA5</i> ; <i>DQB7</i> was more frequent in white anti-HMGCR positive myopathy patients than controls or statin intolerant subjects (p=4.1x10 <sup>-7</sup> & p=5.4x10 <sup>-4</sup> , respectively)  iii) <i>HLA-DR11</i> was more frequent in black anti-HMGCR positive myopathy patients compared to controls (p=0.0002)  iv) In 95% of black/white anti-HMGCR myopathy patients with <i>HLA-DR11</i> , the <i>DRB1*11:01</i> allele was present.  v) Overall, the OR for the presence of <i>HLA-DRB1*11:01</i> in anti-HMGCR myopathy patients vs controls was estimated to be 24.5 (white patients) and 56.5 (black patients)  vi) <i>HLA-DQA1</i> and <i>DQB6</i> were less frequent in white anti-HMGCR positive patients than controls (p=5.5x10 <sup>-4</sup> , p=2.1x10 <sup>-5</sup> , respectively)
		<i>DQA</i>	Intermediate resolution typing				
		<i>DQB</i>					

Table continued							
Study	Design	Genes	Variants	Statin	N	Endpoint	Result
(Limaye <i>et al.</i> , 2015)	Cohort, CG	<i>HLA-DRB1*11</i>	-typing to 'two-digit' resolution	Not specified	207	Anti-HMGCR antibodies in patients with idiopathic inflammatory myositis or immune-mediated necrotizing myopathy	<p>i) Anti-HMGCR antibodies detected in 19 of 207 patients with myopathy</p> <p>ii) In myopathy patients, <i>HLA-DRB1*11</i> was more frequent in those positive than those negative for anti-HMGCR antibodies: OR 56.1 (95% CI 5.0-7739), p=0.001</p> <p>iii) Three myopathy anti-HMGCR positive myopathy patients had high resolution typing and all carried <i>HLA-DRB1*11:01</i></p>
(Siddiqui <i>et al.</i> , 2017)	Case-control,	<i>LILRB5</i>	rs12975366 (T>C)	SVT, others (inc RVT, ATV)	1.034	<p>-General statin intolerance: statin users with CK &gt; ULN and switched statin ≥ 2x or discontinued statin therapy</p> <p>-Low dose intolerance: used ≥ 2 statins, and at least one discontinued statin had to be at the lowest approved daily starting dose before discontinuation, irrespective of CK level</p>	<p>rs12975366 TT vs C carrier:</p> <p>i) General statin intolerance: OR 1.96 (95% CI 1.25-3.07), p=0.003</p> <p>ii) Low dose intolerance: OR 1.43 (95% CI 1.10-1.86), p=0.07</p>
<b>Pain perception</b>							
Ruano <i>et al.</i> , 2007 (Ruano <i>et al.</i> , 2007)	Case-control, CG	<i>HTR3B</i>	rs2276307	ATV, SVT, PVT	195	Myalgia score (definite, probable, no myalgia)	rs2276307 and rs1935349 significantly associated with the myalgia score
		<i>HTR7</i>	rs1935349				
		Multiple SNPs in <i>HTR1D/2A/2C/3A/5A/6 &amp; SLC6A4</i>					

<i>Table continued</i>							
Study	Design	Genes	Variants	Statin	N	Endpoint	Result
<b>Vascular system</b>							
(Ruano <i>et al.</i> , 2005)	Case-control, CG	<i>AGTR1</i> <i>NOS3</i> 8 CGs	rs12695902 rs1799983 15 other SNPs	ATV, SVT	102	Plasma CK level	<i>AGTR1</i> rs12695902 (p=0.002) and <i>NOS3</i> rs1799983 (p=0.005) associated with CK levels

Abbreviations: CG = candidate gene; CI = confidence interval; CK = creatine kinase; D = day; deQTL = differential expression quantitative trait loci; EMG = electromyography; eQTL = expression quantitative trait loci; HR = hazard ratio; MRI = magnetic resonance imaging; OR = odds ratio; RCT = randomized controlled trial; ULN = upper limit of normal; WT = wild type

<sup>1</sup> = Muscle symptoms are a common reason for dose decreases, switching to another cholesterol-lowering agent, and statin discontinuation, and so these studies are included here (Becker *et al.*, 2010; Wei *et al.*, 2013)

### 1.8.2 Statin-induced myocyte dysfunction

Elevated systemic statin plausibly increases intra-myocyte statin concentrations. Statin myocyte entry is likely facilitated by transporters and statins are substrates for several transporters located in the sarcolemma. These include OATP2B1, multidrug resistance-associated protein (MRP) 1 (MRP1), MRP4, MRP5 and MCT4 (monocarboxylate transporter-4) (Sirvent *et al.*, 2005; Knauer *et al.*, 2010). Their tissue distribution may in part account for the apparent lack of statin cardiomyotoxicity (Sirvent *et al.*, 2005). There is preferential accumulation of lipophilic statins (ATV, SVT) in skeletal muscle compared to hydrophilic statins (PVT, RVT) (Schirris *et al.*, 2015a).

Several myotoxicity pathomechanisms have been proposed including: mitochondrial impairment; HMGCR inhibition leading to depletion of myocyte selenoproteins, CoQ<sub>10</sub>, and protein prenylation; depleted cholesterol itself; atrogen-1 mediated muscle atrophy; disruption of calcium signalling; and immunologically-driven.

#### 1.8.2.1 Mitochondrial impairment

*In vitro* work has demonstrated that the statin L forms are markedly more myotoxic than their corresponding acid analytes, with SVT L and FVT L being more myotoxic than ATV L and PVT L metabolites (Skottheim *et al.*, 2008). Following ATV re-challenge, patients with previous SAM had higher systemic exposures to ATV L and 4-OH ATV L (and increased 2-OH ATV and 4-OH ATV) compared to healthy controls (Hermann *et al.*, 2006). Importantly, Ls inhibit mitochondrial complex III within *in vitro* myoblasts, and are associated with reduced complex III enzyme activity and mitochondrial ATP production in SAM patient muscle biopsies, likely attributable to *in silico*-predicted off-target statin L (but not acid) binding to Q<sub>0</sub> of complex III (Schirris *et al.*, 2015a). Interestingly, CVT L showed the greatest degree of complex III inhibition (Schirris *et al.*, 2015a), in keeping with its pronounced rhabdomyolysis risk (Furberg and Pitt, 2001). SVT likely also impairs respiration at mitochondrial

complex I (Kwak *et al.*, 2012). Statin exposure does not however affect mitochondrial membrane potential (Schirris *et al.*, 2015a; Wagner *et al.*, 2011; Wagner *et al.*, 2008), excluding their action as a mitochondrial uncoupler.

Carnitine palmitoyltransferase (CPT) 2 is located within the mitochondrial inner membrane and undertakes oxidation of long-chain fatty acids in mitochondria alongside CPT1. The frequency of *CPT2* variants associated with the clinical syndrome, CPT2 deficiency, is higher in patients with lipid lowering (predominantly statin)-induced myopathy, compared to asymptomatic treated controls (Vladutiu *et al.*, 2006) (Table 1.4). Furthermore, *in vitro* transcriptomics has demonstrated that *CPT2* is amongst the top 1% of genes whose mRNA levels are perturbed by 75 drugs that can cause rhabdomyolysis (Hur *et al.*, 2014).

### **1.8.2.2 Selenoprotein disruption**

As stated earlier, statin-mediated mevalonate depletion via competitive HMGCR inhibition leads to a reduction of several downstream endogenous compounds in addition to cholesterol. It has been suggested that SAM shares phenotypic similarities to selenium deficiency and multi-minicore disease (Moosmann and Behl, 2004a), a recessively inherited neuromuscular disease due to mutations in selenoprotein N (*SEPN1*) or ryanodine receptor I (*RYR1*) (Jungbluth, 2007). Selenoproteins all contain the amino acid, selenocysteine, which requires selenocysteine-transfer ribonucleic acid (Sec-tRNA). In turn, Sec-tRNA requires post-transcriptional modifications to become functional, which include enzymatic isopentenylation using isopentenyl pyrophosphate as substrate, which is a metabolite of mevalonate (Figure 1.2) and depleted by statins (Moosmann and Behl, 2004b). Prominent selenoproteins include deiodinases and glutathione peroxidase antioxidants. However, supplementation with the antioxidant, vitamin E, has not been shown to reduce SAM, albeit in a small trial (n=32) (Caso *et al.*, 2007). Interestingly, clinical hypothyroidism has also been associated with SAM (Jbara and Bricker, 2015; Bar *et al.*, 2007; Bruckert *et al.*,

2005), and therefore further research is required to delineate the role of statin-induced selenoprotein-mediated attenuated deiodination.

### 1.8.2.3 Coenzyme Q<sub>10</sub> depletion

Statins also decrease CoQ<sub>10</sub> by interfering with mevalonate production (Figure 1.2). CoQ<sub>10</sub> is an important cofactor in mitochondrial respiration (Deichmann *et al.*, 2010). Primary CoQ<sub>10</sub> deficiency is a clinically and genetically heterogeneous condition, considered to be inherited in an autosomal recessive manner, and has been associated with isolated myopathy, encephalopathy, nephrotic syndrome, cerebellar ataxia and severe infantile multisystemic disease (Quinzii and Hirano, 2011). In patients on statins, reduced circulating CoQ<sub>10</sub> is routinely observed (Deichmann *et al.*, 2010) and a modest decrease in muscle CoQ<sub>10</sub> has been suggested in some (Lamperti *et al.*, 2005) but not in other studies (Mullen *et al.*, 2010). *COQ2* encodes para-hydroxybenzoate-polyprenyl transferase and defective *COQ2* has been associated with primary CoQ<sub>10</sub> deficiency, which can improve with early CoQ<sub>10</sub> supplementation (Montini *et al.*, 2008). *COQ2* variants, and in particular rs4693075 (1022C>G), have been investigated in relation to SAM with some candidate gene studies (Puccetti *et al.*, 2010; Oh *et al.*, 2007), but not others (Carr *et al.*, 2013), finding evidence of an association. Importantly, a recent meta-analysis of RCTs found that CoQ<sub>10</sub> supplementation likely does not reduce SAM, although larger trials are required to confirm this conclusion (Banach *et al.*, 2015). One possible explanation is that the Q<sub>0</sub> site of mitochondrial complex III, the off-target binding site for statin Ls (Schirris *et al.*, 2015a), is involved in the transfer of electrons from CoQ<sub>10</sub> to cytochrome *c*. Therefore, statins may both reduce circulating CoQ<sub>10</sub> and inhibit its PD effect; CoQ<sub>10</sub> supplementation alone may thus not circumvent the latter.

### 1.8.2.4 Reduced protein prenylation

FPP and GGPP, which are both downstream metabolites of mevalonate (Figure 1.2), enable post-translational prenylation of multiple proteins (Moßhammer *et al.*, 2014). GGPP, rather than FPP, is consistently implicated in *in vitro* statin

myotoxicity (Wagner *et al.*, 2011; Flint *et al.*, 1997; Sakamoto *et al.*, 2007; Itagaki *et al.*, 2009). There is experimental evidence to support that the statin-mediated decrease in GGPP may reduce myotube ATP levels (Wagner *et al.*, 2011), block prenylation of small GTPases including Rab (Wagner *et al.*, 2011; Sakamoto *et al.*, 2007) and RhoA (Itagaki *et al.*, 2009), induce atrogen-1 expression (Cao *et al.*, 2009) and stimulate apoptosis (Wagner *et al.*, 2011; Itagaki *et al.*, 2009). The possible pathways that culminate in apoptosis include RhoA mis-localisation from the cell membrane to the cytoplasm (examined in fibroblasts) (Itagaki *et al.*, 2009), inhibition of AKT (protein kinase B) phosphorylation and activation (Mullen *et al.*, 2011) likely via both statin-mediated ATP depletion through mitochondrial dysfunction and loss of Rab1 activity (Bonifacio *et al.*, 2015), and dose-dependent caspase-3 activation (Itagaki *et al.*, 2009).

#### **1.8.2.4.1 Atrogen-1 upregulation**

The F-box protein, atrogen-1, is a tissue-specific ubiquitin protein E3 ligase that appears central to mediating the proteolysis associated with muscle atrophy observed in multiple diseases, including diabetes and renal failure (Gomes *et al.*, 2001). Atrogen-1 expression is significantly higher in muscle biopsies from patients with SAM, and atrogen-1 knock down in zebrafish embryos prevented LVT-induced myotoxicity (Hanai *et al.*, 2007). It has been shown that SVT-mediated inhibition of AKT phosphorylation is associated with upregulation of atrogen-1 messenger RNA (mRNA) (Bonifacio *et al.*, 2015).

#### **1.8.2.5 Cholesterol depletion**

The depletion of cholesterol itself has been implicated as an aetiological factor in SAM pathogenesis. Slight skeletal muscle damage has been found by electron microscopy in skeletal muscle biopsies from asymptomatic statin-treated patients, with a characteristic pattern involving T-tubular system breakdown and sub-sarcolemmal rupture (Draeger *et al.*, 2006); cholesterol extraction could reproduce these findings *in vitro* in skeletal muscle fibres (Draeger *et al.*,

2006). Nevertheless, although statins inhibit *de novo* cholesterol production in C2C12 myotubes, total intracellular cholesterol pools remain unchanged (Mullen *et al.*, 2010). Furthermore, the PCSK9 inhibitor, evolocumab, which is an even more potent reducer of LDL-C than statins, does not currently appear to have an increased risk of muscle-related events (Sabatine *et al.*, 2017), although the numbers of patients exposure have been relatively low compared to statins.

#### 1.8.2.6 Calcium signalling disruption

RYR1 (chromosome 19) and RYR3 (chromosome 15) mediate the release of stored calcium ions from skeletal muscle sarcoplasmic reticulum, and thereby play a role in triggering muscle contraction (Protasi *et al.*, 2000). Deleterious *RYR1* variants are associated with anaesthesia-induced malignant hyperthermia, central core disease (Robinson *et al.*, 2006) and multi-minicore disease (Jungbluth, 2007); interestingly, disease-causing mutations or variants in *RYR1* appear to be more frequent in statin myopathy patients than controls (Vladutiu *et al.*, 2011). Muscle biopsies from patients with SAM express significantly higher *RYR3* mRNA and have more severe structural damage, including intracellular T-tubular vacuolisation, than both statin-naïve and statin tolerant controls (Mohaupt *et al.*, 2009). Together, these observations suggest SAM involves a disruption of calcium signalling.

It is also noteworthy that the second major published SAM GWAS identified an intronic variant, rs2819742 (1559G>A), in *RYR2* (chromosome one) associated with CVT severe myopathy (Marciante *et al.*, 2011). An additional copy of the minor A allele was associated with *reduced* myopathy risk (OR 0.48, 95% CI 0.36, 0.63) (Marciante *et al.*, 2011). Similarly, a small candidate gene study showed that the rs2819742 A allele was significantly less frequent in 12 statin myalgia cases compared to seven statin tolerant controls ( $p=0.016$ ) (Elam *et al.*, 2017). However unlike RYR1/RYR3, RYR2 is expressed mainly in cardiac muscle tissue where it facilitates cardiac calcium-induced calcium release, and

deleterious *RYR2* mutations are associated with ventricular arrhythmias (Laitinen *et al.*, 2001).

### **1.8.2.7 Immunologically-mediated statin myopathy**

There is increasing evidence for a role of the immune system in the development of SAM. Leucocyte immunoglobulin-like receptor B5 is encoded by *LILRB5* on chromosome five and being homozygous WT at rs12975366 (p.D247G) compared to variant carriers has been associated with increased circulating CK levels, independent of statin use (Dube *et al.*, 2014), and increased lactate dehydrogenase (LDH) levels (Kristjansson *et al.*, 2016). This led to the hypothesis that D247 homozygotes might also be predisposed to SAM independent of CK level. It was subsequently reported that *LILRB5* D247 homozygotes have an increased risk of statin (predominantly SVT) prescription changes indicative of statin intolerance (OR 1.43, 95% CI 1.10-1.86) and this association was replicated in RVT myalgia cases and statin myopathy (CK  $\geq$  4x ULN) cases (Siddiqui *et al.*, 2017). The mechanism underpinning this association is however unknown at present.

In the causality assessment of an adverse event, the observation that the event improves when a drug is stopped or its dose reduced is one indication that the adverse event is likely an ADR (Gallagher *et al.*, 2011). Interestingly, several research groups previously noted that the symptoms and CK elevation in a few patients with SAM persist or progress after statin discontinuation, and these patients respond positively to immunosuppressive therapy (Needham *et al.*, 2007; Grable-Esposito *et al.*, 2010; Christopher-Stine *et al.*, 2010). These features strongly suggest an autoimmune basis, and in 2011 it was reported that these patients, as well as a minority without known prior statin exposure (less than 10% in myopathy patients  $\geq$ 50 years old), are positive for anti-HMGCR autoantibodies (Mammen *et al.*, 2011). Muscle biopsies of patients with anti-HMGCR antibodies often show necrotizing myopathy with minimal lymphocytic infiltration, although histological features indicative of other conditions (e.g.

poly/dermatomyositis) can occur (Mammen, 2016; Limaye *et al.*, 2015). Subsequent pharmacogenomic studies have provided further evidence of an autoimmune aetiology. In white myopathy patients with anti-HMGCR, the human leukocyte antigen (HLA) class II combination of HLA-DR11; DQA5; DQB7 was significantly overrepresented compared to either controls (statin exposure unknown) or statin intolerant subjects (Table 1.4) (Mammen *et al.*, 2012). In black anti-HMGCR myopathy patients, HLA-DR11 alone is markedly elevated compared to black controls (Mammen *et al.*, 2012). When analysing just myopathy cases, HLA-DR11 was strongly associated with anti-HMGCR (Limaye *et al.*, 2015). HLA-DR11 is a serotype associated with the alleles *HLA-DRB1\*11:01*-*\*11:10*; high resolution typing has revealed that *HLA-DRB1\*11:01* is significantly associated with anti-HMGCR positive myopathy (Mammen *et al.*, 2012), and the ORs for the presence of *HLA-DRB1\*11:01* in anti-HMGCR myopathy white or black patients, compared to controls, have been estimated to be ~25 and ~57, respectively (Mammen *et al.*, 2012). *HLA-DRB1\*11:01* has also been associated with the development of anti-Ro antibodies in neonatal lupus. However, similarly to other drug hypersensitivity reactions, the aetiology of statin autoimmune necrotising myopathy remains elusive.

### 1.8.3 Statin-associated myotoxicity summary

Overall, multiple mechanisms likely contribute to SAM pathogenesis. Immune-mediated myotoxicity is pivotal to non-resolving SAM. For myotoxicity that resolves on drug cessation, the evidence is strongest for increased systemic statin (L) exposure predisposing to mitochondrial dysfunction and reduced prenylation with downstream sequelae including atrogen-1 mediated atrophy, calcium signalling disruption and apoptosis.

Multivariable cox proportional analysis using primary care epidemiological data has been used to develop and validate the parsimonious 'QStatin' model for statin moderate-severe myopathy (Hippisley-Cox and Coupland, 2010). The model includes new statin use, ethnicity, co-morbidities (liver disease,

hypothyroidism, diabetes mellitus) and corticosteroids, as well as being adjusted for age and BMI, and has an area under the receiver operator curve of approximately 0.7 for five year myopathy risk (ClinRisk Ltd, 2014). Although not discussed further, corticosteroids are also myotoxic and so interact pharmacodynamically with statins to increase apparent SAM risk. Overall, it is clear that further research is required to refine PK SAM risk factors, elucidate the relative contribution of different risk factors to the different SAM phenotypes (e.g. myalgia, rhabdomyolysis, autoimmune etc), and determine the sequence of statin-induced muscle effects at physiological concentrations.

### **1.9 P450 oxidoreductase**

The flavoprotein, POR, is the major electron donor to several oxygenases including squalene monooxygenase (cholesterol biosynthetic pathway), heme oxygenase, cytochrome b<sub>5</sub> (Cyb5), and importantly all microsomal CYPs including drug-metabolising CYPs (Riddick *et al.*, 2013). POR also directly supplies electrons to specific xenobiotics, such as the one electron activating reduction of the prodrug, mitomycin C (Wang *et al.*, 2007). Thus POR is important in many metabolic processes, and in particular the metabolism of steroid hormones and xenobiotics (Pandey and Fluck, 2013).

The structure of POR (Figure 1.5) consists of an N-terminal membrane-bound domain that associates with the endoplasmic reticulum, a flavin mononucleotide (FMN)-binding domain, a flavin adenine dinucleotide (FAD) domain, a reduced nicotinamide adenine dinucleotide phosphate (NADPH)-binding domain, and a CYP binding domain (Gong *et al.*, 2017). Electrons from NADPH are picked up by the FAD moiety, passed to the FMN domain, and then transferred to the heme iron of a CYP permitting catalysis (Huang *et al.*, 2008). POR is a 'butterfly' shaped enzyme, with each flavin group constituting a 'wing', and undergoes extensive conformational changes during the electron transfer steps (Miller, 2012). POR expression is correlated to total microsomal CYP content with an average molar ratio of 1:7 (Gomes *et al.*, 2009).

**Figure 1.5 Structure of human P450 oxidoreductase**

Image reproduced from (Pandey and Fluck, 2013). POR is a diflavin protein with two distinct cofactor binding domains (red and blue regions). These domains are linked by a flexible bridge that facilitates the electron transfer from NADPH to a wide range of proteins, including microsomal xenobiotic CYP enzymes. The C-terminus (red region) binds NADPH and transfers electrons to the FAD moiety. The N-terminus (blue region) contains the FMN moiety and CYP interaction sites. The FMN moiety receives the electrons from the FAD region and transfers them to a CYP enzyme, or other interacting electron recipient (Pandey and Fluck, 2013).

*POR* is located on chromosome 7q11.2, consists of 15 protein-coding exons and one non-coding exon 38.8kb upstream that initiates transcription (Huang *et al.*, 2008), and produces a 680 amino acid protein (Pandey and Sproll, 2014; Gong *et al.*, 2017). Over 200 variants have been identified including 130 amino acid changes (Gong *et al.*, 2017), although only one missense variant, rs1057868 (*POR*\*28, p.A503V) is appreciably common (Huang *et al.*, 2008) with MAFs of 17%, 36% and 30% in African, Asian and European populations, respectively (Yates *et al.*, 2016). This relatively high rare: common missense variant ratio is in keeping with negative evolutionary selection pressures to conserve *POR* function. Clinically overt *POR* deficiency is rare, due to rare coding deleterious *POR* mutations, and can present as Antley-Bixler syndrome with genital abnormalities and disordered steroidogenesis (ABS-like syndrome), primary amenorrhoea or congenital adrenal hyperplasia following an autosomal

recessive pattern of inheritance (Fluck *et al.*, 2004; Arlt *et al.*, 2004; Huang *et al.*, 2005). ABS was initially described as a skeletal malformation syndrome, including craniosynostosis (Antley and Bixler, 1975), and associated with autosomal dominant mutations in fibroblast growth factor receptor 2 (*FGFR2*). However, patients with severely reduced steroidogenesis with or without ABS-like skeletal malformations were found to harbour *POR* mutations (Huang *et al.*, 2005); A287P and R457H are the best recognised disease-causing mutations in European and Asian patients (Huang *et al.*, 2005).

Williams-Beuren syndrome is characterised by a microdeletion of chromosome seven approximately 1.2 Mb from *POR*. Interestingly, *POR* mRNA expression was significantly reduced in derived cell lines, suggesting regulatory disruption, although clinical implications are unknown (Merla *et al.*, 2006).

**Figure 1.6 The central role of the electron donor, P450 oxidoreductase, in physiology and pharmacology**

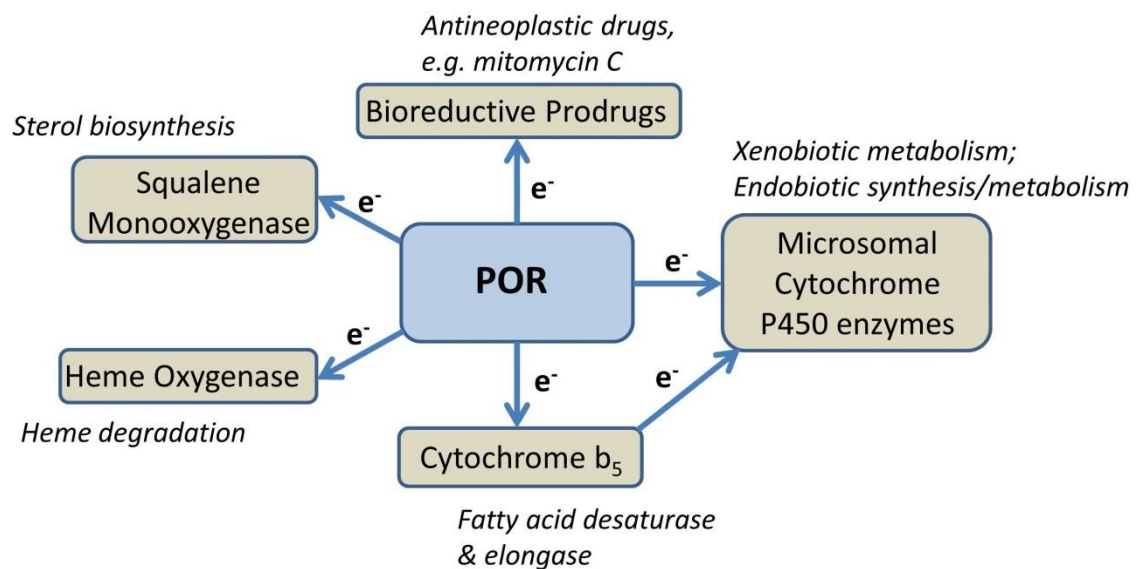


Figure adapted from Riddick *et al.*, 2013. The flavoprotein, P450 oxidoreductase (POR), is a major electron donor necessary for the normal catalytic functioning of several oxygenases. These include squalene monooxygenase, heme oxygenase, cytochrome b<sub>5</sub>, and all microsomal cytochrome P450 (CYP) enzymes, which importantly encompasses drug-metabolising CYPs. POR can also directly biotransform specific xenobiotics through electron donation, such as the one electron activating reduction of the prodrug, mitomycin C (Wang *et al.*, 2007).

### 1.9.1 The role of POR in drug response variability

*In vitro*, animal, and clinical evidence support the hypothesis that POR influences variability in drug response; each are now reviewed below.

### 1.9.2 In vitro observations

*In vitro* studies have demonstrated that different *POR* variants modulate metabolism in a substrate- and CYP-specific manner. Importantly, homozygosity of the 3' untranslated region variant, rs17148944 (MAFs 0-17%) is associated with significantly reduced ATV hydroxylation in *ex vivo* liver microsomes (Gomes *et al.*, 2009). Disease-causing variants, A287P and R457H, have uniformly low *in vitro* activity for CYP3A4 substrates (Agrawal *et al.*, 2010). The missense variant, rs56256515 (L577P), although still rare (MAF 1 in ~700 European-Americans) is nevertheless more common than A287P/R457H and is also associated with reduced activity with most common drug-metabolising CYPs in *ex vivo* liver microsomes (Hart *et al.*, 2008). CYP3A4 activity appears to be modestly reduced for the common A503V polymorphism with some substrates (testosterone, midazolam) and not others (quinidine, erythromycin) (Agrawal *et al.*, 2010). Interestingly, both the flavouring agent, tannic acid, and health supplement, alpha-lipoic acid, have been shown to strongly inhibit POR *in vitro* (Pillai and Mehvar, 2011; Slepneva *et al.*, 1995).

### 1.9.3 Murine observations

Complete *Por* knock-out is embryonically lethal (Shen *et al.*, 2002). However, in 2003 two groups independently reported creation of viable liver-specific conditional *Por* knock out mouse models: the hepatic reductase null (HRN) (Henderson *et al.*, 2003) and liver-specific *Por* null (LCN) (Gu *et al.*, 2003). Both models were created using Cre-Lox recombination technology. The HRN  $POR^{lox/lox} + CRE^{ALB}$  model has been used in this thesis. Briefly, to create the HRN model a replacement-type targeting vector containing *Por* exons 3-16 was created, and loxP sites inserted into introns 4 and 15. The construct was transferred into embryonic cells and clones that had undergone homologous

recombination were selected by resistance to geneticin (G418). These clones were injected into C57BL/6 blastocysts, the male chimera bred with C57BL/6 mice to obtain  $POR^{lox/+}$  mice, which were crossed to produce  $POR^{lox/lox}$  mice. Finally,  $POR^{lox/lox}$  mice were crossed with a transgenic line expressing Cre recombinase under control of the albumin promoter to create  $POR^{lox/lox} + CRE^{ALB}$  liver-specific *Por* conditional knock out mice (Henderson *et al.*, 2003). Several additional models have been created, including *Por* knock out in specific extrahepatic organs (Riddick *et al.*, 2013), a model producing conditional *Por* deficiency in liver and duodenum one week after  $\beta$ -naphthoflavone exposure (Finn *et al.*, 2007), and mice deficient in both hepatic *Por* and *Cyb5a* (HBRN) (Henderson *et al.*, 2013)

Phenotypically, HRN and LCN mice exhibit no overt differences to controls with the same growth rate and no change in survival rates (Henderson *et al.*, 2003). However, they exhibit marked hepatomegaly due to lipid accumulation, which is predominantly triglyceride, and severely reduced circulating cholesterol and triglyceride. They have a profound increase in constitutive hepatic *Cyp* expression (Riddick *et al.*, 2013). Importantly, significantly increased systemic exposures to multiple drugs metabolised by distinct *Cyps* has been measured in HRN and LCN mice, following a typical single intraperitoneal dose (Riddick *et al.*, 2013). These drugs include caffeine (CYP1A2), dextromethorphan (CYP2D6), midazolam (CYP3A4) and omeprazole (CYP2C19) (Riddick *et al.*, 2013). Interestingly, HRN mice are resistant to paracetamol hepatotoxicity, likely due to reduced *Cyp*-mediated production of the toxic metabolite (Henderson *et al.*, 2003).

#### **1.9.4 Clinical observations**

Several clinical PK studies investigating *POR* have been conducted, and the impact of *POR\*28* on lipid lowering response to ATV has been assessed, as outlined below.

#### 1.9.4.1 Cocktail study

*In vivo* cocktail phenotyping has been carried out in a patient with congenital adrenal hyperplasia homozygous for the *POR* A287P mutation and their clinically unaffected mother. The patient had CYP activity consistently lower than the reference 5<sup>th</sup> percentile (CYP1A2, CYP2C9, CYP2D6, CYP3A4); the unaffected mother had more variable CYP activity levels, but consistently less than the referent 25<sup>th</sup> percentile (Tomalik-Scharte *et al.*, 2010).

#### 1.9.4.2 Tacrolimus

The immunosuppressive, tacrolimus, is frequently used after renal transplantation and is a CYP3A substrate. *POR\*28* has been associated with lower concentrations and higher tacrolimus dose requirements that seems to vary by *CYP3A5* expression in most studies (de Jonge *et al.*, 2011; Lunde *et al.*, 2014; Elens *et al.*, 2014; Gijzen *et al.*, 2014), but not all (Kurzawski *et al.*, 2014). These results suggest *POR\*28* may increase CYP3A activity for tacrolimus.

#### 1.9.4.3 Warfarin

The oral anticoagulant, warfarin, is metabolised by CYP2C9 and to a lesser extent by CYP1A1, 1A2 and 3A4. *POR* variants have also been associated with warfarin dose, including the non-coding variant *POR\*37* (rs41301394), two promoter region variants (rs12537282 (-208C>T), rs72553971 (-173C>A) and intronic SNP, rs2868177 (Zhang *et al.*, 2011; Zeng *et al.*, 2016). Nevertheless their effect sizes are modest (Zeng *et al.*, 2016), promoter variant rs12537282 and rs72553971 do not appear to influence transcription (Tee *et al.*, 2011), rs2868177 did not replicate (Tan *et al.*, 2013), *POR\*28* does not appear to affect warfarin (Tan *et al.*, 2013), and their clinical impact remains unknown.

#### 1.9.4.4 Benzodiazepines

The benzodiazepine, midazolam, also serves as a CYP3A probe drug. In *CYP3A5* expressors, but not *CYP3A5\*3/\*3* non-expressors, *POR\*28* carriers have reduced

midazolam metabolic ratios, suggesting reduced CYP3A5-mediated midazolam hydroxylation (Elens *et al.*, 2013a).

#### **1.9.4.5 Atorvastatin**

*POR\*28* carriage has been associated with reduced total and LDL-C lowering on ATV (Drogari *et al.*, 2014), which is hypothesised to be attributable to increased CYP3A4-mediated hydroxylation. However, this observation has not been replicated (Ragia *et al.*, 2014), *POR\*28* does not appear to affect ATV 2-hydroxylation in *ex vivo* microsomes (Gomes *et al.*, 2009), both 2-OH and 4-OH ATV also inhibit HMGCR, and this association has not been found in a GWAS meta-analysis of statin LDL-C levels (Postmus *et al.*, 2014).

#### **1.9.5 *POR* summary**

*POR* is integral to small molecule phase I drug metabolism and there is growing *in vitro*, animal and clinical evidence to support a role for *POR* in the pharmacogenomics of several drugs. The evidence that common *POR* variation impacts drug exposure is strongest for tacrolimus, but heterogeneous for other drugs at present. This is likely due to modest effect sizes, insufficient sample sizes, divergent study populations, and interactions with CYP alleles (e.g. *CYP3A5\*3*) that modulate the effects of *POR* variants. Rare damaging missense variants may well have larger effect sizes.

### **1.10 Major experimental techniques used in thesis**

In this thesis, extensive use of MS is undertaken for both the quantification of statin analytes and proteins. For statin analyte analysis, two approaches to sample collection approaches were employed: conventional use of human plasma stored at -80°C and novel dried blood spot (DBS) collection for murine sampling. In the following sections, an overview of DBS microsampling and MS is provided.

### 1.10.1 Dried blood spots

In 1963, Guthrie and Susi reported the utility of DBS sample collection to enable rapid and economical screening of neonates for elevated phenylalanine levels associated with phenylketonuria (Guthrie and Susi, 1963). Over the last decade there has been a renaissance of interest in DBS microsampling in the pharmaceutical industry and academia. Consequently, there is an expanding repertoire of indications and circumstances where DBS microsampling is being used, including: neonatal screening for multiple inborn errors of metabolism (Chace, 2009; Pourfarzam and Zadhoush, 2013), clinical PK studies (Patel *et al.*, 2013b; Patel *et al.*, 2010), pre-clinical PK (Rahavendran *et al.*, 2012) and toxicokinetic studies (Dainty *et al.*, 2012; Wickremsinhe and Perkins, 2015), therapeutic drug monitoring (Wilhelm *et al.*, 2014; Vu *et al.*, 2012; Lawson *et al.*, 2013), pharmacogenotyping (Hollegaard *et al.*, 2009), human immunodeficiency viral load monitoring and infant diagnosis (Smit *et al.*, 2014; Rutstein *et al.*, 2015), lipid bioanalysis (Koulman *et al.*, 2014), biomarker research (Ostler *et al.*, 2014; Samuelsson *et al.*, 2015), and proteomics (Martin *et al.*, 2013; Ignjatovic *et al.*, 2014). Furthermore, the concept of 'dried matrix spots' has emerged as card based approaches are used to collect samples of biological fluids other than blood for bioanalysis including urine, saliva and breast milk (Olagunju *et al.*, 2015; Numako *et al.*, 2016).

The method for DBS microsampling is straightforward. A whole blood spot is carefully spotted onto filter card and left to dry. The card is kept in an opaque pouch with dessicant and can be stored in ambient conditions until analysis.

#### 1.10.1.1 Advantages of DBS microsampling

This recent 're-discovery' of DBS microsampling has been driven by its notable advantages over traditional plasma-based sampling and facilitated by improvements in the sensitivity of MS analyte detection (Meesters and Hooff, 2013). The advantages of DBS microsampling in bioanalysis include: smaller

sample collection volumes, less invasive sampling collection techniques compared to venepuncture, greater convenience and lower costs for storage and transport, improved (bio)chemical drug stability compared with frozen samples (D'Arienzo *et al.*, 2010; Li *et al.*, 2011), and reduced biohazard risk (Cassol *et al.*, 1992).

With respect to pre-clinical animal studies, in 2010 the European Commission published a directive (2010/63/EU, which updated directive 86/609/EEC) on the protection of animals used for scientific purposes, and is firmly based on the principles of the Three Rs: to replace, reduce and refine the use of animals in scientific research (European Commission, 2010). In the UK, the National Centre for the replacement, refinement and reduction of animals in research (NC3Rs) is the national organisation leading the discovery and implementation of novel approaches to reduce animal use in science (NC3Rs, 2016). Importantly, DBS technology embraces the principles of reduction and refinement, particularly in rodent studies. This is because collection of small blood volumes (typically  $\leq 20\mu\text{L}$ ) enables serial blood monitoring and the generation of a complete PK curve from individual rodents, reducing the number of animals required (Burnett, 2011) and improving study scientific integrity because intraindividual variability is predominantly lower than interindividual variability. Secondly, rodent blood microsampling is typically carried out via the lateral caudal veins. Compared to non-DBS methods that require larger blood volumes, DBS microsampling procedural time is shorter, the warming time to vasodilate the veins is less (in rats), a smaller needle can be used, blood flow will normally stop more quickly following DBS sample collection as the tail puncture is smaller, and overall the stress induced in rodents during blood collection is attenuated (Burnett, 2011).

#### **1.10.1.2 Specific DBS considerations**

DBS microsampling and analysis does involve specific considerations, which can affect the reliability of generated results. These include ensuring a single spot is

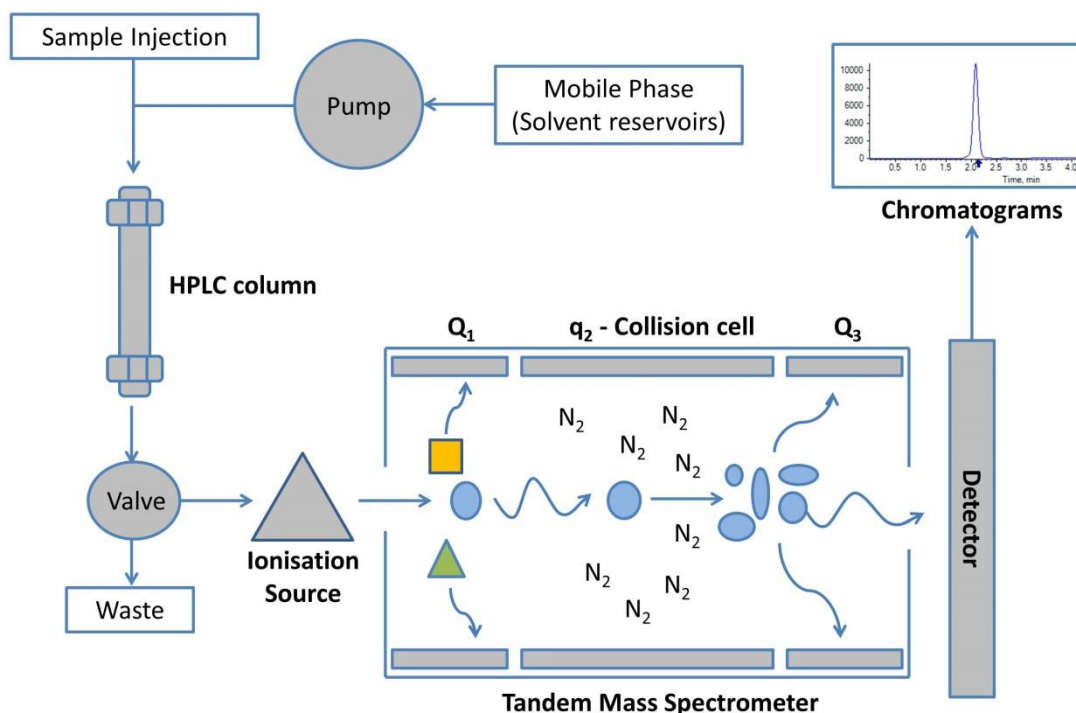
collected avoiding 'double-spotting' or smudging, ensuring sufficient sensitivity to reliably detect analytes in the small blood volumes typically collected, spot size effects, spot homogeneity and haematocrit confounding (Timmerman *et al.*, 2011; Wagner *et al.*, 2016). In general, increases in spot volume and haematocrit increase detected analyte response, and sampling from the outer halo reduces response (Wagner *et al.*, 2016)

### **1.10.2 Liquid chromatography-mass spectrometry**

Coupling of chromatographic apparatus to a mass analyser optimises sensitivity and specificity for analyte identification and quantification. Gas chromatography-MS was developed first, although the crucial development of the electrospray ionisation source led to rapid laboratory uptake of LC-MS.

#### **1.10.2.1 Liquid chromatography**

A high performance liquid chromatography-triple quadrupole (HPLC-MS/MS) system is commonly used for identification, characterisation and quantification of low molecular weight analytes from complex biological matrices, and a schematic of a typical HPLC-MS/MS system is shown in Figure 1.7

**Figure 1.7 Liquid chromatography triple quadrupole system schematic**

This schematic depicts a typical liquid chromatography triple quadrupole mass spectrometry configuration. After off-line extraction of the sample of interest (e.g. protein precipitation extraction of a patient plasma sample), an aliquot of the sample is injected into mobile phase and pumped through a high performance liquid chromatography (HPLC) column to separate the sample matrix components. At the retention time(s) of the analyte(s) of interest, the post-column eluent is diverted via the valve to the mass analyser; at other retention times the eluent is diverted directly to waste to minimise exposure of the mass analyser to the eluent. Electrospray ionisation (ESI) is commonly used to vaporise and ionise the analytes in the eluent, which are then guided and accelerated into the mass spectrometer via a series of focusing voltages (Pitt, 2009). A quadrupole mass analyser separates ions within the lumen based on their mass-to-charge ( $m/z$ ) ratio (Clarke, 2017). A triple quadrupole consists of three quadrupole mass analysers in series:  $Q_1$ ,  $q_2$  and  $Q_3$ .  $Q_1$  and  $Q_3$  act as mass filters whilst  $q_2$  is a collision cell (Clarke, 2017).  $Q_1$  selects the precursor ions injected from the ion source, fragmentation of the precursor ions occurs in  $q_2$  through collisions with nitrogen or argon gas molecules (collision-induced dissociation - CID), and  $Q_3$  selects the fragmented product ions for detection (Pitt, 2009). The primary readout is a chromatogram of analyte intensity (y-axis) versus analysis run time (x-axis).

Chromatography is a physical separation method that separates components in a mixture between a stationary phase and a mobile phase, according to a component's relative affinity to the phases. In most HPLC systems, column chromatography is used in which the stationary phase is attached to the outside of small silica spherical beads housed within a column, and a pump moves the mobile phase from its reservoir through the column at high speed (Malviya *et al.*, 2009). HPLC reduces analysis time and permits the use of smaller beads

(e.g. 2.7 $\mu$ m) that increase surface area to improve separations compared to classic column chromatography (Lakshmi, 2015). Isocratic elution keeps the mobile phase composition constant; in gradient elution the mobile phase is systematically varied during separation by changing its proportions of polar (e.g. water) and organic solvent (e.g. acetonitrile). For analysis of biological matrices, reversed-phase chromatography using a hydrophobic stationary phase and gradient elution are commonly used. The most popular stationary phase is perhaps the octadecyl carbon chain (C<sub>18</sub>) bonded to column silica particles (Lakshmi, 2015). The mobile phase is initially polar (A, aqueous) leading to adsorption of hydrophobic biological components onto the column, but as the proportion of organic (B) solvent in the mobile phase increases, elution of increasing hydrophobic components occurs. The eluent is then transferred to the mass analyser.

#### **1.10.2.2 Mass spectrometry**

Electrospray ionisation (ESI) is a robust ion source that interfaces with LC (Fenn *et al.*, 1989). An ion is a charged atom or molecule. The post-column eluent is pumped through a metal needle, maintained at 3-5 kV, and nebulized at the capillary tip to form a stream of charged droplets (Pitt, 2009). The droplets are rapidly evaporated by nitrogen gas and heat, the residual charge transferred to the analytes (Kearle, 2000), and the analytes guided into the MS via a series of focusing voltages (Pitt, 2009). The mass analyser maintains a high vacuum to smooth analyte transit. Positive or negative ions can be preferentially produced by varying the ion source conditions; positive ionisation mode usually involves addition of a proton (M+H)<sup>+</sup> and negative ionisation mode loss of a proton (M-H)<sup>-</sup>. However, addition of cations (e.g. M+Na<sup>+</sup>) and anions (M+acetate<sup>-</sup>) can also occur (Pitt, 2009). Beyond ESI, other ionisation sources have been developed (Pitt, 2009). As a biological matrix is a complex mixture of multiple components, competition for the ionisation process can occur, leading to a reduced (ion suppression) or increased (ion enhancement) MS signal.

A quadrupole is a type of mass analyser consisting of four cylindrical rods arranged in parallel with a central lumen. A quadrupole separates ions within the lumen based on their mass-to-charge ( $m/z$ ) ratio by varying the stability of their flight trajectory through an oscillating electric field created by applying differential voltages to opposing rods (Clarke, 2017).

A triple quadrupole MS is a type of tandem MS (MS/MS) consisting of three quadrupoles in series: the first ( $Q_1$ ) and third ( $Q_3$ ) act as mass filters whilst the second ( $Q_2$ ) is a collision cell (Figure 1.7) (Clarke, 2017).  $Q_1$  selects the precursor ions injected from the ion source, fragmentation of the precursor ions occurs in  $Q_2$  through collisions with nitrogen or argon gas molecules in a process termed collision-induced dissociation (CID), and  $Q_3$  selects the fragmented product ions for detection (Pitt, 2009). A chromatogram of relative abundance of a specific  $m/z$  versus time is plotted (Clarke, 2017). The requirement to detect both a precursor and product ion for a given analyte optimises analyte specificity.  $Q_1$  and  $Q_3$  can be either fixed to a specific  $m/z$  or set to scan a range of  $m/z$  values to produce a mass spectrum. Single reaction monitoring (SRM) is when both  $Q_1$  and  $Q_3$  are fixed to specifically detect one analyte; multiple reaction monitoring (MRM) is when the voltages of  $Q_1$  and  $Q_3$  are cycled through a number of defined steps to detect a panel of precursors/product ion pairs (mass transitions) to identify a number of specific analytes during a single run (Pitt, 2009).

Analyte quantification is challenging using absolute analyte responses because of inter-day variation in an LC-MS system due to multiple factors including the cleanliness of the ion source, ion suppression, collision cell pressure and MS vacuum (Pitt, 2009). Therefore, an internal standard is added to the sample and the ratio of analyte to internal standard is used to quantify the concentration of analyte within the sample by comparing its response to a calibration curve. Ideally, a stable isotope internal standard is used (e.g. a deuterated version of

the analyte), which has almost identical chemical properties to the analyte but can be easily distinguished by discrete  $m/z$ .

To maximise the sensitivity and specificity of an LC-MS system for the analyte(s) of interest during assay development, several parameters need to be optimised including the assay extraction conditions, column and mobile phases, ion source temperature and gas settings, and collision energy. Assay validation for small molecule quantification involves assessment of selectivity, carryover, accuracy, precision, matrix effects, stability and dilution integrity (Food and Drug Administration, 2001; European Medicines Agency, 2011).

A time-of-flight (TOF) MS is a distinct mass analyser, which accelerates ions generated in the ion source by an electric field into a flight tube. TOF MS separates ions based on their flight times over the defined length of the flight path; the lower an ion's mass, the greater its velocity and so the shorter its flight time. However, TOF analysers can measure all ion masses from each ion pulse. Therefore, TOF analysers are useful in proteomics studies where the relative abundance of multiple (high molecular weight) peptides is of interest (Clarke, 2017).

### **1.11 Thesis research aims and objectives**

This thesis had two major aims. The first aim was to determine whether SAM influences statin utilisation in a secondary prevention UK setting, and if so, whether suboptimal statin use influences the risk of cardiovascular events. Given that SAM is exposure-related, the second aim was to identify novel clinical and genetic factors that affect statin PK and to determine whether identified variants influence the risk of myotoxicity and other adverse outcomes.

To achieve this aim, the objectives were to:

- use a large UK-based cardiovascular secondary prevention prospective cohort study to determine the impact of muscular complaints on statin use, and to assess the impact of suboptimal statin utilisation on cardiovascular events;
- conduct *in vitro* and *in vivo* studies of the HRN murine model to assess the impact of *Por* deficiency on statin disposition;
- identify novel clinical and pharmacogenomic factors associated with plasma levels of ATV and its metabolites in patients on ATV for secondary prevention, and;
- test identified variants for association with muscular complaints, statin utilisation and cardiovascular events.

This thesis involved substantial use of a prospective cardiovascular cohort (PhACS study) (described in detail in Chapter 2), two LC-MS assays were developed and validated, and both an *in vivo* murine single-dose rich PK study and a clinical sparse PK study were conducted.

## **Chapter 2 Investigating the prevalence, predictors and prognosis of suboptimal statin use early after a non-ST elevation acute coronary syndrome**

### **2.1 Introduction**

CVD is the leading cause of mortality worldwide (World Health Organisation, 2014b; World Health Organisation, 2014a). In the US and UK, CVD accounts for the largest and second largest proportions of healthcare expenditure of any disease category, respectively (Cohen and Krauss, 2003; Nuffieldtrust., 2014; Twaddle *et al.*, 2012). Although an acute coronary syndrome (ACS) is a sudden event, most of the morbidity and mortality accrues later, following hospital discharge. Statins inhibit HMGCR and lower circulating LDL-C. Following an ACS, high potency statin therapy, prescribed as ATV 80mg daily, is indicated because it has been demonstrated in RCTs to be highly effective and superior to both placebo and moderate statin therapy for reducing cardiovascular events (Cannon *et al.*, 2004; Waters *et al.*, 2001; Arca and Gaspardone, 2007). However, the effectiveness of drugs in RCTs can be undermined in clinical practice by several factors including poor adherence, discontinuation, and switching prescriptions to a lower equivalent potency. Poor statin adherence has been reported in up to 50% of patients (Blackburn *et al.*, 2005b), statin discontinuation rates vary from 15% (Andrade *et al.*, 1995) to 60-75% (Benner *et al.*, 2002; Simons *et al.*, 1996) and changing to lower potency statin therapy has been noted in ~1% (Hess *et al.*, 2007) to 42% (Colivicchi *et al.*, 2011) of patients.

It is important to understand the clinical consequences of deviating from recommended high potency statin therapy in high-risk patients who have had at least one cardiovascular event. The adverse effects of statin non-adherence and discontinuation on cardiovascular clinical outcomes in patients with existing CVD have been previously investigated separately (Table 2.1), but relatively little is known about the impact of statin dose reductions and/or switching to a

statin of lower equivalent potency in real world secondary prevention (Colivicchi *et al.*, 2011) (Table 2.1). The collective extent to which statin discontinuation, dose reduction, switching and/or non-adherence occur early in secondary prevention is under-reported. Furthermore, few real world statin adherence studies have focussed exclusively on non-ST elevation ACS (NSTEMI-ACS) patients, which as a group are often older, have more comorbidities, are more likely to receive non-interventional medical management and have a worse long term prognosis than patients suffering an ST-elevation myocardial infarction (STEMI) (Docherty, 2010; De Luca *et al.*, 2014; Garcia-Garcia *et al.*, 2011) and so may be more susceptible to insufficient statin therapy.

Therefore, the aims of this study were to investigate: i) the prevalence of, ii) the risk factors for, and iii) the clinical consequences associated with conversion from high potency to 'suboptimal' statin use due to statin discontinuation, dose reduction, switching to an alternative statin of lower equivalent potency and/or statin non-adherence, early after an NSTEMI-ACS in a contemporary prospective cardiovascular cohort.

**Table 2.1 Studies investigating statin non-adherence/discontinuation/persistence/switching in cardiovascular disease**

Study	Country	Setting	Patient population	Study design	Sample size	Endpoints	Main results
<b>Statin adherence studies</b>							
(Blackburn <i>et al.</i> , 2005a)	Canada	Health records database	CAD	Cohort	1221	MACE; Recurrent MI	≥80% vs ≤60% PPF: no significant difference (MACE) ≥80% vs ≤60% PPF: HR 0.45 (95% CI 0.20-0.99) (MI)
(Ho <i>et al.</i> , 2008)	US	Health records databases	CAD	Cohort	13596	ACM Cardiovascular mortality	<80% vs ≥80% PDC: HR 1.85 (95% CI 1.63-2.09) (ACM) <80% vs ≥80% PDC: HR 1.62 (95% CI 1.124-2.13) (Cardiovascular mortality)
(McGinnis <i>et al.</i> , 2009)	USA	Health records database	CAD	Cohort	2201	MACE	>80% vs ≤80% PDC: HR 0.75 (95% CI 0.61-0.93)
(Rasmussen <i>et al.</i> , 2007)	Canada	Health records databases	MI	Cohort	17823	ACM	<40% vs ≥80% PDC: HR 1.25 (95% CI 1.09-1.42) 40-79% vs ≥80% PDC: HR 1.12 (95% CI 1.01-1.25)
(Ruble <i>et al.</i> , 2012)	US	Health records database	CAD	Cohort	15277	MACE	>60% vs ≤60% PDC: HR 0.74 (95% CI 0.66-0.82)
(Tuppin <i>et al.</i> , 2010)	France	Health records databases	MI	Cohort	10501	MACE	≤80% vs >80% PDC: HR 1.58 (95% CI 1.37-1.81)
(Wei <i>et al.</i> , 2002)	Scotland	Health records database	MI	Cohort	5590	Recurrent MI; ACM	≥80% PDC vs no statin: RR 0.19 (95% CI 0.08-0.47) (MI) <80% PDC vs no statin: no significant difference (MI) ≥80% PDC vs no statin: RR 0.47 (95% CI 0.22-0.99) (ACM) <80% PDC vs no statin: no significant difference (ACM)
(Wei <i>et al.</i> , 2008)	Scotland	Health records database	CVD <sup>1</sup>	Cohort	7657	MACE	≥80% vs <80% PDC: RR 0.66 (95% CI 0.47-0.91) (from statin alone cohort, n=671)
<b>Statin discontinuation studies</b>							
(Daskalopoulou <i>et al.</i> , 2008)	UK	Health records database	MI	Cohort	9939	ACM	Statin discontinuation vs no statin use: HR 1.88 (95% CI 1.13-3.07)
(Ho <i>et al.</i> , 2006a)	US	Prospective study	MI	Cohort	2008	ACM	Statin discontinuation vs no discontinuation: HR 2.86 (95% CI 1.47-5.55)
<b>Statin persistence</b>							
(Hippisley-Cox and Coupland, 2006)	UK	Health records database	CAD	Nested case-control	13029	ACM	1-12 months statin vs no statin: OR 0.80 (95% CI 0.66-0.97) >60 months statin vs no statin: OR 0.20 (95% CI 0.08-0.47)

<i>Table continued</i>							
Study	Country	Setting	Patient population	Study design	Sample size	Endpoints	Main results
<b>Statin switching</b>							
(Colivicchi <i>et al.</i> , 2011)	Italy	Prospective study	ACS	Cohort	1321	MACE	Switching from ATV 80mg/day to moderate statin therapy vs constant ATV 80mg/day therapy: HR 2.7 (95% CI 1.7-5.1)

ACM = all-cause mortality; CAD = coronary artery disease; CVD = cardiovascular disease; HR = hazard ratio; MACE = major adverse cardiovascular event; MI = myocardial infarction; OR = odds ratio; PDC = proportion of days covered; PPF = proportion of prescriptions filled.

CAD typically encompasses ACS, percutaneous coronary intervention (PCI) and coronary artery bypass graft (CABG) surgery. MACE typically includes cardiovascular death, myocardial infarction and stroke.

<sup>1</sup> = CVD included angina, MI, heart failure, stroke, transient ischaemic attack (TIA) and peripheral artery disease (PAD).

## 2.2 Methods

### 2.2.1 Prospective study outline

The investigation herein utilises the Pharmacogenetics of Acute Coronary Syndrome (PhACS) prospective observational study, which was conducted at 16 UK hospital sites between 2008-2013. The main inclusion criteria were:

- hospitalisation with a NSTEMI-ACS (both non-ST elevation myocardial infarction (NSTEMI) and unstable angina), and;
- each participant had to be able to provide informed consent.

NSTEMI-ACS was defined by either a positive troponin or appropriate electrocardiography (ECG) changes in the context of a history consistent with an ACS. Permissible ECG changes were: ST-depression, T-wave inversion, ST-segment flattening and transient self-resolving ST-elevation.

The exclusion criteria were:

- unwilling to participate
- inability to consent
- diagnosis of STEMI
- a diagnosis or other pathology likely to account for symptoms or troponin rise
- a diagnosis or other pathology that may lead to death within one year other than cardiac (e.g. terminal lung cancer)
- no fixed address
- no current general practitioner
- not suitable, in the opinion of the Investigator, for participation in the study

In total, 1470 eligible patients were recruited. Patients were followed up at one (visit 2 (V2)) and 12 months (visit 3 (V3)) post recruitment, and annually thereafter until all participants had been followed up for at least 12 months.

V2/V3 were conducted in person, or if not possible by telephone and/or a hospital case notes review (CNR). Subsequent visits were conducted annually thereafter by telephone and/or CNR. Patients that did not have a follow up visit during the last six months of study follow up had another CNR to ensure comprehensive clinical event capture. The general practitioners of patients missing drug data at V3 were contacted to collect V3 drug data and screen for cardiovascular events.

The endpoint clinical events were: death and non-fatal MI or ischaemic stroke. Validation of non-fatal MIs was based on the algorithm used in TRITON-TIMI 38 (Wiviott *et al.*, 2006), with the additional criterion that the treating physician team considered the raised cardiac biomarker (i.e. troponin) to be related to an ACS event, and therefore did not primarily diagnose and treat a non-ACS condition. Validation of non-fatal strokes was based on the HORIZONS-AMI definition, as an acute neurologic deficit lasting for over 24 hours, as classified by a physician, with supporting information, including brain images and neurological/neurosurgical evaluation (Mehran *et al.*, 2008). Non-fatal MIs and strokes were defined as those with no death within seven days and when death did occur within seven days and the death certificate was available, MI/stroke was not listed within part I of the death certificate. Validation of cardiovascular deaths was based on the PLATO trial definition and included deaths due to CVD, cerebrovascular deaths and any other deaths with no clearly documented non-cardiovascular cause (James *et al.*, 2009).

The protocol was approved by the Liverpool (adult) research Ethics Committee, UK; site-specific approval was granted at all sites involved and local informed consent was obtained from all study subjects in accordance with the Declaration of Helsinki.

### 2.2.2 Cohort Selection

Patients were eligible for inclusion in the current study if they were discharged on a high potency statin from their index hospital NSTEMI-ACS admission. High potency statin therapy was: ATV 80mg daily, the equivalently potent RVT 20mg, and RVT 40mg daily. All other statins and doses were considered non-high potency statin therapy. Determination of statin potency is based on the estimated relative LDL-C-lowering potencies of different statins across a range of clinically utilised doses (Table 2.2); the majority of PhACS patients were discharged on ATV 80mg daily because PhACS is a secondary prevention cohort.

Patients were excluded if they died within 30 days of discharge, because this prevented assessment of suboptimal statin status during follow up (see below). Patients were excluded if their V2 occurred during a prolonged index hospital admission or did not actually occur until >180 days after index admission (as ~85% of muscular symptoms occur within 180 days (Bruckert *et al.*, 2005)), or they were lost to follow up following V2.

**Table 2.2 Statin doses estimated to lead to similar reductions in low-density lipoprotein cholesterol**

Fluvastatin	Lovastatin	Pravastatin	Simvastatin	Atorvastatin	Rosuvastatin
40 mg	20 mg	20 mg	10 mg	-	-
80 mg	40 or 80 mg	40 mg	20 mg	10 mg	-
-	80 mg	80 mg	40 mg	20 mg	5 or 10 mg
-	-	-	80 mg	40 mg	-
-	-	-	-	<b>80 mg</b>	<b>20 mg</b>
-	-	-	-	-	<b>40 mg</b>

Based on Smith *et al.*, 2006 (Smith *et al.*, 2009). The doses highlighted in bold represent the high potency statin therapy required at discharge from index hospitalisation for cohort inclusion.

### 2.2.3 Assessment of statin adherence

At V2, cardiac medication adherence was assessed using the Brief Medication Questionnaire (BMQ) (Figure 2.1) (Svarstad *et al.*, 1999). The BMQ is an indirect method of determining medication adherence and incorporates three screens: a regimen screen, belief screen and a recall screen. The BMQ has been

previously compared to the Medication Events Monitoring System in a small validation study (n=20) using angiotensin converting enzyme inhibitors (ACEIs) (Svarstad *et al.*, 1999). This study determined that the regimen screen had a sensitivity of 80% for detecting repetitive non-adherence and did not classify any adherent patients as non-adherent. However, it had 0% sensitivity for detecting sporadic non-adherence, and so the overall accuracy of the regimen screen was 95% (Svarstad *et al.*, 1999). The belief screen had sensitivities of detecting repetitive and sporadic non-adherence of 100% and 10%, respectively. However, it classed ~20% of adherent patients as repetitive non-adherent patients, giving an overall accuracy of 85%. The recall screen had sensitivities of detecting repetitive and sporadic non-adherence of 40% and 90%, respectively. However the respective specificities were only 40% and 80% (Svarstad *et al.*, 1999).

Therefore for the main analysis, assessment of adherence pragmatically utilised the regimen screen; patients were classed as non-adherent if they reported missing at least one statin pill over the past week (BMQ question 1e). For sensitivity analyses B and C4 (see below), the definition of non-adherence was expanded to include all of the available identifiers of potential non-adherence (Svarstad *et al.*, 1999) (listed in sensitivity analysis B).

### Figure 2.1 The Brief Medication Questionnaire

Please list below all of the cardiac medications you took in the past week. For each medication you list, please answer each of the questions in the box below.

#### Question 1

a. Medication name and strength (per tablet)	
b. How many days did you take it?	
c. How many times per day did you take it?	
d. How many pills did you take each time?	
e. How many times did you miss taking a pill?	
f. For what reason were you taking it?	
g. How well does the medicine work for you? 1=well; 2=okay; 3=not well	

#### Question 2 Do any of your medications bother you in any way?

Yes   No   go to question 3

How much did it bother you?					In what way did it bother you?
Medication name	A lot	Some	A little	Never	

**Question 3** Below is a list of problems that people sometimes have with their medicine. Please check how hard it is for you to do each of the following:

	Very hard	Somewhat hard	Not hard at all	Comment (which medicine)
a. <b>Open or close</b> the medication bottle				
b. <b>Read the print</b> on the bottle				
c. <b>Remember</b> to take all the pills				
d. <b>Get your refills</b> in time				
e. <b>Take so many pills</b> at the same time				

#### 2.2.4 Classification of suboptimal and constant statin use

Patients were designated 'suboptimal statin users' if, by V2, they had discontinued, reduced their statin dose, switched to an alternative statin of lower equivalent potency (Table 2.2) and/or were statin non-adherent. Patients that remained on high potency statin therapy between baseline and V2 and were statin adherent represented 'constant statin users'.

### 2.2.5 Outcomes

- i) Suboptimal statin use at V2 was itself the outcome for investigating clinical factors associated with its occurrence.
- ii) For investigating potential sequelae of suboptimal statin use, the primary endpoint was time to first major adverse cardiovascular event (MACE): a composite of death from a CVD (or no known) cause, or non-fatal MI or ischaemic stroke. Time to all-cause mortality (ACM) was the secondary endpoint.

### 2.2.6 Covariates

The following were considered for investigating factors associated with suboptimal statin occurrence: age $\geq$ 75, sex, BMI $\geq$ 30, hypertension, hyperlipidaemia, diabetes mellitus, smoking (current or previous versus non-smokers), chronic kidney disease, chronic obstructive pulmonary disease (COPD), prior CVD (previous MI, stroke, transient ischaemic attack (TIA) or PAD), statin use prior to index admission, raised index troponin, whether the patient was discharge on high potency ATV or RVT, treatment with percutaneous coronary intervention (PCI) or CABG surgery during or within 30 days following discharge from the index admission, New York Heart Association (NYHA) functional class at V2, reported use at V2 of aspirin, a P2Y<sub>12</sub> inhibitor, a beta blocker, an ACEI or angiotensin II receptor blocker (ACEI/ARB), warfarin, or a proton pump inhibitor (PPI), concomitant use of levothyroxine (a surrogate for hypothyroidism diagnosis) or a drug(s) that inhibits CYP3A4, and muscular symptoms recorded at V2.

The following were considered CYP3A4 inhibitors: amiodarone, clarithromycin, ciclosporin, diltiazem, erythromycin, itraconazole, protease inhibitors (indinavir, ritonavir, saquinavir), telithromycin and verapamil (Alfirevic *et al.*, 2014). Levothyroxine and all CYP3A4 inhibitors, except diltiazem and verapamil, were not explicitly referred to in the case report form (CRF), but were accepted for this analysis if they had been noted in the CRF medication

appendix during either baseline or V2. Their absence in the medication appendix was, for the purposes of this investigation, assumed to equate to not being prescribed/taken.

Patients were not explicitly questioned regarding muscular symptoms in PhACS. However, question 2 of the BMQ used at V2 asked if any medications bothered a patient, and if so, in what way; reports of bothersome muscular pains/cramps/aches/weakness whilst on statin therapy herein constituted muscular symptoms.

For the analyses investigating the risks of MACE and ACM, all of the above covariates were included except muscular symptoms, levothyroxine, CYP3A4-inhibiting drugs, and type of high potency statin discharged on. These had only been included in the assessment of suboptimal statin occurrence due to their previous associations with statin-associated myotoxicity (Alfirevic *et al.*, 2014), and so they were *a priori* excluded here. Follow up commenced from the date of V2.

### **2.2.7 Subgroup analyses**

Suboptimal statin use was divided into those who had discontinued or were statin non-adherent, and those who had reduced statin dose or switched statin (but were statin adherent), and the risks of time to MACE and ACM were analysed for both subgroups, compared to constant statin users.

### **2.2.8 Statistical analysis**

For the baseline demographic and comorbidity variables, there was <2% missing data. The percentage of missing cardiovascular and PPI drug data at V2 was 8.4-8.7%. The percentage of missing data for V2 statin status (high dose, low dose, discontinuation) was 9.4%, and ~19% of data were missing for each of V2 NYHA status, V2 muscular symptoms and adherence information. 9.6% of

V2 dates were missing. Overall, 4.3% of data were missing, but 28.6% of cases had at least one missing value. The missing data were handled in three consecutive steps.

First, missing V2 dates were imputed by adding 30 days to baseline discharge date, because 30 days represented the median duration of the non-missing data.

Second, by manual imputation. For missing V2 covariate drug data, if the drug status at baseline and the next recorded visit (predominantly V3) remained unchanged (i.e. a patient remained on or off the drug) then this status was assumed for V2 and was manually imputed. For patients missing V2 statin status, if a patient remained on the same high dose statin therapy between baseline and the next recorded visit then this high dose statin status was manually imputed at V2. Where V2 statin adherence data was missing, if a patient remained on high dose statin therapy and was completely statin adherent at the next recorded follow up visit, then full adherence to high dose statin therapy at V2 was assumed. Only 1.2% of patients openly reported muscular symptoms at V2 and, given a missing data rate of ~19%, it was decided to assume that all patients missing these data did not have muscular symptoms. Following manual imputation, missing data rates for drug covariates, statin therapy, statin adherence and V2 muscular symptoms were reduced to 2.1-4.0, 4.9, 15.9% and 0.0%, respectively. Overall, 2.2% of data remained missing but 27% of cases still had at least one missing data value.

Third, by multiple imputation. Following steps i and ii, the overall missing data rate was negligible, but as the BMQ (and so statin adherence) had a high missing data rate, multiple imputation was undertaken, under the missing at random assumption. Although the missing data pattern had a monotonic trend, this pattern was incomplete and so all missing values were sampled using a fully conditional specification (FCS) method, which uses an iterative Markov chain Monte Carlo procedure (100 iterations), with generation of ten imputation

datasets. Ordinal variables (statin status, statin adherence and NYHA classification) were treated as continuous variables and imputed using linear regression within the FCS procedure. Categorical variables were imputed by logistic regression. Covariate drug status at baseline and 12 months and NYHA status at 12 months were used as auxiliary variables to assist imputation.

#### **2.2.8.1 Investigating factors associated with suboptimal statin use**

Following imputation, potential covariate multicollinearity was first assessed using the variance inflation factor (VIF). Second, the null hypothesis of no association with suboptimal statin occurrence (compared to constant statin use) was tested for each variable using the Wald test, because it generates a pooled value from the ten datasets. Those covariates with univariate  $p < 0.1$  were entered into a multivariable logistic regression model, using forwards stepwise (likelihood ratio) selection. ORs and p-values are pooled from the ten imputed datasets;  $p < 0.05$  indicated significance.

#### **2.2.8.2 Investigating risks of MACE and ACM associated with suboptimal statin use**

For the time to MACE analysis, participants were censored at the earliest date of non-CVD death or date of last recorded visit. For time to ACM, participants were censored at the date of the last recorded visit.

A univariate Cox proportional hazard model was fitted for each covariate to test its association with time to MACE; the same was performed for time to ACM. For each covariate, the Cox proportional hazards assumption was assessed by visual inspection of Kaplan-Meier curves. If a covariate did not meet the proportional hazards assumption, it was excluded from the main analyses (see sensitivity analyses D1 and D2). Covariates meeting the proportional hazards assumption and  $p\text{-value} < 0.1$  in univariate analysis were taken forwards into multivariable Cox proportional hazards modelling, with the final multivariable model covariates chosen by forwards stepwise (likelihood ratio) selection.

After the covariate model had been fitted for both time to MACE and time to ACM, suboptimal statin use was introduced into both models to test its adjusted association with risk of MACE, or ACM. The hazard ratios (HR) and p-values provided in the results section are pooled results across all imputed datasets, except in the complete cases sensitivity analyses.

As two outcomes (MACE, ACM) were investigated here, a Bonferroni correction was used to adjust the significance threshold to  $p \leq 0.025$ . This threshold was also applied to all sensitivity analyses that further examined the risks of MACE or ACM associated with suboptimal statin use (see below).

### **2.2.9 Sensitivity Analyses**

To investigate the robustness of the results, several sensitivity analyses were undertaken.

#### **2.2.9.1 Sensitivity analysis A: Further assessment of the differences between suboptimal and constant statin user groups:**

In sensitivity analysis A, a complete case cohort was used to determine the multivariable (logistic regression) differences in covariate prevalence between the suboptimal and constant statin user groups. This cohort excluded all patients with any missing data that required imputation by any of the three described methods.

#### **2.2.9.2 Sensitivity analyses B-F: Further assessments of the risks of MACE and ACM associated with suboptimal statin therapy**

##### **2.2.9.2.1 Sensitivity analysis B**

Sensitivity analysis B referred to the expanded full statin non-adherence definition, incorporating: patients that missed at least one statin pill (BMQ Qu. 1e), took a statin for six or less days (Qu. 1b) (both from regimen screen),

reported that the statin did not work well for them or they did not know (Qu. 1g), found that the statin bothered them at least a little (Qu. 2) (both from belief screen) and those that found it at least somewhat hard to remember to take all of their pills (Qu. 3c from the recall screen), respectively.

#### **2.2.9.2.2 Sensitivity analyses C1-C4**

Within the complete case cohort (all patients with any missing data excluded), sensitivity analysis C1 assessed the risks of time to MACE and ACM for all patients with suboptimal statin therapy, C2 assessed just those who had discontinued or were statin non-adherent, C3 assessed just those who had reduced the dose or switched statin (but were adherent), and C4 assessed the expanded statin non-adherence definition, compared to constant statin users.

#### **2.2.9.2.3 Sensitivity analyses D1 and D2**

For variables that conspicuously disobeyed the proportional hazards assumption for the full follow up duration upon inspection of unadjusted Kaplan-Meier curves (V2 P2Y<sub>12</sub> inhibitor use for MACE, and sex for ACM), their impact on MACE and ACM was first investigated via univariate and multivariable logistic regression analyses (utilising all endpoint events), as has been previously recommended (Wachtel and Yang, 2014) (D1). Secondly, they were investigated by limiting follow up to 11 months after V2 (essentially 12 months after baseline discharge), because the proportional hazards assumption was upheld for these variables within this shorter duration (D2).

#### **2.2.9.2.4 Sensitivity analyses E1 and E2**

To ensure that all variables that differed significantly between the suboptimal and constant statin user groups at V2 did not affect the adjusted associations between statin utilisation and times to MACE or ACM, multivariable models including these variables were performed. As two of these variables (patient sex and P2Y<sub>12</sub> inhibitor status at V2) did not meet the proportional hazards

assumption, both multivariable logistic regression and Cox proportional hazards modelling censored at 11 months after V2 were carried out.

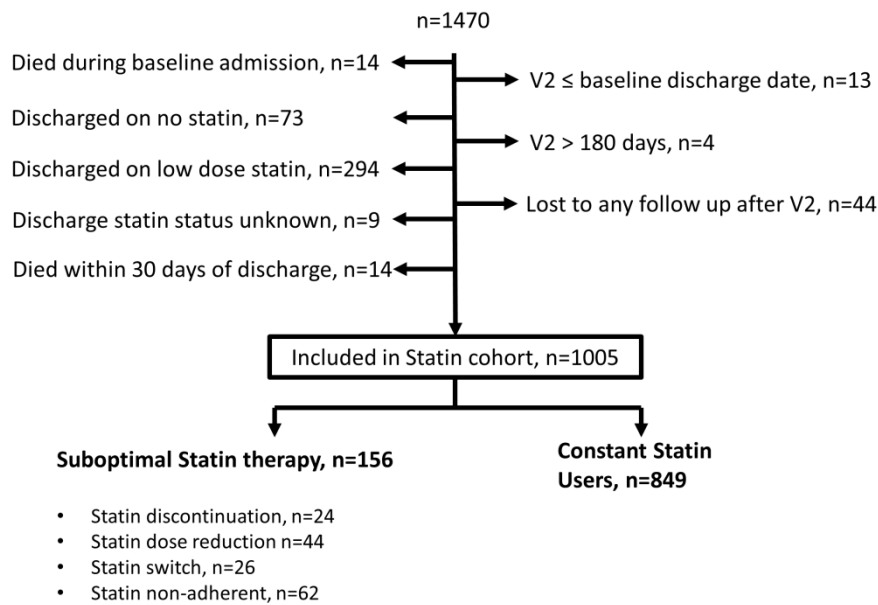
#### **2.2.9.2.5 Sensitivity analyses F1 and F2**

It is possible that statin prescription alterations early after discharge simply identify patients that received more medical attention because they are more ill. Thus, to investigate healthy user bias within this study's cohort, PPI prescription changes were considered. As many patients were not discharged from their index NSTEMI-ACS admission on a PPI, constant PPI status was defined as: not on a PPI or on the same PPI and dose at both baseline and V2. PPI changers were defined as: patients that started, stopped or switched PPI or increased or decreased their PPI dose. When comparing constant to PPI changers for the full follow up duration, the proportional hazards assumption was not met and therefore, healthy user bias was assessed as above using both logistic regression (E1) and limiting follow up to 11 months after V2 (E2).

All analyses were performed using IBM SPSS version 22.0 (IBM Corp, Armonk, NY, USA).

### **2.3 Results**

Figure 2.2 outlines the cohort selection process for this study. 1,005 patients discharged on a high potency statin were included; >99% were prescribed ATV 80mg daily. 156 patients (15.5%) were suboptimal statin users by V2; 849 (84.5%) remained on and adherent to high potency statin therapy, constituting constant statin users. Dose decreases were mainly to 40mg, 20mg or 10mg ATV daily, and switches were almost exclusively to SVT.

**Figure 2.2 A schematic of the study selection process**

### 2.3.1 Factors associated with suboptimal statin occurrence

All covariates had a VIF <1.5 indicating negligible multicollinearity, and so all intended variables were assessed. Suboptimal and constant statin users were broadly similar, as shown in Table 2.3. However, univariate differences between the groups were noted at  $p < 0.1$  for patient sex, diabetes mellitus, use at V2 of a P2Y<sub>12</sub> inhibitor, beta blocker or CYP3A4-inhibiting co-medication, and patient-reported muscle symptoms at V2.

**Table 2.3 Characteristics of suboptimal and constant statin users**

Variable	Suboptimal Statin therapy	Constant Statin users	Unadjusted p-value
<b>Patients (%)</b>	156 (15.6)	849 (84.4)	
Median follow up from V2 (months)	16	15	0.52
<b>Demographics</b>			
Age ≥ 75, n (%)	39 (25.0)	161 (19.0)	0.13
Men, n (%)	102 (65.4)	660 (77.4)	0.004
BMI ≥ 30, n (%)	54 (34.6)	292 (33.4)	0.92
<b>Medical History, n (%)</b>			
Hypertension	93 (59.6)	490 (57.7)	0.63
Hyperlipidaemia	75 (48.1)	455 (53.6)	0.27
Diabetes mellitus	43 (27.6)	43 (27.6)	0.091
Ever smoked	113 (72.4)	588 (69.3)	0.42
CKD (Cr>150µmol/L)	13 (8.3)	48 (5.7)	0.28
COPD	13 (8.3)	74 (8.7)	0.89
Prior CVD <sup>1</sup>	51 (32.7)	287 (33.8)	0.82
On Statin prior to index admission	79 (50.6)	387 (45.6)	0.30
<b>Diagnosis, n (%)<sup>2</sup></b>			
Troponin-raised NSTEMI-ACS	149 (95.5)	828 (97.5)	0.16
Normal troponin NSTEMI-ACS	7 (4.5)	21 (2.5)	
<b>Treatment, n (%)</b>			
PCI/CABG	72 (46.2)	401 (47.2)	0.80
Discharged on ATV 80mg daily	155 (99.4)	843 (99.3)	0.91
<b>NYHA Functional Classification at Visit 2, n (%)</b>			
Class I	82 (52.6)	457 (53.8)	0.61
Class II	56 (35.9)	314 (37.0)	
Class III	18 (11.5)	70 (8.3)	
Class IV	0 (0.0)	8 (0.9)	
<b>Drugs at Visit 2, n (%)</b>			
Aspirin	142 (91.0)	795 (93.6)	0.36
P2Y <sub>12</sub> inhibitor	122 (78.2)	738 (86.9)	0.006
Beta blocker	119 (76.3)	725 (85.4)	0.016
ACEI/ARB	121 (77.6)	706 (83.2)	0.11
Warfarin	6 (3.9)	41 (4.8)	0.57
Proton pump inhibitor	67 (43.0)	358 (42.2)	0.89
CYP3A4-inhibitors	19 (12.2)	66 (7.8)	0.080
Levothyroxine	6 (3.8)	39 (4.6)	0.67
<b>Muscular symptoms at V2, n (%)</b>	5 (3.2)	7 (0.8)	0.020

<sup>1</sup> = Prior CVD encompasses past MI, stroke, TIA or PAD; <sup>2</sup> = raised troponin taken to indicate non-ST elevation myocardial infarction (NSTEMI), and a normal troponin unstable angina.

Importantly, in multivariable logistic regression, being female ( $p=0.010$ ), not on either a P2Y<sub>12</sub> inhibitor ( $p=0.007$ ) or beta blocker at V2 ( $p=0.036$ ), and being bothered by muscular symptoms ( $p=0.017$ ) were all associated with an increased adjusted risk of suboptimal statin occurrence (Table 2.4).

**Table 2.4 Adjusted factors associated with suboptimal statin occurrence**

Risk factor	Suboptimal Statin therapy, n (%)	Constant Statin users, n (%)	Multivariable analysis	
			OR (95% CI)	p-value
Muscular symptoms	5 (3.2)	7 (0.8)	4.28 (1.30-14.08)	0.017
Sex (F vs M)	M: 102 (65.4)	M: 660 (77.4)	1.75 (1.14-2.68)	0.010
P2Y <sub>12</sub> inhibitor at V2	122 (78.2)	738 (86.9)	0.53 (0.34-0.84)	0.007
Beta blocker at V2	119 (76.3)	725 (85.4)	0.59 (0.36-0.96)	0.036

Covariates with univariate  $p<0.1$  were entered into multivariable logistic regression modelling using the forwards likelihood ratio method to select the model ( $p<0.05$  indicated significance).

### 2.3.2 Risks of MACE and ACM associated with suboptimal statin use

The median study duration after V2 was 16 months, and there were 113 MACE and 79 ACM events; 33% of ACM deaths were non-cardiovascular. Table 2.5 shows the univariate analysis results for the clinical variables and time to MACE, or time to ACM. All variables met the Cox proportional hazards assumption, except V2 P2Y<sub>12</sub> status for MACE, and patient sex for ACM (Table 2.5); these were re-considered in sensitivity analyses D1 and D2. Of patients with suboptimal statin use, 32 and 25 suffered MACE and ACM, respectively.

**Table 2.5 Univariate Cox regression analysis results for association with time to MACE or time to ACM**

Variable	Time to MACE (n=113)		Time to ACM (n=79)	
	HR (95% CI)	p-value	HR (95% CI)	p-value
<b>Demographics</b>				
Age ≥ 75	3.02 (2.07-4.40)	<0.001	5.17 (3.31-8.07)	<0.001
Sex (F vs M)	1.31 (0.87-1.97)	NS (p=0.19)	*	*
BMI ≥ 30	1.30 (0.89-1.90)	NS (p=0.18)	1.40 (0.89-2.20)	NS (p=0.14)
<b>Medical History</b>				
Hypertension	1.82 (1.21-2.71)	0.004	2.12 (1.29-3.49)	0.003
Hyperlipidaemia	1.56 (1.06-2.27)	0.023	1.90 (1.20-3.02)	0.007
Diabetes mellitus	2.56 (1.76-3.74)	<0.001	2.77 (1.78-4.33)	<0.001
Ever smoked	1.22 (0.80-1.86)	NS (p=0.35)	1.33 (0.80-2.21)	NS (p=0.27)
CKD (Cr>150)	2.72 (1.65-4.47)	<0.001	3.93 (2.34-6.61)	<0.001
COPD	1.39 (0.79-2.43)	0.26	1.88 (1.03-3.42)	0.039
Prior CVD	3.06 (2.09-4.48)	<0.001	4.25 (2.64-6.87)	<0.001
Statin prior to admission	1.66 (1.14-2.42)	0.009	2.01 (1.26-3.21)	0.003
<b>Diagnosis</b>				
Raised troponin	0.84 (0.34-2.09)	NS (p=0.71)	1.47 (0.36-6.01)	NS (p=0.59)
<b>Treatment</b>				
PCI/CABG	0.42 (0.28-0.63)	<0.001	0.31 (0.18-0.53)	<0.001
<b>Functional statin at V2</b>				
NYHA	1.89 (1.51-2.37)	<0.001	2.07 (1.60-2.70)	<0.001
<b>Drugs at V2</b>				
Suboptimal Statin therapy	2.18 (1.40-3.40)	0.001	2.54 (1.56-4.14)	<0.001
Aspirin	0.49 (0.28-0.86)	0.013	0.23 (0.13-0.38)	<0.001
P2Y <sub>12</sub> inhibitor	*	*	0.66 (0.39-1.12)	NS (p=0.12)
Beta blocker	0.86 (0.53-1.42)	NS (p=0.56)	0.76 (0.43-1.34)	NS (p=0.34)
ACEI/ARB	1.46 (0.84-2.55)	NS (p=0.18)	1.16 (0.63-2.13)	NS (p=0.63)
Warfarin	2.23 (1.13-4.42)	0.022	2.94 (1.41-6.13)	0.004
Proton pump inhibitor	0.97 (0.67-1.42)	NS (p=0.89)	1.40 (0.90-2.18)	NS (p=0.14)

\* = Visit two P2Y<sub>12</sub> status did not meet the proportional hazards assumption for MACE, and patient sex did not meet the proportional hazards assumption for ACM; these variables were considered in sensitivity analyses D1 and D2.

In multivariable analysis, suboptimal statin use was a risk factor for both time to MACE (HR 2.10, 95% CI 1.25-3.53, p=0.005) and time to ACM (HR 2.46, 95% CI 1.38-4.39, p=0.003), after adjusting for age ≥ 75, prior CVD, PCI/CABG treatment, NYHA class, and either diabetes mellitus (time to MACE) or chronic kidney disease (time to ACM) (Table 2.6).

**Table 2.6 Multivariable adjusted Cox regression results for risk of time to MACE or ACM**

Variable	Time to MACE		Time to ACM	
	HR (95% CI)	p-value	HR (95% CI)	p-value
<b>Suboptimal Statin therapy</b>	<b>2.10 (1.25-3.53)</b>	<b>0.005</b>	<b>2.46 (1.38-4.39)</b>	<b>0.003</b>
Age $\geq$ 75	2.05 (1.36-3.09)	0.001	3.47 (2.12-5.68)	<0.001
NYHA	1.48 (1.12-1.96)	0.006	1.62 (1.16-2.27)	0.005
Treatment with PCI/CABG	0.56 (0.37-0.86)	0.008	0.49 (0.28-0.85)	0.011
Prior CVD	2.00 (1.31-3.04)	0.001	2.43 (1.45-4.08)	0.001
Diabetes mellitus	1.52 (1.002-2.30)	0.049	-	-
Chronic kidney disease	-	-	1.65 (0.93-2.93)	0.089

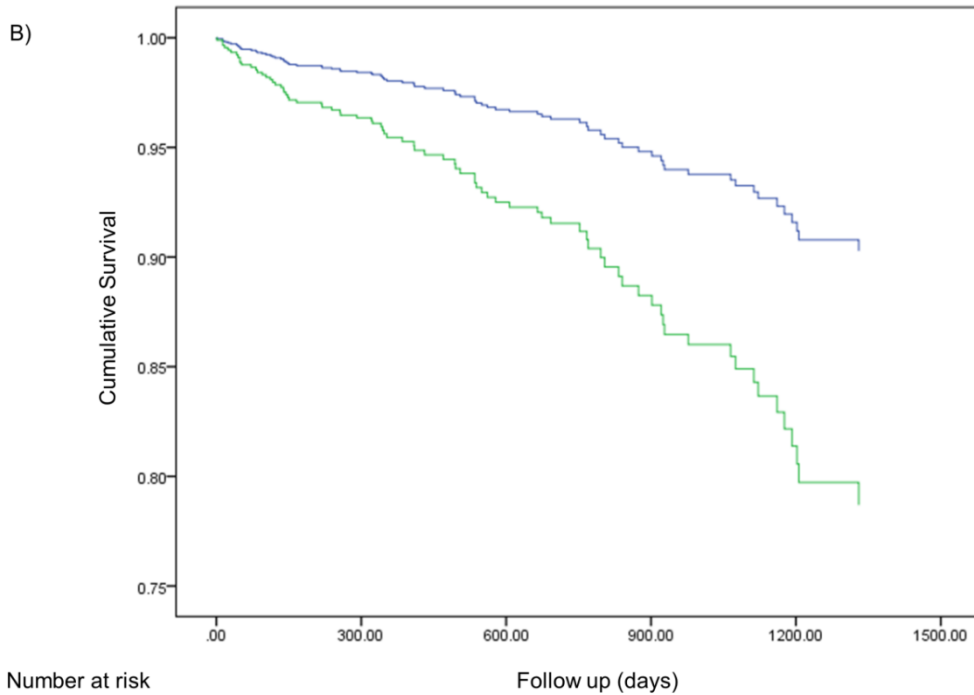
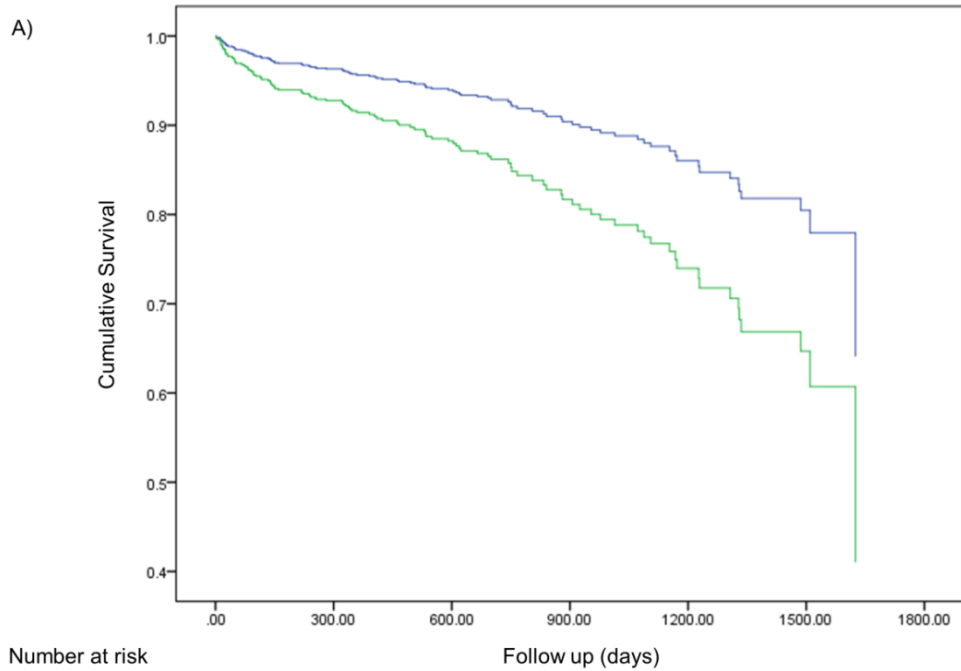
Covariates with  $p < 0.1$  in univariate Cox analysis were entered into multivariable Cox regression modelling using the forwards likelihood ratio method to select the covariate model (variables not in bold font). After these time to MACE or ACM covariate models were selected, the suboptimal statin therapy variable was entered into both models to produce the presented results.

The adjusted survival curves, stratified by suboptimal statin status, are illustrated in Figure 2.3, and demonstrate early separation of hazard risk after V2.

### 2.3.3 Sub-group analyses

The subgroup of suboptimal statin users that had discontinued/were non-adherent ( $n=95$ ) had significantly increased risks of MACE (HR 2.74, 95% CI 1.49-5.04,  $p=0.001$ ) and ACM (HR 3.50, 95% CI 1.69-7.23,  $p=0.001$ ), compared to constant statin users (Table 2.8). The smaller subgroup of patients with reduced statin dose/switched statin ( $n=61$ ), did not have significantly increased risks of MACE ( $p=0.24$ ) or ACM ( $p=0.22$ ) (Table 2.8).

**Figure 2.3 Cumulative survival curves**



The cumulative survival curves compared suboptimal statin (green) and constant statin use (blue) group survival free from; **A)** major adverse cardiovascular events (MACE) and; **B)** all-cause mortality (ACM). Survival curves plotted until last event occurrence.

### 2.3.4 Sensitivity Analyses

The complete cases cohort consisted of 724 patients with complete data available. In this complete cases cohort, muscular symptoms, female sex and beta blocker use remained associated with suboptimal statin occurrence (sensitivity analysis A, shown in Table 2.7), in line with the main study findings.

**Table 2.7 Factors associated with an increased risk of suboptimal statin occurrence in multivariable logistic regression using only participants with complete data available (Sensitivity Analysis A).**

Risk factor	Multivariable adjusted analysis <sup>1</sup>	
	OR (95% CI)	p-value
Muscular symptoms	4.89 (1.38-17.28)	0.014
Sex (F vs M)	1.66 (1.02-2.70)	0.040
Beta blocker at V2	0.45 (0.26-0.78)	0.004

<sup>1</sup> = Variables with p<0.1 in univariate analysis using the complete case cohort (muscular symptoms, CYP3A4-inhibitors, diabetes mellitus, sex, smoking, P2Y<sub>12</sub> inhibitor use and beta blocker use at V2) were entered into multivariable logistic regression modelling using the forwards likelihood ratio method to select the final presented model.

Table 2.8 below is a summary table of results and importantly shows that suboptimal statin use was robustly associated with risks of MACE and ACM irrespective of the adherence definition used (sensitivity analysis B), the missing data imputations (sensitivity analyses C1-C4), the variables that did not meet the proportional hazards assumption (P2Y<sub>12</sub> use for MACE, and sex for ACM) (sensitivity analyses D1, D2), and after inclusion of all variables associated with suboptimal statin occurrence (sensitivity analyses E1, E2).

**Table 2.8 Summary table of all analyses of the multivariable adjusted risks of MACE, or ACM, associated with suboptimal statin users compared to constant statin users**

Analysis	Description	MACE		ACM	
		Risk Estimate (95% CI)	p-value	Risk Estimate (95% CI)	p-value
Main Analysis	Suboptimal statin users (n=156, 15.5%)	HR 2.10 (1.25-3.53) <sup>1</sup>	0.005	HR 2.46 (1.38-4.39) <sup>2</sup>	0.003
	Statin discontinuation/non-adherence (n=95, 10.1%)	HR 2.74 (1.49-5.04) <sup>3</sup>	0.001	HR 3.50 (1.69-7.23) <sup>4</sup>	0.001
	Statin dose reduction/switch (n=61, 6.7%)	HR 1.55 (0.75-3.20) <sup>5</sup>	0.24	HR 1.71 (0.72-4.04) <sup>6</sup>	0.22
Sen analysis B	Expanded statin non-adherence definition (n=272,27.1%)	HR 1.75 (1.17-2.63) <sup>7</sup>	0.007	HR 1.75 (1.06-2.89) <sup>8</sup>	0.030
Sen analysis C: Participants with complete data only. Constant statin users, n=635, versus:					
C1	All suboptimal statin cases (n=89, 12.3%)	HR 2.60 (1.58-4.28) <sup>9</sup>	<0.001	HR 3.41 (1.91-6.06) <sup>10</sup>	<0.001
C2	Statin discontinuation/non-adherence (n=51)	HR 3.94 (2.07-7.48) <sup>11</sup>	<0.001	HR 5.06 (2.35-10.90) <sup>12</sup>	<0.001
C3	Statin dose reduction/ switch (n=38)	HR 1.84 (0.91-3.71) <sup>13</sup>	0.090	HR 2.41 (1.07-5.40) <sup>14</sup>	0.034
C4	Expanded statin non-adherence definition(n=178)	HR 1.83 (1.19-2.84) <sup>15</sup>	0.006	HR 1.85 (1.09-3.12) <sup>16</sup>	0.022
Sen analyses D, E and F: suboptimal statin users, n=156, versus constant statin users, n=849					
Sen analysis D: Covariates that did not meet the proportional hazards assumption during full follow up additionally included:					
D1	Logistic regression	OR 2.61 (1.50-4.54) <sup>17</sup>	0.001	OR 3.18 (1.68-6.01) <sup>18</sup>	<0.001
D2	Censor at 11 months	HR 3.54 (1.90-6.61) <sup>19</sup>	<0.001	HR 5.11 (2.32-11.25) <sup>20</sup>	<0.001
Sen analysis E: variables that differed significantly between suboptimal and constant statin users at visit 2 additionally included:					
E1	Logistic regression	OR 2.65 (1.50-4.65) <sup>21</sup>	0.001	OR 3.17 (1.67-6.04) <sup>22</sup>	<0.001
E2	Censor at 11 months	HR 3.49 (1.85-6.58) <sup>23</sup>	<0.001	HR 5.07 (2.26-11.40) <sup>24</sup>	<0.001
Sen analysis F: Healthy user assessment variable additionally included:					
F1	logistic regression	OR 2.53 (1.46-4.37) <sup>25</sup>	0.001	OR 3.39 (1.80-6.39) <sup>26</sup>	<0.001
F2	Censor at 11 months	HR 3.55 (1.91-6.60) <sup>27</sup>	<0.001	HR 5.52 (2.56-11.89) <sup>28</sup>	<0.001

HR = hazard ratio; OR = odds ratio.

For each analysis (main, subgroup and sensitivity analyses for both MACE and ACM), a multivariable covariate model was fitted before the suboptimal statin variable was added. Covariates with univariate  $p < 0.1$  were entered into multivariable Cox proportional hazards modelling, with the final multivariable covariate model for each analysis chosen by forwards stepwise (likelihood ratio) selection. All analyses adjusted for age  $\geq 75$  and prior CVD. All analyses adjusted for treatment with PCI/CABG except analyses 20, 24 and 28. All analyses adjusted for NYHA functional class at V2 except analysis 12. Other covariates adjusted for in specific analyses were: diabetes mellitus (analyses 1, 6, 7, 9-16, 19, 23, 27); chronic kidney disease (analyses 2, 3, 4, 8, 12, 17, 18, 21, 22, 25, 26); P2Y<sub>12</sub> inhibitor at V2 (analyses 17, 19, 21-24); sex (analyses 18, 20, 21-24); aspirin at V2 (analyses 18, 22, 26); beta blocker at V2 (analyses 21-24); muscular symptoms (analyses 21-24); healthy user assessment (analyses 25-28).

Sensitivity analyses F1 and F2 included the healthy user variable; importantly, suboptimal statin use remained a statistically significant predictor of both MACE and ACM in these sensitivity analyses despite the healthy user variable (Table 2.8). The healthy user variable itself was not associated with MACE (Table 2.9, Table 2.10). Although the healthy user variable was nominally associated with time to ACM up to 11 months after V2 (Table 2.10), it was not significant after correction for multiple testing (p-value threshold 0.025) (Table 2.10). Furthermore, it was not significantly associated with ACM risk in multivariable logistic regression analysis which included all recorded endpoints (Table 2.9). Therefore overall, no substantive healthy user effect was observed.

**Table 2.9 Assessment of potential healthy user bias on the risk of MACE or ACM associated with suboptimal statin use using logistic regression analysis (Sensitivity Analysis F1)**

Variable	MACE		ACM	
	OR (95% CI)	p-value	OR (95% CI)	p-value
<b>Univariate analysis:</b>				
Healthy User Assessment <sup>1</sup>	1.08 (0.66-1.78)	0.76	1.60 (0.94-2.73)	0.083
<b>Multivariable adjusted analysis<sup>2</sup>:</b>				
<b>Suboptimal Statin therapy</b>	<b>2.53 (1.46-4.37)</b>	<b>0.001</b>	<b>3.39 (1.80-6.39)</b>	<b>&lt;0.001</b>
<b>Healthy User Assessment<sup>1</sup></b>	<b>1.01 (0.58-1.74)</b>	<b>0.99</b>	<b>1.59 (0.85-2.98)</b>	<b>0.15</b>
Age ≥ 75	2.38 (1.51-3.76)	<0.001	3.62 (2.10-6.26)	<0.001
NYHA	1.78 (1.32-2.39)	<0.001	1.89 (1.29-2.78)	0.001
Treatment with PCI/CABG	0.57 (0.36-0.91)	0.018	0.45 (0.24-0.83)	0.011
Prior CVD	2.55 (1.63-3.97)	<0.001	2.97 (1.68-5.24)	<0.001
Chronic kidney disease	2.00 (1.05-3.83)	0.036	2.92 (1.44-5.95)	0.003
Aspirin at V2	-	-	0.41 (0.20-0.83)	0.014

<sup>1</sup> = Healthy user assessment is a variable comparing patients with constant proton pump inhibitor (PPI) use, defined as not on a PPI or on the same PPI and dose at both baseline and V2, compared to PPI changers, defined as patients that started, stopped or switched PPI or increased or decreased their PPI dose. <sup>2</sup> = For the multivariable logistic regression MACE/ACM analyses, covariates with univariate p<0.1 were entered into multivariable logistic regression modelling using the forwards likelihood ratio method to select the covariate model (variables not in bold font). After these MACE and ACM logistic regression covariate models were selected, the variables in bold were entered into each model to produce the presented results.

**Table 2.10 Assessment of potential healthy user bias on the risks of time to MACE or ACM associated with suboptimal statin with follow up censored at 11 months after Visit 2 (Sensitivity Analysis F2)**

Variable	Time to MACE		Time to ACM	
	HR (95% CI)	p-value	HR (95% CI)	p-value
<b>Univariate analysis:</b>				
Healthy User Assessment	1.39 (0.76-2.54)	0.28	2.25 (1.09-4.65)	0.029
<b>Multivariable adjusted analysis:</b>				
<b>Healthy User Assessment</b>	<b>1.42 (0.77-2.61)</b>	<b>0.27</b>	<b>2.24 (1.05-4.77)</b>	<b>0.037</b>
<b>Suboptimal Statin therapy</b>	<b>3.55 (1.91-6.60)</b>	<b>&lt;0.001</b>	<b>5.52 (2.56-11.89)</b>	<b>&lt;0.001</b>
Age ≥ 75	2.03 (1.17-3.50)	0.011	3.02 (1.46-6.27)	0.003
NYHA	1.46 (0.99-2.14)	0.054	2.09 (1.28-3.43)	0.004
Treatment with PCI/CABG	0.55 (0.31-0.99)	0.048	-	-
Prior CVD	2.23 (1.26-3.95)	0.006	2.78 (1.29-6.01)	0.009
Diabetes mellitus	1.73 (0.997-2.99)	0.051	-	-

## 2.4 Discussion

The main findings of this study are firstly, by a median of one month after admission for NSTEMI-ACS in patients discharged on high potency statin therapy, ~15% have suboptimal statin utilisation. Expanding the non-adherence definition increased this to 27% (Table 2.8). Secondly, suboptimal statin occurrence was associated with muscular symptoms, female sex, and reduced use of beta blockers and P2Y<sub>12</sub> inhibitors. Thirdly, suboptimal statin use was associated with increased adjusted risks of times to both MACE and ACM, although this was largely attributable to statin discontinuation/non-adherence early after NSTEMI-ACS rather than statin dose reduction/statin switching.

This study is novel because it considered all components of attenuated statin therapy (discontinuation, non-adherence, switching and dose reduction), both collectively and in subgroups. To date, the majority of adherence studies have assessed medication availability (e.g. proportion of days covered) via electronic data sources (Rasmussen *et al.*, 2007; Ho *et al.*, 2008; Wei *et al.*, 2008). Although this approach allows assessment of average adherence over time, it is difficult for healthcare professionals to easily measure and act upon in practice. Importantly, the pragmatic approach used in this study highlights the importance of assessing statin usage early after hospital discharge in CVD

secondary prevention patients. Furthermore, the assessment of statin utilisation used in this study is relatively straightforward and so potentially actionable.

Overall, there were few differences at V2 between suboptimal and constant statin users. However interestingly, females (Rasmussen *et al.*, 2007; Ho *et al.*, 2008; Tuppin *et al.*, 2010; Wei *et al.*, 2013) and a lower rate of beta blocker (Rasmussen *et al.*, 2007; Blackburn *et al.*, 2005a) and antiplatelet (McGinnis *et al.*, 2009) drug use have all previously been associated with poorer statin adherence. In this study, suboptimal statin users were more likely to have not been prescribed P2Y<sub>12</sub> therapy at hospital discharge and to have stopped the beta blocker they were discharged on (data not shown). This study also found that muscular symptoms were a risk factor for suboptimal statin use. Very few other statin utilisation studies have included potential adverse events, although a cross-sectional internet-based survey previously determined that muscular symptoms are reported more frequently in patients that have discontinued, switched statin or are non-adherent, compared to non-switching statin adherent participants (Wei *et al.*, 2013). Overall, there was no evidence that these differences altered the multivariable increased risks of time to MACE or ACM associated with suboptimal statin use (Table 2.8).

Statins are associated with increased myotoxicity, incident diabetes mellitus and probably haemorrhagic stroke (Collins *et al.*, 2016). Statin-associated muscular symptoms are reported in ~1.5-3% of statin users in RCTs (Sathasivam and Lecky, 2008) and in ~7-29% of patients in observational studies (Stroes *et al.*, 2015). However, whilst rare statin-induced severe myopathy/rhabdomyolysis is incontrovertible, the contribution of statins to milder muscle symptoms remains controversial. One informative estimate for the extent of muscular symptoms *attributable* to ATV 80mg daily therapy is ~5% (Parker *et al.*, 2013). The reported rate of bothersome muscular symptoms reported in our observational study was low (~1.2%) (Table 2.3).

This may be a reflection of muscular symptoms not being explicitly asked about, and/or because patients who experienced muscular symptoms shortly after discharge had amended their statin therapy by V2, with potential symptomatic resolution. It should be noted that phenotype verification of the reported SAM (e.g. by statin de-challenge and re-challenge) was not possible. Therefore, it is possible that causes other than statin pharmacological activity contributed to the reported muscle symptoms, including different aetiologies of muscle symptoms (e.g. exercise) and the nocebo effect. Nevertheless it was predictable that muscle symptoms, irrespective of their cause, would lead to suboptimal statin utilisation, because many patients and physicians are likely aware of the link between statin therapy and muscle toxicity.

The largest type of suboptimal statin users in this study was statin non-adherent patients. The aetiology of statin non-adherence is multifactorial and incompletely understood; predictors beyond those identified in this study include age, low income and increased non-cardiovascular medications (Mann *et al.*, 2010). Health beliefs and knowledge affect both perceptions of need for a treatment, and counteracting perceptions of potential treatment adverse effects, are influenced by factors such as patient satisfaction with physician treatment explanations, and likely also modulate non-adherence (Berghlund *et al.*, 2013). Therefore, irrespective of the exact underlying aetiology of mild muscular symptoms, the attribution of these symptoms to statin therapy by a patient will potentially reduce statin utilisation.

Another potential reason for the statin discontinuation/dose reductions/statin switching observed in this study early after an NSTEMI-ACS is a communication breakdown leading to the high potency statin hospital discharge prescription not being transferred and incorporated into a patient's repeat outpatient prescription drug list. Transfer of medical information from secondary to primary care is often incomplete and untimely (Gobel *et al.*, 2012; Viktil *et al.*,

2012), although further research is required to evaluate the extent of its potential impact on early post-ACS suboptimal statin therapy.

Previous secondary prevention cohorts have reported elevated risk estimates for statin non-adherence or discontinuation/minimal persistence/no statin use of 1.01-5.26 for MACE and 1.25-5.00 for mortality, with the majority reporting statistically significant results (De Vera *et al.*, 2014). Our study results of increased adjusted risks of time to MACE or ACM associated with both suboptimal statin use and the statin non-adherence/discontinuation subgroup in particular are in keeping with these findings. This emphasises the generalizability of these clinically relevant findings across secondary prevention populations, settings and study designs.

In this study of NSTEMI-ACS patients, the statin dose reduction/switching statin subgroup was not significantly associated with increased risks of time to MACE or ACM. One other prospective study has investigated statin dose reduction/switching following ACS, but included both NSTEMI-ACS and ST-elevation ACS patients, and reported a significantly increased risk for adverse clinical outcomes (HR 2.7, 95% CI 1.7-5.1) (Colivicchi *et al.*, 2011). Our smaller number of dose reduction/switching cases (n=61) may have accounted for this subgroup only showing a non-significant trend for increased risk. Two other observational studies have investigated the influence of switching from ATV to SVT (Phillips *et al.*, 2007; Jacobson *et al.*, 2013) on cardiovascular events, using mixed primary/secondary prevention populations identified using electronic healthcare databases. The UK-based study found a modestly increased cardiovascular event risk (HR 1.30, 95% CI 1.02-1.64) (Phillips *et al.*, 2007), whilst the US-based study found no association (Jacobson *et al.*, 2013). However in both of these studies the majority of patients were on ATV  $\leq 20$ mg/day, and it has been noted that the proportion of switches from ATV to a lower rather than equivalently potent SVT regimen increases as the initial ATV dose increases (Jacobson *et al.*, 2013). This is particularly relevant in post-ACS

patients, as practically all switches from ATV 80mg/day are to another statin of lower equivalent potency. Overall, persistent adherence to high potency statin therapy after an ACS appears optimal; however, if necessary, reducing the dose or switching statin appears preferable to statin non-adherence or complete discontinuation.

Recently, several interventions have been proposed that attempt to reduce non-adherence/discontinuation and improve statin therapeutic effectiveness, including improving CVD and statin literacy, co-payment reduction, using fixed-dose 'polypill' combinations and behaviour-modification interventions (Phan *et al.*, 2014). For example, brief pharmacist-led face-to-face counselling sessions have been shown to improve statin adherence (Taitel *et al.*, 2012). There is also increasing interest in utilising mobile technology applications (apps) to remind patients to take their medications, and patients are being involved in medication-related app development (DiDonato *et al.*, 2015). It is thus plausible that an intervention based on reminders (e.g. apps and/or posted letters) and face-to-face contact could be targeted to patients early after a CVD event to both screen for and address suboptimal statin utilisation, although further research is required.

This study has limitations. It is a *post hoc* assessment of the PhACS study. The exact reasons for statin prescription changes and the cause(s) for patient non-adherence were not recorded. As stated above, the exact cause of patient reported muscle symptoms is unverified. The data are observational and therefore we cannot confirm causality due to the potential for confounding influences by unmeasured variables, such as cardiac rehabilitation attendance. Although we cannot definitively exclude any healthy user effect, our assessment of PPI utilisation (Table 2.8, Table 2.9, Table 2.10) is in keeping with the lack of healthy user effect reported in other statin utilisation studies (Rasmussen *et al.*, 2007; Ho *et al.*, 2008; Daskalopoulou *et al.*, 2008), and so makes a prominent contribution of this type of influence unlikely. It is acknowledged that both the

assessment of statin adherence at a single time point and basing the primary assessment on the number of pills missed over the preceding week will limit detection of sporadic non-adherence (Svarstad *et al.*, 1999). However, the expanded non-adherence definition (Table 2.8) includes all components of the BMQ and the BMQ recall screen (enquiring about how hard the patient finds it to remember to take all the pills) has a sensitivity of 90% for sporadic non-adherence, albeit with a reduced specificity of 80% (Svarstad *et al.*, 1999). The assessment of statin utilisation at one month is also unlikely long enough to capture full stabilisation of drug use. However, median statin discontinuation in secondary prevention appears to occur at 30-37 days after discharge (Colivicchi *et al.*, 2011; Colivicchi *et al.*, 2007), and our approach does not preclude follow up adherence assessments. Overall, this investigation used a prospective multicentre study with event validation rather than electronic diagnostic codes, and the several sensitivity analyses confer robustness to the main findings.

#### **2.4.1 Conclusion**

In conclusion, patients with an NSTEMI-ACS are at high risk of subsequent MACE and ACM. Following discharge on high potency statin therapy, the intensity of statin therapy is already reduced for a sizeable proportion of patients by one month back in the community, and self-reported muscular symptoms appear to increase the risk for suboptimal statin utilisation. Early statin discontinuation/non-adherence correlates with increased risks of subsequent MACE and ACM. Physicians, pharmacists and cardiac rehabilitation programmes are encouraged to discuss statin therapy with ACS patients early after discharge, reaffirm the benefits of statins, and explore barriers to their effective use in order to maintain and enhance statin utilisation and so potentially improve post NSTEMI-ACS outcomes.

## **Chapter 3 Development and validation of a novel dried murine blood spot high performance liquid chromatography tandem mass spectrometry assay for the quantification of rosuvastatin, atorvastatin and atorvastatin metabolites**

### **3.1 Introduction**

They are hypolipidaemic agents indicated in primary and secondary CVD prevention (Roden *et al.*, 2011). Although generally tolerated, statins are associated with a range of adverse events including SAM, which is considered a dose- and exposure-related ADR (Golomb and Evans, 2008; Alfirevic *et al.*, 2014). Therefore, understanding the factors that affect statin PK is clinically relevant, which requires simple to use quantitative methods.

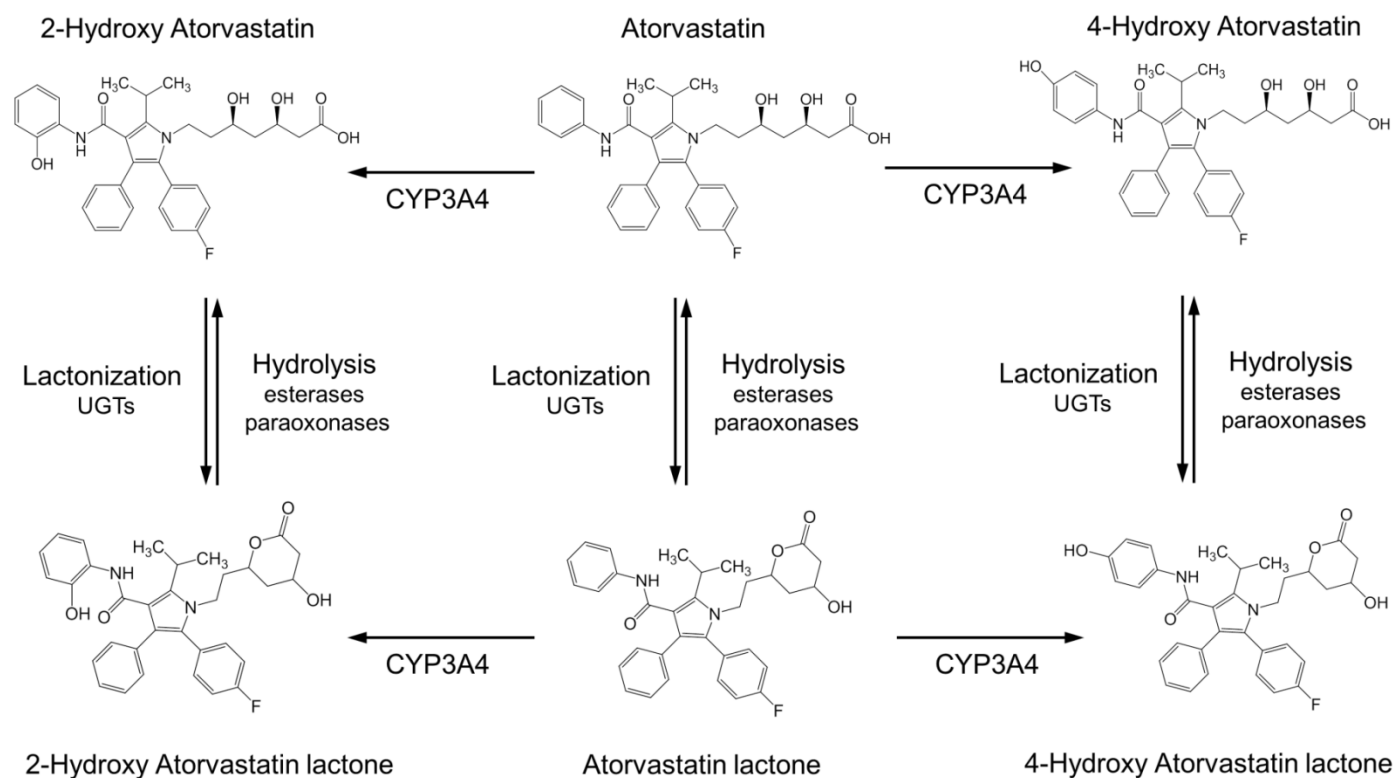
Three statins were considered: ATV, RVT and SVT (Figure 3.1, Figure 3.2). Briefly, ATV (Lipitor) and RVT (Crestor) are administered as calcium salts of their active carboxylic acid form (Pfizer Inc, 2015; AstraZeneca, 2009), and SVT (Zocor) as a therapeutically inactive L. ATV is a CYP3A substrate and can be hydroxylated at the 2- or 4- positions (Jacobsen *et al.*, 2000); ATV is also a substrate for UGT-mediated lactonization (Schirris *et al.*, 2015b). Similarly, both 2-OH ATV and 4-OH ATV can undergo lactonization. ATV L has a higher affinity for CYP3A4 than ATV and inhibits CYP3A ATV metabolism; the primary ATV metabolism pathway is thus postulated to be lactonization followed by hydroxylation (Jacobsen *et al.*, 2000). All three L metabolites (ATV L, 2-OH ATV L, 4-OH ATV L) can be hydrolysed both non-enzymatically and via plasma esterases and paraoxonases to corresponding acids (Riedmaier *et al.*, 2011; Pasanen *et al.*, 2007) (Figure 3.1).

RVT is the most potent statin available for LDL-C reduction. Unlike ATV and SVT that are extensively metabolised, RVT undergoes little metabolism with ~75% of a dose recovered unchanged (Martin *et al.*, 2003); the minor RVT

metabolites, RVT-5S-L and active N-desmethyl RVT (Martin *et al.*, 2003), were not considered further here. SVT is the most lipophilic, followed by ATV and then RVT. SVT is rapidly hydrolysed to its major metabolite, active SVT  $\beta$ -hydroxy acid (SVT-A), by carboxylesterase (CES) enzymes in plasma, liver and intestinal mucosa (Vree *et al.*, 2003). SVT and SVT-A are CYP3A substrates and are converted to a range of metabolites including 3-OH, 3'5'-dihydrodiol and 6'-exomethylene derivatives (Prueksaritanont *et al.*, 1997; Prueksaritanont *et al.*, 2003). SVT-A does not appear to undergo UGT-mediated lactonization (Schirris *et al.*, 2015b) (Figure 3.2).

Although plasma-based statin assays have been developed (Pasanen *et al.*, 2007; Yang *et al.*, 2005), DBS technology is advantageous because it embraces the principles of reduction and refinement to animal experimentation and so is consistent with the aims of the UK NC3Rs programme (NC3Rs, 2016). A murine DBS assay for ATV alone has been used previously (Higgins *et al.*, 2014). Therefore, the aim of this study was to develop and validate a novel DBS-based assay for multiple statin analytes. Nine ATV/RVT/SVT analytes were investigated (ATV, 2-OH ATV, 4-OH ATV, ATV L, 2-OH ATV L, 4-OH ATV L, RVT, SVT, SVT-acid) and a single assay developed and validated for seven of the analytes (ATV analytes and RVT). Extensive hydrolysis of SVT to SVT-A was observed in murine blood, and so SVT analytes were not included in the assay.

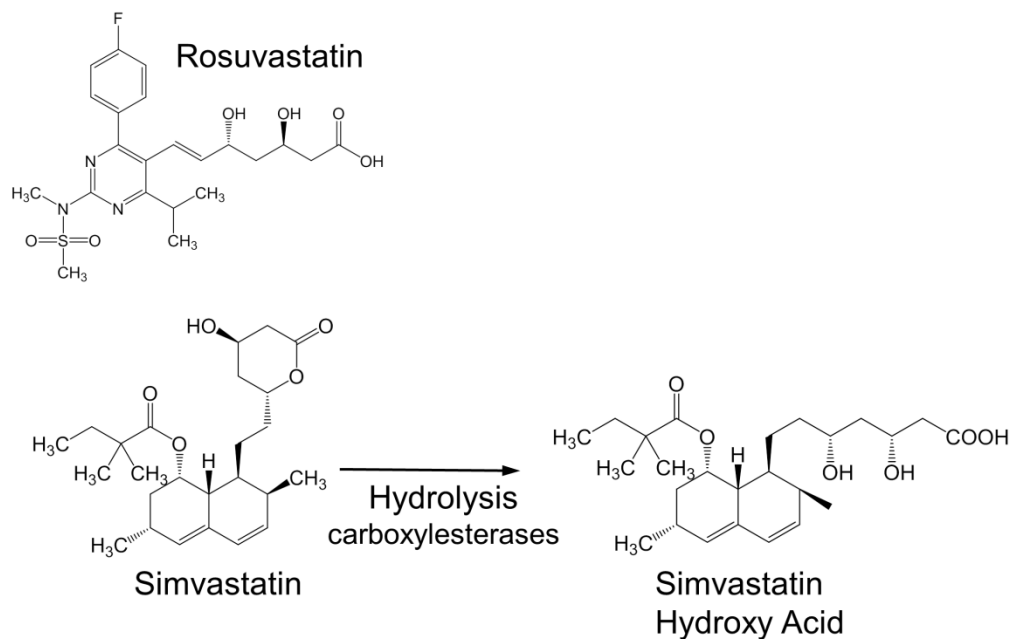
Figure 3.1 Structure and metabolism of atorvastatin analytes



Abbreviations: CYP3A4 = cytochrome P450 3A4; UGTs = uridine 5'-diphospho-glucuronosyltransferases.

ATV is administered as a calcium salt of the carboxylic acid form. ATV can undergo lactonization mediated by UGTs, and hydroxylation via CYP3A4, as well as CYP3A5 and to a lesser extent CYP2C8 (Jacobsen *et al.*, 2000). Parent ATV and its 2-OH and 4-OH hydroxylated metabolites are active in reducing circulating low-density lipoprotein cholesterol. The lactone metabolites of ATV do not lower circulating cholesterol levels, but can be hydrolysed back to their respective acid form both non-enzymatically and via plasma esterases and paraoxonases (Riedmaier *et al.*, 2011; Pasanen *et al.*, 2007).

**Figure 3.2 Structure and metabolism of measured rosuvastatin and simvastatin analytes**



RVT is administered in the therapeutically active carboxylic acid form, whilst SVT is administered as a lactone prodrug. RVT undergoes relatively little metabolism; its minor metabolites are RVT-5S-L and active N-desmethyl RVT, which were not measured in this assay. SVT is rapidly hydrolysed to therapeutically active SVT hydroxy acid (SVT-A) by carboxylesterases in plasma, liver and intestinal mucosa (Vree *et al.*, 2003). SVT-A does not appear to undergo UGT-mediated lactonization (Schirris *et al.*, 2015b). Both SVT and SVT-A are CYP3A substrates, leading to a range of downstream metabolites including 3-OH, 3'5'-dihydrodiol and 6'-exomethylene derivatives, which were not measured in this assay.

## 3.2 Methods

### 3.2.1 Chemicals and reagents

All compounds (analytes and internal standards) were obtained from Toronto Research Chemicals (Toronto, Canada) (Table 3.1). Acetonitrile (Fisher Scientific), water (Fisher Scientific) and all reagents were LC-MS grade unless otherwise stated.

Fresh blood anticoagulated with K3 ethylenediaminetetraacetic acid (EDTA) or lithium heparin (LiHep) from male C57BL/6 mice was used (Charles River, Margate, UK).

**Table 3.1 Formula and purity of compounds used**

Analyte			Internal standard		
Structure	Formula	Purity (%)	Identity	Formula	Purity (%)
Rosuvastatin Calcium	C <sub>22</sub> H <sub>27</sub> FN <sub>3</sub> O <sub>6</sub> S.1/2Ca	98.0	Rosuvastatin-d6 Sodium	C <sub>22</sub> H <sub>21</sub> D <sub>6</sub> FN <sub>3</sub> NaO <sub>6</sub> S	C: 96.0 I: 99.8
Atorvastatin Calcium	C <sub>33</sub> H <sub>34</sub> FN <sub>2</sub> O <sub>5</sub> .1/2Ca	96.0	Atorvastatin-d5 Sodium	C <sub>33</sub> H <sub>29</sub> D <sub>5</sub> FN <sub>2</sub> NaO <sub>5</sub>	C: 98.0 I: 99
2-Hydroxy Atorvastatin Calcium	C <sub>33</sub> H <sub>34</sub> FN <sub>2</sub> O <sub>6</sub> .1/2Ca	96.0	2-Hydroxy Atorvastatin-d5 Disodium	C <sub>33</sub> H <sub>28</sub> D <sub>5</sub> FN <sub>2</sub> Na <sub>2</sub> O <sub>6</sub>	C: 96.0 I: 98.6
4-Hydroxy Atorvastatin Calcium	C <sub>33</sub> H <sub>34</sub> FN <sub>2</sub> O <sub>6</sub> .1/2Ca	98.0	4-Hydroxy Atorvastatin-d5 Calcium	C <sub>33</sub> H <sub>29</sub> D <sub>5</sub> FN <sub>2</sub> O <sub>6</sub> .1/2Ca	C: 94.0 I: 99.3
Atorvastatin Lactone	C <sub>33</sub> H <sub>33</sub> FN <sub>2</sub> O <sub>4</sub>	98.0	Atorvastatin-d5 Lactone	C <sub>33</sub> H <sub>28</sub> D <sub>5</sub> FN <sub>2</sub> O <sub>4</sub>	C: 98.0 I: 98.9
2-Hydroxy Atorvastatin Lactone	C <sub>33</sub> H <sub>33</sub> FN <sub>2</sub> O <sub>5</sub>	98.0	2-Hydroxy Atorvastatin-d5 Lactone	C <sub>33</sub> H <sub>28</sub> D <sub>5</sub> FN <sub>2</sub> O <sub>5</sub>	C: 98.0 I: 99.1
4-Hydroxy Atorvastatin Lactone	C <sub>33</sub> H <sub>33</sub> FN <sub>2</sub> O <sub>5</sub>	97.0	4-Hydroxy Atorvastatin-d5 Lactone	C <sub>33</sub> H <sub>28</sub> D <sub>5</sub> FN <sub>2</sub> O <sub>5</sub>	C: 98.0 I: 98.3
Simvastatin	C <sub>25</sub> H <sub>38</sub> O <sub>5</sub>	98.0	Simvastatin-d6	C <sub>25</sub> H <sub>32</sub> D <sub>6</sub> O <sub>5</sub>	C: 98.0 I: 98.5
Simvastatin hydroxy acid ammonium	C <sub>25</sub> H <sub>43</sub> NO <sub>6</sub>	98.0	Simvastatin-d6 hydroxy acid ammonium	C <sub>25</sub> H <sub>37</sub> D <sub>6</sub> NO <sub>6</sub>	C: 98.0 I: 99.9

Abbreviations: C = chemical; I = isotopic

Stock solutions were prepared by dissolving each compound in dimethyl sulfoxide (DMSO, Sigma-Aldrich) or methanol (Fisher Scientific, Loughborough, UK) and stored at -20°C (Table 3.2).

**Table 3.2 Stock solution solvents and concentrations**

Analyte			Internal standard		
Identity	Solvent	Conc (mM)	Identity	Solvent	Conc (mM)
RVT	DMSO	20	RVT-d6	MeOH	1
ATV	DMSO	20	ATV-d5	MeOH	1
2-OH ATV	DMSO	1	2-OH ATV-d5	MeOH	1
4-OH ATV	DMSO	1	4-OH ATV-d5	DMSO	1
ATV L	DMSO	10	ATV-d5 L	DMSO	1
2-OH ATV L	DMSO	1	2-OH ATV-d5 L	DMSO	1
4-OH ATV L	DMSO	1	4-OH ATV-d5 L	DMSO	1
SVT	DMSO	24	SVT-d6	DMSO	1
SVT-A	DMSO	20	SVT-d6-A	DMSO	1

All stock solutions stored at -20°C

Composite working solutions of RVT plus ATV (RVT/ATV parents), 2-OH ATV and 4-OH ATV (ATV acid metabolites), and ATV L, 2-OH ATV L and 4-OH ATV L (ATV Ls) at three (ATV acids and ATV Ls) or four (RVT/ATV) concentrations were prepared from the stock solutions in 50:50 acetonitrile-water (v/v) (Table 3.3). A composite working solution of all ATV/RVT internal standards at 0.05µg/mL (RVT-d6, ATV-d5, 2-OH ATV-d5, 4-OH ATV-d5, ATV-d5 L, 2-OH ATV-d5 L, 4-OH ATV-d5 L) was similarly prepared from the internal standard stock solutions in 50:50 acetonitrile-water (v/v) (Table 3.3).

Separate 1µg/mL working solutions of SVT and SVT-A in 50:50 acetonitrile-water (v/v), and a single internal standard solution containing both STV-d6 and STV-d6-A at 0.13µg/mL in 100% acetonitrile, was prepared. All working solutions were stored at 4°C.

All pipetting was carried out using positive displacement pipettes (microman pipettes with capillary pistons, Gilson Scientific).

**Table 3.3 Working solution concentrations**

Working solution	RVT/ATV ( $\mu\text{g/mL}$ )				SVT/SVT-A ( $\mu\text{g/mL}$ )		
	RVT/AVT <sup>1</sup>	ATV acid metabolites <sup>2</sup>	ATV lactone metabolites <sup>3</sup>	Internal stds <sup>4</sup>	SVT	SVT-A	Internal stds <sup>5</sup>
XLOW	0.1	-	-	0.05	1.0	1.0	0.13
LOW	0.5	0.2	0.2				
MID	10	2	2				
HIGH	100	20	20				

The working solutions contained the following compounds; <sup>1</sup> = RVT and ATV; <sup>2</sup> = 2-OH ATV and 4-OH ATV; <sup>3</sup> = ATV L, 2-OH ATV L and 4-OH ATV L; <sup>4</sup> = RVT-d6, ATV-d5, 2-OH ATV-d5, 4-OH ATV-d5, ATV-d5 L, 2-OH ATV-d5 L and 4-OH ATV-d5 L; <sup>5</sup> = STV-d6 and STV-d6-A. All working solutions were made in 50:50 acetonitrile-water (v/v) and stored at 4°C.

### 3.2.2 Simvastatin hydrolysis study

Due to a previous observation of no SVT detectable in rats *in vivo* due to hydrolysis (Shanmugam *et al.*, 2011), the proportion of SVT or SVT-A remaining overtime at room temperature or 37°C in EDTA or LiHep blood was tested. Briefly, 200 $\mu\text{L}$  blood was spiked with SVT or SVT-A 1 $\mu\text{g/mL}$  working solution to 10ng/mL. 20 $\mu\text{L}$  aliquots were taken at time 0.0, 0.5 and 2 hours. Proteins were precipitated with 100 $\mu\text{L}$  100% acetonitrile plus 10 $\mu\text{L}$  SVT/SVT-A internal standard, agitated (20 minutes, Vortex genie 2 on setting three, Scientific Industries), centrifuged (18.0g, 4°C, ten minutes, Eppendorf centrifuge 5810R), 50 $\mu\text{L}$  of supernatant diluted in 350 $\mu\text{L}$  50:50 acetonitrile-water, and each sample added to a 2mL 96-well polypropylene block (Thistle Scientific) for analysis.

### 3.2.3 Preparation of RVT/ATV Calibration Standards and Quality Controls

In all aspects of RVT/ATV assay development and validation, due to the potential for ATV acid-L interconversion, statin parents (RVT, ATV), ATV acid metabolites (2-OH ATV, 4-OH ATV), and L metabolites of ATV (ATV L, 2-OH ATV L, 4-OH ATV L) were handled separately. EDTA anticoagulated blood was used only, and samples were prepared on ice.

'Cassette' calibration lines were prepared consisting of a double blood blank (blood spotted onto card, no internal standard, no analyte), double card blank

(only DBS card, no blood, no analyte, no internal standard), a single blood blank (blood on card, internal standard), ten (RVT/ATV) or nine (ATV acid metabolites, and L metabolites of ATV) calibration standards, and a carryover card sample (DBS card only taken immediately after sampling the highest concentration calibration standard, no internal standard, no analyte, no blood). The cassette calibration standards (Table 3.4), and the low, medium and high quality control (QC) samples (Table 3.5), were prepared by spiking fresh pooled blood (50 or 100 $\mu$ L per calibration standard, 200 $\mu$ L per QC) with the appropriate composite working solution and volume; serial dilution was not used. The spiking regimens are in the Appendix (Table 8.2 and Table 8.3). Pooled blood was derived from a minimum of three individual mice, and the percentage of any composite working solution added to blood was limited to  $\leq 12.5\%$  (v/v) of the final volume to preserve the blood matrix.

**Table 3.4 Calibration standard concentrations**

Calibration standard	RVT/ATV (ng/mL)	ATV acid metabolites <sup>1</sup> (ng/mL)	ATV lactones <sup>2</sup> (ng/mL)
1	5	5	5
2	12.5	12.5	12.5
3	25	25	25
4	100	50	50
5	250	100	100
6	500	400	400
7	2,000	800	800
8	4,000	1,500	1,500
9	8,000	2,500	2,500
10	10,000	-	-

<sup>1</sup> = 2-OH ATV and 4-OH ATV; <sup>2</sup> = ATV L, 2-OH ATV L and 4-OH ATV L

**Table 3.5 Quality control concentrations**

Quality control	RVT/ATV (ng/mL)	ATV acid metabolites <sup>1</sup> (ng/mL)	ATV lactones <sup>2</sup> (ng/mL)
Low	15	15	15
Medium	500	75	75
High	7,500	1,000	1,000

<sup>1</sup> = 2-OH ATV and 4-OH ATV; <sup>2</sup> = ATV L, 2-OH ATV L and 4-OH ATV L

After spiking, each sample was pipetted onto a Whatman FTA™ Elute Micro Card (GE Healthcare Life Sciences, hereafter referred to as 'FTA Elute card') in 35µL spots, left to air dry for at least one hour, and then the FTA Elute cards were stored overnight at room temperature in a sealed Whatman multi-barrier pouch (3.75" x 3", GE Healthcare) containing desiccant (MiniPax sorbent packets, Multisorb Technologies). The following day, a 3mm circle from the edge of the main spot interior but avoiding the 'halo' was punched out from each DBS using a Harris Uni-Core 3mm puncher (Sigma-Aldrich) on a Harris cutting map (Sigma-Aldrich), and transferred to a 2mL 96-well polypropylene block (Thistle Scientific). Two extractions were performed using *tert*-butyl methyl ether (TBME, Sigma-Aldrich) containing 2.4% 50:50 acetonitrile-water. For the first extraction, 10µL composite internal standard working solution (for single blank, calibration standards, QC samples) or 10µL 50:50 acetonitrile-water (double blank, carryover samples) was first added to each sample, 400µL TBME added, the block agitated for ten minutes (Vortex genie 2 on setting three), centrifuged (18.0g, 4°C, five minutes, Eppendorf centrifuge 5810R), and the supernatant transferred to a new 0.5mL 96-well polypropylene plate (Agilent Technologies). The second extraction was identical, except 10µL 50:50 acetonitrile-water was initially added to all samples (no additional internal standard added). The supernatant from the second extraction was combined with the first and evaporated to dryness in a vacuum centrifuge (30°C, 40 minutes, vacuum high vapour mode, Eppendorf Concentrator). The dried residues were reconstituted in 200µL of 50:50 acetonitrile-water, agitated (10 minutes), centrifuged (18.0g, 4°C, five minutes), and the supernatant transferred to a new 2mL 96-well block. Another 200µL of 50:50 acetonitrile-water was added (total volume ~400µL), and after a final centrifugation (10.0g, 4°C, ten minutes), the plate was transferred to the autosampler.

### 3.2.4 Comparison of extraction methods

The selected and validated RVT/ATV extraction method is described above. During assay development, additional extraction solvents and methods were tested (Table 3.6). The matrix effect (ME) and extraction recovery (ER)

associated with these different methods were compared for RVT and ATV (see Section 3.2.11 for details on ME and ER testing).

**Table 3.6 Extraction solvents and methods investigated for RVT and ATV**

Solvent	Extraction method
TBME with 2.4% 50:50 acetonitrile-water	Validated method as described in Section 3.2.3
100% TBME	As described in Section 3.2.3, except the two extractions were carried out in TBME only, and the internal standard was added after the second extraction
TBME + 12% water	As described in Section 3.2.3, except 50µL extra water was added to each extraction, and only the top 360µL of supernatant from each extraction was taken
Methanol	As described in Section 3.2.3, but replacing TBME with methanol
50:50 acetonitrile-water	One extraction only with 400µL solvent, 20 minutes agitation, 10 minutes centrifugation, and removal of 360µL supernatant.
50:50 acetonitrile-water + 0.1% formic acid	As per 50:50 acetonitrile-water method

TBME = *tert*-butyl methyl ether. Different extraction solvents and methods were investigated to determine the optimal off-line extraction for RVT and ATV. The validated method (Section 3.2.3) involved two extractions: in the first extraction, 10µL composite internal standard working solution (in 50:50 acetonitrile-water) and 400µL TBME were added to each sample; the samples were agitated (10 minutes), centrifuged (18.0g, 4°C, 5 minutes), and the supernatant retained. The second extraction was identical, except 10µL 50:50 acetonitrile-water was initially added to all samples (no additional internal standard added).

### 3.2.5 Liquid Chromatography Mass Spectrometric instrumentation and operating conditions

The HPLC separation was performed using an Agilent Technologies (Cheadle, UK) 1200 Series quaternary HPLC system. This comprised two binary G1312B pumps, a G1379B degasser and a G1316B column oven set at a standard temperature of 40°C. A 20µL aliquot of each sample was injected into the HPLC system via an HTS Pal autosampler (CTC Analytics, Zwingen, Switzerland) with a cooling facility set to 4°C. A 2.7µm Halo C18 column (50 x 2.1 mm ID, 90Å, Hichrom Limited, Reading, UK, part number: 92812-402) was housed in the column oven. The column was protected by an Upchurch pre-column filter (Sigma-Aldrich) fitted with a 0.5 µm frit. Gradient separation was accomplished using mobile phases containing water with 0.1% v/v formic acid (A) and acetonitrile with 0.1% v/v formic acid (B), at a flow-rate of 500µL/min. The

gradient is detailed in Table 3.7. The run time was 4.5 minutes. Collectively, the Halo C18 column at 40°C and selected eluent gradient achieved good chromatographic separation of all analytes and their corresponding internal standards. RVT and ATV analytes were analysed together in a single acquisition method; SVT analytes were analysed together in a separate acquisition method.

**Table 3.7 Mobile phase gradient used for chromatographic separation**

Step	Time(min)	A (%)	B (%)
0	0.00	75.0	25.0
1	0.50	75.0	25.0
2	2.50	25.0	75.0
3	3.00	25.0	75.0
4	3.10	5.0	95.0
5	3.60	5.0	95.0
6	3.70	75.0	25.0
7	4.50	75.0	25.0

Flow rate = 500µL/min. A = water + 0.1% formic acid; B = acetonitrile + 0.1% formic acid

The MS analysis was carried out using a Sciex triple quadrupole 6500 mass spectrometer (AB Sciex, Warrington, UK) in low mass mode with a Turbo V™ electrospray source operated in positive ionisation mode. An integrated 6-port Valco diverter valve was used so that only the eluate containing the peaks of interest entered the source. Detection and quantification were performed using MRM. The MRM transitions are listed in Table 3.8, with a dwell time of 9.0msec (RVT and ATV analytes) or 20msec (SVT analytes) per transition. Nitrogen was used for all gases (nebuliser, auxiliary, collision, curtain). The main optimised mass spectrometer source/gas parameters were: CID gas 9, curtain gas 35.0, gas 1 (nebuliser gas) 50.0, gas 2 (heater gas) 40.0, turbo ionspray voltage 5500.0 V, entrance potential: 10.0 V, and a source temperature of 500°C. Analyte specific optimised parameters are listed in Table 3.8.

The operation of all parts of the HPLC-MS/MS system, apart from the column oven, data collection and processing were controlled through Analyst® v1.6.2 software (AB Sciex). The temperature of the column oven was set using the Agilent 1200 series Hand Held Control Module. Nitrogen was supplied by a

Genius 3031 nitrogen generator (Peak Scientific, Inchinnan, UK). All automatically operated equipment, apart from the MS, was connected to the controlling computer via an Edgeport 8-port USB Expansion Module (Digi International, Minnetonka, US).

**Table 3.8 Analyte transitions and analyte-specific operating parameters**

Compound	Precursor ion (M+X) <sup>+</sup> (m/z)	Product ion (m/z)	Declustering potential (V)	Collision energy (V)	Collision cell exit potential (V)
RVT	482.3	258.1	141.0	45.0	18.0
RVT-d6	488.3	264.1	141.0	45.0	18.0
ATV	559.2	440.1	56.0	31.0	10.0
ATV-d5	564.2	445.1	56.0	31.0	10.0
2-OH ATV	575.1	250.1	71.0	57.0	16.0
2-OH ATV-d5	580.1	255.1	71.0	57.0	16.0
4-OH ATV	575.1	250.1	56.0	57.0	16.0
4-OH ATV-d5	580.1	255.1	56.0	57.0	16.0
ATV L	541.0	276.2	31.0	57.0	8.0
ATV-d5 L	546.0	281.2	31.0	57.0	8.0
2-OH ATV L	557.0	276.1	76.0	59.0	14.0
2-OH ATV-d5 L	562.0	281.1	76.0	59.0	14.0
4-OH ATV L	557.1	276.1	46.0	61.0	18.0
4-OH ATV-d5 L	562.1	281.1	46.0	61.0	18.0
SVT	441.2	325.1	81.0	35.0	16.0
SVT-d6	447.2	325.1	81.0	35.0	16.0
SVT-A	459.1	343.0	76.0	33.0	16.0
SVT-d6-A	465.1	343.0	76.0	33.0	16.0

Dwell time for all RVT and ATV analytes was 9.0 msec, and 20msec for SVT analytes.

X = H<sup>+</sup> for all RVT and ATV analytes; X = Na<sup>+</sup> for SVT and SVT-A.

### 3.2.6 Validation

RVT/ATV assay validation was carried out according to FDA guidance (Food and Drug Administration, 2001).

### 3.2.7 Selectivity

Selectivity was tested by analysing extracted blank blood from six individuals to investigate for interference occurring at the retention time of each analyte. For each analyte, the mean LLOQ peak area response (from pooled blood) was compared to the individual blank blood responses.

### 3.2.8 Carryover

Carryover was assessed by taking a punch of blank FTA Elute card immediately after punching out the highest calibration standard representing the upper limit of quantification (ULOQ).

### 3.2.9 Accuracy and Precision

Within-run and between-run accuracy and precision was determined for each analyte by analysing three sets of validation samples. Each set consisted of a calibration line, LLOQ, low, medium and high QC samples (n=6 per LLOQ/QC concentration). Set one was analysed first; sets two and three were analysed on the same day, but different to set one. Accuracy was calculated as: mean observed concentration/nominal concentration \* 100. Precision was expressed as the coefficient of variation (CV) (%).

### 3.2.10 Lower Limit of Quantification

The LLOQ for each analyte was defined as the lowest concentration that could be reliably determined with an accuracy of 80-120% and precision  $\leq 20\%$ , and constituted the lowest calibration standard.

### 3.2.11 Matrix Effects and Extraction Recovery

MEs and ER for the assay were determined based on the principles of Matuszewski *et al* (Matuszewski *et al.*, 2003). Three sets of samples were prepared: set one consisted of analyte in solvent (50:50 acetonitrile-water), set two were prepared in blood extracts spiked *after* extraction, and set three were prepared in blood extracts spiked *before* extraction.

The three sets were produced from both pooled fresh blood and fresh blood from six individuals. The pooled fresh blood was used to investigate the average MEs and ERs at the low, medium and high QC concentrations of each analyte. In addition, the ME of FTA Elute card alone was tested by extracting the

card by itself and spiking it *after* extraction. Separately, the six individuals were used to determine interindividual MEs and ERs at the medium QC; the low and high QCs were not included due to limited individual blood availability. For samples spiked *before* extraction, they were prepared at least in triplicate. Samples spiked *after* extraction were prepared in triplicate (pooled blood) or singly (individual blood).

The ME was calculated as:  $\text{set two response} / \text{set one response} * 100$ . The ER was calculated by:  $\text{set three response} / \text{set two response} * 100$ . The primary outcome with the CV (%) of the internal standard-normalised ME response.

### **3.2.12 Dilution Integrity**

Dilution integrity was tested for RVT, ATV and the main ATV metabolite 2-OH ATV, because these were the analytes most likely to exceed ULOQ *in vivo*. Dilution integrity was assessed by spiking fresh pooled blood at x2 ULOQ (i.e. RVT/ATV at 20,000ng/mL, 2-OH ATV at 5,000ng/mL) and diluting it fivefold after extraction in freshly extracted single blank samples (to 4,000ng/mL for RVT/ATV, 1,000ng/mL for 2-OH ATV). Each concentration was assessed in triplicate.

### **3.2.13 Storage and Stability**

Storage and stability was assessed for:

- i) working solutions;
- ii) analyte short term stability in blood matrix, longer term stability on FTA Elute cards, and post-preparative extract stability within the autosampler.

The proportion of analytes in the internal standard composite working solution was assessed. For analyte working solutions, analyte stability was assessed after ~14 days at 4°C at (the same diluted working solution was analysed twice

12-14 days apart) and on the bench top for six hours at room temperature (the diluted working solution was split, with half left on the bench top and half at 4°C for six hours, with both analysed in the same run). To test working solution stability, the solutions were diluted in 50:50 acetonitrile-water to the concentration equivalent to the final concentration of extracted samples spiked at the medium QC concentration. These final concentrations were: 3.4ng/mL (RVT/ATV) and 0.5ng/mL (all ATV metabolites). For 14 day analyte stability tests, internal standard-normalised analyte peak area responses were compared because of the solutions being run on different days. Solution stability was calculated as:  $\text{new solution response/original solution response} * 100$ . Stock solution stability was not tested here, but was tested in Chapter 5.

Short term (30 minute) analyte stability was tested in fresh pooled blood anticoagulated with EDTA chilled on ice (i.e. the assay conditions used). In addition to these assay conditions, the following were tested: blood anticoagulated with either EDTA or LiHep at both room temperature or 37°C. For each condition, blood was spiked at the medium QC and analysed in triplicate. Short term stability (%) was calculated as:  $\text{concentration at 30 minutes/concentration at 0 minutes} * 100$ .

The longer term stability of DBS' on FTA Elute cards stored in Whatman multi-barrier pouches containing desiccant at room temperature was tested at low, medium and high QCs analysed on day 0 and day 14 (RVT, ATV), day 36 (RVT, ATV) and day 7 (all ATV metabolites), against freshly prepared calibration curves (n=3 per QC per run). Post-preparative extract stability in the autosampler (4°C) was tested using low, medium and high QCs analysed on day 0 and re-analysed after 48 (RVT/ATV) or 24 (all ATV metabolites) hours, against a freshly prepared calibration line (n=3 per QC per run). 24 hours exceeds expected run times.

It was aimed for validation accuracy, CV, and stability responses to be within 15% of nominal concentration (accuracy, precision, dilution integrity, long term stability, post-preparative stability) or referent solution response (working solution stability including on the benchtop, short term analyte stability in blood).

### 3.2.14 Atorvastatin analyte interconversion

ATV analyte interconversion was assessed in stability assessments. This was carried out by determining the proportion (%) of *reciprocal* ATV acid/L analyte present as follows:

- I. In RVT/ATV and ATV acid metabolites solutions/spiked with these solutions
  - a.  $\text{ATV} \rightarrow \text{ATV L conversion} = \frac{\text{ATV L}}{(\text{ATV L} + \text{ATV})} * 100$
  - b.  $\text{2-OH ATV} \rightarrow \text{2-OH ATV L conversion} = \frac{\text{2-OH ATV L}}{(\text{2-OH ATV L} + \text{2-OH ATV})} * 100$
  - c.  $\text{4-OH ATV} \rightarrow \text{4-OH ATV L conversion} = \frac{\text{4-OH ATV L}}{(\text{4-OH ATV L} + \text{4-OH ATV})} * 100$
- II. In L metabolites of ATV solution/spiked with this solution
  - a.  $\text{ATV L} \rightarrow \text{ATV conversion} = \frac{\text{ATV}}{(\text{ATV} + \text{ATV L})} * 100$
  - b.  $\text{2-OH ATV L} \rightarrow \text{2-OH ATV} = \frac{\text{2-OH ATV}}{(\text{2-OH ATV} + \text{2-OH ATV L})} * 100$
  - c.  $\text{4-OH ATV L} \rightarrow \text{4-OH ATV} = \frac{\text{4-OH ATV}}{(\text{4-OH ATV} + \text{4-OH ATV L})} * 100$

### 3.2.15 DBS-specific assay assessments

The potential impact of DBS volume and spot homogeneity were investigated. For spot volume, the relative response of each analyte spiked in pooled blood at medium QC and extracted in triplicate from 10, 20 and 50 $\mu$ L spots was compared to the response from 35 $\mu$ L spots; a response  $\leq$  15% was acceptable.

Spot homogeneity was assessed for all analytes by two methods using pooled blood spiked at medium QC. First, the responses of 3mm punches from either the very centre of a spot or from the outer periphery of the spot including the halo were compared to the response from a standard 3mm punch taken from the edge of the main spot interior (excluding the halo) of the same 50 $\mu$ L spot; three 50 $\mu$ L spots were used for each of ATV/RVT, ATV acid metabolites, and L metabolites of ATV. Second, the response precision of two 3mm punches both taken from the edge of the main interior (excluding halo) of the same spot was determined. This was done for both 35 $\mu$ L and 50 $\mu$ L spot volumes (three spots per volume). A CV  $\leq$  15% was acceptable.

### 3.2.16 Data Analysis

All data were processed using Analyst<sup>®</sup> v1.6.2 software (AB Sciex, UK). For calibration and QC data, the ratio of analyte peak area to the peak area of the corresponding deuterated-internal standard was calculated, for each analyte. The linear calibration line fitted was calculated from the equation,  $y = mx + c$ , as determined by the weighted ( $1/y^2$ ) linear regression of the standard line. The regression was not forced through zero. The correlation coefficient ( $r^2$ ) of the calibration curve was accepted if  $>0.99$ . Analyst calculated the empirical concentration of the QC samples by interpolation using the fitted linear calibration line. MEs, ERs, solution stability, L-acid inter-conversion, and the assessments of DBS volume and homogeneity were calculated in Excel 2010 (Microsoft, USA). Pearson correlation coefficients for relating spot volume to area were calculated using IBM SPSS version 22.0 (IBM Corp, Armonk, NY, USA); Pearson p-values were two-sided and  $p < 0.05$  indicated significance.

## 3.3 Results

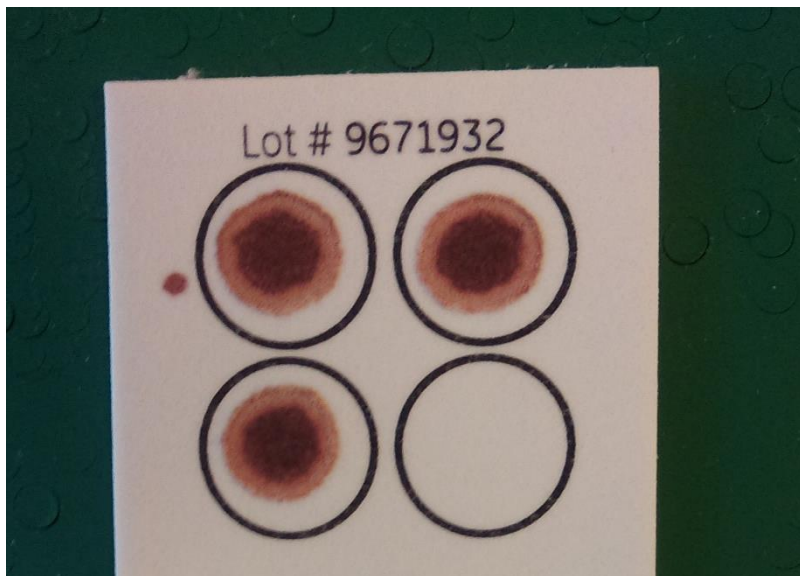
The results of the SVT/SVT-A hydrolysis investigation are shown in Table 3.9. Although the stability of SVT in EDTA was slightly superior to LiHep blood,  $\sim 80\%$  of spiked SVT was converted to SVT-A by two hours at 37 $^{\circ}$ C, indicating substantial hydrolysis. Neither of the SVT analytes were taken forwards for

incorporation into the RVT/ATV assay, although addition of SVT-A could be informative in *in vivo* studies.

### 3.3.1 Representative DBS appearance on FTA Elute cards

Figure 3.3 shows the typical appearance of DBS' on FTA Elute card, with the characteristic pale outer 'halo' surrounding the spot interior. The 3mm circles were punched out from the edge of the main spot interior avoiding the halo.

**Figure 3.3 Representative DBS appearance on FTA Elute cards**



Three dried blood spots are shown on FTA™ Elute Micro Card (GE Healthcare Life Sciences). The paler outer halo and darker interior of each spot are clearly visible.

**Table 3.9 STV is rapidly hydrolysed in murine blood**

Spiked analyte	Condition			Internal standard-normalised response (% relative to analyte T0 response)		Proportion of reciprocal SVT acid/lactone analyte in solution (as a % of total SVT+SVT-A present)
	Time (hr)	Anticoagulant	Temp	SVT	SVT-A	
SVT	0.5	EDTA	RT	75.0	186.9	13.8
	2	EDTA	RT	65.4	499.1	32.8
	0.5	EDTA	37°C	60.2	407.2	27.6
	2	EDTA	37°C	<b>12.2</b>	977.8	<b>81.9</b>
	0.5	LiHep	RT	30.8	116.3	27.3
	2	LiHep	RT	14.7	416.0	73.7
	0.5	LiHep	37°C	30.1	334.3	45.1
	2	LiHep	37°C	<b>6.4</b>	658.1	<b>88.4</b>
SVT-A	0.5	EDTA	RT	168.1	72.8	1.8
	2	EDTA	RT	230.0	80.4	2.2
	0.5	EDTA	37°C	201.7	68.8	2.5
	2	EDTA	37°C	631.2	105.1	<b>5.1</b>
	0.5	LiHep	RT	157.2	69.3	4.1
	2	LiHep	RT	358.3	124.8	5.2
	0.5	LiHep	37°C	359.6	135.2	6.3
	2	LiHep	37°C	608.7	180.3	<b>7.82</b>

SVT is rapidly hydrolysed in rodents *in vivo*, and may not be detectable (Shanmugam *et al.*, 2011). Therefore, the proportion of SVT or SVT-A remaining over time at room temperature (RT) or 37°C in EDTA or LiHep blood was tested (n=3 per condition). Briefly, 200µL blood was spiked with SVT or SVT-A to 10ng/mL. 20µL aliquots were taken at time 0.0, 0.5 and 2 hours. Proteins were precipitated with 100µL 100% acetonitrile plus 10µL SVT+SVT-A internal standard, agitated (20 minutes), centrifuged (18.0g, 4°C, 10 minutes), and 50µL of supernatant was diluted in 350µL 50:50 acetonitrile-water, prior to analysis.

This table shows that by two hours at room temperature after spiking SVT, >80% of total analyte detected (SVT+SVT-A) was SVT-A. In contrast, after spiking SVT-A, by two hours at room temperature SVT made up <8% of total analyte detected.

### 3.3.2 Extraction process development

The influence of extraction method on MEs and ERs of RVT and ATV is tabulated in Table 3.10. Interestingly, TBME alone had a mean ER of less than 4% for both analytes, which increased to over 80% in the presence of 1.2% water (administered as 50: 50 acetonitrile-water to 2.4% of final extraction volume). The addition of further water to TBME reduced ERs. The majority of the MEs were attributable to the FTA Elute card alone. Overall, extraction with TBME and 2.4% 50:50 acetonitrile-water was deemed optimal with minimal MEs and high ERs for RVT and ATV, and was selected. The data also show that extraction with methanol would be an acceptable alternative method.

**Table 3.10 Influence of extraction method on ionisation and extraction**

Analyte	Extraction method	Matrix effects (%)		Extraction recovery (%)	
		Card	Blood + Card	Mean	CV
RVT	TBME	99.7	103.1	2.4	35.6
	TBME + (2.4% 50% aq. MeCN)	103.8	104.8	84.2	2.4
	TBME + 12% water	99.1	100.9	78.7	11.3
	Methanol	114.0	118.5	87.3	3.7
	50% aq. MeCN	135.3	129.6	82.9	22.9
	50% aq. MeCN + 0.1% formic acid	174.1	152.1	78.6	1.8
ATV	TBME	102.8	105.1	3.9	25.5
	TBME + (2.4% 50% aq. MeCN)	105.3	107.6	81.9	2.0
	TBME + 12% water	94.2	97.8	65.8	9.7
	Methanol	101.9	109.2	86.0	2.9
	50% aq. MeCN	123.2	122.4	85.8	24.5
	50% aq. MeCN + 0.1% formic acid	155.9	152.3	80.2	2.8

Matrix effect (ME) was calculated as: analyte response from spiking post extraction (n=4)/ analyte response in 50% acetonitrile-water \*100. The aim was to determine whether it was the card or blood that was the major source of matrix effects, and this could be tested because analyte spiking for MEs occur *after* extraction. Therefore, extractions were carried out using just blank card, or card that had previously had blank pooled blood pipetted onto it.

Extraction recovery (ER) was calculated as: analyte response from spiking before extraction (n=3)/ analyte response from spiking post extraction (n=4) \* 100.

The extraction details are provided in Table 3.6.

This table shows that the addition of water to TBME substantially increased analyte extraction from 2.4 to 84.2%. Extractions via TBME + 2.4% 50% aq. acetonitrile, or methanol were suitable methods.

After selecting to extract using TBME and 2.4% 50:50 acetonitrile-water, the optimal number of extractions was investigated using ATV and RVT (Table 3.11); two extractions per sample was decided on, representing a compromise between 'off-line' extraction time, cost efficiency and ensuring adequate analyte desorption from the FTA Elute card.

**Table 3.11 Optimisation of the number of extractions carried out**

Analyte	Extraction method	Nominal conc. (ng/mL)	Aggregate analyte peak area (cps x 10 <sup>3</sup> )	Proportion of peak area (%)		
				F1	F2	F3
RVT	TBME + (2.5% 50% aq. MeCN)	5	5.079	63.2	25.6	11.2
		500	75.19	81.8	14.5	3.7
		7500	2018.7	78.8	17.8	3.4
ATV	TBME + (2.5% 50% aq. MeCN)	5	12.06	55.6	19.8	24.6
		500	191.72	83.5	13.7	2.8
		7500	4822.0	80.9	16.2	2.9

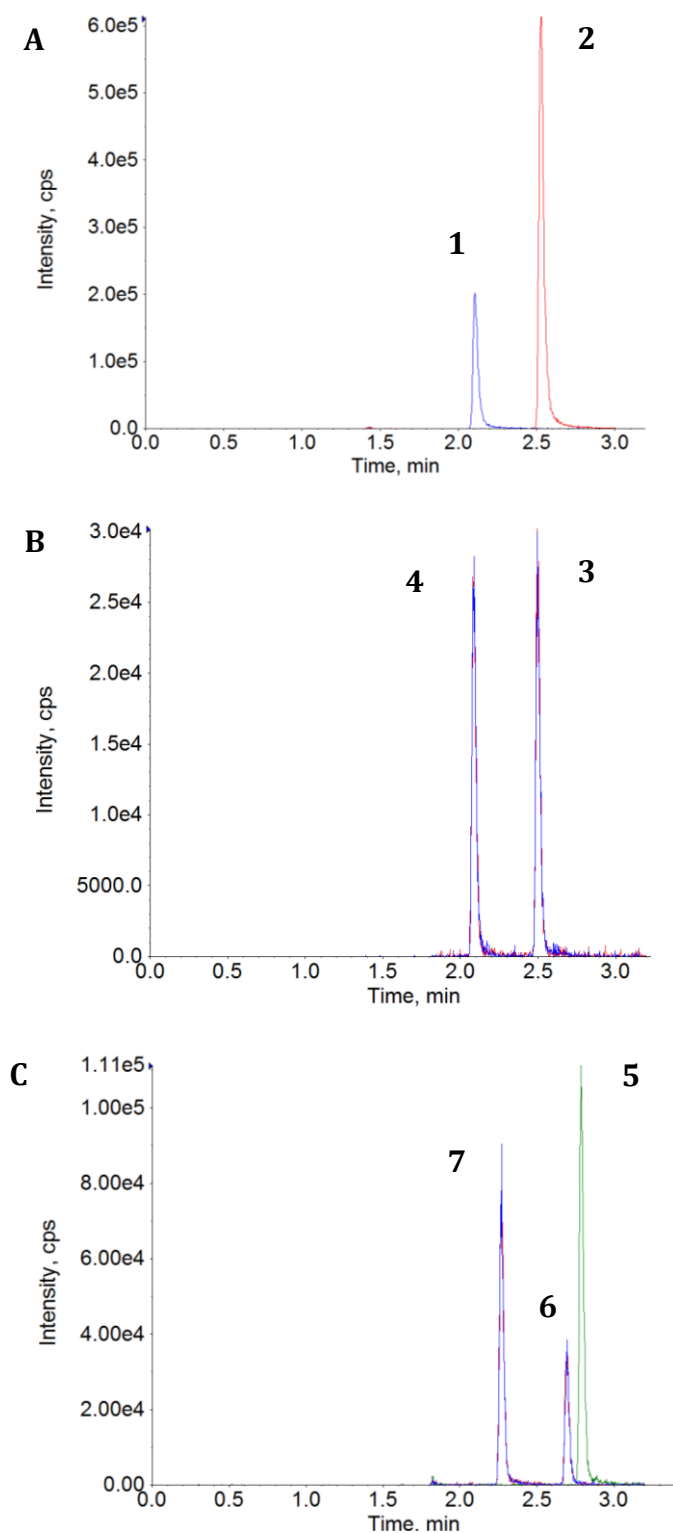
Abbreviations: cps= counts per second; F1/2/3 = 1<sup>st</sup>/2<sup>nd</sup>/3<sup>rd</sup> extraction, respectively.

This analysis was performed by extracting samples (n=1) prepared in pooled blood three times and analysing each extraction separately. For a given concentration, the analyte peak areas for the three extractions were summed and used as the denominator to determine the relative contribution of each extraction. This table shows that after two extractions, the majority of total signal had been extracted.

### 3.3.3 RVT/ATV chromatograms and retention times

The retention times used in assay validation with the Halo C<sub>18</sub> column were: RVT 2.10 (±0.1), ATV 2.52 (±0.1), 2-OH ATV 2.50 (±0.1), 4-OH ATV 2.08 (±0.1), ATV L 2.79 (±0.1), 2-OH ATV L 2.69 (±0.1) and 4-OH ATV L 2.27 (±0.1). Figure 3.4 shows typical chromatograms from pooled spiked blood.

**Figure 3.4 Representative multiple reaction monitoring chromatograms from analyte medium quality control samples**

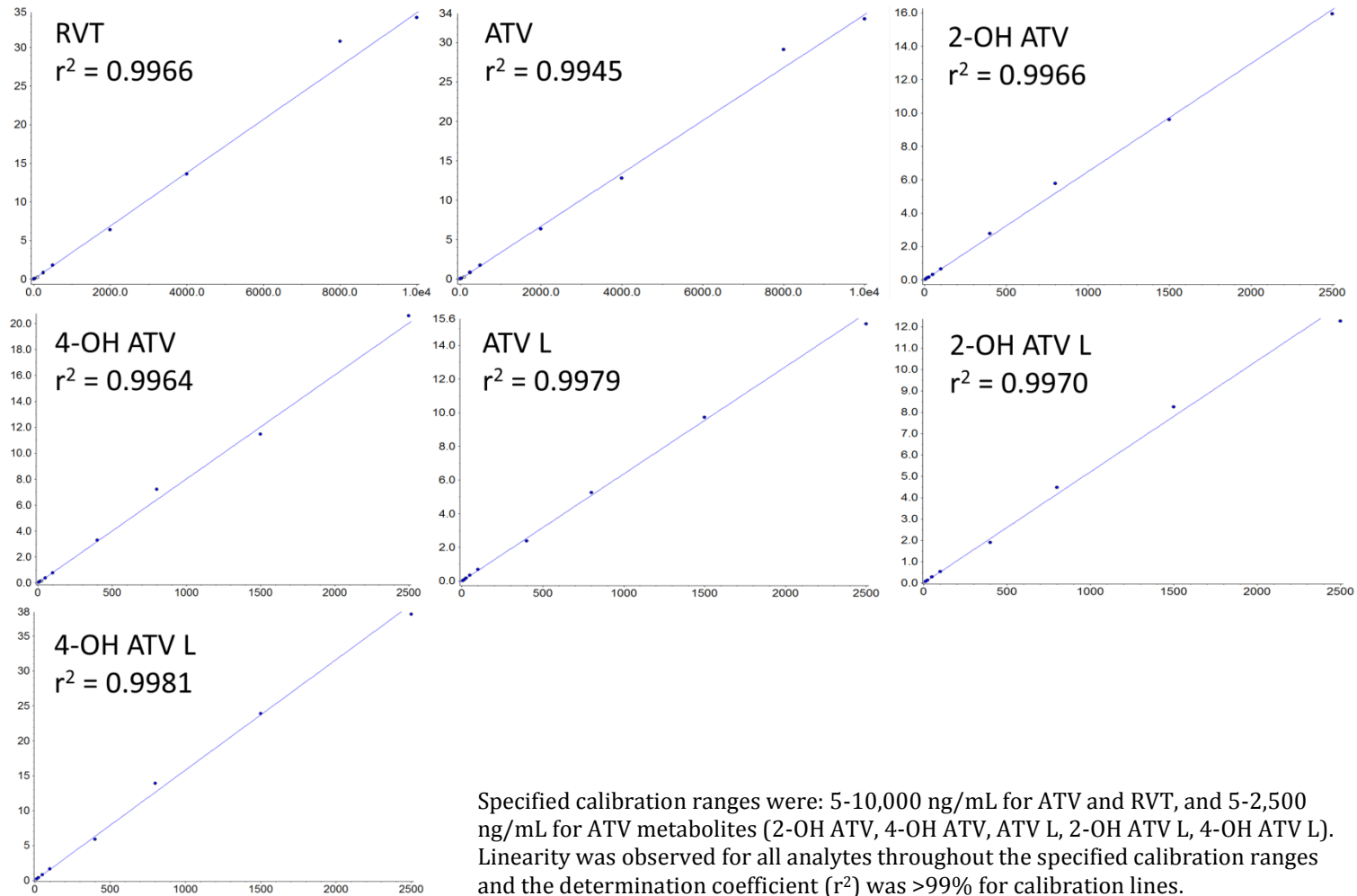


Chromatograms obtained in multiple reaction monitoring mode from medium quality control samples using pooled murine blood spiked with statin parents at 500ng/mL (A), ATV acid metabolites at 75ng/mL (B), and ATV lactones at 75ng/mL (C). 1= RVT; 2=ATV; 3=2-OH ATV; 4=4-OH ATV; 5=ATV L; 6=2-OH ATV L, and; 7=4-OH ATV L. Interestingly, the 4-OH ATV metabolites were consistently eluted earlier than the 2-OH isoforms.

### **3.3.4 Calibration curves**

Specified calibration ranges were: 5-10,000 ng/mL for ATV and RVT, and 5-2,500 ng/mL for ATV metabolites (2-OH ATV, 4-OH ATV, ATV L, 2-OH ATV L, 4-OH ATV L). Linearity was observed for all analytes throughout the specified calibration ranges and the determination coefficient ( $r^2$ ) was >99% for calibration lines (Figure 3.5).

Figure 3.5 Calibration curves



### 3.3.5 Selectivity

The representative chromatograms in Figure 3.6 demonstrate that there was minimal endogenous interference at the retention times of the seven analytes and their internal standards. Importantly, the LLOQ of all analytes was >5x, and the response of each internal standard >20x the background response of each individual blank blood response.

### 3.3.6 Carryover

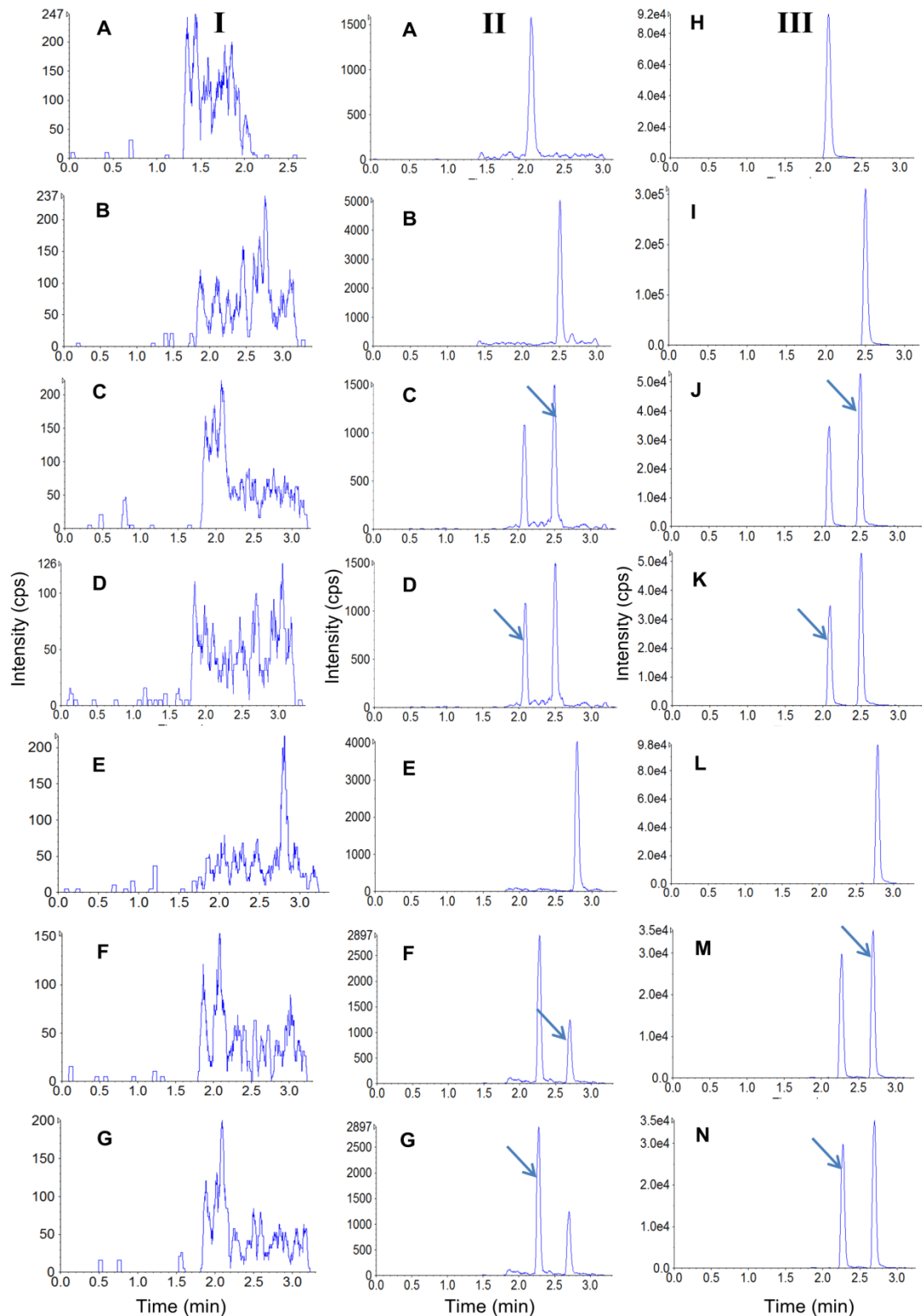
Carryover of RVT, ATV, and ATV metabolites could occur off-line via the 3mm Uni-Core puncher between successive punches. Carryover of analytes and internal standards could also occur on-line within the autosampler between successive samples. Nevertheless, carryover was uniformly negligible after sampling the ULOQ (Table 3.12).

**Table 3.12 Analyte carryover**

Analyte	Upper limit of quantification (ng/mL)	Carryover (%)	
		Analyte	Internal Std.
RVT	10,000	0.06	0.1
ATV	10,000	0.06	0.1
2-OH ATV	2,500	0.1	0.3
4-OH ATV	2,500	0.08	0.3
ATV L	2,500	0.1	0.08
2-OH ATV L	2,500	0.1	0.6
4-OH ATV L	2,500	0.07	0.8

Carryover was determined by taking a 3mm punch of blank FTA Elute card (n=1) immediately after punching out the upper limit of quantification DBS (n=1), with subsequent determination of analyte and internal standard response in the blank card sample. This table shows that carryover was  $\leq 0.1\%$  for all analytes and  $< 1\%$  for all internal standards.

**Figure 3.6 Multiple reaction monitoring chromatograms of blank blood, analytes and internal standards**



Representative MRM chromatograms in: I=blank murine blood; II=blood spiked with analytes at lower limit of quantification (LLOQ) or; III=blood spiked with internal standard. A = RVT; B = ATV; C = 2-OH ATV; D = 4-OH ATV; E = ATV L; F = 2-OH ATV L; G = 4-OH ATV L; H = RVT-d6; I = ATV-d5; J = 2-OH ATV-d5; K = 4-OH ATV-d5; L = ATV-d5 L; M = 2-OH ATV-d5 L; N = 4-OH ATV-d5 L. The molecular weight of 2-OH and 4-OH ATV acid metabolites, and equivalent L metabolites, was equivalent. Therefore, they were detected in the same chromatogram, but are distinguished by retention time – arrows indicate analyte of interest.

### 3.3.7 Accuracy and Precision

Within-run accuracy and precision were within  $\pm 20\%$  at LLOQ and  $\pm 15\%$  at all QC concentrations for all analytes in all three sets, except for the accuracy of 2-OH ATV L and 4-OH ATV L at LLOQ (Table 3.13). Between-run accuracy and precision for all analytes were within  $\pm 20\%$  at LLOQ and  $\pm 15\%$  at all other QC concentrations, except for 4-OH ATV L at LLOQ (Table 3.14). An accuracy at LLOQ of  $\pm 30\%$  was thus accepted for 2-OH and 4-OH ATV L in this assay.

**Table 3.13 Within-run accuracy and precision**

Analyte	Nominal conc. (ng/mL)	Set 1			Set 2			Set 3		
		M (ng/mL)	A (%)	P (%)	M (ng/mL)	A (%)	P (%)	M (ng/mL)	A (%)	P (%)
RVT	5	4.9	97.9	10.5	5.9	118.5	5.3	5.3	106.8	15.7
	15	15.5	103.4	11.1	17.2	114.7	8.4	15.5	103.4	10.0
	500	516.2	103.2	11.5	454.8	91.0	9.2	451.7	90.3	6.5
	7500	7648.1	102.0	9.3	7577.5	101.0	11.6	8563.1	114.2	5.3
ATV	5	5.3	105.4	8.6	5.6	112.0	5.5	5.4	108.1	17.0
	15	16.7	111.1	11.6	17.1	114.0	6.3	16.9	112.8	6.9
	500	532.3	106.5	10.3	444.1	88.8	9.1	462.5	92.5	6.4
	7500	7735.3	103.1	9.9	7429.2	99.1	9.2	8415.9	112.2	2.7
2-OH ATV	5	5.8	115.4	15.4	4.3	85.9	11.6	4.8	96.7	19.4
	15	16.7	111.0	6.1	16.3	108.8	9.6	15.3	101.7	12.1
	75	70.4	93.9	9.0	75.3	100.4	8.7	78.9	105.2	13.1
	1000	867.3	86.7	12.2	937.0	93.7	13.9	1003.0	100.3	10.6
4-OH ATV	5	4.2	84.1	18.7	5.3	106.7	10.7	5.5	109.1	17.0
	15	16.9	112.4	11.0	15.9	106.2	8.6	14.9	99.2	12.0
	75	70.1	93.4	10.2	74.9	99.8	11.6	66.3	88.5	14.8
	1000	866.7	86.7	12.8	943.1	94.3	14.9	934.5	93.4	7.0
ATV L	5	5.6	113.0	3.3	5.7	114.5	4.9	5.2	104.9	15.3
	15	15.2	101.3	9.7	14.9	99.6	7.3	14.0	93.1	4.2
	75	65.9	87.9	6.5	72.2	96.2	6.1	66.5	88.7	8.5
	1000	1112.2	111.2	5.8	1135.2	113.5	10.9	1068.7	106.9	3.5
2-OH ATV L	5	5.8	116.3	8.2	6.2	<b>123.4</b>	15.5	5.9	117.9	16.7
	15	13.9	92.5	8.7	13.4	89.6	9.3	13.2	87.7	7.0
	75	64.2	85.6	8.5	74.8	99.8	12.8	68.5	91.4	14.2
	1000	1110.0	111.0	9.4	1058.6	105.9	5.2	1139.7	114.0	7.1
4-OH ATV L	5	6.4	<b>128.2</b>	5.5	6.4	<b>127.1</b>	7.3	6.1	<b>121.4</b>	18.7
	15	14.9	99.6	10.0	14.4	95.8	7.7	13.4	89.2	8.1
	75	66.4	88.6	11.3	74.3	99.0	9.1	71.3	95.1	12.3
	1000	1141.7	114.2	8.5	1106.0	110.6	13.6	1126.1	112.6	2.0

Abbreviations: A = accuracy; M = mean; P = precision. Accuracy was calculated as: mean observed concentration/nominal concentration \* 100. Precision was determined by the CV (%). Results are shown to 1 decimal place.

The accuracy and precision of each analyte was determined separately in three sets of validation samples (n=6 per LLOQ/QC concentration) to ascertain within-run accuracy and precision. This table shows that all results met the pre-specified criteria except the accuracy of 2-OH ATV L and 4-OH ATV L at LLOQ concentration (highlighted in red).

**Table 3.14 Between-run accuracy and precision**

Analyte	Nominal conc. (ng/mL)	Set 1 Mean (ng/mL)	Set 2 Mean (ng/mL)	Set 3 Mean (ng/mL)	Overall		
					Mean (ng/mL)	Accuracy (%)	Precision (CV, %)
RVT	5	4.9	5.9	5.3	5.4	107.7	9.6
	15	15.5	17.2	15.5	16.1	107.2	6.1
	500	516.2	454.8	451.7	474.2	94.8	7.7
	7500	7648.1	7577.5	8563.1	7929.5	105.7	6.9
	Average						103.9
ATV	5	5.3	5.6	5.4	5.4	108.5	3.0
	15	16.7	17.1	16.9	16.9	112.6	1.3
	500	532.3	444.1	462.5	479.6	95.9	9.7
	7500	7735.3	7429.2	8415.9	7860.1	104.8	6.4
	Average						105.5
2-OH ATV	5	5.8	4.3	4.8	5.0	99.3	15.0
	15	16.7	16.3	15.3	16.1	107.2	4.5
	75	70.4	75.3	78.9	74.9	99.9	5.7
	1000	867.3	937.0	1003.0	935.8	93.6	7.2
	Average						100.0
4-OH ATV	5	4.2	5.3	5.5	5.0	100.0	13.8
	15	16.9	15.9	14.9	15.9	105.9	6.2
	75	70.1	74.9	66.3	70.4	93.9	6.1
	1000	866.7	943.1	934.5	914.7	91.5	4.6
	Average						97.8
ATV L	5	5.6	5.7	5.2	5.5	110.8	4.7
	15	15.2	14.9	14.0	14.7	98.0	4.4
	75	65.9	72.2	66.5	68.2	91.0	5.0
	1000	1112.2	1135.2	1068.7	1105.4	110.5	3.1
	Average						102.6
2-OH ATV L	5	5.8	6.2	5.9	6.0	119.2	3.1
	15	13.9	13.4	13.2	13.5	89.9	2.7
	75	64.2	74.8	68.5	69.2	92.3	7.7
	1000	1110.0	1058.6	1139.7	1102.8	110.3	3.7
	Average						102.9
4-OH ATV L	5	6.4	6.4	6.1	6.3	<b>125.6</b>	2.9
	15	14.9	14.4	13.4	14.2	94.9	5.5
	75	66.4	74.3	71.3	70.7	94.2	5.6
	1000	1141.7	1106.0	1126.1	1124.6	112.5	1.6
	Average						106.8

Between-run accuracy and precision was determined for each analyte from the mean concentration results in the three validation sets (n=6 per LLOQ/QC concentration). Accuracy was calculated as: mean observed concentration/nominal concentration \* 100. Precision was expressed as the coefficient of variation (CV) (%). Results shown are to 1 decimal place. This table shows that all results met the pre-specified criteria except the accuracy of 4-OH ATV L at LLOQ (highlighted in red).

### 3.3.8 Matrix effects and extraction recoveries

The MEs and ERs at the low, medium and high QC concentrations using pooled blood were consistent for each analyte, with internal standard-normalised CVs uniformly <15% (Table 3.15). With blank blood from different mice (n=6), the

CV at the medium QC of the internal standard-normalised ME was again <15% for each analyte, although ER CVs ranged up to 19.5% (Table 3.16).

**Table 3.15 Matrix and extraction recovery effects from pooled blood**

Analyte	Nominal conc. (ng/mL)	Matrix	ME (%) <sup>1</sup>				Analyte ER <sup>2</sup>	
			Analyte	IS	Analyte/IS	<b>Analyte/IS CV</b>	Mean (%)	CV (%)
RVT	15	B	94.8	93.9	100.9	<b>2.7</b>	88.2	6.2
	500	C	88.0	88.7	99.1	<b>0.5</b>	-	-
	500	B	85.2	87.1	97.8	<b>2.5</b>	100.9	11.5
	7500	B	97.5	98.3	99.1	<b>1.5</b>	90.3	4.0
ATV	15	B	94.9	98.6	96.3	<b>2.6</b>	86.0	3.8
	500	C	94.4	94.3	100.1	<b>2.3</b>	-	-
	500	B	98.6	98.9	99.7	<b>3.0</b>	100.8	10.4
	7500	B	97.5	97.6	99.9	<b>1.3</b>	85.8	2.1
2-OH ATV	15	B	115.8	121.8	95.1	<b>5.1</b>	63.2	10.5
	75	C	125.2	124.3	100.8	<b>0.8</b>	-	-
	75	B	125.4	122.5	102.4	<b>1.6</b>	50.8	9.2
	1000	B	108.2	109.9	98.5	<b>1.1</b>	48.6	14.2
4-OH ATV	15	B	117.5	118.2	99.3	<b>5.0</b>	64.1	12.3
	75	C	117.9	123.6	95.4	<b>2.3</b>	-	-
	75	B	118.9	125.6	94.7	<b>2.1</b>	54.6	6.4
	1000	B	105.7	106.1	99.6	<b>1.1</b>	52.4	13.9
ATV L	15	B	85.5	91.4	93.5	<b>5.2</b>	92.4	8.5
	75	C	85.0	79.5	107.1	<b>2.3</b>	-	-
	75	B	87.1	85.7	101.7	<b>3.8</b>	118.2	5.8
	1000	B	79.9	80.3	99.6	<b>0.9</b>	114.5	5.7
2-OH ATV L	15	B	86.2	86.8	99.3	<b>4.6</b>	53.8	9.9
	75	C	75.3	73.2	102.9	<b>5.0</b>	-	-
	75	B	75.5	75.2	100.6	<b>5.7</b>	66.9	10.9
	1000	B	89.8	91.0	98.7	<b>1.6</b>	62.3	7.5
4-OH ATV L	15	B	87.8	92.9	94.5	<b>1.0</b>	56.4	8.9
	75	C	79.8	77.0	104.0	<b>5.4</b>	-	-
	75	B	78.3	74.3	105.6	<b>7.4</b>	70.0	13.7
	1000	B	92.8	92.5	100.3	<b>1.1</b>	68.8	10.3

Abbreviations: B = blood on card; C = just FTA Elute card; CV = coefficient of variation; ER = extraction recovery; IS = internal standard; ME = matrix effect.

<sup>1</sup> = The ME was calculated as: analyte response from spiking post extraction/ analyte response in 50% acetonitrile-water \*100. Extractions were carried out using just blank card (C), or card pipetted with blank blood DBS' (B).

<sup>2</sup>= The ER was calculated as: analyte response from spiking before extraction/ analyte response from spiking post extraction \* 100. As analyte spiking onto card *prior* to extraction was required, ER was only tested in cards pipetted with blood that had been spiked with analyte (rather than from card alone).

The RVT and ATV results are derived from analysis of samples spiked prior to extraction (n=6 for 500ng/mL, n=3 for 15ng/mL and 7,500ng/mL) and samples spiked post extraction (n=6 for 500ng/mL, n=3 for 15ng/mL and 7,500ng/mL samples) in fresh pooled blood. For all ATV metabolites, results are derived from analysis of samples spiked prior to extraction (n=3) and samples spiked post extraction (n=6) in fresh pooled blood.

This table shows that the internal standard-normalise ME CV (in bold), which was the main outcome of interest, was uniformly <10%.

**Table 3.16 Interindividual matrix and recovery assessment**

Analyte	Nominal conc. (ng/mL)	Matrix effect (%)				Analyte Extraction Recovery (%)	
		Mean Analyte	Mean IS	Mean Analyte/IS	Mean Analyte/IS CV	Mean	CV
<b>RVT</b>	500	110.9	113.5	97.6	<b>1.9</b>	60.9	11.5
<b>ATV</b>	500	94.4	97.6	96.2	<b>2.4</b>	63.0	11.2
<b>2-OH ATV</b>	75	133.2	134.6	98.0	<b>1.9</b>	61.2	10.6
<b>4-OH ATV</b>	75	133.2	134.6	99.6	<b>2.2</b>	62.9	13.9
<b>ATV L</b>	75	137.5	139.8	98.9	<b>2.1</b>	108.0	10.3
<b>2-OH ATV L</b>	75	138.0	140.5	101.7	<b>1.2</b>	67.0	16.9
<b>4-OH ATV L</b>	75	124.0	125.3	98.2	<b>2.1</b>	75.3	19.5

Abbreviations: CV = coefficient of variation; IS = internal standard

The ME and ER were determined only from DBS' on FTA Elute card (i.e. not just card alone). Samples were spiked post extraction (n=1) or prior to extraction (n=3) at medium QC concentration per individual murine blood donor (n=6).

The main outcome of interest was the internal standard-normalised ME CV (in bold), which was <3%.

### 3.3.9 Dilution integrity

Acceptable accuracy and precision (<15%) following dilution of 2xULOQ samples back into the calibration range was observed for the analytes tested (RVT, ATV, 2-OH ATV). Furthermore, the high accuracy and precision of the calculated concentrations of the 2xULOQ samples themselves (extrapolated off the calibration curves) denotes that the observed linear concentration-response relationship of these analytes continues above the ULOQ (Table 3.17).

**Table 3.17 Dilution integrity**

Analyte	Nominal concentration (ng/mL)	Mean (ng/mL)	Accuracy (%)	Precision (CV, %)
<b>RVT</b>	4000	3525	<b>88.1</b>	<b>8.2</b>
	20,000 <sup>1</sup>	17,650	88.3	0.4
<b>ATV</b>	4000	4025	<b>100.7</b>	<b>0.4</b>
	20,000 <sup>1</sup>	18350	91.8	5.8
<b>2-OH ATV</b>	1000	1029.3	<b>102.9</b>	<b>10.6</b>
	5000 <sup>1</sup>	5190	103.8	14.4

Dilution integrity was assessed for RVT, ATV and 2-OH ATV by spiking fresh pooled blood at x2 ULOQ (i.e. RVT/ATV at 20,000ng/mL, 2-OH ATV at 5,000ng/mL) and diluting it fivefold after extraction in freshly extracted single blank samples (to 4,000ng/mL for RVT/ATV, 1,000ng/mL for 2-OH ATV). Each concentration was assessed in triplicate. The undiluted 2xULOQ samples were also analysed. As can be seen, the diluted and undiluted samples both have acceptable accuracy and precision, indicating linearity to 2xULOQ.

**3.3.10 Storage and stability****3.3.11 Internal standard solution stability**

The internal standard solution, containing all deuterated internal standards (50ng/mL), had negligible amounts (<1%) of (unlabelled) analytes (Table 3.18).

**Table 3.18 Analytes in internal standard working solution**

Internal standard		Analyte		Analyte relative abundance (%) <sup>1</sup>
Identity	Peak area (cps * 10 <sup>3</sup> )	Identity	Peak area (cps * 10 <sup>3</sup> )	
RVT-d6	311.3	RVT	0.7	0.22
ATV-d5	595.0	ATV	1.1	0.18
2-OH ATV-d5	144.3	2-OH ATV	0.5	0.36
4-OH ATV-d5	166.3	4-OH ATV	0.4	0.22
ATV-d5 L	488.7	ATV L	0.4	0.072
2-OH ATV-d5 L	186.7	2-OH ATV L	0.5	0.28
4-OH ATV-d5 L	116.7	4-OH ATV L	0.3	0.27

The proportion of analytes in the internal standard composite working solution was negligible.

<sup>1</sup> = analyte/(internal standard + analyte)\*100

### 3.3.12 Working solution stability

The 14 day stability of the solutions stored at 4°C was uniformly within 15% of the original response (Table 3.19).

**Table 3.19 Analyte solution stability stored at 4°C**

Specified Analytes in solution	Analyte analysed	IS-normalised analyte peak area responses		Solution stability (%)	Reciprocal ATV acid/lactone analyte in solution (%) <sup>1</sup>	
		Day 0	Day 14		Day 0	Day 14
<b>Statin parents solution</b>						
RVT	RVT	2.20	2.18	<b>99.3</b>	-	-
ATV	ATV	4.19	3.87	<b>92.3</b>	-	-
-	ATV L	0.00056	0.00049	88.2	0.041 <sup>2</sup>	0.038 <sup>2</sup>
<b>ATV acid metabolites solution</b>						
2-OH ATV	2-OH ATV	0.70	0.67	<b>96.6</b>	-	-
4-OH ATV	4-OH ATV	0.87	0.86	<b>98.4</b>	-	-
-	2-OH ATV L	0.0082	0.021	249.1	0.54 <sup>3</sup>	3.30 <sup>3</sup>
-	4-OH ATV L	0.032	0.043	134.4	2.67 <sup>4</sup>	3.62 <sup>4</sup>
<b>ATV lactones solution</b>						
ATV L	ATV L	0.41	0.42	<b>101.9</b>	-	-
2-OH ATV L	2-OH ATV L	0.71	0.69	<b>97.5</b>	-	-
4-OH ATV L	4-OH ATV L	1.88	1.85	<b>98.1</b>	-	-
-	ATV	0.0097	0.027	276.1	3.53 <sup>5</sup>	9.50 <sup>5</sup>
-	2-OH ATV	0.0081	0.029	350.2	1.20 <sup>6</sup>	4.44 <sup>6</sup>
-	4-OH ATV	0.014	0.056	408.4	1.17 <sup>7</sup>	4.92 <sup>7</sup>

To test analyte working solution stability, solutions were diluted in 50:50 acetonitrile-water to the concentration equivalent to the final concentration injected into the MS of extracted samples spiked at the medium QC concentration. These final concentrations were: 3.4ng/mL (RVT/ATV) and 0.5ng/mL (all ATV metabolites). These diluted working solutions were analysed at baseline, stored at 4°C, and re-analysed 12-14 days later. Internal standard-normalised analyte peak area responses were used because of the solutions being run on different days. Solution stability was calculated as: new solution response/original solution response \*100.

The proportion of ATV acid-L interconversion was assessed:

<sup>1</sup>=determined using the peak area responses of analytes alone (i.e. not internal standard normalised)

<sup>2</sup> = ATV L/ (ATV + ATV L)\*100

<sup>3</sup> = 2-OH ATV L/ (2-OH ATV L + 2-OH ATV)\*100; <sup>4</sup> = 4-OH ATV L/ (4-OH ATV L + 4-OH ATV)\*100

<sup>5</sup> = ATV / (ATV + ATV L)\*100; <sup>6</sup> = 2-OH ATV/ (2-OH ATV + 2-OH ATV L)\*100; <sup>7</sup> = 4-OH ATV/ (4-OH ATV + 4-OH ATV L)\*100

This table shows that all analytes in solution were stable (in bold). The conversion of ATV lactone to parent ATV was the most apparent.

### 3.3.13 Benchtop stability of analyte solutions

The six hour bench top stability results for all analytes were acceptable (<15% change in response) (Table 3.20).

**Table 3.20 Six hour bench top stability of working solutions**

Specified Analytes in solution	Analyte analysed	Analyte (cps * 10 <sup>3</sup> )		Solution stability (%)		Reciprocal ATV acid/lactone analyte in solution (%)	
		Time 0	6 hours	Analyte	Analyte/IS	0 hours	6 hours
<b>Statin parents solution</b>							
RVT	RVT	978.3	941.5	96.2	<b>101.4</b>	-	-
ATV	ATV	3277.5	3195.0	97.5	<b>101.0</b>	-	-
-	ATV L	1.2	1.3	107.2	112.9	0.037	0.041
<b>ATV acid metabolites solution</b>							
2-OH ATV	2-OH ATV	179.0	184.5	103.1	<b>102.1</b>	-	-
4-OH ATV	4-OH ATV	235.0	245.5	104.5	<b>104.5</b>	-	-
-	2-OH ATV L	1.0	0.8	81.7	79.1	0.57	0.45
-	4-OH ATV L	0.68	0.7	105.2	109.3	0.29	0.29
<b>ATV lactones solution</b>							
ATV L	ATV L	152.6	148.0	97.0	<b>103.7</b>	-	-
2-OH ATV L	2-OH ATV L	112.6	106.5	94.6	<b>99.8</b>	-	-
4-OH ATV L	4-OH ATV L	207.6	196.0	94.4	<b>97.7</b>	-	-
-	ATV	5.3	7.8	146.3	145.3	3.4	5.0
-	2-OH ATV	1.1	1.9	171.6	169.3	1.0	1.8
-	4-OH ATV	2.3	3.1	135.9	137.1	1.1	1.5

To test the benchtop stability of analyte working solutions, the solutions were diluted in 50:50 acetonitrile-water to the concentration equivalent to the final concentration injected into the MS of extracted samples spiked at the medium QC concentration. These final concentrations were: 3.4ng/mL (RVT/ATV) and 0.5ng/mL (all ATV metabolites). Each diluted solution was then split, with half left on the bench top and half at 4°C for six hours; both aliquots were then analysed in the same run. Solution stability was calculated as: benchtop solution response/4°C solution response \*100.

This table shows that analytes were stable on the benchtop. The conversion of ATV lactone to ATV (which increased from 3.4 to 5.0%) was the most apparent.

### 3.3.14 Short term (30 minute) stability in blood

For all analytes except 4-OH ATV L, the short term (30 minute) stability of spiked fresh pooled blood anticoagulated with EDTA and kept at 4°C (assay extraction conditions) was acceptable with relative changes of <15% (Table 3.21, Table 3.22, Table 3.23). After 30 minutes at 4°C in EDTA, the concentration of 4-OH ATV L had decreased to 77% of its concentration at 0 minutes (Table 3.23).

**Table 3.21 Thirty minute stability of RVT and ATV in blood in different conditions prior to pipetting onto FTA Elute cards**

Conditions	Analytes spiked and analysed				Analysed only	
	RVT		ATV		ATV L	
	Conc. (ng/mL)	Stability (%) <sup>1</sup>	Conc. (ng/mL)	Stability (%) <sup>1</sup>	Conc. (ng/mL)	Stability (%) <sup>1</sup>
EDTA 4C t0	492.0	<b>102.8</b>	474.3	<b>107.9</b>	2.7	<b>119.3</b>
EDTA 4C t30	505.7		511.7		3.2	
EDTA RT t0	498.0	<b>103.9</b>	499.3	<b>103.3</b>	2.8	<b>132.4</b>
EDTA RT t30	517.7		515.7		3.7	
EDTA 37C t0	563.0	<b>102.7</b>	543.0	<b>101.8</b>	3.3	<b>144.6</b>
EDTA 37C t30	578.3		552.7		4.8	
LiHep RT t0	433.0	<b>119.9</b>	441.3	<b>110.7</b>	2.8	<b>133.6</b>
LiHep RT t30	519.0		488.7		3.8	
LiHep 37C t0	479.0	<b>119.5</b>	456.0	<b>119.7</b>	3.1	<b>204.6</b>
LiHep 37C t30	572.3		546.0		6.4	

For each condition, blood was spiked at the medium QC and analysed in triplicate

<sup>1</sup> = Stability: t30 mean concentration /t0 mean concentration \*100

30 minutes after spiking with RVT and ATV, for all conditions, the concentrations of 2-OH and 4-OH ATV acid metabolites were <1ng/mL, indicating negligible conversion (not shown). This table shows that marginal conversion of ATV to ATV L was observed. Analytes were more stable in EDTA than lithium heparin stabilised blood.

**Table 3.22 Thirty minute stability of ATV acid metabolites in blood in different conditions prior to pipetting onto FTA Elute cards**

Conditions	2-OH ATV		4-OH ATV	
	Conc. (ng/mL)	Stability <sup>1</sup> (%)	Conc. (ng/mL)	Stability <sup>1</sup> (%)
EDTA 4C t0	92.1	<b>90.8</b>	95.5	<b>91.7</b>
EDTA 4C t30	83.6		87.6	
EDTA RT t0	83.3	<b>106.2</b>	81.0	<b>113.5</b>
EDTA RT t30	88.5		91.9	
EDTA 37C t0	92.8	<b>104.6</b>	94.3	<b>99.5</b>
EDTA 37Ct30	97.0		93.8	
LiHep RT t0	62.4	<b>154.4</b>	61.3	<b>147.7</b>
LiHep RT t30	96.4		90.6	
LiHep 37C t0	69.6	<b>138.1</b>	69.7	<b>133.5</b>
LiHep 37C t30	96.1		93.0	

For each condition, blood was spiked at the medium QC and analysed in triplicate

<sup>1</sup> = Stability: t30 mean concentration /t0 mean concentration \*100

Negligible conversion to corresponding metabolites of ATV Ls was detected (all below LLOQ); their results are not presented.

This table shows that analytes were more stable in EDTA than lithium heparin stabilised blood.

**Table 3.23 Thirty minute stability of atorvastatin lactone metabolites in blood in different conditions prior to pipetting onto FTA Elute cards**

Conditions	Analytes spiked and analysed						Analytes analysed only					
	ATV L		2-OH ATV L		4-OH ATV L		ATV		2-OH ATV		4-OH ATV	
	Conc. (ng/mL)	Stability (%) <sup>1</sup>	Conc. (ng/mL)	Stability (%) <sup>1</sup>	Conc. (ng/mL)	Stability (%) <sup>1</sup>	Conc. (ng/mL)	Stability (%) <sup>1</sup>	Conc. (ng/mL)	Stability (%) <sup>1</sup>	Conc. (ng/mL)	Stability (%) <sup>1</sup>
EDTA 4C t0	63.5	<b>91.2</b>	65.0	<b>86.5</b>	62.4	<b>77.0</b>	5.0	<b>157.8</b>	4.6	<b>140.4</b>	7.1	<b>194.7</b>
EDTA 4C t30	57.9		56.2		48.0		7.9		6.4		13.9	
EDTA RT t0	71.0	<b>59.6</b>	76.9	<b>51.6</b>	73.9	<b>31.2</b>	6.2	<b>456.1</b>	5.9	<b>523.1</b>	9.0	<b>751.1</b>
EDTA RT t30	42.4		39.7		23.1		28.2		31.0		67.8	
EDTA 37C t0	60.4	<b>27.2</b>	62.3	<b>26.9</b>	61.7	<b>10.0</b>	4.8	<b>908.4</b>	4.2	<b>1281.2</b>	6.5	<b>1415.6</b>
EDTA 37Ct30	16.4		16.8		6.2		43.3		53.8		92.3	
LiHep RT t0	65.8	<b>76.9</b>	74.6	<b>66.5</b>	68.3	<b>55.6</b>	4.8	<b>464.3</b>	4.3	<b>562.8</b>	7.5	<b>663.5</b>
LiHep RT t30	50.6		49.6		38.0		22.1		24.3		49.5	
LiHep 37C t0	70.1	<b>42.2</b>	73.5	<b>35.9</b>	75.4	<b>24.0</b>	4.6	<b>837.1</b>	4.6	<b>1100.5</b>	7.5	<b>1136.5</b>
LiHep 37C t30	29.6		26.4		18.1		38.2		51.1		85.5	

For each condition, blood was spiked at the medium QC and analysed in triplicate

<sup>1</sup> = Stability: t30 mean concentration /t0 mean concentration \*100

This table shows that 30 minutes after spiking with ATV Ls, conversion to corresponding ATV acid analytes was observed. For the assay conditions (4°C in EDTA stabilised blood) the 30 minute responses of ATV L and 2-OH ATV L were still within 15% of original response, but 4-OH ATV L had reduced to 77% of baseline. Rapid pipetting of spiked EDTA blood at 4°C onto DBS card is recommended.

### 3.3.15 Longer term (seven day) stability

Table 3.24 reports the longer term stability results for DBS' on FTA Elute cards kept for up to seven (all ATV metabolites) or 36 days (RVT, ATV). The accuracy and precision of the stored samples for RVT, ATV, 2-OH ATV and 4-OH ATV were uniformly acceptable (<15%). However, the accuracy of the L metabolites of ATV after seven days was reduced to ~80%, with CV ~27%.

**Table 3.24 Longer term DBS storage and stability**

Analyte	Nominal concentration (ng/mL)	Set 1 Day 0 (ng/mL)	Set 2 Day 7 or 14 (ng/mL)	Set 3 Day 36 (ng/mL)	Mean (ng/mL)	Accuracy (%)	Precision (CV, %)
RVT	15	15.2	13.3	13.2	13.9	92.7	8.1
	500	494.4	454.8	445.7	465.0	93.0	5.6
	7500	8467.5	7780.3	6589.6	7612.5	101.5	12.5
ATV	15	15.9	13.3	13.9	14.4	95.8	9.5
	500	500.5	456.4	451.2	469.4	93.9	5.8
	7500	8263.1	7307.1	6402.0	7324.1	97.7	12.7
2-OH ATV	15	14.3	15.2	ND	14.7	98.3	4.5
	75	82.2	71.4	ND	76.8	102.4	10.0
	1000	1068.5	982.4	ND	1025.5	102.5	5.9
4-OH ATV	15	14.9	15.6	ND	15.2	101.4	3.1
	75	71.9	81.0	ND	76.4	101.9	8.4
	1000	934.4	1115.1	ND	1024.8	102.5	12.5
ATV L	15	14.0	12.3	ND	13.1	87.6	8.9
	75	66.5	55.1	ND	60.8	81.1	13.3
	1000	975.2	964.5	ND	969.9	97.0	0.8
2-OH ATV L	15	14.3	10.8	ND	12.6	83.7	20.2
	75	74.1	50.1	ND	62.1	82.8	27.4
	1000	1106.8	887.3	ND	997.0	99.7	15.6
4-OH ATV L	15	13.5	10.5	ND	11.9	79.5	17.3
	75	71.3	49.5	ND	60.4	80.5	25.6
	1000	1064.8	837.4	ND	951.1	95.1	16.9

The longer term stability of DBS' on FTA Elute cards stored in Whatman multi-barrier pouches containing desiccant at room temperature was tested at low, medium and high QCs (n=3 per QC per run). Extracts were analysed on day 0, and compared to extractions on day 14 and 36 (RVT, ATV), or day 7 (all ATV metabolites). Freshly prepared calibration curves were used for each run.

This table shows that the longer term stability of RVT, ATV, 2-OH ATV and 4-OH ATV met the pre-specified accuracy and precision criteria (<15%). However, there was a loss in analyte response over time for all lactone metabolites of ATV leading to inaccurate and imprecise stability.

**Table 3.25 Lactone to acid conversion is only a minor contributor to the decreased response of atorvastatin lactones after storage as DBS on FTA Elute cards**

Spiked analytes	Analyte analysed	Day 7 to 0 change in internal standard-normalised analyte response at Medium QC	
		Relative (%) <sup>1</sup>	Absolute difference (peak area ratio*1000) <sup>2</sup>
ATV L	ATV L	79.7	-89
2-OH ATV L	2-OH ATV L	77.9	-75
4-OH ATV L	4-OH ATV L	74.0	-280
-	ATV	91.9	-11.8
-	2-OH ATV	118.1	4.6
-	4-OH ATV	117.3	26.3

<sup>1</sup> = Day 7 internal standard-normalised analyte peak area/day 0 internal standard-normalised analyte peak area\*100

<sup>2</sup> = Day 7 internal standard-normalised analyte peak area - day 0 internal standard-normalised analyte peak area\*1000. Numbers multiplied by 1000 to aid interpretation.

After storing lactone metabolites of ATV on FTA Elute card, there was a rapid reduction in their extracted response. The aim of this table was to determine the extent to which conversion to reciprocal ATV acid analyte accounted for this loss of signal. Although the *relative* increases in ATV acid analyte responses were similar to the relative decreases observed for the ATV Ls (except for ATV L), the absolute changes highlight that interconversion is only a minor contributor to the loss of signal of ATV Ls. For example, although 4-OH ATV L had an absolute decrease of 280 peak area ratio\*1000, there was only an absolute increase of 26.3 peak area ratio\*1000 in corresponding 4-OH ATV response.

### 3.3.16 Post-preparative stability

Post-preparative stability accuracy and precision after 24 (ATV metabolites) or 48 hours (RVT, ATV) within the autosampler at 4°C was acceptable for all analytes, except for the L metabolites of ATV at medium QC (accuracy of 50-60% relative to nominal concentration) (Table 3.26). Given the accuracy and precision of the low and high QCs were acceptable for the L metabolites of ATV, and the precision of the Ls medium QC was low, this is presumed to be a spiking error.

**Table 3.26 Post-preparative sample stability**

Analyte	Nominal concentration (ng/mL)	Set 1 Day 0 (ng/mL)	Set 1 after 48 or 24 hours (ng/mL)	Mean (ng/mL)	Accuracy (%)	Precision (CV, %)
RVT	15	15.2	14.7	15.0	99.7	2.5
	500	494.4	482.5	488.5	97.7	1.7
	7500	8467.5	8013.2	8240.4	109.9	3.9
ATV	15	15.9	15.7	15.8	105.4	0.9
	500	500.5	475.8	488.2	97.6	3.6
	7500	8263.1	7935.4	8099.3	108.0	2.9
2-OH ATV	15	13.7	14.6	14.2	94.4	4.7
	75	77.1	85.7	81.4	108.5	7.4
	1000	1106.0	1178.6	1142.3	114.2	4.5
4-OH ATV	15	14.2	14.9	14.5	96.9	3.3
	75	78.5	84.5	81.5	108.7	5.2
	1000	1064.9	1124.1	1094.5	109.4	3.8
ATV L	15	15.1	13.5	14.3	95.3	7.6
	75	38.1	40.3	39.2	<b>52.2</b>	4.0
	1000	844.7	907.9	876.3	87.6	5.1
2-OH ATV L	15	14.8	13.6	14.2	94.8	6.0
	75	42.2	41.7	42.0	<b>56.0</b>	0.8
	1000	920.7	990.5	955.6	95.6	5.2
4-OH ATV L	15	16.2	13.3	14.8	98.3	14.0
	75	41.8	41.1	41.4	<b>55.2</b>	1.1
	1000	968.3	962.0	965.2	96.6	0.5

Post-preparative extract stability in the autosampler (4°C) was tested using low, medium and high QCs analysed on day 0 and re-analysed after 48 (RVT/ATV) or 24 (all ATV metabolites) hours, against a freshly prepared calibration line (n=3 per QC per run). 24 hours exceeds expected run times.

The medium quality control (75ng/mL) for ATV Ls was consistently ~50-60% of the nominal concentration. It was thought this was due to a spiking error, but nevertheless was included because the CVs still demonstrate stable post-preparative precision.

Therefore, this table was interpreted to show that all analytes had satisfactory post-preparative stability in the autosampler.

### 3.3.16.1 ATV analyte interconversion

From the stability studies, it is clear that negligible interconversion of ATV acids to Ls occurs. However, conversion of ATV Ls to corresponding acids occurs in both solutions and blood. Notably, after 14 days the concentration of ATV had increased from 3.5% to 9.5% in the L metabolites working solution (Table 3.19). After six hours on the benchtop, ATV acids represented ≤5% of the total ATV analytes present after spiking with ATV lactones (Table 3.20).

L to acid conversion during 30 minutes within blood (short term stability) was most pronounced at physiological temperature (37°C) (Table 3.23); spiking EDTA anticoagulated blood kept at 4°C, constituting the herein assay conditions, was superior in terms of short term stability and relative lack of conversion compared to the other tested conditions. The drop in 4-OH ATV L under assay conditions (to 77% at 30 minutes of baseline response) was however matched by the corresponding largest proportional increase in acid (4-OH ATV to 194.7%) (Table 3.23).

The extent to which the loss of response of L metabolites of ATV after storage for seven days as DBS' on FTA Elute card was attributable to conversion to ATV acid metabolites was estimated (Table 3.25). The standardised absolute differences between day 7 and day 0 responses show that, although L to acid conversion occurred, conversion alone only accounts for a minority of the loss in L response. Interestingly, conversion of ATV L to ATV was not detected (Table 3.25). Therefore, the loss of L signal with storage on FTA Elute card has additional causes, which may include chemical degradation and/or strong binding to the FTA Elute cards.

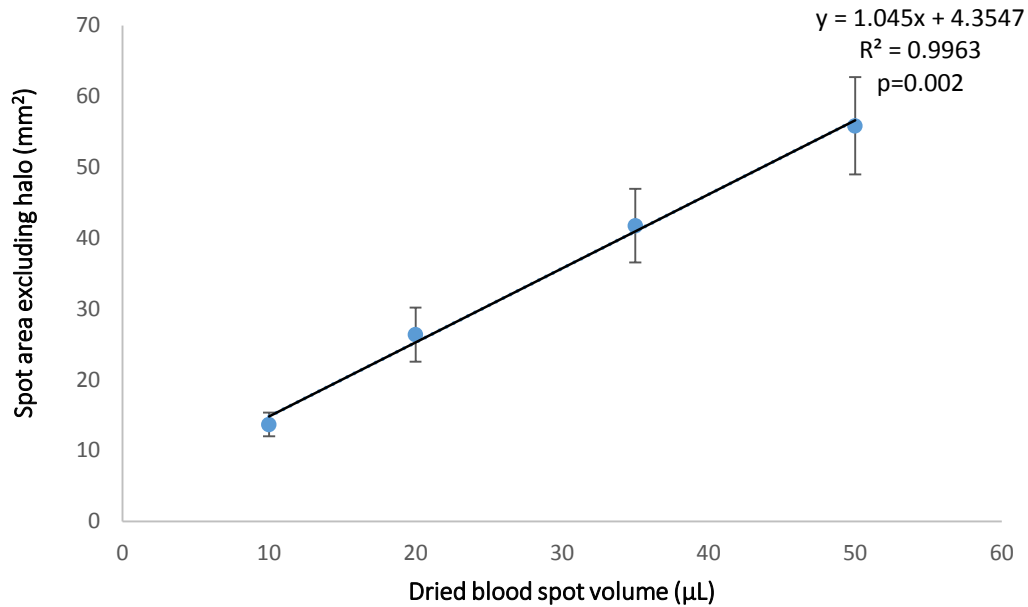
### **3.3.16.2 Stability summary**

The storage and stability results for RVT, ATV and ATV acid metabolites are acceptable. The data show that, although keeping the L metabolites of ATV working solution for 14 days at 4°C is permissible, the time between spiking blood and pipetting onto the FTA Elute cards should be minimised, and immediate analysis of samples (definitely within 7 days) is recommended.

### **3.3.17 DBS volume and homogeneity**

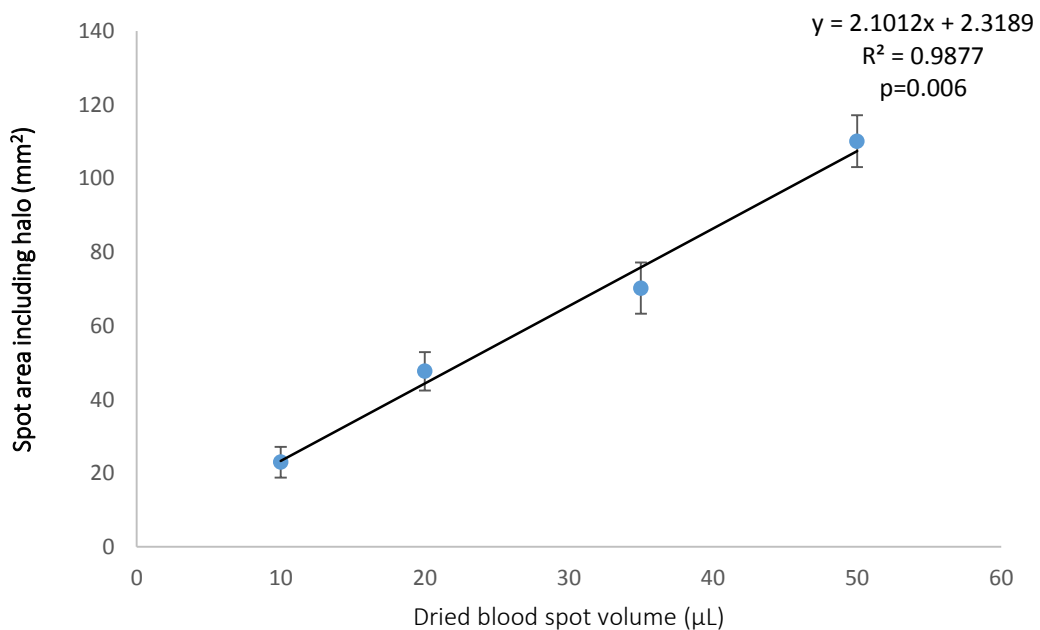
The relationship between pipetted spot volume and DBS area was linear within the investigated volume 10-50µL range, both when measuring only the spot interior (Figure 3.7) and when including the halo (Figure 3.8).

**Figure 3.7 Relationship between DBS pipetted volume and spot area excluding halo**



FTA Elute cards used. Nine spots per volume were used (n=3 ATV/RVT, n=3 ATV acid metabolites, n=3 ATV Ls). Two-sided p-value calculated from Pearson correlation coefficient. The figure shows a linear increase in internal spot area with increasing DBS pipetted volume.

**Figure 3.8 Relationship between DBS pipetted volume and spot area including halo**



FTA Elute cards used. Nine spots per volume were used (n=3 ATV/RVT, n=3 ATV acid metabolites, n=3 ATV lactone metabolites). Two-sided p-value calculated from Pearson correlation coefficient. The figure shows a linear increase in total spot area with increasing DBS pipetted volume.

From Table 3.27 it is clear that for all analytes at medium QC, as DBS volume increases, the internal standard-normalised peak area responses increase. Relative to 35µL spots, all peak area responses varied by <15%, except for the 10µL volumes of 2-OH ATV L and 4-OH ATV L (Table 3.27). The precision of 3mm punches taken from the periphery of the same spot interior (excluding the halo) for both 35µL and 50µL spots was uniformly acceptable (CV < 15%) (Table 3.27). The centre/peripheral (excluding halo) relative responses were near equivalent for each analyte, although there is a suggestion that ATV Ls trend towards higher central concentrations whereas the tested statin acid analytes have slightly lower central compared to peripheral (excluding halo) concentrations (Table 3.27). Expectedly, the response of punches including the halo was substantially lower (Table 3.27).

**Table 3.27 Impact of DBS volume and spot homogeneity on analyte response**

Analyte	IS-normalised analyte peak area responses compared to 35µL volume DBS response (%) <sup>1</sup>			IS-normalised analyte peak area responses within 50µL DBS (%) <sup>2</sup>		Within spot peripheral punch precision, CV (%) <sup>3</sup>	
	10µL	20µL	50 µL	C/P	H/P	35µL	50µL
RVT	95.5	96.9	105.3	98.4	<b>81.1</b>	2.9	4.0
ATV	93.1	97.3	104.3	96.6	<b>82.1</b>	2.7	4.1
2-OH ATV	86.1	98.1	104.5	94.5	<b>82.4</b>	7.8	7.7
4-OH ATV	87.5	96.5	105.5	94.6	<b>77.2</b>	4.0	11.7
ATV L	86.7	94.3	105.0	101.0	<b>78.1</b>	2.6	5.1
2-OH ATV L	<b>84.1</b>	93.5	107.9	99.5	<b>76.6</b>	5.9	4.8
4-OH ATV L	<b>82.2</b>	93.1	103.6	105.4	<b>76.6</b>	2.1	6.5

Abbreviations: C = centre; CV = coefficient of variation; DBS = dried blood spot on FTA Elute card; IS = internal standard; H = halo; P = periphery of DBS excluding halo.

FTA Elute cards and medium QC concentration were used (500ng/mL for ATV/RVT, and 75ng/mL for ATV acid metabolites, and ATV Ls). The results are the average of three spots per spot volume. Responses outside 85-115% are highlighted in red.

<sup>1</sup> = Only punches from the periphery of the spot interior and excluding the halo were used.

<sup>2</sup> = Spot homogeneity was investigated within 50µL DBS' by separately comparing the responses of the DBS centre, or periphery of the interior, to the response from the halo.

<sup>3</sup> = From a given DBS, the precision of two punches taken from the periphery excluding the halo was investigated.

This table shows gradually increasing analyte response with increasing spot volume, homogenous analyte responses from within the spot interior, and greatly reduced analyte response in the spot halo.

### 3.3.18 Assay validation summary

Table 3.28 summarises the assay validation results.

Table 3.28 Assay validation summary

Analyte	RVT	ATV	2-OH ATV	4-OH ATV	ATV L	2-OH ATV L	4-OH ATV L
<b>Calibration range (ng/mL)</b>	5-10,000; linear	5-10,000; linear	5-2,500; linear				
<b>Carry over (%)</b>	0.06	0.06	0.1	0.08	0.1	0.1	0.07
<b>Selectivity</b>	>x5	>x5	>x5	>x5	>x5	>x5	>x5
<b>Accurate<sup>1</sup></b>	Y	Y	Y	Y	Y	Y	Y
<b>Precise<sup>2</sup></b>	Y	Y	Y	Y	Y	Y	Y
<b>Matrix effect CV ≤15%</b>	Y	Y	Y	Y	Y	Y	Y
<b>Dilution integrity</b>	Y	Y	Y	ND	ND	ND	ND
<b>Stability variation ≤15%:</b>							
<b>i) Working solutions:</b>							
<b>14 day, 4°C</b>	Y	Y	Y	Y	Y	Y	Y
<b>6 hours, RT</b>	Y	Y	Y	Y	Y	Y	Y
<b>ii) Blood matrix:</b>							
<b>EDTA blood, 4°C, 0.5hr</b>	Y	Y	Y	Y	Y	Y	N
<b>DBS cards, RT, 7 days</b>	Y	Y	Y	Y	N	N	N
<b>iii) Post extraction:</b>							
<b>Autosampler, 4°C</b>	Y	Y	Y	Y	Y	Y	Y
<b>Spot homogeneity</b>							
<b>CV within main spot interior ≤ 15%</b>	Y	Y	Y	Y	Y	Y	Y

Abbreviations: CV = coefficient of variation; DBS = dried blood spot, N = no; ND = not done; RT = room temperature; Y = yes.

<sup>1,2</sup> = The accuracy and precision (CV) were within ±20% at LLOQ, and ±15% at low (15ng/mL), medium (500ng/mL RVT/ATV, 75ng/mL for all ATV metabolites) and high QC (7,500ng/mL RVT/ATV, 1,000ng/mL for all ATV metabolites) concentrations for RVT, ATV, 2-OH ATV, 4-OH ATV and ATV L. The accuracy of the LLOQ of 2-OH ATV L and 4-OH ATV L was within ±30%.

All pre-specified validation criteria were met except for the accuracy of the LLOQ of 2-OH ATV L and 4-OH ATV L (increased to within ±30%) and the 7-day stability as DBS for all ATV Ls.

### 3.4 Discussion

A novel assay harnessing DBC microsampling with HPLC-MS/MS bioanalysis to advance the Three Rs ethical approach (NC3Rs, 2016) has been developed and validated. Extensive SVT hydrolysis was noted and so SVT analytes were not incorporated in subsequent statin assay development, although addition of SVT-A into the assay would likely be feasible. The RVT/ATV analyte assay met all FDA criteria (Food and Drug Administration, 2001) for RVT, ATV, 2-OH ATV and 4-OH ATV. Most FDA criteria were met for ATV Ls, although the QC accuracy of 2-OH ATV L and 4-OH ATV L at LLOQ was relaxed to  $\pm 30\%$ , and seven day stability on FTA Elute cards for all ATV Ls was suboptimal. Recommendations and suggestions for further research based on the L observations are provided below.

Segregation of acid and L analytes to facilitate investigation of interconversion and reduce any potential impact on quantification has been previously reported (Partani *et al.*, 2014; Jemal *et al.*, 1999a). ATV extraction with TBME from human plasma has been previously reported (Kombu *et al.*, 2011); TBME-based extraction of statins from DBS punches, to the best of knowledge, has not been published previously. This extraction method was selected after comparing the MEs and ERs for RVT and ATV with other desorption solvents. Methanol is a suitable alternative, although the macroscopic appearance of extracts following methanol extraction was cloudy pink, rather than clear as for TBME (data not shown). Therefore, the potential for methanol-based extractions to adversely affect the longevity of the chromatography column and/or effect the ionisation of statin analytes could not be excluded. On the other hand, methanol only requires a single extraction step and may be preferred for high-throughput studies utilising off-line extraction. Interestingly, extraction with 100% TBME extraction was poor, but greatly enhanced with  $\sim 1\%$  (polar) water. Increasing the water content (to 12%) actually reduced RVT and ATV ER, although had little impact on observed MEs. It has been previously noted that DBS solvent mixtures containing a high water content combined with a water-soluble organic solvent (e.g. acetonitrile, methanol) can lead to the co-extraction of

polar blood matrix compounds (e.g. haemoglobin), which may adversely impact MEs (Meesters and Hooff, 2013).

Conversion of 2-OH and 4-OH ATV L to their corresponding acids was noted after seven day's storage, although this only accounted for a proportion of lost L signal. The major cause(s) for the loss of L response after seven days is unclear; possibilities include chemical degradation or strong binding to a constituent(s) of the FTA Elute card, reducing desorption with subsequent TBME extraction. FTA Elute cards are cellulose-based cards treated with a propriety chemical mix (including thiocyanic acid and guanidine) designed to lyse cells and denature enzymes and proteins (Chen *et al.*, 2012b). It is therefore conceivable that an analyte might react with a constituent(s), but perhaps not with alternate 'untreated' DBS card types (e.g. Whatman 903, Ahlstrom 226 cards). Future work should investigate the impact of card type and alternative conditions (e.g. -20°C) on longer term statin L DBS storage stability. Pragmatically, immediate bioanalysis of ATV Ls with minimal storage time is recommended when using the described bioanalytical methodology.

To minimise the impact of the observed short term (30 minute) L to acid conversion, immediate spotting of spiked blood onto DBS card is recommended. Nevertheless, it takes 1-2 hours for liquid blood to fully dry on DBS card (Wagner *et al.*, 2016), and ongoing interconversion after spotting cannot be fully excluded. Suggested method modifications for short term labile analytes include: accelerated drying on the DBA card with either a stream of nitrogen (D'Arienzo *et al.*, 2010) or microwave irradiation (Watanabe *et al.*, 2014), changing DBS card type, modifying sample pH, and impregnating cards with chemical stabilisers (Wagner *et al.*, 2016). Drying in a commercial microwave reduced the drying time of 15µL DBS' for a HIV protease inhibitor assay to just 5 minutes (Watanabe *et al.*, 2014) and could be tested. DBS card type has been observed to affect the 'on-card' initial blood drying phase, as well as longer term stability. Of relevance, FTA Elute cards have superior stability compared to

other card types for the ester analyte, valganciclovir, during the initial drying process (Heinig *et al.*, 2011b). Furthermore, DMPK-B cards, which are re-branded FTA Elute material treated with thiocyanic acid salts (Heinig *et al.*, 2011b), have superior stability during the drying phase for oseltamivir (ester prodrug) in rodent blood compared to 'untreated' Ahlstrom 226 cards (Heinig *et al.*, 2011a). On the other hand, untreated cards were shown to possess the equivalent stability to DMPK-B cards for two propriety prodrugs known to be unstable *ex vivo* due to esterase activity (D'Arienzo *et al.*, 2010). Therefore, although treated cards that denature enzymes might be expected theoretically to optimise the short term stability of analytes that are unstable due to enzymatic action, this cannot be assumed and empirical investigation is recommended.

Modification of pH or chemical stabilisers may reduce enzyme-mediated analyte instability. Compounds can be directly added to blood prior to spotting, although this can prove relatively impractical with DBS microsampling collection techniques (Wagner *et al.*, 2016). Alternatively, cards can be pre-impregnated with a relevant chemical stabiliser and allowed to dry prior to use. Statin L hydrolysis is enzyme mediated (Riedmaier *et al.*, 2011; Pasanen *et al.*, 2007). Furthermore in rodents, statin L hydrolysis is more rapid than in human plasma (Vickers *et al.*, 1990; Heinig *et al.*, 2011a). It is thought to be largely mediated by carboxylesterases (Draganov *et al.*, 2000), which are more prevalent in rodent (mouse > rat) than human plasma (Rudakova *et al.*, 2011), and are not inhibited by EDTA (Draganov *et al.*, 2000). Therefore, blood or DBS card pre-treated with an acetyl/carboxylesterase inhibitor, such as phenylmethanesulfonyl fluoride (D'Arienzo *et al.*, 2010) or dichlorvos (Heinig *et al.*, 2011a), may beneficially stabilise statin L during on-card rodent blood drying.

DBS microsampling has several advantages over conventional larger volume plasma-based approaches, although DBS-specific considerations exist: ensuring

sufficient sensitivity to reliably detect analytes from the small DBS volumes, appropriate use of internal standards, spot size effects, spot homogeneity and haematocrit confounding (Timmerman *et al.*, 2011; Wagner *et al.*, 2016). In this assay, sufficient sensitivity was provided by the Sciex triple quadrupole 6500 mass spectrometer. Second, addition of internal standard is challenging because of the solid nature of DBS. Deuterated internal standards of all analytes were added to the extraction solution (solid-liquid extraction) following standard practice (Wagner *et al.*, 2016). Nevertheless, a limitation of this approach is that the internal standard cannot adjust for variability in sample preparation and ER, and only compensates for post-extraction MEs (Wagner *et al.*, 2016). Potential improvements for DBS solid-liquid extraction include adding internal standard to the blood prior to spiking, although this approach is not applicable in clinical practice, pre-treating DBS cards with internal standard prior to spotting, or spotting the internal standard onto the DBS itself (Li *et al.*, 2012).

The pivotal assumption underlying DBS punch sampling is homogeneity of blood and analyte within the DBS (Wagner *et al.*, 2016). The magnitude of inhomogeneity varies with DBS card type, analyte, haematocrit, spot size and punch location within the DBS (Wagner *et al.*, 2016; Cobb *et al.*, 2013). In this study, DBS area increased linearly with volume (Figure 3.7, Figure 3.8), in agreement with previous findings (Fan *et al.*, 2011). However, for all analytes at medium QC concentration, responses increased with increasing spot volume. Nevertheless, response variation was <15% for all analytes with spot volumes of 20-50 $\mu$ L (compared to 35 $\mu$ L spots) (Table 3.27). Furthermore, mouse microsampling typically collects blood volumes between 10-20 $\mu$ L, and variation between the 10 $\mu$ L and 20 $\mu$ L volumes was also uniformly <15%.

Importantly, analysing punches from the same DBS site (periphery of main spot interior excluding halo) was associated with acceptably low CVs (all <15%) (Table 3.27), and there was minimal difference in analyte responses observed

from central punches compared to punches from the periphery of the spot interior (Table 3.27). Inclusion of the halo led to an unacceptable reduction in response for all analytes (Table 3.27). These findings are in agreement with previous studies (O'Mara *et al.*, 2011; Cobb *et al.*, 2013), and confirm that multiple sampling of a DBS from its interior is acceptable in this assay.

Haematocrit level can affect DBS size, spot homogeneity and analyte recovery rate on an analyte specific basis (de Vries *et al.*, 2013), and has been identified by the European Bioanalysis Forum DBS consortium as a major parameter that can perturb the performance of a DBS-based assay (Timmerman *et al.*, 2011). It is known that increasing haematocrit increases blood viscosity, which reduces blood spread and causes a near linear reduction in final DBS spot size (Denniff and Spooner, 2010). It is important to consider haematocrit during DBS assay development for bioanalysis of human samples, but inter-animal variability in haematocrit is generally confined to a far narrower range, and so haematocrit is less influential in pre-clinical studies (Wagner *et al.*, 2016). For the present assay only blood from male C57BL/6 mice was used, and so the effect of haematocrit was not empirically tested. This is acknowledged to be a limitation of the presented assay validation. Methods to circumvent haematocrit influence, particularly for assays utilising human samples, include measuring haematocrit from a paired blood sample, or estimating it from potassium levels in a DBS spot (Capiou *et al.*, 2013), in conjunction with calibration lines and QCs prepared from a range of different haematocrit levels, and whole-cut DBS analysis following volumetric application of blood by either using pre-cut DBS' or a related whole-cut DBS microsampling technique, such as the 'dried matrix on paper disks' cartridge approach (Meesters *et al.*, 2012).

In conclusion, DBS microsampling is a developing technology (Timmerman *et al.*, 2011) that offers several benefits, including but not limited to a reduction and refinement in the use of animals in scientific research. A novel bioanalytical method for use in murine PK studies has been developed and validated for the identification and quantification of RVT, ATV and ATV metabolites.

## **Chapter 4 Investigating the impact of hepatic cytochrome P450 oxidoreductase deficiency on systemic statin exposure and liver proteomics using the hepatic reductase null mouse model**

### **4.1 Introduction**

Statins are oral hypolipidaemic drugs indicated in the primary and secondary prevention of CVD and are amongst the most widely prescribed drugs. Although generally tolerated, statins are associated with a spectrum of adverse muscle effects, whose aetiology is not fully elucidated, but increased dose and systemic exposure appear significant predisposing factors (Golomb and Evans, 2008; Alfirevic *et al.*, 2014). SAM can range from mild muscular symptoms leading to statin non-adherence and discontinuation (Wei *et al.*, 2013) that increase the risk of cardiovascular events and death (Turner *et al.*, 2017), to life-threatening rhabdomyolysis with acute kidney injury (Stroes *et al.*, 2015).

POR is a diflavin reductase and the major donor of electrons from reduced NADPH to endoplasmic reticulum-located CYPs, including drug-metabolising CYPs; POR is thus a prerequisite for CYP-mediated drug catalysis (Pandey and Fluck, 2013). The first line statin, ATV, is extensively metabolised by CYP3A4, and undergoes UGT-mediated lactonization (Schirris *et al.*, 2015b). Little is known about the impact of POR on statin metabolism. However, decreased *ex vivo* ATV ortho (2)-hydroxylation in liver microsomes has been associated with homozygosity for a *POR* 3'-untranslated region variant, rs17148944 ('SNP2'), in a human liver biobank study (Gomes *et al.*, 2009). RVT is the most potent statin available, but undergoes little metabolism with 90% of an oral dose being recovered in the faeces, and >90% of faecal radioactivity due to parent RVT (Martin *et al.*, 2003; Olsson *et al.*, 2002).

Germline deletion of murine *Por* is embryonically lethal (Shen *et al.*, 2002). The HRN model, however, has a hepatic-specific *Por* deletion. HRN mice are fertile, but develop hepatic steatosis (Henderson *et al.*, 2003). HRN mice have increased systemic exposures to several drugs metabolised by distinct Cyp isoenzymes, including paracetamol, pentobarbital, midazolam, thalidomide, and omeprazole (Henderson *et al.*, 2003; Riddick *et al.*, 2013; Boggs *et al.*, 2014). ATV and RVT have hitherto not been tested.

Therefore, the primary aim of this work was to determine the impact of hepatic *Por* deficiency on the systemic exposures of RVT, ATV and all ATV metabolites. It was hypothesised that HRN mice would exhibit increased circulating ATV, a reduction in hepatic ATV hydroxylation, a possible compensatory increase in ATV lactonization, and little influence on RVT PK. *In vitro* microsomal incubations and comprehensive liver proteomics analyses were undertaken to expound the *in vivo* observations and further characterise the HRN model.

## 4.2 Methods

### 4.2.1 Chemicals and reagents

RVT, ATV, ATV metabolites and deuterated internal standards used in the MS analyses were purchased from Toronto Research Chemicals (Toronto, Canada). Fresh blood anticoagulated with K3 EDTA from male C57BL/6 mice was used to prepare the reference calibration curves and QCs for the *in vivo* PK study (Charles River, Margate, UK). All chemicals associated with the MS analyses were LC-MS grade. All chemicals were from Sigma-Aldrich (Gillingham, UK) unless stated otherwise.

### 4.2.2 Animals

HRN ( $POR^{lox/lox} + Cre^{ALB}$ ) mice were generated as described previously (Henderson *et al.*, 2003). Mice were bred in the Biomedical Research Institute of Ninewells Hospital and Medical School, Dundee, under standard animal

housing conditions with unlimited access to food and water and a 12-hour light/dark cycle.

For tissue harvest for the microsomal and proteomic analyses, six WT (POR<sup>lox/lox</sup>) and six HRN (POR<sup>lox/lox</sup> + Cre<sup>ALB</sup>) male C57BL/6 mice (all over four months old) were sacrificed by rising carbon dioxide in two separate batches (three WT and three HRN mice per batch) by Dr Colin Henderson (senior lecturer, the University of Dundee). Tissues were removed, snap-frozen in liquid nitrogen, transported on dry ice to the University of Liverpool and stored at -80°C.

The live animal work of the main *in vivo* PK study was carried out at the Biomedical Research Institute (Dundee) by Dr Richard Turner and Dr Colin Henderson. All work with animals was carried out in accordance with the Animal Scientific Procedures Act of 1986 and after a local ethics review.

#### **4.2.3 *In vivo* PK study**

Prior to the main PK study, a pilot *in vivo* study was conducted at the University of Liverpool by Dr Richard Turner and Mr Phillip Roberts (senior technician, retired) where WT male C57BL/6 mice received a single intraperitoneal dose of RVT or ATV at 15mg/Kg, and were followed up for five hours. This pilot study confirmed the feasibility of blood sample collection onto DBS but also showed that RVT, 4-OH ATV, ATV L and 2-OH ATV L levels were all below the LLOQ by one to three hours (in WT mice); therefore the dose was increased to 30mg/Kg for the main *in vivo* study.

In the main *in vivo* PK study, three HRN (POR<sup>lox/lox</sup> + Cre<sup>ALB</sup>) and three WT (POR<sup>lox/lox</sup>) male C57BL/6 mice, all over two months old (26-36g), were dosed with RVT (30mg/Kg) and ATV (30mg/Kg) together, via a single intraperitoneal injection (10mL/Kg volume).

The administration solution contained RVT and ATV, both at a final concentration of 3mg/mL dissolved in 8% DMSO (v/v), 20% polyethylene glycol 200 (v/v) and phosphate-buffered saline. This composite injection solution was prepared the day before the PK study at the University of Liverpool using autoclaved solvents, and transported at 4°C.

Blood was collected at 0.13, 0.25, 0.5, 1.0, 1.5, 4.0, 8.0 and 24.0 hours. All blood, except for the final sample, was collected via the lateral caudal veins. The tail was gently warmed in warm water, before a tail nick was made at the first time point using a sterile scalpel. Blood collection at subsequent time points was via removal of the nick scab after gentle warming. Approximately 20µL blood was collected at each time point into a K2 EDTA-coated glass capillary (end-to-end kapillare 20µL K2E, Sarstedt, Germany) attached to a pipette holder (International Medical Supplies, Stockport, UK) and spotted onto a Whatman FTA™ Elute Micro Card (GE Healthcare, Chicago, US, hereafter referred to as 'FTA Elute card'). Each DBS was allowed to air dry for two hours prior to being sealed in a Whatman multi-barrier pouch (3.75" x 3", GE Healthcare) containing desiccant (MiniPax sorbent packets, Multisorb Technologies, Telford, UK). The final blood sample was collected by percutaneous cardiac puncture after culling by rising carbon dioxide, and transferred to a glass capillary for spotting onto the FTA Elute card.

After culling, but prior to cardiac puncture, each mouse was re-weighed. Subsequently the liver was extracted, rinsed in ice-cold phosphate-buffered saline and weighed. A small portion of the large lobe was fixed overnight in 10% (v/v) neutral buffered formalin (Gurr), transferred to 70% alcohol for storage at 4°C, before being embedded in paraffin and transported to the University of Liverpool and stored at room temperature. The remaining liver was snap-frozen in liquid nitrogen, transported to the University of Liverpool on dry ice and stored at -80°C.

The sealed FTA Elute cards were transported to the University of Liverpool for bioanalysis within two days under ambient (temperature, pressure) conditions.

#### **4.2.4 Analysis of livers from PK study**

##### **4.2.4.1 Relative quantification of analyte levels**

24-hour post-dose livers from the *in vivo* PK study were thawed on ice and homogenised in saline (1:3 *w/v*) by oscillation (mixer mill MM 400, Retsch GmbH, Haan, Germany) as follows: one ball/liver oscillating 30x/second for three minutes, with the procedure carried out twice. The homogenised livers were stored at -80°C for 24 hours until use. 300µL of chilled 100% acetonitrile containing internal standard (ATV-d5, 2-OH ATV-d5, ATV-d5 L, RVT-d6 at 0.00625µg/mL) was added to 100µL of each liver homogenate, centrifuged (12000 x *g*, 10 minutes, 4°C, using the Allegra X-30R centrifuge, Beckman Coulter, Brea, USA), before 200µL was diluted in 200µL water to give a final concentration of 37.5% acetonitrile-water. Samples were kept on ice during preparation. 20µL of each sample was injected into the LC-MS/MS system.

##### **4.2.4.2 Liver histology**

The formalin-fixed paraffin-embedded liver tissues were sent to the Institute of Veterinary Science, University of Liverpool, where they were sectioned by microtome and stained with haematoxylin and eosin by Dr Julie Haigh (research associate, Veterinary Pathology and Public Health, University of Liverpool). Feature identification by light microscopy was carried out by Dr Lorenzo Ressel (senior lecturer, Veterinary Pathology and Public Health, University of Liverpool). The PhD candidate (Dr Turner) made a subjective assessment of the relative abundances of the different features in the HRN and WT livers.

#### 4.2.5 Microsome studies

##### 4.2.5.1 Microsome preparation

Liver microsomes were prepared on ice as described previously (Nelson *et al.*, 2001) from three HRN and three WT harvested livers. To ~800mg of each liver, potassium phosphate buffer (0.1M, pH 7.4, containing 0.125M potassium chloride) was added (1:2 w/v) and homogenised with a hand held homogeniser (TissueRuptor using TissueRuptor disposable probes, Qiagen, Hilden, Germany) to form a 33% liver homogenate, before centrifugation (10,000 x *g*, 20 minutes, 4°C, using an Optima™ L-60 Ultracentrifuge, Beckman Coulter). The supernatant (S9 fraction) was re-centrifuged (100,000 x *g*, 4°C) for 60 minutes. The pellet was re-suspended in 1600µL potassium phosphate buffer (0.1M, pH 7.4, containing 0.125M potassium chloride) and another round of centrifugation performed (100,000 x *g*, 4°C) for 60 minutes. The subsequent pellet, representing the liver microsomal fraction, was re-suspended in 200µL phosphate buffer and stored at -80°C.

##### 4.2.5.2 Microsomal incubations

Microsome total protein concentrations were estimated using a bicinchoninic acid (BCA™) assay (Pierce, Rockford, USA). Determination of microsomal Cyp-mediated activity has been described previously (Jacobsen *et al.*, 2000). Briefly, ATV and RVT stock (-20°C, dissolved in DMSO to 20mM) were diluted in autoclaved potassium phosphate buffer to form working solutions (ATV: 50µM, 200µM, 400µM; RVT 200µM) stored at 4°C. Autoclaved potassium phosphate buffer (0.1M, pH 7.4) was added into flat-bottomed glass vials before microsomes (0.5mg/mL), drug (from the above working solutions), and magnesium chloride (5mM) were added; the contents were pre-incubated at 37°C for 4 minutes with agitation in a water bath. The reaction was started by adding reduced NADPH (1mM) to a final reaction volume of 200µL. An aliquot of each reaction was terminated by transfer into 200µL ice-chilled 100% acetonitrile containing internal standard (ATV-d5, 2-OH ATV-d5, ATV-d5 L, RVT-d6 at 0.00625µg/mL). Two types of NADPH-activating experiments were performed. First, the proportion of parent RVT (20µM) or ATV (20µM)

remaining over time was determined by taking 25 $\mu$ L aliquots of the reaction mixtures at 0, 5, 15, 30, 60, and 120 minutes. The proportion of RVT remaining from 5 $\mu$ M RVT was also determined with 25 $\mu$ L aliquots at times 0, 5, 30, 60, 120 and 240 minutes. 20 $\mu$ M parent drug was initially selected because it was consistent with the HRN ATV  $C_{max}$  in the PK study. Second, the production of 2-OH and 4-OH ATV from ATV concentrations of 1, 2, 5, 10, 20, 50, 100, 140, 200 and 250 $\mu$ M was determined by taking a 50 $\mu$ L aliquot of each reaction at 30 minutes.

Determination of Ugt-mediated microsomal activity has been described previously (Dostalek *et al.*, 2011). To the autoclaved potassium phosphate buffer, microsomes (100 $\mu$ g protein per reaction at 0.5mg/mL) and alamethicin (50 $\mu$ g/mg protein, dissolved in 40% methanol *v/v*) were added and incubated on ice for 15 minutes. ATV was added (20 $\mu$ M), the vial contents equilibrated at 37°C for 4 minutes with agitation in the water bath, and the reaction initiated by addition of magnesium chloride (5mM) and uridine 5'-diphosphoglucuronic acid (UDPGA) (5mM) to a final volume of 200 $\mu$ L. The final concentration of methanol was 2% *v/v*. At 30 minutes, 50 $\mu$ L aliquots were similarly transferred to 200 $\mu$ L of ice-chilled 100% acetonitrile containing the internal standards to terminate the reaction.

NADPH/UDPGA active conditions were tested using separate HRN (n=3) and WT (n=3) microsomal incubations. Control conditions tested included microsome inactivation (denatured at 80°C for 10 minutes) and drug metabolism in the presence/absence of NADPH/UDPGA. Unlike the active conditions, all control reactions used HRN or WT pooled microsomes. Two reactions per control condition per strain were used for NADPH controls. Due to a limited microsome supply, each UDPGA control condition was limited to one reaction per strain, and therefore the WT and HRN UDPGA controls for each condition were pooled for data analysis. The maximum final concentration of DMSO in any reaction was 0.6%.

Calibration standards were spiked into pooled (HRN plus WT) denatured microsomes as per Table 4.1, using working solutions containing: 1.) ATV, 2-OH ATV, 4-OH ATV plus RVT in 25:75 acetonitrile-water (v/v); and 2.) ATV L in 50:50 acetonitrile-water. A 50 $\mu$ L aliquot of each standard was added to 200 $\mu$ L ice-chilled 100% acetonitrile containing internal standard.

For all incubations, the chilled samples were vortexed, centrifuged (12000 x g, 10 minutes, 4°C), and 50 $\mu$ L of the supernatant diluted in 450 $\mu$ L (NADPH-activated) or 350 $\mu$ L (UDPGA-activated) of 50% acetonitrile. 20 $\mu$ L of each sample was injected into the LC-MS/MS system.

**Table 4.1 Calibration standard concentrations for microsomal incubations**

Calibration standard	Working solution				
	1.				2.
	RVT (nM)	ATV (nM)	2-OH ATV (nM)	4-OH ATV (nM)	ATV L (nM)
1	12.3	10.6	10.3	0.7	10.9
2	24.3	20.9	20.4	1.4	21.6
3	48.6	41.9	40.7	2.8	43.3
4	97.4	84.0	81.6	5.6	86.8
5	194.8	167.9	163.2	11.3	173.5
6	390.4	336.5	327.2	22.5	347.8
7	779	671	653	45	694
8	1558	1343	1305	90	1387
9	3115	2685	2611	180	2775
10	6230	5370	5221	359	5549
11	12460	10740	10442	719	11099
12	24920	21481	20884	1438	22198

Working solution 1 contained RVT, ATV, 2-OH ATV and 4-OH ATV in 25:75 acetonitrile-water (v/v); and working solution 2 contained ATV L alone in 50:50 acetonitrile-water.

#### 4.2.6 Mass spectrometric bioanalysis of statin analyte levels

Analyte levels from 20 $\mu$ L injections were determined for the *in vivo* PK study blood samples, the 24 hour post-dose liver homogenates, and for all microsomal incubations using an HPLC-MS/MS system consisting of an Agilent Technologies (Santa Clara, US) 1200 Series quaternary HPLC system coupled to a Sciex triple

quadrupole 6500 mass spectrometer (AB Sciex, Warrington, UK). The validated analyte extraction procedure for the FTA Elute card DBS' and associated HPLC-MS/MS settings are in Chapter 3. The same HPLC-MS/MS settings were used for the 24 hour post-dose liver homogenates and microsome samples, with one exception. When determining 2-OH and 4-OH ATV microsomal production, ATV was omitted from the acquisition method to avoid saturating the MS detector with high ATV concentrations.

## **4.2.7 Liver proteomics**

### **4.2.7.1 Preparation of liver homogenates**

The liver homogenates from six HRN and six WT were prepared on ice for proteomic analysis. Briefly, 100mg of whole liver from each mouse was homogenised in 350 $\mu$ L 0.5M triethylammonium bicarbonate buffer (TEAB)/0.1% sodium dodecyl sulphate (SDS) by oscillation (one ball/liver oscillating 30x/second for three minutes). The denatured lysates then underwent a freeze-thaw cycle, sonication (three rounds of 5 $\mu$  sonication for 10 seconds using the Soniprep 150 Plus, MSE, London, UK), a second freeze-thaw cycle, a single round of sonication, centrifugation (18000  $\times g$ , 10 minutes, 4°C), and final re-centrifugation of the supernatant (18000  $\times g$ , 5 minutes, 4°C). The total protein concentration of the resulting liver homogenates was determined using the BCA<sup>TM</sup> assay, and adjusted to 5mg/mL by dilution in 0.5M TEAB/0.1% SDS. A liver homogenate pool consisting of equal volumes of HRN and WT homogenates was also produced, and all homogenates stored at -80°C until use.

### **4.2.7.2 iTRAQ labelling of liver homogenates**

Isobaric tag for relative and absolute quantitation (iTRAQ) reagent labelling was carried out according to the Applied Biosystems protocol for an 8plex study (Applied Biosystems, Thermo Fisher Scientific, Waltham, USA). Three separate iTRAQ experiments were performed: the first was a pilot study using liver microsomes (n=3 HRN, n=3 WT, n=2 of microsome pool); the second and third used liver homogenates and constitute the main study (each batch consisted of

n=3 HRN, n=3 WT, n=2 of the homogenate pool). Briefly, a 20 $\mu$ L aliquot of each thawed homogenate was reduced by addition of 2 $\mu$ L of 50 $\mu$ M tris(2-carboxyethyl)phosphine (TCEP) with incubation at 55°C for 60 minutes, and then capped with addition of 1 $\mu$ L of methylmethanethiosulfate (MMTS) at room temperature. 10 $\mu$ g of sequencing grade modified trypsin (Promega, Madison, USA) was added for overnight digestion at 37°C. Samples were incubated with iTRAQ tags (113-115 for WT, 116-118 for HRN, 191 and 121 for pool) for two hours at room temperature for peptide labelling. The samples were then pooled together, diluted to 4mL in 10mM potassium dihydrogen phosphate/25% acetonitrile, the pH adjusted to <3 using phosphoric acid, and centrifuged (16000 x *g*, 3 minutes, room temperature).

The supernatant was then passed to Dr Rosalind Jenkins (principal experimental officer, Proteomics, University of Liverpool) for fractionation, desalting, bioanalysis and iTRAQ ProteinPilot™ data acquisition. The pooled sample underwent fractionation on a Polysulfoethyl A strong cation-exchange column (200x4.6mm, 5 $\mu$ m, 300 Å; Poly LC, Columbia, MD, USA). Fractions of 2 mL were collected and dried by centrifugation under vacuum (SpeedVac, Eppendorf, Hamburg, Germany). Fractions were reconstituted in 1mL of 0.1% trifluoroacetic acid (TFA) and subsequently desalted using an mRP Hi Recovery protein column 4.6 x 50mm (Agilent Technologies) on a Vision Workstation (Applied Biosystems) prior to mass spectrometric analysis.

#### **4.2.7.3 Mass spectrometric bioanalysis of iTRAQ samples**

This section was undertaken by Dr Rosalind Jenkins. Desalted fractions were reconstituted in 40 $\mu$ L 0.1% formic acid and 5 $\mu$ L aliquots were delivered into a Triple TOF 5600 (AB Sciex) *via* an Eksigent NanoUltra cHiPLC System (AB Sciex) mounted with a microfluidic trap and analytical column (15cm x 75 $\mu$ m) packed with ChromXP C<sub>18</sub>-CL 3 $\mu$ m. A NanoSpray III source was fitted with a 10 $\mu$ m inner diameter PicoTip emitter (New Objective, Woburn, USA). The trap column was washed with 2% acetonitrile/0.1% formic acid for 10 minutes at 2 $\mu$ L/min

before switching in-line with the analytical column. A gradient of 2–50% acetonitrile/0.1% formic acid (v/v) over 90 minutes was applied to the column at a flow rate of 300nL/min. Operating in positive ion mode with survey scans of 250ms, the instrument used an MS/MS accumulation time of 100ms for the 25 most intense ions (total cycle time 2.5s). A threshold for triggering of MS/MS of 100 counts per second was used, with dynamic exclusion for 12 seconds and rolling collision energy, adjusted for the use of iTRAQ reagent in the Analyst method. Information-dependent acquisition was powered by Analyst TF 1.5.1 software, using mass ranges of 400-1600 atomic mass units (amu) in MS and 100-1400 amu in MS/MS. The instrument was calibrated after every fifth sample using a beta-galactosidase digest.

#### **4.2.7.4 iTRAQ data acquisition**

Data were searched using ProteinPilot™ software (Version 4, AB Sciex) against the latest UniProt database with iTRAQ as a variable modification and MMTS as the cysteine alkylating reagent. The reversed database was used as a decoy to determine the false discovery rate (FDR) for protein identification, and only those proteins identified at a  $\leq 1\%$  FDR were evaluated further. Ratios for each HRN or WT iTRAQ label were obtained, using the 121-labelled pool as the denominator.

#### **4.2.7.5 P-gp Immunoblotting**

Western blotting for P-gp was carried out by SDS polyacrylamide gel electrophoresis (SDS-PAGE) as described previously (Henderson and Wolf, 1992). Briefly, aliquots of half the liver homogenates (n=3 HRN, n=3 WT) prepared in 4.2.7.1, were diluted to 1mg/mL. WT heart (n=1) and spleen (n=1) homogenates were also similarly prepared, as described in 4.2.7.1, to serve as relative negative controls (abcam, 2017). An 8% acrylamide gel was freshly prepared in a SE245 dual gel caster (Hoefler, Holliston, USA) as per Table 4.2. 18 $\mu$ L of each sample was denatured with 6 $\mu$ L of SDS/2-mercaptoethanol (3:1 dilution, heated at 55°C for 20 minutes). The gel was transferred to the

electrophoresis running apparatus (Mighty Small II SE250, Hoefer) containing 1% running buffer (0.5M Tris-HCl, 0.5M glycine, 1% w/v SDS); 4 $\mu$ L of ladder (SeeBlue<sup>®</sup> Plus2 Pre-stained protein standard, Invitrogen<sup>™</sup>, Thermo Fisher Scientific) and 10 $\mu$ g sample/lane were loaded into the gel, and electrophoresis was carried out at 30mA/300V (Electrophoresis power supply EPS 500/400, Pharmacia, Pfizer, New York, USA). The gel was electroblotted for 60 minutes onto a nitrocellulose membrane (Amersham Protran 0.45 $\mu$ m pore size premium nitrocellulose membrane, GE healthcare) in transfer buffer (1% running buffer, 20% v/v methanol) at 250mA/300V (EPS 500/400, Pharmacia). The membrane was cut into two at  $\sim$ 90kDa, and both parts blotted in 20mL Tris-buffered saline with tween (TST) containing 2% non-fat milk (non-fat dry milk blotting-grade blocker, Bio-Rad, Hercules, USA) for two hours (room temperature, gentle agitation). The TST was made by adding 8.76g sodium chloride, 1.21g Tris and 1mL Tween into distilled water, with the pH adjusted to 8.0. The top part of the membrane was stained overnight with 1:2,000 rabbit monoclonal anti-P-gp (ab170904, abcam, Cambridge, UK) primary antibody in TST/2% milk at 4 $^{\circ}$ C; the bottom half was similarly stained in 1:10,000 mouse monoclonal anti-beta actin (ab6276, abcam) primary antibody. After the primary antibody was washed off (4x four minute washes in TST/2% milk), the top and bottom parts of the membrane were stained with 1:4000 polyclonal goat anti-rabbit (P0448, Dako, Agilent Technologies) and 1:10000 polyclonal goat anti-mouse (P0447, Dako) secondary antibodies at room temperature for two hours in TST/2% milk, respectively. The secondary antibodies were washed off (4x four minute washes in TST/2% milk), and immunoreactivity was determined by chemiluminescence (western lightning<sup>®</sup> Plus-ECL enhanced chemiluminescence substrate, PerkinElmer, Waltham, USA) onto Amersham Hyperfilm ECL (GE Healthcare) with 30 second exposures. The experiment was carried out twice to confirm findings.

**Table 4.2 8% polyacrylamide gel preparation**

Component	Resolving Gel	Stacking Gel
ProtoGel (30%)	2.66mL	0.65mL
4x ProtoGel resolving buffer	2.6mL	-
ProtoGel stacking buffer	-	1.25mL
Distilled water	4.7mL	3.05mL
TEMED	10 $\mu$ L	5 $\mu$ L
10% ammonium persulphate	100 $\mu$ L	25 $\mu$ L

TEMED = *N,N,N',N'*-tetramethylene-ethylenediamine.

Ultra-pure ProtoGel (30% acrylamide), 4x ProtoGel resolving buffer, and ProtoGel stacking buffer were from national diagnostics (Atlanta, USA).

The resolving gel was made first in a universal tube, then rapidly pipetted into the dual gel caster (Hoefer) and left to air dry for 30-40 minutes. The stacking gel was similarly made, pipetted over the resolving gel with the comb *in situ* and left to air dry for 45 minutes.

## 4.2.8 Data analysis

### 4.2.8.1 PK study parameters

Non-compartmental PK parameters were calculated in Excel 2010 (Microsoft, Redmond, USA) using PK Solver: an add-in program for PK and pharmacodynamic data analysis in Microsoft Excel (Zhang *et al.*, 2010). Only concentrations above the LLOQ were included in the main analysis. For each individual mouse for each analyte, the following were planned to be calculated: the AUC to the last appropriate time point (AUC<sub>0-t</sub>), the terminal elimination half-life ( $t_{1/2}$ ) and both the peak concentration ( $C_{max}$ ) and time taken to reach it ( $t_{max}$ ). The apparent clearance (CL/F) and apparent volume of distribution ( $V_z/F$ ) for parent RVT and ATV were derived from their AUC<sub>0-8</sub>:

- $CL/F = \text{dose}/AUC_{0-8}$
- $V_z/F = (CL/F * t_{1/2})/\ln(2)$

A sensitivity analysis was carried out to assess the potential impact of including concentrations measured below the LLOQ in the determination of the AUC<sub>0-8</sub>,  $C_{max}$ ,  $t_{max}$  and  $t_{1/2}$  for each analyte, and the CL/F and  $V_z/F$  of RVT and ATV within the WT and HRN groups.

### 4.2.8.2 Microsomal enzyme kinetics

The maximum rate of formation ( $V_{max}$ ) and Michaelis-Menten constant ( $K_m$ ) were determined for the microsomal production of 2-OH and 4-OH ATV from

ATV by nonlinear least-squares regression according the equation,  $\text{rate} = V_{\text{max}} \cdot [\text{ATV}] / (K_m + [\text{ATV}])$ . This was carried out in GraphPad Prism (version 7.00 for Windows; GraphPad Software Inc., San Diego, USA) using its *Michaelis-Menten* enzyme kinetics function.

#### 4.2.8.3 Hypothesis testing

All data graphical representation was carried out in Excel 2010; summary statistics are reported as means  $\pm$  standard error. Hypothesis testing was not carried out for the PK study and microsome incubations because it was inappropriate given their low sample size (n=3 per group). However, the results from these studies were interpreted qualitatively. Hypothesis testing for iTRAQ protein expression differences (n=6 per group) was conducted using the Real Statistics Resource Pack Excel add-in (Zaiontz, 2016). Prior to hypothesis testing, the ProteinPilot™ expression ratios (individual mouse/pool) for each identified protein were log<sub>2</sub> transformed and batch mean-centred to remove batch effects between the two iTRAQ liver homogenate experimental runs (Boehm *et al.*, 2007; Lazar *et al.*, 2013). Proteins identified in both or just one iTRAQ run were retained for analysis. Hypothesis testing was carried out using unpaired student's t-test. Following calculation of these raw t-test p-values, Benjamini-Hochberg correction for multiple testing (n=3538 tests) was carried out so that only protein expression changes significant at < 5% FDR were considered statistically significant.

#### 4.2.8.4 Proteomics network analysis

The log<sub>2</sub> transformed batch-corrected expression fold changes of the 199 proteins that remained significant after multiple testing correction were uploaded to Ingenuity® Pathway Analysis (IPA® Version 01-07, Qiagen Bioinformatics, Redwood City, USA). IPA® core expression analysis was undertaken using the Ingenuity® Knowledge Base as reference with the following restrictions applied: experimentally observed confidence (i.e. high confidence of interaction) for any molecule and/or relationship, stringently

limited to results from mouse and either liver organ or hepatoma cell lines; network size was limited to  $\leq 35$  identified molecules per network to aid interpretation. The primary outputs considered were: interaction networks, toxicity lists and toxicity functions. IPA<sup>®</sup> networks are derived from the Ingenuity<sup>®</sup> Knowledge Base Global Molecular Network; networks determined from the uploaded expression data are ranked by calculation of p-scores ( $-\log_{10}$  (p-value)); the p-value is determined using right tailed Fisher's exact test and tests the probability of finding at least the number of identified (focus) molecules in a network of size n, in a set of n genes randomly selected from the Global Molecular Network. Toxicity lists are curated lists of molecules known to be involved in a particular type of toxicity and IPA<sup>®</sup> determines the proportion of molecules affected in each list. Toxicity function represents downstream analysis to identify clinical pathology endpoints given the observed expression changes. For toxicity lists and functions, IPA<sup>®</sup> calculates a p-value to determine the likelihood that the observed changes are due to chance and ranks identified lists/functions in order of decreasing statistical significance.  $p < 0.05$  is statistically significant. Only the top ( $\leq 5$ ) results for each output class from within the IPA<sup>®</sup> results summary were considered.

## 4.3 Results

### 4.3.1 *In vivo* PK study

The characteristics before, during and after the PK study of the mice (HRN=3, WT=3) are shown in Table 4.3. Although mouse body weight did not differ, HRN mice had uniformly larger livers and increased liver: body weight ratios than WT mice, consistent with previous reports (Henderson *et al.*, 2003; Grimsley *et al.*, 2014).

All mice tolerated the PK study adequately except B3, which looked unwell at one hour, did not improve and was culled at 8 hours. Therefore B3 missed blood sampling at the one and 24 hour time points. When undertaking percutaneous cardiac puncture on B3, a pericardial effusion was noted. The

named veterinary surgeon concluded that this individual mouse likely had a congenital/developmental defect in the CVS, and the dose pushed it into overt cardiac failure. The named veterinary surgeon did not think these symptoms were related to statin therapy, considered the dose and injection volume used appropriate, and therefore permissible for future studies. Blood was collected from all other mice at the specified times without exception.

**Table 4.3 Characteristics of the individual mice used in the *in vivo* PK study**

Characteristic	Wild type			Hepatic reductase null		
	A1	A2	A3	B1	B2	B3
<b>Genotype</b>	POR <sup>lox/lox</sup>	POR <sup>lox/lox</sup>	POR <sup>lox/lox</sup>	POR <sup>lox/lox</sup> + Cre <sup>ALB</sup>	POR <sup>lox/lox</sup> + Cre <sup>ALB</sup>	POR <sup>lox/lox</sup> + Cre <sup>ALB</sup>
<b>Start Weight (g)</b>	36.2	30.4	29.4	28.5	26.9	26.3
<b>ATV/RVT Dose (µg)</b>	1,080	900	900	870	810	780
<b>Dose Volume (µL)</b>	360	300	300	290	270	260
<b>Body weight PM (g)</b>	34.4	28.07	28.24	27.54	24.57	26.4
<b>Liver weight PM (g)</b>	1.56	1.46	1.5	2.36	1.93	1.8
<b>Liver; body weight ratio (%)</b>	4.50	5.20	5.30	8.60	7.90	6.80
<b>Weight loss (%)</b>	5	7.70	4	3.90	8.70	0
<b>Max Severity grade</b>	mild	mild	mild	mild	mild	moderate

Abbreviation: PM = post mortem. Statistical hypothesis testing was by unpaired student's t-test.

The QC results from the validated LC-MS analysis of the *in vivo* PK study DBS samples are shown in Table 4.4. The QCs were all acceptable, except for the medium QCs of the three L metabolites, which were consistently ~50% of their nominal concentration (75ng/mL). This was presumed to be a spiking error with the relevant L working solution given that the L low and high QCs were both highly acceptable and the calibration curves were all linear. It was not possible to re-extract and re-analyse the PK study samples because the collected DBS' (~20µL blood per mouse per time point) were insufficiently large for further punches.

**Table 4.4 Results from the quality control extracts included in the analytical run of the *in vivo* PK study dried blood spot extracts**

Analyte	Nominal conc. (ng/mL)	Mean (ng/mL)	Accuracy (%)	Precision, (CV, %)	Number of QC that passed
RVT	15	14.0	93.5	3.2	3 in 3
	500	553.3	110.7	3.9	3 in 3
	7500	7101.5	94.7	6.1	3 in 3
ATV	15	16.3	108.7	7.9	3 in 3
	500	569.3	113.9	1.7	3 in 3
	7500	7081.4	94.4	5.6	3 in 3
2-OH ATV	15	13.7	91.3	4.7	3 in 3
	75	77.1	102.8	4.9	3 in 3
	1000	1106.0	110.6	7.2	2 in 3
4-OH ATV	15	14.2	94.6	7.0	3 in 3
	75	78.5	104.7	6.0	3 in 3
	1000	1064.9	106.5	9.6	3 in 3
ATV L	15	13.9	92.4	0.8	3 in 3
	75	39.2	52.2	8.9	0 in 3
	1000	936.0	93.6	0.4	3 in 3
2-OH ATV L	15	13.6	90.5	4.1	3 in 3
	75	39.3	52.4	13.1	0 in 3
	1000	916.3	91.6	4.3	3 in 3
4-OH ATV L	15	13.2	88.0	8.1	2 in 3
	75	37.2	49.6	8.9	0 in 3
	1000	933.6	93.4	4.3	3 in 3

Three extracts at each quality control (QC) concentration were included in the analytical run. A QC had to be within 85-115% of the nominal QC concentration to pass. All QCs were acceptable except for the medium QC of all three ATV lactones, which was consistently ~50% of the nominal concentration, and presumed to be a spiking error with the relevant lactones working solution because the low and high QCs uniformly passed and the calibration curves are all linear.

#### 4.3.1.1 Individual subject blood statin concentrations

The *in vivo* PK study blood concentrations of RVT, ATV, and ATV metabolites for each subject are reported in Table 4.5. The corresponding individual blood concentration-time profiles for each analyte are presented in Figure 4.1. All 24 hour concentrations were substantially below the LLOQ, did not contribute to data interpretation, and so were not considered further. All measured 4-OH ATV L concentrations were below the LLOQ and so 4-OH ATV L was not investigated further. As seen in Figure 4.1, the degree of exposure to each analyte is correlated within each individual relative to the exposures observed in the other mice; of note, WT A1 had the lowest exposure to all analytes, and in particular all concentrations of both 4-OH ATV and 2-OH ATV L in A1 were below the LLOQ (Table 4.5).

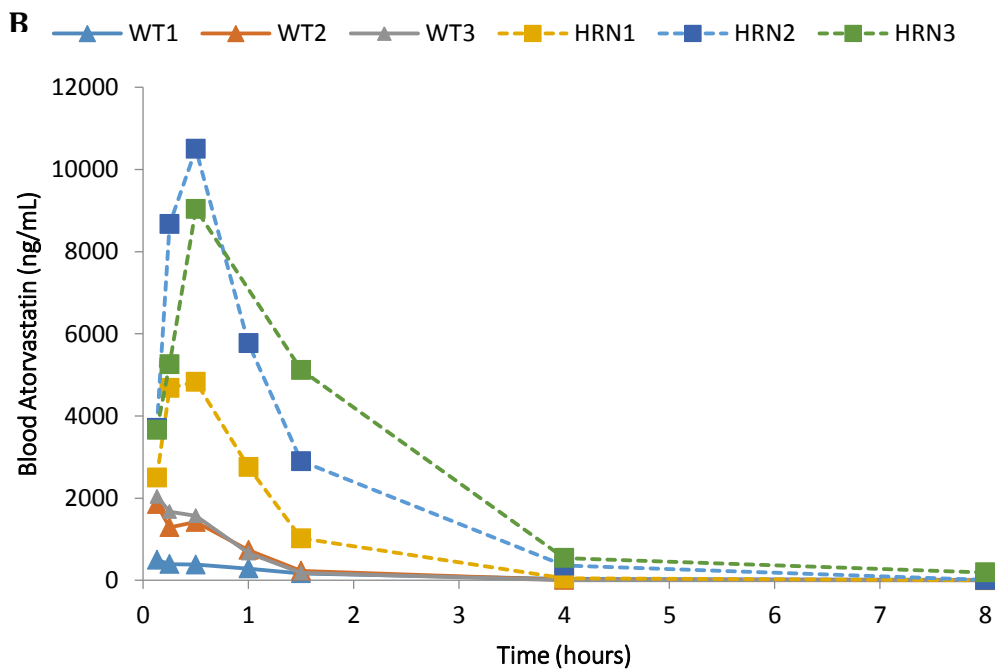
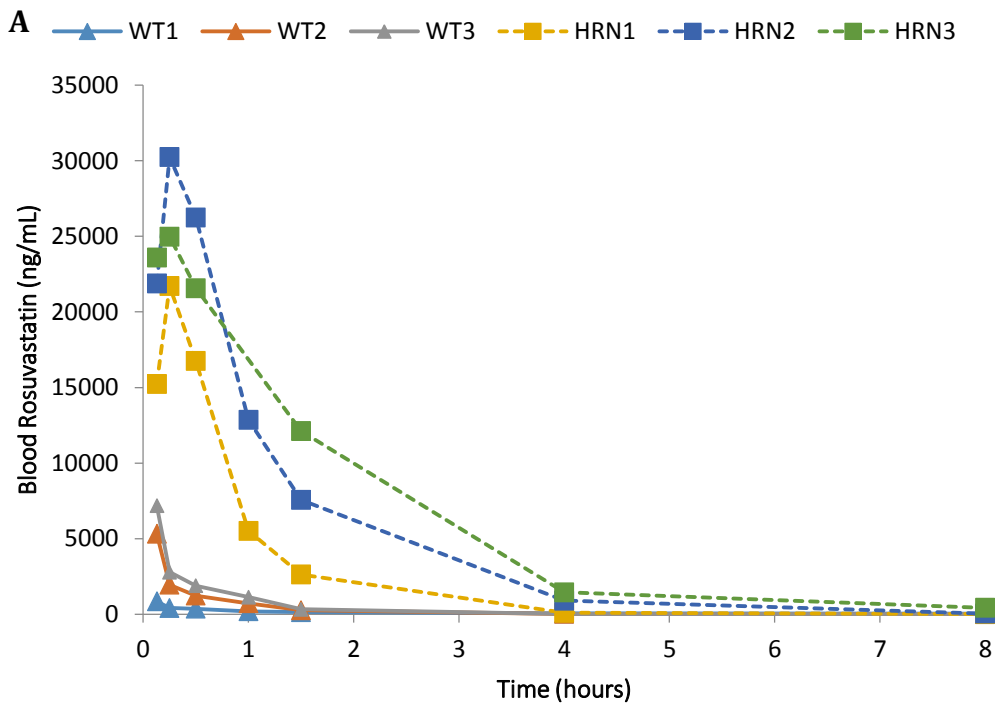
**Table 4.5 Individual subject blood concentrations of RVT, ATV and ATV metabolites**

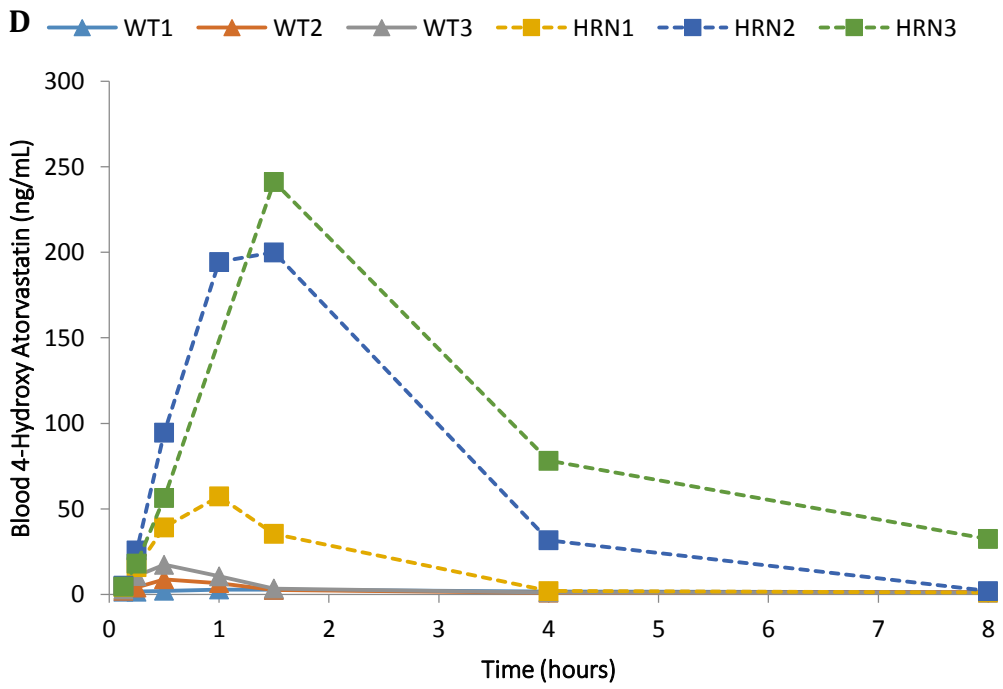
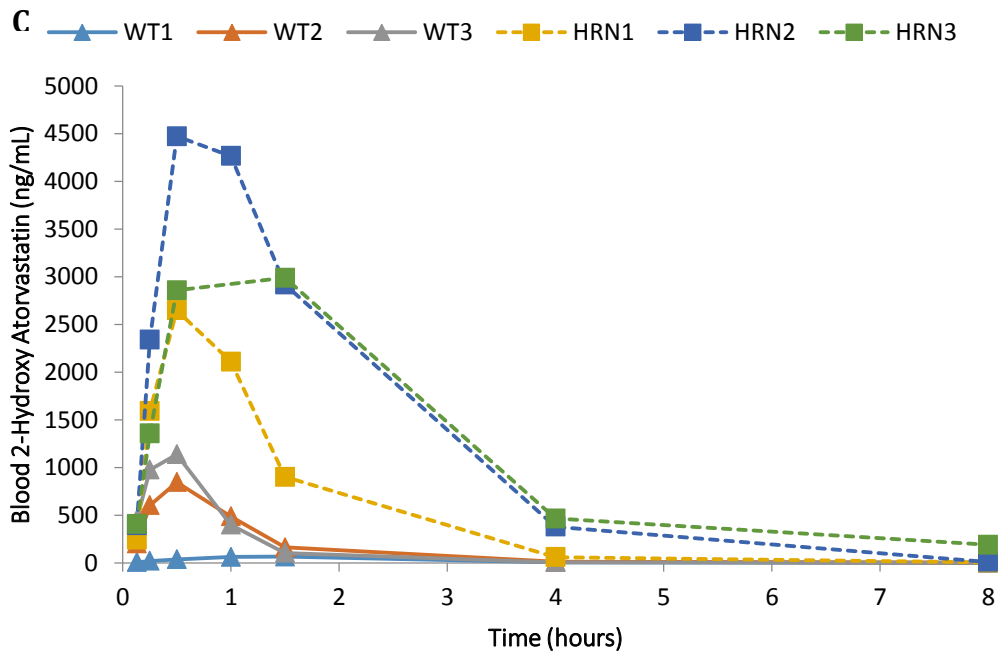
Time (hours)	Concentration (ng/mL)					
	Wild type			Hepatic reductase null		
	A1	A2	A3	B1	B2	B3
<b>RVT</b>						
0.13	844.0	5320.0	7180.0	15244.0	21885.3	23605.8
0.25	411.0	1950.0	2790.0	21713.2	30247.1	24982.2
0.50	362.0	1230.0	1890.0	16758.1	26255.4	21575.6
1	186.0	724.0	1130.0	5520.0	12869.6	ND
1.5	134.0	268.0	326.0	2630.0	7560.0	12112.6
4	49.7	22.9	11.5	98.9	902.0	1450.0
8	27.9	10.3	11.7	16.0	46.8	425.0
24	0.2	0.3	< 0	< 0	0.4	ND
<b>ATV</b>						
0.13	500.0	1850.0	2040.0	2500.0	3710.0	3660.0
0.25	392.0	1290.0	1670.0	4680.0	8670.0	5260.0
0.50	381.0	1420.0	1570.0	4830.0	10500.0	9040.0
1	283.0	738.0	663.0	2760.0	5770.0	ND
1.5	168.0	232.0	182.0	1020.0	2900.0	5120.0
4	33.3	8.2	4.2	45.9	358.0	541.0
8	12.0	1.8	1.1	4.3	6.8	193.0
24	0.8	0.6	0.6	0.4	0.3	ND
<b>2-OH ATV</b>						
0.13	7.8	204.0	454.0	242.9	395.7	409.5
0.25	22.1	606.0	978.0	1593.2	2339.9	1359.2
0.50	39.1	848.0	1140.0	2649.6	4473.4	2859.5
1	64.3	489.0	401.0	2110.0	4266.9	ND
1.5	67.3	165.0	105.0	902.0	2920.0	2990.3
4	9.1	14.3	8.9	62.8	381.0	466.0
8	2.2	5.0	2.7	7.3	11.6	192.0
24	0.6	0.3	0.3	0.5	0.2	ND
<b>4-OH ATV</b>						
0.13	1.5	2.2	2.8	4.3	5.1	4.6
0.25	1.6	4.1	10.8	15.9	25.6	18.1
0.50	2.1	8.8	17.3	39.2	94.6	56.4
1	2.8	6.6	10.6	57.3	194.4	ND
1.5	2.7	2.6	3.4	35.4	200.0	241.2
4	1.6	0.9	1.2	2.0	31.6	78.2
8	1.3	1.2	1.0	1.1	2.0	32.4
24	1.2	1.3	1.1	1.1	0.9	ND
<b>ATV L</b>						
0.13	4.0	14.4	17.8	46.2	43.9	49.5
0.25	4.6	12.6	18.5	110.0	156.0	74.1
0.50	6.2	14.2	18.3	126.0	139.0	109.0
1	3.5	8.5	9.3	66.8	114.0	ND
1.5	2.3	3.9	3.4	31.0	65.4	70.2
4	0.5	0.7	0.4	2.8	10.3	13.0
8	0.4	0.4	0.4	0.6	0.7	1.6
24	0.3	0.3	0.3	0.4	0.3	ND

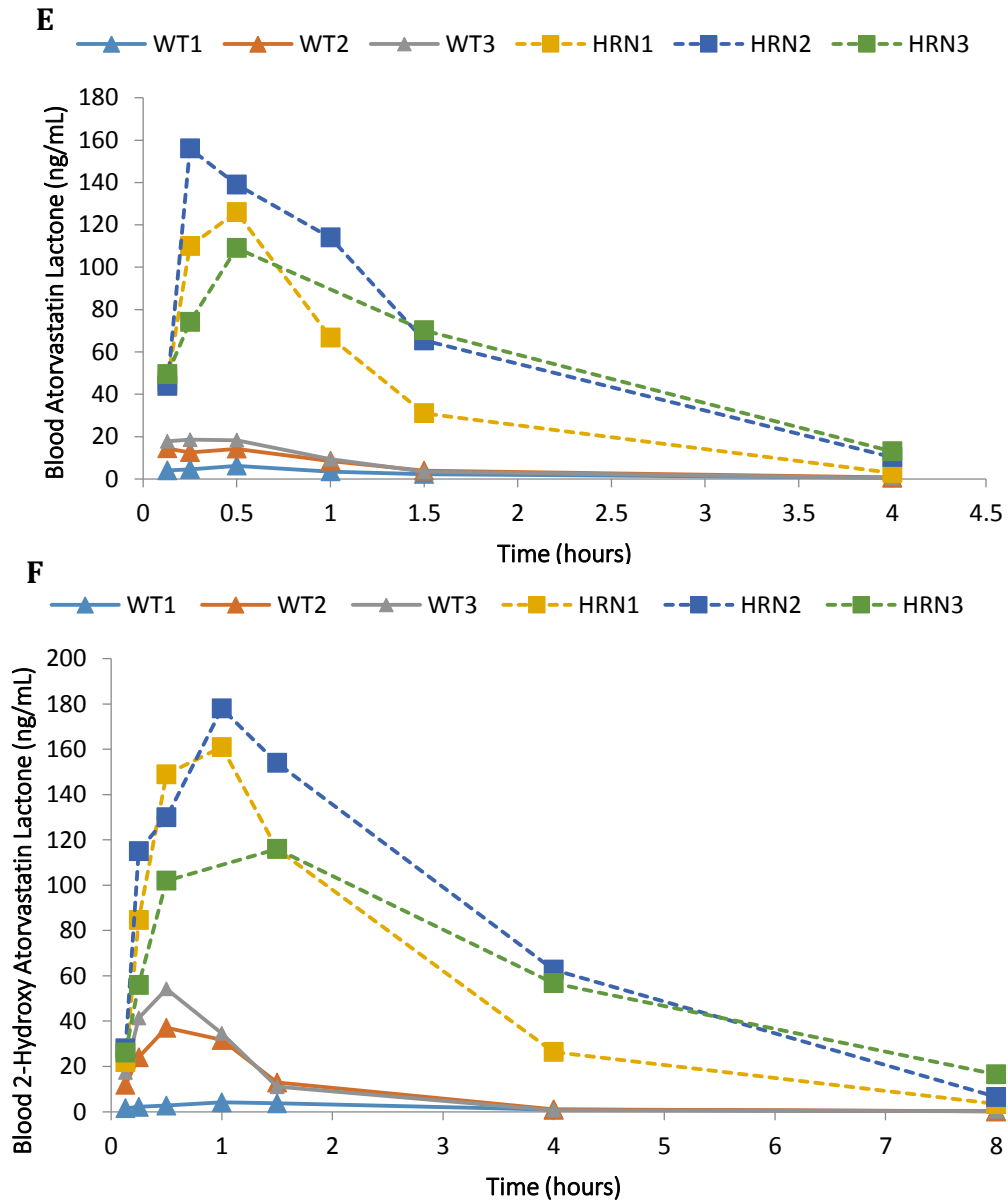
<i>Table continued</i>						
Time (hours)	Concentration (ng/mL)					
	Wild type			Hepatic reductase null		
	A1	A2	A3	B1	B2	B3
<b>2-OH ATV L</b>						
0.13	1.5	11.9	17.4	21.9	28.0	26.1
0.25	2.2	24.1	41.4	84.7	115.0	56.0
0.50	2.7	37.1	54.2	149.0	130.0	102.0
1	4.2	31.7	34.6	161.0	178.0	ND
1.5	3.7	12.9	11.1	116.0	154.0	116.0
4	0.9	1.0	0.7	26.4	62.7	56.8
8	0.2	0.2	0.2	3.4	6.6	16.5
24	0.1	0.1	< 0	0.2	0.1	ND
<b>4-OH ATV L</b>						
0.13	0.3	0.5	0.9	0.4	0.5	0.6
0.25	0.4	1.0	1.8	1.5	1.8	1.0
0.50	0.6	1.5	3.0	2.6	3.2	2.4
1	0.4	1.3	1.6	3.9	4.2	ND
1.5	0.5	0.4	0.6	2.6	3.8	4.1
4	0.3	0.2	0.2	0.1	1.7	2.2
8	0.2	0.1	0.2	0.3	0.5	3.3
24	0.2	0.2	0.1	0.2	0.3	ND

Abbreviation: ND = not done. Three WT and three HRN adult male C57BL/6 mice each received a single intraperitoneal injection containing RVT (30mg/Kg) plus ATV (30mg/Kg). ~20µL blood was collected at 0.13, 0.25, 0.5, 1.0, 1.5, 4.0, 8.0 and 24.0 hours in all mice except HRN B3, which was not sampled at 1.0 and 24 hours. The blood samples were spotted onto FTA Elute card via a K2 EDTA-coated glass capillary. All blood, except for the final sample, was collected via the lateral caudal veins; the final sample was collected by percutaneous cardiac puncture after culling by rising carbon dioxide. The animals were housed under standard conditions with unlimited access to food and water and a 12-hour light/dark cycle throughout the study. LC-MS/MS bioanalysis was carried out within two days of sample collection. The LLOQ was 5ng/mL. Concentrations measured below the LLOQ are reported, but highlighted in red.

**Figure 4.1 Individual subject concentration-time profiles of RVT, ATV and ATV metabolites**







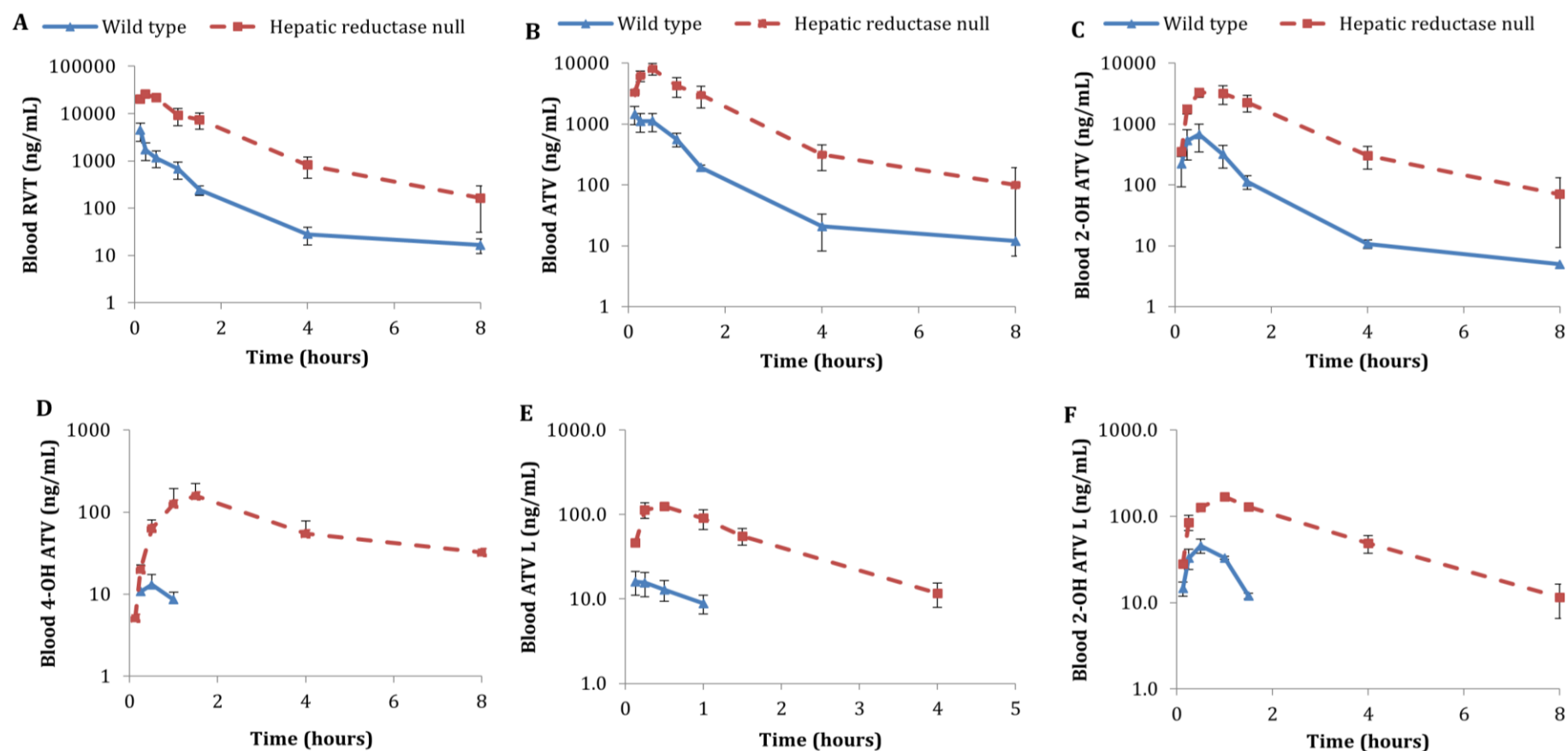
Individual concentration-time profiles of RVT (A), ATV (B), 2-OH ATV (C), 4-OH ATV (D), ATV L (E) and 2-OH ATV L (F) were determined from three individual WT (triangles) and three individual HRN (squares) adult male C57BL/6 mice, following a single intra-peritoneal injection containing RVT and ATV at 30mg/Kg. Blood was sampled at 0.13, 0.25, 0.5, 1.0, 1.5, 4, 8 and 24 hours after dosing in all mice, except HRN B3, which was not sampled at 1.0 and 24 hours. All concentrations determined up to 8 hours are shown (including if less than the LLOQ). However, the 24 hour time point is not shown because it was uniformly below the LLOQ, and did not add significantly to interpretation of the data.

#### 4.3.1.2 Main analysis composite PK results

The main analysis composite concentration-time profiles for each analyte in the HRN (n=3) and WT (n=3) groups are shown in Figure 4.2. Composite PK parameters are reported in Table 4.6. Following visual inspection of Figure 4.2, it was decided to calculate only the mean  $C_{max}$  and  $t_{max}$ , and not the  $AUC_{0-t}$  and  $t_{1/2}$ , for 4-OH ATV, ATV L and 2-OH ATV L in the WT group because there were limited concentrations of these analytes above the LLOQ in the WT mice. Furthermore, the  $t_{1/2}$  of 4-OH ATV was not reported for the WT or HRN groups because its terminal elimination rate constant ( $\lambda_z$ ) could not be derived for five of the six mice (all except HRN B3) because too few points above the LLOQ covered the elimination phase.

The main analysis results showed that  $C_{max}$  was consistently higher in HRN compared to WT mice for all analytes (Table 4.6). The systemic exposures ( $AUC_{0-t}$ ) of RVT, ATV and 2-OH ATV were also consistently higher in the HRN group, with HRN to WT  $AUC_{0-t}$  fold changes of 16, 10 and 11, respectively. Furthermore, although the AUC was not formally determined for 4-OH ATV, ATV L and 2-OH ATV L, it is clear from inspection of Figure 4.2 that the exposures of these analytes were similarly much higher in the HRN group. Interestingly,  $t_{max}$  was prolonged in the HRN mice for RVT, ATV, 4-OH ATV and 2-OH ATV L. On the whole, the  $t_{1/2}$  did not differ substantially between WT and HRN mice. The CL/Fs of parent RVT and ATV were markedly slower in the HRN group (Table 4.6).

**Figure 4.2 Composite concentration-time profiles of RVT, ATV and ATV metabolites**



Mean ( $\pm$  standard error) concentration-time profiles of RVT (A), ATV (B), 2-OH ATV (C), 4-OH ATV (D), ATV L (E) and 2-OH ATV L (F) from three WT (blue continuous line) and three HRN (red dashed line) adult male C57BL/6 mice, following a single intra-peritoneal dose of RVT and ATV (30mg/Kg). Only concentrations above the LLOQ are included in this main analysis

**Table 4.6 Summary of main analysis analyte PK parameters**

PK parameter	WT	HRN
<b>RVT</b>		
<b>AUC<sub>0-t</sub> (ng.hr/mL)</b>	2207.8 ± 729.6	35675.8 ± 8675.5
<b>t<sub>max</sub> (hr)</b>	0.1 ± 0.003	0.3 ± 0.003
<b>C<sub>max</sub> (ng/mL)</b>	4448.0 ± 1880.3	25647.5 ± 2485.9
<b>t<sub>1/2</sub> (hr)</b>	1.5 ± 0.6	1.0 ± 0.2
<b>V<sub>z</sub>/F (mL)</b>	1904.9 ± 1470.5	34.5 ± 6.7
<b>CL/F (mL/min)</b>	10.7 ± 5.4	0.5 ± 0.2
<b>ATV</b>		
<b>AUC<sub>0-t</sub> (ng.hr/mL)</b>	1352.2 ± 277.9	12981.3 ± 3678.7
<b>t<sub>max</sub> (hr)</b>	0.1 ± 0.003	0.5 ± 0.007
<b>C<sub>max</sub> (ng/mL)</b>	1463.3 ± 484.8	8123.3 ± 1699.7
<b>t<sub>1/2</sub> (hr)</b>	0.8 ± 0.3	0.9 ± 0.2
<b>V<sub>z</sub>/F (mL)</b>	1132.8 ± 804.0	84.6 ± 16.3
<b>CL/F (mL/min)</b>	13.6 ± 4.3	1.4 ± 0.5
<b>2-OH ATV</b>		
<b>AUC<sub>0-t</sub> (ng.hr/mL)</b>	719.4 ± 275.6	7786.4 ± 1934.7
<b>t<sub>max</sub> (hr)</b>	0.8 ± 0.3	0.8 ± 0.3
<b>C<sub>max</sub> (ng/mL)</b>	685.1 ± 320.2	3371.1 ± 559.9
<b>t<sub>1/2</sub> (hr)</b>	0.8 ± 0.2	1.1 ± 0.3
<b>4-OH ATV</b>		
<b>AUC<sub>0-t</sub> (ng.hr/mL)</b>	ND	447.8 ± 214.6
<b>t<sub>max</sub> (hr)</b>	0.5 ± 0.0	1.3 ± 0.2
<b>C<sub>max</sub> (ng/mL)</b>	13.1 ± 3.5	166.2 ± 55.7
<b>t<sub>1/2</sub> (hr)</b>	ND	ND
<b>ATV L</b>		
<b>AUC<sub>0-t</sub> (ng.hr/mL)</b>	ND	200.1 ± 44.8
<b>t<sub>max</sub> (hr)</b>	0.3 ± 0.1	0.4 ± 0.07
<b>C<sub>max</sub> (ng/mL)</b>	13.0 ± 3.6	130.3 ± 13.7
<b>t<sub>1/2</sub> (hr)</b>	ND	0.9 ± 0.2
<b>2-OH ATV L</b>		
<b>AUC<sub>0-t</sub> (ng.hr/mL)</b>	ND	496.6 ± 72.5
<b>t<sub>max</sub> (hr)</b>	0.5 ± 0.0	1.2 ± 0.2
<b>C<sub>max</sub> (ng/mL)</b>	45.7 ± 7.0	151.7 ± 18.5
<b>t<sub>1/2</sub> (hr)</b>	ND	1.7 ± 0.3

-Only analyte concentrations above the LLOQ (5ng/mL) in the *in vivo* PK study were included in this main analysis. Mean ± standard error reported.

-Apparent clearance and volume of distribution were limited to parent RVT and ATV as their administered dose was known.

-It was decided that there were too few concentrations of 4-OH ATV, ATV L and 2-OH ATV L above the LLOQ in the WT mice to determine their AUC<sub>0-t</sub> and t<sub>1/2</sub>.

-The t<sub>1/2</sub> of 4-OH ATV could not be estimated in either the WT or HRN groups because, after removal of concentrations below the LLOQ, there were too few remaining points covering the elimination phase to determine the terminal elimination rate constant (lambda z) for all mice except B3.

#### 4.3.1.3 Sensitivity analysis of PK results

In the sensitivity analysis, all concentrations below the LLOQ up to the eight hour post dose time point were also considered; Table 4.7 shows the resulting

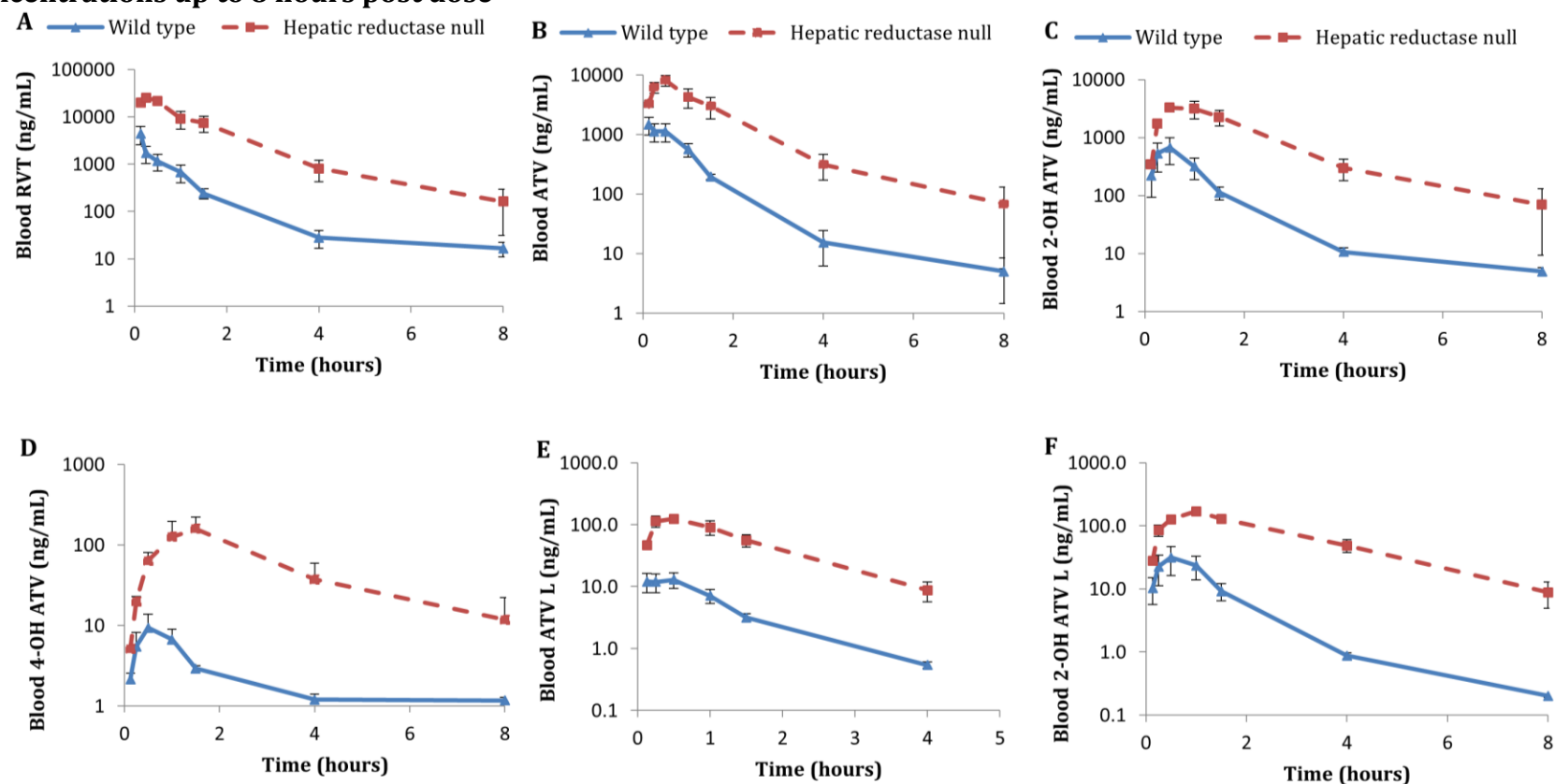
analyte PK parameter estimations, Figure 4.3 the composite concentration-time profiles, and Figure 4.4 the individual and mean analyte systemic exposures. Importantly, on inspection the sensitivity analysis results were consistent with the main results. Of note, the calculated exposure ( $AUC_{0-8}$ ) of all analytes was substantially higher in the HRN compared to WT mice.

**Table 4.7 Sensitivity analysis of analyte PK parameters**

PK parameter	WT	HRN
<b>RVT</b>		
Dose (mg/Kg)	30	30
$AUC_{0-8}$ (ng.hr/mL)	2207.8 ± 729.6	35675.8 ± 8675.5
$t_{max}$ (hr)	0.1 ± 0.003	0.3 ± 0.003
$C_{max}$ (ng/mL)	4448.0 ± 1880.3	25647.5 ± 2485.9
$t_{1/2}$ (hr)	1.4 ± 0.4	1.0 ± 0.2
$V_z/F$ (mL)	1662.9 ± 1228.7	34.5 ± 6.7
CL/F (mL/min)	10.7 ± 5.4	0.5 ± 0.2
<b>ATV</b>		
Dose (mg/Kg)	30	30
$AUC_{0-8}$ (ng.hr/mL)	1443.3 ± 315.3	12953.7 ± 3648.0
$t_{max}$ (hr)	0.1 ± 0.003	0.5 ± 0.007
$C_{max}$ (ng/mL)	1463.3 ± 484.8	8123.3 ± 1699.7
$t_{1/2}$ (hr)	1.0 ± 0.2	0.9 ± 0.2
$V_z/F$ (mL)	1263.4 ± 738.3	97.4 ± 28.5
CL/F (mL/min)	13.1 ± 4.5	1.3 ± 0.5
<b>2-OH ATV</b>		
$AUC_{0-8}$ (ng.hr/mL)	734.2 ± 272.2	7786.4 ± 1934.7
$t_{max}$ (hr)	0.8 ± 0.3	0.8 ± 0.3
$C_{max}$ (ng/mL)	685.1 ± 320.2	3371.1 ± 559.9
$t_{1/2}$ (hr)	1.1 ± 0.1	1.1 ± 0.3
<b>4-OH ATV</b>		
$AUC_{0-8}$ (ng.hr/mL)	18.6 ± 3.0	487.4 ± 200.5
$t_{max}$ (hr)	0.7 ± 0.2	1.3 ± 0.2
$C_{max}$ (ng/mL)	9.7 ± 4.2	166.2 ± 55.7
$t_{1/2}$ (hr)	3.6 ± 1.3	1.5 ± 0.4
<b>ATV L</b>		
$AUC_{0-8}$ (ng.hr/mL)	19.4 ± 4.1	233.6 ± 35.7
$t_{max}$ (hr)	0.3 ± 0.1	0.4 ± 0.1
$C_{max}$ (ng/mL)	13.0 ± 3.6	130.3 ± 13.7
$t_{1/2}$ (hr)	1.5 ± 0.2	1.1 ± 0.1
<b>2-OH ATV L</b>		
$AUC_{0-8}$ (ng.hr/mL)	45.7 ± 16.6	515.9 ± 56.1
$t_{max}$ (hr)	0.7 ± 0.2	1.2 ± 0.2
$C_{max}$ (ng/mL)	31.8 ± 14.7	151.7 ± 18.5
$t_{1/2}$ (hr)	1.1 ± 0.2	1.7 ± 0.3

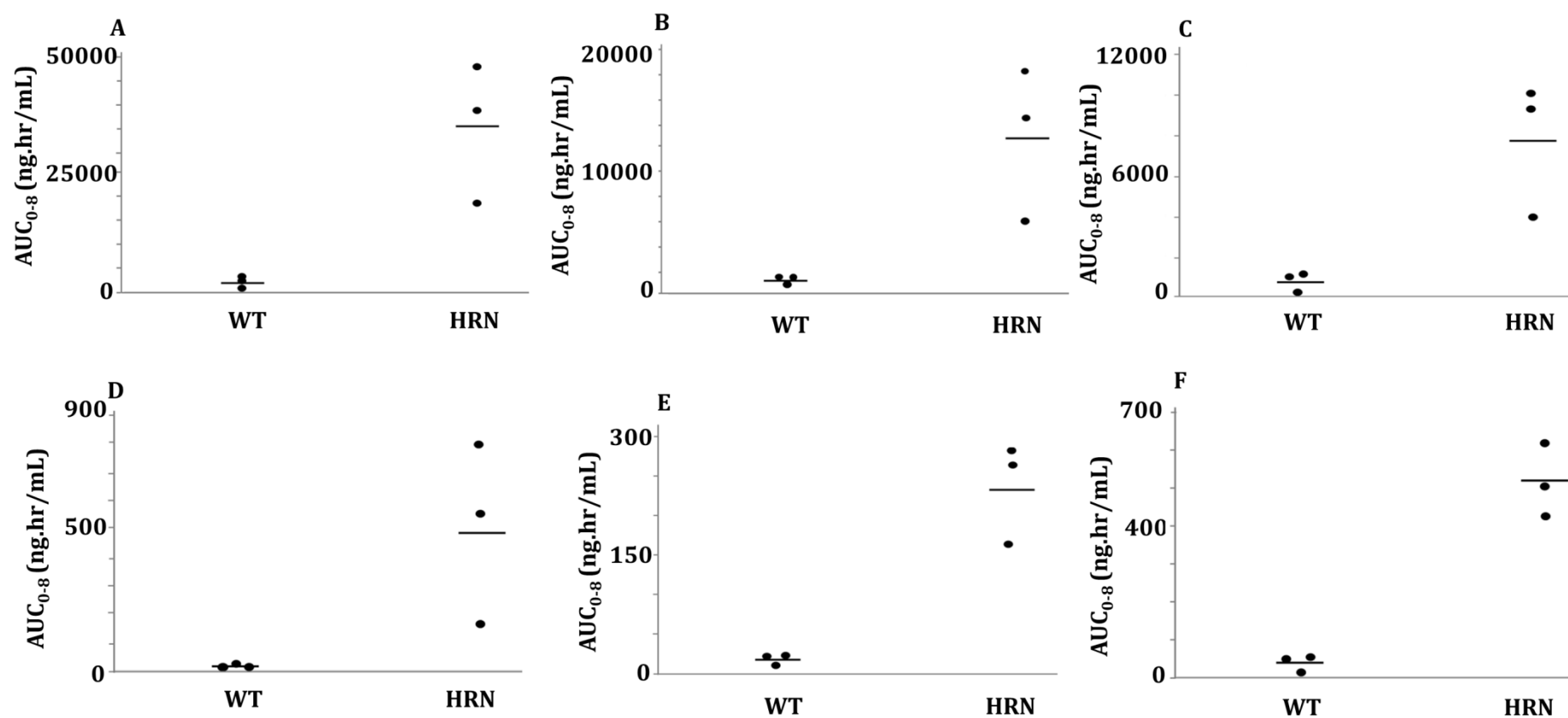
All data points up to the 8 hour time point were used. Mean ± standard error reported. Apparent clearance and volume of distribution were limited to parent RVT and ATV as their administered dose was known.

**Figure 4.3 Sensitivity analysis composite concentration-time profiles of RVT, ATV and ATV metabolites including all concentrations up to 8 hours post dose**



Mean ( $\pm$  standard error) concentration-time profiles of RVT (A), ATV (B), 2-OH ATV (C), 4-OH ATV (D), ATV L (E) and 2-OH ATV L (F) from three WT (blue continuous line) and three HRN (red dashed line) adult male C57BL/6 mice, following a single intra-peritoneal dose of RVT and ATV (30mg/Kg). This figure includes all concentrations (above and below the LLOQ) up to the eight hour time point.

**Figure 4.4 Sensitivity analysis individual and mean analyte systemic exposures including all concentrations up to 8 hours post dose**



Individual mouse (black dots) and mean (horizontal line) systemic exposures (AUC<sub>0-t</sub>, ng/hr/mL) of the three WT and three HRN mice for RVT (A), ATV (B), 2-OH ATV (C), 4-OH ATV (D), ATV L (E) and 2-OH ATV L (F), following a single intra-peritoneal dose containing both RVT and ATV at 30mg/Kg. This figure includes all concentrations (above and below the LLOQ) up to the eight hour time point.

Using the sensitivity analysis  $AUC_{0-8}$  values (because the WT  $AUC_{0-t}$  of ATV L was not calculated in the main analysis), the metabolic ratios of 2-OH ATV to parent ATV, and ATV L to ATV, were determined. However, they did not differ notably between WT and HRN groups (Table 4.8).

**Table 4.8 Ratios of exposure to main acid or lactone metabolite over ATV**

PK parameter	2-OH ATV / ATV		ATV L / ATV	
	WT	HRN	WT	HRN
<b><math>AUC_{0-8}</math> ratio</b>	0.46 ± 0.11	0.62 ± 0.06	0.013 ± 0.00033	0.020 ± 0.0038

For each individual, the ratio of 2-OH ATV/ATV, or ATV L/ATV was determined. The mean ratio ± standard error in the HRN and WT groups is reported.

#### 4.3.1.4 *In vivo* PK study summary

The increased ATV exposure and reduced ATV clearance in the HRN group was expected, given the hepatic Por knock out in HRN mice. However, the PK study produced some surprising results. First, the elevated RVT exposure was unanticipated given that RVT is only minimally metabolised. Second, the apparent elevated levels of Cyp-mediated ATV metabolites (2-OH ATV, 4-OH ATV and 2-OH ATV L) were unexpected given the anticipated reduction in Cyp metabolism in HRN mice. The apparent elevated ATV L and 2-OH ATV L levels suggested increased metabolism in the HRN mice via an alternative pathway. Therefore, subsequent experiments were performed to investigate these findings further.

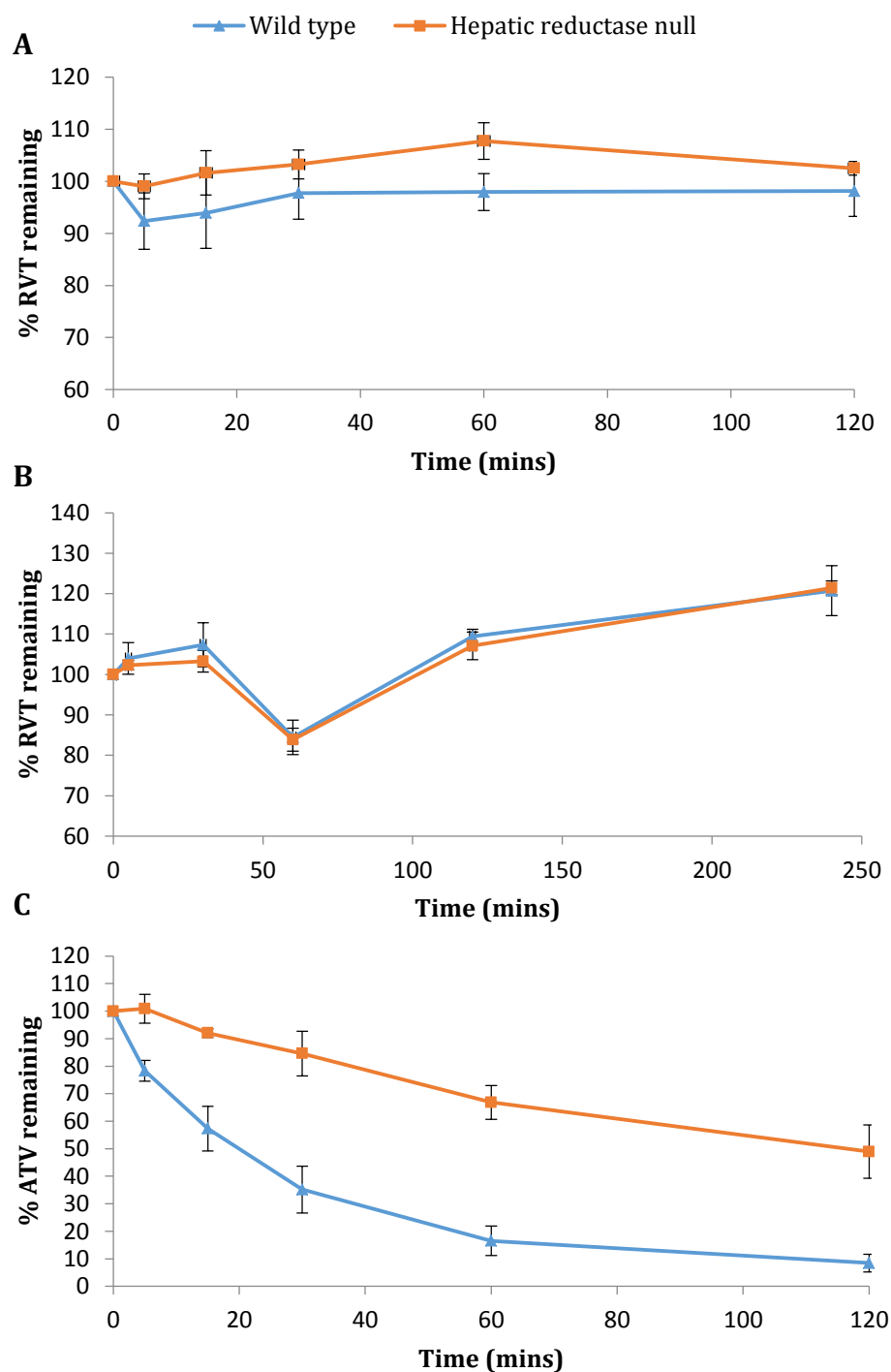
### 4.3.2 Microsomal incubations

The *in vitro* liver NADPH-activated microsomal incubations demonstrated that RVT levels did not differ between WT or HRN incubated microsomes, confirming that RVT undergoes minimal Cyp-mediated metabolism (Figure 4.5 A, B, Figure 4.7 A).

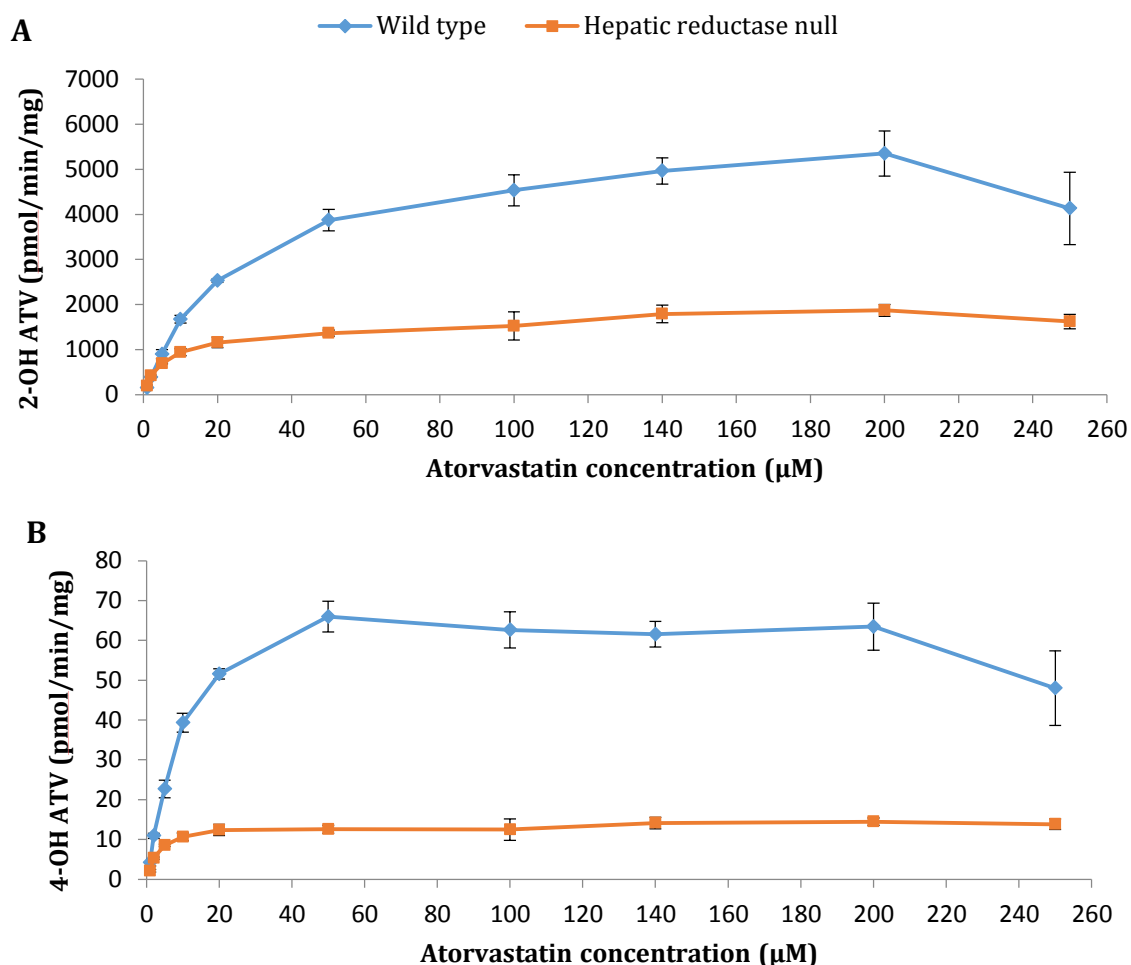
As expected, the proportion of ATV remaining over time reduced substantially more slowly in HRN compared to WT NADPH-activated microsomes (Figure 4.5 C), and the maximal rates of production ( $V_{\max}$ ) of both 2-OH ATV and 4-OH ATV were consistently lower in HRN liver microsomes (Figure 4.6, Table 4.9).

The controls in the hepatic microsomal incubations confirmed that RVT undergoes minimal hydroxylation (Figure 4.7 A) and ATV hydroxylation requires functional NADPH-activated microsomes (Figure 4.7 B).

**Figure 4.5 Proportion of RVT and ATV remaining over time in hepatic microsomes**



Mean (from  $n=3$ )  $\pm$  standard error of the percent remaining over time of RVT (20 $\mu$ M [A] and 5 $\mu$ M [B]) or ATV (20 $\mu$ M [C]) in incubations of hepatic microsomes (0.5mg/mL) from WT or HRN mice, activated with NADPH (1mM) in an initial reaction volume of 200 $\mu$ L agitated in a water bath at 37°C. For the 20 $\mu$ M RVT and ATV experiments, 25 $\mu$ L aliquots were removed from the reaction mixture at 0, 5, 15, 30, 60, and 120 minutes. The proportion of RVT remaining from 5 $\mu$ M RVT was determined with 25 $\mu$ L aliquots at times 0, 5, 30, 60, 120 and 240 minutes. The aliquots were added to 200 $\mu$ L ice-chilled 100% acetonitrile containing internal standard to terminate their reaction, and subsequently analysed by LC-MS/MS. There was no difference in RVT levels, but ATV decreased much more slowly in the HRN compared to WT microsomes.

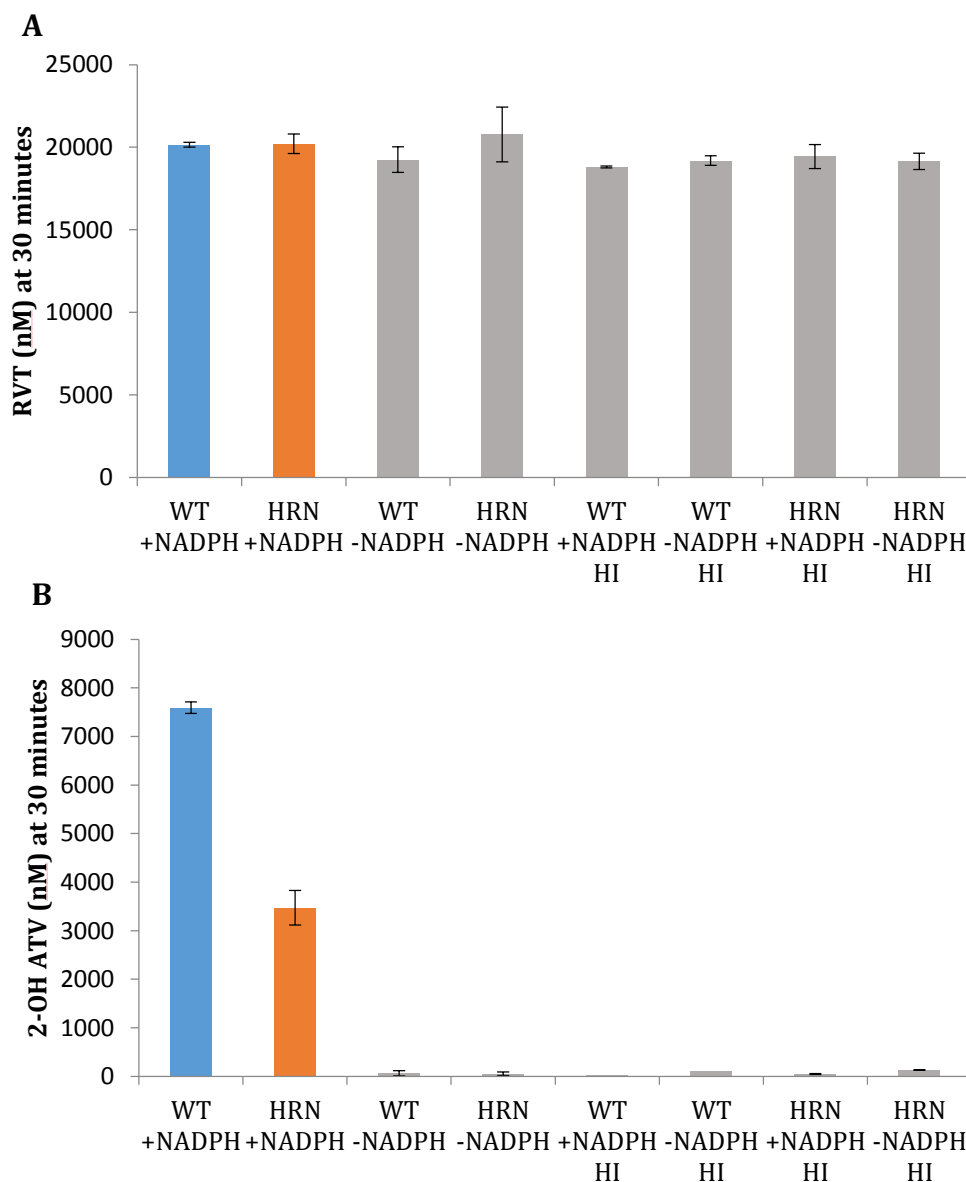
**Figure 4.6 Rates of formation of 2- and 4-OH ATV in hepatic microsomes activated with NADPH**

Mean (n=3)  $\pm$  standard error of formation of 2-OH ATV (A) and 4-OH ATV (B) from increasing concentrations of ATV in WT or HRN hepatic microsomes (0.5mg/mL) activated with NADPH (1mM) in a reaction volume of 200 $\mu$ L agitated at 37°C in a water bath. A 50 $\mu$ L aliquot was taken at 30 minutes and quenched in 200 $\mu$ L of ice-chilled 100% acetonitrile containing internal standard. ATV hydroxylation was consistently attenuated in HRN compared to WT microsomes.

**Table 4.9 Enzyme kinetics for 2-OH and 4-OH ATV microsomal formation**

	WT	HRN
<b>2-OH ATV</b>		
$V_{max}$ (pmol/min/mg microsome protein)	5393 $\pm$ 275.4	1764 $\pm$ 77.9
$K_m$ ( $\mu$ M)	21.6 $\pm$ 4.5	8.8 $\pm$ 1.9
<b>4-OH ATV</b>		
$V_{max}$ (pmol/min/mg microsome protein)	64.0 $\pm$ 2.8	14.1 $\pm$ 0.5
$K_m$ ( $\mu$ M)	6.9 $\pm$ 1.5	3.5 $\pm$ 0.8

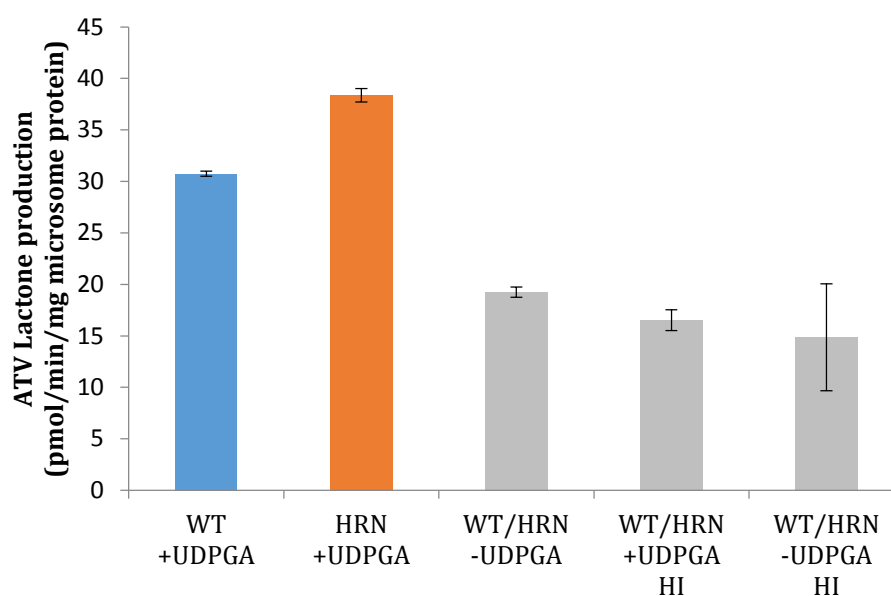
The maximum rate of formation ( $V_{max}$ ) and Michaelis-Menten constant ( $K_m$ ) were determined for the microsomal production of 2-OH and 4-OH ATV from ATV by nonlinear least-squares regression according to the equation, rate =  $V_{max} \cdot [ATV] / (K_m + [ATV])$ . Mean (from n=3)  $\pm$  standard error reported.

**Figure 4.7 Hepatic microsome active and control incubations**

RVT (A) or 2-OH ATV (B) detected after 30 minutes incubation at 37°C in WT or HRN hepatic microsomes (0.5mg/mL) under active (blue and red bars) or control (brown bars) conditions following administration of 20µM RVT (A) or 20µM ATV (B). Mean (from n=3 for active, and n=2 for control conditions) ± standard errors shown. 4-OH ATV production is not shown because no 4-OH ATV was detected in any control condition. HI = heat inactivation of microsomes carried out by heating at 80°C for 10 minutes; +NADPH = nicotinamide adenine dinucleotide phosphate present in reaction mixture (1mM); -NADPH = NADPH omitted from incubation. There was no observed difference between active microsomes and controls for RVT; both active HRN and active WT microsomes produced substantially more 2-OH ATV than any of the control conditions.

As expected, both WT and HRN functional UDPGA-activated microsomes produced more ATV L than controls (Figure 4.8). Interestingly, UDPGA-activated HRN functional microsomes produced demonstrably more ATV L compared to WT microsomes (Figure 4.8).

**Figure 4.8 Apparent rate of formation of ATV L in hepatic microsomal incubations activated with UDPGA**



Mean  $\pm$  standard error of ATV L production after administration of 20 $\mu$ M ATV to WT (active, blue bar), HRN (active, red bar), and combined WT+HRN (controls, grey bars) hepatic microsomes, sampled at 30 minutes. N=3 reactions for UDPGA-activated WT and HRN microsomes, and n=2 reactions for each control condition.

HI = heat inactivation of microsomes carried out by heating at 80°C for 10 minutes; +UDPGA = uridine 5'-diphosphoglucuronic acid present (5mM); -UDPGA = UDPGA absent.

The rate of ATV L production was notably higher in the UDPGA-activated HRN microsomes compared to the WT microsomes.

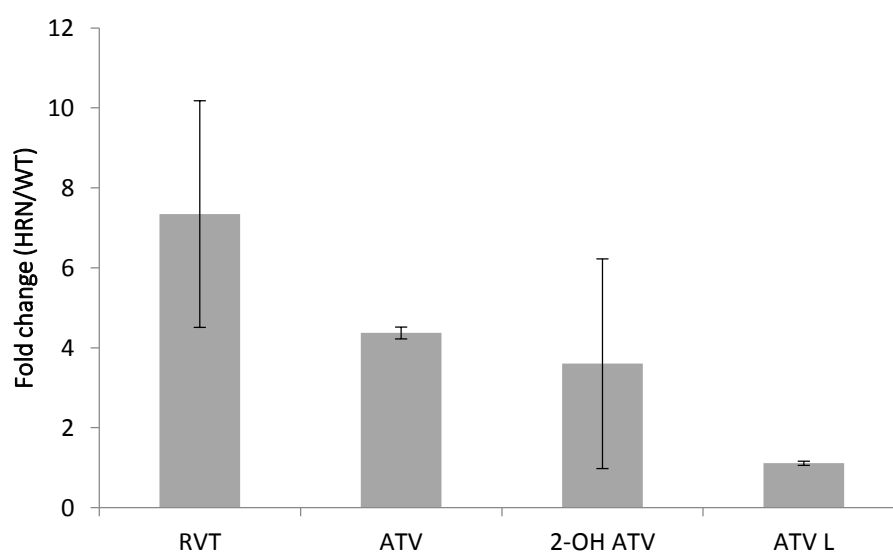
ATV L production was higher for both UDPGA-activated WT and HRN microsomes compared to all controls.

### 4.3.3 *In vivo* PK study liver characterisation

To further investigate the *in vivo* results, analyte levels in liver homogenates from the 5 mice that completed the full 24 hours of the PK study (WT n=3, HRN n=2) underwent exploratory relative quantification (Figure 4.9). Signal: background noise was >3x for RVT, ATV, 2-OH ATV and ATV L, but less for 4-OH and 2-OH ATV L, which were not considered further. Although there was no apparent difference in ATV L levels between strains, there was a trend for

increased abundance of RVT, ATV and 2-OH ATV (Figure 4.9). At 24 hours post dose in both HRN and WT mice, analyte blood concentrations were uniformly low (Table 4.5), precluding accurate calculation of liver to blood ratios. Nevertheless, as the blood concentrations were consistently low, the relative differences were assumed to be due to differences in analyte concentrations within liver parenchymal tissue as opposed to the sampled liver blood vessels.

**Figure 4.9 Relative analyte abundance in post dose liver homogenates**

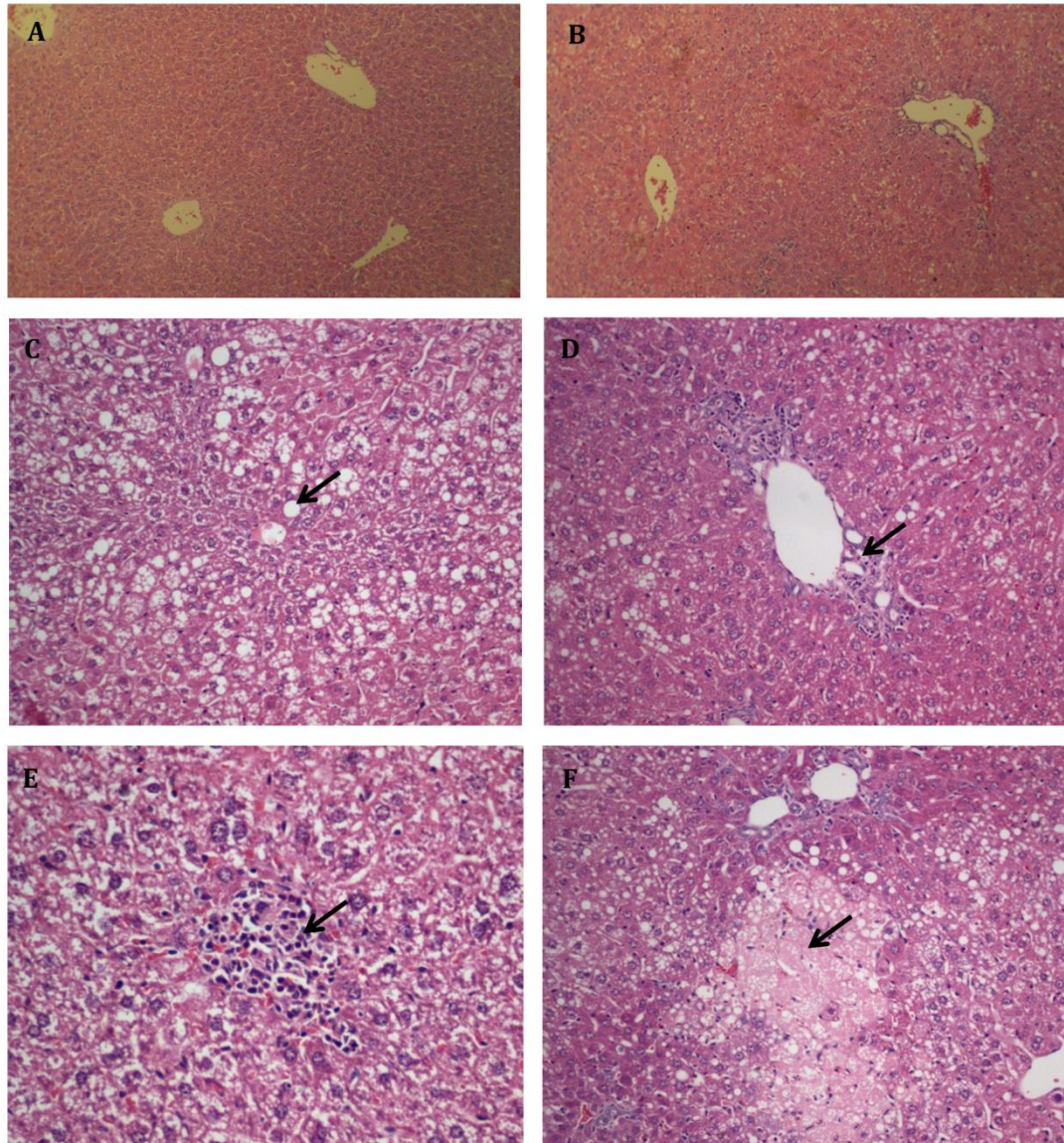


Mean fold change (HRN to WT)  $\pm$  standard error of internal standard-normalised analyte peak areas from liver homogenates of HRN (n=2) and WT (n=3) mice collected 24 hours after a single intraperitoneal dose containing both RVT and ATV at 30mg/Kg. Insufficient 4-OH ATV, 2-OH ATV L or 4-OH ATV L detected for analyte peak determination.

The formalin-fixed paraffin-embedded haematoxylin and eosin stained liver sections showed, as previously reported, enhanced lipid accumulation, bile duct proliferation, inflammatory cell infiltration and some necrosis in HRN livers (

Figure 4.10). The lipid accumulation was in keeping with the macroscopic pallor and hepatomegaly observed for HRN livers. Therefore, it is plausible that the overall function of HRN livers is reduced.

**Figure 4.10 Liver histological changes of the hepatic reductase null model**



Formalin-fixed paraffin-embedded haematoxylin and eosin stained liver sections taken at the end of the *in vivo* PK study. A = Representative section of WT liver (10x magnification); B = representative section of HRN liver (10x); C = a photomicrograph to highlight the clear vacuoles in the livers of HRN mice in keeping with lipid hydrophic degeneration (20x); D = bile duct proliferation in HRN liver (20x); E = lymphocyte aggregation in HRN liver (40x); F = an area of necrosis in HRN liver (20x).

#### 4.3.4 Liver proteomics

Overall, 3538 proteins were identified and 199 proteins remained significant at a FDR of 5% after multiple testing correction; these proteins are listed in the appendix (Table 8.4).

##### 4.3.4.1 DMEs and xenotransporters

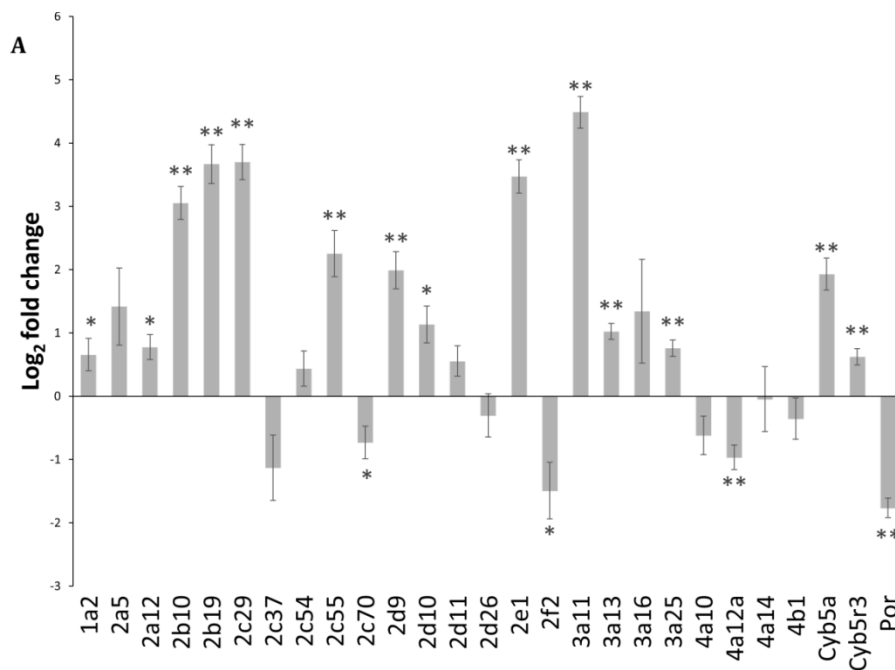
The results of the 92 identified DME and xenotransporter proteins are presented in Figure 4.11 and confirm hepatic Por downregulation in the HRN model (Figure 4.11 A). The expression levels of identified phase I and phase II DMEs were compared to the results from a recent publication, which selectively determined the expression of these proteins by a targeted approach (stable isotope labelling by amino acids in cell culture, SILAC) (MacLeod *et al.*, 2015). A high degree of concordance was observed, serving to externally validate the iTRAQ data.

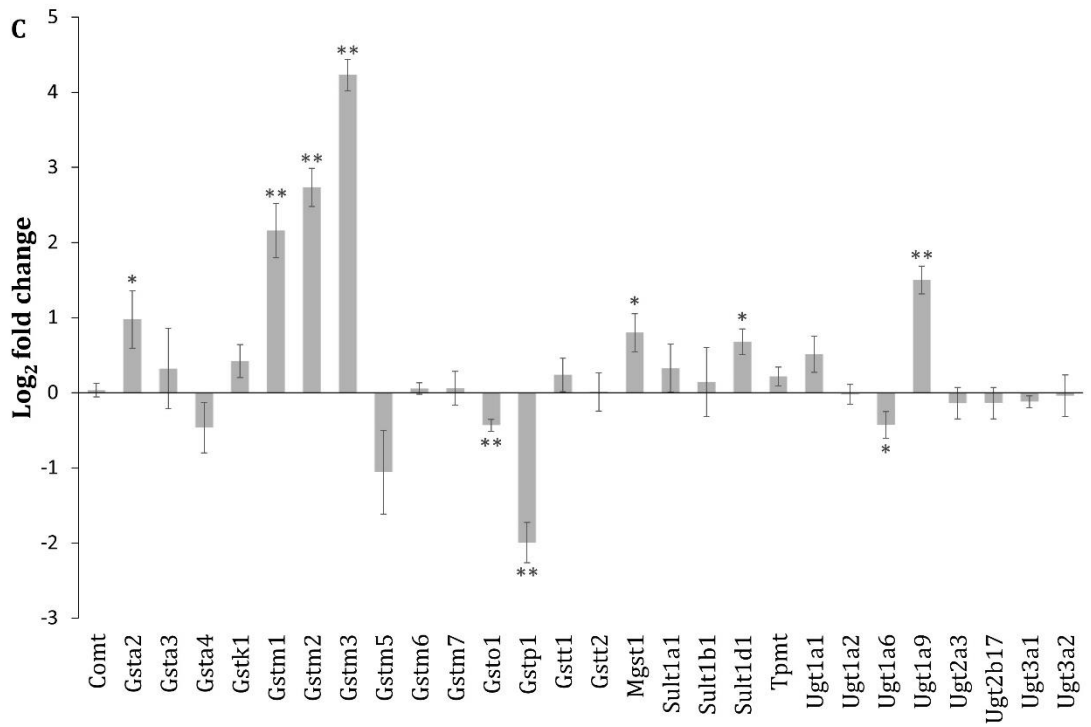
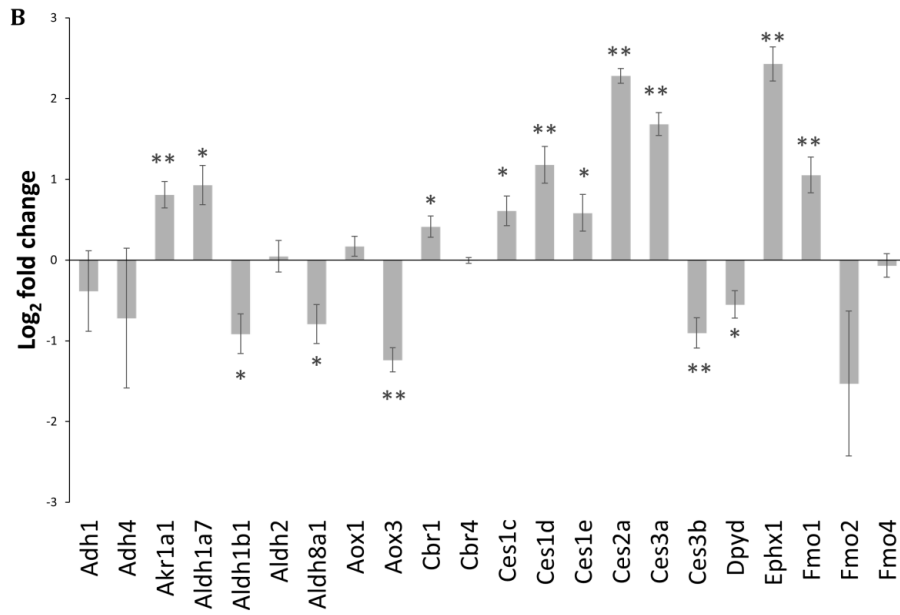
There was significant elevation of multiple CyPs (Cyp2b10, 2b19, 2c29, 2c55, 2d9, 2e1, 3a11, 3a13, 3a25), phase I (aldo-keto reductase 1a1 (Akr1a1), Ces1d, Ces2a, Ces3a, epoxide hydrolase 1 (Ephx1), flavin containing monooxygenase 1 (Fmo1)) and phase II (glutathione S-transferase m1 (Gstm1), Gstm2, Gstm3, Ugt1a9) DMEs, whilst decreases were observed for Cyp4a12a, aldehyde oxidase 3 (Aox3), Ces3b, Gsto1 and Gstp1 in HRN livers (Figure 4.11). The HRN upregulated Ugt1a9 may contribute to the increased ATV lactonization observed in the PK study (Figure 4.2) and UDPGA-activated microsomes (Figure 4.8).

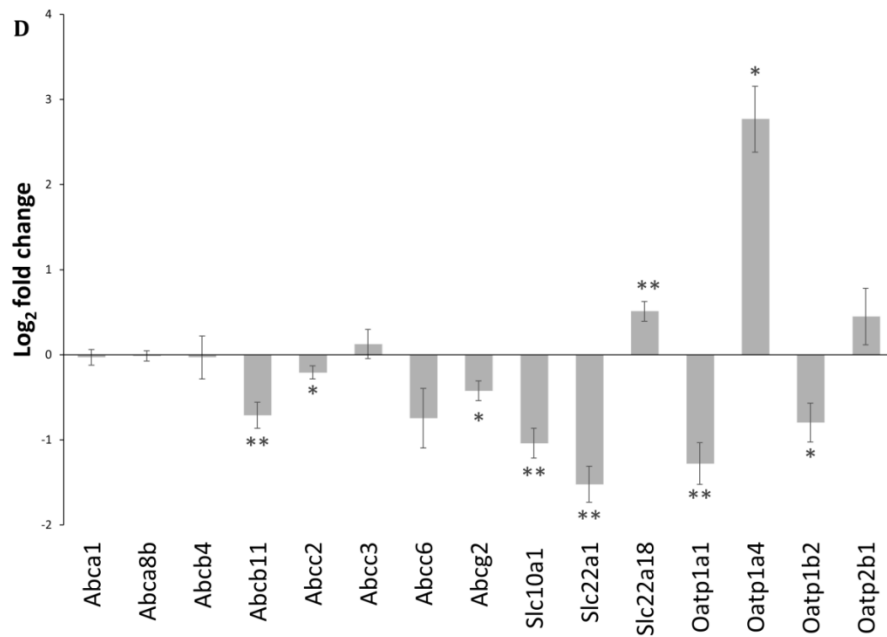
The iTRAQ approach enabled the novel characterisation of previously unquantified proteins including other DMEs (e.g. Cyp2b19, Aox1, Aox3, Ces3b, dihydropyrimidine dehydrogenase (Dpyd), Gsto1 and thiopurine methyltransferase (Tpmt) and importantly, xenotransporters (Figure 4.11 D). Of the transporters implicated in the sinusoidal hepatic influx of RVT and/or ATV, Oatp1a1 and Slc10a1 (Ntcp) were significantly downregulated and a

trend for downregulation was observed for Oatp1b2 (uncorrected raw  $p=0.0091$ ). The rodent-specific transporter, Oatp1a4, is known to transport ATV (Lau *et al.*, 2006) and RVT (Ho *et al.*, 2006b). Although Oatp1a4 was not detected in the liver homogenate iTRAQ, it was identified in the pilot iTRAQ study using liver microsomes, and showed a trend for increased expression (uncorrected raw  $p=0.0034$ ). For transporters involved in biliary excretion and known to handle RVT and/or ATV, Abcb11 (Bsep) was downregulated, and Abcg2 and Abcc2 (Mrp2) showed trends for downregulation (uncorrected raw  $p$ -values of 0.0069 and 0.019, respectively) in HRN livers.

**Figure 4.11 Differential hepatic drug-metabolising enzyme and xenotransporter protein expressions in hepatic reductase null and wild type mice**



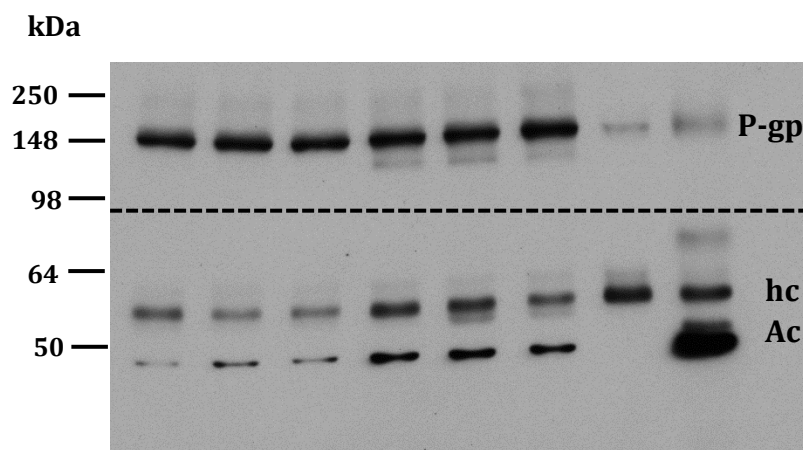




Protein expression mean fold change (HRN to WT)  $\pm$  standard error using  $\log_2$ -transformed batch mean-centred expression data for drug-metabolising cytochrome P450 enzymes (A), other drug-metabolising phase I enzymes (B), phase II enzymes (C), and xenotransporters (D). The protein expressions were determined by iTRAQ in HRN (n=6) versus WT (n=6) liver homogenates. The sole exception is Oatp1a4, which was determined by iTRAQ proteomics using HRN (n=3) and WT (n=3) liver microsome samples, because it was not detected in the liver homogenates. Statistical significance determined by student's t-test. \*\* denotes statistically significant mean fold changes at FDR <0.05 after Benjamini-Hochberg correction for multiple testing (3538 tests, as 3538 proteins detected), \* denotes raw uncorrected p-value <0.05.

Neither murine isoform of P-gp (Abcb1a, Abcb1b) was identified by iTRAQ; therefore P-gp expression was determined by western blot, which revealed no gross changes between HRN and WT livers in relation to the primary band corresponding to P-gp (Figure 4.12). A faint band of slightly lighter mass was consistently observed in the HRN but not the WT liver or control samples; it is of unknown significance but may represent a different P-gp glycosylation pattern or non-P-gp glycoproteins (Figure 4.12) (Greer and Ivey, 2007).

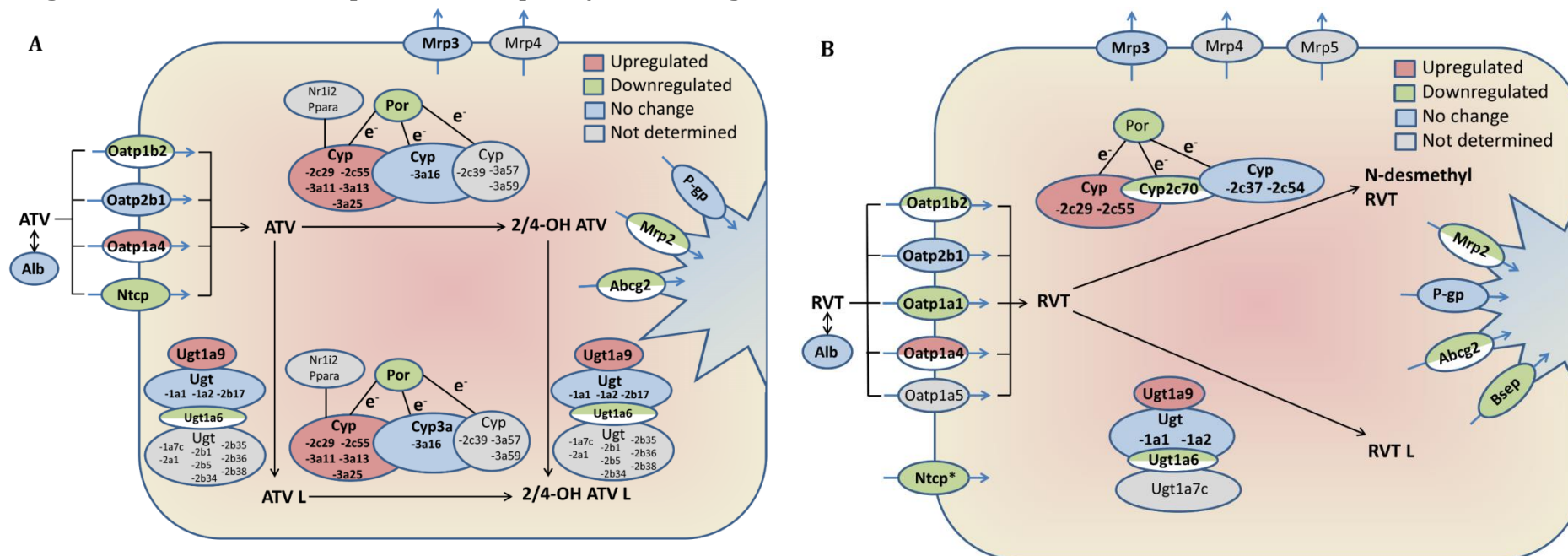
**Figure 4.12 P-gp expression by western blotting**



This western blot shows P-gp expression and beta-actin loading control expression in WT (n=3) and HRN (n=3) liver homogenates, and in two 'relative' negative controls: C = WT murine cardiac homogenate, S = WT murine spleen homogenate. The top half (above dashed line) was incubated with rabbit monoclonal anti-P-gp primary and goat anti-rabbit secondary to show P-gp expression. The bottom half was incubated with mouse monoclonal anti-beta actin and goat anti-mouse secondary; therefore endogenous heavy (hc) and light (lc) chains were detected in addition to beta actin loading control (Ac). The anti-beta actin antibody is known to not cross-react with adult cardiac (or smooth or skeletal muscle) actin, which explains the absence of actin band in lane C. Overall, there was little detectable difference in P-gp expression between WT and HRN liver homogenates.

An illustrative summary of the expression changes of proteins implicated in the hepatic handling RVT and ATV are collated in Figure 4.13.

**Figure 4.13 Schematics of postulated hepatocyte handling of atorvastatin and rosuvastatin in HRN mice**



Schematics of postulated HRN hepatocyte handling of ATV (A) and RVT (B) based on protein expression results. The proteins depicted include rodent proteins known to transport ATV/RVT and murine homologs of human proteins known to transport or metabolise ATV/RVT. For ATV, Cyp2c29, 2c39 and 2c55 were also included because they have been shown to substantially oxidise the prototypical CYP3A4 substrate, midazolam (van Waterschoot et al., 2008). Protein expression results refer to protein changes in HRN compared to WT. Whole colour changes represent protein expression changes significant at a 5% FDR after correction for multiple testing (3538 tests); half colour changes represent protein expression changes with a raw uncorrected t-test p-value <0.05, but were not significant after correction for multiple testing. The minor metabolites of RVT are depicted, although they were not quantified. Broadly, Cyp-mediated metabolism is reduced due to Por knock out despite Cyp upregulation, Ugt-mediated ATV lactonization is likely increased, and biliary excretion for both RVT and ATV is plausibly reduced. Net hepatocyte statin uptake is plausibly reduced in HRN livers, but this cannot be confirmed without further study, particularly because Oatp transporters are thought to be bidirectional (Roth et al., 2012; Li et al., 2000). \* Although RVT is a substrate for NTCP, it does not appear to be a substrate for rodent Ntcp (Ho et al., 2006b).

#### 4.3.4.2 Global proteomics interrogation

The 199 statistically significant proteins underwent IPA® core analysis; the headline results are reported in Table 4.10. Importantly, the top predicted adverse outcomes associated with this protein list (liver cholestasis, steatosis, inflammation, necrosis/cell death) correlated with the macroscopic and microscopic findings observed for HRN livers (Table 4.10).

**Table 4.10 Top significant results from IPA® analysis**

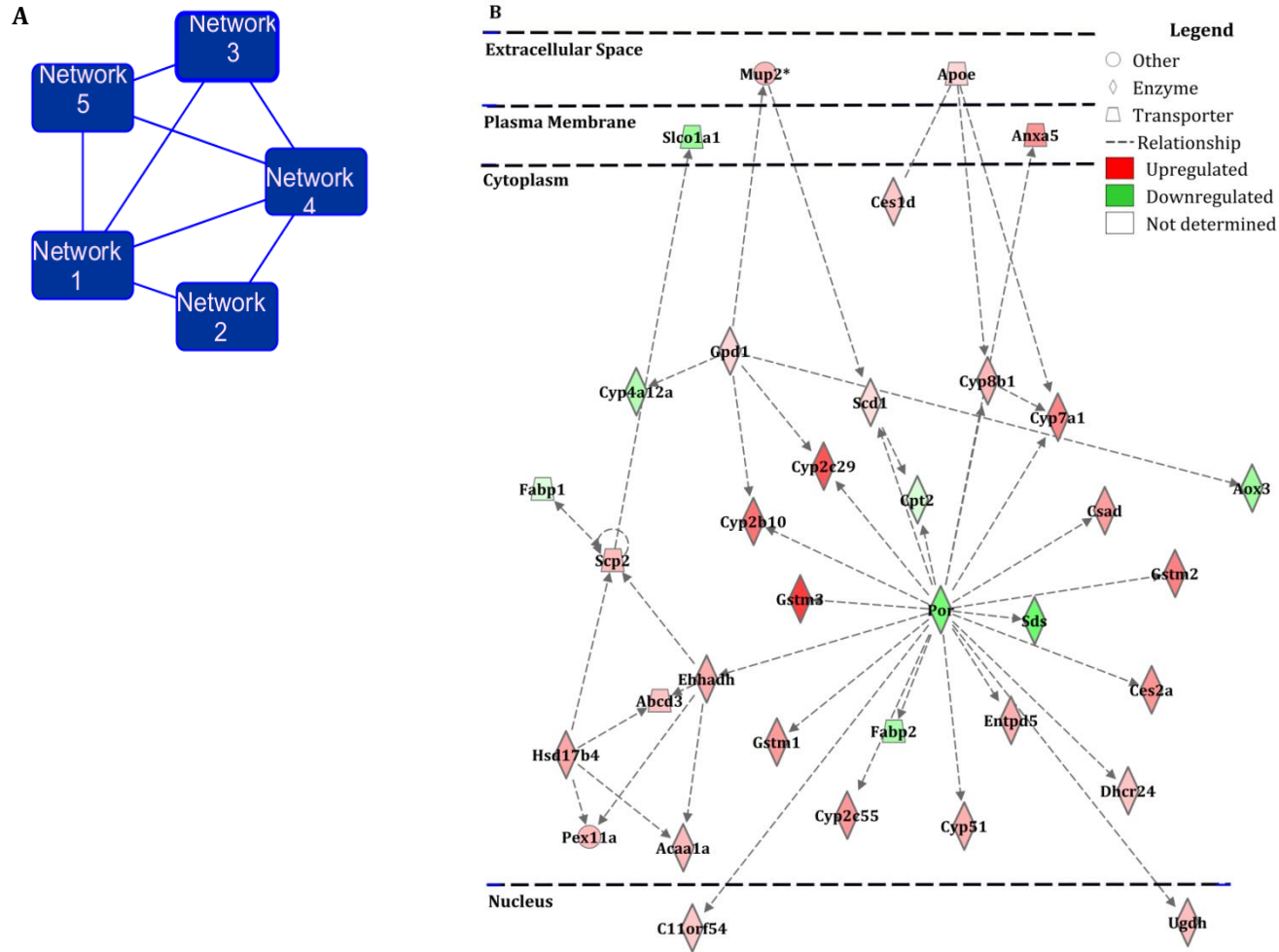
Top Networks	Top Toxicity Lists	Top Toxicity Functions
Energy production, Lipid metabolism, Small molecular biochemistry (p=1E-46)	Fatty acid metabolism (p=5.2E-23)	Liver cholestasis (p=0.02)
Energy production, Lipid metabolism, Small molecular biochemistry (p=1E-21)	LPS/IL-1 mediated inhibition of RXR function (p=9.2E-15)	Liver steatosis (p=0.02)
Lipid metabolism, Small molecule biochemistry, Vitamin and Mineral metabolism (p=1E-14)	NRF2-mediated oxidative stress response (p=2.4E-11)	Liver inflammation/hepatitis (p=0.04)
Metabolic disease, Energy production, Lipid metabolism (p=1E-13)	Xenobiotic metabolism signalling (p=4.7E-10)	Liver necrosis/cell death (p=0.04)
Lipid metabolism, Molecular transport, Small molecule biochemistry (p=1E-12)	Cytochrome P450 panel – substrate is a xenobiotic (mouse) (p=9.4E-10)	

Protein expression in HRN (n=6) and WT (n=6) liver homogenates was determined by iTRAQ. The protein expression fold changes were log<sub>2</sub>-transformed and batch mean-centred prior to statistical hypothesis testing by student's t-test with subsequent Benjamini-Hochberg correction for multiple testing (3538 tests). The 199 proteins with HRN to WT expression ratios that remained significant at a FDR of 5% after multiple testing correction were entered into IPA® core analysis, which used its proprietary Ingenuity® Knowledge Base and analytical software to automatically generate the top networks, toxicity lists and downstream toxicity functions based on the known interactions and functions of the entered protein seed list. Network p-values were estimated from IPA® p-scores within IPA®. Toxicity list and function p-values were taken from the IPA® core analysis results.

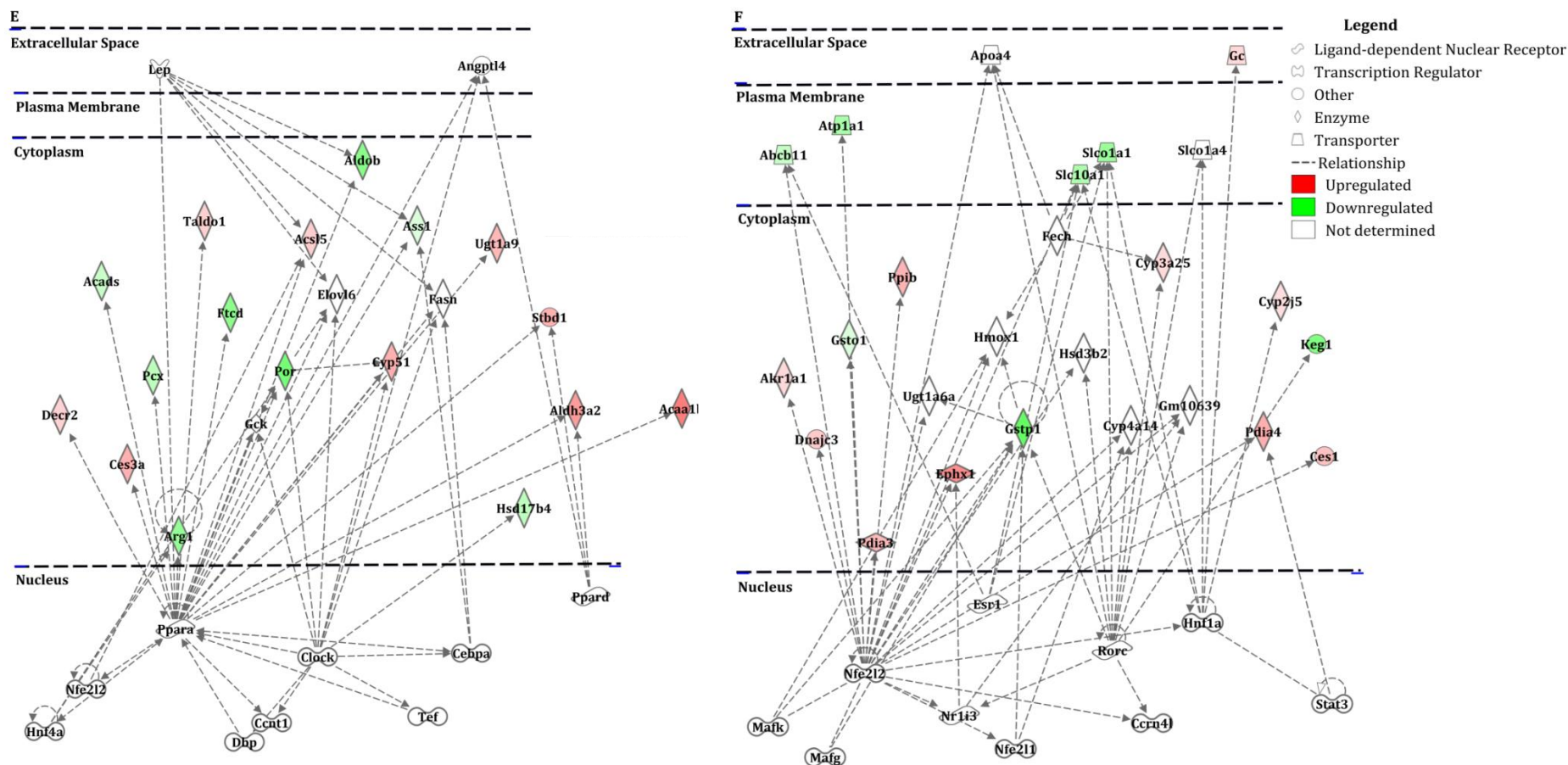
This table shows that the expression of proteins involved in lipid and xenobiotic metabolism are perturbed in HRN livers, and the downstream toxicity function analysis correctly predicted that HRN livers would be steatotic.

Ten networks were identified in the network analysis; the five most significant were overlapping and are presented in Figure 4.14. The latter five were isolated networks containing a median of two proteins and not considered further. The network analysis (Figure 4.14) and related significant toxicity lists (Table 4.10) demonstrate that lipid and xenobiotic metabolism are extensively perturbed in HRN livers, and they highlight a role for the nuclear factor erythroid 2-related factor 2 (Nfe2l2, also known as Nrf2)-mediated oxidative stress response. The IPA<sup>®</sup> upstream regulator analysis predicted significantly increased activity of Ppar $\alpha$ , Nfe2l2, nuclear receptor subfamily 1 group i (Nr1i) member 3 (Nr1i3, also known as constitutive androstane receptor, Car) and Nr1i2 (pregnane X receptor, Pxr).

Figure 4.14 Main protein networks detected by IPA core analysis comparing HRN to WT liver homogenates







This figure shows the top five networks generated by IPA® core analysis. Figure A provides an overview that shows how the five networks overlap with one another; figures B-F display the individual networks 1-5, respectively. To generate these networks, 199 proteins whose expression in HRN compared to WT liver homogenates remained statistically significant after applying a 5% FDR Benjamini-Hochberg multiple testing correction were entered into the IPA® core analysis. IPA® networks are derived from the Ingenuity® Knowledge Base Global Molecular Network, and are ranked based on the number of identified molecules in a network. Network size was limited to  $\leq 35$  identified molecules and the interacting proteins not in the seed list were retained to aid interpretation.

Using the full list of identified proteins, those involved in lipid metabolism were categorised into major functional classes for further evaluation (Table 4.11). As expected, Cyp enzymes involved in the classic (neutral) pathway of bile acid synthesis (Cyp7a1, Cyp8b1) and steroid synthesis (Cyp51a1) were upregulated in response to Por deficiency. Overall, fatty acid biosynthetic and elongation processes were not differentially perturbed. However, there was differential expression of multiple proteins involved in fatty acid degradation with a preference for upregulation (Acaa1b, Aldh3a2, Acsl5, Decr2, Acox2, Acad11), although some downregulation occurred (Cpt2, Acads, Acaa2) in HRN livers. Interestingly, the expression of several proteins involved in intracellular lipid transport (Scp2, Abcd3, Mttp) was noticeably increased, although no changes in proteins involved in mediating the influx into/extrusion of lipids out of cells was detected (Table 4.11).

**Table 4.11 Expression fold changes for identified proteins involved in lipid metabolism**

Protein	Description	Log <sub>2</sub> Fold change (±SE) (HRN to WT)	p-value <sup>1</sup>
<b>Nuclear receptor</b>			
Hnf4	Hepatocyte nuclear factor 4-alpha	0.2 ± 0.1	0.046
<b>Bile acid biosynthesis</b>			
<u>Cyp7a1</u>	<u>Cholesterol 7-alpha-monooxygenase</u>	<u>2.6 ± 0.4</u>	<u>&lt;0.001</u>
<u>Cyp8b1</u>	<u>7-alpha-hydroxycholest-4-en-3-one 12-alpha-hydroxylase</u>	<u>1.5 ± 0.2</u>	<u>&lt;0.001</u>
Hsd3b7	3 beta-hydroxysteroid dehydrogenase type 7	0.9 ± 0.3	0.08
Slc27a2	Very long-chain acyl-CoA synthetase	0.3 ± 0.2	0.22
Akr1d1	3-oxo-5-beta-steroid 4-dehydrogenase	0.0 ± 0.2	0.85
Slc27a5	Bile acyl-CoA synthetase	-0.3 ± 0.2	0.20
Cyp7b1	25-hydroxycholesterol 7-alpha-hydroxylase	-0.7 ± 0.3	0.032
<b>Fatty acid biosynthesis/metabolism</b>			
<u>Scd1</u>	<u>Acyl-CoA desaturase 1</u>	<u>0.7 ± 0.2</u>	<u>0.002</u>
Acot13	Acyl-coenzyme A thioesterase 13	0.7 ± 0.2	0.017
Fads2	Fatty acid desaturase 2	0.7 ± 0.3	0.040
Acaca	Acetyl-CoA carboxylase 1	0.2 ± 0.1	0.14
Fasn	Fatty acid synthase	0.1 ± 0.0	0.026
Acss3	Acyl-CoA synthetase short-chain family member 3, mitochondrial	0.1 ± 0.3	0.82
Mcat	Malonyl-CoA-acyl carrier protein transacylase, mitochondrial	0.1 ± 0.1	0.32
Acacb	Acetyl-CoA carboxylase 2	0.0 ± 0.1	0.94
Oxsm	3-oxoacyl-[acyl-carrier-protein] synthase, mitochondrial	-0.1 ± 0.3	0.76

<i>Table continued</i>			
<b>Protein</b>	<b>Description</b>	<b>Log<sub>2</sub> Fold change (±SE) (HRN to WT)</b>	<b>p-value<sup>1</sup></b>
Acsf3	Acyl-CoA synthetase family member 3, mitochondrial	-0.6 ± 0.2	0.032
Acsf2	Acyl-CoA synthetase family member 2, mitochondrial	-0.8 ± 0.1	<0.001
Acly	ATP-citrate synthase	-0.9 ± 0.3	0.011
<b>Fatty acid elongation</b>			
Hacd3	Very-long-chain (3R)-3-hydroxyacyl-CoA dehydratase 3	0.7 ± 0.2	0.003
Hsd17b12	Very-long-chain 3-oxoacyl-CoA reductase	0.6 ± 0.2	0.005
Hacd2	Very-long-chain (3R)-3-hydroxyacyl-CoA dehydratase 2	0.5 ± 0.2	0.06
Tecr	Very-long-chain enoyl-CoA reductase	0.5 ± 0.2	0.047
<b>Steroid biosynthesis</b>			
<u>Cyp51a1</u>	<u>Lanosterol 14-alpha demethylase</u>	<u>1.7 ± 0.3</u>	<u>&lt;0.001</u>
<u>Dhcr24</u>	<u>Delta(24)-sterol reductase</u>	<u>1.2 ± 0.2</u>	<u>&lt;0.001</u>
Sc5d	Lathosterol oxidase	0.7 ± 0.5	0.30
Sqle	Squalene monooxygenase	0.3 ± 0.3	0.41
Dhcr7	7-dehydrocholesterol reductase	0.0 ± 0.2	0.93
Lss	Lanosterol synthase	-0.1 ± 0.2	0.76
Fdft1	Squalene synthase	-0.1 ± 0.2	0.55
<b>Fatty acid degradation</b>			
<u>Acaa1b</u>	<u>3-ketoacyl-CoA thiolase B, peroxisomal</u>	<u>2.8 ± 0.2</u>	<u>&lt;0.001</u>
<u>Aldh3a2</u>	<u>Fatty aldehyde dehydrogenase</u>	<u>2.1 ± 0.4</u>	<u>&lt;0.001</u>
<u>Acs15</u>	<u>Long-chain-fatty-acid--CoA ligase 5</u>	<u>1.1 ± 0.1</u>	<u>&lt;0.001</u>
Acs14	Long-chain-fatty-acid--CoA ligase 4	1.0 ± 0.3	0.012
<u>Decr2</u>	<u>Peroxisomal 2,4-dienoyl-CoA reductase</u>	<u>0.9 ± 0.2</u>	<u>&lt;0.001</u>
<u>Acox2</u>	<u>Peroxisomal acyl-coenzyme A oxidase 2</u>	<u>0.8 ± 0.1</u>	<u>&lt;0.001</u>
Acox1	Peroxisomal acyl-coenzyme A oxidase 1	0.6 ± 0.3	0.09
Eci2	Enoyl-CoA delta isomerase 2, mitochondrial	0.6 ± 0.2	0.012
<u>Acad11</u>	<u>Acyl-CoA dehydrogenase family member 11</u>	<u>0.5 ± 0.1</u>	<u>0.002</u>
Acadm	Medium-chain specific acyl-CoA dehydrogenase, mitochondrial	0.1 ± 0.1	0.50
Cpt1a	Carnitine O-palmitoyltransferase 1, liver isoform	0.0 ± 0.2	0.82
Eci1	Enoyl-CoA delta isomerase 1, mitochondrial	0.0 ± 0.2	0.99
Echdc2	Enoyl-CoA hydratase domain-containing protein 2, mitochondrial	-0.3 ± 0.2	0.22
Echs1	Enoyl-CoA hydratase, mitochondrial	-0.3 ± 0.3	0.36
Acadl	Long-chain specific acyl-CoA dehydrogenase, mitochondrial	-0.5 ± 0.2	0.07
<u>Cpt2</u>	<u>Carnitine O-palmitoyltransferase 2, mitochondrial</u>	<u>-0.5 ± 0.1</u>	<u>0.001</u>
Acadvl	Very long-chain specific acyl-CoA dehydrogenase, mitochondrial	-0.6 ± 0.2	0.045
<u>Acads</u>	<u>Short-chain specific acyl-CoA dehydrogenase, mitochondrial</u>	<u>-0.7 ± 0.1</u>	<u>0.001</u>
Acs11	Long-chain-fatty-acid--CoA ligase 1	-0.7 ± 0.2	0.015
Hsd17b10	3-hydroxyacyl-CoA dehydrogenase type-2	-0.8 ± 0.3	0.031
<u>Acaa2</u>	<u>3-ketoacyl-CoA thiolase, mitochondrial</u>	<u>-1.7 ± 0.3</u>	<u>&lt;0.001</u>

<i>Table continued</i>			
Protein	Description	Log <sub>2</sub> Fold change (±SE) (HRN to WT)	p-value <sup>1</sup>
<b>Lipid transport</b>			
<b>i) Within cell</b>			
<u>Scp2</u>	<u>Non-specific lipid-transfer protein</u>	<u>1.4 ± 0.2</u>	<u>&lt;0.001</u>
<u>Abcd3</u>	<u>ATP-binding cassette sub-family D member 3</u>	<u>1.3 ± 0.2</u>	<u>&lt;0.001</u>
<u>Mttp</u>	<u>Microsomal triglyceride transfer protein large subunit</u>	<u>1.0 ± 0.2</u>	<u>&lt;0.001</u>
Pctp	Phosphatidylcholine transfer protein	0.0 ± 0.2	0.93
<u>Fabp1</u>	<u>Fatty acid-binding protein, liver</u>	<u>-0.2 ± 0.0</u>	<u>&lt;0.001</u>
<b>ii) Into/out of cell</b>			
Slc27a4	Long-chain fatty acid transport protein 4	1.0 ± 2.0	0.68
Slc27a1	Long-chain fatty acid transport protein 1	0.4 ± 0.4	0.45
Cd36	Platelet glycoprotein 4	0.3 ± 0.3	0.36
Abcg8	ATP-binding cassette sub-family G member 8	0.2 ± 0.1	0.23
Ldlr	Low-density lipoprotein receptor	0.2 ± 0.4	0.73
Abca1	ATP-binding cassette sub-family A member 1	0.0 ± 0.1	0.78
Lrp1	Prolow-density lipoprotein receptor-related protein 1	-0.3 ± 0.2	0.15
Scarb1	Scavenger receptor class B member 1	-0.5 ± 0.3	0.09
<b>Lipoproteins</b>			
Apof	Apolipoprotein F	1.7 ± 1.8	0.44
Apoc4	Apolipoprotein C-IV	1.4 ± 1.8	0.55
<u>Apoe</u>	<u>Apolipoprotein E</u>	<u>0.9 ± 0.2</u>	<u>0.001</u>
Apoc1	Apolipoprotein C-I	0.8 ± 0.2	0.004
Apoa5	Apolipoprotein A-V	0.7 ± 0.3	0.10
Apob	Apolipoprotein B-100	0.4 ± 0.2	0.05
Apoa2	Apolipoprotein A-II	0.3 ± 0.3	0.28
Apoa4	Apolipoprotein A-IV	0.3 ± 0.2	0.21
Apoa1	Apolipoprotein A-I	0.0 ± 0.2	0.96
Apoc3	Apolipoprotein C-III	0.0 ± 0.2	0.98

From the full list of proteins identified in the HRN and WT liver homogenates (n=3538), those involved in lipid metabolism were categorised into major functional classes.

<sup>1</sup> = raw t-test p-value is shown. Proteins that remained significant at a FDR<0.05 after correction for multiple testing (n=3538 protein tests) are underlined.

#### 4.4 Discussion

The primary finding in this study was increased *in vivo* exposure of RVT, ATV and ATV metabolites in HRN mice following a 30mg/Kg intraperitoneal dose. The increased exposure of RVT and ATV metabolites was unanticipated and led to further investigation. Hepatic microsomal incubations confirmed that RVT does not undergo Cyp-mediated metabolism *in vitro*, and HRN microsomes expectedly have impaired ATV hydroxylation capacity. Furthermore, UDPGA-activated HRN microsomes have notably increased ATV L production compared to WT microsomes. Histologically, the HRN livers showed features in keeping

with lipid accumulation and potential liver dysfunction. Liver proteomic analysis confirmed that hepatocyte-specific Por knock out has a dramatic effect on DME levels, and to a lesser extent on transporters. Global proteomic interrogation highlighted perturbations in both lipid and xenobiotic metabolism in HRN livers.

#### 4.4.1 RVT and ATV disposition

Following intraperitoneal administration, the increased  $C_{max}$  for all analytes suggests increased systemic exposure due to reduced liver extraction. The increased systemic exposure and reduced clearance of RVT and ATV will have contributed to the increased observed  $AUC_{0-8}$  exposures.

The NADPH-activated microsomal incubations confirmed the expected findings. RVT has previously been observed to undergo no metabolism in human liver microsomes (1-4 $\mu$ M RVT) after a 3-hour incubation, and very slow metabolism (5-50%) via CYP2C9 to *N*-desmethyl RVT in cultured human hepatocytes over three days (Olsson *et al.*, 2002). Although the HRN NADPH-activated liver microsomal incubations showed a substantial reduction in ATV hydroxylation, mean HRN 2'-hydroxylation  $V_{max}$  was still ~one third of the mean WT  $V_{max}$  (1764 to 5393 pmol/min/mg microsome protein, respectively). Given the dramatic reduction in hepatic Por expression and cytochrome c reduction (>90%) activity by 6-8 weeks postpartum (Henderson *et al.*, 2003), the remaining ATV hydroxylation is likely attributable to the NADH-cyb5 system. There are several lines of evidence to support this hypothesis. First, this study has shown that both the electron donor, Cyb5r3, and electron carrier, Cyb5a, are upregulated in HRN livers. Second, previous microsomal and recombinant expression studies have demonstrated that CYP3A4 and 2E1 can accept electrons from cyb5 as well as POR (Porter, 2012; Yamazaki *et al.*, 1996). Third, oral midazolam administration to mice with conditional deletion of Cyb5a (HBN mice) results in increased AUC and  $C_{max}$ , and lower midazolam clearance (Finn *et al.*, 2008). Fourth, oral midazolam dosing in HBRN mice, which are deficient

of both hepatic Por and Cyb5a, results in higher midazolam exposures than in either HRN or HBN models (Henderson *et al.*, 2013).

Interestingly, this study showed that HRN mice have increased circulating L metabolites of ATV *in vivo*. HRN mice have been previously reported to have higher circulating levels of 1'-hydroxymidazolam-*O*-glucuronide following oral midazolam (Grimsley *et al.*, 2014), and higher levels of urinary glucuronide and taurine amide conjugated diclofenac metabolites following oral diclofenac (Pickup *et al.*, 2012). These observations suggest increased phase II activity and/or altered metabolite elimination due to reduced biliary excretion. The work herein has confirmed and extended these findings by demonstrating an increased rate of microsomal ATV lactonization in the presence of the UGT cofactor, UDPGA. UGTs catalyse a major pathway of statin lactonization by metabolising statin acid forms into unstable acyl-glucuronide intermediates, which then undergo spontaneous cyclization to the corresponding L species (Prueksaritanont *et al.*, 2002). Furthermore, this study has shown that there is significant upregulation of Ugt1a9 in HRN livers, which shares ~63% homology with UGT1A3, the principal enzyme involved in ATV lactonization in supersomes of human recombinant UGTs (Schirris *et al.*, 2015b). Therefore, increased lactonization rate due to Ugt1a9 plausibly contributes to the increased ATV Ls observed systemically *in vivo* (Figure 4.2).

Apparent increased RVT, ATV and 2-OH ATV retention were observed in this study in HRN livers 24 hours post-dose Figure 4.9. This observation is in keeping with the previous findings from whole body autoradiography studies of increased radioactivity retention in HRN livers compared to WT livers at 24-hours following oral [<sup>14</sup>C]-diclofenac (Pickup *et al.*, 2012), and HRN liver retention of [<sup>14</sup>C]-fenclozic acid at 72-hours post-dose (Pickup *et al.*, 2014). Cellular macromolecule covalent binding studies showed no difference in liver binding between strains for [<sup>14</sup>C]-diclofenac (Pickup *et al.*, 2012); minor covalent binding of [<sup>14</sup>C]-fenclozic was detected in HRN livers, although it was

not assessed in WT mice (Pickup *et al.*, 2014). Furthermore, at 24 hours, significantly less [<sup>14</sup>C]-diclofenac was recovered from HRN faeces (~2%) compared to WT faecal excreta (~15%), whilst significantly more was found in HRN (~87%) compared to WT (~52%) urine (Pickup *et al.*, 2012). Abcg2, Bsep, Mrp2 and P-gp are implicated in the excretion of statins into biliary canaliculi, and in this study reduced protein expression in HRN livers was observed for Abcg2 (p=0.0069), Bsep (p=0.0012) and Mrp2 (p=0.019), although only the decrease in Bsep remained statistically significant after correction for multiple testing. In contrast, mRNA levels of Abcb1a (one of two isoforms encoding rodent P-gp) and Abcc2 (encoding Mrp2) have been reported to be elevated in HRN livers (Cheng *et al.*, 2014; Gonzalez *et al.*, 2011a), suggesting that expression changes for these proteins may be potentially regulated through post-translational mechanisms. Interestingly, immunohistochemistry has shown that MRP2 is improperly localised away from the canalicular membrane of hepatocytes in patients with non-alcoholic steatohepatitis (NASH), and this was thought to contribute to increased serum levels of the glucuronide primary metabolite of paracetamol (Canet *et al.*, 2015). This finding is likely relevant because the fatty liver phenotype of HRN livers has characteristics of non-alcoholic fatty liver disease (Gonzalez *et al.*, 2011a; Riddick *et al.*, 2013), and Mrp2 is the rodent orthologue of MRP2. Overall on balance, although not definitively proven, it is likely that HRN mice have reduced biliary drug excretion, which will have contributed to the elevated levels of analytes *in vivo*.

The protein expression findings of sinusoidal transporters suggest possible decreased hepatic statin uptake, with decreased expression for Oatp1a1 (raw p=0.00053), Oatp1b2 (raw p=0.0091) and Ntcp (raw p=0.00023), although only reduced Oatp1a1 and Ntcp remained significant after multiple testing correction. In contrast, HRN Oatp1a4 (p=0.0034) expression was increased, albeit non-significantly after adjustment for multiple testing. Similarly, HRN mRNA levels of Oatp1a1 (Cheng *et al.*, 2014) and Oatp1a4 (Cheng *et al.*, 2014; Gonzalez *et al.*, 2011a) have been reported to be decreased and increased, respectively, alongside non-significant mild trends of reduced Oatp1b2 and

Ntcp mRNA (Cheng *et al.*, 2014). Clinically, non-alcoholic fatty liver disease represents a spectrum of disease from simple fatty liver to NASH. It is worth noting that hepatic mRNA levels of multiple sinusoidal transporters (Ntcp, Oatp1a1, 1a4, 1b2, 2b1; Oat2 and 3) were found to be decreased in rat models of fatty liver and NASH, and Oatp1b2 protein expression progressively decreased with increasing liver damage (Fisher *et al.*, 2009). This suggests that the degree of liver pathology and so potentially HRN mouse age, as well as the class of biological molecule measured (mRNA versus protein), may contribute to the slight differences in sinusoidal/canalicular transporter expression observed between this study and previous HRN studies.

Oatp1b2 is the single rodent orthologue (Roth *et al.*, 2012) of the major statin transporters, OATP1B1 and OATP1B3 (Pasanen *et al.*, 2007; Vildhede *et al.*, 2014), and has been shown to have the highest transport capacity for RVT *in vitro* out of any rodent sinusoidal transporter (Ho *et al.*, 2006b). On the other hand, Oatp1a4 is one of four mouse orthologues of OATP1A2 (Roth *et al.*, 2012); both Oatp1a4 and OATP1A2 can contribute to statin transport (Knauer *et al.*, 2010). The reason(s) for the isolated increased Oatp1a4 expression is unknown. However, Oatp1a4 is markedly induced during cholestatic liver injury in mice alongside other efflux transporters (Bsep, Mrp1-5) (Slitt *et al.*, 2007), and so may represent an adaptive response to the lipid accumulation observed in HRN livers.

The mechanism(s) of Oatp-mediated transport remain uncertain, although it is established that Oatps are capable of bidirectional transport and the driving force is ATP- and sodium-independent (Roth *et al.*, 2012; Li *et al.*, 2000). Therefore, reduced biliary excretion and liver retention may predispose to reduced Oatp-mediated statin uptake (e.g. due to reduced Oatp1a1) and/or increased basolateral efflux (e.g. due to increased Oatp1a4), reducing net hepatic statin uptake. Further research is required to quantify absolutely transporter expression in HRN mice, determine their individual transport rates

for statin substrates, and define the mechanism(s) of Oatp transport, to better understand statin HRN hepatic distribution. Furthermore, the role of HRN enterohepatic recycling on net biliary excretion needs study.

Besides considering hepatic protein expression, it is important to consider the liver tissue and its architecture as a whole when evaluating *in vivo* drug PK results. Macroscopically, HRN mice have hepatomegaly. The liver histology from this study and others (Akingbasote *et al.*, 2016; Akingbasote *et al.*, 2017), and the elevated plasma levels of liver biomarkers (alanine aminotransferase, glutamate dehydrogenase and alkaline phosphatase) in HRN mice (Akingbasote *et al.*, 2016) indicate lipid accumulation in keeping with fatty liver and underlying liver dysfunction. Fatty liver is associated with reduced sinusoidal perfusion in human fatty livers (Seifalian *et al.*, 1998) as well as in rabbit (Seifalian *et al.*, 1999) and rodent models (Ito *et al.*, 2006; McCuskey *et al.*, 2004). The reduction in sinusoidal perfusion, which impairs hepatic tissue perfusion, is attributable to both the enlarged lipid-laden hepatic parenchymal cells and associated oxidative stress that markedly narrow sinusoid lumens, alter the sinusoidal network architecture and so reduce the number of adequately perfused sinusoids per microscopic field (Farrell *et al.*, 2008). With the progression to steatohepatitis, there is capillarization of sinusoids with loss of sinusoidal endothelial cell fenestrae and collagen deposition in the space of Disse, which further restricts microvascular blood flow and hepatocyte blood exposure (Farrell *et al.*, 2008). Therefore, microcirculatory dysfunction with reduced hepatocyte blood exposure may underlie the increased  $t_{max}$  of RVT and parent ATV and contribute significantly to the increased apparent absorption and reduced clearance of analytes observed *in vivo* in HRN mice in this study.

The elevated circulating levels of hydroxylated ATV metabolites in HRN mice was unanticipated. However, following a single midazolam oral dose (2mg/Kg), HRN mice had increased systemic levels of both 1'-hydroxymidazolam-*O*-glucuronide, as stated above, and 4'-hydroxymidazolam, as well as parent

midazolam. These HRN mice did however have slightly lower systemic 1'-hydroxymidazolam (Grimsley *et al.*, 2014). Co-administration of the pan-Cyp inhibitor, 1'-aminobenzotriazole, led to equivalence of parent midazolam levels between strains (Grimsley *et al.*, 2014). Thus, extra-hepatic Cyp metabolism is clearly relevant in HRN mice. Importantly, intestinal expression of Cyp2b, 2c and 3a proteins are increased two to three fold in the related liver-specific Por null LCN mouse model, associated with increased small intestinal microsomal hydroxylase activity (Zhu *et al.*, 2014). Lung and kidney Cyp3a protein levels are unchanged (Zhu *et al.*, 2014). Following intraperitoneal injection, drug absorption is largely via the portal system (Lukas *et al.*, 1971); the extent to which drugs have access to intestinal epithelial metabolism during absorption, and once in the systemic circulation, requires further study. The observed increased systemic exposure of parent ATV would have also provided more substrate for lung, kidney and small intestine Cyp3a-mediated hydroxylation.

In summary, the elevated *in vivo* analyte systemic exposures are likely due to a combination of factors including reduced hepatic drug extraction and clearance. The underlying mechanisms for these changes plausibly include fatty liver-associated microvascular alterations and protein transporter expression changes leading to reduced biliary excretion and potentially reduced hepatocyte uptake. There appears to be upregulation of both hepatic glucuronide conjugation and extra-hepatic Cyp-mediated oxidation to compensate for the reduction in liver Cyp activity.

#### **4.4.1.1 Global HRN liver proteomics**

This study represents the first large-scale proteomics evaluation using HRN mice. Importantly, this study confirms that hepatic-specific Por deletion leads to major changes in hepatic xenobiotic and lipid metabolism protein expression, and upregulation of some oxidative stress response proteins, as collectively implicated in previous HRN liver transcriptomic studies (Mutch *et al.*, 2007; Wang *et al.*, 2005; Gonzalez *et al.*, 2011a).

The iTRAQ liver protein expression patterns of phase I and phase II DMEs (Figure 4.11 A, B, C) were congruent to those in a recent publication, which selectively quantified phase I/phase II DME protein expression via SILAC; this was considered external validation of the iTRAQ results (MacLeod *et al.*, 2015). For example, the expression levels of several Cyps (e.g. 2b10, 2b29, 2c55, 2e1, 3a11, 3a13), Gstm2 and Gstm3 were significantly upregulated in HRN livers using both methodologies. Although the SILAC testing was limited to 106 proteins (reducing the multiple testing burden), it was carried out using up to three mice/genotype, whereas the iTRAQ results are predominantly based on six liver samples/genotype, which can increase the power to detect protein expression differences. Accordingly, several protein expression trends observed in the previous SILAC data (MacLeod *et al.*, 2015) reached statistical significance here, including: increased expression in HRN livers of Cyb5a, Cyb5r3, Akr1a1, Ces3a, Ephx1 and Ugt1a9, and decreased expression of Gstp1 (Figure 4.11). The broader iTRAQ approach used here also facilitated the novel characterisation of previously unquantified DME and transporter proteins.

HRN mice exhibit hepatic lipid accumulation in association with severely reduced circulating cholesterol and triglyceride levels (Henderson *et al.*, 2003). The accumulated liver lipids are predominantly triglycerides (~2000% increase) with smaller contributions from diglycerides (~150% increase) and cholesterol esters (~130% increase) (Mutch *et al.*, 2007). In this study, two Por-mediated electron recipients involved in cholesterol synthesis, squalene monooxygenase (Sqle) and lanosterol 14- $\alpha$  demethylase (Cyp51a1), were detected; there was no change in Sqle expression but Cyp51a1 protein expression was increased in HRN livers. These changes may reflect the observation that Sqle retains partial activity in response to Por deficiency whilst Cyp51a1 appears to be fully Por-dependent (Porter, 2012). Therefore, the increased hepatic cholesterol content is unlikely to be due to *de novo* hepatic cholesterol synthesis, which is impaired in HRN livers, but rather from exogenous sources.

Overall little change was observed in the levels of proteins involved in fatty acid biosynthesis and elongation (Table 4.11), in keeping with previous transcriptomic observations (Mutch *et al.*, 2007). For example, fatty acid synthase (Fasn) expression is unchanged at both mRNA (Mutch *et al.*, 2007; Wang *et al.*, 2005) and protein (Table 4.11) levels. Furthermore, the mRNA of the sterol biosynthesis transcription factor upregulator, sterol regulatory element-binding protein 1c (*Sreb1c*), is unaltered (Mutch *et al.*, 2007) or reduced (Wang *et al.*, 2005) in HRN livers; however its protein was not identified here. These observations suggest that the origin of HRN excess liver triglyceride is not *de novo* liver synthesis but uptake from the circulation, akin to the proposed mechanism of cholesterol accumulation in HRN livers. Interestingly, HRN livers have increased transcription (Mutch *et al.*, 2007) and protein level expression (Table 4.11) of acyl-CoA desaturase 1 (*Scd1*), which is important to the synthesis of monounsaturated oleic acid (n-9 C<sub>18:1</sub>) by desaturating the saturated fatty acid, stearic acid. This may underlie the observation that HRN hepatic cholesterol esters preferentially incorporate monounsaturated fatty acids and in particular, oleic acid (Mutch *et al.*, 2007), and suggests that hepatic triglycerides preferentially contain unsaturated fatty acid chains.

A fat-deficient diet has been shown to prevent the widespread Cyp induction and hepatic triglyceride induction associated with hepatic Por deficiency, indicating that diet is the origin of HRN excess liver lipids (Finn *et al.*, 2009). This is consistent with the lack of induction of fatty acid biosynthetic pathways in HRN livers. Furthermore, a fat-deficient diet specifically replenished with sunflower oil (~88% unsaturated fatty acids) led to re-emergence of Cyp induction, hepatic lipid accumulation and liver enlargement. Subsequent work identified the dietary essential polyunsaturated fatty acid, linoleic acid (n-6, C<sub>18:2</sub>), as one key driver of Cyp induction and lipid accumulation. HRN mice additionally nullled for *Nr1i3* (*Car*) interestingly had reduced expression of some CyPs (e.g. Cyp2b, Cyp2c enzymes but not Cyp3a11) and decreased hepatic

lipid content, and linoleic acid was shown to directly activate Nr1i3 (Finn *et al.*, 2009). A role for Nr1i3 is in keeping with the increased Nr1i3 activity predicted from the IPA<sup>®</sup> analysis. Nevertheless, this Nr1i3 pathway was not responsible for the observed reduction in circulating lipids in HRN mice (Finn *et al.*, 2009). Furthermore, the aforementioned increased HRN liver capacity to convert (diet-derived) saturated to desaturated fatty acids, such as oleic acid, may exacerbate the effect of exogenous unsaturated fatty acids on HRN liver Cyp and lipid homeostasis. Thus, it appears that the accumulation of unsaturated fatty acids drive both the Cyp induction, which may represent a compensatory mechanism, and the hepatomegaly (Finn *et al.*, 2009).

The main difference between previous transcriptomic findings and this proteomic analysis is that, whereas transcript expression of lipid influx transporters were increased (e.g. *Cd36*, *Scarb1*, *Ptcp*) and the mRNA of the cholesterol efflux pump, *Abcg8*, decreased (Mutch *et al.*, 2007), no changes in the protein levels of these transporters were detected (Table 4.11). This may relate to differences in post-transcriptional regulation or methodological differences in sample extraction efficiency of membrane bound proteins. Nevertheless, transcriptomic and proteomic analyses both indicate that the HRN liver adapts to its increased localised lipid content by activation of peroxisomal fatty acid oxidation (Table 4.11) and oxidative stress response pathways (Wang *et al.*, 2005; Gonzalez *et al.*, 2011a) (Table 4.10). For example, increased protein levels of peroxisomal 2,4-dienoyl-CoA reductase (*Decr2*) and peroxisomal acyl-coenzyme A oxidase 2 (*Acox2*) indicate peroxisomal oxidation, whereas elevated *Gstm1*, *m2* and *m3* (Wang *et al.*, 2005) (Table 4.10) indicate induction of protective stress response systems; the latter are predicted to be due, in part, to increased *Nfe2l2* activity (Table 4.10). Despite no change in *Ppara* mRNA expression (Wang *et al.*, 2005), *Ppara* is predicted to be activated (Figure 4.14) (Mutch *et al.*, 2007) and may contribute to the upregulation of fatty acid peroxisomal oxidative mechanisms (Hashimoto *et al.*, 1999). In contrast, the reduction in *Cpt2* suggests that mitochondrial beta-oxidation is inefficient in HRN livers (Table 4.11). Previously, it has been postulated that HRN

mitochondrial oxidation may be inefficient due to observed increased transcription of acetyl-CoA carboxylase 2 (*Acacb*) (Mutch *et al.*, 2007), which could lead to elevated intracellular malonyl-CoA, which is an allosteric inhibitor of Cpt isoforms (Ghadiminejad and Saggerson, 1990). Nevertheless, the protein levels of acetyl-CoA carboxylases (*Acaca*, *Acacb*) were unchanged here, unlike the reduced *Cpt2*.

In contrast to HRN lipid disposition, HRN mice have decreased hepatic bile acid content (~60% reduction) but almost double the normal serum total bile acid concentration (Cheng *et al.*, 2014). *Cyp7a1* and *Cyp8b1* are central to the classic pathway of primary bile acid synthesis and, in keeping with the HRN hepatic widespread Cyp induction, both are upregulated (Table 4.11). However, *Por*-deficiency nullifies primary hepatic bile acid synthesis (Cheng *et al.*, 2014). Several mechanisms for the surprising observation of increased circulating bile acids have been proposed, including increased activity of the alternative (acidic) pathway of bile acid synthesis, induction of intestinal transporters (apical sodium-bile acid transporter (*Asbt*), organic solute transporter  $\alpha$  (*Ost $\alpha$* ) and *Ost $\beta$* ) and increased intestinal generation of secondary bile acids (Cheng *et al.*, 2014). This study has identified reduced *Ntcp*, which suggests another potential mechanism for increased circulating bile acids is reduced hepatic uptake, particularly of conjugated bile acids (Dawson *et al.*, 2009).

In summary, global proteomic profiling of HRN livers has confirmed and built upon the previous transcriptomic studies (Wang *et al.*, 2005; Mutch *et al.*, 2007; Gonzalez *et al.*, 2011a). Hepatic *Por* deficiency leads to hepatic lipid accumulation, predicted increased activity of several regulators, and compensatory adaptive mechanisms including co-ordinated Cyp-induction and upregulation of both fatty acid peroxisomal oxidation and oxidative stress response proteins.

#### 4.4.1.2 Study limitations

This study had certain limitations. First, the PK study and microsome incubations were limited to three mice/strain precluding hypothesis testing. Furthermore, the limited size of the blood samples collected using the DBS method in the PK study did not readily permit re-extraction for additional LC-MS analyses. Nevertheless, the PK profiles were consistently different between strains. Although inter-animal haematocrit is generally confined to a narrow range (Wagner *et al.*, 2016) and not expected to differ between strains, it was not determined in this study. However, experimental manipulation of haematocrit to the theoretical extremes has shown that its maximal effect on drug measurements from DBS is  $\pm 20\%$  (Wagner *et al.*, 2016), which cannot account for the multiple fold change differences in analyte levels observed between HRN and WT subjects. Third, the effect, if any, of co-administration of RVT and ATV is unknown. Fourth, the impact of RVT/ATV on the observed liver histology is unknown as baseline liver histology was unavailable.

#### 4.4.1.3 Conclusion

In conclusion, this study has shown that Por-deficiency markedly impairs ATV hydroxylation *in vitro*. There is increased systemic exposures to RVT, ATV and ATV metabolites in HRN mice *in vivo*, which are likely due to several factors including microvascular aberrations associated with fatty liver, altered hepatic transporter expression, extra-hepatic Cyp-mediated metabolism, and increased hepatic glucuronidation. HRN hepatic proteomic analysis reinforced and built upon previous transcriptomic analyses, indicating that *de novo* hepatic lipid synthesis is unlikely to contribute to liver lipid accumulation. Nevertheless, the liver responds to increased local lipid content through Cyp induction and activation of fatty acid oxidation and oxidative stress response mechanisms. To further understand the observed *in vivo* statin disposition, PK statin studies using additional murine models should be conducted. These would include the HBN and HBRN models, and a novel model of conditional Por deficiency in both the liver and duodenum one week after exposure to  $\beta$ -naphthoflavone (Finn *et al.*, 2007). The latter model could be further refined by maintenance on a fat-free diet to prevent liver lipid accumulation (Finn *et al.*, 2009).

## **Chapter 5 Development, validation and application of a novel plasma high performance liquid chromatography tandem mass spectrometry assay for the quantification of six analytes from atorvastatin, bisoprolol and clopidogrel**

### **5.1 Introduction**

CVD is a leading cause of morbidity and is responsible for 30% of all deaths worldwide (World Health Organisation, 2014b). The pathogenesis of CVD is multifactorial (Sing *et al.*, 2003; Low Wang *et al.*, 2016) and, as a result, a multi-drug strategy has been iteratively developed for secondary CVD prevention that includes statins, beta blockers and antiplatelet agents (e.g. clopidogrel (CLP)). The overlapping pathophysiology of distinct cardiovascular disorders means that statins are also commonly used in primary CVD prevention and beta blockers in cardiac arrhythmias and hypertension.

Cardiovascular drugs are dosed empirically. Nevertheless, drug effectiveness and toxicity are related to drug concentration, which varies between individuals due to a constellation of clinical (e.g. age, comorbidities), environmental (e.g. drug-drug and drug-food interactions) and genetic factors (Turner and Pirmohamed, 2014). A large proportion of interindividual variation in drug response remains currently unexplained, despite intensive research (Turner *et al.*, 2015). Therefore, there is the need to develop straightforward quantitative multi-drug assays and apply them to large patient cohorts to parse the PK factors of cardiovascular drug exposure, to determine the associations between dose, exposure and outcome for cardiovascular drugs, and to potentially guide dosing of cardiovascular drugs.

Most prior assays are limited to one cardiovascular drug (Hermann *et al.*, 2005; Partani *et al.*, 2014) or therapeutic class (Wang *et al.*, 2015; Umezawa *et al.*, 2008). Alternatively, one assay has been developed for screening 34 (Dias *et al.*,

2013) and another for quantifying 55 (Gonzalez *et al.*, 2011b) cardiovascular drugs. Nevertheless, full validation is not undertaken with assays of this impressive size, they do not employ analyte-specific deuterated internal standards, extraction requires a time consuming evaporation stage and importantly, they have only been reported to be used on modest sample sizes of 294 (Dias *et al.*, 2013) and 13 (Gonzalez *et al.*, 2011b) patients.

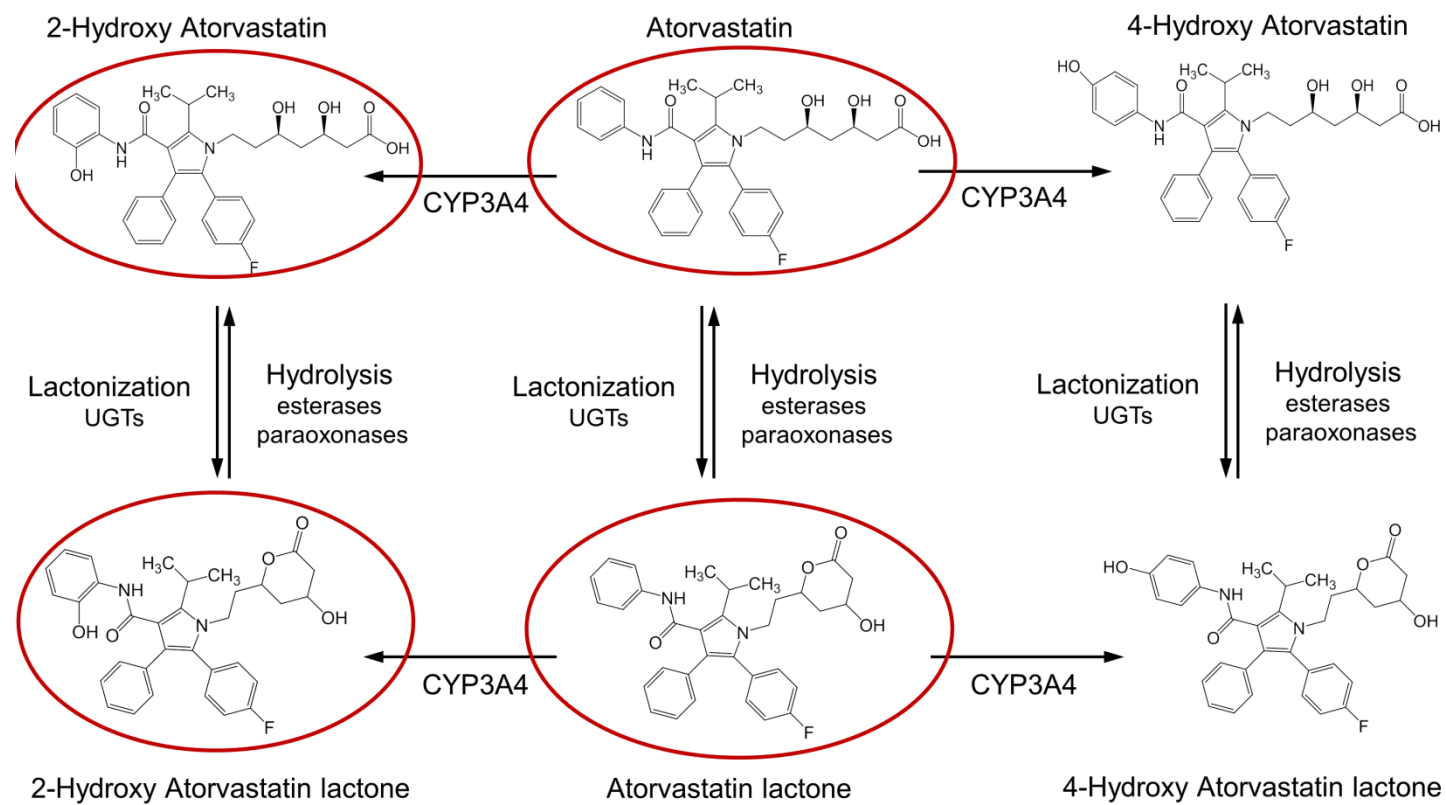
Therefore, the aims here were to: i) develop and fully validate a novel LC-MS/MS assay for quantification of commonly used ATV, bisoprolol (BSP) and CLP-carboxylic acid (CLP-CA) in plasma, and; ii) apply this assay to 1,283 samples from 1,026 patients in the PhACS study (Turner *et al.*, 2016).

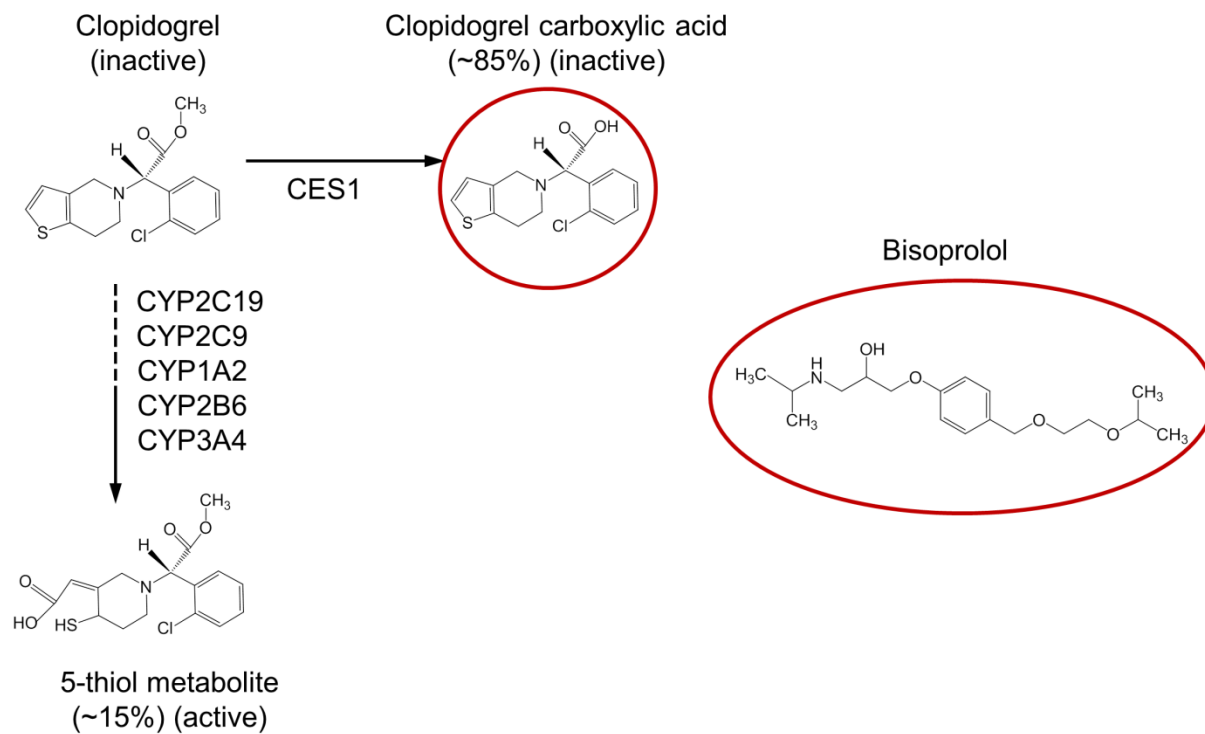
The assay herein quantifies six clinically relevant analytes from these three mechanistically distinct drugs: ATV, 2-OH ATV, ATV L, 2-OH ATV L, BSP, and CLP-CA (Figure 5.1). ATV and 2-OH ATV were selected because they are both active inhibitors of HMGCR and contribute to ATV's hypolipidaemic therapeutic effect (Pfizer Inc, 2015); ATV L and 2-OH ATV L were selected because statin Ls are implicated in SAM (Skottheim *et al.*, 2008; Schirris *et al.*, 2015a). 4-OH ATV and 4-OH ATV L were pragmatically excluded because they represent minor derivatives compared to 2-OH metabolites, and undergo the same biotransformation processes as 2-OH metabolites (Partani *et al.*, 2014; Keskitalo *et al.*, 2009c) (Figure 5.1).

BSP is a cardioselective beta-1 adrenergic receptor antagonist racemate with high oral bioavailability (~80-90%), peak plasma concentrations within 2-4 hours of dosing, low plasma protein-binding (30%) and an elimination half-life of ~9-12 hours. Approximately 50% of BSP is renally excreted unchanged and 50% undergoes hepatic metabolism into labile or inactive metabolites prior to predominant renal excretion (Duramed Pharmaceuticals Inc, 2010; Leopold, 1986).

The second generation thienopyridine, CLP, is a prodrug that is rapidly absorbed and its peak concentration occurs at ~45 minutes post dose (Bristol-Myers Squibb Company, 2009). Approximately 85% of CLP is metabolised by esterases to the major circulating inactive metabolite, CLP-CA; the other ~15% undergoes two sequential hepatic oxidation steps mediated by several CYPs, and in particular CYP2C19, to produce the active thiol group-containing metabolite that irreversibly inhibits platelet P2Y<sub>12</sub> receptors (Turner and Pirmohamed, 2014). CLP-CA is highly protein bound (~94%) with an elimination half-life of 8 hours (Bristol-Myers Squibb Company, 2009). The active metabolite is labile, and requires addition of a preservative (2-bromo-3'-methoxyacetophenone (MPB)) to collected samples to enable quantification (Karaźniewicz-Łada *et al.*, 2014; Lewis *et al.*, 2013), precluding LC-MS/MS analysis in routinely collected samples. The extensive metabolism of parent CLP means that CLP-CA peak levels are a thousand-fold greater than those of CLP (Karaźniewicz-Łada *et al.*, 2014). Furthermore, CLP-CA has been correlated to platelet inhibition indices (Serebruany *et al.*, 2009) and demonstrated utility in identifying CLP non-adherence and variable metabolism (Mani *et al.*, 2008; Serebruany *et al.*, 2009), and was therefore included in this assay.

**Figure 5.1 Chemical structures and relevant metabolism of analytes analysed**





Abbreviations: CES1 = carboxylesterase 1; CYP = cytochrome P450; UGTs = uridine 5'-diphospho-glucuronosyltransferases.

The red rings denote the analytes quantified in this assay. The analytes were: parent ATV, its major hydroxylated metabolite (2-OH ATV), their corresponding lactones (ATV L and 2-OH ATV L, parent BSP, and the major CLP inactive metabolite, CLP -CA.

## 5.2 Methods

### 5.2.1 Chemicals and reagents

All compounds (analytes and internal standards) were purchased from Toronto Research Chemicals (Toronto, Canada) (Table 5.1). Acetic acid, DMSO and formic acid were obtained from Sigma-Aldrich (St. Louis, MO, USA).

Acetonitrile, methanol and water were obtained from Fisher Scientific (Loughborough, UK). All reagents were LC-MS grade unless otherwise stated.

Pooled gender unfiltered human healthy volunteer plasma in K3 EDTA was purchased from Sera Laboratories International (Seralab, West Sussex, UK) and stored at -80°C.

**Table 5.1 Compounds**

Analyte			Internal standard		
Structure	Formula	Purity (%)	Identity	Formula	Purity (%)
Atorvastatin Calcium	C <sub>33</sub> H <sub>34</sub> FN <sub>2</sub> O <sub>5</sub> .1/2Ca	96.0	Atorvastatin-d5 Sodium	C <sub>33</sub> H <sub>29</sub> D <sub>5</sub> FN <sub>2</sub> NaO <sub>5</sub>	C: 98.0 I: 99
2-Hydroxy Atorvastatin Calcium	C <sub>33</sub> H <sub>34</sub> FN <sub>2</sub> O <sub>6</sub> .1/2Ca	96.0	2-Hydroxy Atorvastatin-d5 Disodium	C <sub>33</sub> H <sub>28</sub> D <sub>5</sub> FN <sub>2</sub> Na <sub>2</sub> O <sub>6</sub>	C: 96.0 I: 98.6
Atorvastatin Lactone	C <sub>33</sub> H <sub>33</sub> FN <sub>2</sub> O <sub>4</sub>	98.0	Atorvastatin-d5 Lactone	C <sub>33</sub> H <sub>28</sub> D <sub>5</sub> FN <sub>2</sub> O <sub>4</sub>	C: 98.0 I: 98.9
2-Hydroxy Atorvastatin Lactone	C <sub>33</sub> H <sub>33</sub> FN <sub>2</sub> O <sub>5</sub>	98.0	2-Hydroxy Atorvastatin-d5 Lactone	C <sub>33</sub> H <sub>28</sub> D <sub>5</sub> FN <sub>2</sub> O <sub>5</sub>	C: 98.0 I: 99.1
Bisoprolol Hemifumarate	C <sub>18</sub> H <sub>31</sub> NO <sub>4</sub> .1/2[C <sub>4</sub> H <sub>4</sub> O <sub>4</sub> ]	98.0	Bisoprolol-d5	C <sub>18</sub> H <sub>26</sub> D <sub>5</sub> NO <sub>4</sub>	C: 98.0 I: 98.3
Clopidogrel Carboxylic Acid Hydrochloride	C <sub>15</sub> H <sub>15</sub> Cl <sub>2</sub> NO <sub>2</sub> S	97.0	Rac-Clopidogrel-d4 Carboxylic Acid	C <sub>15</sub> H <sub>10</sub> D <sub>4</sub> ClNO <sub>2</sub> S	C: 97.0 I: 99.4

Abbreviations: C = chemical; I = isotopic

### 5.2.2 Preparation of stock solutions, working solutions, internal standards solution, calibration standards, and quality controls

Stock solutions were prepared by dissolving each compound (Table 5.1) in DMSO or methanol and stored at -20°C (Table 5.2).

**Table 5.2 Stock solutions**

Analyte			Internal standard		
Identity	Solvent	Concentration	Identity	Solvent	Concentration
ATV	DMSO	20mM	ATV-d5	MeOH	1mM
2-OH ATV	DMSO	1mM	2-OH ATV-d5	MeOH	1mM
ATV L	DMSO	10mM	ATV-d5 L	DMSO	1mM
2-OH ATV L	DMSO	1mM	2-OH ATV-d5 L	DMSO	1mM
BSP	MeOH	2mg/mL	BSP-d5	MeOH	4mg/mL
CLP-CA	MeOH	2mg/mL	CLP-d4 CA	MeOH	1mg/mL

All stock solutions stored at -20°C. DMSO = dimethyl sulfoxide; MeOH = methanol

The analytes were divided into two sets of working solutions: i) a 'joint' composite working solution, consisting of ATV, 2-OH ATV, BSP and CLP-CA and; ii) an 'ATV lactones' composite working solution consisting of ATV L and 2-OH ATV L. The joint and ATV lactones working solutions were prepared in 25:75 acetonitrile-water and 100% acetonitrile (v/v), respectively. Solutions for each calibration standard and each QC concentration were prepared at 10x the required concentration in individual glass vials, for both joint and ATV lactones (Table 5.3).

**Table 5.3 Analyte working solutions**

Working solution name	Composite working solution			
	Joint <sup>1</sup> (ng/mL)		ATV lactones <sup>2</sup> (ng/mL)	
	ATV, 2-OH ATV, BSP	CLP-CA	ATV L	2-OH ATV L
CAL 1	5	150	X	5
CAL 2	10	300	X	10
CAL 3	15	450	12	15
CAL 4	30	900	24	30
CAL 5	100	3000	80	100
CAL 6	250	7500	200	250
CAL 7	500	15000	400	500
CAL 8	800	24000	640	800
CAL 9	1000	30000	800	1000
CAL 10	1250	37500	1000	1250
LLOQ	5	150	12 <sup>3</sup>	5 <sup>3</sup>
LOW	15	450	36	15
MID	450	13500	360	450
HIGH	950	28500	760	950

<sup>1</sup> = Each joint solution consisted of ATV, 2-OH ATV, BSP and CLP-CA in 25:75 acetonitrile-water;

<sup>2</sup> = each lactone solution was composed of ATV L and 2-OH ATV L in 100% acetonitrile;

<sup>3</sup>= for the ATV lactones lower limit of quantification (LLOQ), two separate solutions rather than one composite were used.

For each analyte, a deuterated internal standard was used. An internal standard 'intermediate' working solution containing all six deuterated internal standards in 100% acetonitrile (v/v) was prepared and stored at 4°C. On each day of analysis, an aliquot of the internal standard intermediate solution was diluted 10x in 25:75 acetonitrile-water to produce the internal standard working solution; the concentrations in the daily internal standard working solution are in Table 5.4.

**Table 5.4 Composite internal standard daily working solution**

Internal standard	Concentration (ng/mL)
ATV-d5	25
2-OH ATV-d5	25
ATV-d5 L	55
2-OH ATV-d5 L	55
BSP-d5	25
CLP-d4 CA	750

All six deuterated internal standards were prepared in a single 'intermediate' working solution in 100% acetonitrile (v/v), which was stored at 4°C. On each day of analysis, an aliquot of this solution was diluted 10x in 25:75 acetonitrile-water to produce the internal standard working solution shown in this table.

All working solutions were stored at 4°C, and kept on ice during use. Positive displacement pipettes were used to prepare all solutions, and for plasma spiking (microman pipettes with capillary pistons, Gilson Scientific, Luton, UK).

The calibration standard and QC concentrations are listed in Table 5.5. Each calibration line consisted of a double blank, single blank and 10 calibration standards (eight for ATV L). To prepare calibration and QC samples, pooled human plasma was defrosted for ~one hour and vortexed (SciQuip VariMix Vortex) for homogenisation. For each sample, 180µL plasma was spiked with 20µL of the appropriate working solution (i.e. a 10x dilution). For the double and single blanks, 180µL was spiked with 20µL 25:75 acetonitrile-water. Each spiked plasma sample was briefly vortexed before 50µL was transferred into a 96-well plate (1.2mL square well, U-bottomed ABgene storage plate, ThermoFisher Scientific). 20µL internal standard working solution was added

to all samples using an electronic repeat dispensing pipette (Eppendorf Multipette Xstream dispenser) except the double blank, to which 20µL 25:75 acetonitrile-water was added. The plate containing the samples was gently agitated (750rpm) for 8 minutes using an Orbit™ P2 digital shaker (Labnet International). 180µL of 100% acetonitrile containing 0.3% acetic acid (v/v) was then added to each sample using the repeat dispenser, the block re-agitated for 2 minutes, and centrifuged for 10 minutes at 2,038 x *g* in 4°C (Eppendorf™ 54030 R microcentrifuge). 100µL supernatant was transferred to a new 96-well plate and 200µL water added using the repeat dispenser (producing a final concentration of acetic acid of 0.1%). The plate was centrifuged for 5 minutes (2,038 x *g*, 4°C), and was then ready for the autosampler. Fresh calibration and QC samples were prepared on each day of analysis during both validation and patient sample analyses. Full calibration lines were injected at the beginning and end of each analytical run.

**Table 5.5 Calibration standard and quality control concentrations**

	Joint (ng/mL)		ATV lactones (ng/mL)	
	ATV, 2-OH ATV, BSP	CLP-CA	ATV L	2-OH ATV L
<b>Calibration standard</b>				
1	0.5	15	X	0.5
2	1.0	30	X	1.0
3	1.5	45	1.2	1.5
4	3.0	90	2.4	3.0
5	10.0	300	8.0	10.0
6	25.0	750	20.0	25.0
7	50.0	1500	40.0	50.0
8	80.0	2400	64.0	80.0
9	100.0	3000	80.0	100.0
10	125.0	3750	100.0	125.0
<b>Quality control</b>				
LOW	1.5	45	3.6	1.5
MID	45.0	1350	36.0	45.0
HIGH	95.0	2850	76.0	95.0

The quality control concentrations were chosen to be 3x the lower limit of quantification (low), and 36% (mid) and 76% (high) of the calibration range. For each analytical run, two sets of calibration standards and quality control samples were prepared – the first for the joint analytes (ATV, 2-OH ATV, BSP, CLP-CA), and the second for the ATV lactones (ATV L, 2-OH ATV L).

### 5.2.3 LC-MS/MS conditions

A Shimadzu Nexera X2 modular system (Kyoto, Japan) was coupled to a Sciex triple quadrupole 6500 QTRAP mass spectrometer (AB Sciex, Warrington, UK). The Shimadzu system comprised a SIL-30AC autosampler, two LC-30AD pumps, a CTO-20A column oven and a CBM-20A controller. The autosampler temperature was set to 4°C, and a 5µL aliquot of each sample was injected from the autosampler into the system. The column oven was set to 40°C and housed a 2.7µm Halo C18 column (50 x 2.1 mm ID, 90Å, Hichrom Limited, Reading, UK, part number: 92812-402). Gradient separation was performed using standard mobile phases containing water with 0.1% v/v formic acid (A) and acetonitrile with 0.1% v/v formic acid (B), at a flow-rate of 500µL/min. A standard gradient procedure, as detailed in Table 5.6, was used that started with a high proportion of non-organic solvent (A), and transitioned to a high proportion of organic solvent (B). The column oven setting, Halo C18 column and eluent gradient collectively accomplished good HPLC separation of analytes and their corresponding internal standards. The run time of 6.0 minutes was chosen in particular to adequately separate the more hydrophilic CLP-CA and BSP peaks.

**Table 5.6 Eluent gradient**

Step	Time(min)	A (%)	B (%)
0	0.50	90	10
1	2.50	70	30
2	2.51	50	50
3	3.75	30	70
4	3.76	5	95
5	4.25	5	95
6	4.26	90	10
7	6.00	90	10

Flow rate used was 500µL/min.

A = water + 0.1% formic acid; B = acetonitrile + 0.1% formic acid (v/v)

The MS analysis was carried out in the low mass setting with a Turbo V™ electrospray source operated in positive ionisation mode. An integrated 6-port Valco diverter valve was used so that only the eluate containing the peaks of interest entered the source (Table 5.7).

**Table 5.7 Valco diverter valve setup**

Step	Time(min)	Valve position
1	0.00	A
2	1.90	B
3	2.70	A
4	3.20	B
5	4.10	A
6	6.00	A

The Valco valve diverted the eluate to either the waster (position A) or into the mass spectrometer (position B).

Detection and quantification were performed using MRM. The MRM transitions are listed in Table 5.8. A dwell time of 9.0msec per transition was used for all ATV analytes and internal standards, and 7.0msec per transition for BSP and CLP-CA analytes and internal standards. Nitrogen was used for all gases (nebuliser, auxiliary, collision, curtain), supplied by a Genius 3031 nitrogen generator (Peak Scientific, Inchinnan, UK). The main optimised mass spectrometer source/gas parameters were: CID gas 'medium'; curtain gas 25.0; gas 1 (nebuliser gas) 50.0; gas 2 (heater gas) 40.0; turbo ionspray voltage 5500.0 V; entrance potential 10.0 V and; a source temperature of 500°C. Analyte specific optimised parameters are listed in Table 5.8. All hardware was controlled using Analyst® software (Version 1.6.2, Sciex).

**Table 5.8 Transitions and specific operating parameters for the mass spectrometer**

Analyte/ Internal Std	Precursor ion (M+H <sup>+</sup> ) (m/z)	Product ion (m/z)	Declustering potential (V)	Collision energy (V)	Collision cell exit potential (V)
ATV	559.3	440.3	116	31	32
ATV-d5	564.1	445.1	46	29	38
2-OH ATV	575.3	250.2	111	57	50
2-OH ATV-d5	580.2	255.1	51	57	16
ATV L	541.3	276.2	50	55	24
ATV-d5 L	546.3	281.2	70	57	25
2-OH ATV L	557.3	276.2	60	57	24
2-OH ATV-d5 L	562.2	281.1	70	48	25
BSP	326.2	116.2	96	25	8
BSP-d5	331.0	121.1	96	23	10
CLP-CA	308.0	198.1	62	15	14
CLP-d4 CA	312.2	202.0	41	21	18

#### **5.2.4 Method Validation**

The developed assay was validated for selectivity, carryover, accuracy, precision, MEs, stability and dilution integrity according to the European Medicines Agency guidelines (European Medicines Agency, 2011).

#### **5.2.5 Selectivity**

Selectivity was tested by analysing extracted blank plasma from six individuals, including one lipaemic sample and one 2% haemolysed sample, to investigate interference at the retention time of each compound. Selectivity was accepted if the blank response of each individual plasma sample was less than 20% of the mean (n=6) LLOQ response for an analyte, and less than 5% of the mean internal standard response for an internal standard.

#### **5.2.6 Carryover**

Carryover into injected double blank extracted plasma, or injected 25:75 acetonitrile-water, immediately following injection of the top calibration standard (ULOQ), was separately assessed. Carryover was calculated by: detector response in extracted double blank plasma/ULOQ response\*100, or response in 25:75 acetonitrile-water/ULOQ\*100. Carryover was accepted if it was less than 20% of the LLOQ for an analyte, and if it was less than 5% of internal standard response for an internal standard.

#### **5.2.7 Lower limit of quantification**

The lowest calibration standard constituted the LLOQ. The LLOQ for each analyte could be reliably quantified (see below), and had a response at least 5x the mean blank response.

#### **5.2.8 Accuracy and Precision**

Within-run and between-run accuracy and precision was determined for each analyte by analysing three sets of validation samples. Each set consisted of a

calibration line, LLOQ samples, low, medium and high QC samples (n=6 for each concentration), all freshly prepared. Each set was prepared and analysed on a different day; different operators prepared different sets to assess the potential impact of operator on assay robustness. Accuracy was calculated as: mean observed concentration/nominal concentration \* 100. Precision was expressed as the CV (%). For each analyte, accuracy was acceptable if it was within 15% of the nominal concentration for each QC, and within 20% at the LLOQ. Similarly for each analyte, precision was acceptable if the CV did not exceed 15% for each QC, and was within 20% at the LLOQ.

### 5.2.9 Matrix Effect and Recovery

MEs, ER, and process efficiency (PE) for the assay were determined based on the principles of Matuszewski *et al* (Matuszewski *et al.*, 2003), using plasma from six individuals including one hyperlipidaemic sample and one 2% haemolysed sample. Three sets of samples from the six individuals were prepared: set one was neat analyte in 25:75 acetonitrile-water, set two consisted of samples prepared in plasma spiked *after* extraction, and set three consisted of samples prepared in plasma spiked *before* extraction (i.e. normal sample preparation).

MEs were calculated as: set two peak area response/set one peak area response \* 100. The MEs for each analyte and internal standard were determined separately in each sample by assessment of their individual peak area response, and the internal standard-normalised ME for each analyte was calculated as the analyte ME/internal standard ME in each sample. A CV  $\leq$  15% for the internal standard-normalised ME was considered acceptable.

ER was calculated by: set three peak area response/set two peak area response \* 100. PE was calculated by: set three peak area response /set one peak area response \* 100. ER and PE were both determined without internal standard normalisation.

In addition, the effect of 2% haemolysis on the joint analytes was further investigated by comparing the accuracy and precision on six replicates of low and high QC concentrations, prepared in 2% haemolysed and non-haemolysed plasma. This was undertaken because a signal for potential enhanced ME was identified for CLP-CA.

#### **5.2.10 Stability**

The stability of the analytes in solution (stock, working) and in plasma (bench top, freeze-thaw, 24-hour re-injection reproducibility, long term, and analytical run length) was determined.

Stock solution stability was determined by comparing six replicates of the old stock of each analyte stored at -20°C for three (ATV L, 2-OH ATV L) or six (ATV, 2-OH ATV, BSP, CLP-CA) months, to six replicates of new stock. Working solution stability was determined by comparing four replicates of old working solutions stored at 4°C for four (joint analytes) or seven (L analytes) weeks, to four replicates of newly prepared working solutions; all working solutions were prepared from the same stock. Peak area analyte responses for the old solutions that were within 15% of the new solution responses were considered acceptable. Conversion of deuterated internal standard to unlabelled analytes in the composite internal standard working solution after storage for 20 days at 4°C was also assessed.

Six replicates of spiked plasma at low and high QC concentrations were used to determine bench top, freeze-thaw, and long term stability. Bench top stability of spiked plasma after four hours at room temperature was assessed for joint analytes; stability at one, two and four hours on ice (4°C) and at room temperature on the bench top was determined for Ls. To assess the impact of freeze-thawing, QC samples underwent three freeze-thaw cycles which involved

at least 12 hours of freezing prior to thawing, and were compared to fresh calibration standards. To assess long term stability, QC samples were stored at -80°C and then compared to fresh calibration standards at three and six months. It was estimated that the analytical run length would not exceed 24 hours. Therefore, re-injection reproducibility after 24 hours in the autosampler was determined by re-injecting full calibration lines and six low, medium and high QCs. Mean responses within 15% of nominal concentrations were considered acceptably accurate for the above stability assessments. Lastly, joint and L calibration and QC samples were continually injected (n=261) for over 24 hours to determine analytical run length viability. Each calibration/QC sample had to be within 15% of its nominal concentration (except calibration one, which needed to be within 20%) to pass; the percentage of passes at each concentration for each analyte was recorded.

#### 5.2.11 Atorvastatin analyte interconversion

In all stability assessments (stock/working solutions, spiked plasma conditions), potential ATV analyte interconversion was assessed. This was carried out by determining the proportion (%) of *reciprocal* ATV acid/L analyte present as follows:

##### III. In joint solutions/spiking

- a.  $\text{ATV} \rightarrow \text{ATV L conversion} = \frac{\text{ATV L}}{(\text{ATV L} + \text{ATV})} * 100$
- b.  $\text{2-OH ATV} \rightarrow \text{2-OH ATV L conversion} = \frac{\text{2-OH ATV L}}{(\text{2-OH ATV L} + \text{2-OH ATV})} * 100$

##### IV. In lactone solutions/spiking

- a.  $\text{ATV L} \rightarrow \text{ATV conversion in ATV L stock} = \frac{\text{ATV}}{(\text{ATV} + \text{ATV L})} * 100$
- b.  $\text{ATV L} \rightarrow \text{ATV conversion in all other stability experiments} = \frac{\text{ATV}}{(\text{ATV} + \text{ATV L})} * 100 - \% \text{ of ATV in ATV L stock}$
- c.  $\text{2-OH ATV L} \rightarrow \text{2-OH ATV} = \frac{\text{2-OH ATV}}{(\text{2-OH ATV} + \text{2-OH ATV L})} * 100$

After identification of the high proportion of ATV in ATV L stock, ATV L to ATV conversions assessments in all subsequent stability experiments took this stock impurity into account.

When determining interconversion in plasma QC samples, only the high QC was considered because at the low QC, the reciprocal ATV analyte peaks (e.g. an ATV L peak after spiking with ATV) could not be reliably distinguished from background interference.

#### **5.2.12 Dilution Integrity**

To determine dilution integrity, pooled plasma was first spiked with joint or Ls to give high plasma concentrations of: 800ng/mL (ATV L), 1,000ng/mL (ATV, 2-OH ATV, 2-OH ATV L and BSP), and 30,000ng/mL (CLP-CA). These high plasma samples were diluted 20x in plasma to bring them back into the calibration standard range with final plasma concentrations of: 40ng/mL (ATV L), 50ng/mL (ATV, 2-OH ATV, 2-OH ATV L, BSP) and 1500ng/mL (CLP-CA). Six joint and six L replicates were extracted for analysis. Accuracy and precision (CV) of the diluted samples within 15% was considered acceptable.

#### **5.2.13 Application to sparse pharmacokinetics study in patients**

The developed, validated HPLC-MS/MS assay was successfully applied to simultaneously determine the concentrations of the analytes in one (n=1,026) or two (n=257) EDTA plasma samples from 1,026 patients. The included patients were taken from the PhACS study, which has been described previously (Turner *et al.*, 2016) and in Chapter 2. Briefly, PhACS was a multicentre UK-based prospective observational study that ran from 2008-2013 and recruited 1,470 patients hospitalised with a NSTEMI-ACS from 16 sites; participants were followed up for further cardiovascular events for at least 12 months. Blood-derived samples were taken at baseline, and at a median of one month and 12 months after discharge from index hospitalisation, and stored at -80°C. For participants on ATV (80mg or 40mg daily), BSP (any dose) or CLP (75mg daily),

EDTA plasma samples collected at one month were analysed to ensure steady-state had been reached; participants from all sites were included. Plasma samples taken at 12 months were also analysed in a subgroup of patients. 12 analytical runs were carried out; rows A and B of each 96-well plate were used for the joint and L calibration lines; the QCs were distributed throughout the remaining plate amongst the patient samples.

#### 5.2.14 Data Analysis

Raw data were processed using MultiQuant™ Version 1.6.2 (Sciex). The analyte to internal standard peak area ratio was calculated for the six analytes for calibration, QC and patient samples. The linearity of calibration standards was assessed. Separate weighted least squares regression analyses were applied to the calibration lines ( $1/x$  for ATV, 2-OH ATV, CLP-CA;  $1/x^2$  for BSP, ATV L, 2-OH ATV L). For each analyte, MultiQuant™ calculated the empirical concentration of the calibration, QC and patient samples by interpolation from the fitted calibration line. Acceptance criteria for a calibration line were: correlation coefficient ( $r^2$ )  $>0.99$ , and 75% of standards were within 15% of their nominal concentration, except for standard 1, which could be within 20%. For the patient sample runs, at least 67% of QCs had to be within 15% of their nominal concentration. This latter stipulation is in accordance with the Food and Drug Administration (FDA) bioanalytical guidance (Food and Drug Administration, 2001). Excel 2010 (Microsoft, USA) was used during assay validation for four purposes: i) to calculate the accuracy and precision of MultiQuant™-calculated concentrations in reference to nominal concentrations; ii) to carry out a student's t-test to determine the impact of haemolysis on joint QC concentrations; iii) to compare analyte (alone) peak areas when appropriate during validation, and; iv) to quantify ATV analyte acid/L interconversion.

Dose-specific analyte concentrations from the PhACS study are reported as medians and interquartile ranges, with exclusion of values  $<LLOQ$ . The influence of five key sample characteristics on  $\log_{10}$  transformed patient analyte

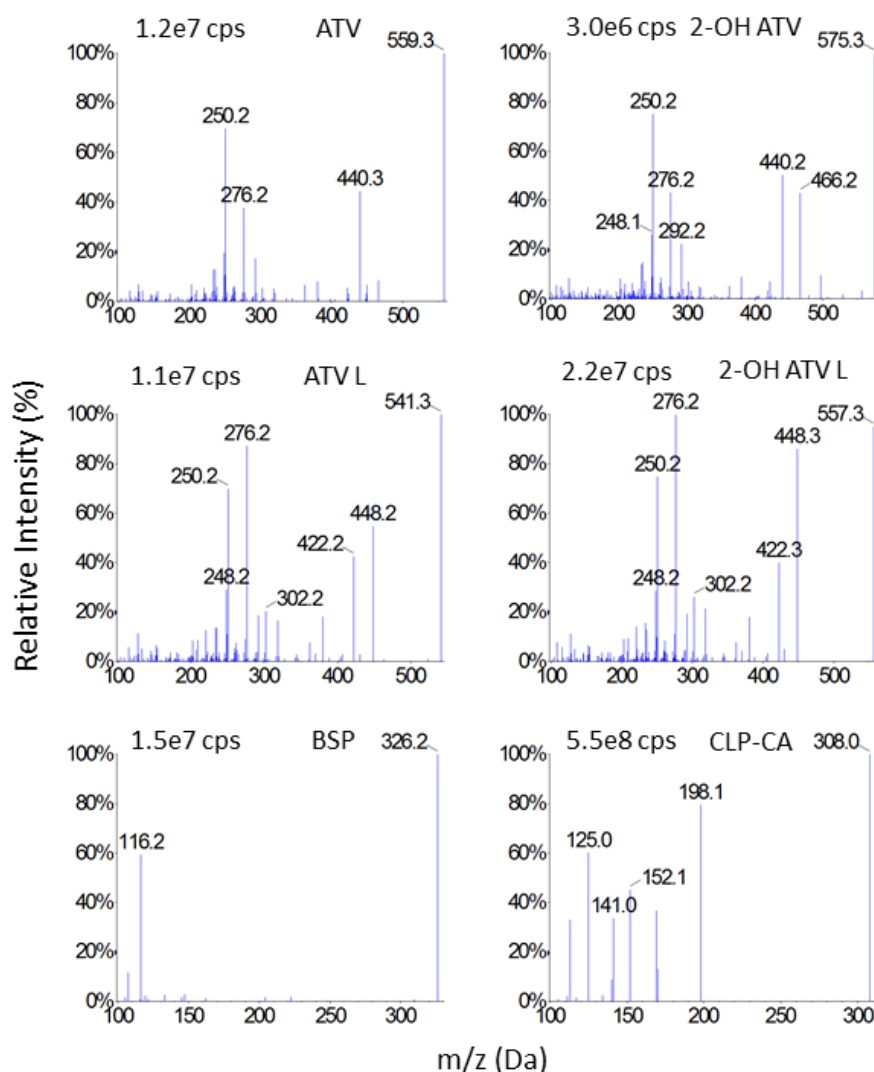
levels was determined by univariate linear regression. These variables are: time since last drug administration, dose (for ATV analytes and BSP), non-adherence, sample storage duration (days), and the duration between blood collection and laboratory processing of blood into plasma (hours). Time since last dose was estimated as 22:00 until blood collection time for ATV analytes, and 07:00 until blood collection time for BSP/CLP-CA. For each drug, non-adherence was defined as the number of tablets not taken during the seven days preceding the one month follow up visit (ordinal variable). For each variable, effect (unstandardized coefficient, B) and p-values are reported. All determined one month analyte levels, including those <LLOQ, were used in the regression analyses to avoid exclusion bias. For each variable,  $\leq 1.5\%$  of patients had missing data, except for sample collection to processing duration which was missing in  $\sim 1/3$  of patients. P-values were two-sided and  $p < 0.05$  indicated significance. Univariate regression analyses were performed in IBM SPSS version 22.0 (IBM Corp, Armonk, NY, USA).

All laboratory work described in this chapter only was jointly carried out by Dr Richard Turner and Dr Vanessa Fontana (post-doc, Molecular and Clinical Pharmacology, University of Liverpool).

## **5.3 Results**

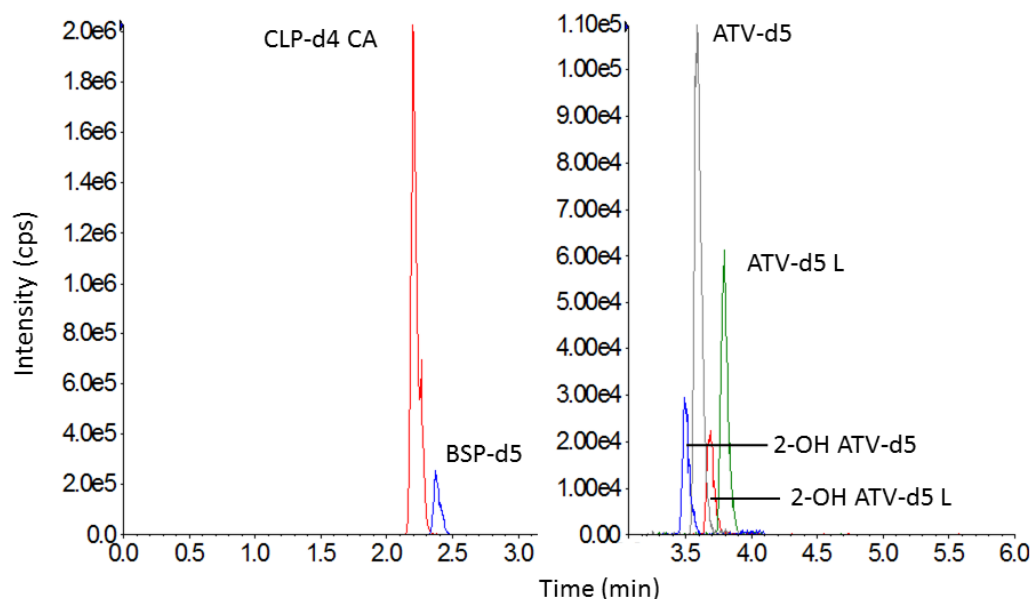
### **5.3.1 Optimisation of LC-MS/MS conditions**

The 2.7 $\mu\text{m}$  Halo C18 column was selected because it provided a symmetrical peak shape for all analytes, and in combination with the mobile phase used, analytes were eluted at high intensities. For all analytes, ESI and Q2 collision parameters were optimised. The stable and intense selected reaction monitoring transitions for the six analytes are presented in Figure 5.2, and a chromatogram of the six internal standards is shown in Figure 5.3.

**Figure 5.2 MS/MS spectra of analytes**

Cps = counts per second. This figure shows the tandem mass spectrometry (MS/MS) precursor and product ion m/z (mass-to-charge ratio) spectra for each analyte. The cited cps refers to the highest peak (at 100%). The selected precursor and product ions for each analyte are: ATV 559.3 & 440.3; 2-OH ATV 575.3 & 250.2; ATV L 541.3 & 276.2; 2-OH ATV L 557.3 & 276.2; BSP 326.2 & 116.2; CLP-CA 308.0 & 198.1.

During assay development, the calibration curve for CLP-CA consistently showed a weak quadratic fit at the higher end. This remained despite optimising the eluent gradient to ensure no overlap between the CLP-CA and adjacent BSP peaks, injecting only a 5  $\mu$ L sample, and purposely reducing the CLP-CA collision energy to keep the 6500 mass spectrometer detector response under its reported dynamic range ceiling ( $\sim 2 \times 10^8$  counts per second) (AB Sciex, 2012).

**Figure 5.3 Chromatograms of deuterated internal standards**

This figure shows the typical chromatograms from a single blank plasma sample spiked with the composite internal standard daily working solution. The figure represents one spiked sample but has been split into two graphs to permit two y-axes, because the CLP-d4 CA signal is more intense compared to the other internal standards. The internal standard solution concentrations were: 25ng/mL for ATV-d5, 2-OH ATV-d5 & BSP-d5; 55ng/mL for ATV-d5 L & 2-OH ATV-d5 L; 750ng/mL for CLP-d4 CA.

### 5.3.2 Optimisation of extraction procedure

Initially a one-step protein precipitation pilot extraction method was trialled in which 200 $\mu$ L of a solution of 100% acetonitrile with 0.3% acetic acid containing all internal standards was added directly to the 50 $\mu$ L spiked plasma. However, the accuracy of QCs using this pilot method was poor when derived from analyte to internal standard peak area ratios, but acceptable interestingly when considering analyte peak areas alone (Table 5.9). This suggested incomplete mixing of the internal standard, and therefore the optimised method required two-steps: the first to add 20 $\mu$ L of internal standard (at 10x higher concentration than the pilot method) and to agitate, and the second to add 180 $\mu$ L of the protein precipitation solvent (100% acetonitrile with 0.3% acetic acid) and to re-agitate. The importance of agitating again after the proteins had been precipitated on QC accuracy is confirmed in Table 5.9. The 0.1% acetic acid final concentration and autosampler temperature of 4°C were selected to reduce the conversion of ATV Ls to acid as previously reported (Macwan *et al.*, 2011; Jemal *et al.*, 1999a).

Table 5.9 Assay extraction method development

Analyte	Quality control conc. (ng/mL)	Analyte/IS Pilot method (n=3) (A)			Analyte alone Pilot method (n=3) (B)			Analyte/IS Assay method (n=6) (C)			Analyte/IS Assay without 2 min shake (n=6) (D)			
		M (ng/mL)	A (%)	P (%)	M (ng/mL)	A (%)	P (%)	M (ng/mL)	A (%)	P (%)	Nominal conc. (ng/mL)	M (ng/mL)	A (%)	P (%)
ATV	0.5	ND			ND			0.42	83.6	6.9	0.5	0.46	91.2	22.5
	1.5	1.77	117.9	7.3	1.49	99.2	3.3	1.34	89.2	11.6	1.5	1.58	105.0	6.0
	4.5	6.20	137.7	14.6	3.71	82.5	2.1	4.38	97.3	4.4	ND			
	51.2	74.68	145.9	5.2	47.48	92.7	3.7	49.90	97.5	3.0	45	57.30	127.3	8.5
	96	162.90	169.7	8.0	87.81	91.5	3.4	95.86	99.9	3.6	95	119.00	125.2	5.3
2-OH ATV	0.5	ND			ND			0.52	103.2	11.7	0.5	0.39	77.0	34.5
	1.5	1.70	113.6	5.4	1.45	96.7	9.7	1.42	95.0	6.0	1.5	1.43	95.4	9.6
	4.5	5.72	127.1	13.2	3.81	84.7	6.1	4.60	102.1	4.1	ND			
	51.2	68.07	133.0	2.8	47.66	93.1	4.9	49.46	96.6	3.2	45	51.45	114.3	12.4
	96	140.30	146.1	7.4	87.51	91.2	1.3	93.91	97.8	3.4	95	111.90	117.8	4.6
BSP	0.5	ND			ND			0.46	92.4	6.6	0.5	0.58	116.8	6.3
	1.5	1.89	125.9	6.3	1.55	103.5	1.5	1.37	91.3	4.7	1.5	1.73	115.2	4.4
	4.5	6.92	153.8	20.8	4.15	92.2	2.4	4.26	94.7	2.1	ND			
	51.2	76.72	149.8	7.7	51.41	100.4	3.6	50.02	97.7	3.4	45	53.52	118.9	8.5
	96	180.90	188.5	8.7	90.82	94.6	1.4	95.10	99.1	2.9	95	110.10	115.9	4.1
CLP-CA	15	ND			ND			0.49	97.9	4.8	15	11.30	75.3	15.1
	47	41.85	89.1	0.3	49.15	104.7	1.2	1.44	95.7	5.1	45	45.59	101.3	9.5
	141	140.30	99.6	1.3	131.40	93.2	6.2	4.43	98.4	2.1	ND			
	1600	1803.00	112.7	1.2	1741.00	108.8	3.2	51.82	101.2	2.1	1350	1470.00	108.9	8.1
	3000	3180.00	106.0	0.6	2916.00	97.2	2.8	96.74	100.8	3.6	2850	3103.00	108.9	6.4

Abbreviations: A = accuracy; IS = internal standard; M = mean; ND = not done; P = precision. Precision was determined by the coefficient of variation (%).

A and B show the quality control results from the same pilot analytical run, which added the 100% acetonitrile (to precipitate the plasma proteins) and internal standards in the same step, with (A) or without (B) considering the internal standard peak areas when calculating the analyte concentrations. Consideration of the internal standard areas (A) resulted in poorer analyte accuracy (red font) and precision compared to considering the analyte responses alone (B).

C shows early results from the validated assay extraction method, which added the internal standards and 100% acetonitrile in two sequential steps, with acceptable accuracy (green font) and precision.

D shows the negative impact of neglecting the final two minute agitation step (after protein precipitation) from the validated method.

### 5.3.3 Method validation

#### 5.3.3.1 Selectivity

The representative chromatograms of Figure 5.4 demonstrate that the method produced extracts with minimal endogenous interference at the retention times of the six analytes and their deuterated internal standards. The expected retention times reflect the increased hydrophilic nature of CLP-CA and BSP compared to ATV analytes, and so were 2.14, 2.33, 3.48, 3.57, 3.66 and 3.77 minutes for CLP-CA, BSP, 2-OH ATV, ATV, 2-OH ATV L and ATV L, respectively. Importantly, interference within each individual plasma sample was less than 20% of LLOQ (calibration 1) response for all analytes except ATV, and less than 5% of internal standard response for all internal standards (Table 5.10). In one individual blank sample, the ATV response was 258% of the LLOQ response, which was presumed to be a contaminant or sample mislabelling, and needs repeating.

**Table 5.10 Analyte and internal standard selectivity**

Analyte	Mean blank sample peak area response (cps) (n=6) <sup>1</sup>	Mean analyte LLOQ peak area (cps) (n=6) <sup>2</sup>	Mean interference (%)
<b>Analyte</b>			
ATV	653.7	5927.5	11.0 <sup>3</sup>
2-OH ATV	402.5	2812.6	14.3
ATV L	281.4	6606.0	4.3
2-OH ATV L	181.3	2481.1	7.3
BSP	280.4	13385.8	2.1
CLP-CA	2381.8	73750.0	3.2
<b>Internal standard</b>			
ATV-d5	997.7	163955.1	0.7
2-OH ATV-d5	449.7	51931.4	0.9
ATV-d5 L	471.9	170642.6	0.28
2-OH ATV-d5 L	818.5	60748.5	1.35
BSP-d5	344.7	399988.8	0.09
CLP-d4 CA	3079.6	3895025.8	0.08

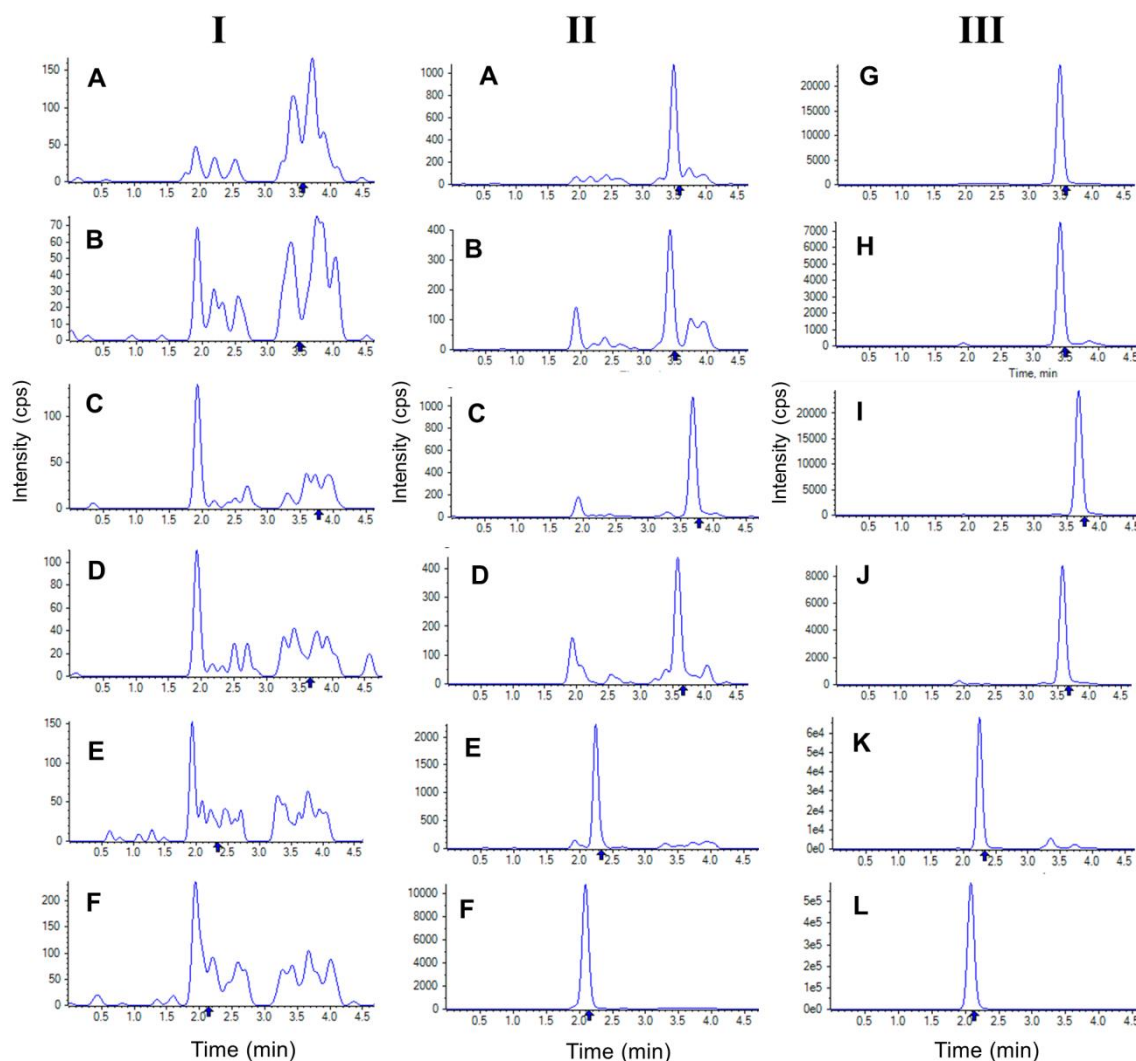
Cps = counts per second.

<sup>1</sup> = The six blank plasma samples analysed were four from healthy volunteers, one hyperlipidaemic sample and one 2% haemolysis sample

<sup>2</sup> = The mean lower limit of quantification area response was determined using spiked plasma from one volunteer injected for analysis six times.

<sup>3</sup> = calculated using the ATV response from five of the six blank plasma samples, excluding the very high (258% of LLOQ) response.

This table shows the 'mean interference' for each analyte and internal standard. However, interference was assessed for each individual blank plasma sample, and was accepted for all analytes and internal standards except ATV, for which one blank sample had a response 258% higher than the ATV LLOQ response. Therefore, ATV selectivity needs repeating.

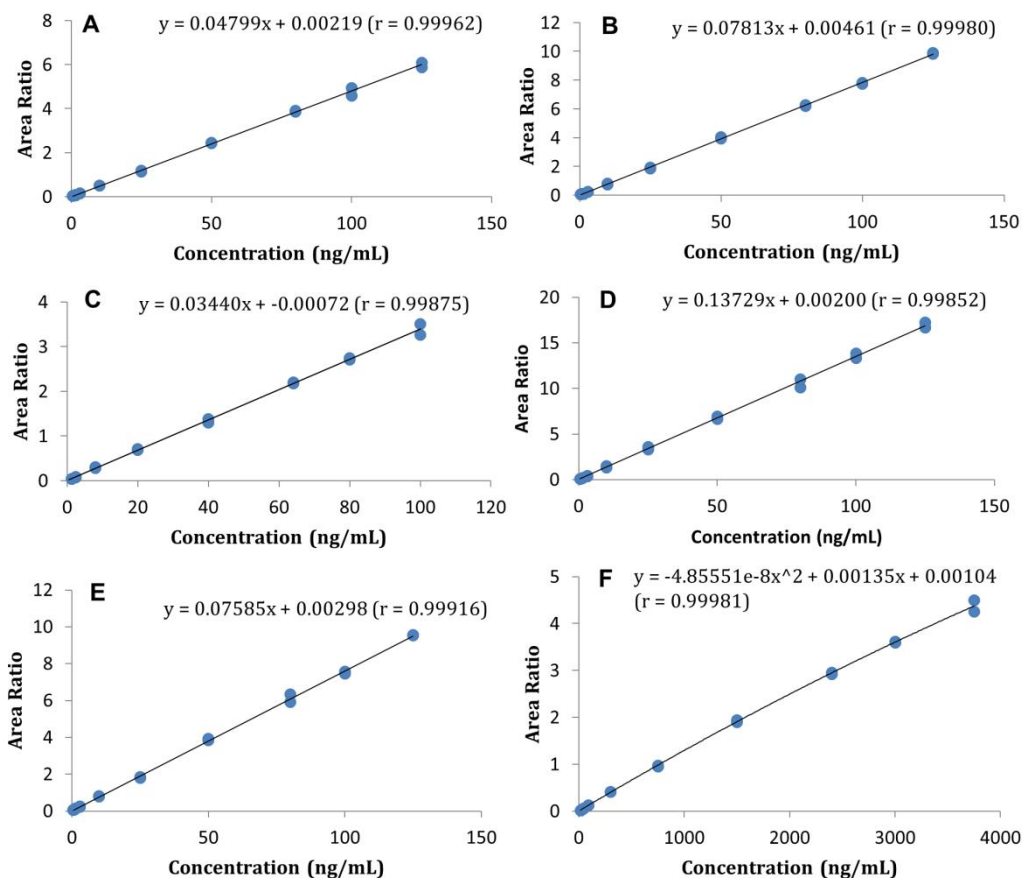
**Figure 5.4 Representative multiple reaction monitoring chromatograms**

A = ATV; B = 2-OH ATV; C = ATV L; D = 2-OH ATV L; E = BSP; F = CLP-CA; G = ATV-d5; H = 2-OH ATV-d5; I = ATV-d5 L; J = 2-OH ATV-d5 L; K = BSP-d5; L = CLP-d4 CA

This figure shows representative multiple reaction monitoring chromatograms of blank human plasma (I) and blank human plasma spiked with analytes at the LLOQ (II), or with internal standard (III).

### 5.3.3.2 Calibration curves

Validated calibration ranges were: 0.5-125ng/mL for ATV, 2-OH ATV, 2-OH ATV L and BSP, 1.2-100ng/mL for ATV L, and 15-3,750ng/mL for CLP-CA. Linearity was observed for all analytes throughout these concentration ranges, except for CLP-CA for which a quadratic line fit the calibration standard data better. Representative calibration lines, equations and correlation coefficients are provided in Figure 5.5.

**Figure 5.5 Representative calibration curves**

A = ATV; B = 2-OH ATV; C = ATV L; D = 2-OH ATV L; E = BSP; F = CLP-CA

This figure shows representative calibration lines for each analyte. All calibration lines were linear except for CLP-CA, which was best fit using a quadratic function. Separate weighted least squares regression analyses were applied to the calibration lines ( $1/x$  for ATV, 2-OH ATV, CLP-CA;  $1/x^2$  for BSP, ATV L, 2-OH ATV L). 10 calibration standards were used for all analytes except ATV L, which required eight standards because of a higher LLOQ (1.2ng/mL). The standards were injected at the beginning and end of each analytical run, and so two points per concentration are visible.

### 5.3.3.3 Carryover

Carryover after ULOQ injection into blank plasma was slightly higher than into 25:75 acetonitrile-water solvent, likely due to an additive contribution from endogenous interference (Table 5.11). Nevertheless, carryover into both solutions was uniformly less than 20% of LLOQ response for all analytes, and less than 5% of internal standard response for all internal standards (Table 5.11).

**Table 5.11 Carryover of analytes and internal standards**

Compound	ULOQ (ng/mL)	Carryover (% of LLOQ)	
		Into blank plasma	Into 25:75 acetonitrile-water
<b>Analyte</b>			
ATV	125	11.0	6.2
2-OH ATV	125	15.7	3.7
ATV L	100	3.8	2.7
2-OH ATV L	125	14.8	10.9
BSP	125	0.6	1.1
CLP-CA	3750	5.9	5.2
<b>Internal standard</b>	<b>Concentration (ng/mL)</b>		
ATV-d5	25	0.5	0.1
2-OH ATV-d5	25	1.2	0.5
ATV-d5 L	55	0.6	0.1
2-OH ATV-d5 L	55	1.2	0.1
BSP-d5	25	0.3	0.1
CLP-d4 CA	750	0.1	0.1

Carryover from the top calibration standard (the upper limit of quantification) into either blank plasma or 25:75 acetonitrile-water was determined. This table shows that internal standard carryover was uniformly negligible. Analyte carryover was acceptable. However, carryover into blank plasma was higher than into 25:75 acetonitrile-water, likely due to a contribution from endogenous interference.

#### 5.3.3.4 Accuracy and Precision

Within-run (intra-day) and between-run (inter-day) accuracy and precision results for all analytes at the specified LLOQ, low, middle and high QCs were acceptable, as shown in Table 5.12 and Table 5.13, respectively. Although ATV L selectivity was acceptable at 0.5ng/mL (not shown), a higher LLOQ was used for ATV L (1.2ng/mL) because calculated ATV L concentrations at 0.5ng/mL were found to be insufficiently accurate during assay optimisation (not shown).

**Table 5.12 Within-run (intra-day) accuracy and precision**

Analyte	Nominal conc. (ng/mL)	Set 1 (n=6)			Set 2 (n=6)			Set 3 (n=6)		
		M (ng/mL)	A (%)	CV (%)	M (ng/mL)	A (%)	CV (%)	M (ng/mL)	A (%)	CV (%)
ATV	0.5	0.47	95.0	11.1	0.49	99.0	6.7	0.46	92.0	8.5
	1.5	1.57	104.5	8.2	1.54	102.8	6.3	1.55	103.7	5.1
	45	44.53	99.0	1.6	45.78	101.7	3.3	45.3	100.8	2.3
	95	91.25	96.1	4.5	96.14	101.2	2.6	94.8	99.8	2.9
2-OH ATV	0.5	0.48	97.0	6.0	0.49	98.7	10.0	0.46	92.5	8.1
	1.5	1.53	102.2	7.7	1.55	103.2	8.0	1.49	99.2	10.8
	45	44.90	99.8	2.2	45.68	101.5	4.1	43.29	96.2	4.3
	95	89.58	94.3	4.0	94.30	99.3	4.7	93.37	98.3	4.3
ATV L	1.2	1.08	90.3	9.5	1.29	107.8	7.9	1.22	101.8	7.9
	3.6	3.56	98.8	6.0	3.54	98.4	2.7	3.51	97.4	8.3
	36	35.79	99.4	2.3	33.76	93.8	4.7	33.14	92.1	2.3
	76	75.25	99.0	4.7	74.87	98.5	2.8	73.30	96.5	4.4
2-OH ATV L	0.5	0.54	107.6	12.1	0.43	86.2	15.1	0.54	107.7	4.3
	1.5	1.63	108.6	8.7	1.40	93.3	10.9	1.53	101.8	12.9
	45	42.23	93.8	4.2	41.76	92.8	7.7	44.23	98.3	3.7
	95	92.95	97.8	5.8	96.00	101.1	4.0	95.56	100.6	7.3
BSP	0.5	0.46	92.8	2.3	0.47	93.7	7.8	0.48	96.7	3.8
	1.5	1.54	102.8	4.3	1.56	104.2	4.4	1.52	101.5	5.0
	45	44.61	99.1	2.0	45.32	100.7	3.1	44.78	99.5	2.6
	95	91.18	96.0	4.3	97.91	103.1	6.2	92.95	97.8	1.6
CLP-CA	15	15.23	101.5	3.3	14.11	94.0	3.8	14.32	95.4	3.1
	45	46.22	102.7	3.4	44.81	99.6	2.7	45.46	101.0	4.5
	1350	1345.83	99.7	2.3	1334.00	98.8	4.0	1331.67	98.6	4.4
	2850	2706.55	95.0	5.5	2821.50	99.0	3.6	2848.17	99.9	4.0

Abbreviations: A = accuracy; M = mean.

Each set consisted of a calibration line, LLOQ samples, low, medium and high QC samples (n=6 for each concentration), all freshly prepared. Each set was prepared and analysed on a different day.

**Table 5.13 Between-run (inter-day) accuracy and precision**

Analyte	Nominal conc. (ng/mL)	n=18		
		Mean (ng/mL)	Accuracy (%)	CV (%)
ATV	0.5	0.48	95.3	8.9
	1.5	1.56	103.7	6.3
	45	45.22	100.5	2.6
	95	94.06	99.0	3.9
	Overall		99.6	6.5
2-OH ATV	0.5	0.48	96.1	8.2
	1.5	1.52	101.5	8.5
	45	44.62	99.2	4.1
	95	92.42	97.3	4.7
	Overall		98.5	6.9
ATV L	1.2	1.20	100.0	10.9
	3.6	3.54	98.2	5.8
	36	34.23	95.1	4.6
	76	74.47	98.0	4.0
	Overall		97.8	7.0
2-OH ATV L	0.5	0.50	100.5	14.6
	1.5	1.52	101.2	12.1
	45	42.74	95.0	5.7
	95	94.84	99.8	5.7
	Overall		99.1	10.5
BSP	0.5	0.47	94.4	5.2
	1.5	1.54	102.8	4.4
	45	44.90	99.8	2.6
	95	94.02	99.0	5.3
	Overall		99.0	5.4
CLP-CA	15	14.55	97.0	4.7
	45	45.50	101.1	3.7
	1350	1337.17	99.0	3.5
	2850	2792.07	98.0	4.7
	Overall		98.8	4.4

This table shows the overall average concentration, accuracy and precision of each analyte from the three separate accuracy and precision analytical runs.

### 5.3.3.5 Matrix effects and recovery

The mean MEs, ER and PE for low and high QCs for all analytes are in Table 5.14. Analyte ERs ranged from 93 to ~100%, indicating complete recovery. ER precision (CV) was <14% at low or high QCs, and <11% for any analyte overall, which demonstrates no substantial loss of analytes during extraction. There was consistent ion enhancement for all analytes and internal standards, although importantly, the CV of the internal standard-normalised MEs was <13% for any analyte, meeting the acceptance criterion.

**Table 5.14 Interindividual Matrix effects and recovery assessment**

Analyte	Nominal conc. (ng/mL)	N=6							
		Analyte Extraction Recovery (%)		Matrix Effect (%)				Analyte Process Efficiency (%)	
		Mean	CV	Mean Analyte	Mean IS	Mean Analyte/IS	Mean Analyte/IS CV	Mean	CV
ATV	1.5	102.4	13.3	118.6	115.0	103.9	<b>12.3</b>	120.8	11.1
	95	99.1	5.7	123.0	109.7	112.2	<b>5.8</b>	121.7	5.8
	Overall	100.8	9.5	120.8	112.3	108.0	<b>9.1</b>	121.3	8.5
2-OH ATV	1.5	96.5	13.9	118.9	121.6	98.0	<b>12.2</b>	113.6	9.9
	95	98.8	6.8	119.6	122.0	98.4	<b>4.7</b>	118.0	6.2
	Overall	97.6	10.3	119.3	121.8	98.2	<b>8.5</b>	115.8	8.0
ATV L	3.6	102.5	8.9	136.8	126.5	113.1	<b>11.6</b>	139.2	5.1
	76	98.2	5.1	153.3	134.3	114.7	<b>3.5</b>	150.4	6.3
	Overall	100.3	7.1	145.1	130.4	113.9	<b>7.5</b>	144.8	5.7
2-OH ATV L	1.5	108.5	5.4	116.0	130.8	88.9	<b>8.8</b>	125.6	6.9
	95	100.6	6.6	133.5	130.5	102.8	<b>8.8</b>	134.5	9.2
	Overall	104.6	6.0	124.8	130.6	95.9	<b>8.8</b>	130.0	8.1
BSP	1.5	98.5	11.0	120.2	112.6	107.4	<b>7.0</b>	118.0	8.9
	95	97.4	7.0	111.4	104.9	106.3	<b>4.3</b>	108.4	4.6
	Overall	97.9	9.0	115.8	108.8	106.8	<b>5.6</b>	113.2	6.8
CLP-CA	45	93.8	12.4	114.0	108.0	106.5	<b>8.8</b>	106.3	8.8
	2850	92.7	3.9	112.5	111.6	100.9	<b>2.2</b>	104.3	2.5
	Overall	93.3	8.2	113.3	109.8	103.7	<b>5.5</b>	105.3	5.7

Abbreviations: CV = coefficient of variation; IS = internal standard. 'Overall' is the mean of the low and high quality control results.

Plasma from six separate sources was used to determine matrix effects, extraction recovery and process efficiency: four from healthy volunteers, one hyperlipidaemic sample and one 2% haemolysed sample. Plasma from each source was spiked both pre-extraction at the low and high quality control concentrations (normal extraction procedure), and spiked post-extraction at the appropriate equivalent low and high quality control concentration. Referent low and high quality control concentration solutions were spiked in 25:75 acetonitrile-water (instead of plasma). These samples were made for both the composite joint analytes (ATV, 2OH ATV, BSP, CLP-CA) and ATV lactones (ATV L, 2-OH ATV L) working solutions. This table shows that, for all analytes, the internal standard-normalised matrix effect CV, and the CVs for the extraction recovery and process efficiency were uniformly <15%.

When determining the MEs for CLP-CA, the 2% haemolysed sample was associated with higher ion enhancement (126.1%) than any of the other five individual matrices. However, there was no statistical difference in the accuracy or precision between low or high QCs prepared in normal non-haemolysed or 2% haemolysed plasma for any of the joint analytes (Table 5.15), which indicates minimal impact of haemolysis overall in this assay on empirical concentration determination.

**Table 5.15 Haemolysis impact on accuracy and precision of joint analytes**

Analyte	Nominal conc. (ng/mL)	Control (n=6)			2% haemolysed (n=6)			t-test (comparing concentrations)
		M (ng/mL)	A (%)	CV (%)	M (ng/mL)	A (%)	CV (%)	
ATV	1.5	1.72	114.6	7.7	1.59	106.0	9.1	0.14
	95	87.63	92.2	3.2	90.53	95.3	4.4	0.18
	Overall		103.4	12.8		100.7	9.0	0.94
2-OH ATV	1.5	1.64	109.2	6.8	1.71	113.9	12.8	0.51
	95	93.31	113.9	12.8	96.37	101.4	6.7	0.36
	Overall		103.7	7.9		107.6	11.7	0.94
BSP	1.5	1.56	104.0	15.7	1.64	109.6	6.1	0.46
	95	99.30	104.5	8.5	98.82	104.0	3.3	0.90
	Overall		104.3	12.0		106.8	5.5	0.99
CLP-CA	45	45.87	101.9	6.7	48.79	108.4	7.7	0.17
	2850	3054.54	107.2	4.7	3115.79	109.3	8.7	0.64
	Overall		104.6	6.1		108.9	7.8	0.96

Abbreviations: A = accuracy; M = mean. 'Overall' is the mean of the low and high quality control results. This table shows the results of an experiment that compared the accuracy and precision of joint analytes in six replicates prepared in pooled human blank plasma (control) compared to six replicates prepared in 2% haemolysed plasma. No statistically significant difference was detected between matrices and so it was concluded that 2% haemolysis did not have a substantial impact on joint analyte responses.

### 5.3.3.6 Stability

The stability of analytes in all conditions tested was <15% different compared to the reference, except for 2-OH ATV in the six month long term stability test. Therefore overall, stability was considered acceptable. All analytes were thus stable in: stock stored at -20°C (Table 5.16), working solutions stored at 4°C (Table 5.18), plasma on the bench top for four hours at room temperature (Table 5.19, Table 5.20), after three freeze-thaw cycles (Table 5.21), and after three months at -80°C (Table 5.23). At six months, only two of six 2-OH ATV low QCs passed, and the 2-OH ATV low QC mean accuracy was 118.1% (Table 5.23).

There was negligible analyte presence in the internal standard solution after 20 days at 4 °C (Table 5.17). A 96-well plate could be accurately and precisely re-injected after 24 hours in the autosampler at 4°C (Table 5.22). Furthermore, throughout 24 hours of continual re-injection, >90% of all calibration standard and QC injections were accurate. This indicates that this run length could be used to accurately determine patient drug concentrations and that the calibration lines and QCs used in the patient analytical runs should be expected to consistently meet the acceptance criteria.

#### **5.3.3.7 Atorvastatin analyte acid/lactone interconversion**

In all tested stability conditions, ATV analyte interconversion was assessed. Acid to L conversion (ATV to ATV L, and 2-OH ATV to 2-OH ATV L) was uniformly negligible with a difference of  $\leq 0.3\%$  in all conditions compared to controls.

A high proportion (~18-20%) of ATV was noted in the ATV L new and old stock (Table 5.16). Therefore as detailed in Methods, the initial ATV proportion present in the new ATV L stock was subtracted from the proportion of ATV calculated to be present in all other stability experiments. This subtraction was carried out for determination of ATV L to ATV conversion only. ATV L new stock was used to prepare all working solutions for assay validation and patient sample analysis. Taking the unexpected high ATV L stock impurity into account, all ATV L calibration standard and QC initial concentrations were back-calculated (multiplication by 0.8) to determine accurate ATV L calibration and QC concentrations, which are those reported.

ATV L to acid conversion was higher than acid to L conversion. After 24 hours in the autosampler at 4°C (Table 5.22), the increase in the proportion of acid between time 0 and 24 hours was 1.4% and 1.2% for ATV L and 2-OH ATV L, respectively. Higher conversion to acids of 10.6% and 3.7% was seen after three freeze-thaw cycles (Table 5.21) for ATV L and 2-OH ATV L, respectively.

This effect of thawing may explain why the fresh L working solution had a higher proportion of ATV in compared to the solution stored at 4°C for 7 weeks (7.2% versus 3.7%), since the ATV L stock had to be thawed in the preparation of the fresh composite L working solution. Nevertheless, minimal ATV (3.7%) and 2-OH ATV (1.5%) were present overall in the L working solution after seven weeks storage (Table 5.18). The highest conversion to acids, which was particularly pronounced for ATV L, was seen after four at room temperature on the bench top (Table 5.20). However, it was attenuated by reducing the length of time samples were left at room temperature, and negated by keeping samples on ice on the bench top (Table 5.20). Limited conversion occurred during three months storage at -80°C (Table 5.23).

**Table 5.16 Stock solution stability at -20°C**

Stock solution	Solution concentration (ng/mL)	Analyte mean peak area (cps * 10 <sup>5</sup> ) (n=6)		Stability (%)	Reciprocal ATV acid/lactone analyte in solution (%) <sup>1</sup>	
		Old stock	New stock		Old stock	New stock
ATV	135	639.9	642.2	99.7	0.02 <sup>2</sup>	0.02 <sup>2</sup>
2-OH ATV	45	71.8	73.9	97.2	0.07 <sup>3</sup>	0.1 <sup>3</sup>
ATV L	45	65.1	64.1	101.6	20.3 <sup>4</sup>	18.8 <sup>4</sup>
2-OH ATV L	45	85.4	84.3	101.3	0.4 <sup>5</sup>	1.1 <sup>5</sup>
BSP	45	649.4	606.8	107.0	-	-
CLP-CA	45	96.0	84.2	114.0	-	-

Cps = counts per second.

Stock stability was tested after 3 (ATV L, 2-OH ATV L) or 6 (ATV, 2-OH ATV, BSP, CLP-CA) months, and calculated by: old stock response/new stock response\*100. The solution concentration represents the concentration directly injected for analysis. The nominal concentration of a plasma sample would need to be 15x greater than these solution concentrations to generate the same detector response after extraction.

<sup>1</sup> = To assess ATV analyte acid/lactone interconversion, the proportion of *reciprocal* ATV analyte in solution was determined; as follows:

<sup>2</sup> = ATV L / (ATV + ATV L)\*100; <sup>3</sup> = 2-OH ATV L / (2-OH ATV L + 2-OH ATV)\*100;

<sup>4</sup> = ATV / (ATV + ATV L)\*100; <sup>5</sup> = 2-OH ATV / (2-OH ATV + 2-OH ATV L)\*100.

This table shows that the stock solutions were stable at -20°C for the durations tested. However, ~18-20% of analyte was ATV in the ATV L stock solution.

**Table 5.17 Determination of unlabelled analyte abundance in composite internal standards working solution after 20 days at 4°C**

Internal standard		Unlabelled analyte		Relative abundance unlabelled analyte (%) <sup>1</sup>
Identity	Mean peak area (cps * 10 <sup>3</sup> ) (n=4)	Identity	Mean peak area (cps * 10 <sup>3</sup> ) (n=4)	
ATV-d5	254.0	ATV	0.27	0.1
2-OH ATV-d5	72.1	2-OH ATV	0.19	0.3
ATV-d5 L	118.3	ATV L	0.20	0.2
2-OH ATV-d5 L	41.8	2-OH ATV L	0.12	0.3
BSP-d5	728.4	BSP	0.24	0.04
CLP-d4 CA	7423.8	CLP-CA	1.08	0.02

<sup>1</sup> = unlabelled analyte/(internal standard + unlabelled analyte)\*100

This table shows that negligible (<0.4%) analyte was detected in the internal standard solution.

**Table 5.18 Stability of working solutions stored at 4°C**

Analytes in solution	Solution concentration (ng/mL)	Analyte mean peak area (cps * 10 <sup>3</sup> ) (n=4)		Stability (%)	Reciprocal ATV acid/lactone analyte in solution (%)	
		Old WS	New WS		Old WS	New WS
<b>Joint (4 week stability)</b>						
ATV	5	1300.6	1348.8	<b>96.2</b>	0.09	0.03
2-OH ATV	5	487.3	516.3	<b>94.4</b>	0.4	0.3
BSP	5	2904.0	2966.5	<b>97.9</b>	-	-
CLP-CA	150	9528.9	9555.9	<b>99.9</b>	-	-
<b>Lactones (7 week stability)</b>						
ATV L	4	260.0	228.5	<b>114.2</b>	3.7 <sup>1</sup>	7.2 <sup>1</sup>
2-OH ATV L	5	383.7	371.8	<b>103.4</b>	1.5	1.5

Cps = counts per second; WS = working solution.

Stability was calculated as: old working solution/new working solution\*100.

The solution concentration represents the concentration directly injected for analysis. The nominal concentration of a plasma sample would need to be 15x greater than these solution concentrations to generate the same detector response after extraction.

<sup>1</sup> = to generate these tabulated results for ATV L only, the notable proportion of ATV present in the new ATV L stock was also subtracted from the proportion of ATV present in the lactones working solutions (i.e. ATV/(ATV + ATV L)\*100 - % ATV in new ATV L stock).

This table shows that all working solutions met the pre-specified stability criterion (<15%).

**Table 5.19 Four hour room temperature bench top stability of Joint analytes**

Analyte	Nominal concentration (ng/mL)	N=6				Reciprocal ATV lactone analyte in solution (%) <sup>1</sup>	
		Mean (ng/mL)	Accuracy (%)	Precision (CV, %)	Time 0		
					4 hours		
ATV	1.5	1.72	<b>114.3</b>	5.8			
	95	101.71	<b>107.1</b>	2.7	0.3	0.3	
	Overall		<b>111.4</b>	5.7			
2-OH ATV	1.5	1.62	<b>107.7</b>	13.5			
	95	107.24	<b>112.9</b>	4.8	0.8	0.7	
	Overall		<b>109.8</b>	10.6			
BSP	1.5	1.48	<b>98.5</b>	3.4	-	-	
	95	91.31	<b>96.1</b>	3.9			
	Overall		<b>97.3</b>	3.7			
CLP-CA	45	48.45	<b>107.7</b>	4.1	-	-	
	2850	2940.82	<b>103.2</b>	3.7			
	Overall		<b>105.4</b>	4.4			

<sup>1</sup> = For assessment of ATV acid to lactone conversion, only high quality control samples were considered because the peak areas of the reciprocal ATV analytes could not be reliably distinguished from background interference at the low quality control concentration.

This table shows that the joint analytes were stable after four hours on the benchtop.

Table 5.20 Bench top stability of ATV lactones

Analyte	Temperature	Duration (hours)	Nominal concentration (ng/mL)	N=6				
				Mean (ng/mL)	Accuracy (%)	Precision (CV, %)	Reciprocal ATV acid analyte in solution (%)	
							Time 0	4 hours
ATV L	RT	4	3.6	3.77	<b>104.8</b>	4.9		
			76	75.14	<b>98.9</b>	2.2	3.1	<b>21.4</b>
			Overall		<b>101.8</b>	4.8		
		2	3.6	3.49	<b>96.9</b>	1.9	3.1	13.3
			76	71.28	<b>93.8</b>	6.4		
			Overall		<b>95.3</b>	4.8		
		1	3.6	3.60	<b>99.9</b>	8.9	3.1	8.0
			76	73.52	<b>96.7</b>	3.1		
			Overall		<b>98.3</b>	6.7		
	4°C	4	3.6	4.08	<b>113.5</b>	2.7		
			76	85.65	<b>112.7</b>	3.5	3.1	1.8
			Overall		<b>113.1</b>	3.0		
2-OH ATV L	RT	4	1.5	1.58	<b>105.6</b>	7.8		
			95	102.41	<b>107.8</b>	4.0	3.2	9.0
			Overall		<b>106.7</b>	6.0		
		2	1.5	1.58	<b>105.4</b>	6.1		
			95	91.09	<b>95.9</b>	7.3	3.2	5.8
			Overall		<b>100.6</b>	8.0		
		1	1.5	1.51	<b>100.9</b>	4.4		
			95	92.37	<b>97.2</b>	3.8	3.2	4.3
			Overall		<b>99.1</b>	4.4		
	4°C	4	1.5	1.64	<b>109.1</b>	4.3		
			95	108.26	<b>114.0</b>	5.0	3.2	2.8
			Overall		<b>111.5</b>	5.0		

RT = room temperature. Six replicates of spiked plasma at low and high quality control concentrations were used to determine bench top stability. This table shows that ATV L and 2-OH ATV L were accurate and precise at four hours on the benchtop at both room temperature and 4°C. Conversion to reciprocal ATV acid analyte (i.e. ATV L -> ATV, and 2-OH ATV L -> 2-OH ATV) was greater at room temperature than if the samples were kept on ice.

**Table 5.21 Freeze-thaw stability**

Analyte	Nominal concentration (ng/mL)	N=6				Reciprocal ATV acid/lactone analyte in solution (%)	
		Mean (ng/mL)	Accuracy (%)	Precision (CV, %)	Fresh		
					x3 F-T		
ATV	1.5	1.65	<b>110.2</b>	8.5			
	95	98.39	<b>103.6</b>	1.8	0.3	0.3	
	Overall		<b>106.9</b>	6.8			
2-OH ATV	1.5	1.71	<b>114.5</b>	7.3			
	95	97.29	<b>102.4</b>	2.6	0.8	0.8	
	Overall		<b>108.5</b>	8.0			
ATV L	3.6	3.23	<b>89.7</b>	2.9			
	76	66.94	<b>88.2</b>	4.7	5.2	15.8	
	Overall		<b>88.9</b>	3.8			
2-OH ATV L	1.5	1.45	<b>96.6</b>	6.2			
	95	91.04	<b>96.0</b>	6.4	4.8	8.5	
	Overall		<b>96.3</b>	6.0			
BSP	1.5	1.54	<b>102.5</b>	4.5	-	-	
	95	95.75	<b>100.9</b>	4.8			
	Overall		<b>101.7</b>	4.5			
CLP-CA	45	47.95	<b>106.6</b>	3.4	-	-	
	2850	2825.26	<b>99.2</b>	3.0			
	Overall		<b>102.9</b>	4.9			

x3 F-T = 3 freeze-thaw cycles.

Six replicates of spiked plasma at low and high quality control concentrations were used to determine bench top stability. This table shows that all analyte responses were acceptably accurate and precise after undergoing three freeze-thaw cycles. Conversion from ATV L to ATV was prominent.

**Table 5.22 Re-injection reproducibility after 24-hours in autosampler**

Analyte	Nominal concentration (ng/mL)	N=6				Reciprocal ATV acid/lactone analyte in solution (%)	
		Mean (ng/mL)	Accuracy (%)	Precision (CV, %)	Time 0		24 hours
ATV	1.5	1.38	<b>91.9</b>	2.9			
	45	45.36	<b>100.8</b>	4.0			
	95	98.73	<b>103.9</b>	4.9	0.2	0.4	
	Overall		<b>98.9</b>	6.5			
2-OH ATV	1.5	1.63	<b>108.7</b>	7.9			
	45	46.33	<b>103.0</b>	4.1			
	95	96.07	<b>101.1</b>	4.1	0.8	1.1	
	Overall		<b>104.3</b>	6.3			
ATV L	3.6	3.66	<b>101.7</b>	4.6			
	36	34.84	<b>96.8</b>	2.3			
	76	74.04	<b>97.4</b>	4.4	2.0	3.4	
	Overall		<b>98.6</b>	4.4			
2-OH ATV L	1.5	1.56	<b>103.8</b>	7.3			
	45	43.87	<b>97.5</b>	4.2			
	95	94.07	<b>99.0</b>	4.4	3.0	4.2	
	Overall		<b>100.1</b>	5.9			
BSP	1.5	1.52	<b>101.0</b>	2.2	-	-	
	45	45.19	<b>100.4</b>	3.5	-	-	
	95	94.76	<b>99.7</b>	4.7	-	-	
	Overall		<b>100.4</b>	3.4	-	-	
CLP-CA	45	47.05	<b>104.5</b>	6.2	-	-	
	1350	1457.77	<b>108.0</b>	2.3	-	-	
	2850	2961.97	<b>103.9</b>	2.6	-	-	
	Overall		<b>105.5</b>	4.2	-	-	

Re-injection reproducibility was determined by re-injecting full calibration lines and six low, medium and high quality controls after they had been stored for 24 hours in the autosampler at 4°C.

This table shows that the accuracy and precision of all re-injected quality controls for all analytes were acceptable. Minimal reciprocal ATV analyte interconversion was observed.

Table 5.23 Long term stability stored at -80°C

Analyte	Nominal conc. (ng/mL)	Day 0 (n=6)			3 Months (n=6)			6 Months (n=6)			Reciprocal ATV acid/lactone analyte in solution (%)		
		M (ng/mL)	A (%)	CV (%)	M (ng/mL)	A (%)	CV (%)	M (ng/mL)	A (%)	CV (%)	Day 0	3 months	6 months
ATV	1.5	1.52	101.6	7.9	1.61	<b>107.5</b>	7.3	1.66	<b>110.4</b>	8.5			
	95	97.70	102.8	2.0	99.21	<b>104.4</b>	6.6	99.96	<b>105.2</b>	4.4	0.3	0.4	0.3
	Overall		102.2	5.5		<b>105.9</b>	6.8		<b>107.8</b>	7.0			
2-OH ATV	1.5	1.55	103.4	6.2	1.67	<b>111.4</b>	4.6	1.77	<b>118.1</b>	10.3			
	95	95.5	100.5	3.2	100.74	<b>106.0</b>	6.7	103.92	<b>109.4</b>	2.5	0.8	1.0	0.8
	Overall		102.0	5.0		<b>108.7</b>	6.0		<b>113.8</b>	8.4			
ATV L	3.6	3.53	98.0	2.7	3.95	<b>109.7</b>	4.7	3.84	<b>106.8</b>	6.9			
	76	75.78	99.7	2.8	80.84	<b>106.4</b>	3.2	77.58	<b>102.1</b>	4.2	3.1	-2.9	0.02
	Overall		98.9	2.8		<b>108.0</b>	4.2		<b>104.4</b>	6.0			
2-OH ATV L	1.5	1.40	93.3	10.9	1.69	<b>112.5</b>	3.8	1.71	<b>113.9</b>	10.1			
	95	96.00	101.1	4.0	98.05	<b>103.2</b>	3.7	102.04	<b>107.4</b>	2.9	3.2	2.7	3.3
	Overall		97.2	8.6		<b>107.8</b>	5.8		<b>110.6</b>	7.9			
BSP	1.5	1.53	102.1	5.8	1.55	<b>103.3</b>	4.6	1.56	<b>104.2</b>	7.5	-	-	-
	95	97.84	103.0	3.3	99.28	<b>104.5</b>	6.4	99.56	<b>104.8</b>	5.6			
	Overall		102.5	4.5		<b>103.9</b>	5.4		<b>104.5</b>	6.3			
CLP-CA	45	46.70	103.8	8.6	46.74	<b>103.9</b>	4.2	46.56	<b>103.5</b>	7.0	-	-	-
	2850	2975.90	104.4	4.8	2843.99	<b>99.8</b>	6.2	2841.83	<b>99.7</b>	3.1			
	Overall		104.1	6.6		<b>101.8</b>	5.4		<b>101.6</b>	5.6			

Abbreviations: A = accuracy; M = mean

To assess long term stability, six replicates of each low and high quality control were analysed on day 0, and then after three and six months storage at -80°C in comparison to fresh calibration standards. This table shows that all analytes met the accuracy and precision acceptability criteria at three months and six months, except for the accuracy of the low quality control of 2-OH ATV (highlighted in red). Minimal ATV analyte interconversion was observed.

**Table 5.24 Analytical run length validation**

Sample	No. injections	% passed <sup>1</sup>					
		ATV	2-OH ATV	ATV L <sup>2</sup>	2-OH ATV L	BSP	CLP-CA
<b>Calibration standards</b>							
1	6	100	100	x	66.7	100	100
2	6	100	100	x	50	100	100
3	6	100	66.7	100	100	100	100
4	6	100	100	100	100	100	100
5	6	100	100	100	100	100	100
6	6	100	100	100	100	100	100
7	6	100	100	100	100	100	100
8	6	100	100	100	100	100	100
9	6	100	100	100	100	100	100
10	6	100	100	100	100	100	100
Overall	<b>60</b>	<b>100</b>	<b>96.7</b>	<b>100</b>	<b>91.7</b>	<b>100</b>	<b>100</b>
<b>Quality controls</b>							
LOW	18	100	72.2	100	77.8	100	77.8
MID	18	100	100	100	100	100	100
HIGH	18	100	100	100	100	100	100
Overall	<b>54</b>	<b>100</b>	<b>90.7</b>	<b>100</b>	<b>92.6</b>	<b>100</b>	<b>92.6</b>

261 samples were injected, including 114 joint and 114 lactone calibration and quality control samples. The length of this run exceeded the expected maximum patient batch run time.

<sup>1</sup> = the percentage of analyte calibration or quality control samples that passed. To pass, a sample had to be within 15% of its nominal concentration, except for the calibration 1 standard that could be within 20% of its nominal concentration.

<sup>2</sup> = the validated ATV L calibration line (1.2-100ng/mL) consists of only eight concentrations (calibration standards 3 to 10).

This table shows that over the expected run time the majority of calibration and quality control extracts will be suitably accurate.

### 5.3.3.8 Dilution integrity

The precision and accuracy following a one in 20 dilution was acceptable for all analytes (Table 5.25), and therefore, dilution up to 20 times for patient samples higher than the ULOQ was deemed acceptable.

**Table 5.25 Integrity of 20-times dilution**

Analyte	Nominal concentration (ng/mL)	N=6		
		Mean (ng/mL)	Accuracy (%)	Precision (CV, %)
ATV	50	49.3	98.7	11.7
2-OH ATV	50	46.9	93.7	6.2
ATV L	40	41.2	102.9	3.4
2-OH ATV L	50	53.3	106.7	4.9
BSP	50	54.5	109.0	14.0
CLP-CA	1500	1446.0	96.4	3.3

The nominal concentration was produced by diluting a plasma sample spiked at 1µg/mL (for all analytes except CLP-CA, which was spiked at 30µg/mL) 20x in plasma, prior to extraction. Six replicates for each analyte were analysed. This table shows that every analyte has acceptable dilution integrity.

### 5.3.4 Method validation summary

Table 5.26 summarises the assay validation results and indicates acceptable selectivity, carryover, accuracy, precision, MEs, stability and dilution integrity.

**Table 5.26 Summary of assay validation results**

Analyte	ATV	2-OH ATV	ATV L	2-OH ATV L	BSP	CLP-CA
<b>Calibration range (ng/mL)</b>	0.5-125	0.5-125	1.2-100	0.5-125	0.5-125	15-3750
<b>Selectivity (% of LLOQ)</b>	11.0 <sup>1</sup>	14.3	4.3	7.3	2.1	3.2
<b>Carryover (% of LLOQ)</b>	9.2	16.8	4.6	11.4	1.0	3.0
<b>Accuracy (%)</b>	99.6	98.5	97.8	99.1	99.0	98.8
<b>Precision (CV %)</b>	6.5	6.9	7.0	10.5	5.4	4.4
<b>Matrix effect (CV %)</b>	9.1	8.5	7.5	8.8	5.6	5.5
<b>Extraction recovery (CV %)</b>	8.5	8.0	5.7	8.1	6.8	5.7
<b>Dilution integrity (% relative to nominal conc.)</b>	98.7	93.7	102.9	106.7	109.0	96.4
<b>Stability</b>						
<b>iv) Solutions (relative to new solution, %):</b>						
<b>Stock, -20°C<sup>2</sup></b>	99.7	97.2	101.6	101.3	107.0	114.0
<b>Working sols, 4°C<sup>3</sup></b>	96.2	94.4	114.2	103.4	97.9	99.9
<b>% in Internal std sol, 20 days, 4°C</b>	0.1	0.3	0.2	0.3	0.04	0.02
<b>v) Plasma matrix (relative to QC nominal concentrations, %):</b>						
<b>3 freeze-thaw cycles</b>	106.9	108.5	88.9	96.3	101.7	102.9
<b>4 hours on benchtop, RT</b>	111.4	109.8	101.8	106.7	97.3	105.4
<b>6 month stability, -80°C</b>	107.8	113.8	104.4	108.5	104.5	101.6
<b>24 hour re-injection reproducibility, ~26 hours, 4°C</b>	98.9	104.3	98.6	100.1	100.4	105.5
<b>% Cal/QC samples passed in analytical run length</b>	100.0	93.9	100.0	92.1	100.0	96.5

<sup>1</sup> = Calculated for ATV using five of the six individual blank plasma samples, excluding the blank sample with a very high response (258% of LLOQ)

<sup>2</sup> = Stock stored at -20°C for 3 (ATV L, 2-OH ATV L) or 6 (ATV, 2-OH ATV, BSP, CLP-CA) months

<sup>3</sup> = Working solutions stored at 4°C for 4 (ATV, 2-OH ATV, BSP, CLP-CA) or 7 (ATV L, 2-OH ATV L) weeks

For the accuracy, precision, matrix effect, extraction recovery and all stability assessments using plasma matrix, the tabulated figure is the mean of the results of the different quality control concentrations used for each analyte.

This table shows that all analytes met the pre-specified validation criteria, although the accuracy of 2-OH ATV low quality control was 118.1%.

### 5.3.5 Application to sparse pharmacokinetics study in patients

The developed HPLC-MS/MS method was successfully applied to determine the concentrations of the six analytes in the plasma of PhACS patients (n=1,026). The QC results from the 12 analytical runs are provided in the Appendix (Table 8.5, Table 8.6). The key sample characteristics are described in Table 5.27.

**Table 5.27 Summary of patient one month sample characteristics and analyte concentrations**

	ATV	2-OH ATV	ATV L	2-OH ATV L	BSP	CLP-CA
<b>Concentration<sup>1</sup> (median + IQR, ng/mL) at each dose</b>						
<b>1.25mg</b>					5.67 (4.31-7.63)	
<b>2.50mg</b>					10.83 (8.24-14.05)	
<b>3.75mg</b>					17.50 (12.53-23.05)	
<b>5mg</b>					23.14 (17.08-28.86)	
<b>6.25</b>					55.34 <sup>3</sup>	
<b>7.5mg</b>					36.74 (27.35-45.67)	
<b>10mg</b>					43.93 (28.06-52.73)	
<b>20mg</b>					105.5 <sup>4</sup>	
<b>40mg</b>	4.86 (1.92-9.53)	5.85 (2.80-8.81)	3.98 (2.51-8.90)	4.64 (2.74-9.73)		
<b>75mg</b>						736.94 (392.13-1211.11)
<b>80mg</b>	5.67 (3.18-10.98)	7.49 (4.26-12.76)	4.94 (2.87-9.41)	7.49 (4.39-13.22)		
<b>Time since last dose (median + IQR, hours)<sup>2</sup></b>	13.4 (12.5-15.8)				4.5 (3.5-7.0)	4.5 (3.5-7.0)
<b>Storage duration (median + IQR, days)<sup>2</sup></b>	2195 (1948-2719)				2166 (1964-2693)	2165 (1961-2683)
<b>Collection to processing (median + IQR, hours)<sup>2</sup></b>	24 (6-51)				28 (6-67)	28 (6-67)
<b>Number of patients that missed ≥1 tablet within last week, n (%)<sup>2</sup></b>	40 (5.6)				18 (2.4)	24 (3.0)

<sup>1</sup> = Concentrations reported from values within calibration ranges only; <sup>2</sup> = All patient samples (including those with concentrations <LLOQ) were considered; <sup>3</sup> = n=2; <sup>4</sup> = n=3.

The developed, validated HPLC-MS/MS assay was successfully applied to simultaneously determine the concentrations of the six analytes in stored EDTA plasma samples from 1,026 patients in the PhACS study. This table shows the mean results following analysis of samples collected at one month (n=1,026) after the index hospitalisation for a NSTEMI-ACS. Although not shown, a sub-group of these 1,026 patients (n=257) also had their 12 month sample analysed as well.

Table 5.28 shows the univariate linear regression analysis results for the association between the sample characteristics and one month analyte concentrations. Notably, estimated time to last dose and non-adherence were both significantly associated with levels of all analytes except BSP, although administered dose was strongly associated with BSP levels. Storage duration was associated with 2-OH ATV level, and blood collection to processing duration was associated with levels of all analytes except ATV and BSP (Table 5.28).

## 5.4 Discussion

In summary, a novel LC-MS/MS assay has been developed and validated for quantification of six clinically relevant analytes from three mechanistically distinct commonly used cardiovascular drugs, and applied to a large cohort of patients on secondary prevention cardiovascular medications. The assay requires only 50µL of sample, involves simple protein precipitation extraction, and rapidly separates analytes within a 6.0 minute run time. The best fit for the CLP-CA calibration line was a quadratic curve; however, all CLP-CA validation criteria were met.

Other LC-MS/MS assays that analyse some (Partani *et al.*, 2014; Bullen *et al.*, 1999) or all ATV (Hermann *et al.*, 2005; Macwan *et al.*, 2011; Jemal *et al.*, 1999a) analytes have been reported. Most use either solid phase extraction (Hermann *et al.*, 2005; Partani *et al.*, 2014) or liquid-liquid extraction (Bullen *et al.*, 1999; Jemal *et al.*, 1999a) requiring time limiting evaporation to dryness and reconstitution. To the best of knowledge, only one ATV assay has reported use of comparably low sample volumes and protein precipitation extraction (Macwan *et al.*, 2011). The assay herein has built on this foundation by both incorporation of hydrophilic CLP-CA and BSP and application to a large patient sample set.

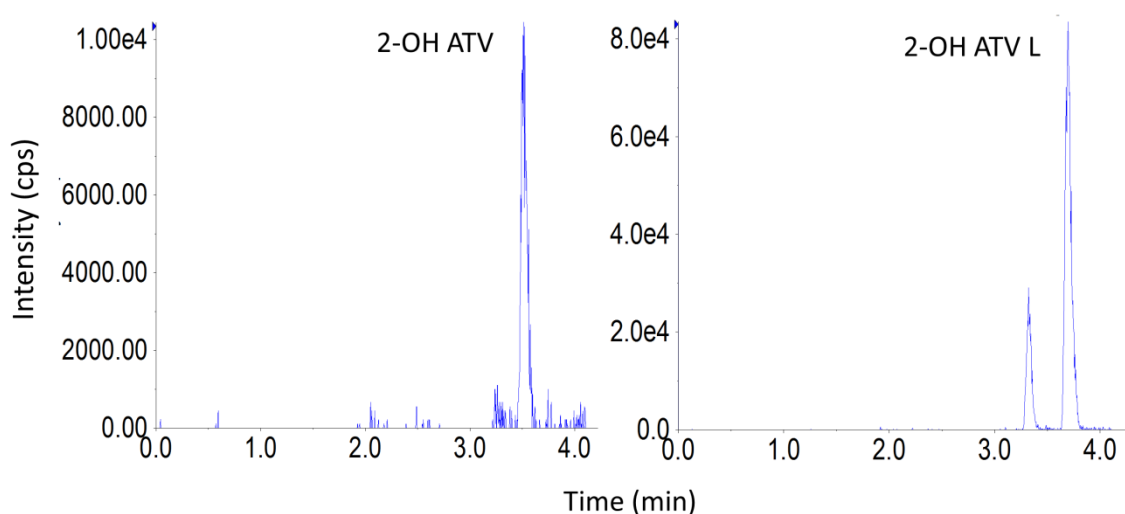
**Table 5.28 Univariate regression analyses to assess the impact of sample characteristics on patient one month analyte concentrations, determined using the validated assay**

Univariate analysis	ATV (n=718)		2-OH ATV (n=718)		ATV L (n=718)		2-OH ATV L (n=718)		BSP (n=742)		CLP-CA (n=811)	
	Effect (B)	p-value	Effect (B)	p-value	Effect (B)	p-value	Effect (B)	p-value	Effect (B)	p-value	Effect (B)	p-value
<b>Time since last dose (hours)</b>	-0.001	<b>1.0x10<sup>-6</sup></b>	-0.001	<b>0.001</b>	-0.001	<b>0.008</b>	-0.001	<b>0.002</b>	-2.9x10 <sup>-5</sup>	0.9	-0.001	<b>0.001</b>
<b>Dose</b>	0.001	0.7	0.001	0.6	0.003	0.4	0.003	0.1	0.08	<b>2.8x 10<sup>-23</sup></b>	NA	NA
<b>Non-adherence<sup>1</sup></b>	-0.2	<b>2.1x10<sup>-7</sup></b>	-0.2	<b>2.8x10<sup>-8</sup></b>	-0.3	<b>3.8x10<sup>-9</sup></b>	-0.2	<b>2.5x10<sup>-9</sup></b>	-0.01	0.9	-0.5	<b>4.0x10<sup>-11</sup></b>
<b>Storage (days)</b>	-0.0001	0.06	-0.0003	<b>1.5x 10<sup>-5</sup></b>	7.7x10 <sup>-5</sup>	0.3	2.0x10 <sup>-5</sup>	0.7	1.7x10 <sup>-5</sup>	0.7	-0.0001	0.1
<b>Collection to processing (hrs)<sup>2</sup></b>	3.2x10 <sup>-5</sup>	>0.9	0.001	<b>0.009</b>	-0.002	<b>3.6x 10<sup>-4</sup></b>	-0.001	<b>0.02</b>	0.0005	0.3	0.002	<b>0.03</b>

The tabulated analyses were carried out using all available one month analyte concentration results (including those below the lower limit of quantification and those with very high measured concentrations likely near  $C_{max}$  due to drug administration close to blood sampling time). NA = not applicable. Effect (B) is the predictor variable unstandardized coefficient, which has been determined from univariate linear regression analysis using  $\log_{10}$  transformed analyte levels as the dependent variable. Statistically significant p-values ( $p < 0.05$ ) are highlighted in bold. <sup>1</sup> = number of pills missed in the preceding week; <sup>2</sup> = Only available for 479 (66.7%, ATV analytes), 487 (65.6%, BSP) and 567 (69.9%, CLP-CA) patients. All other variables had  $\leq 1.5\%$  data missing.

ATV, BSP and CLP-CA were uniformly stable under the reported extraction and operating conditions. 2-OH ATV was stable, except for its low QC at six months (Table 5.23), which needs repeating to exclude experimental error. Although ATV Ls met the validation stability criteria, they showed notable hydrolysis to their acid form, as previously reported (Jemal *et al.*, 1999a), particularly on the bench top at room temperature and after three freeze-thaw cycles. Indeed, L hydrolysis to acid form in human serum has been reported to be almost 100% complete after 24 hours at room temperature (Jemal *et al.*, 1999a). Importantly, L hydrolysis in plasma is time- and temperature-dependent (Table 5.20). Therefore, it is recommended that calibration/QC spiking and patient sample extraction are carried out within one hour if done at room temperature, which is feasible with this assay. Alternatively, samples can be prepared on ice-water slurry (Macwan *et al.*, 2011). Minimisation of freeze-thaw cycling will especially benefit L quantification integrity.

The patient study reported concentrations of ATV, BSP and CLP-CA that are in keeping with levels previously reported in small PK studies (DeGorter *et al.*, 2013; Kirch *et al.*, 1987; Karażniewicz-Łada *et al.*, 2014). 4-OH ATV was predominantly not detectable in the patient samples. However, a discrete small peak was consistently detected with the 2-OH ATV L transitions, which eluted earlier than 2-OH ATV L (or 2-OH ATV-d5 L). This peak likely represents the minor 4-OH ATV L metabolite (Figure 5.6), and therefore, if needed, it could be included in an extended version of the assay. The minor presence of 4-OH ATV L, but virtually no 4-OH ATV, is in keeping with a healthy volunteer ATV PK rich sampling study (Keskitalo *et al.*, 2009c).

**Figure 5.6 Detection of likely 4-OH ATV L in patient samples**

This figure is representative of 2-OH ATV and 2-OH ATV L chromatograms from a patient sample. Interestingly, there is a smaller peak with an earlier elution time detected with the 2-OH ATV L MRM, which is not present with 2-OH ATV. This small peak likely represents the minor 4-OH ATV L metabolite.

Daily dose was strongly associated with BSP, for which eight doses were analysed (Table 5.28). Estimated time to last dose was strongly associated with all analytes except BSP (Table 5.28). Further subgroup analysis similarly found no association when BSP levels were split and analysed separately for those estimated to have had their blood collected within, or after, four hours since the last dose for patients on the most common BSP dose (2.5mg daily) (data not shown). The reason(s) for this is unclear but may represent a limitation of only knowing the exact time of sample collection and not also the exact time of last administration. Similarly, non-adherence was strongly associated with levels of all analytes except BSP (Table 5.28), and when limited again to the 2.5mg BSP dose group, non-adherence was still not associated with BSP (data not shown). The level of reported BSP non-adherence was lower than for ATV/CLP (Table 5.27) and so insufficient sensitivity to detect a signal is possible. The clinical impact of patient-reported statin non-adherence on cardiovascular outcomes in the PhACS study has been previously reported (Turner *et al.*, 2017) (Chapter 2). However, the impact of CLP non-adherence and of biochemically determined non-adherence on adverse clinical outcomes warrant further investigation. A limitation of the present study is that the long term stability validation for the

assay is of shorter duration (six months) than the patient sample storage durations. Interestingly, storage duration was associated with 2-OH ATV level (Table 5.28), and 2-OH ATV was the least accurate analyte in the six month stability assessment (Table 5.23). Therefore, it will be beneficial to consider adjusting for these variables in future analyses.

In summary, a novel LC-MS/MS cardiovascular assay for ATV, BSP and CLP-CA has been developed and validated. The levels of the six analytes determined in a large patient cohort will be used for adherence-related, PK and pharmacogenomic analyses.

## Chapter 6 A genome-wide association study of atorvastatin and metabolite systemic exposures and their impact on clinical outcomes in secondary prevention patients

### 6.1 Introduction

Statins are hypolipidaemic drugs and amongst the most highly prescribed medications worldwide. ATV 20mg daily is currently recommended as first line hypolipidaemic treatment for primary CVD prevention, reducing LDL-C by ~43% (NICE, 2016a). ATV 80mg daily is first line for secondary CVD prevention and decreases LDL-C by ~55% (NICE, 2016a). Overall statins are safe and well tolerated, although they are associated with a variety of ADRs, including incident diabetes mellitus (Collins *et al.*, 2016; Lakey *et al.*, 2016) and notably SAM (Alfirevic *et al.*, 2014).

SAM ranges from common benign muscle symptoms (~5% (Parker *et al.*, 2013)) through to uncommon myopathies (~0.1%) and rarely rhabdomyolysis (0.1-8.4/100,000 patient-years) (Alfirevic *et al.*, 2014). Increased exposure contributes to the risk of SAM. Increased statin dose and concomitant use of CYP3A4-inhibiting co-medications with statins metabolised by CYP3A4 (ATV, SVT, LVT) are both associated with an increased risk of myotoxicity (Zhou *et al.*, 2005; Armitage, 2007). A nonsynonymous variant, rs4149056 (p.V174A) within *SLC01B1*, which encodes the hepatic xenobiotic influx transporter, OATP1B1, is associated with increased systemic exposures to all statins (except FVT) (Elsby *et al.*, 2012), and SVT-associated myotoxicity (Link *et al.*, 2008; Voora *et al.*, 2009; Donnelly *et al.*, 2011). However to date, rs4149056 has not been convincingly associated with ATV, PVT or RVT myotoxicity (Voora *et al.*, 2009; Brunham *et al.*, 2012; Danik *et al.*, 2013). A GWAS meta-analysis has also confirmed that *SLC01B1* rs4149056 is associated with a reduced LDL-C response to statin therapy (Postmus *et al.*, 2014). Small healthy volunteer studies have demonstrated that variation in several other candidate genes,

including *ABCB1* (Keskitalo *et al.*, 2008; Lee *et al.*, 2010), *ABCG2* (Keskitalo *et al.*, 2009c), *CYP3A4* and *PPARA* (Klein *et al.*, 2012) affect ATV PK.

Despite this progress, to date there has been no comprehensive analysis of the clinical and PGx factors differentially affecting the PK of ATV and its metabolites in real world clinical practice. Therefore, the aim of this study was to conduct a large GWAS of steady state ATV levels, ATV metabolite levels, and analyte ratios in a cohort of NSTEMI patients and to relate identified variants to adverse events.

## **6.2 Methods**

### **6.2.1 Prospective study outline**

This investigation utilised the PhACS study, which was a UK multicentre prospective cardiovascular pharmacogenomics observational study that has been described in detail previously (Chapter 2, (Turner *et al.*, 2017)). Briefly, 1470 patients hospitalised with an NSTEMI-ACS between 2008-2012 were recruited and followed up at one (V2) and 12 months (V3), and annually thereafter until all participants had been followed up for at least 12 months. The study ended in 2013. Demographic, comorbidity and prescription information was collected at baseline; current drug use, drug adherence, functional status, and new clinical events were captured during follow up. Blood samples were collected at baseline, V2 and V3, and bio-banked at -80°C for future analyses.

The protocol was approved by the Liverpool (adult) research Ethics Committee, UK; site-specific approval was granted at all sites involved and local informed consent was obtained from all study subjects in accordance with the Declaration of Helsinki.

### 6.2.2 Assay of ATV analyte concentrations

The concentrations of four ATV analytes (ATV, 2-OH ATV, ATV L and 2-OH ATV L) were determined in V2 EDTA plasma samples using an HPLC-MS/MS method, which additionally quantified BSP and CLP-CA levels, and was validated according to EMA criteria (European Medicines Agency, 2011), as detailed in Chapter 5. Briefly, samples were mixed with a composite internal standard solution containing deuterated internal standards of all six analytes, and acetonitrile with 0.3% acetic acid, to precipitate protein and minimise lactone to acid interconversion (Macwan *et al.*, 2011). Following centrifugation, the supernatant was diluted 1:2 in water and a 5 $\mu$ L aliquot injected for analysis. Analytes were separated using an 2.7 $\mu$ m Halo C18 column (50 x 2.1 mm ID, 90 $\text{\AA}$ , Hichrom Limited, Reading, UK, part number: 92812-402) with gradient elution, housed within a Shimadzu Nexera X2 modular system (Kyoto, Japan). Analytes were detected in low mass positive ionisation mode using multiple reaction monitoring (Sciex triple quadrupole 6500 QTRAP mass spectrometer with a Turbo V<sup>TM</sup> electrospray source, AB Sciex, Warrington, UK). The ATV analyte transitions were ([M+H<sup>+</sup>] *m/z*): ATV 559.3 $\rightarrow$ 440.3, 2-OH ATV 575.3 $\rightarrow$ 250.2, ATV L 541.3 $\rightarrow$ 276.2, 2-OH ATV L 557.3 $\rightarrow$ 276.2, ATV-d5 564.1 $\rightarrow$ 445.1, 2-OH ATV-d5 580.2 $\rightarrow$ 255.1, ATV-d5 L 546.3 $\rightarrow$ 281.2, 2-OH ATV-d5 L 562.2 $\rightarrow$ 281.1. Calibration and QC samples were prepared in pooled healthy human volunteer K3 EDTA plasma (Sera Laboratories International, West Sussex, UK). The dynamic range of the ATV analytes in the validated assay was 0.5-125ng/mL (ATV, 2-OH ATV, 2-OH ATV L) and 1.2-100ng/mL (ATV L); at 0.5ng/mL, the accuracy and precision (CV) of ATV L was 88.8% and 28.2%, respectively. Data acquisition was via Analyst<sup>®</sup> software (v1.6.2, Sciex); MultiQuant<sup>TM</sup> v1.6.2 (Sciex) was used for analyte quantification with separate weighted least squares regression applied to the linear calibration lines (1/x for ATV, 2-OH ATV; 1/x<sup>2</sup> for ATV L, 2-OH ATV L).

### 6.2.3 Genotyping, imputation and quality control

Genotyping of PhACS participants was carried out using the Illumina HumanOmniExpressExome-8 v1.0 BeadChip at Edinburgh Genomics (Roslin

Institute, Scotland). Dr Peng Yin (previous research associate at the Department of Biostatistics, University of Liverpool) carried out the genetic QC procedures and imputation (Yin *et al.*, 2016). The QC steps have been previously described (Anderson *et al.*, 2010). Briefly, 1442 participants were successfully genotyped. Per-individual QC was carried out excluding participants with genotype call rate <95% (n=54), discordant clinical/X-chromosome-derived gender (n=7), and aberrant heterozygosity (<0.2 in PhACS) (n=1). For each pair of individuals with an identity by descent (IBD) >0.1875 using pruned genetic data, the individual with the worse call rate and/or absence of cardiovascular events during follow up, was removed (n=5). Potential confounding due to population stratification was assessed by principal component (PC) analysis (PCA). The reference PCA model was built using international HapMap 3 data from European (CEU), Asian (CHB+JPT) and African (YRI) individuals (Altshuler *et al.*, 2010) and the first two PCs achieved adequate separation. After application of the PCA model to the PhACS cohort, genetically non-European participants were excluded (n=18), leaving 1,357 participants. Per-marker QC excluded SNPs with call rate <95%, MAF <5% and SNPs deviating from Hardy-Weinberg equilibrium ( $p < 0.0001$ ), resulting in a reduction of variants from 951,117 to 598,054. The QC steps were carried out in PLINK v1.07 (<http://zzz.bwh.harvard.edu/plink/> (Purcell *et al.*, 2007)).

Following QC, the genotype scaffold was imputed up to the 1000 Genomes Phase I reference panel (all ancestries, March 2012 release) (The 1000 Genomes Project Consortium, 2012); PhACS pre-phasing was performed using SHAPEIT v2 ([https://mathgen.stats.ox.ac.uk/genetics\\_software/shapeit/shapeit.html](https://mathgen.stats.ox.ac.uk/genetics_software/shapeit/shapeit.html) (Delaneau *et al.*, 2011)) and imputation using IMPUTE2 ([http://mathgen.stats.ox.ac.uk/impute/impute\\_v2.html](http://mathgen.stats.ox.ac.uk/impute/impute_v2.html) (Howie *et al.*, 2009)). The total number of SNPs post-imputation was 8,788,191. Further QC steps were performed after each GWAS analysis (see below).

## 6.2.4 Cohort selection

Three cohorts were selected: cohort 1 for the ATV PK study, and cohorts 2 and 3 to study the clinical impact of biologically plausible genetic variants identified through the analyses undertaken in cohort 1.

### 6.2.4.1 Cohort 1

The inclusion criteria for ATV analyte quantification were:

- all PhACS participants on 80mg ATV daily at both baseline and V2, OR
- all PhACS participants on ATV 40mg at both baseline and V2, AND
- both drug adherence data and a stored plasma EDTA sample available from V2.

Three exclusion criteria were applied, resulting in cohort 1 - the main study cohort:

- Participants that failed the genetic QC procedures (n=43);
- Participants that had two or more ATV analyte levels  $<0.5\text{ng/mL}$  (i.e.  $<\text{LLOQ}$ ) (n=44), leading to formation of a single participant cohort to facilitate comparisons between ATV PK analyses. This approach was chosen because participants with  $\geq 2$  analytes  $<0.5\text{ng/mL}$  (n=44) were significantly more likely to be statin non-adherent (p=0.001) compared to participants with no low ATV analytes. However, those with only one analyte  $<0.5\text{ng/mL}$  (n=20) were not statin non-adherent (p=0.88), could be thus exhibiting unorthodox ATV disposition/metabolism, and so were retained.
- Participants with ATV concentrations  $\geq 31\text{ng/mL}$  (if on 80mg ATV) or  $\geq 15.5\text{ng/mL}$  (if on 40mg ATV) were excluded (n=41). This is because, whilst sample collection time was known, time of last ATV administration was not. Consequently, time since last ATV was estimated by assuming all participants took their last ATV dose at 2200 the previous evening. However, clearly some participants would have taken their ATV in the morning and so have near  $C_{\text{max}}$  levels. Therefore, a ceiling limit was set, based on the mean ATV concentration ( $6\text{ng/mL}$ )

plus three standard deviations (8.2ng/mL) (SD) of patients on ATV 80mg in a previous small ATV PK patient study (DeGorter *et al.*, 2013); the ceiling concentration was halved for ATV 40mg patients.

#### **6.2.4.2 Cohort 2**

Cohort 2 consisted of PhACS patients discharged from index NSTEMI-ACS hospitalisation on *any* ATV dose, and at V2 their statin status (continued statin use or discontinued), statin prescription (specific statin and dose) and statin adherence status were known, and they have quality controlled genetic data available.

#### **6.2.4.3 Cohort 3**

Cohort 3 was composed of PhACS patients discharged from index NSTEMI-ACS hospitalisation on *any* ATV dose with quality controlled genetic data available.

#### **6.2.5 Covariates**

Demographic and comorbidity covariates considered were: sex, age, BMI, smoking status, hypertension, hyperlipidaemia prior to recruitment, diabetes mellitus, CKD, prior CVD (previous MI, stroke, TIA or PAD), and hepatic disease (liver diagnosis and/or history of alcohol excess). Co-medications used at V2 considered were: aspirin, a P2Y<sub>12</sub> inhibitor, a beta blocker, an ACEI/ARB, a loop diuretic, a thiazide diuretic, amiodarone, a PPI, CYP3A4 inducers, moderate and strong CYP3A4 inhibitors, and an OATP1B1 inhibitor. ATV non-adherence was determined by the number of ATV pills self-reported to have been missed during the week preceding V2. Blood sample characteristics considered were: the estimated time since last dose (see 6.2.4.1), and sample storage duration.

CYP3A inducers and inhibitors were based on drugs within the US FDA lists (Food and Drug Administration, 2016) available as a prescription in the UK. Only strong and moderate CYP3A inhibitors were considered (Table 6.1).

Amiodarone was considered separately because its potency of CYP3A inhibition is unspecified and it also inhibits P-glycoprotein (Flockhart, 2007). OAT1B1 inhibitors were defined as drugs with >75% inhibition of *in vitro* OATP1B1-mediated transport of oestradiol-17 $\beta$ -glucuronide at 20 $\mu$ M (Table 6.1) (Karlgrén *et al.*, 2012).

**Table 6.1 CYP3A inducers, inhibitors, and OATP1B1 potential inhibitors**

CYP3A inducers <sup>1</sup>	CYP3A strong/moderate inhibitors <sup>1</sup>	OATP1B1 inhibitors <sup>2</sup>
<b>Detected in at least one participant</b>		
carbamazepine	ciclosporin	ciclosporin
phenytoin	cimetidine	clarithromycin
-	ciprofloxacin	diclofenac
-	clarithromycin	dipyridamole
-	diltiazem	glibenclamide
-	dronedarone	indometacin
-	erythromycin	rosiglitazone
-	fluconazole	spironolactone
-	itraconazole	sulfasalazine
-	verapamil	-
<b>Available in UK but not detected in PhACS cohort<sup>3</sup></b>		
bosentan	aprepitant	atazanavir
efavirenz	boceprevir	indinavir
enzalutamide	clotrimazole	lopinavir
etravirine	cobicistat	mifepristone
mitotane	idelalisib	paclitaxel
modafinil	imatinib	repaglinide
phenobarbital	ketoconazole	rifampicin
rifampicin	luvoxamine	ritonavir
rufinamide	posaconazole	telmisartan
St John's wort	voriconazole	tipranavir
-	Ritonavir alone or in combination with other antivirals (elvitegravir, indinavir, lopinavir, paritaprevir, saquinavir, teleprevir, tipranavir)	-

<sup>1</sup> = from (Food and Drug Administration, 2016). <sup>2</sup> = OATP1B1 inhibitors were all drugs with >75% inhibition of *in vitro* OATP1B1-mediated transport of oestradiol-17 $\beta$ -glucuronide at 20 $\mu$ M except for ATV and other statins (Karlgrén *et al.*, 2012). <sup>3</sup> = grapefruit juice and crizotinib are two FDA listed strong/moderate CYP3A inhibitors. However, it was not possible to detect their use in the PhACS study because the study closed in 2013 before crizotinib was licensed in the UK, and food consumption was not specifically captured in the case report form.

### 6.2.5.1 PK Endpoints

The primary endpoints of this study were: the concentrations of individual ATV analytes, the sum total of all analytes (ATV+2-OH ATV+ATV L+2-OH ATV L), and

specific analyte metabolic ratios (2-OH ATV/ATV, 2-OH ATV L/ATV L, ATV L/ATV), hereafter collectively termed 'PK endpoints'. All PK endpoints were tested in cohort 1.

#### **6.2.5.2 Clinical Endpoints**

Significant biologically plausible variants identified by the ATV PK genetic analyses in cohort 1 were subsequently tested in cohorts 2 and 3 for their association with the following 'clinical endpoints':

- i) Any V2 adverse event attributed by the patient to their statin, and specifically muscular symptoms reported at V2 whilst on statin therapy (in cohort 2);
- ii) ATV intolerance, defined as discontinued ATV, reduced ATV dose, switched to a different statin at lower equivalent dose and/or classed ATV non-adherent (missed at least one ATV pill in the last week) at V2, versus ATV tolerant users (in cohort 2);
- iii) MACE and ACM (in cohort 3).

#### **6.2.6 Statistical analysis**

As expected, the raw ATV analyte levels in cohort 1 showed a right-skew distribution. Therefore, the analytes, their total and ratios (i.e. all PK endpoints) were  $\log_{10}$  transformed to normalise the distribution of (observed) residuals and optimise homoscedasticity. Clinical covariate multicollinearity was assessed using VIF. For each (transformed) PK endpoint, univariate linear regression was conducted for all clinical covariates. Covariates with univariate  $p \leq 0.1$  were entered into multivariable linear regression modelling, using stepwise selection to determine the parsimonious clinical covariate model for each PK endpoint ( $p < 0.05$  taken to indicate clinical covariate multivariable significance).

Prior to GWAS, new PCs were calculated for each participant within the fully quality controlled PhACS sample set by Dr Eunice Zhang (post-doc, Molecular and Clinical Pharmacology, University of Liverpool). The first two PCs were included in all GWAS analyses, alongside the model clinical covariates for each PK endpoint, to adjust for fine-scale European ancestry population structure.

A GWAS of each  $\log_{10}$  transformed PK endpoint was carried out using frequentist association testing assuming an additive model of SNP effect and considering genotype dosages within SNPtest v2.5 ([https://mathgen.stats.ox.ac.uk/genetics\\_software/snpctest/snpctest.html](https://mathgen.stats.ox.ac.uk/genetics_software/snpctest/snpctest.html) (Marchini and Howie, 2010)). Post-analysis QC steps involved exclusion of SNPs with info score (a measure of imputation quality)  $<0.4$ , MAF  $<1\%$  or deviation from Hardy-Weinberg equilibrium ( $p < 1.0 \times 10^{-6}$ ). Manhattan plots were created using the qqman package (Turner, 2014) within the R statistical framework (R Core Team, 2017). A genome-wide statistical significance threshold of  $5.0 \times 10^{-8}$  was applied;  $p \leq 1.0 \times 10^{-5}$  indicated suggestive signals, and  $0.05 \leq p < 1.0 \times 10^{-5}$  nominal significance.

For ATV, ATV L and 2-OH ATV/ATV analyses, suggestive loci ( $p < 1.0 \times 10^{-5}$ ) were investigated further, as follows:

- Regional locus plots were created using LocusZoom (<http://locuszoom.sph.umich.edu/> (Pruim *et al.*, 2010)).
- The predicted effect of all variants with  $p < 1.0 \times 10^{-5}$  was assessed using Ensembl Variant Effect Predictor to screen for non-synonymous variants (<http://www.ensembl.org/info/docs/tools/vep/index.html> (McLaren *et al.*, 2016)); non-coding SNPs and SNPs in moderate LD (LD,  $r^2 > 0.6$ ) with each locus lead SNP were subsequently assessed for eQTLs using HaploReg Version 4.1 (<http://archive.broadinstitute.org/mammals/haploreg/haploreg.php> (Ward and Kellis, 2016)) and the Genotype-Tissue-Expression (GTEx)

project (<https://www.gtexportal.org/home/> (The GTEx Consortium, 2013)), considering all tissues.

- Where appropriate, haplotype and LD structure computations were performed with Haploview 4.2 (<https://www.broadinstitute.org/haploview/haploview> (Barrett *et al.*, 2005)).

The above investigations led to the identification of biologically plausible SNPs (lead locus SNPs, or known biologically relevant locus SNPs), which were further examined as follows:

- Dot plots were produced in GraphPad Prism (version 5.00 for Windows: GraphPad Software Inc., San Diego, USA) to visualise the effect of the identified SNPs on their associated analyte level/ratio using non-transformed PK data.
- For each locus, regional genetic analyses were conducted with inclusion of the lead/biologically relevant SNP as an additional covariate in the regression model in SNPtest v2.5, to search for evidence of distinct association signals within the locus.
- The SNPs were added to the appropriate multivariable clinical covariate model to determine the additional proportion of variation ( $r^2$ ) in the PK endpoint explained by the variant.

Lastly, the impact of biologically plausible SNPs on clinical endpoints was assessed. Logistic regression was used in cohort 2 to determine the association with SNPs, and i) V2 statin adverse events; ii) muscular symptoms; and iii) ATV intolerance. Any SNP associated with ATV intolerance was additionally tested for association with the subgroups of ATV discontinuation/non-adherence, and ATV dose reduction/switching (but adherent). SNPs with univariate  $p$ -value  $\leq 0.1$  were entered into multivariable logistic regression modelling. Similarly, clinical covariates required univariate  $p \leq 0.1$  for entry into multivariable modelling, with the final logistic regression model chosen by forwards likelihood ratio selection. All clinical variables used with the PK endpoints were

considered as potential covariates except blood sample characteristics (storage duration, and time since last ATV) and V2 ATV dose, which was replaced with NSTE-ACS index hospitalisation discharge ATV dose to avoid potential protopathic bias. When investigating ATV intolerance, V2 statin adverse events and the subset of muscular symptoms were themselves considered as covariates in separate multivariable models to assess their association with ATV intolerance.

In cohort 3, univariate Cox proportional hazards regression was used to assess the impact of identified biologically plausible SNPs on time to MACE and time to ACM. For MACE, participants were censored at the earliest of the date of non-CVD death or date of last recorded visit. For ACM, participants were censored at the date of the last recorded visit. P-values  $<0.05$  were taken to indicate significance for all clinical endpoint analyses.

For any biologically plausible imputed variant tested for association with the clinical endpoints, a probability threshold of  $\geq 0.9$  was applied to accept the imputation; patients with imputation probabilities  $<0.9$  were excluded. In the clinical endpoint analyses, SNPs were first tested using an additive model with genotypes coded as 0, 1 or 2 to represent homozygous WT, heterozygous and homozygous variant patients, respectively. Any borderline significant associations were investigated further using a dominant model with genotypes coded as 0 or 1 to represent homozygous WT and variant allele carriers, respectively.

#### **6.2.6.1 Sensitivity analyses**

Sensitivity analyses for both PK and clinical endpoints were conducted.

For the PK endpoints, sensitivity analyses to investigate identified associations with both clinical and genetic factors were undertaken. The sensitivity analyses

of clinical factors were: determination of the adjusted associations between clopidogrel (vs no P2Y<sub>12</sub> inhibitor), furosemide (vs no loop diuretic), omeprazole (vs no PPI) and lansoprazole (vs no PPI) with PK endpoints using the multivariable linear regression models (clinical covariates only). In addition, the adjusted association of furosemide with ATV concentration was determined following cohort stratification by *ABCG2* rs2231142 (Q141K) status. This is because furosemide inhibits BCRP *in vitro* (Ebner *et al.*, 2015) and rs2231142 can be deleterious (Keskitalo *et al.*, 2009c); thus the effect size of a BCRP-mediated furosemide-ATV interaction may be attenuated in 141K carrier patients. Two PK endpoint genetic sensitivity analyses were conducted. First, a GWAS of ATV level with no drug concentration upper limit was carried out. Second, a localised chromosome two analysis (234Mb-235Mb) of 2-OH ATV/ATV was conducted after exclusion of all outliers (outside two SDs for each genotype for both non-transformed and transformed 2-OH ATV/ATV results) to determine any outlier effect impact.

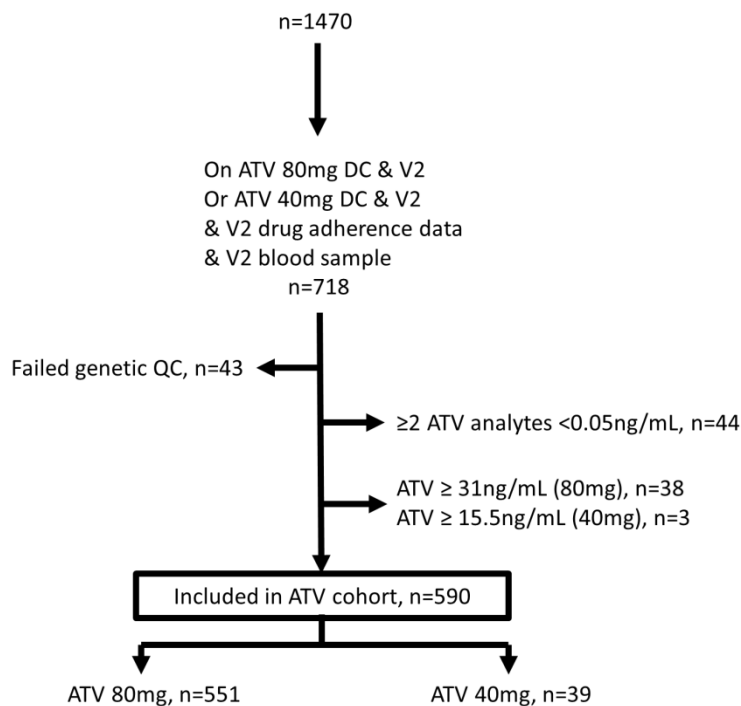
The main clinical endpoint sensitivity analysis was to test any biologically plausible SNP associated with muscle symptoms and/or ATV intolerance (in cohort 2 - discharged on *any* ATV dose) for association with muscle symptoms and/or ATV intolerance (discontinuation, dose reduction, switching, missed  $\geq$ one statin pills in the preceding week) in those discharged on ATV 80mg only. This sensitivity analysis cohort (n=786) is very similar to the complete case sensitivity analysis cohort used in Chapter 2 (n=724), except that the Chapter 2 cohort included patients on RVT 20/40mg daily and excluded patients missing data in *any* clinical covariate. For avoidance of doubt, when limited to patients discharged on high potency ATV (80mg daily), the definitions of 'suboptimal statin therapy' (Chapter 2 terminology) and 'ATV intolerance' (Chapter 6 terminology) are identical. Multiple imputation was not used here.

All clinical analyses were conducted using IBM SPSS v22.0 (IBM Corp, Armonk, NY, USA).

### 6.3 Results

590 patients were selected for inclusion in the main study (cohort 1) (Figure 6.1); their clinical characteristics are presented in Table 6.2. 551 (93.4%) were taking 80mg ATV daily, and 39 (6.6%) ATV 40mg. As expected from a NSTEMI-ACS cohort, the majority were male with a high prevalence of cardiometabolic co-morbidities and concomitant use of CVD secondary prevention medications.

**Figure 6.1 A schematic of the study cohort selection process**



DC = discharge from index hospitalisation; QC = quality control; V2 = visit 2 (month one follow up). From 1470 patients eligible for inclusion in the PhACS study, 590 were included in the main study cohort used in this chapter. Inclusion criteria were: prescribed ATV 80mg or 40mg daily at both discharge from index hospitalisation and V2, with drug adherence data and a plasma sample both available at V2. Exclusion criteria were: failure of genetic quality control steps,  $\geq 2$  analytes were below the LLOQ ( $0.05\text{ng/mL}$ ), or ATV concentration above the implemented ceiling threshold ( $31\text{ng/mL}$  for ATV 80mg, and  $>15.5\text{ng/mL}$  for ATV 40mg).

**Table 6.2 Clinical characteristics of study patients**

<b>Characteristic</b>	<b>ATV</b>
Patients (n)	590
ATV dose: 80mg 40mg	551 (93.4%) 39 (6.6%)
<b>Demographics:</b>	
Male	456 (77.3%)
Age, mean $\pm$ SD (years)	63.6 $\pm$ 11.5
BMI, mean $\pm$ SD (Kg/m <sup>2</sup> )	28.9 $\pm$ 6.0
Smoking: Previous Current	256 (43.4%) 161 (27.3%)
<b>Co-morbidities:</b>	
Hypertension	326 (55.3%)
Hyperlipidaemia prior to index NSTEMI	304 (51.5%)
Diabetes mellitus	109 (18.5%)
CKD (Cr>150 $\mu$ mol/L)	34 (5.8%)
Prior CVD (previous MI, stroke, TIA or PAD)	177 (30.0%)
Hepatic disease	5 (0.8%)
<b>Drugs at Visit 2:</b>	
Aspirin	555 (94.1%)
P2Y <sub>12</sub> inhibitor	503 (85.3%)
Beta blocker	501 (84.9%)
ACEI/ARB	499 (84.6%)
Loop diuretic	100 (16.9%)
Thiazide diuretic	19 (3.2%)
Amiodarone	7 (1.2%)
Proton pump inhibitor	235 (39.8%)
CYP3A4 inducer	3 (0.5%)
CYP3A4 inhibitor	24 (4.1%)
OATP1B1 inhibitor	18 (3.1%)
ATV non-adherence: Missed 1 pill in last 7 days Missed 2 pills in last 7 days	21 (3.6%) 7 (1.2%)
<b>Blood sample characteristics:</b>	
Sample storage duration, mean $\pm$ SD (years)	6.3 $\pm$ 1.2
Time since last ATV, mean $\pm$ SD (hours)	14.0 $\pm$ 1.9

Expectedly, inter-ATV analyte correlations were relatively high (Table 6.3). Nevertheless, they varied between analyte-pairs ranging from 0.18 (ATV L-2-OH ATV) to 0.66 (ATV L-2-OH ATV L); the low ATV L-2-OH ATV correlation plausibly reflects the different metabolic routes (lactonization versus hydroxylation) available for primary ATV metabolism.

**Table 6.3 Correlation between analytes concentrations ( $r^2$ )**

Analyte	ATV	2-OH ATV	ATV L	2-OH ATV L
ATV	x	0.56	0.61	0.48
2-OH ATV	0.56	x	0.18	0.39
ATV L	0.61	0.18	x	0.66
2-OH ATV L	0.48	0.39	0.66	x

The  $r^2$  correlation between the untransformed concentrations of pairs of ATV analytes within the main cohort (n=590) were determined from the calculated line of best fit from scatter plots.

### 6.3.1 Clinical factors associated with ATV analytes

The VIF was <1.5 for all clinical covariates, indicating negligible multicollinearity. The clinical factors significantly associated in multivariable linear regression are presented in Table 6.4 and Table 6.5; the univariate analysis results are in the Appendix (Table 8.7 and Table 8.8). ATV dose was positively associated with the concentration of each ATV analyte and their total, but not with any analyte ratio. Time since last ATV was strongly inversely correlated with analyte and total concentrations, but positively associated with 2-OH ATV/ATV and ATV L/ATV ratios, suggesting progressive ATV metabolism over time. Mean sample storage time was 6.3 years (Table 6.2); therefore, it was not unexpected that storage duration was associated with analyte concentrations and ratios. The composite of strong/moderate CYP3A4 drug inhibitors, and amiodarone itself, were associated with higher ATV concentrations and lower ratios of 2-OH ATV/ATV and 2-OH ATV L/ATV L, reflecting inhibition of CYP3A-mediated hydroxylation. Loop diuretics (88% furosemide, 12% bumetanite) and PPIs (58% lansoprazole, 38% omeprazole, 4% other) were both associated with higher concentrations of ATV analytes and total, and P2Y<sub>12</sub> inhibitor use (99% clopidogrel, 1% prasugrel) was associated with increased hydroxylation.

**Table 6.4 Clinical variables associated with ATV analyte levels in multivariable linear regression**

Variable	ATV		2-OH ATV		ATV L		2-OH ATV L	
	B (SE)	p-value	B (SE)	p-value	B (SE)	p-value	B (SE)	p-value
ATV Dose	0.004 (0.001)	0.0050	0.005 (0.001)	0.000011	0.006 (0.002)	0.00048	0.006 (0.001)	0.000012
Sex (M vs F)	-0.128 (0.034)	0.00018	-	-	-0.104 (0.037)	0.0056	-	-
Age	0.004 (0.001)	0.0017	0.007 (0.001)	1.17x10 <sup>-10</sup>	-	-	0.005 (0.001)	3.00x10 <sup>-6</sup>
BMI	-	-	-0.006 (0.002)	0.0042	-0.007 (0.003)	0.012	-0.006 (0.002)	0.0050
Diabetes mellitus	-	-	0.081 (0.031)	0.010	-	-	-	-
CLD	-	-	-	-	-	-	-0.292 (0.134)	0.029
Loop diuretic	0.103 (0.039)	0.0085	-	-	0.129 (0.042)	0.0023	0.084 (0.035)	0.016
Proton pump inhibitor	0.081 (0.029)	0.0050	0.063 (0.024)	0.0093	0.130 (0.032)	0.000056	0.097 (0.025)	0.00015
CYP3A4 inhibitor	0.174 (0.073)	0.017	-	-	-	-	-	-
Amiodarone	0.262 (0.0128)	0.041	-	-	0.326 (0.141)	0.022	-	-
Sample storage duration	-	-	-0.0001 (0.00003)	2.00x10 <sup>-6</sup>	0.0002 (0.00004)	9.47x10 <sup>-9</sup>	0.0001 (0.00003)	1.00x10 <sup>-6</sup>
Time since last ATV	-0.001 (0.0001)	4.20x10 <sup>-14</sup>	-0.001 (0.0001)	1.23x10 <sup>-12</sup>	-0.001 (0.0001)	1.61x10 <sup>-7</sup>	-0.001 (0.0001)	3.49x10 <sup>-8</sup>

Variables associated ( $p \leq 0.1$ ) with  $\log_{10}$  transformed ATV analyte concentrations in univariate linear regression were entered into multivariable linear regression modelling, using stepwise selection, and retained in the final model if adjusted  $p < 0.05$ .

B is the unstandardized coefficient; B and standard error (SE) represent the change in  $\log_{10}$  transformed analyte concentration for a unit change in a given clinical variable, with all other variables held constant. A positive B value indicates a higher analyte concentration, and a negative B a lower level.

**Table 6.5 Clinical variables associated with ATV analyte total or ratios in multivariable linear regression**

Variable	2-OH ATV/ATV		2-OH ATV L/ATV L		ATV L/ATV		TOTAL <sup>1</sup>	
	B (SE)	p-value	B (SE)	p-value	B (SE)	p-value	B (SE)	p-value
ATV Dose	-	-	-	-	-	-	0.005 (0.001)	5.00x10 <sup>-6</sup>
Sex (M vs F)	0.119 (0.021)	2.74x10 <sup>-8</sup>	0.091 (0.021)	0.000016	-	-	-	-
Age	0.003 (0.001)	0.00044	0.003 (0.001)	7.00x10 <sup>-6</sup>	-	-	0.005 (0.001)	6.00x10 <sup>-6</sup>
BMI	-	-	-	-	-	-	-0.005 (0.002)	0.006
Diabetes mellitus	-	-	-	-	-0.060 (0.024)	0.013	-	-
P2Y <sub>12</sub> inhibitor	0.070 (0.025)	0.006	0.074 (0.025)	0.003	-	-	-	-
Loop diuretic	-	-	-	-	-	-	0.095 (0.032)	0.003
Proton pump inhibitor	-	-	-	-	0.038 (0.019)	0.041	0.086 (0.023)	0.00028
CYP3A4 inducer	-	-	-	-	0.256 (0.128)	0.046	-	-
CYP3A4 inhibitor	-0.148 (0.045)	0.001	-0.133 (0.044)	0.002	-	-	-	-
Amiodarone	-0.170 (0.081)	0.037	-0.167 (0.080)	0.038	-	-	-	-
Sample storage duration	-0.0001 (0.00002)	2.46x10 <sup>-7</sup>	-7.08x10 <sup>-5</sup> (0.00002)	0.001	0.0002 (0.00002)	2.03x10 <sup>-24</sup>	-	-
Time since last ATV	0.0002 (0.00008)	0.011	-	-	0.0003 (0.00008)	0.001	-0.001 (0.0001)	1.13x10 <sup>-13</sup>

<sup>1</sup> = ATV + 2-OH ATV + ATV L + 2-OH ATV L. Variables associated (p≤0.1) with log<sub>10</sub> transformed ATV analyte ratios or total in univariate linear regression were entered into multivariable linear regression modelling, using stepwise selection, and retained in the final model if adjusted p<0.05.

B is the unstandardized coefficient; B and standard error (SE) represent the change in log<sub>10</sub> transformed analyte ratio or total for a unit change in a given clinical variable, with all other variables held constant. A positive B value indicates a higher level, and a negative B a lower level.

### 6.3.2 Sensitivity analyses of clinical factors associated with PK endpoints

Multivariable analysis showed that the identified associations with loop diuretics and P2Y<sub>12</sub> inhibitors are driven by furosemide and clopidogrel, respectively (Table 6.6). The PPI associations are potentially a class effect as the majority of PPI associations remained when considering omeprazole and lansoprazole (vs no PPI) separately (Table 6.6). Based on *in vitro* research suggesting that furosemide inhibits BCRP (Ebner *et al.*, 2015), the cohort was stratified into wild-type (n=452) and carriers (n=138) of the *ABCG2* deleterious missense variant, rs2231142 (Q141K). Interestingly, furosemide was associated in multivariable analysis with increased ATV concentration in rs2231142 wild-type homozygotes (B (SE) = 0.123 (0.046), adjusted p=0.007), but not in 141K carriers (B (SE) = 0.044 (0.091), adjusted p=0.63).

**Table 6.6 Sensitivity analysis to determine the association between specific drugs and ATV PK endpoints in multivariable linear regression**

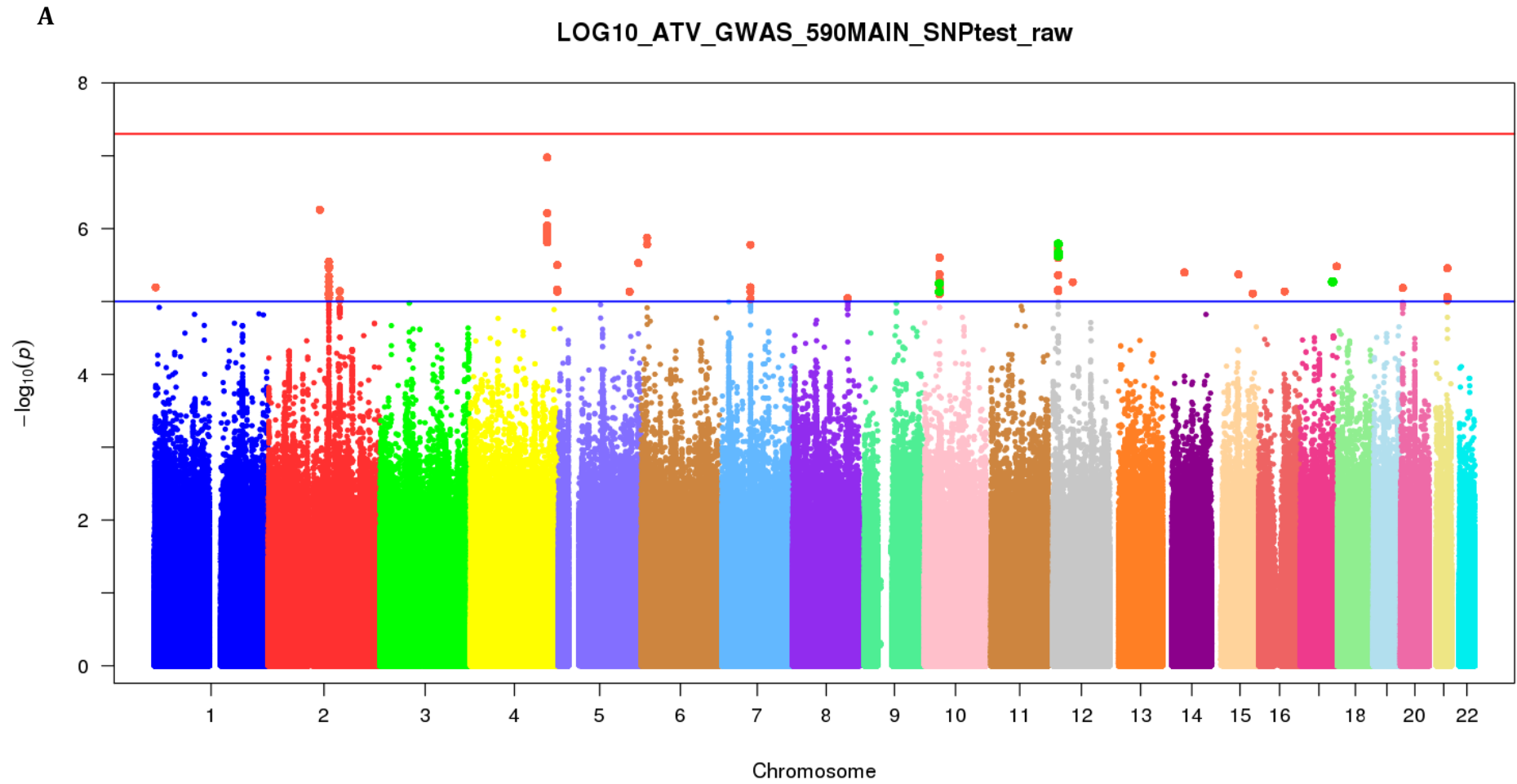
PK endpoint	Furosemide (n=88)		Clopidogrel (n=496)		Omeprazole (n=90)		Lansoprazole (n=136)	
	B (SE)	p-value	B (SE)	p-value	B (SE)	p-value	B (SE)	p-value
ATV	0.105 (0.041)	0.010	-	-	0.064 (0.040)	0.11	0.089 (0.034)	0.010
2-OH ATV	-	-	-	-	0.072 (0.034)	0.036	0.055 (0.029)	0.054
ATV L	0.143 (0.044)	0.001	-	-	0.116 (0.045)	0.010	0.125 (0.039)	0.001
2-OH ATV L	0.089 (0.036)	0.014	-	-	0.111 (0.035)	0.002	0.079 (0.031)	0.012
2-OH ATV/ATV	-	-	0.072 (0.025)	0.005	-	-	-	-
2-OH ATV L/ATV L	-	-	0.076 (0.025)	0.003	-	-	-	-
ATV L/ATV	-	-	-	-	0.034 (0.027)	0.21	0.036 (0.023)	0.12
TOTAL	0.100 (0.033)	0.003	-	-	0.101 (0.032)	0.002	0.067 (0.028)	0.017

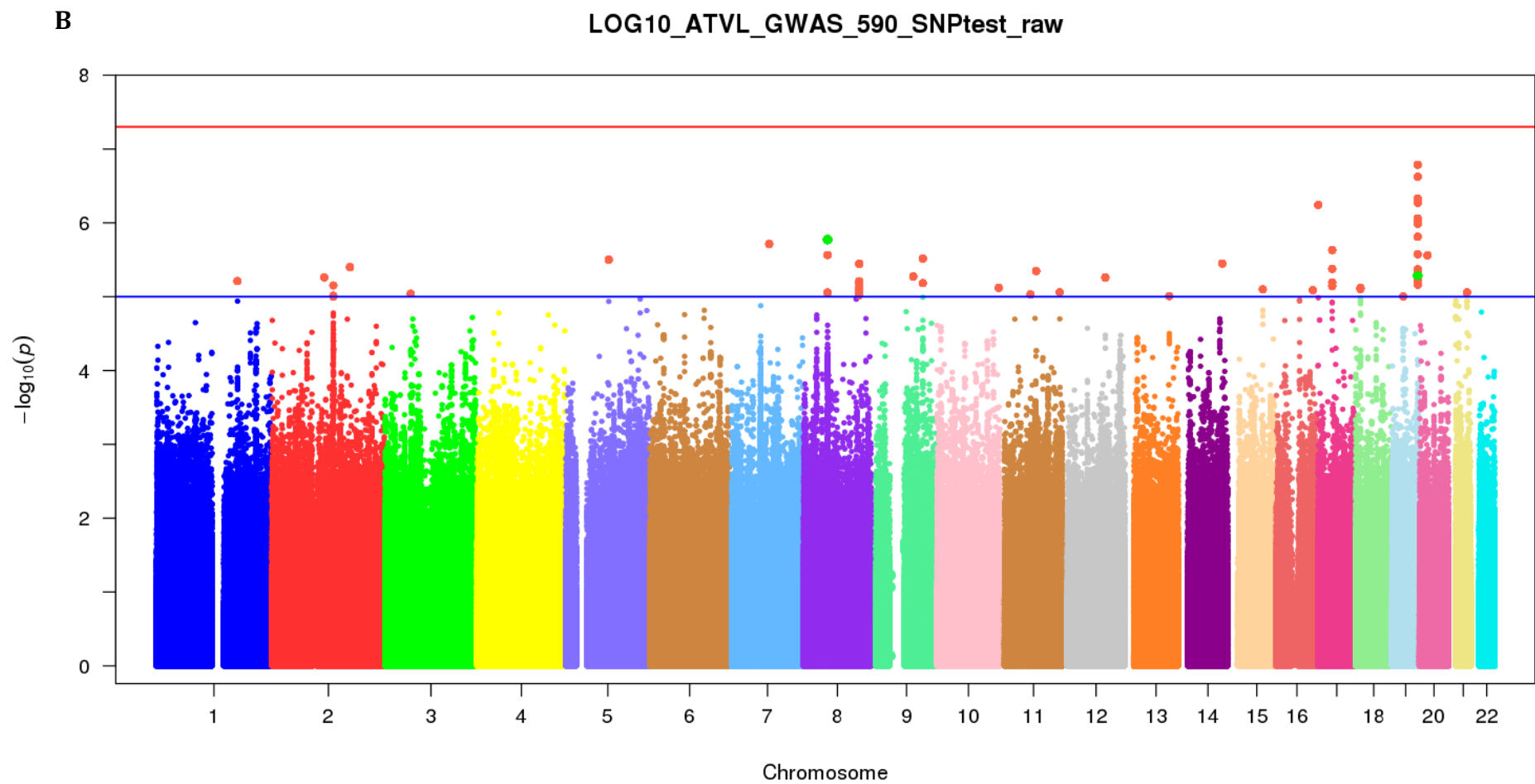
Loop diuretics, P2Y<sub>12</sub> inhibitors and PPI drug classes were associated with several PK endpoints ( $p < 0.05$ ) (Table 6.4, Table 6.5). This sensitivity analysis was restricted to the predominant drug(s) in each class to determine whether they are driving the drug class association. Presented results are from multivariable linear regression using the clinical covariate models, with substitution of each drug class (e.g. loop diuretics) for the specific drug (e.g. furosemide) in the model. For each specific drug, the comparator was the absence of any drug from the drug class (e.g. omeprazole vs no PPI). For each drug, only PK endpoints significantly associated with the respective drug class were analysed.

### 6.3.3 Genome-wide association analyses of PK endpoints

Two strong genome-wide significant associations between the *UGT1A* locus in chromosome two and the ratios of both 2-OH ATV/ATV (top SNP, rs887829,  $p=7.25 \times 10^{-16}$ ) and 2-OH ATV L/ATV L (top SNP, rs887829,  $p=3.95 \times 10^{-15}$ ) were detected, which shared the same lead SNP: rs887829. The 2-OH ATV/ATV and 2-OH ATV L/ATV L GWAS analyses had 89 and 99 SNPs with  $p < 5.0 \times 10^{-8}$  in total, all mapping to the same chromosome two locus, respectively. These genome-wide significant results and the other suggestive signals from the ATV, ATV L and 2-OH ATV/ATV analyses were explored further; the Manhattan plots for these analyses are in Figure 6.2. Overall the ATV, ATV L and 2-OH ATV/ATV analyses had 156, 63 and 227 suggestive SNPs with  $p < 1.0 \times 10^{-5}$ , respectively; the lead SNPs are summarised in Table 6.7. The Manhattan plots of the other PK endpoints are available in the Appendix (Figure 8.1).

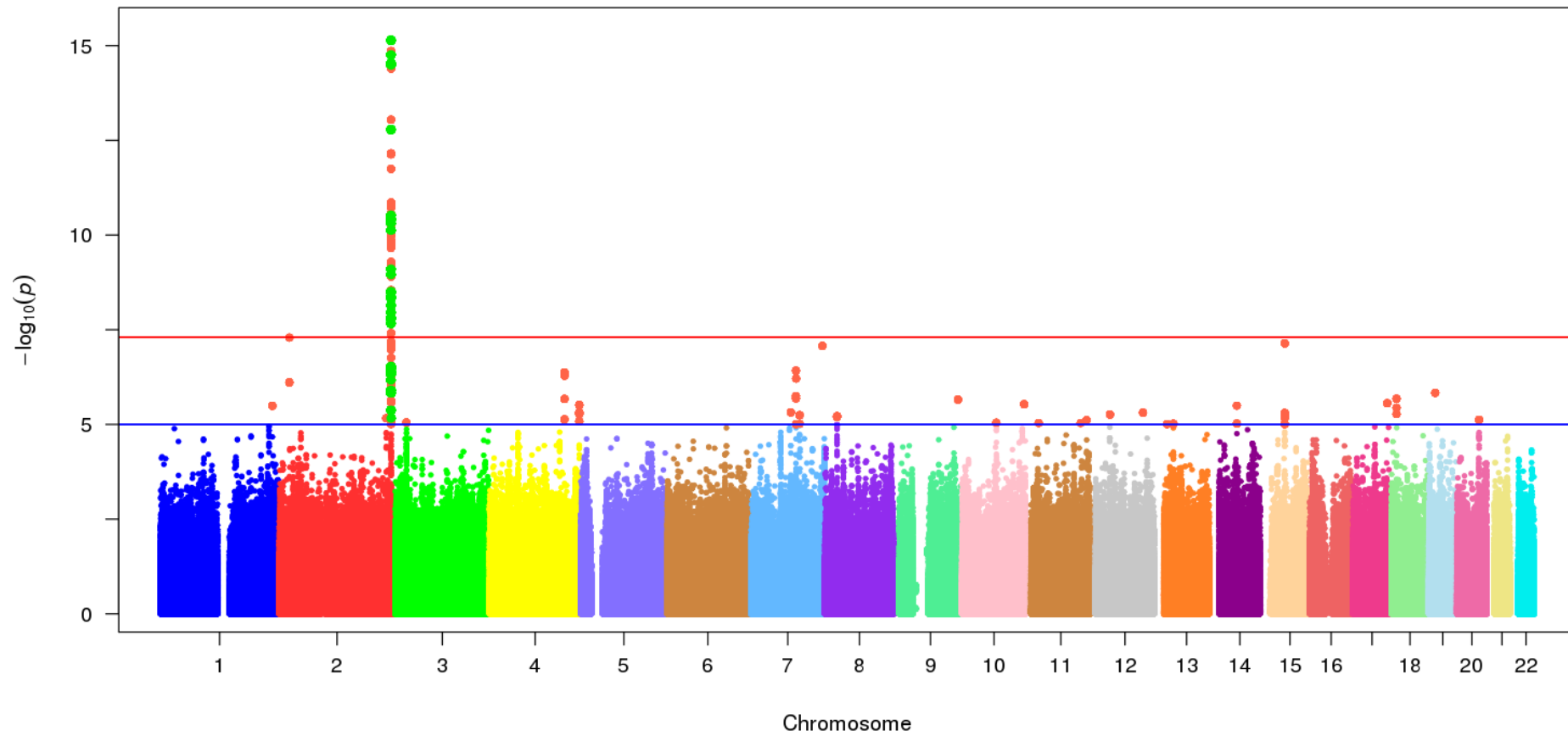
Figure 6.2 Manhattan plots of key genome-wide association analyses

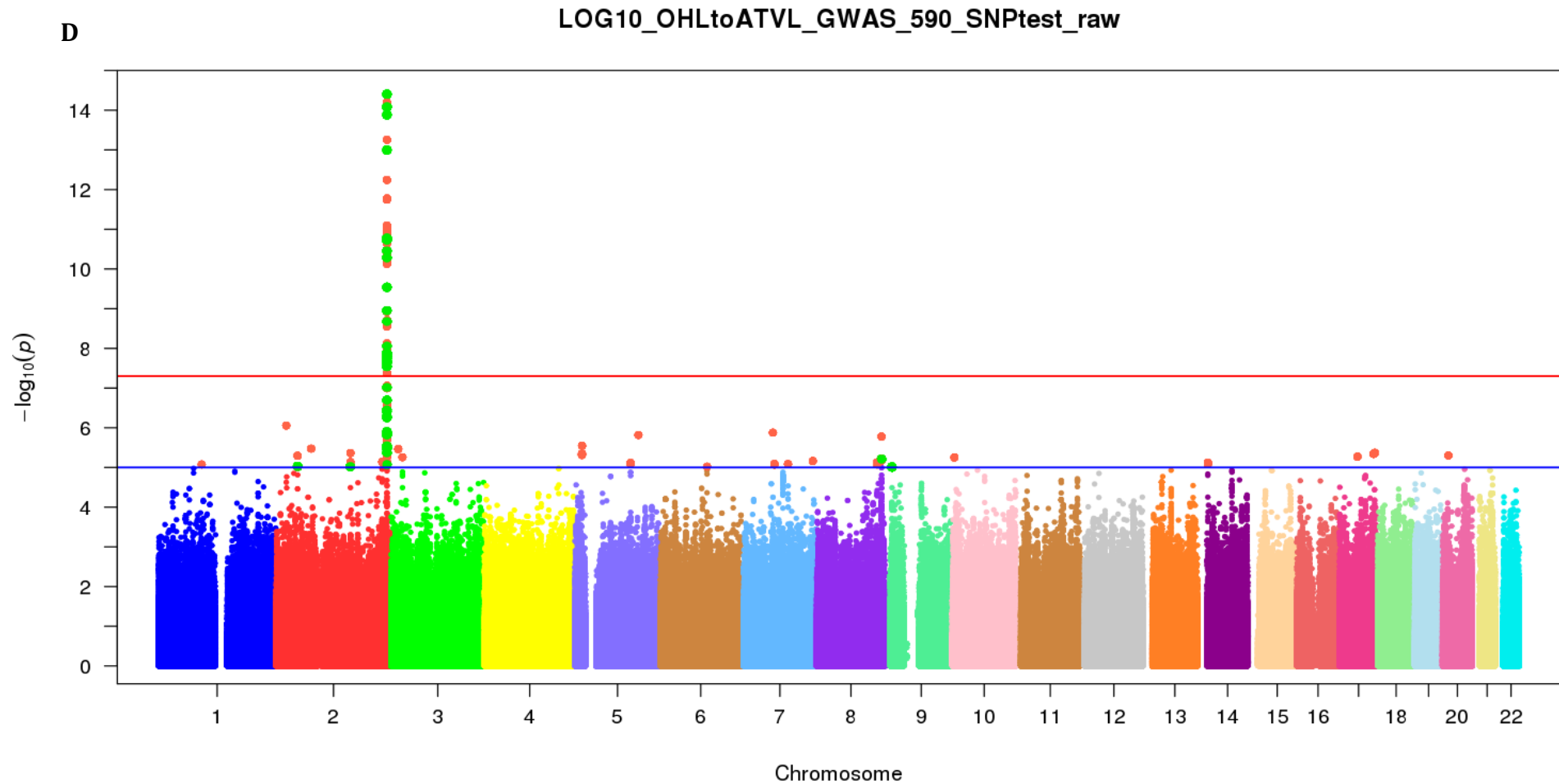




C

LOG10\_OHtoATV\_GWAS\_590\_SNPtest\_raw





Genome-wide association analyses were carried out using  $\log_{10}$  transformed analyte concentrations or ratios within the main cohort ( $n=590$ ), adjusted for the first two principal components and the clinical covariates of the relevant PK endpoint multivariable linear regression model, in SNPtest v2.5 by frequentist association testing assuming an additive model of SNP effect and considering genotype dosage. The analyses of ATV (A), ATV L (B), 2-OH ATV/ATV (C), and just the genome-wide significant association in 2-OH ATV L/ATV L (D), were focused on and so presented here.

**Table 6.7 Lead SNPs from ATV, ATV L and 2-OH ATV/ATV genome-wide association analyses**

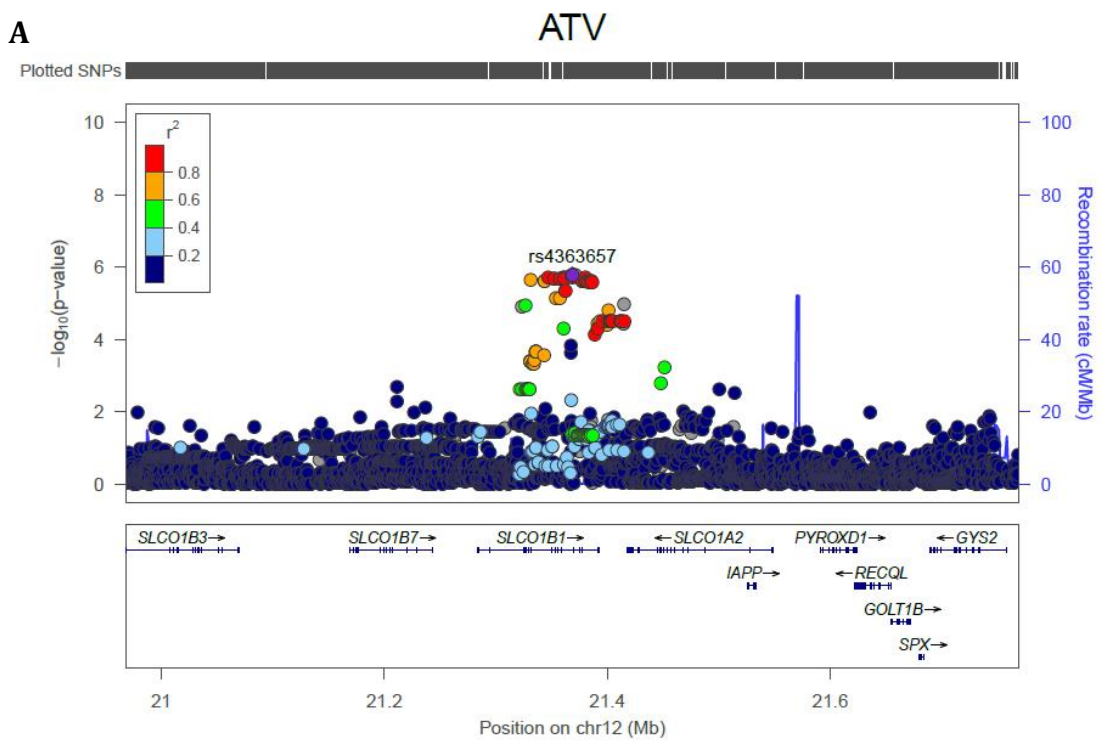
Lead SNP	Chr	Position	Locus	Reference allele	Variant allele	Study MAF	1000G MAF <sup>4</sup>	Genome-wide association result <sup>5</sup>		
								Analysis	B (SE)	p-value
<b>Biologically plausible loci</b>										
rs4363657 <sup>1</sup>	12	21368722	<i>SLCO1B1</i>	T	C	0.16	0.19	ATV	0.125 (0.026)	1.63x10 <sup>-6</sup>
								2-OH ATV	0.105 (0.022)	1.57x10 <sup>-6</sup>
rs887829 <sup>3</sup>	2	234668570	<i>UGT1A</i>	C	T	0.346	0.30	2-OH ATV/ATV	0.100 (0.012)	7.25x10 <sup>-16</sup>
								2-OH ATV L/ATV L	0.096 (0.012)	3.95x10 <sup>-15</sup>
rs45446698 <sup>3</sup>	7	99332948	5' of <i>CYP3A7</i>	T	G	0.046	0.04	2-OH ATV/ATV	0.154 (0.031)	6.18x10 <sup>-7</sup>
								2-OH ATV L/ATV L	0.128 (0.030)	2.91x10 <sup>-5</sup>
<b>Putative loci</b>										
rs78192210 <sup>1</sup>	2	132162134	LINC01120	T	G	0.036	0.03	ATV	-0.239 (0.050)	2.85x10 <sup>-6</sup>
								TOTAL	-0.196 (0.041)	2.14x10 <sup>-6</sup>
rs2322579 <sup>1</sup>	4	167097209	Intergenic	A	C	0.012	0.01	ATV	-0.559 (0.104)	1.05x10 <sup>-7</sup>
rs73323405 <sup>2</sup>	8	119984870	<i>RNU6-12P</i>	T	C	0.026	0.03	ATV L	-0.327 (0.070)	3.58x10 <sup>-6</sup>
rs11008865 <sup>1</sup>	10	32574842	<i>EPC1</i>	C	T	0.172	0.15	ATV	-0.117 (0.025)	5.67x10 <sup>-6</sup>
								2-OH ATV	-0.077 (0.022)	0.000440
rs17806387 <sup>2</sup>	17	30836040	<i>MYO1D</i>	A	G	0.020	0.02	ATV L	0.392 (0.082)	2.33x10 <sup>-6</sup>
rs62124643 <sup>2</sup>	19	55492610	<i>NLRP2</i>	C	T	0.071	0.05	ATV L	-0.231 (0.044)	1.63x10 <sup>-7</sup>

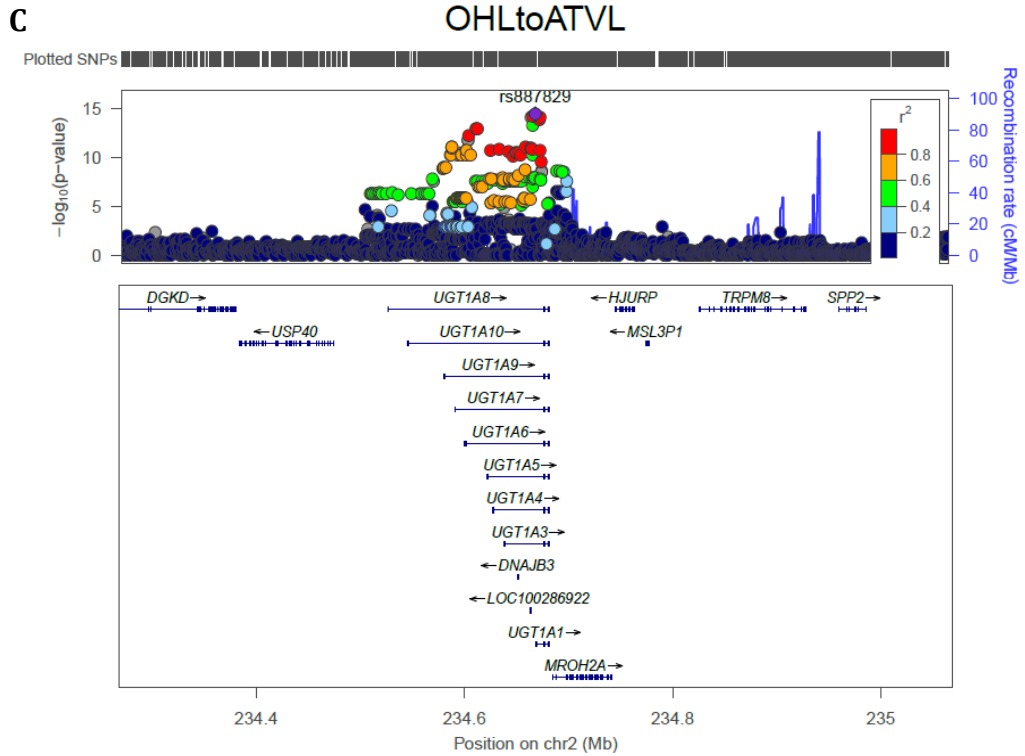
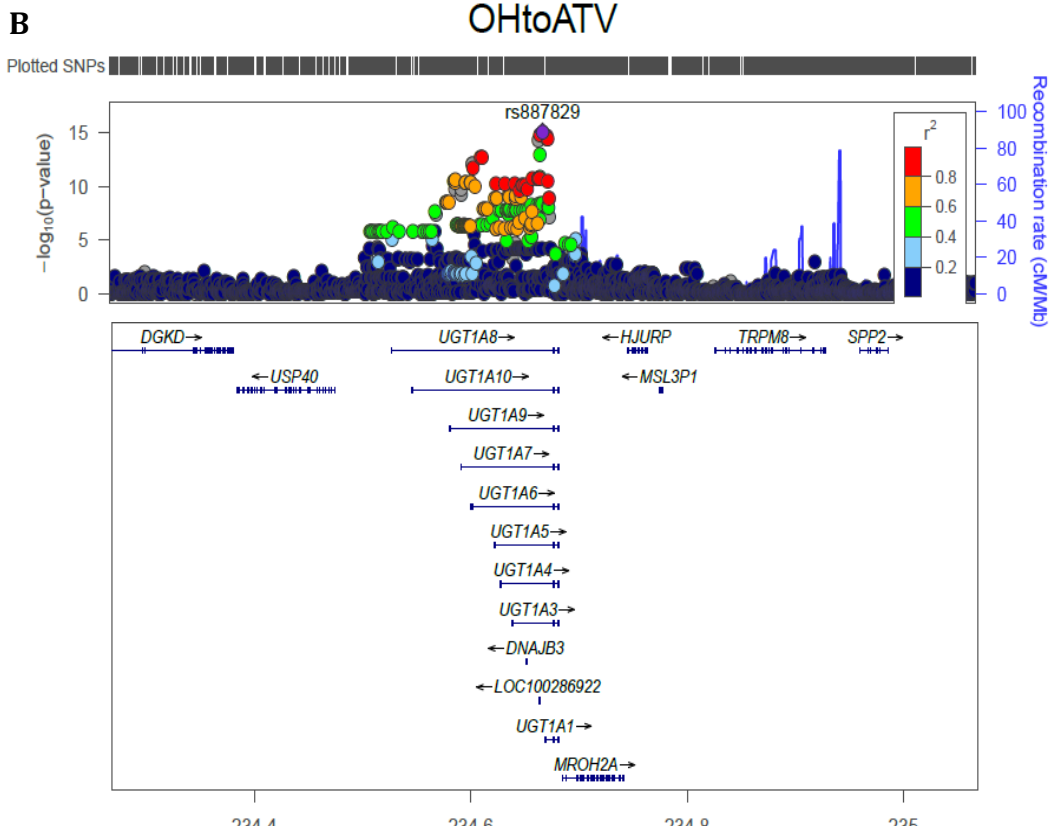
Locus lead SNPs were selected from: <sup>1</sup> = ATV; <sup>2</sup> = ATV L; <sup>3</sup> = 2-OH ATV/ATV. <sup>4</sup> = 1000 Genomes Project Phase 3 European allele frequencies. <sup>5</sup> = where appropriate, the GWAS result for a given lead SNP from another PK endpoint analysis is presented. B and standard error represent the change in log<sub>10</sub> transformed analyte level for a change in genotype using an additive model, with all clinical covariates held constant; a positive B indicates an increased level and a negative B a reduced level.

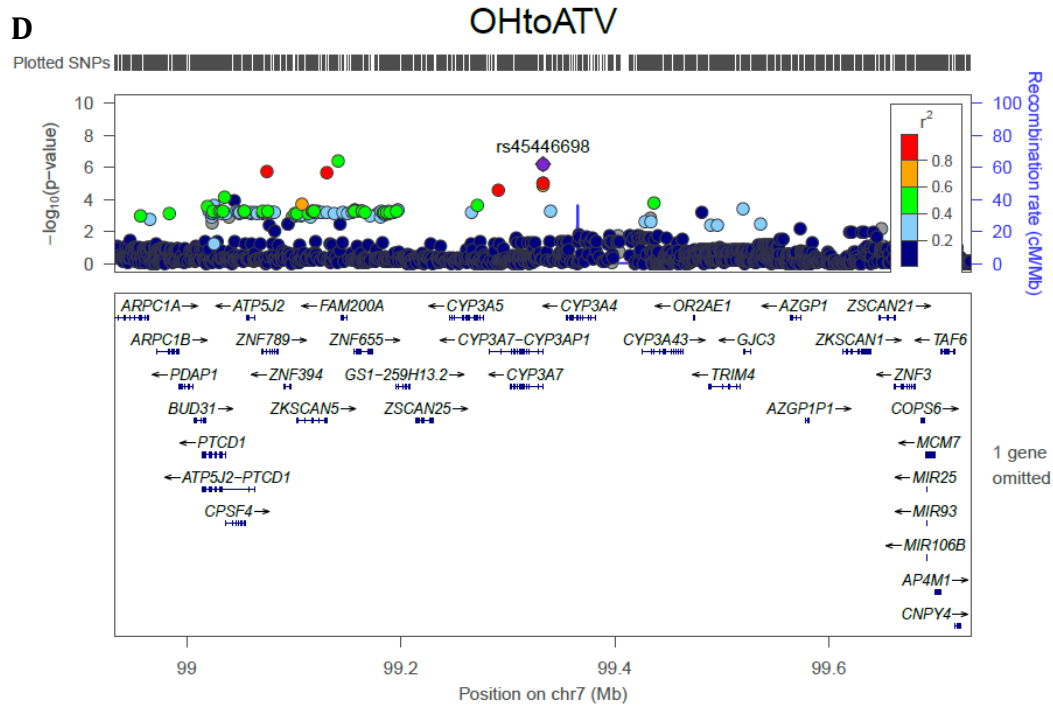
### 6.3.4 Biologically plausible candidate signals

From the Manhattan-identified suggestive signals, *in silico* functional analysis identified three biologically plausible loci: the genome-wide significant *UGT1A* locus, and the suggestively associated *SLCO1B1* and *CYP3A7* loci (Table 6.7). Regional plots of these loci are shown in Figure 6.3. Although eQTLs for both *MZT2A* (mitotic spindle organising protein 2A) and *EPC1* (enhancer of polycomb homolog 1) were identified in at least one tissue (see Appendix Table 8.9), they were not considered further due to lack of established biological plausibility.

**Figure 6.3 Regional locus plots of biologically plausible loci**







Biologically plausible loci were selected from the ATV, ATV L and 2-OH ATV/ATV genome-wide association analyses, based on proximity to genes with plausible biological relevance, identification of non-synonymous variants and eQTL analysis. The regional plots were produced in 'Locus Zoom' using a 400Kb flanking size and LD based on the 1000 Genomes Phase I 2012 European ancestry reference panel. The presented regional locus plots are: A = *SLC01B1* with ATV; B = *UGT1A* locus with 2-OH ATV/ATV; C = *UGT1A* locus with 2-OH ATV L/ATV L; D = *CYP3A* locus with 2-OH ATV/ATV.

### 6.3.5 Characterisation of biologically plausible signals

#### 6.3.5.1 *SLC01B1* locus

Importantly, the ATV chromosome 12 lead SNP (rs4363657,  $p=1.63 \times 10^{-6}$ , Figure 6.3A) was located in *SLC01B1* and was in strong LD with the known *SLC01B1* missense SNP, rs4149056 ( $r^2 = 0.7$ ,  $D' = 0.93$ ). SNP rs4149056 was itself suggestively associated with higher ATV ( $B=0.127$ ,  $SE=0.026$ ,  $p=2.21 \times 10^{-6}$ ) and 2-OH ATV ( $B=0.110$ ,  $SE=0.022$ ,  $p=1.09 \times 10^{-6}$ ) concentrations, but only nominally associated with higher ATV L ( $p=0.0032$ ) and 2-OH ATV L (0.0042) levels. A dot plot to show the impact of rs4149056 by genotype on ATV concentrations is shown in Figure 6.5A. Conditioning on rs4149056 led to complete loss of signal with ATV and 2-OH ATV levels, indicating a single association was responsible for the locus signal. Addition of rs4149056 to the multivariable clinical variable

ATV model increased the proportion of ATV concentration variance explained from 16.9 to 20.2% (Table 6.8).

### 6.3.5.2 *CYP3A7* locus

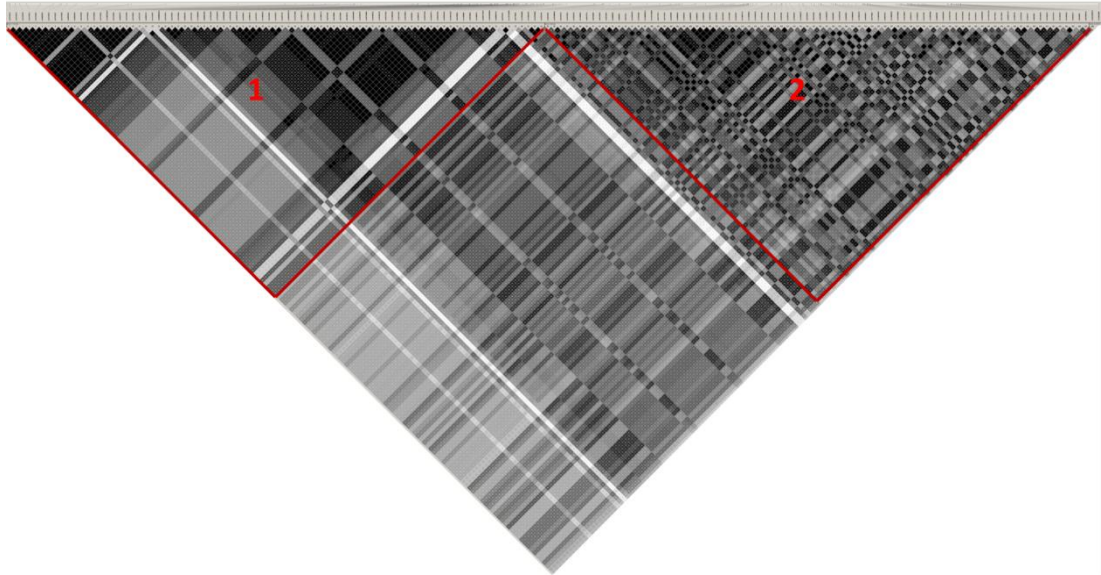
Secondly, the 2-OH ATV/ATV lead chromosome seven SNP (rs45446698) is one of seven highly correlated SNPs (rs11568824, rs45494802, rs45575938, rs45467892, rs11568825, rs11568826, and rs45446698) that cluster within the *CYP3A7* promoter and constitute the *CYP3A7\*1C* allele, which is associated with adult *CYP3A7* liver expression (Kuehl *et al.*, 2001; Johnson *et al.*, 2016). Similarly, the GTEx project identified rs45446698 (but none of the other six *\*1C* SNPs) as an eQTL, specifically for higher *CYP3A7* expression in the adrenal gland and transverse colon (The GTEx Consortium, 2013). Although no rs45446698 variant homozygotes were detected, rs45446698 heterozygosity was associated with increased 2-OH ATV/AVT ( $p=6.18 \times 10^{-7}$ ) and 2-OH ATV L/ATV L ( $p=2.91 \times 10^{-5}$ ) (Table 6.7) ratios compared to wild-type participants, implicating *CYP3A7* for the first time in ATV metabolism. The effect of rs45446698 by genotype on 2-OH ATV/ATV levels is portrayed by dot plot in Figure 6.5B. Conditioning on rs45446698 led to loss of locus signal for both 2-OH ATV/ATV and 2-OH ATV L/ATV L endpoints. Neither of the common established reduced function alleles, *CYP3A4\*22* (rs35599367) and *CYP3A5\*3* (rs776746), were in LD with rs45446698. Although *CYP3A4\*22* was nominally associated with lower ratios of 2-OH ATV/ATV ( $p=0.016$ ) and 2-OH ATV L/ATV L ( $p=0.005$ ), it was not associated with ATV or ATV L concentrations; *CYP3A5\*3* was not associated with hydroxylation ratios, ATV or ATV L concentrations.

### 6.3.5.3 *UGT1A* locus

Thirdly, haplotype analysis of the 89 genome-wide significant SNPs in the 2-OH ATV/ATV *UGT1A* SNP tower revealed two nominal haplotype blocks, although all SNPs were in strong LD with one another ( $r^2 = 0.71-1.0$ , Figure 6.4). After conditional analysis adjusted for the lead SNP, rs887829, there was complete

loss of locus signal. The impact of rs887829 genotype on hydroxylation ratios is shown in Figure 6.5C and D.

**Figure 6.4 Haplotype structure of *UGT1A* SNPs associated with 2-hydroxy atorvastatin to atorvastatin ratio with  $p < 5.0 \times 10^{-8}$**



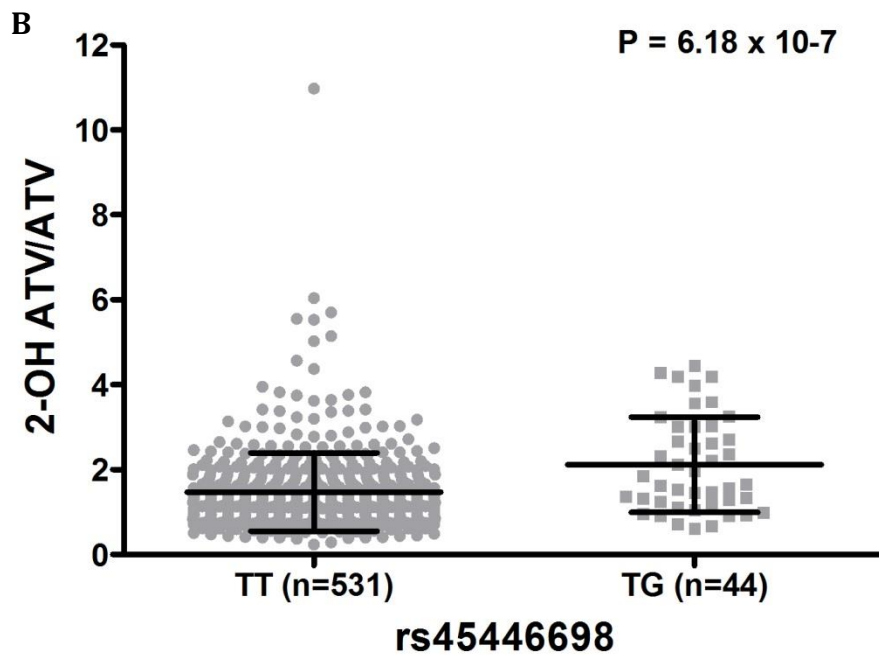
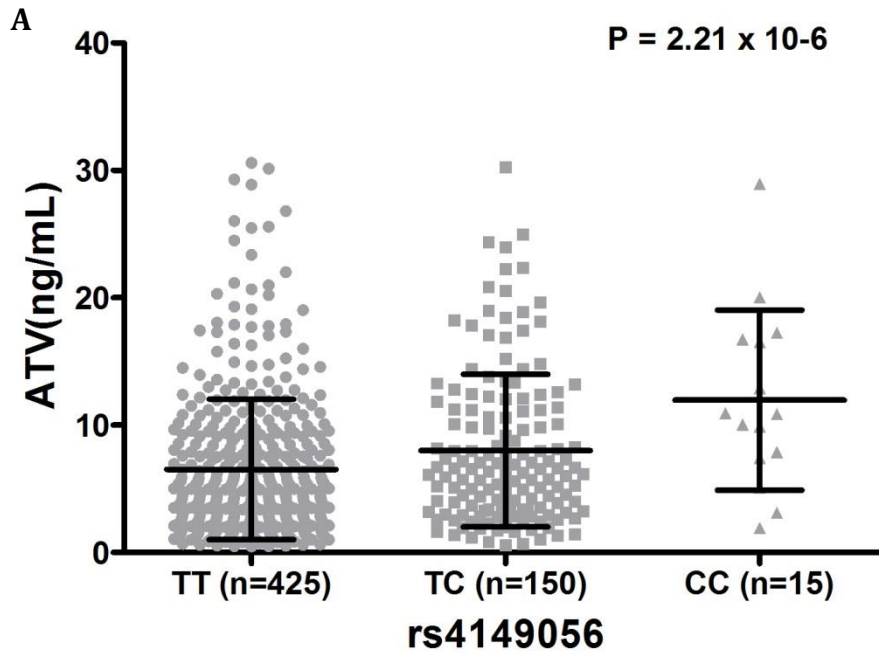
This figure shows the haplotype structure of the 89 *UGT1A* genome-wide significant SNPs for 2-OH ATV/ATV. Although two haplotype blocks were nominally identified according to the solid spine of LD (identified by the red lines), the SNPs were all in high LD with one another ( $r^2 = 0.71-1.0$ ). Increasing blackness indicates higher LD ( $R^2 = 1$  for black, and 0 for white). The lead SNP, rs887829, and the two correlated *UGT1A3\*2* SNPs (rs2008584, rs1983023) were all in haploblock 2.

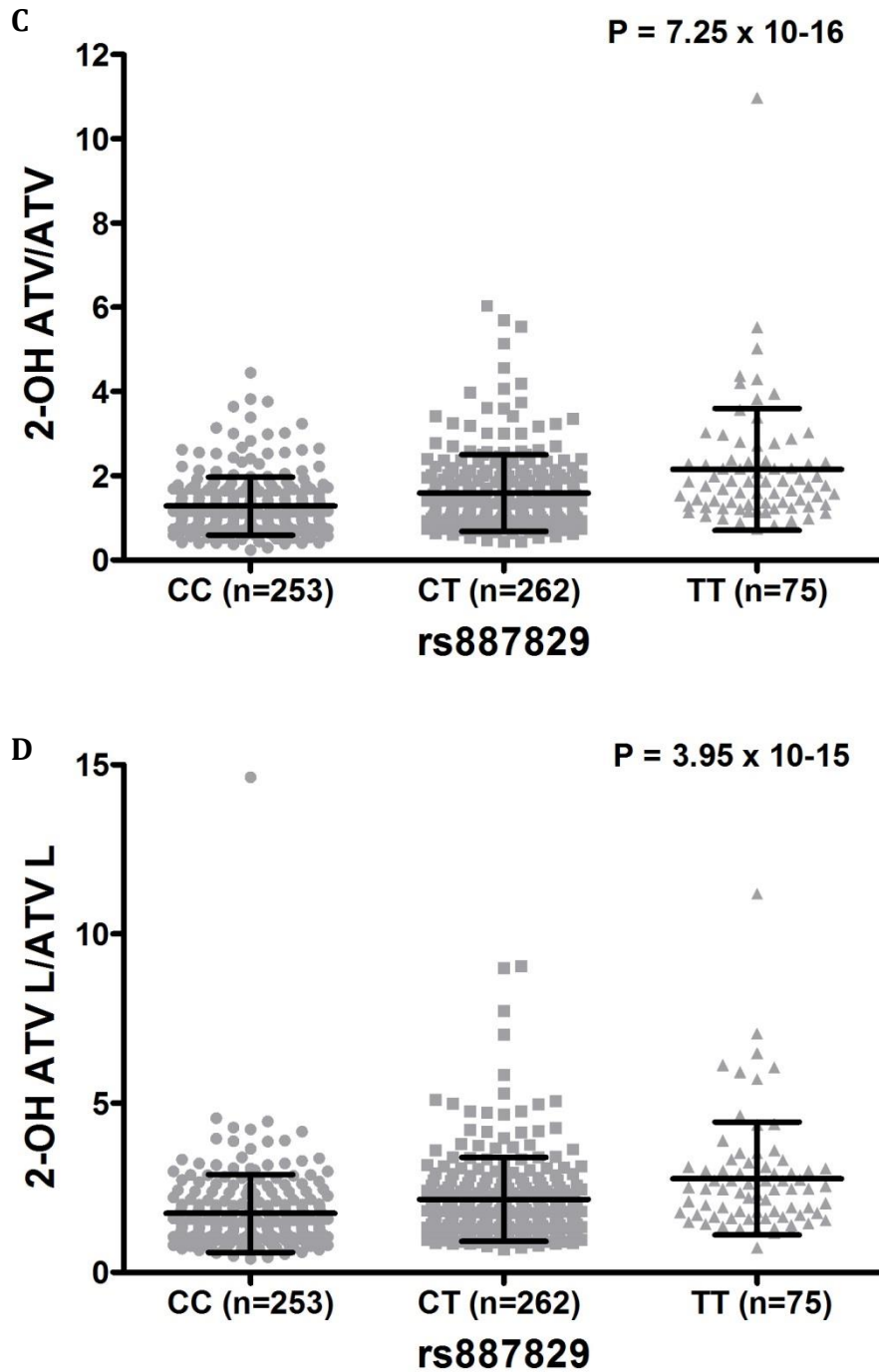
The common low expression *UGT1A1* allele, *UGT1A1\*28*, was not present in the genotype array. However, *UGT1A1\*28* is known to be strongly correlated with the variant T allele of rs887829 (Horsfall *et al.*, 2011). Furthermore, rs887829 is in moderate LD with two of the three *UGT1A3\*2*-defining SNPs (rs2008584,  $r^2 = 0.53$ ,  $D' = 0.93$ ; rs1983023  $r^2 = 0.71$ ,  $D' = 0.93$ ). Interestingly, rs2008584 and rs1983023 were themselves associated with increased 2-OH ATV/ATV ( $p = 3.93 \times 10^{-8}$  and  $6.60 \times 10^{-10}$ , respectively) and increased 2-OH ATV L/ATV L ( $p = 4.20 \times 10^{-8}$ ,  $1.03 \times 10^{-8}$ , respectively). The third *UGT1A3\*2* SNP, rs45449995, was not in LD with rs887829, but was nominally associated with higher 2-OH ATV/ATV ( $p = 5.46 \times 10^{-5}$ ) and 2-OH ATV L/ATV L ( $p = 0.00051$ ) ratios. The impact of *UGT1A3* haplotypes on increasing 2-OH ATV/ATV is available in the Appendix

(Figure 8.5). In conditional analyses that adjusted for the three *UGT1A3*\*2 defining-SNPs, the signal of the lead SNP, rs887829, was attenuated but not extinguished (from  $7.25 \times 10^{-16}$  to  $4.63 \times 10^{-7}$  for 2-OH ATV/ATV). The sequential addition of rs887829 (*UGT1A* cluster) and rs45446698 (*CYP3A7*) to the 2-OH ATV/ATV multivariable clinical model increased the proportion of variation explained from 15.8% to 25.2% to 28.6%, respectively (Table 6.8).

Regional plots of all ATV and ATV L suggestive loci, and the effect sizes for rs4149056 (*SLCO1B1*), rs45446698 (*CYP3A7*) and rs887829 (*UGT1A*) with all PK endpoints are available in the Appendix (Figure 8.2, Figure 8.3 and Table 8.10, respectively). There was no clear signal in the *POR* region of chromosome seven for any PK endpoint (see Appendix Figure 8.4 for regional plots of *POR* in relation to ATV concentration and hydroxylation).

Figure 6.5 The impact of the biologically-plausible identified variants by genotype on atorvastatin and hydroxylation levels illustrated by dot plots





Figures show mean  $\pm$  SD of ATV concentration (A) or ratios of 2-OH ATV/ATV (B,C) or 2-OH ATV L/ATV L (D) by variant genotype. P-values taken from GWAS analysis of  $\log_{10}$  transformed results using frequentist association testing assuming an additive model. The SNPs illustrated are the common missense variant in *SLCO1B1* (rs4149056, V174A), and the lead SNPs at the identified *CYP3A7* locus (rs45446698) and *UGT1A* locus (rs887829).

**Table 6.8 Additional proportion of analyte level variation explained by biologically plausible identified SNPs**

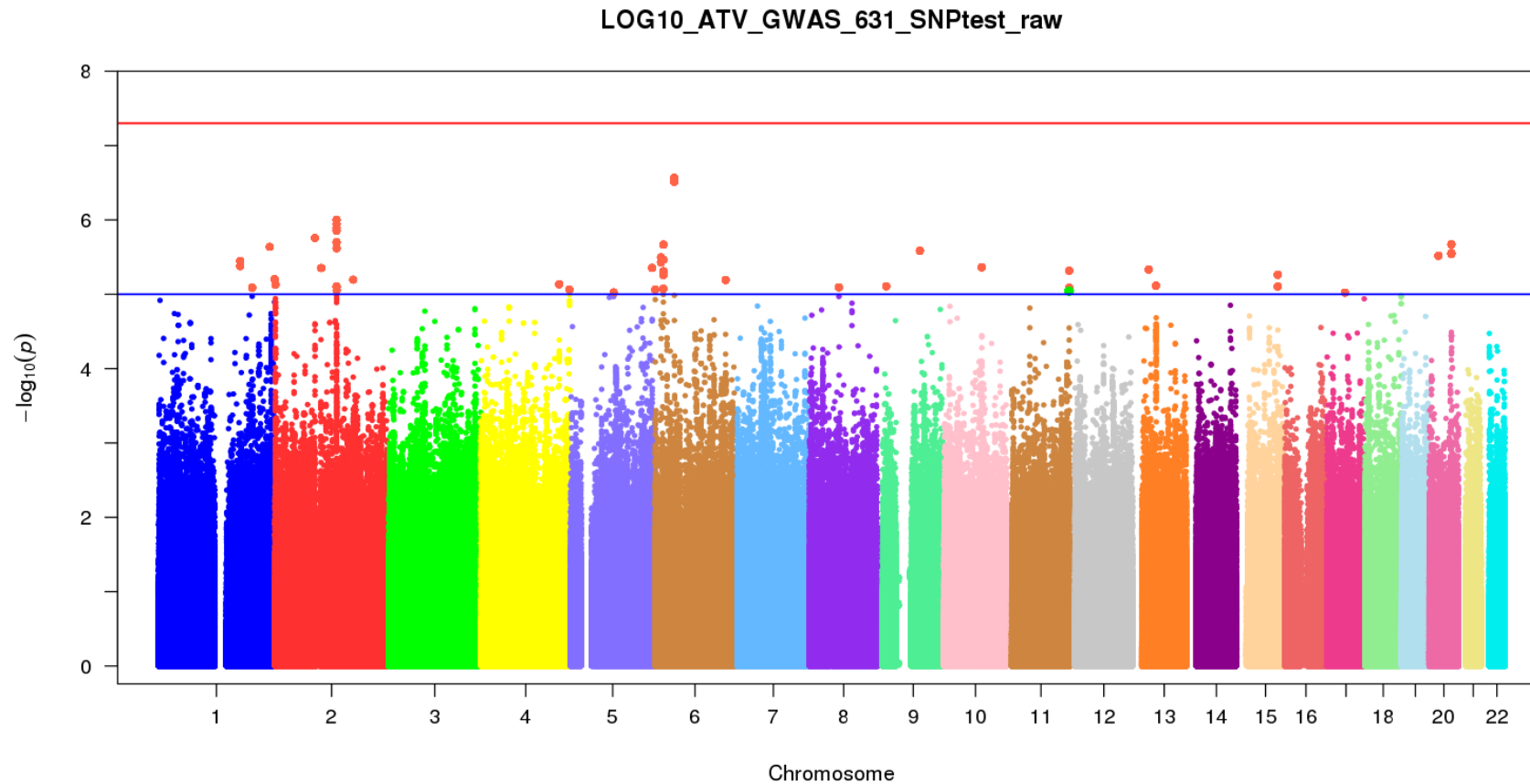
Model	Variables	Final regression equation	Model p-value	R <sup>2</sup> (%)
ATV clinical	ATV dose, Age, Sex, LD, PPI, Amiodarone, CYP3A4 inhibitor, Time since last ATV	-	1.92x10 <sup>-19</sup>	16.9
ATV PGx	ATV clinical + rs4149056 ( <i>SLCO1B1</i> )	Log <sub>10</sub> (ATV) = 1.004 + 0.004(ATV dose) -0.132(Female) + 0.004(Age) + 0.106(LD) + 0.080(PPI) + 0.285(Amiodarone) + 0.181(CYP3A4 inhibitor) - 0.001(Time since last ATV) + 0.128(rs4149056)	1.41x10 <sup>-23</sup>	20.2
2-OH ATV/ATV clinical	Age, Sex, P2Y <sub>12</sub> inhibitor, CYP3A4 inhibitor, Amiodarone, Sample storage duration, Time since last ATV	-	6.02x10 <sup>-18</sup>	15.8
2-OH ATV/ATV PG <sub>x</sub> <sub>i</sub>	2-OH ATV/ATV clinical + rs887829 ( <i>UGT1A</i> )	Log <sub>10</sub> (2-OH ATV/ATV) = -0.276 + 0.114(Female) + 0.003(Age) + 0.076(P2Y <sub>12</sub> inhibitor) -0.168(CYP3A4 inhibitor) -0.150(Amiodarone) - 0.0001(Sample storage duration) + 0.0002(Time since last ATV) +0.102(rs887829)	3.58x10 <sup>-31</sup>	25.2
2-OH ATV/ATV PG <sub>x</sub> <sub>ii</sub>	2-OH ATV/ATV clinical + rs887829 ( <i>UGT1A</i> ) + rs45446698 (5' of <i>CYP3A7</i> )	Log <sub>10</sub> (2-OH ATV/ATV) = -0.264 + 0.112(Female) + 0.003(Age) + 0.075(P2Y <sub>12</sub> inhibitor) -0.178(CYP3A4 inhibitor) -0.136(Amiodarone) - 0.0001(Sample storage duration) + 0.0002(Time since last ATV) + 0.104(rs887829) + 0.156(rs45446698)	6.36x10 <sup>-36</sup>	28.6

Biologically plausible SNPs were entered into the main study cohort multivariable linear regression model for their relevant PK endpoint to determine the additional proportion of variation in log<sub>10</sub> transformed PK endpoint explained by the variant.

### 6.3.6 Sensitivity analyses of genetic association with PK endpoints

As shown in Figure 6.6, inclusion of all high ATV concentrations with no upper limit applied (n=631) led to a large reduction of significance of the *SLCO1B1* signal (from  $p=2.21 \times 10^{-6}$  to  $p=0.00013$  for ATV concentration). Given the prior knowledge linking *SLCO1B1* rs4149056 to ATV exposure (Pasanen *et al.*, 2007), this provides support that these high concentrations are likely due to temporal proximity to the last ATV dose rather than a genotype-mediated effect. Furthermore, the significance of univariate time since last ATV dose with, for example ATV concentration, reduced from  $p=1.14 \times 10^{-12}$  to  $p=1.03 \times 10^{-10}$  with inclusion of all high outlying ATV concentrations.

Exclusion of all participants with 2-OH ATV/ATV ratios outside two SDs of the mean for each rs887829 genotype (for both the non-transformed and transformed ratio) had minimal impact on rs887829 association signal ( $p=7.25 \times 10^{-16}$  to  $p=3.31 \times 10^{-14}$ ), indicating that the *UGT1A* signal is not attributable to an outlier effect.

**Figure 6.6 Sensitivity genome-wide association analysis that included all patients with high ATV concentrations**

This sensitivity genome-wide association analysis of  $\log_{10}$  transformed ATV concentration applied no ATV concentration upper limit ( $n=631$ ). It demonstrates loss of the chromosome 12 *SLC01B1* suggestive signal, in keeping with the hypothesis that the high measured ATV concentrations are more likely related to ATV dose timing than a genotype-mediated effect.

### 6.3.7 Impact of biologically plausible SNPs on clinical adverse events

870 patients were included in cohort 2: 118 and 752 were ATV intolerant and tolerant, respectively. Of those ATV intolerant by V2, 23 had discontinued statin therapy, 26 reduced their ATV dose, 22 switched statin to a lower equivalent dose, and 55 were non-adherent. Of these 55 non-adherent patients, 47 remained on their discharge ATV dose, and 8 had discontinued/reduced dose/switched statin. In the full PhACS cohort (n=1470), 16 patients spontaneously reported muscle symptoms whilst on a statin at V2. However, one was discharged on SVT and two did not meet genetic QC steps, leaving 13 on ATV for inclusion in cohort 2.

*SLCO1B1* rs4149056 was associated with muscular symptoms, particularly under a dominant model (p=0.016) (Table 6.9). Although rs4149056 was associated with any adverse event in multivariable regression, this was driven by muscular symptoms (i.e. p=0.42 with non-muscular adverse events). Importantly, rs4149056 was associated with ATV intolerance (Table 6.10). In further subgroup analysis, rs4149056 was associated with ATV dose reduction/statin switching but not ATV discontinuation/non-adherence (Table 6.10). As shown in Table 6.10, any adverse event (multivariable model 1) and muscular symptoms (multivariable model 2) were important clinical covariates associated with ATV intolerance. However, rs4149056 was not associated with MACE or ACM (Table 6.11). Neither rs887829 (*UGT1A*) nor rs45446698 (*CYP3A7*) were associated with any clinical endpoint.

### 6.3.8 Sensitivity analyses with clinical endpoints

In the sensitivity analysis restricted to patients discharged on 80mg ATV daily only (n=786), rs4149056 (*SLCO1B1*) remained associated with muscular symptoms (n=12 ATV myotoxicity cases, p=0.039) (Table 6.9) and with ATV intolerance in univariate (p=0.033) and multivariable analysis (Table 6.10).

**Table 6.9 Impact of biologically plausible identified SNPs on statin-attributable adverse events**

	Discharged on <i>any</i> ATV dose (n=870) <sup>1</sup>				Muscle symptoms (n=12) in those discharged on ATV 80mg (n=786) <sup>2</sup>	
	All adverse events (n=51)		Muscle symptoms (n=13)		OR (95% CI)	p-value
	OR (95% CI)	p-value	OR (95% CI)	p-value		
<b>Univariate</b>						
rs4149056 (additive) ( <i>SLCO1B1</i> )	1.47 (0.90-2.38)	0.12	2.32 (1.01-5.33)	0.048	2.16 (0.89-5.28)	0.090
rs4149056 (dominant) ( <i>SLCO1B1</i> )	1.76 (0.99-3.14)	0.055	3.97 (1.29-12.27)	0.016	3.40 (1.07-10.81)	0.039
rs887829 (additive) ( <i>UGT1A</i> )	0.95 (0.62-1.46)	0.83	0.45 (0.17-1.20)	0.11	0.51 (0.19-1.37)	0.18
rs887829 (dominant) ( <i>UGT1A</i> )	0.98 (0.56-1.74)	0.96	0.33 (0.10-1.07)	0.064 <sup>3</sup>	0.38 (0.11-1.28)	0.12
rs45446698 (additive) ( <i>5' of CYP3A7</i> )	0.79 (0.25-2.54)	0.70	1.06 (0.15-7.68)	0.96	1.11 (0.15-8.05)	0.92
<b>Multivariable</b>						
rs4149056 (dominant) ( <i>SLCO1B1</i> )	1.92 (1.04-3.54)	0.036	3.97 (1.29-12.27)	0.016	3.40 (1.07-10.81)	0.039
ACEI/ARB	4.41 (1.21-16.12)	0.025	-	-	-	-
Statin non-adherence (missed ≥1 pill in last week)	1.78 (1.39-2.25)	3.0x10 <sup>-6</sup>	-	-	-	-

Univariate logistic regression was used to assess the impact of biologically plausible SNPs on statin adverse events and muscle symptoms. SNPs were first tested using an additive model; any borderline significant associations were investigated further using a dominant model. SNPs with univariate  $p \leq 0.1$  were entered into multivariable logistic regression modelling alongside clinical covariates with univariate  $p \leq 0.1$ ; the final multivariable model was chosen by forwards likelihood ratio selection (significance defined as  $p < 0.05$ ). The analysis was restricted to patients discharged from index hospitalisation on: <sup>1</sup> = any dose of ATV (cohort 2, n=870); or <sup>2</sup> = only ATV 80mg daily (n=786) - with V2 statin status, prescription and adherence known, and quality controlled SNP information available. All clinical covariates were considered except blood sample characteristics (storage duration, and time since last ATV) and V2 ATV dose - the latter was replaced with index hospitalisation discharge ATV dose. <sup>3</sup> = this association had  $p \leq 0.1$ ; however, no variables were selected in multivariable analysis and so it is not shown.

**Table 6.10 Impact of biologically plausible identified SNPs on risk of ATV intolerance**

	Discharged on <i>any</i> ATV dose (n=870) <sup>1</sup>						ATV intolerance (n=106) in those discharged on ATV 80mg (n=786) <sup>2</sup>	
	ATV intolerance (n=118)		ATV discontinuation/non-adherence (n=75) <sup>3</sup>		ATV dose reduction/switch (adherent) (n=43) <sup>4</sup>		OR (95% CI)	p-value
	OR (95% CI)	p-value	OR (95% CI)	p-value	OR (95% CI)	p-value		
<b>Univariate</b>								
rs4149056 (additive)	1.44 (1.02-2.03)	0.036	1.27 (0.82-1.95)	0.28	1.76 (1.06-2.91)	0.028	1.48 (1.03-2.13)	0.033
rs887829 (additive)	0.98 (0.73-1.31)	0.89	-	-	-	-	1.01 (0.74-1.37)	0.97
rs45446698(additive)	0.80 (0.37-1.77)	0.59	-	-	-	-	0.73 (0.31-1.70)	0.46
<b>Multivariable 1.</b>								
rs4149056 (additive)	1.53 (1.07-2.18)	0.019	-	-	1.86 (1.12-3.10)	0.016	1.58 (1.09-2.31)	0.017
P2Y <sub>12</sub> inhibitor	0.50 (0.31-0.82)	0.006	-	-	0.34 (0.17-0.68)	0.002	0.42 (0.25-0.70)	0.001
Beta blocker	0.52 (0.33-0.83)	0.006	-	-	-	-	0.44 (0.27-0.74)	0.002
ACEI/ARB	-	-	-	-	-	-	-	-
Any AE at V2 attributed to statin	3.55 (1.89-6.67)	7.8x10 <sup>-5</sup>	-	-	-	-	4.05 (2.09-7.85)	3.6x10 <sup>-5</sup>
<b>Multivariable 2.</b>								
rs4149056 (additive)	1.52 (1.07-2.17)	0.019	-	-	1.83 (1.09-3.07)	0.022	1.59 (1.10-2.31)	0.015
P2Y <sub>12</sub> inhibitor	0.51 (0.32-0.83)	0.007	-	-	0.33 (0.16-0.66)	0.002	0.45 (0.27-0.74)	0.002
Beta blocker	0.50 (0.31-0.79)	0.003	-	-	-	-	0.43 (0.26-0.70)	0.001
ACEI/ARB	-	-	-	-	-	-	-	-
Myalgia at V2 on statin	4.56 (1.44-14.4)	0.010	-	-	7.10 (1.77-28.46)	0.006	3.76 (1.09-12.95)	0.036

Univariate logistic regression was used to assess the impact of biologically plausible SNPs on ATV intolerance. SNPs with univariate  $p \leq 0.1$  were entered into multivariable logistic regression modelling alongside clinical covariates with univariate  $p \leq 0.1$ ; the final multivariable model was chosen by forwards likelihood ratio selection (significance defined as  $p < 0.05$ ). The SNPs shown are the common missense variant in *SLCO1B1* (rs4149056, V174A), and the lead SNPs at the identified *CYP3A7* locus (rs45446698) and *UGT1A* locus (rs887829). The analysis was restricted to patients discharged from index hospitalisation on: <sup>1</sup> = any dose of ATV (cohort 2, n=870); or <sup>2</sup> = only ATV 80mg daily (n=786) - with V2 statin status, prescription and adherence known, and quality controlled SNP information available. Subgroup analysis was also conducted restricted to: <sup>3</sup> = ATV intolerant patients that discontinued ATV or were non-adherent at V2, and; <sup>4</sup> = ATV intolerant patients that reduced ATV dose or switched statin to another at lower equivalent dose but were statin adherent at V2. In the multivariable logistic regression analyses all clinical covariates were considered except blood sample characteristics (storage duration, and time since last ATV) and V2 ATV dose – the latter was replaced with index hospitalisation discharge ATV dose. In multivariable analysis 1, any adverse event attributed by the patient to their statin at V2 was also included. In multivariable analysis 2, muscular symptoms on statin therapy at V2 were also included.

**Table 6.11 Impact of biologically plausible identified SNPs on cardiovascular events and mortality**

	MACE (n=142 events)		ACM (n=93 events)	
	HR (95% CI)	p-value	HR (95% CI)	p-value
<b>Univariate</b>				
rs4149056 (additive) ( <i>SLCO1B1</i> )	1.08 (0.79-1.48)	0.64	1.29 (0.90-1.86)	0.17
rs887829 (additive) ( <i>UGT1A</i> )	1.04 (0.82-1.33)	0.74	1.25 (0.93-1.67)	0.14
rs45446698 (additive) ( <i>5' of CYP3A7</i> )	0.76 (0.38-1.53)	0.44	0.45 (0.15-1.42)	0.17

Univariate Cox proportional hazards regression was used to assess the impact of biologically plausible SNPs on time to MACE and time to ACM. The analysis was restricted to patients discharged from index admission on *any* dose of ATV with quality controlled SNP information available (cohort 3, n=1,081); median follow up from discharge was 17 months.

## 6.4 Discussion

This study constitutes the largest ATV PK study to date, included both ATV and acid and lactone metabolites, and is the first reported GWAS of ATV exposure. The main study findings are: confirmation of the roles of several clinical factors on exposure to ATV analytes, putative identification of new drug-ATV PK interactions involving PPIs, furosemide and clopidogrel, novel genome-wide significant associations involving the *UGT1A* locus, a suggestive association between *CYP3A7* and ATV hydroxylation, reaffirmation of the impact of *SLC01B1* rs4149056 on ATV and 2-OH ATV exposure, and demonstration of rs4149056 associated with muscular symptoms and ATV intolerance.

### 6.4.1 Clinical factor associations with PK endpoints

Increasing age was associated with higher concentrations of ATV analytes, in keeping with previous findings (Gibson *et al.*, 1996). Women had lower ATV and ATV L concentrations but increased 2-OH ATV/ATV and 2-OH ATV L/ATV L ratios, in keeping with the known ~2-fold increased CYP3A4 protein levels present in female compared to male livers (Zanger and Schwab, 2013). Higher BMI was associated with lower concentrations of all analytes and total, except for parent ATV. However, a previous sparse PK study limited to only parent ATV similarly found no association with BMI (DeGorter *et al.*, 2013). ATV L and 2-OH ATV L are both relatively lipophilic and therefore reduced plasma levels within increasing BMI were anticipated. The reason(s) for the lack of effect of BMI on ATV circulating levels is unclear, but possibly relates to the increased prevalence of fatty liver in obesity, which is associated with reduced CYP3A4 (Kolwankar *et al.*, 2007). This in turn may contribute to the reduced plasma levels of hydrophilic 2-OH ATV observed with increasing BMI, and offset the anticipated reduction in ATV levels at higher body masses. Furthermore, murine studies have shown that *Oatp1b2* mRNA and protein expression are reduced in simple fatty liver and NASH, respectively (Fisher *et al.*, 2009); *Oatp1b2* is the murine orthologue of OATP1B1 and OATP1B3, and so reduced OATP1B1 in obesity could increase ATV bioavailability and so further nullify any decrease in systemic ATV levels expected from higher body masses.

Diabetes was associated with a significantly lower ATV L/ATV ratio in this study. However, in a study of renal transplant recipients, ATV L concentrations were significantly higher in patients with diabetes mellitus, due to reduced clearance (Dostalek *et al.*, 2012). The reason(s) for this disparity are unknown, but differences in diabetes severity and anti-diabetic concurrent medications may be contributory. Less than 2% of ATV is excreted through the kidneys (Pfizer Inc, 2015), and therefore renal dysfunction had no impact on the concentration of any individual ATV analyte, metabolic ratio, or the analyte sum total (ATV + 2-OH ATV + ATV L + 2-OH ATV L) following multivariable adjustment. No conclusions can be made from these data regarding the influence of hepatic dysfunction as only five participants reported liver disease, although chronic alcoholic liver disease is known to markedly increase ATV and ATV acid metabolite levels (Pfizer Inc, 2015).

CYP3A4 drug inhibitors were associated with a higher ATV concentration and lower 2-OH ATV/ATV and 2-OH ATV L/ATV L ratios, which was expected as CYP3A4 is the major enzyme responsible for ATV and ATV L hydroxylation (Jacobsen *et al.*, 2000). Cases of ATV severe myotoxicity involving a possible interaction with a PPI (predominantly omeprazole) have been reported (Elazzazy *et al.*, 2012; Sipe *et al.*, 2003; Kanth *et al.*, 2013; Clark and Strandell, 2006; Marusic *et al.*, 2012) and myotoxicity is a possible PPI adverse class effect (Clark and Strandell, 2006). Furthermore, it has been suggested that PPIs may modestly boost statin-mediated LDL-C reduction (Barkas *et al.*, 2015). Nevertheless, to the best of knowledge, this is the first study demonstrating that PPIs (omeprazole/lansoprazole) increase the concentration of all four measured ATV analytes, including the myotoxic L metabolites. However, the mechanism is uncertain. Furthermore, neither omeprazole (Shah *et al.*, 2016) nor pantoprazole (Huguet *et al.*, 2016) altered RVT PK in healthy volunteers. Lansoprazole and omeprazole are substrates and inhibitors of CYP2C19 and CYP3A4 (Ko *et al.*, 1997; Shirasaka *et al.*, 2013), but CYP3A4-mediated inhibition would not account for the uniform increase in ATV analytes; possible

explanations include an increase in ATV bioavailability because of PPI-induced raised gastric pH, or inhibition of an elimination transporter such as P-gp.

The loop diuretic, furosemide, was surprisingly associated with increased concentrations of individual ATV analytes (ATV, ATV L, 2-OH ATV L) and the analyte sum total, which to the best of knowledge have not been reported previously. An *in vitro* evaluation of furosemide identified that it is a substrate of OAT1, OAT3, BCRP, OATP1B1 and OATP1B3, and importantly an inhibitor of BCRP (Ebner *et al.*, 2015). Interestingly, the exploratory stratification of patients according to *ABCG2* rs2231142 (Q141K) carrier status in this study supports the hypothesis that furosemide increases ATV bioavailability through BCRP inhibition.

The potential for ATV to reduce clopidogrel's antiplatelet inhibitory effects has been extensively studied because CYP3A4 is involved in the bioactivation of prodrug clopidogrel into its active 5-thiol metabolite (Trenk *et al.*, 2013), and ATV competes for CYP3A4. However, both *ex vivo* platelet aggregometry studies and clinical outcome studies investigating this PD interaction have had heterogeneous results (Bates *et al.*, 2011), perhaps influenced by clopidogrel loading dose (Bates *et al.*, 2011), the irreversible nature of clopidogrel P2Y<sub>12</sub> antagonism, and because ATV itself inhibits platelet activity (Xu *et al.*, 2016). Nevertheless, the influence of clopidogrel on ATV PK has been under-investigated. In this study, clopidogrel was associated with increased 2-OH ATV/ATV and 2-OH ATV L/ATV L ratios. This finding is surprising because clopidogrel is not a CYP3A4 inducer (Food and Drug Administration, 2016). CYP2C8 can metabolise ATV to 4-OH ATV, but not 2-OH ATV, to a minor extent (Jacobsen *et al.*, 2000). Clopidogrel is a strong CYP2C8 inhibitor (Food and Drug Administration, 2016) and so one hypothesis is that clopidogrel further shunts CYP3A-mediated ATV metabolism to 2-OH ATV (and 4-OH ATV) through CYP2C8 antagonism. Alternatively, both ATV (Pfizer Inc, 2015) and clopidogrel

(Ganesan *et al.*, 2013) are extensively protein-bound and so perhaps clopidogrel increases free ATV levels, leading to greater CYP-mediated hydroxylation.

It will be important to replicate these novel ATV interactions with PPIs, furosemide and clopidogrel, characterise the PK interactions further in rich PK studies, determine underlying mechanisms and delineate their clinical relevance.

#### **6.4.2 GWAS associations**

This study found that *SLCO1B1* rs4149056 (V174A) was suggestively associated with increased ATV and 2-OH ATV concentrations using GWAS methodology. Furthermore, rs4149056 was only nominally associated with ATV L and 2-OH ATV L levels in GWAS, indicating that the impact of the *OATP1B1* 174A missense variant is confined to statin acid analytes. Together, these results were interpreted as confirmation of the findings of previous healthy volunteer rich PK studies (Pasanen *et al.*, 2007; Pasanen *et al.*, 2006; Tornio *et al.*, 2015). It is thought that rs4149056 perturbs intrinsic *OATP1B1* substrate transport as opposed to altering membrane transporter expression (Nies *et al.*, 2013). When added to the ATV clinical model, rs4149056 increased the proportion of observed ATV levels explained by 3.3% to 20.2% (Table 6.8); whilst significant, almost 80% of variability in interindividual ATV levels thus remains unaccounted. Furthermore, the increase in explained ATV variation attributed here to rs4149056 is likely an overestimation of its effect on population ATV level variation because the same patient cohort was used for both SNP identification and SNP testing; this principle similarly applies to the other tested SNPs (rs45446698 and rs887829).

Importantly, *SLCO1B1* rs4149056 was significantly associated with an increased risk of muscular symptoms (OR 3.97, 95% CI 1.29-12.27,  $p=0.016$ ) and ATV intolerance, which was driven by the ATV dose reduction/statin switching subgroup (adjusted OR 1.86, 95% CI 1.12-3.10,  $p=0.016$ ). Previous studies have

not found rs4149056 to be associated with ATV clinical myotoxicity using 10 severe myopathy (Brunham *et al.*, 2012) or 11 myopathy (Carr *et al.*, 2013) ATV cases. Whilst a false positive result cannot be excluded given the low number of self-reported muscular symptom cases (n=13) in this study, the different myotoxicity phenotype employed and/or the high ATV doses (predominantly 80mg daily) of PhACS participants may contribute to this divergent finding. A previous smaller study found rs4149056 was associated with dose decreases or statin switches in patients prescribed ATV at >20mg daily (de Keyser *et al.*, 2014), and this present study supports these findings. Although the minor allele of rs4149056 is associated with a moderately smaller LDL-C reduction in response to statin therapy (Postmus *et al.*, 2014), no association was found here with MACE or ACM, although power was low to detect cardiovascular endpoints.

For the first time, a potential contribution of CYP3A7 in the metabolism of ATV in patients has been uncovered, with the lead variant, rs45446698, suggestively associated with increased 2-OH ATV/ATV ( $p=6.18 \times 10^{-7}$ ) and nominally associated with increased ATV, ATV L and 2-OH ATV L/ATV L. The human CYP3A subfamily consists of CYP3A4, 3A5, 3A7 and 3A43 located on chromosome 7q22.1 (Zanger and Schwab, 2013). CYP3A7 is the predominant CYP expressed in the foetus, accounting for 30-50% of foetal liver total CYP content (Shimada *et al.*, 1996). However on average, 85.4% of total microsomal CYP3A protein content in human adult livers is CYP3A4 and 3.4% ( $\leq 9.4\%$ ) is CYP3A7 (Zanger and Schwab, 2013). Nevertheless, human liver *CYP3A7* mRNA expression varies >700-fold (Burk *et al.*, 2002) and CYP3A7 liver protein increases with increasing adult age (Ohtsuki *et al.*, 2012). The *CYP3A7\*1C* allele, which includes rs45446698, results from 60bp of the *CYP3A7* promoter (-188 to -129, relative to the transcription start site) being replaced by the corresponding *CYP3A4* region. This results in seven bases differing between *CYP3A7* wild-type and *\*1C* alleles (Kuehl *et al.*, 2001), and high *CYP3A7* mRNA expression in both adult livers and intestine (Burk *et al.*, 2002). Two SNPs within *CYP3A7\*1C*, rs11568825 and rs11568826, modify the *CYP3A7* proximal promoter ER6 (everted repeat separated by 6 base pairs) motif to its *CYP3A4*

isoform leading to markedly stronger PXR/RXR heterodimer binding and activation compared to wild-type *CYP3A7* (Burk *et al.*, 2002); interestingly these SNPs were themselves suggestively associated with increased ATV hydroxylation (both  $p=6.82 \times 10^{-6}$ ). Similarly *\*1C* is associated with increased CAR-mediated activation (Burk *et al.*, 2002), which requires both the *CYP3A4-ER* motif isoform and especially variant rs11568824 ( $p=1.23 \times 10^{-5}$ ). Clinically, rs45446698 has been identified by GWAS to be associated with progesterone and dehydroepiandrosterone sulphate (DHEAS) levels (Ruth *et al.*, 2016). Furthermore, rs45446698 has been recently associated with breast cancer mortality, all-cause mortality in lung cancer patients and chronic lymphocytic leukaemia progression (Johnson *et al.*, 2016). These novel associations across a diverse range of cancers suggest an underlying common pharmacogenomic interaction, and indeed a borderline interaction ( $p=0.06$ ) between *CYP3A7\*1C* allele, treatment using a cytotoxic agent that is a CYP3A substrate, and adverse clinical outcomes, was identified (Johnson *et al.*, 2016). Currently, the clinical implications of altering the extent of ATV (L) hydroxylation are unknown, given that both parent ATV and its acid metabolites actively inhibit HMGCR, but L metabolites do not; rs45446698 was not associated with either total adverse events or muscular symptoms in this study. However, CYP3A plays a major role in the metabolism of ~30% of clinically used drugs (Zanger and Schwab, 2013) and rs45446698 has an appreciable MAF of ~4-5%. Therefore, further research is clearly required to define the clinical sequelae of enhanced *CYP3A7\*1C*-mediated drug metabolism across medical specialties. Lastly, *CYP3A7\*1C* is only present in half of adults with high *CYP3A7* mRNA expression, *CYP3A7\*1B* is also associated with increased hepatic, but not intestinal, adult *CYP3A7* expression (Burk *et al.*, 2002), and therefore the pharmacogenomic impact of *CYP3A7* likely extends beyond *\*1C*.

The principal genome-wide significant findings in this study were the associations between rs887829, within the *UGT1A* cluster, and both increased 2-OH ATV/ATV and 2-OH ATV L/ATV L ratios. In total, 89 strongly correlated

variants had p-values less than  $5.0 \times 10^{-8}$ , and conditional analysis for rs887829 led to total loss of signal.

SNP rs887829 is located 311bp upstream of the *UGT1A1* TATA box promoter (Cox *et al.*, 2013), which contains the indel polymorphism, rs8175347. Variant alleles of rs8175347 have different numbers of thymine-adenine repeats (TA)<sub>n</sub> within the *UGT1A1* TATA box; (TA)<sub>6</sub> is wild-type (\*1), (TA)<sub>5</sub> (\*36) is also considered fully functional, whilst (TA)<sub>7</sub> (\*28) and (TA)<sub>8</sub> (\*37) are reduced expression alleles (Dean, 2015). *UGT1A1*\*28 is common across a number of populations (e.g. MAF 0.26-0.31 in Caucasians), whilst *UGT1A1*\*36 and \*37 are found almost exclusively in populations of African origin (Dean, 2015). The rs887829 variant T allele is in strong LD with (TA)<sub>7</sub> in those of European ( $r^2 = 0.99$ ) (Namjou *et al.*, 2015) and Chinese ancestry ( $r^2 = 0.86$ ) (Zhou *et al.*, 2014). In 98.7% of cases in African populations, the ancestral C allele of rs887829 is found with (TA)<sub>5</sub> or (TA)<sub>6</sub>, and the variant T allele with (TA)<sub>7</sub> or (TA)<sub>8</sub> (Horsfall *et al.*, 2011). rs887829 has also been found to be in strong LD with rare (MAF < 1%) missense variants in the first exon of *UGT1A1* (rs4148323, rs144398951, rs35003977, rs57307513) by exome array (Oussalah *et al.*, 2015). *UGT1A1* can lactonize ATV (Schirris *et al.*, 2015b) and carrying *UGT1A1*\*28 has been associated with lower ATV L levels in a small CG study (Stormo *et al.*, 2013); therefore, it was surprising that rs887829 was associated with increased hydroxylation, and not differential lactonization. One possibility is reduced ATV lactonization leads to increased shunting of ATV to CYP3A-mediated hydroxylation, increasing the 2-OH ATV/ATV ratio. A uniform (reduced) rate of UGT-mediated lactonization of both 2-OH ATV and ATV would then elevate the 2-OH ATV L/ATV L ratio.

An alternative explanation is based on the observation that reduced function *UGT1A1*\*28 is known to be in strong LD with *UGT1A3*\*2 (Riedmaier *et al.*, 2010; Cho *et al.*, 2012). *UGT1A3* also lactonizes ATV (Schirris *et al.*, 2015b), and *UGT1A3*\*2 has been previously associated *ex vivo* with increased *UGT1A3* mRNA,

protein, and microsomal ATV lactonization (Riedmaier *et al.*, 2010). Furthermore, *UGT1A3\*2/\*2* homozygosity has been associated with modestly lower (but non-significant) ATV, and 65%, 72% and 160% higher AUCs of 2-OH ATV, ATV L and 2-OH ATV L, respectively. Although previous ATV studies understandably focussed on increased L/acid analyte ratios (Cho *et al.*, 2012; Riedmaier *et al.*, 2010), these findings also appear to be in keeping with the increased hydroxylation observed in this study. ATV L has a significantly higher affinity for CYP3A4 than ATV. Thus, CYP-dependent hydroxylation is 20-83-fold higher for ATV L than ATV, and ATV L is a strong inhibitor of ATV hydroxylation (Jacobsen *et al.*, 2000). Therefore, the increased hydroxylation ratios are perhaps attributable to elevated ATV L leading to preferential CYP-mediated ATV L hydroxylation. This could lead to the increased 2-OH ATV L/ATV L ratio, and a subsequent constant rate of hydrolysis would produce the increased 2-OH ATV/ATV ratio. Nevertheless, the rs887829 signal remained despite conditioning on the three *UGT1A3\*2* SNPs, suggesting that *UGT1A3\*2* does not fully account for the observed locus association. The *UGT1A* locus is complex and further functional studies will be needed to resolve the causal variant(s).

Functionally, *UGT1A3\*2* has been associated with reduced ATV LDL-C lowering efficacy (Cho *et al.*, 2012). Previous GWAS studies have also identified rs887829 to be strongly associated with increased total (Cox *et al.*, 2013; Namjou *et al.*, 2015; Chen *et al.*, 2012a; Oussalah *et al.*, 2015), unconjugated (Oussalah *et al.*, 2015) and conjugated (Oussalah *et al.*, 2015) serum bilirubin levels, cholelithiasis (Milton *et al.*, 2012), gallstone-related cholecystectomy (Oussalah *et al.*, 2015), and in patients with diabetes, an increased risk of ACM was identified (Cox *et al.*, 2013). However, rs887829 was not associated with MACE or ACM in this study, perhaps due to a lack of power to detect a signal or because both parent ATV and 2-OH ATV actively inhibit HMGCR. In terms of pharmacogenomics, *UGT1A1\*28* is itself associated with an increased risk of irinotecan toxicity (Dean, 2015) and an increased risk of hyperbilirubinaemia-related discontinuation in patients taking the *UGT1A1*-inhibiting antiretroviral, atazanavir (Gammal *et al.*, 2016).

Beyond rs4149056 (*SLCO1B1*), rs45446698 (*CYP3A7*) and the *UGT1A* locus, other putative loci were identified. Interestingly, the minor variant of rs62124643 (C>T) was suggestively associated with reduced ATV L concentrations ( $p=1.63 \times 10^{-7}$ ). Although no functional role was ascribed to this chromosome 19 gene-dense locus, rs62124643 is within 0.8Mb of *LILRB5*, which has been associated with elevated serum CK and LDH levels (Dube *et al.*, 2014; Kristjansson *et al.*, 2016) and statin intolerance/myalgia (Siddiqui *et al.*, 2017).

### 6.4.3 Study limitations

This study had two main and several minor limitations. First, although sample collection time was recorded, time of last ATV administration was not known. However, as most patients take ATV at night, daytime blood collection will occur long after  $C_{max}$  (1-2 hours post-dose (Pfizer Inc, 2015)) on the gently declining phase of the concentration-time PK curve, mitigating the impact of time. Thus, whilst estimating the time of last ATV dose as 22:00 for all patients will inevitably lead to some inaccuracy, the association between analyte levels and this estimated time was uniformly strong (e.g.  $p=4.20 \times 10^{-14}$  for the association between time since last dose and adjusted ATV level). Second, linear regression was implemented in preference of non-linear mixed effects modelling (NONMEM) to facilitate the GWAS analyses. However, NONMEM may be beneficial to further characterise the effects of identified factors on the PK profile of ATV analytes. It is also noted that the GWAS findings from the ATV, ATV L and 2-OH ATV/ATV analyses were preferentially focussed on. In depth analysis of the other GWAS results, as well as GWAS analyses conditioned on identified associations (e.g. rs4149056) may reveal further pharmacogenomic signatures. However, the sample size ( $n=590$ ) may preclude detection of additional statistically significant signals of small effect size. It is noteworthy that grapefruit juice is a moderate CYP3A inhibitor (Bailey *et al.*, 1998) and so influences ATV levels. However, grapefruit juice consumption was not recorded in the PhACS study. Similarly, it can never be guaranteed that all concomitant

medications taken were captured in the CRF. Lastly, as discussed in Chapter 2, verification of the patient reported muscle symptoms being due to statin pharmacological effects was not possible, and so other causes for these muscle symptoms, including other diagnoses (e.g. symptomatic vitamin D deficiency) and the nocebo effect, cannot be excluded.

#### **6.4.4 Conclusion**

ATV is one of the most commonly prescribed medications worldwide, and is metabolised to acid and L derivatives. This study uniquely conducted a clinical and GWAS interrogation of ATV analytes, identifying potential new ATV-drug interactions, confirmed the importance of *SLCO1B1* rs4149056 on ATV systemic exposure, and identified novel associations with both *CYP3A7\*1C* and the *UGT1A* locus. This study found that rs4149056 is associated with both on-statin muscular symptoms and ATV intolerance. Further research is required to determine the underlying *UGT1A* causal variant.

## Chapter 7 Discussion

This thesis was built on the premises that SAM occurrence can alter statin utilisation (Wei *et al.*, 2013), and increased systemic statin exposure increases the risk of SAM (Alfirevic *et al.*, 2014; Armitage, 2007; Davidson and Robinson, 2007). Therefore, the main aims were to: 1.) determine the impact of SAM on statin utilisation and the resultant cardiovascular consequences in a secondary prevention UK setting, and; 2.) identify novel clinical and genetic factors associated with altered statin PK, which may contribute to myotoxicity risk and other adverse outcomes. In summary, the main results of this thesis are:

- Recommended high potency statin therapy (principally ATV 80mg daily) for patients hospitalised with an NSTEMI-ACS becomes suboptimal due to prescribing/adherence decisions for a sizeable proportion within one month post discharge
- Suboptimal statin utilisation at one month following discharge for an NSTEMI-ACS is associated with increased subsequent risks of both MACE and ACM;
- All adverse events attributed by patients to ATV (Chapter 6), and specifically muscular symptoms (Chapters 2 and 6), have been associated with suboptimal statin therapy;
- Multiple clinical factors affect ATV and metabolite systemic levels, and novel DDIs between ATV and furosemide, PPIs and clopidogrel have been identified;
- The *UGT1A* locus has been newly associated with ATV hydroxylation at genome-wide significance (lead SNP, rs887829, associated with increased ATV hydroxylation, and ATV L hydroxylation, with p-values of  $p=7.25 \times 10^{-16}$  and  $p=3.95 \times 10^{-15}$ , respectively);
- A novel association between *CYP3A7\*1C* and increased ATV hydroxylation has been identified (lead SNP, rs45446698, was suggestively associated with increased ATV hydroxylation,  $p=6.18 \times 10^{-7}$ );

- *SLCO1B1* rs4149056 has been suggestively associated with increased ATV and 2-OH ATV concentrations (ATV  $p=2.21 \times 10^{-6}$ ) but not with levels of ATV Ls, consistent with previous healthy volunteer findings (Pasanen *et al.*, 2007; Pasanen *et al.*, 2006);
- The variant allele of *SLCO1B1* rs4149056 was associated with patient-reported muscular symptoms and ATV dose reduction/statin switching, but not MACE or ACM;
- ATV hydroxylation is reduced whilst lactonization appears modestly increased in HRN liver microsomes *in vitro*;
- Systemic exposures of RVT, ATV and ATV metabolites are all dramatically increased (c.10-fold) in HRN relative to WT mice *in vivo*, although *in vitro* microsomal incubations demonstrated that RVT undergoes little metabolism and ATV hydroxylation is significantly impaired in HRN livers;
- The expression of proteins involved in lipid and xenobiotic metabolism are extensively perturbed in HRN livers;
- Two LC-MS/MS assays have been developed and validated for identification and quantification of analytes from murine DBS (RVT, ATV, ATV metabolites) and human plasma (ATV, ATV metabolites, BSP, CLP-CA).

The principal purpose of statin therapy is to reduce MACE to improve quality and longevity of life. To maximise statin utility, two processes must be optimised:

1. The identification of patients likely to benefit from statin therapy
2. Statin utilisation in these patients

## 7.1 Patient identification

The first line role of high potency statin therapy (ATV 80mg daily) in secondary prevention is largely accepted. This is because of both the unequivocally high risk of recurrent MACE and ACM in this patient group (Turner *et al.*, 2017) and

because of the documented advantage of intensive over placebo and moderate statin therapy in reducing cardiovascular events seen in RCTs (Cannon *et al.*, 2004; Arca and Gaspardone, 2007; Waters *et al.*, 2001; Cholesterol Treatment Trialists, 2010). Statin therapy is also indicated in familial hypercholesterolaemia, due to the elevated life time risk of CVD (NICE, 2016b).

The main area of discourse is the use of statins in primary CVD prevention (Godlee, 2014), largely because of disagreements over their benefit-risk profile in lower cardiovascular risk patients. There is general approval for statin therapy in primary prevention for patients with an estimated  $\geq 20\%$  risk of CVD over the next 10 years. However in 2013, the American College of Cardiology/American Heart Association (ACC/AHA) taskforce published new guidelines recommending primary prevention statin therapy in individuals with no diabetes but a 10 year risk of atherosclerotic CVD of  $\geq 7.5\%$ , although statin therapy could reasonably be offered to those with a risk of 5-7.5% (Stone *et al.*, 2014). Similarly in 2014, NICE reduced the threshold for initiating statin therapy in primary prevention from a predicted 10-year risk of CVD of 20% to 10% (NICE, 2016a; NICE, 2014). This was estimated to increase the number of individuals eligible for a statin in England by up to 4.5 million (NICE, 2014) to  $\sim 10$ -12 million (Hawkes, 2017; Ueda *et al.*, 2017). Neither guideline recommended routine lipid monitoring and target lipid levels. This was based on evidence that increasing relative and absolute reductions in LDL-C are associated with an increasing reduction in cardiovascular events, with no threshold for loss of benefit identified (Grundy, 2016). This evidence was largely derived from CTT meta-analyses of individual participant data from statin RCTs in a wide range of patients (combined secondary and primary prevention) (Cholesterol Treatment Trialists, 2010) and when limited to individuals with low risk (e.g. 5-year CVD risk of  $< 10\%$ ) of vascular disease (Cholesterol Treatment Trialists, 2012). The updated Cochrane systematic review of primary prevention statin RCTs suggests that the numbers needed to treat (NNT) with a statin (compared to placebo) for five years is 96 (95% CI 64-

244) and 56 (95% CI 46-75) to prevent one all-cause death, and one combined fatal/non-fatal coronary event, respectively (Taylor *et al.*, 2013).

Therefore, it appears commendable to increase primary prevention statin eligibility. However, further risk stratification remains attractive to identify the asymptomatic individuals most likely to benefit from statin therapy. The current QRISK2 calculator is based on UK epidemiological data (Hippisley-Cox *et al.*, 2008). Multiple additional biomarkers have been associated with CVD, including genetic SNPs (The CARDIoGRAMplusC4D Consortium, 2013), circulating micro-RNAs (Romaine *et al.*, 2015), proteins (Ganz *et al.*, 2016), and radiographic findings (Nasir *et al.*, 2015). Most novel risk factors, however, have low ORs (e.g. 1.10-1.50) and do not significantly increase the C-statistic beyond QRISK2/Framingham risk scores. Nevertheless, a genetic risk score of 27 variants was associated with both incident CAD events and response to statin therapy; importantly, the NNT to prevent one CAD event over 10 years decreased from ~57-66 in the low genetic risk group to ~20-25 in the high genetic risk group (Mega *et al.*, 2015). However, germline genetic testing does not account for environmental exposures (e.g. diet). Interestingly, the MESA study has demonstrated that detecting a coronary artery calcium (CAC) score of 0 Agatston units reclassifies 44% of participants eligible for statin therapy according to the new ACC/AHA guidelines as no longer statin eligible (cardiovascular event rate 4.2 per 1,000 person-years) (Nasir *et al.*, 2015). However, CAC scoring requires computed tomography, which is of limited availability. Therefore, further research is required to amalgamate biomarkers and prospectively test their clinical utility and cost-effectiveness to optimise the identification of patients most likely to benefit from statin therapy.

## **7.2 Statin utilisation in statin eligible patients**

After identification of appropriate statin eligible individuals, optimisation of statin usage to realise cardiovascular benefits is vital. In the primary prevention statin RCTs, ~77% of participants were statin adherent (Taylor *et al.*, 2013). In

contrast, only ~50% of real world patients remain adherent to primary prevention statin therapy at one year (García-Gil *et al.*, 2016; McGinnis *et al.*, 2007). Importantly, statin adherence/discontinuation reduces treatment efficacy (Turner *et al.*, 2017) and can make statin therapy cost-ineffective for most patients, even with low cost generic statins (Aarnio *et al.*, 2015).

Drug adherence is multidimensional and is determined by interrelated patient factors, physician factors, and healthcare system-related factors (Casula *et al.*, 2012). Patient factors include the knowledge, attitudes, beliefs, perceptions, resources, treatment expectations and on-treatment experience (Casula *et al.*, 2012). Physician factors include poor patient-doctor relationships, complex drug regimens and inadequate explanations about the benefits and risks of a new medication (Maningat *et al.*, 2013). The direct economics of healthcare systems can impinge on adherence through reducing consultation length, seeing different physicians at each clinic attendance, and co-payment sizes. Measured patient-related factors appear to explain statin adherence to a greater extent than either physician factors or co-payments (Chan *et al.*, 2010). Interventions to improve statin adherence can be classified into different classes, including: patient education and information, (electronic) reminders, regimen simplification, cost coverage, and multifaceted approaches (Rash *et al.*, 2016). A systematic review found that these interventions generally had small positive effects on improving statin adherence, but the effect sizes were small and identified RCTs exhibited methodological weaknesses (Rash *et al.*, 2016). The investigation of pharmacogenomics on statin adherence is in its infancy. However interestingly, small studies that provided pharmacogenomic information for either *SLCO1B1* rs4149056 (Li *et al.*, 2014; Callier, 2017) in patients previously statin intolerant, or kinesin family member six (Charland *et al.*, 2014) in patients first commencing statin therapy, suggest that improved adherence may be an un-envisaged benefit of pharmacogenomics. Overall, further research into resource-economic strategies to bolster statin adherence are required.

Importantly, SAM is a major cause of statin discontinuation/non-adherence/switching (Wei *et al.*, 2013). This is mainly due to commonly reported muscular symptoms at the 'milder' end of the SAM spectrum. Rarely, SAM directly causes considerable patient harm by precipitating rhabdomyolysis, leading to hospitalisation. Therefore, to prevent harm the FDA have advised against prescribing SVT 80mg daily unless patients have been taking this dose for over one year without harm (Food and Drug Administration, 2011), and the summary of product characteristics recommend to avoid SVT 80mg in patients known to have the *SLCO1B1* CC genotype (Actavis UK Ltd, 2016). Furthermore, guidance has been published to mitigate against statin-drug interactions to reduce SAM (Wiggins *et al.*, 2016). Nevertheless, further research is required to understand, predict, diagnose and mitigate SAM to improve real world statin utility.

In this thesis, both ATV adverse events and specifically muscular symptoms were associated with ATV intolerance. Furthermore, *SLCO1B1* rs4149056 was associated with both ATV intolerance, driven by an increased risk of ATV dose reduction/switching, and with muscular complaints. Some previous studies have suggested (Voora *et al.*, 2009; de Keyser *et al.*, 2014; Bakar *et al.*, 2017) or reported (Puccetti *et al.*, 2010) an association between rs4149056 and ATV myotoxicity, whilst other studies found no association (Carr *et al.*, 2013; Brunham *et al.*, 2012; Santos *et al.*, 2012; Hubacek *et al.*, 2015). Interestingly, rs4149056 was previously associated with dose decreases or statin switches in participants on ATV  $\geq 20$ mg daily in the Rotterdam Study, although this finding was not confirmed in a meta-analysis (de Keyser *et al.*, 2014). This heterogeneity may stem from different doses of ATV being studied, the placebo effect influencing case selection (Tobert and Newman, 2016), and the low number of ATV myotoxicity cases included in the studies compared to SVT cases; indeed, given the low number of eligible PhACS self-reported ATV-associated myotoxicity cases (n=13, with 12 discharged on 80mg ATV), one cannot exclude the possibility that the positive association between rs4149056 and muscle symptoms on ATV identified in this thesis is a false positive.

Nevertheless, SAM is considered dose-related and this thesis investigated the association between rs4149056 and ATV 80mg, rather than low ATV doses.

*SLCO1B1* rs4149056 was associated with increased ATV concentrations, alongside ATV dose, time since last ATV dose, sex, age, and concurrent loop diuretic, proton pump inhibitor, amiodarone and other CYP3A4-inhibiting drugs. Nevertheless, only 20% of ATV concentration variability was explained by these clinical factors and rs4149056. The positive predictive value of rs4149056 for myopathy in patients on SVT 80mg daily for five years was 4%, although its negative predictive value was >99% (Stewart, 2013). The high negative predictive value suggests that rs4149056 may have clinical utility in patients at high risk of CVD to identify WT homozygotes who are more likely to be able to tolerate higher SVT doses. Secondly, testing for rs4149056 may be clinically relevant in patients treated with SVT 80mg daily and presenting with myopathy, because the absence of the rs4149056 minor C allele suggests that SVT is unlikely to be the cause of the myopathy. This genotype-informed 'rule out' approach may improve statin adherence and lipid levels (Callier, 2017).

The low positive predictive value of rs4149056 indicates that the test cannot be used in isolation to predict incident myopathy in patient's starting SVT, or to distinguish between statin-induced myotoxicity and other aetiologies of muscle pathology (e.g. viral, metabolic etc.) in patients on statin therapy presenting with muscular symptoms. Further studies will need to integrate *SLCO1B1* rs4149056 with *LILRB5* rs12975366 (Siddiqui *et al.*, 2017) to improve prognostication. However, it remains unlikely that these two SNPs alone will be sufficient. Indeed, n-of-1 trials of patients with previous SAM have demonstrated that muscular symptoms attributable to statin therapy only occur in approximately one third of SAM patients, highlighting the difficulties of determining myotoxicity aetiology in routine clinical practice (Taylor *et al.*, 2015; Nissen *et al.*, 2016). Therefore, an n-of-1 approach will be crucial to improve prospective SAM phenotype specificity and facilitate identification of

novel biomarkers specific to statin-induced myotoxicity. To that end, an n-of-1 trial is currently recruiting 200 participants with previous SAM; each participant will receive ATV 20mg or identical placebo daily for six alternating two-month treatment periods (ClinicalTrials.gov, 2017).

To systematically identify novel biomarkers, interrogation of multiple 'omics' levels using a systems pharmacology approach may be beneficial (Turner *et al.*, 2015). For example, statin-potentiated muscle injury during exercise is accompanied with augmented extracellular release of the muscle specific microRNA, c-miR-499-5p, which is not released by statin exposure or muscle contraction alone (Min *et al.*, 2016). It is hoped that assimilation of n-of-1 trial and systems pharmacology methodologies will lead to the identification and integration of additional factors beyond rs4149056 associated with the different SAM phenotypes, which will enable myotoxicity due to statin medication to be adequately predicted and/or diagnosed for clinical utility. Furthermore, PCSK9 inhibitors are now being studied for their use in patients with statin intolerance (Nissen *et al.*, 2016). Therefore, biomarker-assisted patient stratification into statin- and non-statin-mediated myotoxicity groups will help not just individual patient management but may improve the cost effectiveness of hypolipidaemic management.

### **7.3 Novel genetic associations**

#### **7.3.1 UGT1A locus**

In this thesis, the UGT1A locus was strongly associated by GWAS with increased 2-OH ATV/ATV (rs887829  $p=7.25 \times 10^{-16}$ ) and 2-OH ATV L/ATV L (rs887829  $p=3.95 \times 10^{-15}$ ) hydroxylation ratios; 89 and 99 SNPs were associated with each ratio at  $p < 5.0 \times 10^{-8}$ , respectively. Conditioning for the lead SNP, rs887829, led to total loss of signal, suggesting the association identified is a single signal. Two studies previously reported that hyperfunctional *UGT1A3\*2* is associated with increased ATV lactonization (Riedmaier *et al.*, 2010; Cho *et al.*, 2012), and one study found hypofunctional *UGT1A1\*28* is associated with reduced ATV

lactonization (Stormo *et al.*, 2013). The work herein is thus the first to describe *UGT* variation associated with differential ATV *hydroxylation*. Interestingly, from the tabulated AUC data in Cho *et al.*, carrying increasing numbers of *UGT1A3\*2* variants appeared to be associated with increased ATV (L) hydroxylation (Cho *et al.*, 2012), although this was not supported by the results from Riedmaier *et al.* (2010), and insufficient data were reported in Stormo *et al.* (2013) to make any inference.

The *UGT1A* locus is complex; rs887829 is strongly associated with *UGT1A1\*28*, and moderately associated with *UGT1A3\*2* (Chapter 6). Further investigation is required to determine the causal variant(s) to provide a mechanistic explanation for the observed hydroxylation. This could include genotyping *UGT1A1\*28* in the PhACS cohort, and working with groups that have access to human liver banks. A future experiment could study ATV hydroxylation *in vitro* using human liver microsomes activated with NADPH, UDPGA, and NADPH plus UDPGA together, alongside sequencing the samples for *UGT1A1* and *UGT1A3*. My hypothesis remains that the causal *UGT1A* variant(s) leads to reduced ATV lactonization, predisposing to increased hydroxylation, but this needs testing.

The lead variant, rs887829, has previously been associated with increased total, unconjugated and conjugated serum bilirubin levels (Oussalah *et al.*, 2015), cholelithiasis (Milton *et al.*, 2012), gallstone-related cholecystectomy (Oussalah *et al.*, 2015), reduced risk of CAD in a Han Chinese population (Lin *et al.*, 2009), and increased ACM in European Americans with diabetes (Cox *et al.*, 2013). *UGT1A1\*28* is associated with Gilbert's syndrome (*\*28/\*28*) (Gil and Sasiadek, 2012), irinotecan toxicity (Dean, 2015) and potentially increased breast cancer risk in Caucasians (Yao *et al.*, 2010); exonic variants in *UGT1A1* are associated with Crigler-Najjar type I and type II syndromes (Gil and Sasiadek, 2012). However in this study, rs887829 was not associated with all ATV adverse events, muscular symptoms, ATV intolerance, MACE or ACM. This lack of clinical association is perhaps not surprising, given that both 2-OH ATV and ATV

are active inhibitors of HMGCR (Pfizer Inc, 2015), and Ls are considered more myotoxic (Skottheim *et al.*, 2008; Hermann *et al.*, 2006). Nevertheless, the relative myotoxicity of ATV L versus 2-OH ATV L is not established. Furthermore, rs887829 may be clinically relevant for other UGT1A-metabolised drugs, such as ezetimibe, raltegravir, raloxifene, mycophenolic acid, ketoprofen and irinotecan (Zhang, 2009); therefore it will be important to functionally understand this novel pharmacogenomic association and assess its impact on the efficacy and ADRs of other drugs.

### 7.3.2 CYP3A7 locus

For the first time, *CYP3A7* has been implicated in ATV metabolism in this thesis. Specifically, rs45446698 was suggestively associated with increased hydroxylation of ATV ( $p=6.18 \times 10^{-7}$ ) and ATV L ( $p=2.91 \times 10^{-5}$ ). SNP rs45446698 is one of seven SNPs in strong LD with one another within the *CYP3A7* proximal promoter region and collectively constitute *CYP3A7\*1C*. *CYP3A7\*1B* and *CYP3A7\*1D* are two other recognised *CYP3A7* promoter region haplotypes (Burk *et al.*, 2002; Kuehl *et al.*, 2001).

*CYP3A7* is the predominant CYP in human foetal liver, accounting for 30-50% of total CYP (Shimada *et al.*, 1996; Pang *et al.*, 2012) and 87-100% of total CYP3A in foetal hepatic tissue (Stevens *et al.*, 2003; Pang *et al.*, 2012). *CYP3A7* had been considered a foetus-specific CYP (Sim *et al.*, 2005). However, *CYP3A7* mRNA expression varies 333 to >700-fold in human adult livers, with a distinct subgroup of 11-15% of livers with high *CYP3A7* expression (Burk *et al.*, 2002; Koch *et al.*, 2002). For comparison, *CYP3A4* interindividual hepatic mRNA expression varies 118 to 224-fold (Koch *et al.*, 2002; Burk *et al.*, 2002). Furthermore, significant levels of *CYP3A7* protein were found in ~10% of 59 human adult livers, contributing 9-36% of total CYP3A in these livers (Sim *et al.*, 2005). In Europeans, average *CYP3A7* mRNA levels (Koch *et al.*, 2002) and protein levels (Sim *et al.*, 2005; Westlind-Johnsson *et al.*, 2003) are marginally higher than for *CYP3A5*. Importantly, *CYP3A7\*1C* has been associated with

significantly higher hepatic and intestinal *CYP3A7* expression, and *CYP3A7\*1B* with higher hepatic expression (Burk *et al.*, 2002). *CYP3A7\*1C* represents a 60bp substitution within the *CYP3A7* promoter region to the corresponding *CYP3A4* region. Unlike *CYP3A4*, *CYP3A7* is expressed in additional foetal and adult tissues, including the adrenal gland and prostate (Koch *et al.*, 2002). Interestingly, rs45446698 is associated with increased *CYP3A7* expression in adrenal tissue in the GTEx dataset (The GTEx Consortium, 2013); therefore, it is possible that *CYP3A7\*1C* leads to appreciable adult *CYP3A7* expression in tissues beyond the gut and liver.

*CYP3A4* contributes to the metabolism of ~50% of clinically used drugs (Guengerich, 1999), and *CYP3A7* shares nearly 90% of sequence homology with *CYP3A4* (Pang *et al.*, 2012). *CYP3A7* has high catalytic activity for endogenous steroids, estrone and retinoic acid (Pang *et al.*, 2012; Lee *et al.*, 2003), and *CYP3A7\*1C* has been associated with reduced serum levels of dehydroepiandrosterone sulphate (DHEAS) and testosterone (Goodarzi *et al.*, 2008). An *in vitro* study found *CYP3A7* had reduced metabolic activity to specific *CYP3A4* substrates at equimolar recombinant CYP concentrations compared to *CYP3A4*, although this was limited to 10 substrates (Williams *et al.*, 2002). Importantly, rs45446698 has been associated with adverse outcomes across a range of cancers and a borderline interaction between *CYP3A7\*1C*, *CYP3A*-substrate chemotherapy and outcome was observed (Johnson *et al.*, 2016).

Overall, it will be important to confirm the observed association with ATV hydroxylation in an independent cohort, such as an existing rich ATV PK healthy volunteer dataset. Similarly to rs887829, increased ATV hydroxylation is of unknown clinical significance. However, the range of *CYP3A* substrate drugs suggests that *CYP3A7\*1C* may be an underappreciated pharmacogenomic variant that might reduce drug efficacy across a range of therapeutic areas including organ transplantation (e.g. tacrolimus), cancer (e.g. docetaxel,

erlotinib, vemurafenib, vincristine) and infectious diseases (e.g. clarithromycin, itraconazole, protease inhibitors). *CYP3A7\*1C* may also further complicate drug-drug CYP3A PK interactions. For example, one therapeutic strategy within highly active antiretroviral therapy is to use low dose ritonavir to inhibit CYP3A in order to boost the activity of another protease inhibitor. Ritonavir inhibits CYP3A4, but 3A7 to a lesser extent; therefore the benefit of ritonavir may be attenuated in *CYP3A7\*1C* carriers (Granfors *et al.*, 2006).

#### 7.4 P450 oxidoreductase

The HRN *in vitro* hepatic microsome incubations demonstrate that complete *Por* deficiency is associated with markedly reduced ATV hydroxylation, and modestly increased lactonization. Consistent with these *in vitro* results, the murine *in vivo* PK study found that HRN mice have increased systemic levels of parent ATV and ATV Ls. However, the HRN mice also had unexpectedly elevated levels of hydroxylated ATV metabolites, and RVT, which undergoes little metabolism. The cause(s) of these *in vivo* findings is not clear but plausibly multifactorial; possibilities include underlying hepatic dysfunction resulting from the marked HRN liver steatosis, downregulation of hepatic xenotransporters (except *Oatp1a4*), and compensatory increases in intestinal Cyp expression. To investigate the *in vivo* results further, it would be reasonable to repeat the experiment, but administering ATV and RVT to separate mice in a larger study (e.g. n=4 per strain per statin) with analyte quantification by DBS with additional LC-MS/MS analyte quantification using a plasma sample from the last time point (eight hours post dose). In HRN mice of different ages, both serum liver function tests and the histology of drug unexposed livers examined for sinusoid numbers per microscopic field, could be investigated. It would be beneficial to repeat the study in mice with conditional hepatic and intestinal *Por* deletion that do not develop hepatic steatosis (Finn *et al.*, 2007), to further tease apart the reported *in vivo* findings.

The ATV PK GWAS results from the PhACS study suggest that common *POR* variants (MAF>1%) do not significantly impact ATV analyte levels or metabolic ratios. This is in contrast to, for example, the reported association between *POR\*28* (A503V) and lower tacrolimus exposure (Elens *et al.*, 2014; Gijzen *et al.*, 2014). Furthermore, we have investigated the impact of rare variants (individual SNP MAF<1%) on ATV PK within the PhACS cohort. The included rare variants were the 'exm' variants on the Illumina HumanOmniExpressExome-8 v1.0 BeadChip and the genotypes of the low frequency variants was called using the zCall algorithm (Goldstein *et al.*, 2012). The variants were combined in 'gene units' to determine each participant's rare variant burden per gene and analysed for association with the  $\log_{10}(\text{ATV})$  PK endpoint. Similar to the GWAS findings, no association between *POR* and ATV exposure was found (unpublished data). However, this approach was limited to the exm variants on the chip and the sample size (n=590).

Nevertheless, the essential role of *POR* in CYP-mediated catalysis suggests that *POR* dysfunction could perturb drug PK. Indeed, the only human rich PK (micro-dosing) study to date found that autosomal recessive *POR* deficiency is associated with subnormal drug metabolising activity of multiple CYPs (Tomalik-Scharte *et al.*, 2010). Therefore, it may just be that rare deleterious missense variants, such as rs121912974 (A287P, European MAF ~0.05%) or rs56256515 (L577P, European MAF ~0.1%) (Yates *et al.*, 2016) are relevant to drug PK, even in heterozygotes, but are too rare for investigating in a non-selected conventional study populations. Therefore, endeavours such as the FUTURE Initiative (Pirmohamed *et al.*, 2017), which is recruiting 3,000 healthy participants to undergo exome analysis and are willing to be contacted for future genotype-guided rich PK studies, will be invaluable to define the role of rare *POR* variation in drug PK. Furthermore, the large size and whole-genome sequencing approach of the UK-wide 100,000 Genomes Project (Marx, 2015) will be valuable for assessing if *POR* rare variants are collectively associated with specific type A (excessive exposure-related) ADRs.

## 7.5 Conclusion

In conclusion, this thesis has explored statin utilisation and the PK of ATV and RVT. It has confirmed known and identified novel clinical and genetic factors associated with altered ATV PK, shown that *SLCO1B1* rs4149056 carriage is a risk factor for muscular symptoms and ATV intolerance, and demonstrated that suboptimal statin utilisation following an NSTEMI-ACS is associated with poorer cardiovascular outcomes. As statin prescriptions and co-medications continue to increase upon a backdrop of increasingly tight healthcare resource constraints, it will become increasingly important to maximise benefits from statins, whilst minimising patient harm. It is envisaged that pharmacogenomics may have a role in promoting adherence and reducing SAM. However, this is unlikely to be as an isolated companion diagnostic. Rather, it is anticipated that a pre-emptive multi-SNP/sequencing approach integrated with patient electronic medical records will facilitate genotype-informed prescribing for multiple drugs (van der Wouden *et al.*, 2017), reduce test costs, and improve overall drug outcomes. It is an exciting time, although much remains to be done.

## Chapter 8 Appendix

This appendix contains:

- Table 8.1, which tabulates the clinical factors associated with altered statin PK (relating to the Introduction)
- Table 8.2 and Table 8.3, which summarise the spiking regimens used to prepare the calibration lines and quality controls, respectively, for the DBS LC-MS/MS assay (Chapter 3)
- Table 8.4, which is a table of proteins and their expression fold changes in HRN compared to WT mice liver homogenates that were statistically significant after correction for multiple testing (Chapter 4)
- Table 8.7 and Table 8.8, which detail the univariate linear regression analysis results for the association between each clinical covariate and all ATV PK endpoints in the main study cohort (n=590) (Chapter 6)
- Figure 8.1, which shows the Manhattan plots from the genome-wide association analyses of: 2-OH ATV, 2-OH ATV L, the total sum of all four ATV analytes, and the ratio of ATV L/ATV (Chapter 6)
- Figure 8.2 and Figure 8.3, which show the regional locus plots from the genome-wide association analyses of ATV and ATV L for the main suggestively associated signals ( $p < 1.0 \times 10^{-5}$ ), respectively (Chapter 6)
- Figure 8.4, which includes regional locus plots that demonstrate that there was no discernible association between variants in the *POR* region and either ATV or 2-OH ATV/ATV (Chapter 6)
- Table 8.9, which details all loci that had functional effects identified *in silico* and were associated with atorvastatin analytes (Chapter 6)
- Figure 8.5, which highlights the effect of *UGT1A3* haplotypes on ATV hydroxylation (Chapter 6)
- Table 8.10, which summarises the results for the effects of the three biologically plausible identified SNPs (rs4149056 in *SLCO1B1*, rs887829 in *UGT1A*, and rs45446698 near *CYP3A7*) and the *UGT1A3*\*2 haplotype on all ATV PK endpoints (Chapter 6).

**Table 8.1 Clinical factors associated with altered statin pharmacokinetics (Introduction)**

Factor	Statin	Effect	Reference
<b>Clinical</b>			
Advanced age	ATV, LVT, PIT, PVT, SVT,	-Increased AUC: <b>ATV</b> (30%), <b>PIT</b> (30%), <b>PVT</b> (~37%) -Increased mean plasma level of HMG-CoA reductase inhibitory activity: <b>LVT</b> (45%), <b>SVT</b> (45%)	(Pfizer Inc, 2015; Merck & Co, 2014; Kowa Pharmaceuticals, 2012; Bristol-Myers Squibb Company, 2013; Merck & Co, 2015)
	FVT, RVT	No significant difference	(Novartis, 2012; AstraZeneca, 2010)
Gender	ATV	Women: 20% higher <b>ATV</b> C <sub>max</sub> , 10% lower AUC	(Pfizer Inc, 2015)
	FVT, PIT	Women: increased <b>FVT</b> or <b>PIT</b> AUC	(RxList, 2016; Novartis, 2012)
	PVT	Women: increased <b>PVT</b> AUC (in subjects homozygous wild type at <i>SLCO1B1</i> rs4149056)	(Niemi <i>et al.</i> , 2006b)
	RVT	No significant difference	(AstraZeneca, 2010; Zhou <i>et al.</i> , 2013c)
	SVT	- <b>SVT acid</b> : increased exposure in women - SVT: no significant difference	(Yang <i>et al.</i> , 2014)
Dose	ATV, FVT, LVT, PIT, PVT, RVT, SVT,	Increased statin plasma exposure	(AstraZeneca, 2010; Pfizer Inc, 2015; Novartis, 2012; Merck & Co, 2014; Bristol-Myers Squibb Company, 2013; Kowa Pharmaceuticals, 2012; Merck & Co, 2015)
Evening compared to morning dosing	ATV, PVT	- <b>ATV</b> AUC decreased by 29% - <b>PVT</b> bioavailability decreased by 60%	(Pfizer Inc, 2015; Bristol-Myers Squibb Company, 2013; Cilla <i>et al.</i> , 1996)
	PIT, RVT	No significant difference in AUC	(Kowa Pharmaceuticals, 2012; AstraZeneca, 2010; Martin <i>et al.</i> , 2002)
<b>Ethnicity (compared to Caucasian)</b>			
African American	PVT	1.4 fold increased <b>PVT</b> AUC	(Ho <i>et al.</i> , 2007)
Asian	ATV	No significant difference in ATV AUC	(Gandelman <i>et al.</i> , 2012)
Asian-Indian	RVT	26% non-significant increase in RVT AUC	(Birmingham <i>et al.</i> , 2015)
East Asian	RVT	64-84% increased <b>RVT</b> AUC	(Birmingham <i>et al.</i> , 2015)
Japanese	SVT, PIT	- 68% increased exposure to <b>SVT acid</b> - no significant difference for PIT	(Tsamandouras <i>et al.</i> , 2014; Kowa Pharmaceuticals, 2012)
Mexican	PVT	No significant difference in AUC	(Escobar <i>et al.</i> , 2005)

<i>Table continued</i>			
<b>Factor</b>	<b>Statin</b>	<b>Effect</b>	<b>Reference</b>
Alcohol	FVT	- 30% increased <b>FVT</b> AUC in chronic alcohol consumption - no significant difference in FVT AUC in acute alcohol consumption:	(Scripture and Pieper, 2001)
Co-administration with food	LVT	~50% increased <b>LVT</b> AUC	(Merck & Co, 2014)
	PVT	Decreased <b>PVT</b> C <sub>max</sub> (by 49%) and AUC (by 31%)	(Pan <i>et al.</i> , 1993)
	ATV, FVT, PIT	- Significant decrease in C <sub>max</sub> ( <b>ATV</b> by 47.9%, <b>FVT</b> by 40-60%, <b>PIT</b> by 43%) - Non-significant decrease in AUC ( <b>ATV</b> 9-13%, <b>FVT</b> by 11%)	(Radulovic <i>et al.</i> , 1995; Kowa Pharmaceuticals, 2012; Novartis, 2012; Smith <i>et al.</i> , 1993)
	RVT, SVT	No significant difference in AUC	(AstraZeneca, 2010; Merck & Co, 2015)
Diabetes mellitus	ATV	Increased plasma concentrations of ATV and metabolites when sampled >5-24 hours post dose	(Dostalek <i>et al.</i> , 2012)
Hepatic impairment	ATV, FVT, PIT, PVT	Increased AUC: <b>ATV</b> (4-11 fold), <b>FVT</b> (2.5 fold), <b>PIT</b> (1.6-3.8 fold) <b>PVT</b> (34%)	(Pfizer Inc, 2015; Novartis, 2012; Kowa Pharmaceuticals, 2012; Hatanaka, 2000)
	RVT	No significant difference	(Simonson <i>et al.</i> , 2003)
Renal impairment	LVT, PIT, PVT, RVT	Increased AUC: <b>LVT</b> (2 fold), <b>PIT</b> (2 fold), <b>PVT</b> (69%), <b>RVT</b> (3 fold)	(AstraZeneca, 2010; Merck & Co, 2014; Kowa Pharmaceuticals, 2012; Bristol-Myers Squibb Company, 2013)
	ATV, FVT	No significant difference	(Pfizer Inc, 2015; Appel-Dingemanse <i>et al.</i> , 2002)
	SVT	Potentially no difference	(Launay-Vacher <i>et al.</i> , 2005)
Following bariatric surgery	ATV	- 2 fold increased <b>ATV</b> AUC 3-8 weeks after surgery -Decreased <b>ATV</b> AUC ~2 years after surgery	(Jakobsen <i>et al.</i> , 2013)
<b>Selected co-medications</b>			
<u>Strong CYP3A4 inhibitors</u>			
Itraconazole	ATV, LVT, PVT, RVT, SVT	Increased AUC: <b>ATV</b> (3.3 fold), <b>LVT</b> (>15-20 fold), <b>LVT acid</b> (15-20 fold), <b>PVT</b> (11-72%), <b>RVT</b> (28-39%), <b>SVT</b> (10 fold), <b>SVT acid</b> (19 fold)	(Cooper <i>et al.</i> , 2003c; Neuvonen and Jalava, 1996; Pfizer Inc, 2015; Neuvonen <i>et al.</i> , 1998; Mazzu <i>et al.</i> , 2000; Bristol-Myers Squibb Company, 2013; Kivisto <i>et al.</i> , 1998)
	PIT	<b>PIT</b> AUC decreased by 23%	(Nakagawa <i>et al.</i> , 2013)
	FVT	No significant difference	(Kivisto <i>et al.</i> , 1998)

<i>Table continued</i>			
<b>Factor</b>	<b>Statin</b>	<b>Effect</b>	<b>Reference</b>
Ketoconazole	RVT	No significant difference	(Cooper <i>et al.</i> , 2003b)
Clarithromycin	ATV, PVT, SVT	Increased AUC: <b>ATV</b> (4.4. fold), <b>PVT</b> (2.1 fold), <b>SVT</b> (10 fold), <b>SVT acid</b> (12 fold)	(Jacobson, 2004; Pfizer Inc, 2015; Bristol-Myers Squibb Company, 2013)
<u>Moderate CYP3A4 inhibitors</u>			
Erythromycin	ATV, PIT, SVT	Increased AUC: <b>ATV</b> (33%), <b>PIT</b> (2.8 fold), <b>SVT</b> (6.2 fold), <b>SVT acid</b> (3.9 fold)	(Kantola <i>et al.</i> , 1998; Pfizer Inc, 2015; Kowa Pharmaceuticals, 2012; Siedlik <i>et al.</i> , 1999)
	RVT	<b>RVT</b> AUC decreased by 20%	(Cooper <i>et al.</i> , 2003a)
	FVT	No significant difference	(Scripture and Pieper, 2001)
Grapefruit juice (low dose)	ATV, LVT, PIT, SVT	Increased AUC: <b>ATV</b> (40-83%), <b>LVT</b> (1.94 fold), <b>PIT</b> (14%), <b>SVT</b> (1.9-3.6 fold), <b>SVT acid</b> (1.3-3.3 fold)	(Merck & Co, 2015; Ando <i>et al.</i> , 2005; Fukazawa <i>et al.</i> , 2004; Lilja <i>et al.</i> , 2004; Rogers <i>et al.</i> , 1999; Hu <i>et al.</i> , 2013)
	PVT	No significant difference	(Fukazawa <i>et al.</i> , 2004)
Diltiazem	ATV, LVT, SVT	Increased AUC: <b>ATV</b> (51%), <b>LVT</b> (3.57 fold), <b>SVT</b> (3.10-4.6 fold), <b>SVT acid</b> (2.69 fold)	(Pfizer Inc, 2015; Merck & Co, 2014; Merck & Co, 2015)
	PIT	10% increased PIT AUC, but statistical significance unknown	(Kowa Pharmaceuticals, 2012)
	PVT	No significant difference	(Bristol-Myers Squibb Company, 2013)
<u>Weak CYP3A4 inhibitors</u>			
Amlodipine	ATV, SVT	Increased AUC: <b>ATV</b> (18%), <b>SVT</b> (1.77 fold), <b>SVT acid</b> (1.58 fold)	(Merck & Co, 2015; Drugs.com, 2016)
	FVT	No significant different	(Prasad <i>et al.</i> , 2004)
<u>Other drugs</u>			
Ciclosporin	ATV, FVT, LVT, PIT, PVT, RVT, SVT	Increased AUC: <b>ATV</b> (8.7 fold), <b>FVT</b> (90%), <b>LVT</b> (5-8 fold), <b>PIT</b> (4.6 fold), <b>PVT</b> (3.8 fold), <b>RVT</b> (7 fold), <b>SVT</b> (8 fold)	(Ichimaru <i>et al.</i> , 2001; Pfizer Inc, 2015; Novartis, 2012; Merck & Co, 2014; Kowa Pharmaceuticals, 2012; Bristol-Myers Squibb Company, 2013; AstraZeneca, 2010; Merck & Co, 2015)
Fluconazole	FVT	84% increased <b>FVT</b> AUC	(Kantola <i>et al.</i> , 2000)
	PVT, RVT	No significant difference	(Cooper <i>et al.</i> , 2002; Kantola <i>et al.</i> , 2000)

<i>Table continued</i>			
<b>Factor</b>	<b>Statin</b>	<b>Effect</b>	<b>Reference</b>
Gemfibrozil	ATV, LVT acid, PIT, PVT, RVT, SVT	Increased AUC: <b>ATV</b> (35%), <b>LVT acid</b> (2.8 fold), LVT (no significant difference), <b>PIT</b> (45%), <b>PVT</b> (2 fold), <b>RVT</b> (1.9 fold), <b>SVT</b> (1.35 fold), <b>SVT acid</b> (2.85 fold)	(Kyrklund <i>et al.</i> , 2003; Whitfield <i>et al.</i> , 2011; Matthew <i>et al.</i> , 2004; Schneck <i>et al.</i> , 2004; Backman <i>et al.</i> , 2000; Kyrklund <i>et al.</i> , 2001)
	FVT	No significant difference	(Spence <i>et al.</i> , 1995; Kyrklund <i>et al.</i> , 2001)
Rifampicin	ATV	- 7 fold increased <b>ATV</b> AUC if single rifampicin dose co-administered with a single ATV dose - 30% increased <b>ATV</b> AUC if ATV/rifampicin co-administered after a 5 day course of rifampicin - <b>ATV</b> AUC decreased by 80% if ATV given separately after a 5 day course of rifampicin	(Pfizer Inc, 2015; Backman <i>et al.</i> , 2005; Rhoda Lee <i>et al.</i> , 2012)
	PIT	6.7 fold increased <b>PIT</b> AUC if single rifampicin dose co-administered with a single PIT dose	(Chen <i>et al.</i> , 2013)
	PVT	- 2.3 fold increased <b>PVT</b> AUC if single rifampicin dose co-administered with a single PVT dose - <b>PVT</b> AUC decreased by 31% if PVT given separately after a 5 day course of rifampicin	(Deng <i>et al.</i> , 2009; Kyrklund <i>et al.</i> , 2004)
	FVT, SVT	Decreased AUC if statin given separately following rifampicin pre-treatment: <b>FVT</b> (by 53%), <b>SVT</b> (by 87%), <b>SVT acid</b> (by 93%). (Probable decrease in LVT AUC)	(Novartis, 2012; Kyrklund <i>et al.</i> , 2000; Neuvonen <i>et al.</i> , 2008)
	RVT	No significant difference when RVT given separately after a 6 day course of rifampicin	(Zhang <i>et al.</i> , 2008)
Tocilizumab	SVT	<b>SVT</b> AUC decreased by 57%	(Schmitt <i>et al.</i> , 2011)

This table summarises the clinical factors that have been associated with altered statin pharmacokinetics and published in the literature. Unless otherwise stated, reported changes are statistically significant (statin with significant change highlighted in bold font).

**Table 8.2 Cassette calibration line spiking regimens (Chapter 3)**

Cal std	RVT/ATV				ATV metabolites <sup>1</sup>			
	Cal std conc. (ng/mL)	WS (µg/mL)	Volume (µL)		Cal std conc. (ng/mL)	WS (µg/mL)	Volume (µL)	
			WS	Blood			WS	Blood
1	5	0.1	2.63	50	5	0.2	2.56	100
2	12.5	0.1	7.14	50	12.5	0.2	3.33	50
3	25	0.5	5.26	100	25	0.2	7.14	50
4	100	10	1.01	100	50	2	2.56	100
5	250	10	2.56	100	100	2	2.63	50
6	500	10	2.63	50	400	20	2.04	100
7	2,000	100	2.04	100	800	20	2.08	50
8	4,000	100	2.08	50	1,500	20	4.05	50
9	8,000	100	8.70	100	2,500	20	7.14	50
10	10,000	100	5.56	50	-	-	-	-

Abbreviations: Cal std = calibration standard, WS = composite working solution

<sup>1</sup> = ATV acid metabolites (2-OH ATV, 4-OH ATV), and ATV lactones (ATV L, 2-OH ATV L, 4-OH ATV L). The calibration standards of the ATV acid metabolites and ATV lactones were prepared separately using their own composite working solutions, but at the same concentrations.

Briefly, 50 or 100µL of fresh pooled blood per calibration standard was pipetted into a 0.5mL Eppendorf tube, and the appropriate volume of the correct working solution was spiked in. After vortexing, each spiked sample was pipetted onto an FTA Elute card in 35µL spots, left to air dry for at least one hour, and then the FTA Elute cards were stored overnight at room temperature in a sealed Whatman multi-barrier pouch containing desiccant, prior to extraction.

**Table 8.3 Cassette quality control sample spiking regimens (Chapter 3)**

QC sample	RVT/ATV				ATV metabolites <sup>1</sup>			
	Cal std conc. (ng/mL)	WS (µg/mL)	Volume (µL)		Cal std conc. (ng/mL)	WS (µg/mL)	Volume (µL)	
			WS	Blood			WS	Blood
Low	15	0.5	6.19	200	15	0.2	16.22	200
Medium	500	10	10.53	200	75	2	7.79	200
High	7,500	100	16.22	200	1,000	20	10.53	200

Abbreviations: QC = quality control; WS = composite working solution

<sup>1</sup> = ATV acid metabolites (2-OH ATV, 4-OH ATV), and ATV lactones (ATV L, 2-OH ATV L, 4-OH ATV L). The quality control samples of the ATV acid metabolites and ATV lactones were prepared separately using their own composite working solutions, but at the same concentrations.

Briefly, 200µL of fresh pooled blood per quality control was pipetted into a 0.5mL Eppendorf tube, and the appropriate volume of the correct working solution was spiked in. After vortexing, each spiked sample was pipetted onto an FTA Elute card in 35µL spots, left to air dry for at least one hour, and then the FTA Elute cards were stored overnight at room temperature in a sealed Whatman multi-barrier pouch containing desiccant, prior to extraction.

**Table 8.4 Protein expression changes in liver homogenates from hepatic reductase null compared to wild type mice determined by iTRAQ and remained statistically significant after multiple testing correction (Chapter 4)**

Protein	Uniprot ID	Fold change (HRN to WT)	P-value
Pyrethroid hydrolase Ces2a	Q8QZR3	2.281822	6.01E-10
Glutathione S-transferase Mu 3	P19639	4.226929	1.34E-09
Cytochrome P450 3A11	Q64459	4.485966	9.84E-09
Cytochrome P450 2C29	Q64458	3.699818	1.3E-08
Ornithine carbamoyltransferase, mitochondrial	P11725	-2.19203	2.11E-08
Protein disulfide-isomerase A6	Q922R8	2.413683	3.85E-08
Cytochrome P450 2B10	P12791	3.053026	5.11E-08
Cytochrome P450 2E1	Q05421	3.47122	5.96E-08
78 kDa glucose-regulated protein	P20029	0.363213	7.05E-08
Endoplasmic reticulum chaperone	P08113	1.929555	1.34E-07
3-ketoacyl-CoA thiolase B, peroxisomal	Q8VCH0	2.799127	3.27E-07
Dimethylaniline monooxygenase [N-oxide-forming] 5	P97872	1.425862	3.93E-07
Cytochrome P450 2B19	O55071	3.666855	4.03E-07
Protein disulfide-isomerase	P09103	0.29671	5.83E-07
NADPH--cytochrome P450 reductase	P37040	-1.76524	6.67E-07
Protein disulfide-isomerase A3	P27773	1.51274	6.73E-07
Epoxide hydrolase 1	Q9D379	2.428847	8.24E-07
Histidine ammonia-lyase	P35492	-2.89886	9.34E-07
Carboxylesterase 3A	Q63880	1.682812	9.8E-07
Ornithine aminotransferase, mitochondrial	P29758	1.68764	1.13E-06
Peroxisomal multifunctional enzyme type 2	P51660	1.904974	1.26E-06
Glutathione S-transferase Mu 2	P15626	2.733217	1.39E-06
Kynurenine 3-monooxygenase	Q91WN4	-0.94079	1.71E-06
Histone H1.5	P43276	1.465752	2.24E-06
Annexin A5	P48036	2.322103	2.45E-06
Ester hydrolase C11orf54 homolog	Q91V76	1.184346	3.96E-06
Hypoxia up-regulated protein 1	Q9JKR6	1.614333	5E-06
Glycine N-acyltransferase-like protein Keg1	Q9DCY0	-1.608	9.24E-06
Fructose-bisphosphate aldolase B	Q91Y97	-1.51042	1.12E-05

<i>Table continued</i>			
<b>Protein</b>	<b>Uniprot ID</b>	<b>Fold change (HRN to WT)</b>	<b>P-value</b>
Mesencephalic astrocyte-derived neurotrophic factor	Q9CXI5	2.08656	1.21E-05
Alanine aminotransferase 2	Q8BGT5	1.208863	1.51E-05
Galectin-1	P16045	1.922435	1.77E-05
Glutathione S-transferase P 1	P19157	-1.99542	1.81E-05
Leukotriene-B4 omega-hydroxylase 3	Q9EP75	-2.23242	1.82E-05
UDP-glucuronosyltransferase 1-9	Q62452	1.501695	1.85E-05
Cytochrome P450 3A13	Q64464	1.023223	1.93E-05
Formimidoyltransferase-cyclodeaminase	Q91XD4	-1.47962	2.03E-05
Long-chain-fatty-acid--CoA ligase 5	Q8JZR0	1.053819	2.16E-05
ATP synthase subunit alpha, mitochondrial	Q03265	-0.14824	2.3E-05
Ectonucleoside triphosphate diphosphohydrolase 5	Q9WUZ9	1.674163	2.44E-05
Aldehyde oxidase 3	G3X982	-1.23578	2.62E-05
Interferon-inducible GTPase 1	Q9QZ85	-1.64963	2.67E-05
Protein disulfide-isomerase A4	P08003	1.731389	2.78E-05
Glutaredoxin-1	Q9QUH0	1.266238	2.79E-05
Large proline-rich protein BAG6	Q9Z1R2	-0.61391	2.91E-05
Cysteine sulfinic acid decarboxylase	Q9DBE0	2.08832	2.95E-05
Fatty acid-binding protein, intestinal	P55050	-1.09343	3.4E-05
Vimentin	P20152	1.460995	3.64E-05
Glutaminase liver isoform, mitochondrial	Q571F8	-1.82877	3.74E-05
Electron transfer flavoprotein subunit beta	Q9DCW4	-0.98575	3.88E-05
Ribonuclease UK114	P52760	-1.53001	4.09E-05
UDP-glucose 6-dehydrogenase	O70475	1.397372	4.36E-05
Non-specific lipid-transfer protein	P32020	1.428466	4.41E-05
ATP synthase subunit e, mitochondrial	Q06185	-0.91461	4.64E-05
Cytochrome b5	P56395	1.929255	5.06E-05
ATP-binding cassette sub-family D member 3	P55096	1.25975	5.38E-05
Peptidyl-prolyl cis-trans isomerase B	P24369	1.62246	5.72E-05
Solute carrier family 22 member 1	O08966	-1.52164	5.84E-05
Peroxisomal bifunctional enzyme	Q9DBM2	1.7675	6.31E-05
Elongation factor Tu, mitochondrial	Q8BFR5	-0.61788	6.76E-05

<i>Table continued</i>			
<b>Protein</b>	<b>Uniprot ID</b>	<b>Fold change (HRN to WT)</b>	<b>P-value</b>
Urocanate hydratase	Q8VC12	-1.57205	6.79E-05
7-alpha-hydroxycholest-4-en-3-one 12-alpha-hydroxylase	O88962	1.52124	8E-05
Sarcosine dehydrogenase, mitochondrial	Q99LB7	-1.56067	8.15E-05
Corticosteroid 11-beta-dehydrogenase isozyme 1	P50172	-2.31166	8.38E-05
Fatty acid-binding protein, liver	P12710	-0.16627	8.46E-05
Calreticulin	P14211	1.867503	8.77E-05
Plastin-2	Q61233	0.868072	8.81E-05
Kynurenine/alpha-aminoadipate aminotransferase, mitochondrial	Q9WVM8	-1.15148	8.82E-05
Cholesterol 7-alpha-monooxygenase	Q64505	2.629703	8.83E-05
3-hydroxyanthranilate 3,4-dioxygenase	Q78JT3	-1.09611	9.11E-05
Cytochrome P450 2D9	P11714	1.988457	9.13E-05
Pyruvate carboxylase, mitochondrial	Q05920	-0.85675	9.82E-05
Cysteine-rich protein 2	Q9DCT8	0.429842	0.000109
ATP synthase-coupling factor 6, mitochondrial	P97450	-1.17098	0.000112
Carbamoyl-phosphate synthase [ammonia], mitochondrial	Q8C196	-0.11756	0.000124
Cytochrome b-c1 complex subunit Rieske, mitochondrial	Q9CR68	-0.83267	0.000136
Peroxisomal membrane protein PEX14	Q9R0A0	0.637912	0.000137
Starch-binding domain-containing protein 1	Q8C7E7	1.641222	0.000143
Peroxisomal acyl-coenzyme A oxidase 2	Q9QXD1	0.783898	0.000151
Pyrethroid hydrolase Ces2e	Q8BK48	0.657713	0.000159
Cytochrome P450 2C55	Q9D816	2.252735	0.000162
Acyl-CoA synthetase family member 2, mitochondrial	Q8VCW8	-0.81281	0.000178
Alcohol dehydrogenase [NADP(+)]	Q9JII6	0.808708	0.000178
Pyruvate kinase PKLR	P53657	-0.93915	0.00018
Major vault protein	Q9EQK5	1.259719	0.000183
3-ketoacyl-CoA thiolase, mitochondrial	Q8BWT1	-1.68781	0.0002
Mannose-P-dolichol utilization defect 1 protein	Q9R0Q9	1.277912	0.000216
Peroxisomal 2,4-dienoyl-CoA reductase	Q9WV68	0.940826	0.000226
Electron transfer flavoprotein-ubiquinone oxidoreductase, mitochondrial	Q921G7	-0.84383	0.000227
Sodium/bile acid cotransporter	O08705	-1.03824	0.000228
Fatty aldehyde dehydrogenase	P47740	2.149125	0.000233

<i>Table continued</i>			
<b>Protein</b>	<b>Uniprot ID</b>	<b>Fold change (HRN to WT)</b>	<b>P-value</b>
Microsomal triglyceride transfer protein large subunit	O08601	1.009445	0.000236
Thioredoxin-dependent peroxide reductase, mitochondrial	P20108	0.600168	0.000243
Mitochondrial pyruvate carrier 2	Q9D023	-1.00953	0.000258
Arginase-1	Q61176	-1.3509	0.000272
Glutathione S-transferase Mu 1	P10649	2.159203	0.000305
Choline/ethanolamine kinase	O55229	-1.43208	0.000308
Adenylate kinase 2, mitochondrial	Q9WTP6	-0.71531	0.000316
Lanosterol 14-alpha demethylase	Q8K0C4	1.704777	0.00035
GrpE protein homolog 1, mitochondrial	Q99LP6	0.659724	0.000363
Delta(24)-sterol reductase	Q8VCH6	1.239968	0.000365
3-ketoacyl-CoA thiolase A, peroxisomal	Q921H8	1.479331	0.000368
Lipoamide acyltransferase component of branched-chain alpha-keto acid dehydrogenase complex, mitochondrial	P53395	-0.84342	0.000377
ATP synthase subunit g, mitochondrial	Q9CPQ8	-1.12306	0.000378
Sodium/potassium-transporting ATPase subunit alpha-1	Q8VDN2	-1.10111	0.000399
Cytochrome P450 3A25	O09158	0.759768	0.000404
L-serine dehydratase/L-threonine deaminase	Q8VBT2	-1.89093	0.000419
Tubulin alpha-4A chain	P68368	-0.65968	0.000438
Quinone oxidoreductase	P47199	0.841792	0.000452
Complement factor B	P04186	0.861663	0.000472
Glutathione S-transferase omega-1	O09131	-0.43422	0.000501
Solute carrier organic anion transporter family member 1A1	Q9QXZ6	-1.27792	0.000534
Liver carboxylesterase 1	Q8VCC2	1.302007	0.000545
Major urinary protein 3	P04939	-1.1849	0.000597
Acetolactate synthase-like protein	Q8BU33	1.080481	0.0006
Methylmalonate-semialdehyde dehydrogenase [acylating], mitochondrial	Q9EQ20	-1.0735	0.000601
Transmembrane emp24 domain-containing protein 5	Q9CXE7	0.87668	0.000607
Cytochrome P450 4V2	Q9DBW0	-2.32789	0.000617
Polyadenylate-binding protein 2	Q8CCS6	0.314101	0.000646
40S ribosomal protein S10	P63325	-0.38541	0.000672
ATP synthase subunit delta, mitochondrial	Q9D3D9	-1.24275	0.000701

<i>Table continued</i>			
<b>Protein</b>	<b>Uniprot ID</b>	<b>Fold change (HRN to WT)</b>	<b>P-value</b>
Major urinary protein 2	P11589	1.520971	0.000707
Carboxylesterase 1D	Q8VCT4	1.180302	0.000724
Ubiquitin-like modifier-activating enzyme 1	Q02053	-0.3455	0.000752
B-cell receptor-associated protein 31	Q61335	1.049546	0.000783
Glutamate dehydrogenase 1, mitochondrial	P26443	-1.19548	0.000785
Isovaleryl-CoA dehydrogenase, mitochondrial	Q9JHI5	-0.85018	0.000802
ATP synthase subunit O, mitochondrial	Q9DB20	-0.91453	0.000822
Retinol dehydrogenase 7	O88451	1.115976	0.000833
Argininosuccinate synthase	P16460	-0.15073	0.000837
Thioredoxin domain-containing protein 5	Q91W90	1.16242	0.000846
Thymosin beta-4	P20065	1.886002	0.000868
Peroxisomal membrane protein 2	P42925	1.368378	0.00087
Carnitine O-palmitoyltransferase 2, mitochondrial	P52825	-0.49585	0.000887
Methyltransferase-like protein 7B	Q9DD20	1.624868	0.000888
THO complex subunit 2	B1AZI6	0.683818	0.000894
Eukaryotic translation initiation factor 5A-1	P63242	0.976769	0.00092
Phytanoyl-CoA dioxygenase, peroxisomal	O35386	0.837109	0.000924
DnaJ homolog subfamily C member 3	Q91YW3	1.104977	0.000941
Estradiol 17-beta-dehydrogenase 8	P50171	-0.83051	0.000962
Protein WWC2	Q6NXJ0	0.385344	0.00098
NADH-cytochrome b5 reductase 3	Q9DCN2	0.624546	0.000981
Citrate synthase, mitochondrial	Q9CZU6	0.489088	0.001001
NLR family member X1	Q3TL44	-1.80675	0.001012
Cytochrome P450 4A12A	Q91WL5	-0.96575	0.001025
Aldo-keto reductase family 1 member C13	Q8VC28	-0.76643	0.001045
Retinol-binding protein 4	Q00724	1.364458	0.001068
Peptidyl-prolyl cis-trans isomerase FKBP2	P45878	0.568848	0.001069
Talin-1	P26039	0.376226	0.001073
NADH dehydrogenase [ubiquinone] iron-sulfur protein 2, mitochondrial	Q91WD5	-0.57325	0.001078
Isocitrate dehydrogenase [NADP], mitochondrial	P54071	1.24004	0.001115
Nucleotide exchange factor SIL1	Q9EPK6	1.507812	0.001122

<i>Table continued</i>			
<b>Protein</b>	<b>Uniprot ID</b>	<b>Fold change (HRN to WT)</b>	<b>P-value</b>
Short-chain specific acyl-CoA dehydrogenase, mitochondrial	Q07417	-0.68181	0.001126
Carboxylesterase 3B	Q8VCU1	-0.90128	0.00122
Dimethylaniline monooxygenase [N-oxide-forming] 1	P50285	1.053968	0.001236
Bile salt export pump	Q9QY30	-0.71093	0.001278
Stromal interaction molecule 2	P83093	-0.9922	0.001402
Transaldolase	Q93092	0.978473	0.001413
Apolipoprotein E	P08226	0.859597	0.001482
C-1-tetrahydrofolate synthase, cytoplasmic	Q922D8	-0.70644	0.001493
MICOS complex subunit Mic19	Q9CRB9	-0.63748	0.001523
High mobility group protein B2	P30681	0.996551	0.001571
Myosin-9	Q8VDD5	0.839252	0.001588
L-lactate dehydrogenase A chain	P06151	-0.80595	0.001593
Death-associated protein 1	Q91XC8	1.361565	0.001601
Calnexin	P35564	0.518331	0.001609
Solute carrier family 22 member 18	Q78KK3	0.51133	0.001627
Ketohexokinase	P97328	-0.93917	0.001735
Probable imidazolonepropionase	Q9DBA8	-0.81277	0.001737
Electron transfer flavoprotein subunit alpha, mitochondrial	Q99LC5	-1.43818	0.001746
Dihydrolipoyllysine-residue succinyltransferase component of 2-oxoglutarate dehydrogenase complex, mitochondrial	Q9D2G2	-0.65978	0.001746
N(G),N(G)-dimethylarginine dimethylaminohydrolase 1	Q9CWS0	-0.74184	0.001803
Serotransferrin	Q921I1	0.801313	0.001908
Cytochrome P450 2J5	O54749	0.609095	0.001925
Glycerol-3-phosphate dehydrogenase [NAD(+)], cytoplasmic	P13707	0.879297	0.001942
Transgelin-2	Q9WVA4	0.702118	0.002043
2-amino-3-ketobutyrate coenzyme A ligase, mitochondrial	O88986	-0.64201	0.002054
Vitamin D-binding protein	P21614	0.794977	0.002082
Acyl-CoA desaturase 1	P13516	0.739709	0.002087
Copper transport protein ATOX1	O08997	1.561613	0.002115
Peroxisomal membrane protein 11A	Q9Z211	1.411243	0.002168
Pro-cathepsin H	P49935	-0.74871	0.002172

<i>Table continued</i>			
<b>Protein</b>	<b>Uniprot ID</b>	<b>Fold change (HRN to WT)</b>	<b>P-value</b>
Fetuin-B	Q9QXC1	0.635725	0.002176
Lactoylglutathione lyase	Q9CPU0	-1.0455	0.002178
Prothrombin	P19221	1.446014	0.002207
Calmodulin	P62204	0.688632	0.002224
RNA-binding protein 14	Q8C2Q3	-0.77069	0.002226
Cystatin-B	Q62426	0.843393	0.002348
Phenazine biosynthesis-like domain-containing protein 2	Q9CXN7	-1.37079	0.002348
Succinyl-CoA ligase [ADP-forming] subunit beta, mitochondrial	Q9Z2I9	-0.44512	0.002349
Acyl-CoA dehydrogenase family member 11	Q80XL6	0.455944	0.002488
Triokinase/FMN cyclase	Q8VC30	-0.85308	0.002593
Protein FAM210B	Q9D8B6	-0.57086	0.002623
Serine protease hepsin	O35453	0.879412	0.002623
Cytochrome b-c1 complex subunit 6, mitochondrial	P99028	-0.78832	0.00269
ATP synthase subunit f, mitochondrial	P56135	-0.69111	0.00275
Tropomyosin alpha-4 chain	Q6IRU2	0.84581	0.002761
Protein S100-A11	P50543	2.400858	0.002768
Heme oxygenase 2	O70252	0.529262	0.002794

Protein identification and relative quantification in liver homogenates from six hepatic reductase null mice compared to six wild type mouse liver homogenates was carried out by isobaric tag for relative and absolute quantitation (iTRAQ) in two separate batches (each batch contained three HRN and WT liver homogenates and the same homogenate pool). Protein identification harnessed ProteinPilot™ software, and 3538 proteins were identified at a false discovery rate of  $\leq 1\%$ . Proteins identified in both or just one iTRAQ run were included. The ProteinPilot™ expression ratios (individual mouse/homogenate pool) for each identified protein were  $\log_2$  transformed and batch mean-centred, prior to hypothesis testing using student's unpaired t-test. These raw t-test p-values then underwent Benjamini-Hochberg correction for multiple testing (n=3538 tests) so that only the proteins whose expression changes remained significant at a 5% FDR were considered statistically significant; these 199 proteins are presented in this table.

**Table 8.5 A summary of the quality control results from the 12 analytical runs carried out to determine the concentrations of cardiovascular drug analytes in patient samples from the PhACS study using the validated liquid chromatography-mass spectrometry assay (Chapter 5)**

Run	QC	ATV			2-OH ATV			ATV L			2-OH ATV L			BSP			CLP-CA		
		M (ng/mL)	A (%)	CV (%)															
1	LOW	1.6	104.7	3.0	1.6	103.8	6.1	3.4	95.4	3.6	1.6	107.8	5.9	1.6	104.2	7.1	45.7	101.6	0.7
	MID	48.7	108.1	1.2	48.0	106.6	3.1	36.6	101.8	1.7	43.6	97.0	4.6	47.2	104.9	2.7	1423.2	105.4	3.4
	HIGH	100.9	106.2	2.0	95.2	100.2	3.1	77.4	101.8	3.7	98.2	103.4	1.6	94.2	99.1	1.0	2748.3	96.4	0.7
2	LOW	1.6	109.7	6.8	1.6	103.6	6.9	3.5	97.1	5.5	1.7	111.1	4.0	1.5	102.9	2.6	51.8	115.2	3.7
	MID	50.0	111.1	6.0	48.6	107.9	9.8	35.8	99.4	3.5	43.5	96.7	2.0	46.8	103.9	7.3	1474.7	109.2	8.4
	HIGH	103.1	108.5	4.3	95.8	100.8	1.9	74.1	97.5	1.5	91.5	96.4	3.3	98.7	103.9	4.9	3058.4	107.3	4.2
3	LOW	1.6	108.2	14.2	1.6	108.8	5.0	3.6	99.8	7.1	1.7	112.4	18.4	1.5	102.4	5.0	48.9	108.8	0.4
	MID	47.7	106.1	7.9	47.5	105.6	7.5	35.2	97.7	3.2	40.6	90.1	9.0	48.4	107.5	14.8	1446.6	107.2	0.9
	HIGH	101.5	106.8	3.7	113.2	119.1	12.7	73.6	96.8	15.5	96.0	101.1	1.8	104.5	110.0	0.0	3218.5	112.9	7.0
4	LOW	1.6	104.2	1.5	1.5	97.5	7.1	3.8	106.6	2.3	1.7	116.1	13.6	1.5	97.3	4.9	44.3	98.4	7.2
	MID	46.2	102.8	1.9	44.6	99.1	6.9	34.7	96.3	8.3	46.0	102.3	7.3	48.0	106.6	6.3	1262.4	93.5	4.5
	HIGH	88.4	93.1	3.6	89.2	93.9	12.3	78.0	102.6	6.1	92.1	97.0	3.9	99.8	105.1	5.1	2470.7	86.7	0.7
5	LOW	1.6	103.6	8.7	1.9	125.3	10.1	3.6	100.6	6.8	1.6	109.8	2.4	1.6	104.9	5.7	49.0	108.9	5.5
	MID	46.1	102.5	6.2	44.7	99.2	6.9	34.6	96.2	5.2	43.7	97.0	5.0	44.3	98.4	11.8	1383.0	102.4	11.4
	HIGH	99.1	104.3	6.9	93.9	98.9	2.4	75.1	98.8	4.2	97.8	103.0	5.8	96.8	101.9	9.1	2986.7	104.8	4.7
6	LOW	1.6	109.4	9.1	1.5	100.0	10.6	3.7	102.4	3.9	1.6	105.5	2.2	1.6	105.8	13.3	48.2	107.1	6.0
	MID	48.4	107.5	8.9	47.4	105.3	5.5	35.7	99.2	8.0	49.8	110.7	2.1	45.0	99.9	10.5	1403.9	104.0	18.5
	HIGH	107.3	113.0	16.5	98.0	103.1	14.9	77.5	101.9	4.4	99.3	104.5	11.9	99.5	104.7	7.8	2790.3	97.9	7.4
7	LOW	1.7	114.5	10.2	1.6	103.7	17.9	3.3	92.1	11.8	1.4	95.0	16.2	1.7	112.3	8.7	46.2	102.7	13.3
	MID	50.6	112.3	7.3	46.2	102.7	9.2	36.6	101.6	7.0	46.5	103.4	14.5	49.9	110.9	15.1	1560.0	115.6	9.4
	HIGH	100.3	105.6	8.2	96.7	101.8	7.2	80.3	105.7	4.4	101.3	106.7	7.2	101.2	106.6	8.2	3083.8	108.2	5.2
8	LOW	1.4	94.5	4.8	1.6	104.4	4.3	3.5	96.0	3.5	1.4	95.3	1.1	1.6	104.5	7.9	45.1	100.1	6.8

<i>Table continued</i>																			
	QC	ATV			2-OH ATV			ATV L			2-OH ATV L			BSP			CLP-CA		
		M (ng/mL)	A (%)	CV (%)															
	MID	46.1	102.5	8.7	47.8	106.2	2.4	37.7	104.7	2.9	48.1	106.8	4.6	40.8	90.8	7.5	1377.3	102.0	4.5
	HIGH	99.5	104.7	3.6	102.0	107.3	6.8	82.0	107.9	0.9	97.1	102.2	8.9	96.1	101.2	6.3	2801.9	98.3	3.5
9	LOW	1.5	101.6	14.0	1.4	96.5	7.8	ND	ND	ND	ND	ND	ND	1.7	110.9	14.1	55.1	122.4	15.1
	MID	51.2	113.9	6.3	43.1	95.7	7.3	ND	ND	ND	ND	ND	ND	44.5	99.0	5.2	1520.9	112.7	16.5
	HIGH	97.3	102.5	9.8	89.3	94.0	2.8	ND	ND	ND	ND	ND	ND	97.3	102.4	17.7	2966.1	104.1	6.1
10	LOW	1.4	92.2	0.0	1.6	103.5	5.9	ND	ND	ND	ND	ND	ND	1.5	101.8	3.0	45.4	100.9	5.2
	MID	44.5	98.8	0.6	44.2	98.1	1.2	ND	ND	ND	ND	ND	ND	47.6	105.7	0.7	1347.8	99.8	0.9
	HIGH	89.0	93.7	1.7	89.6	94.3	2.1	ND	ND	ND	ND	ND	ND	97.2	102.3	1.2	2719.1	95.4	0.7
11	LOW	1.6	107.7	5.5	1.7	115.9	5.9	3.3	91.4	8.5	1.6	108.3	10.5	1.7	111.5	11.3	49.3	109.6	12.0
	MID	47.1	104.6	3.6	46.0	102.2	9.0	34.9	96.9	5.6	43.0	95.5	4.2	48.9	108.6	8.6	1556.8	115.3	8.7
	HIGH	108.4	114.2	12.2	97.3	102.4	10.8	79.3	104.3	8.7	88.3	92.9	9.0	107.0	112.6	19.1	3309.2	116.1	1.8
12	LOW	1.6	108.3	9.2	1.6	106.8	5.4	3.2	90.0	0.8	1.7	113.7	0.3	1.6	103.5	17.4	50.4	112.0	5.7
	MID	47.8	106.3	7.1	46.2	102.7	5.6	38.4	106.8	10.0	47.2	104.9	6.8	49.2	109.3	7.0	1547.4	114.6	11.1
	HIGH	102.4	107.8	10.5	95.7	100.8	4.0	72.9	95.9	12.9	91.4	96.2	1.4	91.1	95.9	17.2	2794.3	98.0	4.4

12 analytical runs were carried out to analyse 1,026 patient plasma samples. Each run consisted of one or two 96-well plates that contained six (two low, two mid, two high) quality control extracts for both joint and lactone analytes per plate. For the joint analytes (ATV, 2-OH ATV, BSP, CLP-CA) runs 1, 3, 4 and 10 consisted of one 96-well plate (six QC extracts), and runs 2, 5, 6, 7, 8, 9, 11 and 12 consisted of two 96-well plates (12 QC extracts). The run composition was the same for the lactones (ATV L, 2-OH ATV L), except that lactone QCs and calibration line were not included in runs 9 and 10 as these runs did not include any patient samples designated for ATV analyte quantification, and runs 8 and 12 only had one 96-well plate containing samples for ATV analyte analysis (thus runs 8 and 12 only had two of each QC concentration for the lactones). A = accuracy; CV = coefficient of variation; M = mean concentration. ND = not done.

**Table 8.6 A summary of the quality control extracts that passed from the 12 analytical runs carried out to determine the concentration of cardiovascular drug analytes in patient samples from the PhACS study using the validated liquid chromatography-mass spectrometry assay (Chapter 5)**

Analytical run		ATV	2-OH ATV	ATV L	2-OH ATV L	BSP	CLP-CA
1	LOW	2 in 2	2 in 2	2 in 2	2 in 2	2 in 2	2 in 2
	MID	2 in 2	2 in 2	2 in 2	2 in 2	2 in 2	2 in 2
	HIGH	2 in 2	2 in 2	2 in 2	2 in 2	2 in 2	2 in 2
2	LOW	3 in 4	4 in 4	4 in 4	4 in 4	4 in 4	2 in 4
	MID	3 in 4	3 in 4	4 in 4	4 in 4	4 in 4	3 in 4
	HIGH	4 in 4	4 in 4	4 in 4	4 in 4	4 in 4	4 in 4
3	LOW	1 in 2	2 in 2	2 in 2	1 in 2	2 in 2	2 in 2
	MID	2 in 2	2 in 2	2 in 2	1 in 2	1 in 2	2 in 2
	HIGH	2 in 2	1 in 2	2 in 2	2 in 2	2 in 2	1 in 2
4	LOW	2 in 2	2 in 2	2 in 2	1 in 2	2 in 2	2 in 2
	MID	2 in 2	2 in 2	2 in 2	2 in 2	2 in 2	2 in 2
	HIGH	2 in 2	2 in 2	2 in 2	2 in 2	2 in 2	2 in 2
5	LOW	3 in 4	1 in 4	4 in 4	4 in 4	4 in 4	3 in 4
	MID	4 in 4	4 in 4	4 in 4	4 in 4	3 in 4	4 in 4
	HIGH	4 in 4	4 in 4	4 in 4	4 in 4	4 in 4	4 in 4
6	LOW	3 in 4	4 in 4	4 in 4	4 in 4	3 in 4	4 in 4
	MID	4 in 4	4 in 4	4 in 4	4 in 4	4 in 4	1 in 4
	HIGH	3 in 4	3 in 4	4 in 4	3 in 4	4 in 4	4 in 4
7	LOW	2 in 4	2 in 4	3 in 4	2 in 4	3 in 4	3 in 4
	MID	2 in 4	4 in 4	4 in 4	3 in 4	2 in 4	1 in 4
	HIGH	4 in 4	4 in 4	4 in 4	4 in 4	4 in 4	4 in 4
8	LOW	4 in 4	4 in 4	2 in 2	2 in 2	4 in 4	4 in 4
	MID	4 in 4	4 in 4	2 in 2	2 in 2	3 in 4	4 in 4
	HIGH	4 in 4	3 in 4	2 in 2	2 in 2	4 in 4	4 in 4
9	LOW	3 in 4	4 in 4	ND	ND	2 in 4	2 in 4
	MID	2 in 4	4 in 4	ND	ND	4 in 4	3 in 4
	HIGH	3 in 4	4 in 4	ND	ND	3 in 4	4 in 4
10	LOW	2 in 2	2 in 2	ND	ND	2 in 2	2 in 2
	MID	2 in 2	2 in 2	ND	ND	2 in 2	2 in 2
	HIGH	2 in 2	2 in 2	ND	ND	2 in 2	2 in 2
11	LOW	4 in 4	2 in 4	3 in 4	3 in 4	3 in 4	3 in 4
	MID	4 in 4	4 in 4	4 in 4	4 in 4	3 in 4	3 in 4
	HIGH	2 in 4	4 in 4	4 in 4	3 in 4	3 in 4	4 in 4
12	LOW	3 in 4	4 in 4	2 in 2	2 in 2	3 in 4	3 in 4
	MID	4 in 4	4 in 4	2 in 2	2 in 2	3 in 4	2 in 4
	HIGH	3 in 4	4 in 4	2 in 2	2 in 2	2 in 4	4 in 4

12 analytical runs were carried out to analyse 1,026 patient plasma samples. For a run to 'pass', two thirds of all QCs had to be within 85-115% of their nominal concentration and at least one QC extract had to pass at each QC concentration in the run for each analyte. As can be seen, all runs satisfied these criteria.

**Table 8.7 Univariate linear regression analysis of association between clinical variables and ATV analyte levels in PhACS patients (Chapter 6)**

Variable	ATV		2-OH ATV		ATV L		2-OH ATV L	
	B (SE)	p-value	B (SE)	p-value	B (SE)	p-value	B (SE)	p-value
ATV dose	0.003 (0.001)	0.068	0.004 (0.001)	0.0033	0.005 (0.002)	0.0039	0.004 (0.001)	0.0011
<b>Demographics:</b>								
Sex (M vs F)	-0.086 (0.035)	0.016	0.025 (0.031)	0.41	-0.077 (0.039)	0.051	0.012 (0.032)	0.71
Age	0.004 (0.001)	0.00075	0.007 (0.001)	3.92x10 <sup>-11</sup>	0.003 (0.001)	0.020	0.007 (0.001)	3.20x10 <sup>-9</sup>
BMI	-0.002 (0.003)	0.37	-0.006 (0.002)	0.0046	-0.006 (0.003)	0.024	-0.008 (0.002)	0.00069
Smoking	0.010 (0.018)	0.58	0.009 (0.015)	0.57	0.014 (0.020)	0.47	0.010 (0.016)	0.54
<b>Co-morbidities:</b>								
Hypertension	0.074 (0.030)	0.014	0.061 (0.026)	0.019	0.068 (0.033)	0.040	0.086 (0.027)	0.0014
Hyperlipidaemia prior to index NSTEMI	0.060 (0.030)	0.043	0.044 (0.026)	0.088	0.068 (0.033)	0.039	0.059 (0.027)	0.029
Diabetes mellitus	0.072 (0.038)	0.062	0.089 (0.033)	0.0074	0.007 (0.043)	0.87	0.049 (0.035)	0.16
CKD (Cr>150µmol/L)	0.097 (0.064)	0.13	0.097 (0.056)	0.083	0.109 (0.071)	0.12	0.121 (0.058)	0.036
Prior CVD	0.080 (0.032)	0.014	0.101 (0.028)	0.00035	0.051 (0.036)	0.16	0.080 (0.029)	0.0062
Hepatic disease	-0.311 (0.163)	0.056	-0.380 (0.141)	0.0072	-0.263 (0.180)	0.15	-0.332 (0.147)	0.024
<b>Drugs at Visit 2:</b>								
Aspirin	-0.144 (0.063)	0.023	-0.091 (0.055)	0.097	-0.168 (0.070)	0.016	-0.113 (0.057)	0.048
P2Y12 inhibitor	-0.044 (0.042)	0.29	0.052 (0.037)	0.15	-0.147 (0.046)	0.002	-0.059 (0.038)	0.12
Beta blocker	-0.052 (0.042)	0.22	-0.068 (0.036)	0.059	-0.021 (0.046)	0.65	-0.033 (0.038)	0.38
ACEI/ARB	-0.035 (0.041)	0.40	0.027 (0.036)	0.45	-0.090 (0.046)	0.048	-0.032 (0.037)	0.39
Loop diuretic	0.124 (0.040)	0.0017	0.092 (0.034)	0.0078	0.140 (0.044)	0.0014	0.135 (0.036)	0.00016

<i>Table continued</i>								
Variable	ATV		2-OH ATV		ATV L		2-OH ATV L	
	B (SE)	p-value	B (SE)	p-value	B (SE)	p-value	B (SE)	p-value
Thiazide diuretic	-0.012 (0.085)	0.89	0.062 (0.074)	0.40	-0.070 (0.094)	0.45	0.002 (0.076)	0.98
Amiodarone	0.225 (0.138)	0.10	0.042 (0.120)	0.73	0.318 (0.152)	0.037	0.126 (0.125)	0.31
Proton pump inhibitor	0.093 (0.030)	0.0022	0.073 (0.026)	0.0060	0.137 (0.033)	0.000042	0.121 (0.027)	0.000010
CYP3A4 inducer	-0.162 (0.210)	0.44	-0.173 (0.183)	0.34	0.193 (0.232)	0.41	0.210 (0.190)	0.27
CYP3A4 inhibitor	0.209 (0.075)	0.0056	0.080 (0.066)	0.22	0.129 (0.083)	0.12	0.025 (0.068)	0.72
OATP1B1 inhibitor	0.035 (0.087)	0.68	0.082 (0.075)	0.28	0.040 (0.096)	0.67	0.133 (0.078)	0.091
ATV non-adherence	-0.046 (0.053)	0.38	-0.058 (0.046)	0.21	-0.111 (0.058)	0.057	-1.03 (0.048)	0.031
<b>Blood sample characteristics:</b>								
Sample storage duration	-6.99x10 <sup>-6</sup> (0.00004)	0.84	-0.0001 (0.00003)	0.000041	0.0002 (0.00004)	2.49x10 <sup>-9</sup>	0.0002 (0.00003)	1.00x10 <sup>-6</sup>
Time since last ATV	-0.001 (0.0001)	1.14x10 <sup>-12</sup>	-0.001 (0.0001)	1.13x10 <sup>-10</sup>	-0.001 (0.0001)	8.00x10 <sup>-6</sup>	-0.001 (0.0001)	2.00x10 <sup>-6</sup>

ATV, 2-hydroxy ATV, ATV lactone and 2-hydroxy ATV lactone levels were quantified, log<sub>10</sub> transformed and then analysed in 590 patients from the PhACS study who had been taking 80mg or 40mg ATV daily from their index hospitalisation for a non-ST elevation acute coronary syndrome until their month one visit, and in whom an EDTA plasma sample at one month was available and their statin adherence was known.

Univariate linear regression analysis was conducted with all included covariates (tabulated here) and those variables with univariate p≤0.1 were entered into multivariable linear regression modelling, using stepwise selection, and retained in the final model if they had an adjusted p<0.05.

B is the unstandardized coefficient; B and standard error (SE) represent the change in log<sub>10</sub> transformed analyte concentration for a unit change in a given clinical variable, with all other variables held constant. A positive B value indicates a higher analyte concentration, and a negative B a lower level.

**Table 8.8 Univariate linear regression analysis of association between clinical variables and ATV analyte total and ratios (Chapter 6)**

Variable	2-OH ATV/ATV		2-OH ATV L/ATV L		ATV L/ATV		TOTAL <sup>1</sup>	
	B (SE)	p-value	B (SE)	p-value	B (SE)	p-value	B (SE)	p-value
ATV dose	0.001 (0.001)	0.24	-0.0004 (0.001)	0.68	0.002 (0.001)	0.044	0.004 (0.001)	0.0014
<b>Demographics:</b>								
Sex (M vs F)	0.111 (0.022)	4.60x10 <sup>-7</sup>	0.089 (0.021)	0.000035	0.009 (0.024)	0.72	-0.024 (0.029)	0.42
Age	0.003 (0.001)	0.00024	0.004 (0.001)	6.00x10 <sup>-6</sup>	-0.001 (0.001)	0.24	0.006 (0.001)	1.69x10 <sup>-8</sup>
BMI	-0.004 (0.002)	0.013	-0.001 (0.002)	0.35	-0.004 (0.002)	0.019	-0.006 (0.002)	0.0038
Smoking	-0.001 (0.011)	0.92	-0.004 (0.011)	0.69	0.004 (0.012)	0.72	0.011 (0.015)	0.47
<b>Co-morbidities:</b>								
Hypertension	-0.012 (0.019)	0.52	0.018 (0.018)	0.31	-0.005 (0.020)	0.79	0.066 (0.025)	0.0078
Hyperlipidaemia prior to index NSTEMI	-0.016 (0.019)	0.39	-0.009 (0.018)	0.61	0.008 (0.020)	0.70	0.050 (0.025)	0.044
Diabetes mellitus	0.018 (0.024)	0.46	0.042 (0.023)	0.072	-0.065 (0.026)	0.013	0.058 (0.032)	0.068
CKD (Cr>150µmol/L)	-0.001 (0.040)	0.99	0.012 (0.039)	0.75	0.012 (0.043)	0.79	0.109 (0.053)	0.039
Prior CVD	0.021 (0.020)	0.31	0.029 (0.020)	0.14	-0.029 (0.022)	0.19	0.083 (0.027)	0.0020
Hepatic disease	-0.069 (0.102)	0.50	-0.069 (0.099)	0.48	0.048 (0.11)	0.66	-0.336 (0.134)	0.013
<b>Drugs at Visit 2:</b>								
Aspirin	0.053 (0.039)	0.18	0.055 (0.038)	0.15	-0.024 (0.043)	0.58	-0.120 (0.052)	0.022
P2Y12 inhibitor	0.097 (0.026)	0.00022	0.088 (0.025)	0.00055	-0.102 (0.028)	0.00033	-0.040 (0.035)	0.25
Beta blocker	-0.017 (0.026)	0.53	-0.013 (0.025)	0.62	0.031 (0.028)	0.27	-0.051 (0.034)	0.14
ACEI/ARB	0.062 (0.026)	0.017	0.058 (0.025)	0.020	-0.056 (0.28)	0.047	-0.025 (0.034)	0.46
Loop diuretic	-0.032 (0.025)	0.19	-0.005 (0.024)	0.83	0.016 (0.027)	0.56	0.125 (0.033)	0.00014
Thiazide diuretic	0.074 (0.053)	0.16	0.073 (0.051)	0.16	-0.058 (0.057)	0.31	-0.005 (0.070)	0.95
Amiodarone	-0.183 (0.086)	0.033	-0.192 (0.083)	0.021	0.094 (0.093)	0.32	0.156 (0.114)	0.17
Proton pump inhibitor	-0.020 (0.019)	0.29	-0.016 (0.018)	0.38	0.044 (0.021)	0.032	0.102 (0.025)	0.000050
CYP3A4 inducer	-0.010 (0.131)	0.94	0.017 (0.127)	0.89	0.355 (0.142)	0.012	0.026 (0.174)	0.88
CYP3A4 inhibitor	-0.129 (0.047)	0.0063	-0.104 (0.046)	0.022	-0.080 (0.051)	0.12	0.101 (0.062)	0.11
OATP1B1 inhibitor	0.047 (0.054)	0.39	0.092 (0.052)	0.079	0.005 (0.059)	0.93	0.078 (0.072)	0.28
ATV non-adherence	-0.012 (0.033)	0.72	0.008 (0.032)	0.80	-0.065 (0.036)	0.069	-0.073 (0.044)	0.094

<i>Table continued</i>								
Variable	2-OH ATV/ATV		2-OH ATV L/ATV L		ATV L/ATV		TOTAL <sup>1</sup>	
	B (SE)	p-value	B (SE)	p-value	B (SE)	p-value	B (SE)	p-value
<b>Blood sample characteristics:</b>								
Sample storage duration	-0.0001 (0.00002)	5.81x10 <sup>-8</sup>	7.79x10 <sup>-5</sup> (0.00002)	0.00027	0.0002 (0.00002)	5.39x10 <sup>-25</sup>	4.47x10 <sup>-5</sup> (0.00003)	0.13
Time since last ATV	0.0002 (0.00008)	0.019	7.78x10 <sup>-5</sup> (0.00008)	0.33	0.0003 (0.00009)	0.0023	-0.001 (0.0001)	2.03x10 <sup>-11</sup>

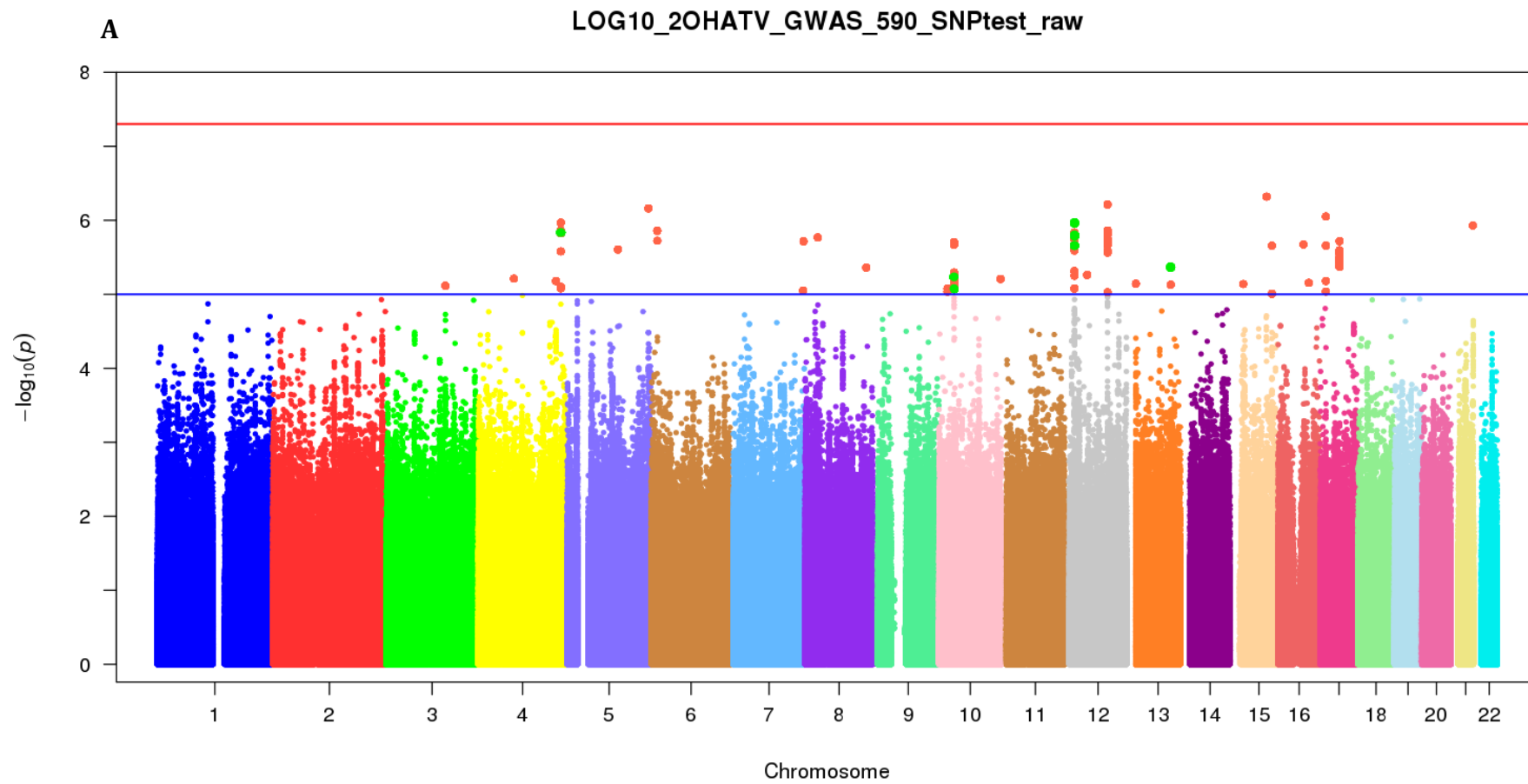
<sup>1</sup> = ATV + 2-OH ATV + ATV L + 2-OH ATV L.

ATV, 2-hydroxy ATV, ATV lactone and 2-hydroxy ATV lactone levels were quantified, log<sub>10</sub> transformed and then analysed in 590 patients from the PhACS study who had been taking 80mg or 40mg ATV daily from their index hospitalisation for a non-ST elevation acute coronary syndrome until their month one visit, and in whom an EDTA plasma sample at one month was available and their statin adherence was known.

Univariate linear regression analysis was conducted with all included covariates (tabulated here) and those variables with univariate p≤0.1 were entered into multivariable linear regression modelling, using stepwise selection, and retained in the final model if they had an adjusted p<0.05.

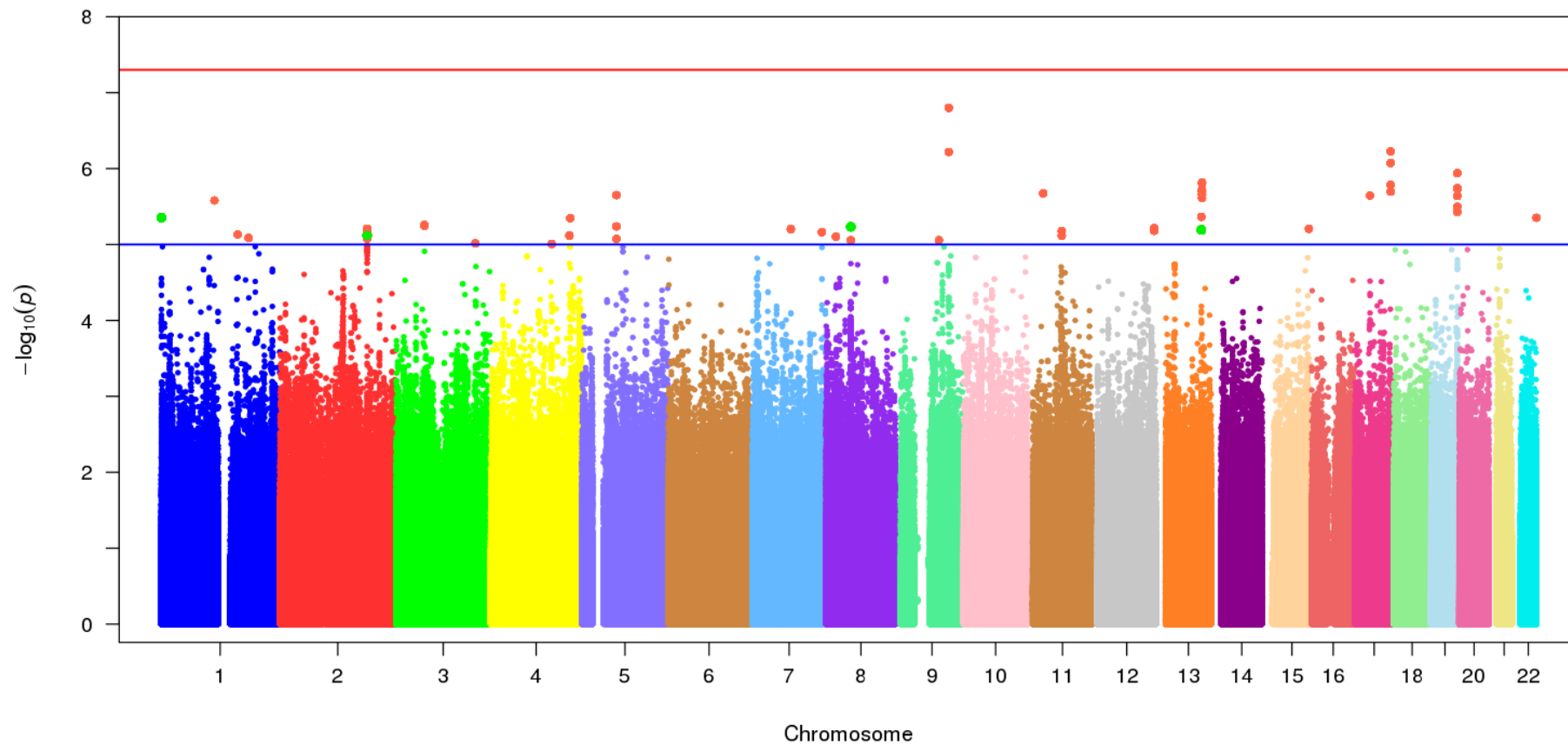
B is the unstandardized coefficient; B and standard error (SE) represent the change in log<sub>10</sub> transformed analyte concentration for a unit change in a given clinical variable, with all other variables held constant. A positive B value indicates a higher analyte concentration, and a negative B a lower level.

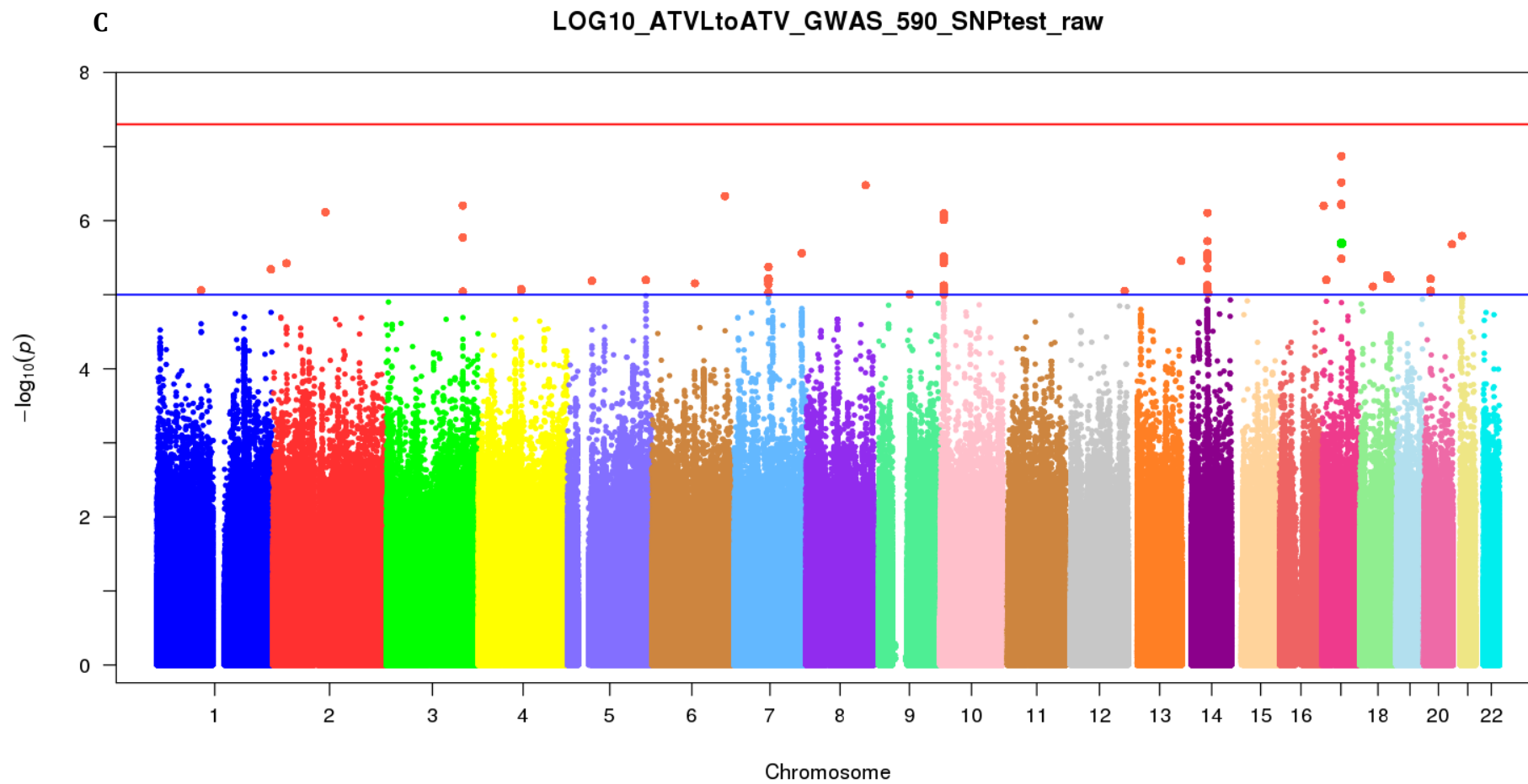
Figure 8.1 Additional Manhattan plots for the following dependent variables: 2-hydroxy ATV, 2-hydroxy ATV lactone, the total sum of all four ATV analytes, and the ratio of ATV lactone/ATV (Chapter 6)

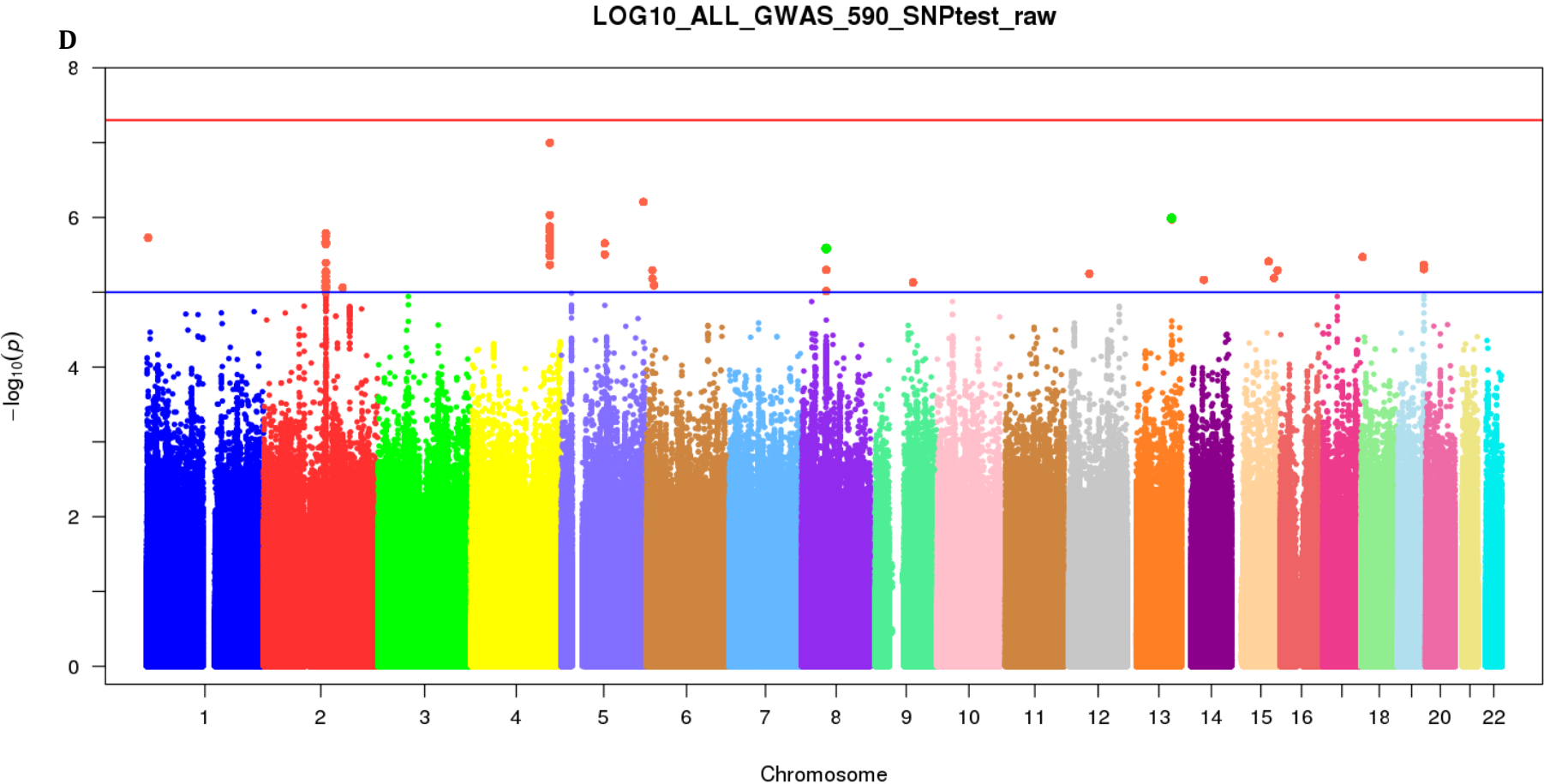


B

LOG10\_2OHATVL\_GWAS\_590\_SNPtest\_raw

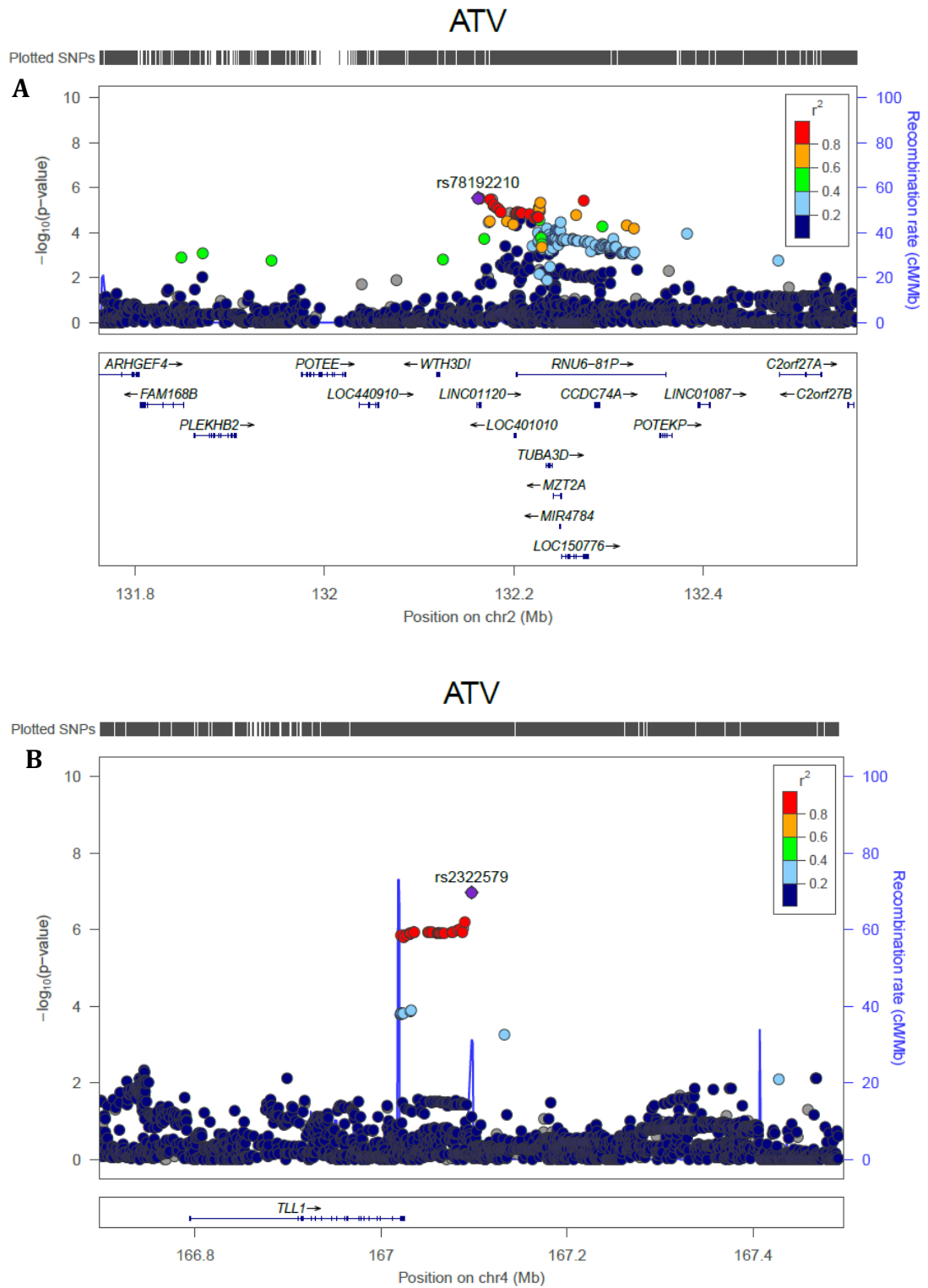


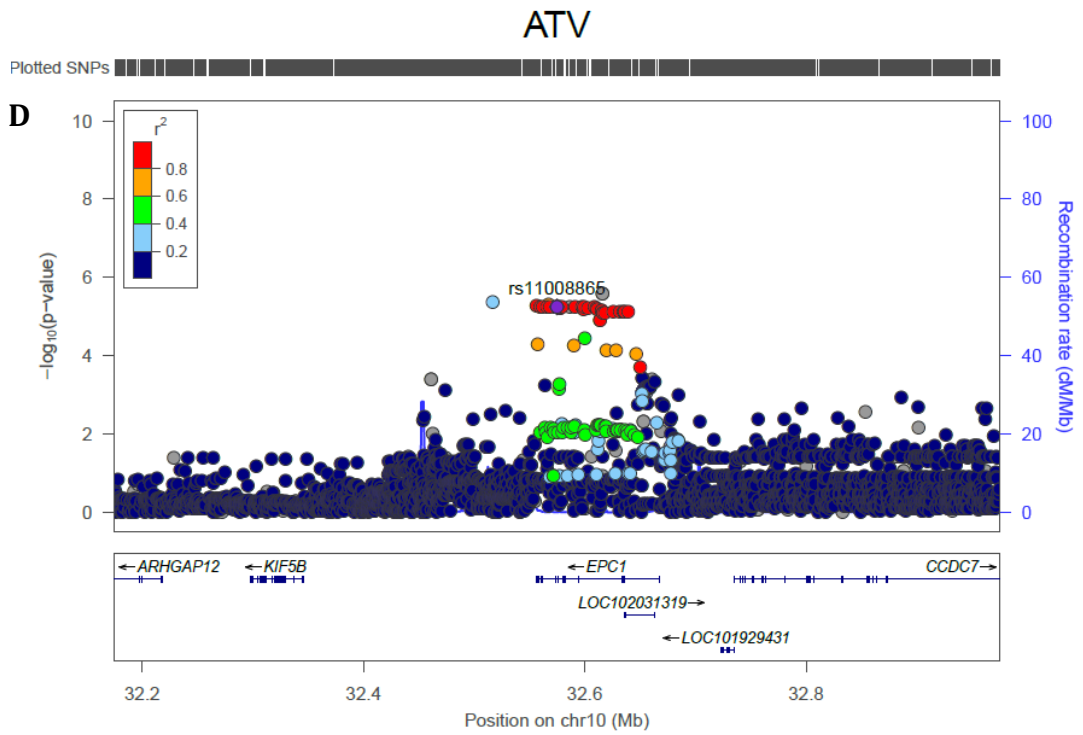
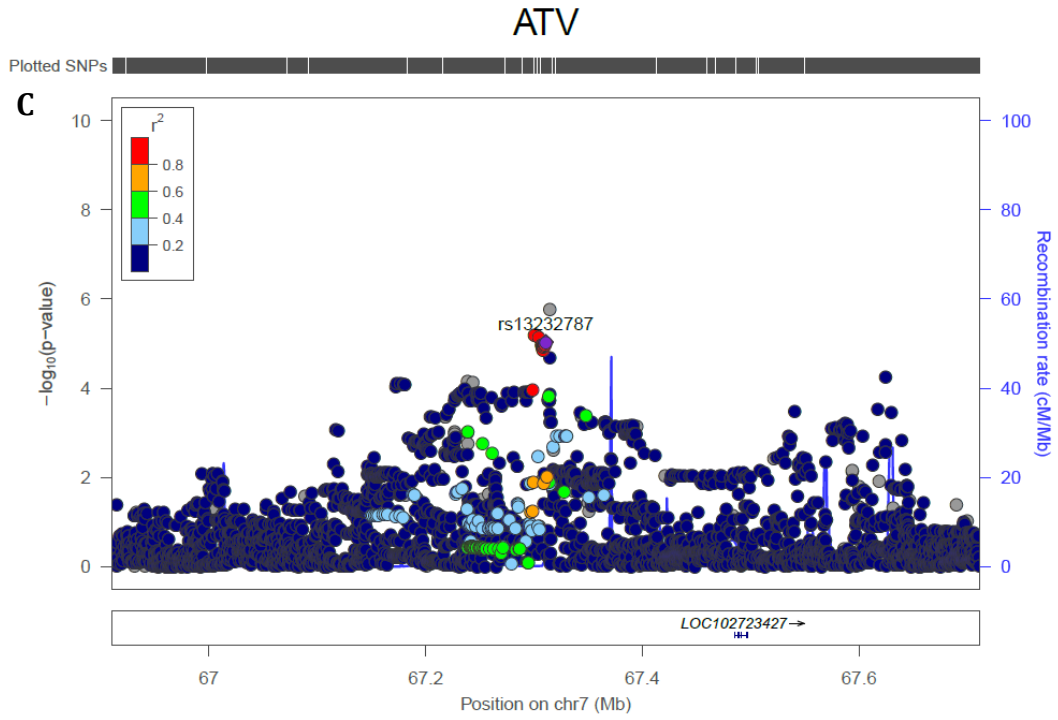


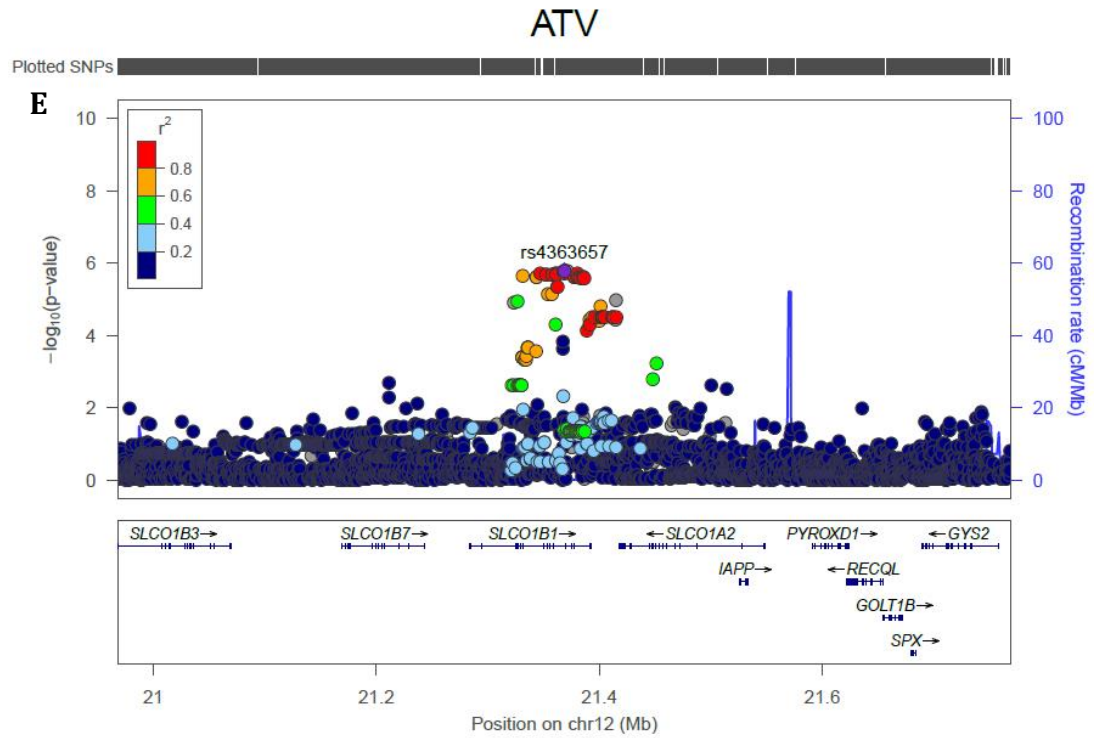


Genome-wide association analyses were carried out using  $\log_{10}$  transformed ATV analyte concentrations or ratios within the main PhACS cohort (n=590), adjusted for the first two principal components and the clinical covariates of the relevant PK endpoint multivariable linear regression model, in SNPtest v2.5 by frequentist association testing assuming an additive model of SNP effect and considering genotype dosage. A = 2-OH ATV; B = 2-OH ATV L; C = ATV L/ATV; D = ATV+2-OH ATV+ATV L+2-OH ATV L

**Figure 8.2 Regional locus plots for loci associated with atorvastatin concentration at  $p < 1.0 \times 10^{-5}$  (Chapter 6)**

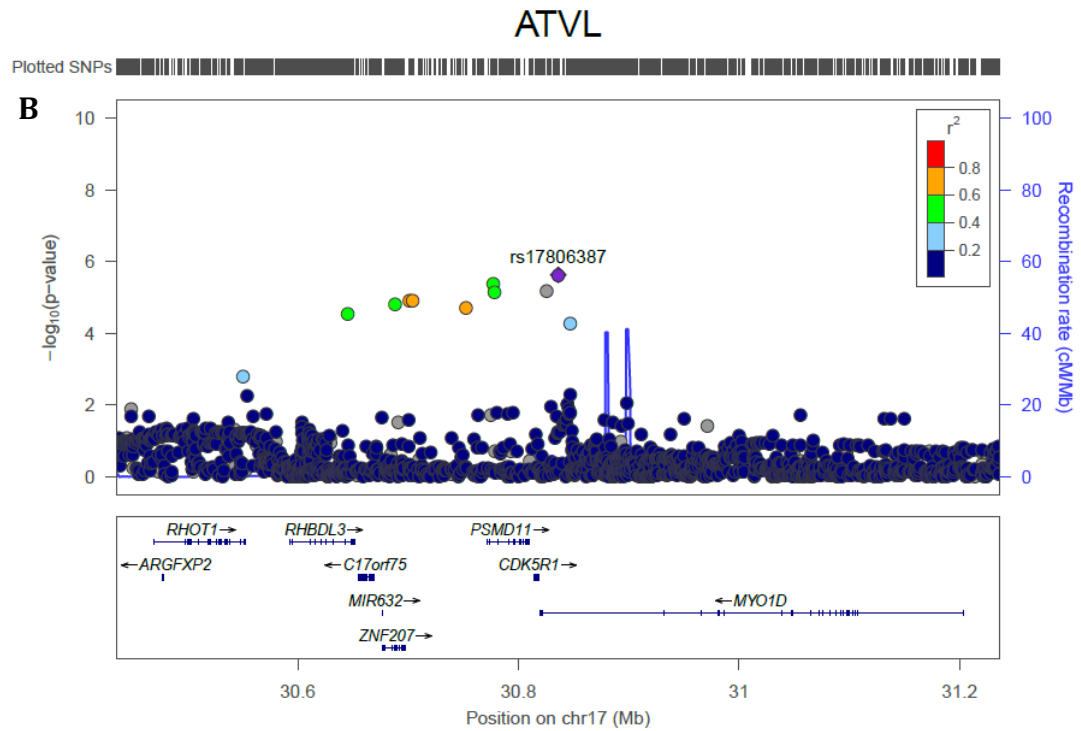
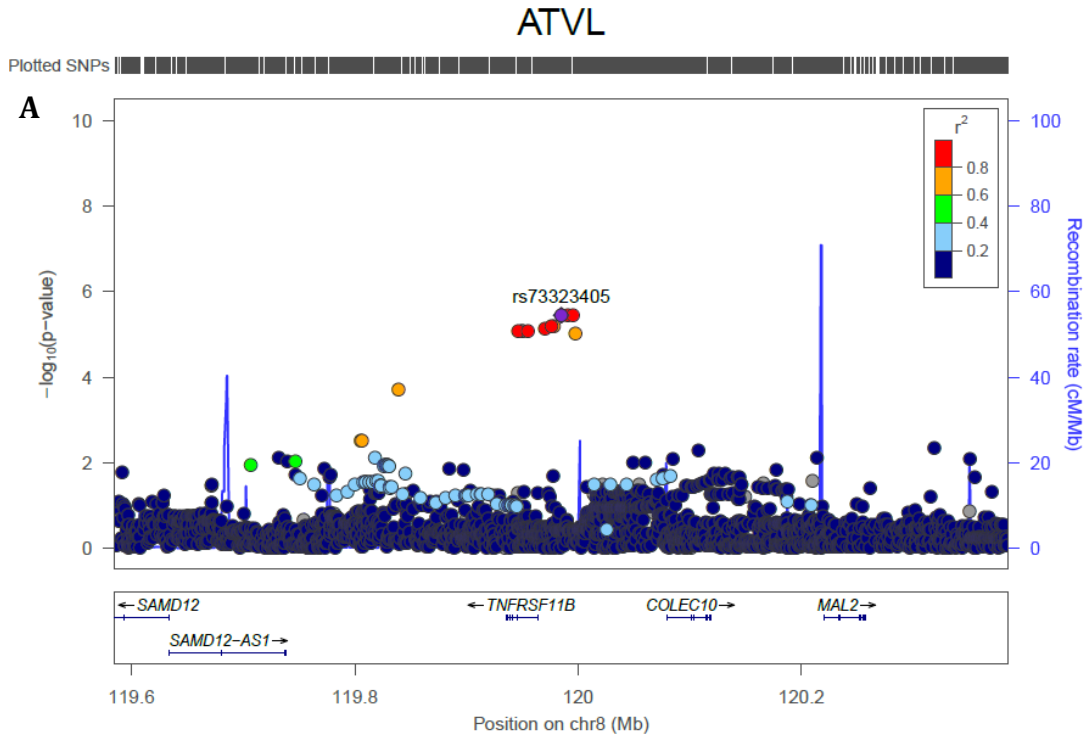


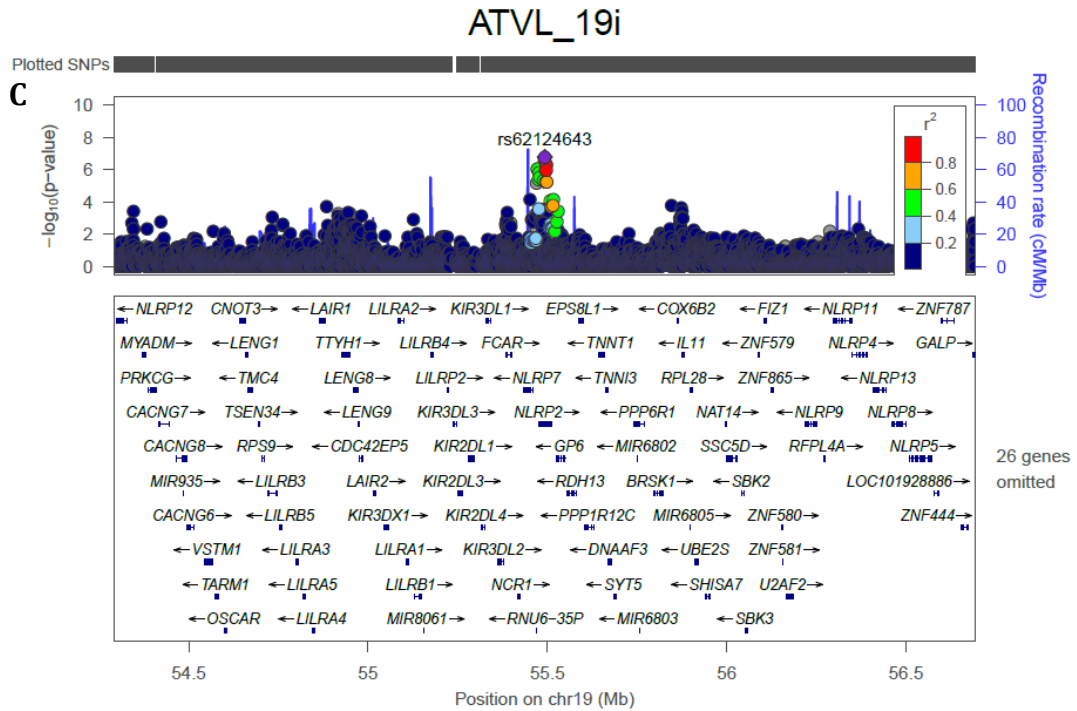




This figure shows the regional plots around the main SNP signals suggestively associated with ATV concentration at  $p < 1.0 \times 10^{-5}$  in the genome-wide association analysis using the main study cohort ( $n=590$ ). The regional plots were produced in 'Locus Zoom' using a 400Kb flanking size and linkage disequilibrium based on the 1000 Genomes Phase I 2012 European ancestry reference panel. The presented atorvastatin regional locus plots are from chromosome 2 (A), 4 (B), 7 (C), 10 (D) and 12 (E).

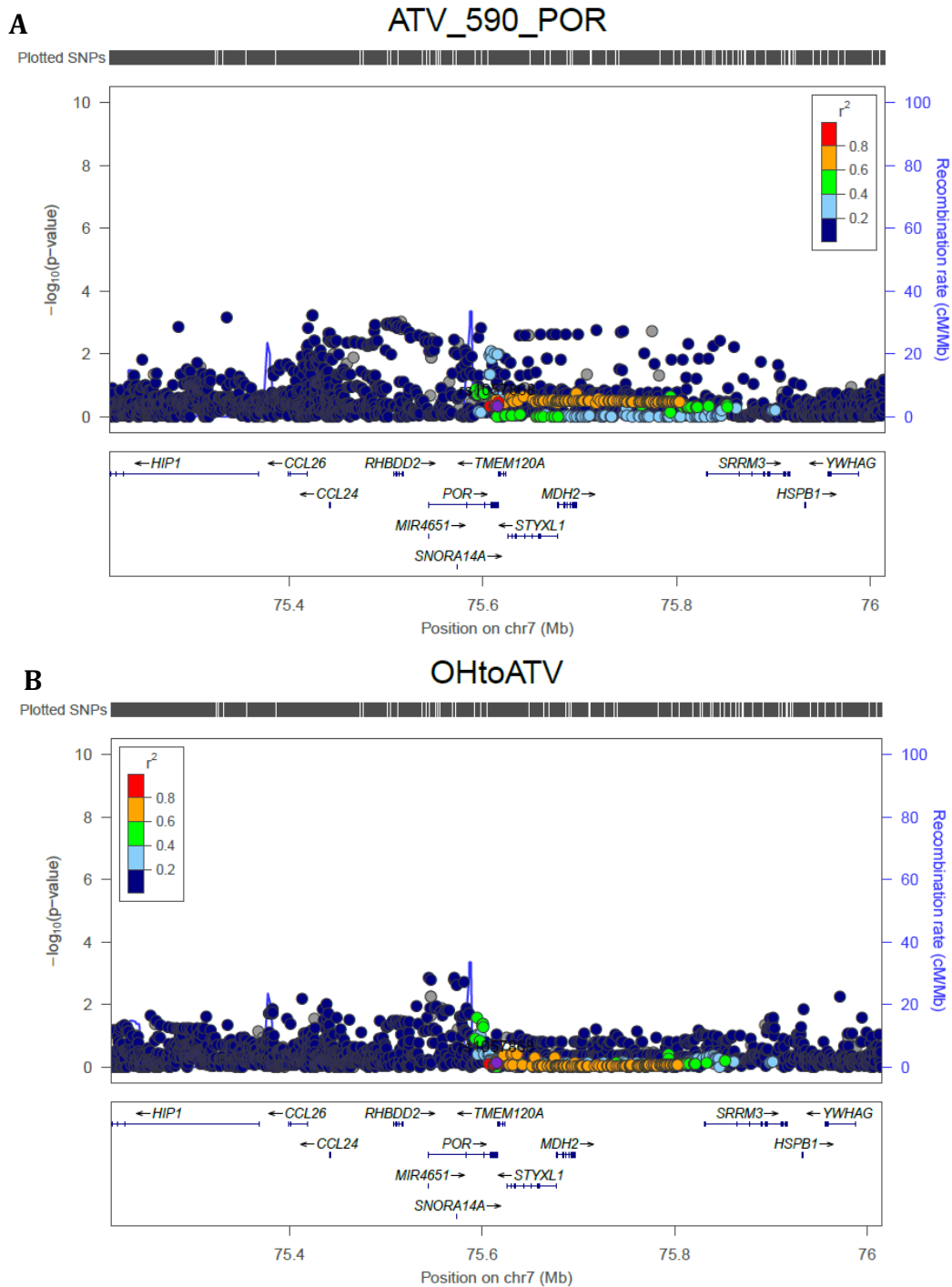
**Figure 8.3 Regional locus plots for loci associated with atorvastatin lactone concentration at  $p < 1.0 \times 10^{-5}$  (Chapter 6)**





This figure shows the regional plots around the main SNP signals suggestively associated with atorvastatin lactone concentration at  $p < 1.0 \times 10^{-5}$  in the genome-wide association analysis using the main study cohort ( $n=590$ ). The regional plots were produced in 'Locus Zoom' with linkage disequilibrium based on the 1000 Genomes Phase I 2012 European ancestry reference panel. The presented atorvastatin lactone regional locus plots are from chromosome 8 (A), 17 (B) and 19 (C).

**Figure 8.4 The lack of genetic association between P450 oxidoreductase and atorvastatin concentration or hydroxylation (Chapter 6)**



This figure shows the regional plots of P450 oxidoreductase (*POR*) from the genome-wide association analyses of atorvastatin (A) or the ratio of 2-hydroxyatorvastatin to parent atorvastatin (B) from the main study cohort (n=590). The regional plots were produced in 'Locus Zoom' with linkage disequilibrium based on the 1000 Genomes Phase I 2012 European ancestry reference panel. No SNPs in the *POR* region were associated with either PK endpoint.

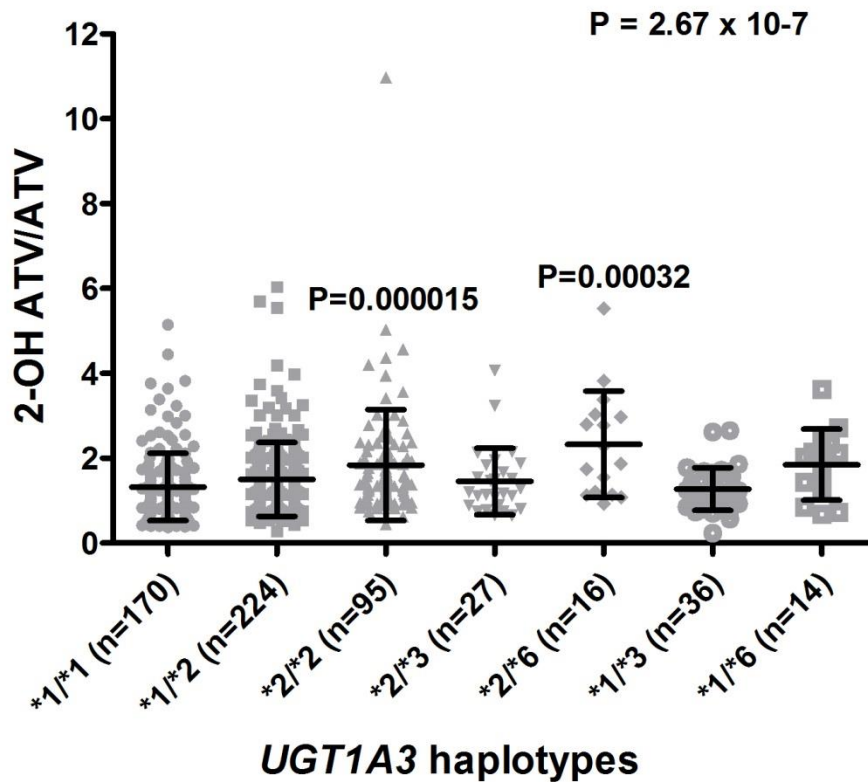
**Table 8.9 Loci with functional effects identified *in silico* and are at least suggestively associated with atorvastatin analytes**

Functional SNP	Lead SNP	LD		Chr	Function	ATV pharmacokinetics		
		r <sup>2</sup>	D'			Analysis	B (SE)	p-value
<b>Likely</b>								
rs4149056	rs4363657	0.7	0.93	12	<i>SLCO1B1</i> deleterious missense SNP (V174A) (Pasanen <i>et al.</i> , 2007)	ATV	0.127 (0.026)	2.21x10 <sup>-6</sup>
						2-OH ATV	0.110 (0.022)	1.09x10 <sup>-6</sup>
rs45446698	rs45446698	NA	NA	7	rs45446698: <i>CYP3A7</i> upregulation eQTL in adrenal gland (p=1.5x10 <sup>-8</sup> ) and transverse colon (p=7.4x10 <sup>-4</sup> ) (The GTEx Consortium, 2013) <i>CYP3A7*1C</i> includes rs45446698, and is associated with increased <i>CYP3A7</i> expression in human adult liver and intestine (Burk <i>et al.</i> , 2002)	2-OH ATV/ATV	0.154 (0.031)	6.18x10 <sup>-7</sup>
						2-OH ATV L/ATV L	0.128 (0.030)	2.91x10 <sup>-5</sup>
rs887829	rs887829	NA	NA	2	<i>UGT1A6</i> downregulation eQTL in oesophagus mucosa (p=3.0x10 <sup>-9</sup> ) (The GTEx Consortium, 2013)	2-OH ATV/ATV	0.100 (0.012)	7.25x10 <sup>-16</sup>
						2-OH ATV L/ATV L	0.096 (0.012)	3.95x10 <sup>-15</sup>
						2-OH ATV	0.068 (0.017)	8.38x10 <sup>-5</sup>
<i>UGT1A3*2</i> : rs2008584, rs1983023, rs45449995	rs887829	0.53 0.71 -	0.93 0.93 -	2	<i>UGT1A3*2</i> increases <i>UGT1A3</i> mRNA, protein and ATV lactonization (Riedmaier <i>et al.</i> , 2010)	2-OH ATV/ATV	0.066 (0.013)	4.64x10 <sup>-7</sup>
						2-OH ATV L/ATV L	0.064 (0.013)	1.00x10 <sup>-6</sup>
						2-OH ATV	0.069 (0.018)	1.11x10 <sup>-4</sup>
<b>Putative</b>								
rs78192210	rs78192210	NA	NA	2	<i>MZT2A</i> downregulation eQTL in pancreas (p=3.3x10 <sup>-6</sup> ), oesophagus muscularis & skin (The GTEx Consortium, 2013)	ATV	-0.239 (0.050)	2.85x10 <sup>-6</sup>
						TOTAL	-0.196 (0.041)	2.14x10 <sup>-6</sup>
rs11008865	rs11008865	NA	NA	10	<i>EPC1</i> eQTL in peripheral blood (Westra <i>et al.</i> , 2013)	ATV	-0.117 (0.025)	5.67x10 <sup>-6</sup>
						2-OH ATV	-0.077 (0.022)	0.000440

The suggestive loci (p<1.0x10<sup>-5</sup>) from the genome-wide association analyses of atorvastatin, atorvastatin lactone and the ratio of 2-hydroxyatorvastatin to atorvastatin were investigated further by *in silico* methods to identify nonsynonymous variants and eQTLs. All of the variants with identified functional effects are reported in this table. For these variants, their effect size and significance is shown for all PK endpoints with which they were at least modestly associated.

No functional effects could be assigned to the lead SNP (or SNPs in linkage disequilibrium with it) at the remaining suggestive loci, which were rs2322579 on chromosome 4 for atorvastatin, and rs73323405 on chromosome 8, rs17806387 on chromosome 17 and rs62124643 on chromosome 19 for atorvastatin lactone.

**Figure 8.5 The effect of *UGT1A3* haplotypes on atorvastatin hydroxylation (Chapter 6)**



The Levene statistic was used to confirm homogeneity of variance across haplotypes, and statistical significance was determined using the  $\log_{10}$  transformed ratio of 2-hydroxyatorvastatin concentration to parent atorvastatin concentration by analysis of variance (ANOVA), with post-hoc Bonferroni testing relative to \*1/\*1. Overall, the groups were statistically different ( $P=2.67 \times 10^{-7}$ ), and the \*2/\*2 and \*2/\*6 haplotypes had significantly higher ratios compared to the \*1/\*1 subgroup.

**Table 8.10 Summary of results for the effect of biologically plausible identified single nucleotide polymorphisms on all atorvastatin pharmacokinetic endpoints (Chapter 6)**

SNP	ATV	2-OH ATV	ATV L	2-OH ATV L	2-OH ATV/ ATV	2-OH ATV L/ ATV L	ATV L/ATV	TOTAL <sup>1</sup>
rs4149056 ( <i>SLCO1B1</i> )	<b>B=0.127</b> <b>SE=0.026</b> <b>P=2.21x10<sup>-6</sup></b>	<b>B=0.110</b> <b>SE=0.022</b> <b>P=1.09x10<sup>-6</sup></b>	B=0.088 SE=0.030 P=0.0032	B=0.068 SE=0.024 P=0.0042	B= -0.021 SE=0.017 P=0.22	B= -0.022 SE=0.017 P=0.19	B= -0.047 SE=0.018 P=0.0085	B=0.092 SE=0.022 P=2.58x10 <sup>-5</sup>
rs45446698 ( <i>5' CYP3A7</i> )	B= -0.204 SE=0.049 P=4.11x10 <sup>-5</sup>	B= -0.060 SE=0.042 P=0.16	B= -0.201 SE=0.055 P=0.00028	B= -0.083 SE=0.044 P=0.063	<b>B=0.154</b> <b>SE=0.031</b> <b>P=6.18x10<sup>-7</sup></b>	B=0.128 SE=0.030 P=2.91x10 <sup>-5</sup>	B=0.002 SE=0.033 P=0.94	B= -0.115 SE=0.041 P=0.0050
rs887829 ( <i>UGT1A</i> )	B= -0.032 SE=0.020 P=0.12	B=0.068 SE=0.017 P=8.38x10 <sup>-5</sup>	B= -0.059 SE=0.023 P=0.0092	B=0.035 SE=0.018 P=0.055	<b>B=0.100</b> <b>SE=0.012</b> <b>P=7.25x10<sup>-16</sup></b>	<b>B=0.096</b> <b>SE=0.012</b> <b>P=3.95x10<sup>-15</sup></b>	B= -0.030 SE=0.014 P=0.028	B=0.014 SE=0.017 P=40
<i>UGT1A3</i> *2: rs2008584, rs1983023, rs45449995	B=0.004 SE=0.021 P=0.19	B=0.069 SE=0.018 P=1.11x10 <sup>-4</sup>	B= -0.006 SE=0.023 P=0.78	B=0.054 SE=0.018 P=0.003	<b>B=0.066</b> <b>SE=0.013</b> <b>P=4.64x10<sup>-7</sup></b>	<b>B=0.064</b> <b>SE=0.013</b> <b>P=1.00x10<sup>-6</sup></b>	B= -0.012 SE=0.014 P=0.38	B=0.038 SE=0.017 P=0.028

<sup>1</sup> = ATV + 2-OH ATV + ATV L + 2-OH ATV L. Bold indicates  $p \leq 1.0 \times 10^{-5}$ . B and standard error represent the change in  $\log_{10}$  transformed analyte level for a change in genotype using an additive model, with all clinical covariates held constant; a positive B indicates an increased level and a negative B a reduced level.

## Chapter 9 References

1. Aarnio E, Korhonen M J, Huupponen R & Martikainen J 2015. Cost-effectiveness of statin treatment for primary prevention in conditions of real-world adherence--estimates from the Finnish prescription register. *Atherosclerosis*, 239, 240-7.
2. Ab Sciex. 2012. The AB SCIEX Triple Quad™ 6500 and QTRAP® 6500 Systems for Bioanalysis – A New Level of Sensitivity (Online). Available: <http://www.absciex-korea.com/Documents/Downloads/Literature/6500%20System%20for%20High%20Sensitivity%20Bioanalysis%20TN%205780212-01.pdf> (Accessed 15 March 2017).
3. Abcam. 2017. Product datasheet for Anti-P Glycoprotein antibody [EPR10364-57] ab170904 (Online). Available: <http://www.abcam.com/p-glycoprotein-antibody-epr10364-57-ab170904.html> (Accessed 3 May 2017).
4. Abd T T & Jacobson T A 2011. Statin-induced myopathy: a review and update. *Expert Opin Drug Saf*, 10, 373-87.
5. Actavis UK Ltd. 2016. Simvastatin (Online). Available: <https://www.medicines.org.uk/emc/medicine/24536> (Accessed 17 November 2017).
6. Agrawal V, Choi J H, Giacomini K M & Miller W L 2010. Substrate-specific modulation of CYP3A4 activity by genetic variants of cytochrome P450 oxidoreductase. *Pharmacogenet Genomics*, 20, 611-8.
7. Ahmed W, Khan N, Glueck C J, Pandey S, Wang P, Goldenberg N, Uppal M & Khanal S 2009. Low serum 25 (OH) vitamin D levels (<32 ng/mL) are associated with reversible myositis-myalgia in statin-treated patients. *Transl Res*, 153, 11-6.
8. Akingbasote J A, Foster A J, Jones H B, David R, Gooderham N J, Wilson I D & Kenna J G 2017. Improved hepatic physiology in hepatic cytochrome P450 reductase null (HRN[trade mark sign]) mice dosed orally with fenclizic acid. *Toxicology Research*, 6, 81-88.
9. Akingbasote J A, Foster A J, Wilson I, Sarda S, Jones H B & Kenna J G 2016. Hepatic effects of repeated oral administration of diclofenac to hepatic cytochrome P450 reductase null (HRN) and wild-type mice. *Arch Toxicol*, 90, 853-62.
10. Alakhali K, Hassan Y, Mohamed N & Mordi M N 2013. Pharmacokinetic of simvastatin study in Malaysian subjects. *ISOR Journal of Pharmacy*, 3, 46-51.
11. Alfirevic A, Neely D, Armitage J, Chinoy H, Cooper R G, Laaksonen R, Carr D F, Bloch K M, Fahy J, Hanson A, Yue Q Y, Wadelius M, Maitland-Van Der Zee A H, Voora D, Psaty B M, Palmer C N & Pirmohamed M 2014. Phenotype standardization for statin-induced myotoxicity. *Clin Pharmacol Ther*, 96, 470-6.
12. Altshuler D M, Gibbs R A, Peltonen L, Altshuler D M, Gibbs R A, Dermitzakis E, Schaffner S F, Yu F, Peltonen L, Dermitzakis E, Bonnen P E, Altshuler D M, Gibbs R A, De Bakker P I, Deloukas P, Gabriel S B, Gwilliam R, Hunt S, Inouye M, Jia X, Palotie A, Parkin M, Whittaker P, Yu F, Chang K, Hawes A, Lewis L R, Ren Y, Wheeler D, Gibbs R A, Muzny D M, Barnes C, Darvishi K, Hurles M, Korn J M, Kristiansson K, Lee C, Mccarroll S A, Nemes J, Dermitzakis E, Keinan A, Montgomery S B, Pollack S, Price A L, Soranzo N, Bonnen P E, Gibbs R A, Gonzaga-Jauregui C, Keinan A, Price A L, Yu F, Anttila V, Brodeur W, Daly M J, Leslie S, Mcvean G, Moutsianas L, Nguyen H, Schaffner S F, Zhang Q, Ghorji M J, McGinnis R, McLaren W, Pollack S, Price A L, Schaffner S F, Takeuchi F, Grossman S R, Shlyakhter I, Hostetter E B, Sabeti P C, Adebamowo C A, Foster M W, Gordon D R, Licinio J, Manca M C, Marshall P A, Matsuda I, Ngare D, Wang V O, Reddy D, Rotimi C N, Royal C D, Sharp R R, Zeng C, Brooks L D & McEwen J E 2010. Integrating common and rare genetic variation in diverse human populations. *Nature*, 467, 52-8.
13. Amundsen R, Asberg A, Ohm I K & Christensen H 2012. Cyclosporine A- and tacrolimus-mediated inhibition of CYP3A4 and CYP3A5 in vitro. *Drug Metab Dispos*, 40, 655-61.
14. Anderson C A, Pettersson F H, Clarke G M, Cardon L R, Morris A P & Zondervan K T 2010. Data quality control in genetic case-control association studies. *Nature protocols*, 5, 1564-1573.
15. Ando H, Tsuruoka S, Yanagihara H, Sugimoto K, Miyata M, Yamazoe Y, Takamura T, Kaneko S & Fujimura A 2005. Effects of grapefruit juice on the pharmacokinetics of pitavastatin and atorvastatin. *Br J Clin Pharmacol*, 60, 494-7.
16. Andrade S E, Walker A M, Gottlieb L K, Hollenberg N K, Testa M A, Saperia G M & Platt R 1995. Discontinuation of antihyperlipidemic drugs--do rates reported in clinical trials reflect rates in primary care settings? *N Engl J Med*, 332, 1125-31.
17. Antley R & Bixler D 1975. Trapezoidocephaly, midfacial hypoplasia and cartilage abnormalities with multiple synostoses and skeletal fractures. *Birth Defects Orig Artic Ser*, 11, 397-401.
18. Appel-Dingemanse S, Smith T & Merz M 2002. Pharmacokinetics of fluvastatin in subjects with renal impairment and nephrotic syndrome. *J Clin Pharmacol*, 42, 312-8.
19. Arca M & Gaspardone A 2007. Atorvastatin efficacy in the primary and secondary prevention of cardiovascular events. *Drugs*, 67 Suppl 1, 29-42.

20. Arlt W, Walker E A, Draper N, Ivison H E, Ride J P, Hammer F, Chalder S M, Borucka-Mankiewicz M, Hauffa B P, Malunowicz E M, Stewart P M & Shackleton C H 2004. Congenital adrenal hyperplasia caused by mutant P450 oxidoreductase and human androgen synthesis: analytical study. *Lancet*, 363, 2128-35.
21. Armitage J 2007. The safety of statins in clinical practice. *Lancet*, 370, 1781-90.
22. Astrazeneca. 2009. Crestor highlights of prescribing information (Online). Available: [http://www.accessdata.fda.gov/drugsatfda\\_docs/label/2009/021366s015lbl.pdf](http://www.accessdata.fda.gov/drugsatfda_docs/label/2009/021366s015lbl.pdf) (Accessed 22 April 2016).
23. Astrazeneca. 2010. Crestor (rosuvastatin calcium tablets) - highlights of prescribing information (Online). FDA. Available: [http://www.accessdata.fda.gov/drugsatfda\\_docs/label/2010/021366s016lbl.pdf](http://www.accessdata.fda.gov/drugsatfda_docs/label/2010/021366s016lbl.pdf) (Accessed 7 July 2016).
24. Backman J T, Kyrklund C, Kivisto K T, Wang J S & Neuvonen P J 2000. Plasma concentrations of active simvastatin acid are increased by gemfibrozil. *Clin Pharmacol Ther*, 68, 122-9.
25. Backman J T, Luurila H, Neuvonen M & Neuvonen P J 2005. Rifampin markedly decreases and gemfibrozil increases the plasma concentrations of atorvastatin and its metabolites. *Clin Pharmacol Ther*, 78, 154-67.
26. Bailey D G, Malcolm J, Arnold O & David Spence J 1998. Grapefruit juice–drug interactions. *British Journal of Clinical Pharmacology*, 46, 101-110.
27. Bakar N S, Neely D, Avery P, Brown C, Daly A K & Kamali F 2017. Genetic and Clinical Factors Are Associated With Statin-Related Myotoxicity of Moderate Severity: A Case-Control Study. *Clin Pharmacol Ther*.
28. Banach M, Serban C, Sahebkar A, Ursoniu S, Rysz J, Muntner P, Toth P P, Jones S R, Rizzo M, Glasser S P, Lip G Y, Dragan S & Mikhailidis D P 2015. Effects of coenzyme Q10 on statin-induced myopathy: a meta-analysis of randomized controlled trials. *Mayo Clin Proc*, 90, 24-34.
29. Bar S L, Holmes D T & Frohlich J 2007. Asymptomatic hypothyroidism and statin-induced myopathy. *Canadian Family Physician*, 53, 428-431.
30. Barkas F, Elisaf M, Rizos C V, Klouras E, Kostapanos M S & Liberopoulos E 2015. Proton pump inhibitors and statins: a possible interaction that favors low-density lipoprotein cholesterol reduction? *Hippokratia*, 19, 332-337.
31. Barrett J C, Fry B, Maller J & Daly M J 2005. Haploview: analysis and visualization of LD and haplotype maps. *Bioinformatics*, 21, 263-5.
32. Bates E R, Lau W C & Angiolillo D J 2011. Clopidogrel–Drug Interactions. *Journal of the American College of Cardiology*, 57, 1251-1263.
33. Becker M L, Visser L E, Van Schaik R H, Hofman A, Uitterlinden A G & Stricker B H 2010. Influence of genetic variation in CYP3A4 and ABCB1 on dose decrease or switching during simvastatin and atorvastatin therapy. *Pharmacoepidemiol Drug Saf*, 19, 75-81.
34. Benner J S, Glynn R J, Mogun H, Neumann P J, Weinstein M C & Avorn J 2002. Long-term persistence in use of statin therapy in elderly patients. *Jama*, 288, 455-61.
35. Berglund E, Lytsy P & Westerling R 2013. Adherence to and beliefs in lipid-lowering medical treatments: a structural equation modeling approach including the necessity-concern framework. *Patient Educ Couns*, 91, 105-12.
36. Birmingham B K, Bujac S R, Azumaya C T, Zalikowski J, Chen Y, Kim K & Ambrose H J 2015. Rosuvastatin pharmacokinetics and pharmacogenetics in Caucasian and Asian subjects residing in the United States. *Eur J Clin Pharmacol*, 71, 329-40.
37. Black A E, Sinz M W, Hayes R N & Woolf T F 1998. Metabolism and excretion studies in mouse after single and multiple oral doses of the 3-hydroxy-3-methylglutaryl-CoA reductase inhibitor atorvastatin. *Drug Metab Dispos*, 26, 755-63.
38. Blackburn D F, Dobson R T, Blackburn J L & Wilson T W 2005a. Cardiovascular morbidity associated with nonadherence to statin therapy. *Pharmacotherapy*, 25, 1035-43.
39. Blackburn D F, Dobson R T, Blackburn J L, Wilson T W, Stang M R & Semchuk W M 2005b. Adherence to statins, beta-blockers and angiotensin-converting enzyme inhibitors following a first cardiovascular event: a retrospective cohort study. *Can J Cardiol*, 21, 485-8.
40. Boehm A M, Putz S, Altenhofer D, Sickmann A & Falk M 2007. Precise protein quantification based on peptide quantification using iTRAQ. *BMC Bioinformatics*, 8, 214.
41. Boggs J W, Hop C E, Mcnamara E, Deng Y, Messick K, West K & Choo E F 2014. Assessment of the hepatic CYP reductase null mouse model and its potential application in drug discovery. *Mol Pharm*, 11, 1062-8.
42. Bonifacio A, Sanvee G M, Bouitbir J & Krähenbühl S 2015. The AKT/mTOR signaling pathway plays a key role in statin-induced myotoxicity. *Biochimica et Biophysica Acta (BBA) - Molecular Cell Research*, 1853, 1841-1849.
43. Bristol-Myers Squibb Company. 2009. Plavix clopidogrel bisulfate tablets product information (Online). Available: [http://www.accessdata.fda.gov/drugsatfda\\_docs/label/2009/020839s044lbl.pdf](http://www.accessdata.fda.gov/drugsatfda_docs/label/2009/020839s044lbl.pdf) (Accessed 14 March 2017).
44. Bristol-Myers Squibb Company. 2013. Pravachol (pravastatin) tablets - highlights of prescribing information (Online). Available: [http://packageinserts.bms.com/pi/pi\\_pravachol.pdf](http://packageinserts.bms.com/pi/pi_pravachol.pdf) (Accessed 7 July 2016).

45. Bruckert E, Hayem G, Dejager S, Yau C & Begaud B 2005. Mild to moderate muscular symptoms with high-dosage statin therapy in hyperlipidemic patients--the PRIMO study. *Cardiovasc Drugs Ther*, 19, 403-14.
46. Brunham L R, Lansberg P J, Zhang L, Miao F, Carter C, Hovingh G K, Visscher H, Jukema J W, Stalenhoef A F, Ross C J, Carleton B C, Kastelein J J & Hayden M R 2012. Differential effect of the rs4149056 variant in SLCO1B1 on myopathy associated with simvastatin and atorvastatin. *Pharmacogenomics J*, 12, 233-7.
47. Bullen W W, Miller R A & Hayes R N 1999. Development and validation of a high-performance liquid chromatography tandem mass spectrometry assay for atorvastatin, ortho-hydroxy atorvastatin, and para-hydroxy atorvastatin in human, dog, and rat plasma. *J Am Soc Mass Spectrom*, 10, 55-66.
48. Burk O, Tegude H, Koch I, Hustert E, Wolbold R, Glaeser H, Klein K, Fromm M F, Nuessler A K, Neuhaus P, Zanger U M, Eichelbaum M & Wojnowski L 2002. Molecular mechanisms of polymorphic CYP3A7 expression in adult human liver and intestine. *J Biol Chem*, 277, 24280-8.
49. Burnett J E 2011. Dried blood spot sampling: practical considerations and recommendation for use with preclinical studies. *Bioanalysis*, 3, 1099-107.
50. Callier V. 2017. Genetic test helps people avoid statins that may cause them pain (Online). New Scientist. Available: <https://www.newscientist.com/article/2144394-genetic-test-helps-people-avoid-statins-that-may-cause-them-pain/> (Accessed 17 November 2017).
51. Camm A J & Bunce N H 2012. Chapter 14: Cardiovascular disease. In: Kumar P & Clark M (eds.) *Clinical Medicine*. 8 ed.
52. Canestaro W J, Austin M A & Thummel K E 2014. Genetic factors affecting statin concentrations and subsequent myopathy: a HuGENet systematic review. *Genet Med*, 16, 810-9.
53. Canet M J, Merrell M D, Hardwick R N, Bataille A M, Campion S N, Ferreira D W, Xanthakos S A, Manautou J E, Hesham a-Kader H, Erickson R P & Cherrington N J 2015. Altered Regulation of Hepatic Efflux Transporters Disrupts Acetaminophen Disposition in Pediatric Nonalcoholic Steatohepatitis. *Drug Metabolism and Disposition*, 43, 829-835.
54. Cannon C P, Braunwald E, McCabe C H, Rader D J, Rouleau J L, Belder R, Joyal S V, Hill K A, Pfeffer M A & Skene A M 2004. Intensive versus moderate lipid lowering with statins after acute coronary syndromes. *N Engl J Med*, 350, 1495-504.
55. Cao P, Hanai J-I, Tanksale P, Imamura S, Sukhatme V P & Lecker S H 2009. Statin-induced muscle damage and atrogen-1 induction is the result of a geranylgeranylation defect. *The FASEB Journal*, 23, 2844-2854.
56. Capiou S, Stove V V, Lambert W E & Stove C P 2013. Prediction of the hematocrit of dried blood spots via potassium measurement on a routine clinical chemistry analyzer. *Anal Chem*, 85, 404-10.
57. Carr D F, O'meara H, Jorgensen A L, Campbell J, Hobbs M, Mccann G, Van Staa T & Pirmohamed M 2013. SLCO1B1 genetic variant associated with statin-induced myopathy: a proof-of-concept study using the clinical practice research datalink. *Clin Pharmacol Ther*, 94, 695-701.
58. Caso G, Kelly P, Mcnurlan M A & Lawson W E 2007. Effect of coenzyme q10 on myopathic symptoms in patients treated with statins. *Am J Cardiol*, 99, 1409-12.
59. Cassol S, Salas T, Gill M J, Montpetit M, Rudnik J, Sy C T & O'shaughnessy M V 1992. Stability of dried blood spot specimens for detection of human immunodeficiency virus DNA by polymerase chain reaction. *J Clin Microbiol*, 30, 3039-42.
60. Casula M, Tragni E & Catapano A L 2012. Adherence to lipid-lowering treatment: the patient perspective. *Patient preference and adherence*, 6, 805-814.
61. Catapano A L 2010. Pitavastatin - pharmacological profile from early phase studies. *Atheroscler Suppl*, 11, 3-7.
62. Ceckova-Novotna M, Pavek P & Staud F 2006. P-glycoprotein in the placenta: expression, localization, regulation and function. *Reprod Toxicol*, 22, 400-10.
63. Chace D H 2009. Mass spectrometry in newborn and metabolic screening: historical perspective and future directions. *J Mass Spectrom*, 44, 163-70.
64. Chan D C, Shrank W H, Cutler D, Jan S, Fischer M A, Liu J, Avorn J, Solomon D, Brookhart M A & Choudhry N K 2010. Patient, physician, and payment predictors of statin adherence. *Med Care*, 48, 196-202.
65. Chanson N, Bossi P, Schneider L, Bourry E & Izzedine H 2008. Rhabdomyolysis after ezetimibe/simvastatin therapy in an HIV-infected patient. *NDT Plus*, 1, 157-161.
66. Charland S L, Agatep B C, Herrera V, Schrader B, Frueh F W, Ryvkin M, Shabbeer J, Devlin J J, Superko H R & Stanek E J 2014. Providing patients with pharmacogenetic test results affects adherence to statin therapy: results of the Additional KIF6 Risk Offers Better Adherence to Statins (AKROBATS) trial. *Pharmacogenomics J*, 14, 272-80.
67. Chen G, Ramos E, Adeyemo A, Shriner D, Zhou J, Doumatey A P, Huang H, Erdos M R, Gerry N P, Herbert A, Bentley A R, Xu H, Charles B A, Christman M F & Rotimi C N 2012a. UGT1A1 is a major locus influencing bilirubin levels in African Americans. *Eur J Hum Genet*, 20, 463-8.
68. Chen X, Zhao H, Hatsis P & Amin J 2012b. Investigation of dried blood spot card-induced interferences in liquid chromatography/mass spectrometry. *J Pharm Biomed Anal*, 61, 30-7.
69. Chen Y, Zhang W, Huang W H, Tan Z R, Wang Y C, Huang X & Zhou H H 2013. Effect of a single-dose rifampin on the pharmacokinetics of pitavastatin in healthy volunteers. *Eur J Clin Pharmacol*, 69, 1933-8.

70. Cheng C H, Miller C, Lowe C & Pearson V E 2002. Rhabdomyolysis due to probable interaction between simvastatin and ritonavir. *Am J Health Syst Pharm*, 59, 728-30.
71. Cheng X, Zhang Y & Klaassen C D 2014. Decreased Bile-Acid Synthesis in Livers of Hepatocyte-Conditional NADPH–Cytochrome P450 Reductase–Null Mice Results in Increased Bile Acids in Serum. *The Journal of Pharmacology and Experimental Therapeutics*, 351, 105-113.
72. Cho S K, Oh E S, Park K, Park M S & Chung J Y 2012. The UGT1A3\*2 polymorphism affects atorvastatin lactonization and lipid-lowering effect in healthy volunteers. *Pharmacogenet Genomics*, 22, 598-605.
73. Choi H Y, Bae K S, Cho S H, Ghim J L, Choe S, Jung J A, Jin S J, Kim H S & Lim H S 2015. Impact of CYP2D6, CYP3A5, CYP2C19, CYP2A6, SLCO1B1, ABCB1, and ABCG2 gene polymorphisms on the pharmacokinetics of simvastatin and simvastatin acid. *Pharmacogenet Genomics*, 25, 595-608.
74. Cholesterol Treatment Trialists C 2010. Efficacy and safety of more intensive lowering of LDL cholesterol: a meta-analysis of data from 170 000 participants in 26 randomised trials. *Lancet*, 376, 1670-1681.
75. Cholesterol Treatment Trialists C 2012. The effects of lowering LDL cholesterol with statin therapy in people at low risk of vascular disease: meta-analysis of individual data from 27 randomised trials. *Lancet*, 380, 581-590.
76. Cholesterol Treatment Trialists Collaboration 1995. Protocol for a prospective collaborative overview of all current and planned randomized trials of cholesterol treatment regimens. Cholesterol Treatment Trialists' (CTT) Collaboration. *Am J Cardiol*, 75, 1130-4.
77. Christopher-Stine L, Casciola-Rosen L A, Hong G, Chung T, Corse A M & Mammen A L 2010. A novel autoantibody recognizing 200-kd and 100-kd proteins is associated with an immune-mediated necrotizing myopathy. *Arthritis Rheum*, 62, 2757-66.
78. Cilla D D, Jr., Gibson D M, Whitfield L R & Sedman A J 1996. Pharmacodynamic effects and pharmacokinetics of atorvastatin after administration to normocholesterolemic subjects in the morning and evening. *J Clin Pharmacol*, 36, 604-9.
79. Clark D W & Strandell J 2006. Myopathy including polymyositis: a likely class adverse effect of proton pump inhibitors? *Eur J Clin Pharmacol*, 62, 473-9.
80. Clarke W 2017. Chapter 1 - Mass spectrometry in the clinical laboratory: determining the need and avoiding pitfalls. *Mass Spectrometry for the Clinical Laboratory*. San Diego: Academic Press.
81. Clinical Gene Networks. 2012. Market analysis (Online). Available: <http://cgnetworks.se/page/market/> (Accessed 9 November 2016).
82. Clinicaltrials.Gov. 2017. STATIN: Web-based Investigation of Side Effects (STATINWISE) (Online). Available: [https://clinicaltrials.gov/ct2/show/study/NCT02781064?show\\_desc=Y#desc](https://clinicaltrials.gov/ct2/show/study/NCT02781064?show_desc=Y#desc) (Accessed 2 October 2017).
83. Clinrisk Ltd. 2014. QStatin - 2014 update information (Online). Available: <http://qintervention.org/QStatin-2014-Update-Information.pdf> (Accessed 24 July 2017).
84. Cobb Z, De Vries R, Spooner N, Williams S, Staelens L, Doig M, Broadhurst R, Barfield M, Van De Merbel N, Schmid B, Siethoff C, Ortiz J, Verheij E, Van Baar B, White S & Timmerman P 2013. In-depth study of homogeneity in DBS using two different techniques: results from the EBF DBS-microsampling consortium. *Bioanalysis*, 5, 2161-9.
85. Cohen J W & Krauss N A 2003. Spending and service use among people with the fifteen most costly medical conditions, 1997. *Health Aff (Millwood)*, 22, 129-38.
86. Colivicchi F, Bassi A, Santini M & Caltagirone C 2007. Discontinuation of statin therapy and clinical outcome after ischemic stroke. *Stroke*, 38, 2652-7.
87. Colivicchi F, Tubaro M & Santini M 2011. Clinical implications of switching from intensive to moderate statin therapy after acute coronary syndromes. *Int J Cardiol*, 152, 56-60.
88. Collins R, Reith C, Emberson J, Armitage J, Baigent C, Blackwell L, Blumenthal R, Danesh J, Smith G D, Demets D, Evans S, Law M, Macmahon S, Martin S, Neal B, Poulter N, Preiss D, Ridker P, Roberts I, Rodgers A, Sandercock P, Schulz K, Sever P, Simes J, Smeeth L, Wald N, Yusuf S & Peto R 2016. Interpretation of the evidence for the efficacy and safety of statin therapy. *Lancet*.
89. Cooper K J, Martin P D, Dane A L, Warwick M J, Raza A & Schneck D W 2003a. The effect of erythromycin on the pharmacokinetics of rosuvastatin. *Eur J Clin Pharmacol*, 59, 51-6.
90. Cooper K J, Martin P D, Dane A L, Warwick M J, Raza A & Schneck D W 2003b. Lack of effect of ketoconazole on the pharmacokinetics of rosuvastatin in healthy subjects. *British Journal of Clinical Pharmacology*, 55, 94-99.
91. Cooper K J, Martin P D, Dane A L, Warwick M J, Schneck D W & Cantarini M V 2002. The effect of fluconazole on the pharmacokinetics of rosuvastatin. *Eur J Clin Pharmacol*, 58, 527-31.
92. Cooper K J, Martin P D, Dane A L, Warwick M J, Schneck D W & Cantarini M V 2003c. Effect of itraconazole on the pharmacokinetics of rosuvastatin. *Clin Pharmacol Ther*, 73, 322-9.
93. Cox A J, Ng M C, Xu J, Langefeld C D, Koch K L, Dawson P A, Carr J J, Freedman B I, Hsu F C & Bowden D W 2013. Association of SNPs in the UGT1A gene cluster with total bilirubin and mortality in the Diabetes Heart Study. *Atherosclerosis*, 229, 155-60.

94. D'ariento C J, Ji Q C, Discenza L, Cornelius G, Hynes J, Cornelius L, Santella J B & Olah T 2010. DBS sampling can be used to stabilize prodrugs in drug discovery rodent studies without the addition of esterase inhibitors. *Bioanalysis*, 2, 1415-22.
95. Dainty T C, Richmond E S, Davies I & Blackwell M P 2012. Dried blood spot bioanalysis: an evaluation of techniques and opportunities for reduction and refinement in mouse and juvenile rat toxicokinetic studies. *Int J Toxicol*, 31, 4-13.
96. Danik J S, Chasman D I, Macfadyen J G, Nyberg F, Barratt B J & Ridker P M 2013. Lack of association between SLCO1B1 polymorphisms and clinical myalgia following rosuvastatin therapy. *Am Heart J*, 165, 1008-14.
97. Daskalopoulou S S, Delaney J A, Filion K B, Brophy J M, Mayo N E & Suissa S 2008. Discontinuation of statin therapy following an acute myocardial infarction: a population-based study. *Eur Heart J*, 29, 2083-91.
98. Davidson M H & Robinson J G 2007. Safety of aggressive lipid management. *J Am Coll Cardiol*, 49, 1753-62.
99. Davies E C, Green C F, Taylor S, Williamson P R, Mottram D R & Pirmohamed M 2009. Adverse drug reactions in hospital in-patients: a prospective analysis of 3695 patient-episodes. *PLoS One*, 4, e4439.
100. Dawson P A, Lan T & Rao A 2009. Bile acid transporters. *Journal of Lipid Research*, 50, 2340-2357.
101. De Jonge H, Metalidis C, Naesens M, Lambrechts D & Kuypers D R 2011. The P450 oxidoreductase \*28 SNP is associated with low initial tacrolimus exposure and increased dose requirements in CYP3A5-expressing renal recipients. *Pharmacogenomics*, 12, 1281-91.
102. De Keyser C E, Peters B J, Becker M L, Visser L E, Uitterlinden A G, Klungel O H, Verstuyft C, Hofman A, Maitland-Van Der Zee A H & Stricker B H 2014. The SLCO1B1 c.521T>C polymorphism is associated with dose decrease or switching during statin therapy in the Rotterdam Study. *Pharmacogenet Genomics*, 24, 43-51.
103. De Luca L, Leonardi S, Cavallini C, Lucci D, Musumeci G, Caporale R, Abrignani M G, Lupi A, Rakar S, Gulizia M M, Bovenzi F M & De Servi S 2014. Contemporary antithrombotic strategies in patients with acute coronary syndrome admitted to cardiac care units in Italy: The EYESHOT Study. *Eur Heart J Acute Cardiovasc Care*.
104. De Vera M A, Bhole V, Burns L C & Lacaille D 2014. Impact of statin adherence on cardiovascular disease and mortality outcomes: a systematic review. *Br J Clin Pharmacol*, 78, 684-98.
105. De Vries R, Barfield M, Van De Merbel N, Schmid B, Siethoff C, Ortiz J, Verheij E, Van Baar B, Cobb Z, White S & Timmerman P 2013. The effect of hematocrit on bioanalysis of DBS: results from the EBF DBS-microsampling consortium. *Bioanalysis*, 5, 2147-60.
106. Dean L 2015. Irinotecan Therapy and UGT1A1 Genotype. Medical Genetics Summaries [Internet]. Bethesda (MD): National Center for Biotechnology Information (US); 2012.
107. Degorter M K, Tirona R G, Schwarz U I, Choi Y-H, Dresser G K, Suskin N, Myers K, Zou G, Iwuchukwu O, Wei W-Q, Wilke R A, Hegele R A & Kim R B 2013. Clinical and Pharmacogenetic Predictors of Circulating Atorvastatin and Rosuvastatin Concentration in Routine Clinical Care. *Circulation. Cardiovascular genetics*, 6, 400-408.
108. Deichmann R, Lavie C & Andrews S 2010. Coenzyme Q10 and Statin-Induced Mitochondrial Dysfunction. *The Ochsner Journal*, 10, 16-21.
109. Delaneau O, Marchini J & Zagury J F 2011. A linear complexity phasing method for thousands of genomes. *Nat Methods*, 9, 179-81.
110. Deng S, Chen X P, Cao D, Yin T, Dai Z Y, Luo J, Tang L & Li Y J 2009. Effects of a concomitant single oral dose of rifampicin on the pharmacokinetics of pravastatin in a two-phase, randomized, single-blind, placebo-controlled, crossover study in healthy Chinese male subjects. *Clin Ther*, 31, 1256-63.
111. Denniff P & Spooner N 2010. The effect of hematocrit on assay bias when using DBS samples for the quantitative bioanalysis of drugs. *Bioanalysis*, 2, 1385-95.
112. Dias E, Hachey B, Mcnaughton C, Nian H, Yu C, Straka B, Brown N J & Caprioli R M 2013. An LC-MS assay for the screening of cardiovascular medications in human samples. *J Chromatogr B Analyt Technol Biomed Life Sci*, 937, 44-53.
113. Didonato K L, Liu Y, Lindsey C C, Hartwig D M & Stoner S C 2015. Community pharmacy patient perceptions of a pharmacy-initiated mobile technology app to improve adherence. *Int J Pharm Pract*.
114. Docherty A 2010. Acute medical management of the non-ST-segment elevation acute coronary syndromes (NSTE-ACS) in older patients. *Arch Gerontol Geriatr*, 51, 129-34.
115. Donnelly L A, Doney A S, Tavendale R, Lang C C, Pearson E R, Colhoun H M, McCarthy M I, Hattersley A T, Morris A D & Palmer C N 2011. Common nonsynonymous substitutions in SLCO1B1 predispose to statin intolerance in routinely treated individuals with type 2 diabetes: a go-DARTS study. *Clin Pharmacol Ther*, 89, 210-6.
116. Dostalek M, Court M H, Hazarika S & Akhlaghi F 2011. Diabetes mellitus reduces activity of human UDP-glucuronosyltransferase 2B7 in liver and kidney leading to decreased formation of mycophenolic acid acyl-glucuronide metabolite. *Drug Metab Dispos*, 39, 448-55.
117. Dostalek M, Sam W J, Paryani K R, Macwan J S, Gohh R Y & Akhlaghi F 2012. Diabetes mellitus reduces the clearance of atorvastatin lactone: results of a population pharmacokinetic analysis in renal transplant recipients and in vitro studies using human liver microsomes. *Clin Pharmacokinet*, 51, 591-606.

118. Draeger A, Monastyrskaya K, Mohaupt M, Hoppeler H, Savolainen H, Allemann C & Babiyshuk E B 2006. Statin therapy induces ultrastructural damage in skeletal muscle in patients without myalgia. *J Pathol*, 210, 94-102.
119. Draganov D I, Stetson P L, Watson C E, Billecke S S & La Du B N 2000. Rabbit serum paraoxonase 3 (PON3) is a high density lipoprotein-associated lactonase and protects low density lipoprotein against oxidation. *J Biol Chem*, 275, 33435-42.
120. Dreier J P & Endres M 2004. Statin-associated rhabdomyolysis triggered by grapefruit consumption. *Neurology*, 62, 670.
121. Drogari E, Ragia G, Mollaki V, Elens L, Van Schaik R H & Manolopoulos V G 2014. POR\*28 SNP is associated with lipid response to atorvastatin in children and adolescents with familial hypercholesterolemia. *Pharmacogenomics*, 15, 1963-72.
122. Drugs.Com. 2016. Amlodipine and Atorvastatin Tablets (Online). drugs.com. Available: <https://www.drugs.com/pro/amlodipine-and-atorvastatin-tablets.html> (Accessed 12 July 2016).
123. Dube M P, Zetler R, Barhdadi A, Brown A, Mongrain I, Normand V, Laplante N, Asselin G, Feroz Zada Y, Provost S, Bergeron J, Kouz S, Dufour R, Diaz A, Dedenus S, Turgeon J, Rheume E, Phillips M S & Tardif J C 2014. CKM and LILRB5 Are Associated with Serum Levels of Creatine Kinase. *Circ Cardiovasc Genet*.
124. Duramed Pharmaceuticals Inc. 2010. ZEBETA (BISOPROLOL FUMARATE) TABLETS - bisoprolol fumarate tablet (Online). Available: [http://www.accessdata.fda.gov/drugsatfda\\_docs/label/2011/019982s016lbl.pdf](http://www.accessdata.fda.gov/drugsatfda_docs/label/2011/019982s016lbl.pdf) (Accessed 8 March 2017).
125. Ebner T, Ishiguro N & Taub M E 2015. The Use of Transporter Probe Drug Cocktails for the Assessment of Transporter-Based Drug-Drug Interactions in a Clinical Setting-Proposal of a Four Component Transporter Cocktail. *J Pharm Sci*, 104, 3220-8.
126. Elam M B, Majumdar G, Mozhui K, Gerling I C, Vera S R, Fish-Trotter H, Williams R W, Childress R D & Raghov R 2017. Patients experiencing statin-induced myalgia exhibit a unique program of skeletal muscle gene expression following statin re-challenge. *PLoS One*, 12, e0181308.
127. Elazzazy S, Eziada S S & Zaidan M 2012. Rhabdomyolysis secondary to drug interaction between atorvastatin, omeprazole, and dexamethasone. *Int Med Case Rep J*, 5, 59-61.
128. Elens L, Hesselink D A, Bouamar R, Budde K, De Fijter J W, De Meyer M, Mourad M, Kuypers D R, Haufroid V, Van Gelder T & Van Schaik R H 2014. Impact of POR\*28 on the pharmacokinetics of tacrolimus and cyclosporine A in renal transplant patients. *Ther Drug Monit*, 36, 71-9.
129. Elens L, Nieuweboer A J, Clarke S J, Charles K A, De Graan A J, Haufroid V, Van Gelder T, Mathijssen R H & Van Schaik R H 2013a. Impact of POR\*28 on the clinical pharmacokinetics of CYP3A phenotyping probes midazolam and erythromycin. *Pharmacogenet Genomics*, 23, 148-55.
130. Elens L, Van Gelder T, Hesselink D A, Haufroid V & Van Schaik R H 2013b. CYP3A4\*22: promising newly identified CYP3A4 variant allele for personalizing pharmacotherapy. *Pharmacogenomics*, 14, 47-62.
131. Elsby R, Hilgendorf C & Fenner K 2012. Understanding the critical disposition pathways of statins to assess drug-drug interaction risk during drug development: it's not just about OATP1B1. *Clin Pharmacol Ther*, 92, 584-98.
132. Endo A 2004. The origin of the statins. 2004. *Atheroscler Suppl*, 5, 125-30.
133. Endo A, Kuroda M & Tsujita Y 1976. ML-236A, ML-236B, and ML-236C, new inhibitors of cholesterologenesis produced by *Penicillium citrinum*. *J Antibiot (Tokyo)*, 29, 1346-8.
134. Escobar Y, Venturelli C R & Hoyo-Vadillo C 2005. Pharmacokinetic properties of pravastatin in Mexicans: An open-label study in healthy adult volunteers. *Curr Ther Res Clin Exp*, 66, 238-46.
135. European Commission. 2010. Legislation for the protection of animals used for scientific purposes (Online). Available: [http://ec.europa.eu/environment/chemicals/lab\\_animals/legislation\\_en.htm](http://ec.europa.eu/environment/chemicals/lab_animals/legislation_en.htm) (Accessed 22 April 2016).
136. European Medicines Agency. 2011. Guideline on bioanalytical method validation (Online). Available: [http://www.ema.europa.eu/ema/index.jsp?curl=pages/includes/document/document\\_detail.jsp?webContentId=WC500109686%26mid=WC0b01ac058009a3dc](http://www.ema.europa.eu/ema/index.jsp?curl=pages/includes/document/document_detail.jsp?webContentId=WC500109686%26mid=WC0b01ac058009a3dc) (Accessed 6 March 2017).
137. Fan L, Lee J, Hall J, Tolentino E J, Wu H & El-Shourbagy T 2011. Implementing DBS methodology for the determination of Compound A in monkey blood: GLP method validation and investigation of the impact of blood spreading on performance. *Bioanalysis*, 3, 1241-52.
138. Farrell G C, Teoh N C & Mccuskey R S 2008. Hepatic microcirculation in fatty liver disease. *Anat Rec (Hoboken)*, 291, 684-92.
139. Fenn J B, Mann M, Meng C K, Wong S F & Whitehouse C M 1989. Electrospray ionization for mass spectrometry of large biomolecules. *Science*, 246, 64-71.
140. Ferrari M, Guasti L, Maresca A, Mirabile M, Contini S, Grandi A M, Marino F & Cosentino M 2014. Association between statin-induced creatine kinase elevation and genetic polymorphisms in SLCO1B1, ABCB1 and ABCG2. *Eur J Clin Pharmacol*, 70, 539-47.
141. Fiegenbaum M, Da Silveira F R, Van Der Sand C R, Van Der Sand L C, Ferreira M E, Pires R C & Hutz M H 2005. The role of common variants of ABCB1, CYP3A4, and CYP3A5 genes in lipid-lowering efficacy and safety of simvastatin treatment. *Clin Pharmacol Ther*, 78, 551-8.

142. Finkelman R D, Wang T D, Wang Y, Azumaya C T, Birmingham B K, Wissmar J & Mosqueda-Garcia R 2015. Effect of CYP2C19 polymorphism on the pharmacokinetics of rosuvastatin in healthy Taiwanese subjects. *Clin Pharmacol Drug Dev*, 4, 33-40.
143. Finn Robert d, Henderson Colin j, Scott Claire I & Wolf C r 2009. Unsaturated fatty acid regulation of cytochrome P450 expression via a CAR-dependent pathway. *Biochemical Journal*, 417, 43-54.
144. Finn R D, McLaren A W, Carrie D, Henderson C J & Wolf C R 2007. Conditional deletion of cytochrome P450 oxidoreductase in the liver and gastrointestinal tract: a new model for studying the functions of the P450 system. *J Pharmacol Exp Ther*, 322, 40-7.
145. Finn R D, Mclaughlin L A, Ronseaux S, Rosewell I, Houston J B, Henderson C J & Wolf C R 2008. Defining the in Vivo Role for cytochrome b5 in cytochrome P450 function through the conditional hepatic deletion of microsomal cytochrome b5. *J Biol Chem*, 283, 31385-93.
146. Fisher C D, Lickteig A J, Augustine L M, Oude Elferink R P J, Besselsen D G, Erickson R P & Cherrington N J 2009. Experimental non-alcoholic fatty liver disease results in decreased hepatic uptake transporter expression and function in rats. *European journal of pharmacology*, 613, 119-127.
147. Flint O P, Masters B A, Gregg R E & Durham S K 1997. HMG CoA reductase inhibitor-induced myotoxicity: pravastatin and lovastatin inhibit the geranylgeranylation of low-molecular-weight proteins in neonatal rat muscle cell culture. *Toxicol Appl Pharmacol*, 145, 99-110.
148. Flockhart D A. 2007. Drug interactions: cytochrome P450 drug interaction table. Indiana University School of Medicine. (Online). Available: <http://medicine.iupui.edu/CLINPHARM/ddis/main-table> (Accessed 4 July 2017).
149. Fluck C E, Tajima T, Pandey A V, Arlt W, Okuhara K, Verge C F, Jabs E W, Mendonca B B, Fujieda K & Miller W L 2004. Mutant P450 oxidoreductase causes disordered steroidogenesis with and without Antley-Bixler syndrome. *Nat Genet*, 36, 228-30.
150. Food and Drug Administration. 2001. Guidance for Industry. Bioanalytical method validation (Online). Available: <http://www.fda.gov/downloads/Drugs/Guidance/ucm070107.pdf> (Accessed 22 April 2016).
151. Food and Drug Administration. 2011. FDA: Limit Use of 80 mg Simvastatin (Online). Available: <http://www.fda.gov/ForConsumers/ConsumerUpdates/ucm257884.htm> (Accessed 28 October 2016).
152. Food and Drug Administration. 2016. Drug Development and Drug Interactions: Table of Substrates, Inhibitors and Inducers (Online). Available: <https://www.fda.gov/drugs/developmentapprovalprocess/developmentresources/druginteractionslabeling/ucm093664.htm> (Accessed 23 January 2017).
153. Frudakis T N, Thomas M J, Gijnjupalli S N, Handelin B, Gabriel R & Gomez H J 2007. CYP2D6\*4 polymorphism is associated with statin-induced muscle effects. *Pharmacogenet Genomics*, 17, 695-707.
154. Fujino H, Yamada I, Shimada S, Yoneda M & Kojima J 2003. Metabolic fate of pitavastatin, a new inhibitor of HMG-CoA reductase: human UDP-glucuronosyltransferase enzymes involved in lactonization. *Xenobiotica*, 33, 27-41.
155. Fukazawa I, Uchida N, Uchida E & Yasuhara H 2004. Effects of grapefruit juice on pharmacokinetics of atorvastatin and pravastatin in Japanese. *British Journal of Clinical Pharmacology*, 57, 448-455.
156. Furberg C D & Pitt B 2001. Withdrawal of cerivastatin from the world market. *Curr Control Trials Cardiovasc Med*, 2, 205-207.
157. Furihata T, Satoh N, Ohishi T, Ugajin M, Kameyama Y, Morimoto K, Matsumoto S, Yamashita K, Kobayashi K & Chiba K 2009. Functional analysis of a mutation in the SLCO1B1 gene (c.1628T>G) identified in a Japanese patient with pravastatin-induced myopathy. *Pharmacogenomics J*, 9, 185-93.
158. Gallagher R M, Kirkham J J, Mason J R, Bird K A, Williamson P R, Nunn A J, Turner M A, Smyth R L & Pirmohamed M 2011. Development and inter-rater reliability of the Liverpool adverse drug reaction causality assessment tool. *PLoS One*, 6, e28096.
159. Gammal R S, Court M H, Haidar C E, Iwuchukwu O F, Gaur A H, Alvarellos M, Guillemette C, Lennox J L, Whirl-Carrillo M, Brummel S S, Ratain M J, Klein T E, Schackman B R, Caudle K E & Haas D W 2016. Clinical Pharmacogenetics Implementation Consortium (CPIC) Guideline for UGT1A1 and Atazanavir Prescribing. *Clinical Pharmacology and Therapeutics*, 99, 363-369.
160. Gandelman K, Fung G L, Messig M & Laskey R 2012. Systemic exposure to atorvastatin between Asian and Caucasian subjects: a combined analysis of 22 studies. *Am J Ther*, 19, 164-73.
161. Ganesan S, Williams C, Maslen C L & Cherala G 2013. Clopidogrel variability: role of plasma protein binding alterations. *British Journal of Clinical Pharmacology*, 75, 1468-1477.
162. Ganz P, Heidecker B, Hveem K, Jonasson C, Kato S, Segal M R, Sterling D G & Williams S A 2016. Development and Validation of a Protein-Based Risk Score for Cardiovascular Outcomes Among Patients With Stable Coronary Heart Disease. *Jama*, 315, 2532-41.
163. Garcia-Garcia C, Subirana I, Sala J, Bruguera J, Sanz G, Valle V, Aros F, Fiol M, Molina L, Serra J, Marrugat J & Elosua R 2011. Long-term prognosis of first myocardial infarction according to the electrocardiographic pattern (ST elevation myocardial infarction, non-ST elevation myocardial infarction and non-classified myocardial infarction) and revascularization procedures. *Am J Cardiol*, 108, 1061-7.

164. García-Gil M, Blanch J, Comas-Cufí M, Daunis-I-Estadella J, Bolívar B, Martí R, Ponjoan A, Alves-Cabratos L & Ramos R 2016. Patterns of statin use and cholesterol goal attainment in a high-risk cardiovascular population: A retrospective study of primary care electronic medical records. *Journal of Clinical Lipidology*, 10, 134-142.
165. Gauthier J M & Massicotte A 2015. Statins and their effect on cognition: Let's clear up the confusion. *Canadian Pharmacists Journal : CPJ*, 148, 150-155.
166. Gene Ncbi. 2017. UGT1A UDP glucuronosyltransferase family 1 member A complex locus [ Homo sapiens (human) ] (Online). Available: <https://www.ncbi.nlm.nih.gov/gene/7361> (Accessed 18 July 2017).
167. Generaux G T, Bonomo F M, Johnson M & Doan K M 2011. Impact of SLCO1B1 (OATP1B1) and ABCG2 (BCRP) genetic polymorphisms and inhibition on LDL-C lowering and myopathy of statins. *Xenobiotica*, 41, 639-51.
168. Ghadiminejad I & Saggerson E D 1990. Carnitine palmitoyltransferase (CPT2) from liver mitochondrial inner membrane becomes inhibitable by malonyl-CoA if reconstituted with outer membrane malonyl-CoA binding protein. *FEBS Lett*, 269, 406-8.
169. Gibson D M, Bron N J, Richens A, Hounslow N J, Sedman A J & Whitfield L R 1996. Effect of age and gender on pharmacokinetics of atorvastatin in humans. *J Clin Pharmacol*, 36, 242-6.
170. Gijzen V M, Van Schaik R H, Soldin O P, Soldin S J, Nulman I, Koren G & De Wildt S N 2014. P450 oxidoreductase \*28 (POR\*28) and tacrolimus disposition in pediatric kidney transplant recipients--a pilot study. *Ther Drug Monit*, 36, 152-8.
171. Gil J & Sasiadek M M 2012. Gilbert syndrome: the UGT1A1\*28 promoter polymorphism as a biomarker of multifactorial diseases and drug metabolism. *Biomark Med*, 6, 223-30.
172. Gobel B, Zwart D, Hesselink G, Pijnenborg L, Barach P, Kalkman C & Johnson J K 2012. Stakeholder perspectives on handovers between hospital staff and general practitioners: an evaluation through the microsystems lens. *BMJ Qual Saf*, 21 Suppl 1, i106-13.
173. Godlee F 2014. Adverse effects of statins. *BMJ : British Medical Journal*, 348.
174. Goldstein J I, Crenshaw A, Carey J, Grant G B, Maguire J, Fromer M, O'dushlaine C, Moran J L, Chambert K, Stevens C, Swedish Schizophrenia C, Consortium A a S, Sklar P, Hultman C M, Purcell S, Mccarroll S A, Sullivan P F, Daly M J & Neale B M 2012. zCall: a rare variant caller for array-based genotyping: Genetics and population analysis. *Bioinformatics*, 28, 2543-2545.
175. Goldstein J L & Brown M S 2009. The LDL receptor. *Arterioscler Thromb Vasc Biol*, 29, 431-8.
176. Golomb B A & Evans M A 2008. Statin Adverse Effects: A Review of the Literature and Evidence for a Mitochondrial Mechanism. *American journal of cardiovascular drugs : drugs, devices, and other interventions*, 8, 373-418.
177. Golomb B A, Evans M A, Dimsdale J E & White H L 2012. Effects of statins on energy and fatigue with exertion: results from a randomized controlled trial. *Arch Intern Med*, 172, 1180-2.
178. Gomes A M, Winter S, Klein K, Turpeinen M, Schaeffeler E, Schwab M & Zanger U M 2009. Pharmacogenomics of human liver cytochrome P450 oxidoreductase: multifactorial analysis and impact on microsomal drug oxidation. *Pharmacogenomics*, 10, 579-99.
179. Gomes M D, Lecker S H, Jagoe R T, Navon A & Goldberg A L 2001. Atrogin-1, a muscle-specific F-box protein highly expressed during muscle atrophy. *Proceedings of the National Academy of Sciences of the United States of America*, 98, 14440-14445.
180. Gong L, Zhang C M, Lv J F, Zhou H H & Fan L 2017. Polymorphisms in cytochrome P450 oxidoreductase and its effect on drug metabolism and efficacy. *Pharmacogenet Genomics*.
181. Gonzalez M, Sealls W, Jesch E D, Brosnan M J, Ladunga I, Ding X, Black P N & Dirusso C C 2011a. Defining a relationship between dietary fatty acids and the cytochrome P450 system in a mouse model of fatty liver disease. *Physiol Genomics*, 43, 121-35.
182. Gonzalez O, Alonso R M, Ferreiros N, Weinmann W, Zimmermann R & Dresen S 2011b. Development of an LC-MS/MS method for the quantitation of 55 compounds prescribed in combined cardiovascular therapy. *J Chromatogr B Analyt Technol Biomed Life Sci*, 879, 243-52.
183. Goodarzi M O, Xu N & Azziz R 2008. Association of CYP3A7\*1C and serum dehydroepiandrosterone sulfate levels in women with polycystic ovary syndrome. *J Clin Endocrinol Metab*, 93, 2909-12.
184. Gordon A S, Tabor H K, Johnson A D, Snively B M, Assimes T L, Auer P L, Ioannidis J P, Peters U, Robinson J G, Sucheston L E, Wang D, Sotoodehnia N, Rotter J I, Psaty B M, Jackson R D, Herrington D M, O'donnell C J, Reiner A P, Rich S S, Rieder M J, Bamshad M J & Nickerson D A 2014. Quantifying rare, deleterious variation in 12 human cytochrome P450 drug-metabolism genes in a large-scale exome dataset. *Hum Mol Genet*, 23, 1957-63.
185. Grable-Esposito P, Katzberg H D, Greenberg S A, Srinivasan J, Katz J & Amato A A 2010. Immune-mediated necrotizing myopathy associated with statins. *Muscle Nerve*, 41, 185-90.
186. Granfors M T, Wang J S, Kajosaari L I, Laitila J, Neuvonen P J & Backman J T 2006. Differential inhibition of cytochrome P450 3A4, 3A5 and 3A7 by five human immunodeficiency virus (HIV) protease inhibitors in vitro. *Basic Clin Pharmacol Toxicol*, 98, 79-85.
187. Greenwell C. 2015. Heart disease and stroke cost American nearly \$1 billion a day in medical costs, lost productivity (Online). CDC Foundation. Available: <https://www.cdcfoundation.org/pr/2015/heart->

- [disease-and-stroke-cost-america-nearly-1-billion-day-medical-costs-lost-productivity](#) (Accessed 12 July 2017).
188. Greer D A & Ivey S 2007. Distinct N-Glycan Glycosylation of P-glycoprotein Isolated from the Human Uterine Sarcoma Cell Line MES-SA/Dx5. *Biochimica et biophysica acta*, 1770, 1275-1282.
  189. Grimsley A, Foster A, Gallagher R, Hutchison M, Lundqvist A, Pickup K, Wilson I D & Samuelsson K 2014. A comparison of the metabolism of midazolam in C57BL/6J and hepatic reductase null (HRN) mice. *Biochem Pharmacol*, 92, 701-711.
  190. Grundy S M 2016. Primary prevention of cardiovascular disease with statins: assessing the evidence base behind clinical guidance. *Clinical Pharmacist*, 8.
  191. Gu J, Weng Y, Zhang Q Y, Cui H, Behr M, Wu L, Yang W, Zhang L & Ding X 2003. Liver-specific deletion of the NADPH-cytochrome P450 reductase gene: impact on plasma cholesterol homeostasis and the function and regulation of microsomal cytochrome P450 and heme oxygenase. *J Biol Chem*, 278, 25895-901.
  192. Guengerich F P 1999. Cytochrome P-450 3A4: regulation and role in drug metabolism. *Annu Rev Pharmacol Toxicol*, 39, 1-17.
  193. Gunde-Cimerman N & Cimerman A 1995. Pleurotus fruiting bodies contain the inhibitor of 3-hydroxy-3-methylglutaryl-coenzyme A reductase-lovastatin. *Exp Mycol*, 19, 1-6.
  194. Gupta A, Thompson D, Whitehouse A, Collier T, Dahlof B, Poulter N, Collins R & Sever P 2017. Adverse events associated with unblinded, but not with blinded, statin therapy in the Anglo-Scandinavian Cardiac Outcomes Trial-Lipid-Lowering Arm (ASCOT-LLA): a randomised double-blind placebo-controlled trial and its non-randomised non-blind extension phase. *Lancet*, 389, 2473-2481.
  195. Guthrie R & Susi A 1963. A SIMPLE PHENYLALANINE METHOD FOR DETECTING PHENYLKETONURIA IN LARGE POPULATIONS OF NEWBORN INFANTS. *Pediatrics*, 32, 338-43.
  196. Hamann P, Cooper R, Mchugh N & Chinoy H 2013. Statin-induced necrotizing myositis – A discrete autoimmune entity within the “statin-induced myopathy spectrum”. *Autoimmunity reviews*, 12, 1177-1181.
  197. Hanai J, Cao P, Tanksale P, Imamura S, Koshimizu E, Zhao J, Kishi S, Yamashita M, Phillips P S, Sukhatme V P & Lecker S H 2007. The muscle-specific ubiquitin ligase atrogin-1/MAFbx mediates statin-induced muscle toxicity. *J Clin Invest*, 117, 3940-51.
  198. Hart S N, Wang S, Nakamoto K, Wesselman C, Li Y & Zhong X B 2008. Genetic polymorphisms in cytochrome P450 oxidoreductase influence microsomal P450-catalyzed drug metabolism. *Pharmacogenet Genomics*, 18, 11-24.
  199. Hashimoto T, Fujita T, Usuda N, Cook W, Qi C, Peters J M, Gonzalez F J, Yeldandi A V, Rao M S & Reddy J K 1999. Peroxisomal and mitochondrial fatty acid beta-oxidation in mice nullizygous for both peroxisome proliferator-activated receptor alpha and peroxisomal fatty acyl-CoA oxidase. Genotype correlation with fatty liver phenotype. *J Biol Chem*, 274, 19228-36.
  200. Hatanaka T 2000. Clinical pharmacokinetics of pravastatin: mechanisms of pharmacokinetic events. *Clin Pharmacokinet*, 39, 397-412.
  201. Hawkes N 2017. NICE guidelines could put 12 million UK adults on statins. *BMJ*, 358.
  202. Heinig K, Wirz T, Bucheli F & Gajate-Perez A 2011a. Determination of oseltamivir (Tamiflu(R)) and oseltamivir carboxylate in dried blood spots using offline or online extraction. *Bioanalysis*, 3, 421-37.
  203. Heinig K, Wirz T, Gajate-Perez A & Belli S 2011b. Determination of Ganciclovir and its prodrug Valganciclovir by hydrophilic interaction liquid chromatography-tandem mass spectrometry. *J Chromatogr B Analyt Technol Biomed Life Sci*, 879, 436-42.
  204. Henderson C J, McLaughlin L A & Wolf C R 2013. Evidence that cytochrome b5 and cytochrome b5 reductase can act as sole electron donors to the hepatic cytochrome P450 system. *Mol Pharmacol*, 83, 1209-17.
  205. Henderson C J, Otto D M, Carrie D, Magnuson M A, McLaren A W, Rosewell I & Wolf C R 2003. Inactivation of the hepatic cytochrome P450 system by conditional deletion of hepatic cytochrome P450 reductase. *J Biol Chem*, 278, 13480-6.
  206. Henderson C J & Wolf C R 1992. Immunodetection of proteins by western blotting. In: Manson M M (ed.) *Immunochemical protocols*. Totowa, NJ: Humana Press.
  207. Hermann M, Bogsrud M P, Molden E, Asberg A, Mohebi B U, Ose L & Retterstol K 2006. Exposure of atorvastatin is unchanged but lactone and acid metabolites are increased several-fold in patients with atorvastatin-induced myopathy. *Clin Pharmacol Ther*, 79, 532-9.
  208. Hermann M, Christensen H & Reubsæet J L 2005. Determination of atorvastatin and metabolites in human plasma with solid-phase extraction followed by LC-tandem MS. *Anal Bioanal Chem*, 382, 1242-9.
  209. Hess G, Sanders K N, Hill J & Liu L Z 2007. Therapeutic dose assessment of patient switching from atorvastatin to simvastatin. *Am J Manag Care*, 13 Suppl 3, S80-5.
  210. Higgins J W, Bao J Q, Ke A B, Manro J R, Fallon J K, Smith P C & Zamek-Gliszczyński M J 2014. Utility of Oatp1a/1b-knockout and OATP1B1/3-humanized mice in the study of OATP-mediated pharmacokinetics and tissue distribution: case studies with pravastatin, atorvastatin, simvastatin, and carboxydichlorofluorescein. *Drug Metab Dispos*, 42, 182-92.

211. Hippisley-Cox J & Coupland C 2006. Effect of statins on the mortality of patients with ischaemic heart disease: population based cohort study with nested case-control analysis. *Heart*, 92, 752-8.
212. Hippisley-Cox J & Coupland C 2010. Unintended effects of statins in men and women in England and Wales: population based cohort study using the QRResearch database. *BMJ*, 340.
213. Hippisley-Cox J, Coupland C, Vinogradova Y, Robson J, Minhas R, Sheikh A & Brindle P 2008. Predicting cardiovascular risk in England and Wales: prospective derivation and validation of QRISK2. *BMJ*, 336, 1475-1482.
214. Hirano M, Maeda K, Hayashi H, Kusuhara H & Sugiyama Y 2005. Bile salt export pump (BSEP/ABCB11) can transport a nonbile acid substrate, pravastatin. *J Pharmacol Exp Ther*, 314, 876-82.
215. Ho P M, Magid D J, Shetterly S M, Olson K L, Maddox T M, Peterson P N, Masoudi F A & Rumsfeld J S 2008. Medication nonadherence is associated with a broad range of adverse outcomes in patients with coronary artery disease. *Am Heart J*, 155, 772-9.
216. Ho P M, Spertus J A, Masoudi F A, Reid K J, Peterson E D, Magid D J, Krumholz H M & Rumsfeld J S 2006a. Impact of medication therapy discontinuation on mortality after myocardial infarction. *Arch Intern Med*, 166, 1842-7.
217. Ho R H, Choi L, Lee W, Mayo G, Schwarz U I, Tirona R G, Bailey D G, Stein C M & Kim R B 2007. Effect of drug transporter genotypes on pravastatin disposition in European- and African-American participants. *Pharmacogenet Genomics*, 17, 647-56.
218. Ho R H, Tirona R G, Leake B F, Glaeser H, Lee W, Lemke C J, Wang Y & Kim R B 2006b. Drug and bile acid transporters in rosuvastatin hepatic uptake: function, expression, and pharmacogenetics. *Gastroenterology*, 130, 1793-806.
219. Hoenig M R, Walker P J, Gurnsey C, Beadle K & Johnson L 2011. The C3435T polymorphism in ABCB1 influences atorvastatin efficacy and muscle symptoms in a high-risk vascular cohort. *J Clin Lipidol*, 5, 91-6.
220. Hoffman M F, Preissner S C, Nickel J, Dunkel M, Preissner R & Preissner S 2014. The Transformer database: biotransformation of xenobiotics. *Nucleic Acids Res*, 42, 1113-7.
221. Hollegaard M V, Grove J, Thorsen P, Norgaard-Pedersen B & Hougaard D M 2009. High-throughput genotyping on archived dried blood spot samples. *Genet Test Mol Biomarkers*, 13, 173-9.
222. Horsfall L J, Zeitlyn D, Tarekegn A, Bekele E, Thomas M G, Bradman N & Swallow D M 2011. Prevalence of clinically relevant UGT1A alleles and haplotypes in African populations. *Ann Hum Genet*, 75, 236-46.
223. Howie B N, Donnelly P & Marchini J 2009. A flexible and accurate genotype imputation method for the next generation of genome-wide association studies. *PLoS Genet*, 5, e1000529.
224. Hu M, Mak V W, Yin O Q, Chu T T & Tomlinson B 2013. Effects of grapefruit juice and SLCO1B1 388A>G polymorphism on the pharmacokinetics of pitavastatin. *Drug Metab Pharmacokinet*, 28, 104-8.
225. Huang N, Agrawal V, Giacomini K M & Miller W L 2008. Genetics of P450 oxidoreductase: Sequence variation in 842 individuals of four ethnicities and activities of 15 missense mutations. *Proceedings of the National Academy of Sciences of the United States of America*, 105, 1733-1738.
226. Huang N, Pandey A V, Agrawal V, Reardon W, Lapunzina P D, Mowat D, Jabs E W, Van Vliet G, Sack J, Fluck C E & Miller W L 2005. Diversity and function of mutations in p450 oxidoreductase in patients with Antley-Bixler syndrome and disordered steroidogenesis. *Am J Hum Genet*, 76, 729-49.
227. Hubacek J A, Dlouha D, Adamkova V, Zlatohlavek L, Viklicky O, Hruby P, Ceska R & Vrablik M 2015. SLCO1B1 polymorphism is not associated with risk of statin-induced myalgia/myopathy in a Czech population. *Med Sci Monit*, 21, 1454-9.
228. Huguot J, Lu J, Gaudette F, Chiasson J L, Hamet P, Michaud V & Turgeon J 2016. No effects of pantoprazole on the pharmacokinetics of rosuvastatin in healthy subjects. *Eur J Clin Pharmacol*, 72, 925-31.
229. Hur J, Liu Z, Tong W, Laaksonen R & Bai J P 2014. Drug-induced rhabdomyolysis: from systems pharmacology analysis to biochemical flux. *Chem Res Toxicol*, 27, 421-32.
230. Ichimaru N, Takahara S, Kokado Y, Wang J D, Hatori M, Kameoka H, Inoue T & Okuyama A 2001. Changes in lipid metabolism and effect of simvastatin in renal transplant recipients induced by cyclosporine or tacrolimus. *Atherosclerosis*, 158, 417-23.
231. Ieiri I, Suwannakul S, Maeda K, Uchimaru H, Hashimoto K, Kimura M, Fujino H, Hirano M, Kusuhara H, Irie S, Higuchi S & Sugiyama Y 2007. SLCO1B1 (OATP1B1, an uptake transporter) and ABCG2 (BCRP, an efflux transporter) variant alleles and pharmacokinetics of pitavastatin in healthy volunteers. *Clin Pharmacol Ther*, 82, 541-7.
232. Ignjatovic V, Pitt J, Monagle P & Craig J M 2014. The utility of dried blood spots for proteomic studies: looking forward to looking back. *Proteomics Clin Appl*, 8, 896-900.
233. Isackson P J, Ochs-Balcom H M, Ma C, Harley J B, Peltier W, Tarnopolsky M, Sripathi N, Wortmann R L, Simmons Z, Wilson J D, Smith S A, Barboi A, Fine E, Baer A, Baker S, Kaufman K, Cobb B, Kilpatrick J R & Vladutiu G D 2011. Association of common variants in the human eyes shut ortholog (EYS) with statin-induced myopathy: evidence for additional functions of EYS. *Muscle Nerve*, 44, 531-8.
234. Itagaki M, Takaguri A, Kano S, Kaneta S, Ichihara K & Satoh K 2009. Possible mechanisms underlying statin-induced skeletal muscle toxicity in L6 fibroblasts and in rats. *J Pharmacol Sci*, 109, 94-101.

235. Ito Y, Abril E R, Bethea N W, Mccuskey M K & Mccuskey R S 2006. Dietary steatotic liver attenuates acetaminophen hepatotoxicity in mice. *Microcirculation*, 13, 19-27.
236. Iyer L V, Ho M N, Furimsky A M, Green C E, Green A G, Sharp L E, Koch S, Li Y, Catz P, Furniss M, Kapetanovic I M & Nath S S 2004. In vitro metabolism and interaction studies with celecoxib and lovastatin. *Cancer Research*, 64, 488-488.
237. Jacobsen W, Kuhn B, Soldner A, Kirchner G, Sewing K F, Kollman P A, Benet L Z & Christians U 2000. Lactonization is the critical first step in the disposition of the 3-hydroxy-3-methylglutaryl-CoA reductase inhibitor atorvastatin. *Drug Metab Dispos*, 28, 1369-78.
238. Jacobson T A 2004. Comparative pharmacokinetic interaction profiles of pravastatin, simvastatin, and atorvastatin when coadministered with cytochrome P450 inhibitors. *Am J Cardiol*, 94, 1140-6.
239. Jacobson T A, Wertz D A, Kuznik A & Cziraky M 2013. Cardiovascular event rates in atorvastatin patients versus patients switching from atorvastatin to simvastatin. *Curr Med Res Opin*, 29, 773-81.
240. Jakobsen G S, Skottheim I B, Sandbu R, Christensen H, Roislien J, Asberg A & Hjelmessaeth J 2013. Long-term effects of gastric bypass and duodenal switch on systemic exposure of atorvastatin. *Surg Endosc*, 27, 2094-101.
241. James S, Akerblom A, Cannon C P, Emanuelsson H, Husted S, Katus H, Skene A, Steg P G, Storey R F, Harrington R, Becker R & Wallentin L 2009. Comparison of ticagrelor, the first reversible oral P2Y<sub>12</sub> receptor antagonist, with clopidogrel in patients with acute coronary syndromes: Rationale, design, and baseline characteristics of the PLATElet inhibition and patient Outcomes (PLATO) trial. *Am Heart J*, 157, 599-605.
242. Jbara Y & Bricker D 2015. Rhabdomyolysis in the setting of induced hypothyroidism and statin therapy: a case report. *Eur Thyroid J*, 4, 62-4.
243. Jemal M, Ouyang Z, Chen B C & Teitz D 1999a. Quantitation of the acid and lactone forms of atorvastatin and its biotransformation products in human serum by high-performance liquid chromatography with electrospray tandem mass spectrometry. *Rapid Commun Mass Spectrom*, 13, 1003-15.
244. Jemal M, Rao S, Salahudeen I, Chen B C & Kates R 1999b. Quantitation of cerivastatin and its seven acid and lactone biotransformation products in human serum by liquid chromatography-electrospray tandem mass spectrometry. *J Chromatogr B Biomed Sci Appl*, 736, 19-41.
245. Jemnitz K, Veres Z, Tugyi R & Vereczkey L 2010. Biliary efflux transporters involved in the clearance of rosuvastatin in sandwich culture of primary rat hepatocytes. *Toxicol In Vitro*, 24, 605-10.
246. Johnson N, De Ieso P, Migliorini G, Orr N, Broderick P, Catovsky D, Matakidou A, Eisen T, Goldsmith C, Dudbridge F, Peto J, Dos-Santos-Silva I, Ashworth A, Ross G, Houlston R S & Fletcher O 2016. Cytochrome P450 allele CYP3A7\*1C associates with adverse outcomes in chronic lymphocytic leukemia, breast and lung cancer. *Cancer research*, 76, 1485-1493.
247. Jungbluth H 2007. Multi-minicore Disease. *Orphanet Journal of Rare Diseases*, 2, 31-31.
248. Kanth R, Shah M S & Flores R M 2013. Statin-associated polymyositis following omeprazole treatment. *Clin Med Res*, 11, 91-5.
249. Kantola T, Backman J T, Niemi M, Kivisto K T & Neuvonen P J 2000. Effect of fluconazole on plasma fluvastatin and pravastatin concentrations. *Eur J Clin Pharmacol*, 56, 225-9.
250. Kantola T, Kivisto K T & Neuvonen P J 1998. Erythromycin and verapamil considerably increase serum simvastatin and simvastatin acid concentrations. *Clin Pharmacol Ther*, 64, 177-82.
251. Karaźniewicz-Łada M, Danielak D, Burchardt P, Kruszyna Ł, Komosa A, Lesiak M & Główska F 2014. Clinical Pharmacokinetics of Clopidogrel and Its Metabolites in Patients with Cardiovascular Diseases. *Clinical Pharmacokinetics*, 53, 155-164.
252. Karlgren M, Vildhede A, Norinder U, Wisniewski J R, Kimoto E, Lai Y, Haglund U & Artursson P 2012. Classification of inhibitors of hepatic organic anion transporting polypeptides (OATPs): influence of protein expression on drug-drug interactions. *J Med Chem*, 55, 4740-63.
253. Kashani A, Phillips C O, Foody J M, Wang Y, Mangalmurti S, Ko D T & Krumholz H M 2006. Risks associated with statin therapy: a systematic overview of randomized clinical trials. *Circulation*, 114, 2788-97.
254. Kavalipati N, Shah J, Ramakrishan A & Vasawala H 2015. Pleiotropic effects of statins. *Indian Journal of Endocrinology and Metabolism*, 19, 554-562.
255. Kearney A S, Crawford L F, Mehta S C & Radebaugh G W 1993. The interconversion kinetics, equilibrium, and solubilities of the lactone and hydroxyacid forms of the HMG-CoA reductase inhibitor, CI-981. *Pharm Res*, 10, 1461-5.
256. Kebarle P 2000. A brief overview of the present status of the mechanisms involved in electrospray mass spectrometry. *J Mass Spectrom*, 35, 804-17.
257. Keskitalo J E, Kurkinen K J, Neuvonen M, Backman J T, Neuvonen P J & Niemi M 2009a. No significant effect of ABCB1 haplotypes on the pharmacokinetics of fluvastatin, pravastatin, lovastatin, and rosuvastatin. *British Journal of Clinical Pharmacology*, 68, 207-213.
258. Keskitalo J E, Kurkinen K J, Neuvonen P J & Niemi M 2008. ABCB1 haplotypes differentially affect the pharmacokinetics of the acid and lactone forms of simvastatin and atorvastatin. *Clin Pharmacol Ther*, 84, 457-61.

259. Keskitalo J E, Pasanen M K, Neuvonen P J & Niemi M 2009b. Different effects of the ABCG2 c.421C>A SNP on the pharmacokinetics of fluvastatin, pravastatin and simvastatin. *Pharmacogenomics*, 10, 1617-24.
260. Keskitalo J E, Zolk O, Fromm M F, Kurkinen K J, Neuvonen P J & Niemi M 2009c. ABCG2 polymorphism markedly affects the pharmacokinetics of atorvastatin and rosuvastatin. *Clin Pharmacol Ther*, 86, 197-203.
261. Khayznikov M, Kumar A, Wang P & Glueck C J 2015. Statin Intolerance and Vitamin D Supplementation. *North American Journal of Medical Sciences*, 7, 339-340.
262. Kim K A, Park P W, Lee O J, Kang D K & Park J Y 2007. Effect of polymorphic CYP3A5 genotype on the single-dose simvastatin pharmacokinetics in healthy subjects. *J Clin Pharmacol*, 47, 87-93.
263. Kirch W, Rose I, Demers H G, Leopold G, Pabst J & Ohnhaus E E 1987. Pharmacokinetics of bisoprolol during repeated oral administration to healthy volunteers and patients with kidney or liver disease. *Clin Pharmacokinet*, 13, 110-7.
264. Kirchheiner J, Kudlicz D, Meisel C, Bauer S, Meineke I, Roots I & Brockmoller J 2003. Influence of CYP2C9 polymorphisms on the pharmacokinetics and cholesterol-lowering activity of (-)-3S,5R-fluvastatin and (+)-3R,5S-fluvastatin in healthy volunteers. *Clin Pharmacol Ther*, 74, 186-94.
265. Kitzmiller J P, Luzum J A, Baldassarre D, Krauss R M & Medina M W 2014. CYP3A4\*22 and CYP3A5\*3 are associated with increased levels of plasma simvastatin concentrations in the cholesterol and pharmacogenetics study cohort. *Pharmacogenet Genomics*, 24, 486-91.
266. Kivisto K T, Kantola T & Neuvonen P J 1998. Different effects of itraconazole on the pharmacokinetics of fluvastatin and lovastatin. *Br J Clin Pharmacol*, 46, 49-53.
267. Klein K, Thomas M, Winter S, Nussler A K, Niemi M, Schwab M & Zanger U M 2012. PPARA: a novel genetic determinant of CYP3A4 in vitro and in vivo. *Clin Pharmacol Ther*, 91, 1044-52.
268. Knauer M J, Urquhart B L, Meyer Zu Schwabedissen H E, Schwarz U I, Lemke C J, Leake B F, Kim R B & Tirona R G 2010. Human skeletal muscle drug transporters determine local exposure and toxicity of statins. *Circ Res*, 106, 297-306.
269. Ko J W, Sukhova N, Thacker D, Chen P & Flockhart D A 1997. Evaluation of omeprazole and lansoprazole as inhibitors of cytochrome P450 isoforms. *Drug Metab Dispos*, 25, 853-62.
270. Koch I, Weil R, Wolbold R, Brockmoller J, Hustert E, Burk O, Nuessler A, Neuhaus P, Eichelbaum M, Zanger U & Wojnowski L 2002. Interindividual variability and tissue-specificity in the expression of cytochrome P450 3A mRNA. *Drug Metab Dispos*, 30, 1108-14.
271. Kolwankar D, Vuppalanchi R, Ethell B, Jones D R, Wrighton S A, Hall S D & Chalasani N 2007. Association between nonalcoholic hepatic steatosis and hepatic cytochrome P-450 3A activity. *Clin Gastroenterol Hepatol*, 5, 388-93.
272. Kombu R S, Batta N, Mohan L, Pallapothu K, Pigili R K, Yarramraju S & Agilent Technologies Inc. 2011. Development of an LC/MS/MS assay for atorvastatin in human plasma using a 6460 triple quadrupole LC/MS system (Online). Available: [https://www.agilent.com/cs/library/applications/5990-9128en\\_lo.pdf](https://www.agilent.com/cs/library/applications/5990-9128en_lo.pdf) (Accessed 25 April 2016).
273. Koulman A, Prentice P, Wong M C Y, Matthews L, Bond N J, Eiden M, Griffin J L & Dunger D B 2014. The development and validation of a fast and robust dried blood spot based lipid profiling method to study infant metabolism. *Metabolomics*, 10, 0.
274. Kowa Pharmaceuticals. 2012. Livalo (pitavastatin) tablet - highlights of prescribing information (Online). Available: [http://www.accessdata.fda.gov/drugsatfda\\_docs/label/2012/022363s008s009lbl.pdf](http://www.accessdata.fda.gov/drugsatfda_docs/label/2012/022363s008s009lbl.pdf) (Accessed 7 July 2016).
275. Krajcsi P 2013. Drug-transporter interaction testing in drug discovery and development. *World Journal of Pharmacology*, 2, 35-46.
276. Kristjansson R P, Oddsson A, Helgason H, Sveinbjornsson G, Arnadottir G A, Jensson B O, Jonasdottir A, Jonasdottir A, Bragi Walters G, Sulem G, Oskarsdottir A, Benonisdottir S, Davidsson O B, Masson G, Th Magnusson O, Holm H, Sigurdardottir O, Jonsdottir I, Eyjolfsson G I, Olafsson I, Gudbjartsson D F, Thorsteinsdottir U, Sulem P & Stefansson K 2016. Common and rare variants associating with serum levels of creatine kinase and lactate dehydrogenase. *Nature Communications*, 7, 10572.
277. Kuehl P, Zhang J, Lin Y, Lamba J, Assem M, Schuetz J, Watkins P B, Daly A, Wrighton S A, Hall S D, Maurel P, Relling M, Brimer C, Yasuda K, Venkataramanan R, Strom S, Thummel K, Boguski M S & Schuetz E 2001. Sequence diversity in CYP3A promoters and characterization of the genetic basis of polymorphic CYP3A5 expression. *Nat Genet*, 27, 383-91.
278. Kurzawski M, Malinowski D, Dziwanowski K & Drozdziak M 2014. Impact of PPARA and POR polymorphisms on tacrolimus pharmacokinetics and new-onset diabetes in kidney transplant recipients. *Pharmacogenet Genomics*, 24, 397-400.
279. Kwak H-B, Thalacker-Mercer A, Anderson E J, Lin C-T, Kane D A, Lee N-S, Cortright R N, Bamman M M & Neuffer P D 2012. Simvastatin impairs ADP-stimulated respiration and increases mitochondrial oxidative stress in primary human skeletal myotubes. *Free Radical Biology and Medicine*, 52, 198-207.
280. Kyrklund C, Backman J T, Kivisto K T, Neuvonen M, Laitila J & Neuvonen P J 2000. Rifampin greatly reduces plasma simvastatin and simvastatin acid concentrations. *Clin Pharmacol Ther*, 68, 592-7.

281. Kyrklund C, Backman J T, Kivisto K T, Neuvonen M, Laitila J & Neuvonen P J 2001. Plasma concentrations of active lovastatin acid are markedly increased by gemfibrozil but not by bezafibrate. *Clin Pharmacol Ther*, 69, 340-5.
282. Kyrklund C, Backman J T, Neuvonen M & Neuvonen P J 2003. Gemfibrozil increases plasma pravastatin concentrations and reduces pravastatin renal clearance. *Clin Pharmacol Ther*, 73, 538-44.
283. Kyrklund C, Backman J T, Neuvonen M & Neuvonen P J 2004. Effect of rifampicin on pravastatin pharmacokinetics in healthy subjects. *British Journal of Clinical Pharmacology*, 57, 181-187.
284. Laitinen P J, Brown K M, Piippo K, Swan H, Devaney J M, Brahmbhatt B, Donarum E A, Marino M, Tiso N, Viitasalo M, Toivonen L, Stephan D A & Kontula K 2001. Mutations of the cardiac ryanodine receptor (RyR2) gene in familial polymorphic ventricular tachycardia. *Circulation*, 103, 485-90.
285. Lakey W C, Greyschok N G, Kelley C E, Siddiqui M A, Ahmad U, Lokhnygina Y V & Guyton J R 2016. Statin intolerance in a referral lipid clinic. *J Clin Lipidol*, 10, 870-879.e3.
286. Lakshmi S 2015. A Review on Chromatography with High Performance Liquid Chromatography (HPLC) and its Functions. *Research and Reviews: Journal of Pharmaceutical Analysis*, 4.
287. Lamperti C, Naini A B, Lucchini V, Prella A, Bresolin N, Moggio M, Sciacco M, Kaufmann P & Dimauro S 2005. Muscle coenzyme Q10 level in statin-related myopathy. *Arch Neurol*, 62, 1709-12.
288. Laslett L J, Alagona P, Clark B A, Drozda J P, Saldivar F, Wilson S R, Poe C & Hart M 2012. The Worldwide Environment of Cardiovascular Disease: Prevalence, Diagnosis, Therapy, and Policy Issues A Report From the American College of Cardiology. *Journal of the American College of Cardiology*, 60, S1-S49.
289. Lau Y Y, Okochi H, Huang Y & Benet L Z 2006. Multiple transporters affect the disposition of atorvastatin and its two active hydroxy metabolites: application of in vitro and ex situ systems. *J Pharmacol Exp Ther*, 316, 762-71.
290. Launay-Vacher V, Izzedine H & Deray G 2005. Statins' dosage in patients with renal failure and cyclosporine drug-drug interactions in transplant recipient patients. *Int J Cardiol*, 101, 9-17.
291. Lawson G, Cocks E & Tanna S 2013. Bisoprolol, ramipril and simvastatin determination in dried blood spot samples using LC-HRMS for assessing medication adherence. *J Pharm Biomed Anal*, 81-82, 99-107.
292. Lazar C, Meganck S, Taminau J, Steenhoff D, Coletta A, Molter C, Weiss-Solis D Y, Duque R, Bersini H & Nowe A 2013. Batch effect removal methods for microarray gene expression data integration: a survey. *Brief Bioinform*, 14, 469-90.
293. Lee A J, Conney A H & Zhu B T 2003. Human cytochrome P450 3A7 has a distinct high catalytic activity for the 16 $\alpha$ -hydroxylation of estrone but not 17 $\beta$ -estradiol. *Cancer Res*, 63, 6532-6.
294. Lee D S, Markwardt S, Goeres L, Lee C G, Eckstrom E, Williams C, Fu R, Orwoll E, Cawthon P M, Stefanick M L, Mackey D, Bauer D C & Nielson C M 2014. Statins and physical activity in older men: the osteoporotic fractures in men study. *JAMA Intern Med*, 174, 1263-70.
295. Lee H K, Hu M, Lui S, Ho C S, Wong C K & Tomlinson B 2013. Effects of polymorphisms in ABCG2, SLCO1B1, SLCO10A1 and CYP2C9/19 on plasma concentrations of rosuvastatin and lipid response in Chinese patients. *Pharmacogenomics*, 14, 1283-94.
296. Lee Y J, Lee M G, Lim L A, Jang S B & Chung J Y 2010. Effects of SLCO1B1 and ABCB1 genotypes on the pharmacokinetics of atorvastatin and 2-hydroxyatorvastatin in healthy Korean subjects. *Int J Clin Pharmacol Ther*, 48, 36-45.
297. Lees R S & Lees A M 1995. Rhabdomyolysis from the Coadministration of Lovastatin and the Antifungal Agent Itraconazole. *New England Journal of Medicine*, 333, 664-665.
298. Leopold G 1986. Balanced pharmacokinetics and metabolism of bisoprolol. *J Cardiovasc Pharmacol*, 8 Suppl 11, S16-20.
299. Lewis J P, Horenstein R B, Ryan K, O'connell J R, Gibson Q, Mitchell B D, Tanner K, Chai S, Bliden K P, Tantry U S, Peer C J, Figg W D, Spencer S D, Pacanowski M A, Gurbel P A & Shuldiner A R 2013. The functional G143E variant of carboxylesterase 1 is associated with increased clopidogrel active metabolite levels and greater clopidogrel response. *Pharmacogenet Genomics*, 23, 1-8.
300. Li C, Subramanian R, Yu S & Prueksaritanont T 2006. Acyl-coenzyme a formation of simvastatin in mouse liver preparations. *Drug Metab Dispos*, 34, 102-10.
301. Li J H, Joy S V, Haga S B, Orlando L A, Kraus W E, Ginsburg G S & Voora D 2014. Genetically guided statin therapy on statin perceptions, adherence, and cholesterol lowering: a pilot implementation study in primary care patients. *J Pers Med*, 4, 147-62.
302. Li L, Meier P J & Ballatori N 2000. Oatp2 mediates bidirectional organic solute transport: a role for intracellular glutathione. *Mol Pharmacol*, 58, 335-40.
303. Li W, Zhang J & Tse F L 2011. Strategies in quantitative LC-MS/MS analysis of unstable small molecules in biological matrices. *Biomed Chromatogr*, 25, 258-77.
304. Li Y, Henion J, Abbott R & Wang P 2012. Semi-automated direct elution of dried blood spots for the quantitative determination of guanfacine in human blood. *Bioanalysis*, 4, 1445-56.
305. Lilja J J, Neuvonen M & Neuvonen P J 2004. Effects of regular consumption of grapefruit juice on the pharmacokinetics of simvastatin. *British Journal of Clinical Pharmacology*, 58, 56-60.
306. Limaye V, Bundell C, Hollingsworth P, Rojana-Udomsart A, Mastaglia F, Blumbergs P & Lester S 2015. Clinical and genetic associations of autoantibodies to 3-hydroxy-3-methyl-glutaryl-coenzyme a

- reductase in patients with immune-mediated myositis and necrotizing myopathy. *Muscle Nerve*, 52, 196-203.
307. Lin R, Wang Y, Wang Y, Fu W, Zhang D, Zheng H, Yu T, Wang Y, Shen M, Lei R, Wu H, Sun A, Zhang R, Wang X, Xiong M, Huang W & Jin L 2009. Common variants of four bilirubin metabolism genes and their association with serum bilirubin and coronary artery disease in Chinese Han population. *Pharmacogenet Genomics*, 19, 310-8.
  308. Linde R, Peng L, Desai M & Feldman D 2010. The role of vitamin D and SLCO1B1\*5 gene polymorphism in statin-associated myalgias. *Dermatoendocrinol*, 2, 77-84.
  309. Link E, Parish S, Armitage J, Bowman L, Heath S, Matsuda F, Gut I, Lathrop M & Collins R 2008. SLCO1B1 variants and statin-induced myopathy--a genomewide study. *N Engl J Med*, 359, 789-99.
  310. Liu J, Zhang J, Shi Y, Grimsgaard S, Alraek T & Fonnebo V 2006. Chinese red yeast rice (*Monascus purpureus*) for primary hyperlipidemia: a meta-analysis of randomized controlled trials. *Chin Med*, 1, 4.
  311. Lou X Y, Zhang W, Wang G, Hu D L, Guo D, Tan Z R, Zhou H H, Chen Y & Bao H H 2014. The effect of Na<sup>+</sup>/taurocholate cotransporting polypeptide (NTCP) c.800C > T polymorphism on rosuvastatin pharmacokinetics in Chinese healthy males. *Pharmazie*, 69, 775-9.
  312. Low Wang C C, Hess C N, Hiatt W R & Goldfine A B 2016. Clinical Update: Cardiovascular Disease in Diabetes Mellitus: Atherosclerotic Cardiovascular Disease and Heart Failure in Type 2 Diabetes Mellitus - Mechanisms, Management, and Clinical Considerations. *Circulation*, 133, 2459-502.
  313. Lukas G, Brindle S D & Greengard P 1971. The route of absorption of intraperitoneally administered compounds. *J Pharmacol Exp Ther*, 178, 562-4.
  314. Lunde I, Bremer S, Midtvedt K, Mohebi B, Dahl M, Bergan S, Asberg A & Christensen H 2014. The influence of CYP3A, PPARA, and POR genetic variants on the pharmacokinetics of tacrolimus and cyclosporine in renal transplant recipients. *Eur J Clin Pharmacol*, 70, 685-93.
  315. Macleod A K, Fallon P G, Sharp S, Henderson C J, Wolf C R & Huang J T J 2015. An Enhanced In Vivo Stable Isotope Labeling by Amino Acids in Cell Culture (SILAC) Model for Quantification of Drug Metabolism Enzymes. *Molecular & Cellular Proteomics : MCP*, 14, 750-760.
  316. Macwan J S, Ionita I A, Dostalek M & Akhlaghi F 2011. Development and validation of a sensitive, simple, and rapid method for simultaneous quantitation of atorvastatin and its acid and lactone metabolites by liquid chromatography-tandem mass spectrometry (LC-MS/MS). *Anal Bioanal Chem*, 400, 423-33.
  317. Malviya R, Bansal V, Pal O P & Sharma P K 2009. High performance liquid chromatography: a short review. *Journal of Global Pharma Technology*.
  318. Mammen A L 2016. Statin-Associated Autoimmune Myopathy. *New England Journal of Medicine*, 374, 664-669.
  319. Mammen A L, Chung T, Christopher-Stine L, Rosen P, Rosen A & Casciola-Rosen L A 2011. Autoantibodies against 3-Hydroxy-3-Methylglutaryl-Coenzyme A Reductase (HMGCR) in Patients with Statin-Associated Autoimmune Myopathy. *Arthritis and Rheumatism*, 63, 713-721.
  320. Mammen A L, Gaudet D, Brisson D, Christopher-Stine L, Lloyd T E, Leffell M S & Zachary A A 2012. Increased frequency of DRB1\*11:01 in anti-hydroxymethylglutaryl-coenzyme A reductase-associated autoimmune myopathy. *Arthritis Care Res (Hoboken)*, 64, 1233-7.
  321. Mangravite L M, Engelhardt B E, Medina M W, Smith J D, Brown C D, Chasman D I, Mecham B H, Howie B, Shim H, Naidoo D, Feng Q, Rieder M J, Chen Y D, Rotter J I, Ridker P M, Hopewell J C, Parish S, Armitage J, Collins R, Wilke R A, Nickerson D A, Stephens M & Krauss R M 2013. A statin-dependent QTL for GATM expression is associated with statin-induced myopathy. *Nature*, 502, 377-80.
  322. Mani H, Toennes S W, Linnemann B, Urbanek D A, Schwonberg J, Kauert G F & Lindhoff-Last E 2008. Determination of clopidogrel main metabolite in plasma: a useful tool for monitoring therapy? *Ther Drug Monit*, 30, 84-9.
  323. Maningat P, Gordon B R & Breslow J L 2013. How Do We Improve Patient Compliance and Adherence to Long-Term Statin Therapy? *Current atherosclerosis reports*, 15, 291-291.
  324. Mann D M, Woodward M, Muntner P, Falzon L & Kronish I 2010. Predictors of nonadherence to statins: a systematic review and meta-analysis. *Ann Pharmacother*, 44, 1410-21.
  325. Mao Q 2008. BCRP/ABCG2 in the placenta: expression, function and regulation. *Pharm Res*, 25, 1244-55.
  326. Marchini J & Howie B 2010. Genotype imputation for genome-wide association studies. *Nat Rev Genet*, 11, 499-511.
  327. Marcianti K D, Durda J P, Heckbert S R, Lumley T, Rice K, Mcknight B, Totah R A, Tamraz B, Kroetz D L, Fukushima H, Kaspera R, Bis J C, Glazer N L, Li G, Austin T R, Taylor K D, Rotter J I, Jaquish C E, Kwok P Y, Tracy R P & Psaty B M 2011. Cerivastatin, genetic variants, and the risk of rhabdomyolysis. *Pharmacogenet Genomics*, 21, 280-8.
  328. Martin N J, Bunch J & Cooper H J 2013. Dried Blood Spot Proteomics: Surface Extraction of Endogenous Proteins Coupled with Automated Sample Preparation and Mass Spectrometry Analysis. *Journal of the American Society for Mass Spectrometry*, 24, 1242-1249.

329. Martin P D, Mitchell P D & Schneck D W 2002. Pharmacodynamic effects and pharmacokinetics of a new HMG-CoA reductase inhibitor, rosuvastatin, after morning or evening administration in healthy volunteers. *British Journal of Clinical Pharmacology*, 54, 472-477.
330. Martin P D, Warwick M J, Dane A L, Hill S J, Giles P B, Phillips P J & Lenz E 2003. Metabolism, excretion, and pharmacokinetics of rosuvastatin in healthy adult male volunteers. *Clin Ther*, 25, 2822-35.
331. Marusic S, Lisicic A, Horvatic I, Bacic-Vrca V & Bozina N 2012. Atorvastatin-related rhabdomyolysis and acute renal failure in a genetically predisposed patient with potential drug-drug interaction. *Int J Clin Pharm*, 34, 825-7.
332. Marx V 2015. The DNA of a nation. *Nature*, 524, 503-505.
333. Matthew P, Cuddy R, Tracewell W G & Salazar D 2004. An open-label study on the pharmacokinetics (PK) of pitavastatin (NK-104) when administered concomitantly with fenofibrate or gemfibrozil in healthy volunteers (abstract). *Clin Pharmacol Ther*, 75, 33.
334. Matuszewski B K, Constanzer M L & Chavez-Eng C M 2003. Strategies for the assessment of matrix effect in quantitative bioanalytical methods based on HPLC-MS/MS. *Anal Chem*, 75, 3019-30.
335. Mazzu A L, Lasseter K C, Shamblen E C, Agarwal V, Lettieri J & Sundaresen P 2000. Itraconazole alters the pharmacokinetics of atorvastatin to a greater extent than either cerivastatin or pravastatin. *Clin Pharmacol Ther*, 68, 391-400.
336. McClure D L, Valuck R J, Glanz M, Murphy J R & Hokanson J E 2007. Statin and statin-fibrate use was significantly associated with increased myositis risk in a managed care population. *J Clin Epidemiol*, 60, 812-8.
337. McCormick A D, Mckillop D, Butters C J, Miles G S, Baba T, Touchi A & Yamaguchi Y 2000. ZD4522 – an HMG-CoA reductase inhibitor free of metabolically mediated drug interactions: metabolic studies in human in vitro systems (abstract 46). *J Clin Pharmacol*, 40, 1055.
338. Mccuskey R S, Ito Y, Robertson G R, Mccuskey M K, Perry M & Farrell G C 2004. Hepatic microvascular dysfunction during evolution of dietary steatohepatitis in mice. *Hepatology*, 40, 386-93.
339. McGill H C, Jr., McMahan C A, Herderick E E, Malcom G T, Tracy R E & Strong J P 2000. Origin of atherosclerosis in childhood and adolescence. *Am J Clin Nutr*, 72, 1307s-1315s.
340. Mcginnis B, Olson K L, Magid D, Bayliss E, Korner E J, Brand D W & Steiner J F 2007. Factors related to adherence to statin therapy. *Ann Pharmacother*, 41, 1805-11.
341. Mcginnis B D, Olson K L, Delate T M & Stolpart R S 2009. Statin adherence and mortality in patients enrolled in a secondary prevention program. *Am J Manag Care*, 15, 689-95.
342. McLaren W, Gil L, Hunt S E, Riat H S, Ritchie G R, Thormann A, Flicek P & Cunningham F 2016. The Ensembl Variant Effect Predictor. *Genome Biol*, 17, 122.
343. Meador B M & Huey K A 2010. Statin-associated myopathy and its exacerbation with exercise. *Muscle Nerve*, 42, 469-79.
344. Meesters R J & Hooff G P 2013. State-of-the-art dried blood spot analysis: an overview of recent advances and future trends. *Bioanalysis*, 5, 2187-208.
345. Meesters R J, Zhang J, Van Huizen N A, Hooff G P, Gruters R A & Luidert T M 2012. Dried matrix on paper disks: the next generation DBS microsampling technique for managing the hematocrit effect in DBS analysis. *Bioanalysis*, 4, 2027-35.
346. Mega J L, Stitzel N O, Smith J G, Chasman D I, Caulfield M, Devlin J J, Nordio F, Hyde C, Cannon C P, Sacks F, Poulter N, Sever P, Ridker P M, Braunwald E, Melander O, Kathiresan S & Sabatine M S 2015. Genetic risk, coronary heart disease events, and the clinical benefit of statin therapy: an analysis of primary and secondary prevention trials. *Lancet*, 385, 2264-2271.
347. Mehran R, Brodie B, Cox D A, Grines C L, Rutherford B, Bhatt D L, Dangas G, Feit F, Ohman E M, Parise H, Fahy M, Lansky A J & Stone G W 2008. The Harmonizing Outcomes with Revascularization and Stents in Acute Myocardial Infarction (HORIZONS-AMI) Trial: study design and rationale. *Am Heart J*, 156, 44-56.
348. Merck & Co I. 2014. Mevacor (lovastatin) tablets description (Online). Available: [https://www.merck.com/product/usa/pi\\_circulars/m/mevacor/mevacor\\_pi.pdf](https://www.merck.com/product/usa/pi_circulars/m/mevacor/mevacor_pi.pdf) (Accessed 7 July 2016).
349. Merck & Co I. 2015. Zocor (simvastatin) tablets - highlights of prescribing information (Online). Available: [https://www.merck.com/product/usa/pi\\_circulars/z/zocor/zocor\\_pi.pdf](https://www.merck.com/product/usa/pi_circulars/z/zocor/zocor_pi.pdf) (Accessed 7 July 2016).
350. Merla G, Howald C, Henrichsen C N, Lyle R, Wyss C, Zobot M T, Antonarakis S E & Reymond A 2006. Submicroscopic deletion in patients with Williams-Beuren syndrome influences expression levels of the nonhemizygous flanking genes. *Am J Hum Genet*, 79, 332-41.
351. Miller W L 2012. P450 oxidoreductase deficiency: a disorder of steroidogenesis with multiple clinical manifestations. *Sci Signal*, 5, pt11.
352. Milton J N, Sebastiani P, Solovieff N, Hartley S W, Bhatnagar P, Arking D E, Dworkis D A, Casella J F, Barron-Casella E, Bean C J, Hooper W C, Debaun M R, Garrett M E, Soldano K, Telen M J, Ashley-Koch A, Gladwin M T, Baldwin C T, Steinberg M H & Klings E S 2012. A genome-wide association study of total bilirubin and cholelithiasis risk in sickle cell anemia. *PLoS One*, 7, e34741.

353. Min P-K, Park J, Isaacs S, Taylor B A, Thompson P D, Troyanos C, D'hemecourt P, Dyer S, Chan S Y & Baggish A L 2016. Influence of statins on distinct circulating microRNAs during prolonged aerobic exercise. *Journal of Applied Physiology*, 120, 711-720.
354. Mirosevic Skvrce N, Bozina N, Zibar L, Barisic I, Pejnovic L & Macolic Sarinic V 2013. CYP2C9 and ABCG2 polymorphisms as risk factors for developing adverse drug reactions in renal transplant patients taking fluvastatin: a case-control study. *Pharmacogenomics*, 14, 1419-31.
355. Mohaupt M G, Karas R H, Babiychuk E B, Sanchez-Freire V, Monastyrskaya K, Iyer L, Hoppeler H, Breil F & Draeger A 2009. Association between statin-associated myopathy and skeletal muscle damage. *CMAJ : Canadian Medical Association Journal*, 181, E11-E18.
356. Montini G, Malaventura C & Salviati L 2008. Early coenzyme Q10 supplementation in primary coenzyme Q10 deficiency. *N Engl J Med*, 358, 2849-50.
357. Moosmann B & Behl C 2004a. Selenoprotein synthesis and side-effects of statins. *Lancet*, 363, 892-4.
358. Moosmann B & Behl C 2004b. Selenoproteins, cholesterol-lowering drugs, and the consequences: revisiting of the mevalonate pathway. *Trends Cardiovasc Med*, 14, 273-81.
359. Morimoto K, Oishi T, Ueda S, Ueda M, Hosokawa M & Chiba K 2004. A novel variant allele of OATP-C (SLCO1B1) found in a Japanese patient with pravastatin-induced myopathy. *Drug Metab Pharmacokinet*, 19, 453-5.
360. Moßhammer D, Schaeffeler E, Schwab M & Mörike K 2014. Mechanisms and assessment of statin-related muscular adverse effects. *British Journal of Clinical Pharmacology*, 78, 454-466.
361. Muck W 2000. Clinical pharmacokinetics of cerivastatin. *Clin Pharmacokinet*, 39, 99-116.
362. Muck W, Park S, Jager W, Voith B, Wandel E, Galle P R & Schwarting A 2001. The pharmacokinetics of cerivastatin in patients on chronic hemodialysis. *Int J Clin Pharmacol Ther*, 39, 192-8.
363. Mulder A B, Van Lijf H J, Bon M A, Van Den Bergh F A, Touw D J, Neef C & Vermes I 2001. Association of polymorphism in the cytochrome CYP2D6 and the efficacy and tolerability of simvastatin. *Clin Pharmacol Ther*, 70, 546-51.
364. Mullen P J, Luscher B, Scharnagl H, Krahenbuhl S & Brecht K 2010. Effect of simvastatin on cholesterol metabolism in C2C12 myotubes and HepG2 cells, and consequences for statin-induced myopathy. *Biochem Pharmacol*, 79, 1200-9.
365. Mullen P J, Zahno A, Lindinger P, Maseneni S, Felser A, Krähenbühl S & Brecht K 2011. Susceptibility to simvastatin-induced toxicity is partly determined by mitochondrial respiration and phosphorylation state of Akt. *Biochimica et Biophysica Acta (BBA) - Molecular Cell Research*, 1813, 2079-2087.
366. Mutch D M, Klocke B, Morrison P, Murray C A, Henderson C J, Seifert M & Williamson G 2007. The disruption of hepatic cytochrome p450 reductase alters mouse lipid metabolism. *J Proteome Res*, 6, 3976-84.
367. Nakagawa S, Gosho M, Inazu Y & Hounslow N 2013. Pitavastatin Concentrations Are Not Increased by CYP3A4 Inhibitor Itraconazole in Healthy Subjects. *Clin Pharmacol Drug Dev*, 2, 195-200.
368. Namjou B, Marsolo K, Lingren T, Ritchie M D, Verma S S, Cobb B L, Perry C, Kitchner T E, Brilliant M H, Peissig P L, Borthwick K M, Williams M S, Grafton J, Jarvik G P, Holm I A & Harley J B 2015. A GWAS Study on Liver Function Test Using eMERGE Network Participants. *PLoS One*, 10, e0138677.
369. Nasir K, Bittencourt M S, Blaha M J, Blankstein R, Agatson A S, Rivera J J, Miedema M D, Sibley C T, Shaw L J, Blumenthal R S, Budoff M J & Krumholz H M 2015. Implications of Coronary Artery Calcium Testing Among Statin Candidates According to American College of Cardiology/American Heart Association Cholesterol Management Guidelines. *Journal of the American College of Cardiology*, 66, 1657-1668.
370. National Statistics. 2015. Prescriptions dispensed in the community, England 2004-14 (Online). Available: <http://content.digital.nhs.uk/catalogue/PUB17644/pres-disp-com-eng-2004-14-rep.pdf> (Accessed 19 July 2017).
371. Nc3rs. 2016. National centre for the replacement refinement and reduction of animals in research (Online). Available: <https://www.nc3rs.org.uk/> (Accessed 22 April 2016).
372. Nebert D W, Adesnik M, Coon M J, Estabrook R W, Gonzalez F J, Guengerich F P, Gunsalus I C, Johnson E F, Kemper B, Levin W & Et Al. 1987. The P450 gene superfamily: recommended nomenclature. *Dna*, 6, 1-11.
373. Needham M, Fabian V, Knezevic W, Panegyres P, Zilko P & Mastaglia F L 2007. Progressive myopathy with up-regulation of MHC-I associated with statin therapy. *Neuromuscul Disord*, 17, 194-200.
374. Nelson A C, Huang W & Moody D E 2001. Variables in human liver microsomes preparation: impact on the kinetics of l-alpha-acetylmethadol (LAAM) n-demethylation and dextromethorphan O-demethylation. *Drug Metab Dispos*, 29, 319-25.
375. Neuvonen P J, Backman J T & Niemi M 2008. Pharmacokinetic comparison of the potential over-the-counter statins simvastatin, lovastatin, fluvastatin and pravastatin. *Clin Pharmacokinet*, 47, 463-74.
376. Neuvonen P J & Jalava K M 1996. Itraconazole drastically increases plasma concentrations of lovastatin and lovastatin acid. *Clin Pharmacol Ther*, 60, 54-61.
377. Neuvonen P J, Kantola T & Kivisto K T 1998. Simvastatin but not pravastatin is very susceptible to interaction with the CYP3A4 inhibitor itraconazole. *Clin Pharmacol Ther*, 63, 332-41.

378. Neuvonen P J, Niemi M & Backman J T 2006. Drug interactions with lipid-lowering drugs: mechanisms and clinical relevance. *Clin Pharmacol Ther*, 80, 565-81.
379. Nhs Choices. 2014. NICE publishes new draft guidelines on statins use (Online). Available: <http://www.nhs.uk/news/2014/02February/Pages/NICE-publishes-new-draft-guidelines-on-statins-use.aspx> (Accessed 19 October 2016).
380. Nice. 2014. Wider use of statins could cut deaths from heart disease (Online). Available: <https://www.nice.org.uk/news/article/wider-use-of-statins-could-cut-deaths-from-heart-disease> (Accessed 19 October 2016).
381. Nice. 2016a. Cardiovascular disease: risk assessment and reduction, including lipid modification (Online). Available: <https://www.nice.org.uk/guidance/cg181/chapter/1-Recommendations> (Accessed 12 July 2017).
382. Nice. 2016b. Familial hypercholesterolaemia: identification and management (Online). Available: <https://www.nice.org.uk/guidance/cg71/chapter/Introduction> (Accessed 2 October 2017).
383. Niemi M, Arnold K A, Backman J T, Pasanen M K, Godtel-Armbrust U, Wojnowski L, Zanger U M, Neuvonen P J, Eichelbaum M, Kivisto K T & Lang T 2006a. Association of genetic polymorphism in ABC2 with hepatic multidrug resistance-associated protein 2 expression and pravastatin pharmacokinetics. *Pharmacogenet Genomics*, 16, 801-8.
384. Niemi M, Pasanen M K & Neuvonen P J 2006b. SLCO1B1 polymorphism and sex affect the pharmacokinetics of pravastatin but not fluvastatin. *Clin Pharmacol Ther*, 80, 356-66.
385. Nies A T, Niemi M, Burk O, Winter S, Zanger U M, Stieger B, Schwab M & Schaeffeler E 2013. Genetics is a major determinant of expression of the human hepatic uptake transporter OATP1B1, but not of OATP1B3 and OATP2B1. *Genome Med*, 5, 1.
386. Nishizato Y, Ieiri I, Suzuki H, Kimura M, Kawabata K, Hirota T, Takane H, Irie S, Kusahara H, Urasaki Y, Urae A, Higuchi S, Otsubo K & Sugiyama Y 2003. Polymorphisms of OATP-C (SLC21A6) and OAT3 (SLC22A8) genes: consequences for pravastatin pharmacokinetics. *Clin Pharmacol Ther*, 73, 554-65.
387. Nissen S E, Stroes E, Dent-Acosta R E, Rosenson R S, Lehman S J, Sattar N, Preiss D, Bruckert E, Ceska R, Lepor N, Ballantyne C M, Gouni-Berthold I, Elliott M, Brennan D M, Wasserman S M, Somaratne R, Scott R & Stein E A 2016. Efficacy and Tolerability of Evolocumab vs Ezetimibe in Patients With Muscle-Related Statin Intolerance: The GAUSS-3 Randomized Clinical Trial. *Jama*, 315, 1580-90.
388. Novartis. 2012. Lescol (fluvastatin dosium) - highlights of prescribing information (Online). Available: <https://www.pharma.us.novartis.com/sites/www.pharma.us.novartis.com/files/Lescol.pdf> (Accessed 7 July 2016).
389. Nuffieldtrust. 2014. NHS spending on the top three disease categories in England (Online). Available: <http://www.nuffieldtrust.org.uk/data-and-charts/nhs-spending-top-three-disease-categories-england> (Accessed 04 May 2016).
390. Numako M, Takayama T, Noge I, Kitagawa Y, Todoroki K, Mizuno H, Min J Z & Toyo'oka T 2016. Dried Saliva Spot (DSS) as a Convenient and Reliable Sampling for Bioanalysis: An Application for the Diagnosis of Diabetes Mellitus. *Anal Chem*, 88, 635-9.
391. O'mara M, Hudson-Curtis B, Olson K, Yueh Y, Dunn J & Spooner N 2011. The effect of hematocrit and punch location on assay bias during quantitative bioanalysis of dried blood spot samples. *Bioanalysis*, 3, 2335-47.
392. Oh E S, Kim C O, Cho S K, Park M S & Chung J Y 2013. Impact of ABC2, ABCG2 and SLCO1B1 polymorphisms on the pharmacokinetics of pitavastatin in humans. *Drug Metab Pharmacokinet*, 28, 196-202.
393. Oh J, Ban M R, Miskie B A, Pollex R L & Hegele R A 2007. Genetic determinants of statin intolerance. *Lipids Health Dis*, 6, 7.
394. Ohtsuki S, Schaefer O, Kawakami H, Inoue T, Liehner S, Saito A, Ishiguro N, Kishimoto W, Ludwig-Schwellinger E, Ebner T & Terasaki T 2012. Simultaneous absolute protein quantification of transporters, cytochromes P450, and UDP-glucuronosyltransferases as a novel approach for the characterization of individual human liver: comparison with mRNA levels and activities. *Drug Metab Dispos*, 40, 83-92.
395. Olagunju A, Bolaji O O, Amara A, Waitt C, Else L, Soyinka J, Adeagbo B, Adejuyigbe E, Siccardi M, Back D, Owen A & Khoo S 2015. Development, validation and clinical application of a novel method for the quantification of efavirenz in dried breast milk spots using LC-MS/MS. *J Antimicrob Chemother*, 70, 555-61.
396. Olsson A G, Mctaggart F & Raza A 2002. Rosuvastatin: a highly effective new HMG-CoA reductase inhibitor. *Cardiovasc Drug Rev*, 20, 303-28.
397. Ostler M W, Porter J H & Buxton O M 2014. Dried Blood Spot Collection of Health Biomarkers to Maximize Participation in Population Studies. *Journal of Visualized Experiments : JoVE*, 50973.
398. Oussalah A, Bosco P, Anello G, Spada R, Guéant-Rodriguez R-M, Chery C, Rouyer P, Josse T, Romano A, Elia M, Bronowicki J-P & Guéant J-L 2015. Exome-Wide Association Study Identifies New Low-Frequency and Rare UGT1A1 Coding Variants and UGT1A6 Coding Variants Influencing Serum Bilirubin in Elderly Subjects: A Strobe Compliant Article. *Medicine*, 94, e925.

399. Pan H Y, Devault A R, Brescia D, Willard D A, MCGovern M E, Whigan D B & Ivashkiv E 1993. Effect of food on pravastatin pharmacokinetics and pharmacodynamics. *Int J Clin Pharmacol Ther Toxicol*, 31, 291-4.
400. Pandey A V & Fluck C E 2013. NADPH P450 oxidoreductase: structure, function, and pathology of diseases. *Pharmacol Ther*, 138, 229-54.
401. Pandey A V & Sproll P 2014. Pharmacogenomics of human P450 oxidoreductase. *Front Pharmacol*, 5, 103.
402. Pang X-Y, Cheng J, Kim J-H, Matsubara T, Krausz K W & Gonzalez F J 2012. Expression and Regulation of Human Fetal-Specific CYP3A7 in Mice. *Endocrinology*, 153, 1453-1463.
403. Parker B A, Capizzi J A, Grimaldi A S, Clarkson P M, Cole S M, Keadle J, Chipkin S, Pescatello L S, Simpson K, White C M & Thompson P D 2013. Effect of statins on skeletal muscle function. *Circulation*, 127, 96-103.
404. Partani P, Verma S M, Gurule S, Khuroo A & Monif T 2014. Simultaneous quantitation of atorvastatin and its two active metabolites in human plasma by liquid chromatography/(-) electrospray tandem mass spectrometry *J Pharm Anal*, 4, 26-36.
405. Pasanen M K, Fredrikson H, Neuvonen P J & Niemi M 2007. Different effects of SLCO1B1 polymorphism on the pharmacokinetics of atorvastatin and rosuvastatin. *Clin Pharmacol Ther*, 82, 726-33.
406. Pasanen M K, Neuvonen M, Neuvonen P J & Niemi M 2006. SLCO1B1 polymorphism markedly affects the pharmacokinetics of simvastatin acid. *Pharmacogenet Genomics*, 16, 873-9.
407. Pasternak R C, Smith S C, Bairey-Merz C N, Grundy S M, Cleeman J I & Lenfant C 2002. ACC/AHA/NHLBI Clinical Advisory on the Use and Safety of Statins. *Circulation*, 106, 1024.
408. Patel A M, Shariff S, Bailey D G, Juurlink D N, Gandhi S, Mamdani M, Gomes T, Fleet J, Hwang Y J & Garg A X 2013a. Statin toxicity from macrolide antibiotic coprescription: a population-based cohort study. *Ann Intern Med*, 158, 869-76.
409. Patel P, Mulla H, Kairamkonda V, Spooner N, Gade S, Della Pasqua O, Field D J & Pandya H C 2013b. Dried blood spots and sparse sampling: a practical approach to estimating pharmacokinetic parameters of caffeine in preterm infants. *British Journal of Clinical Pharmacology*, 75, 805-813.
410. Patel P, Mulla H, Tanna S & Pandya H 2010. Facilitating pharmacokinetic studies in children: a new use of dried blood spots. *Arch Dis Child*, 95, 484-7.
411. Pfizer Inc. 2015. LIPITOR- atorvastatin calcium trihydrate tablet, film coated. Highlights of prescribing information (Online). Available: <http://labeling.pfizer.com/ShowLabeling.aspx?id=587> (Accessed 7 July 2016).
412. Phan K, Gomez Y H, Elbaz L & Daskalopoulou S S 2014. Statin Treatment Non-adherence and Discontinuation: Clinical Implications and Potential Solutions. *Curr Pharm Des*, 20, 6314-24.
413. Phillips B, Roberts C, Rudolph A E, Morant S, Aziz F & O'regan C P 2007. Switching statins: the impact on patient outcomes. *Br J Cardiol*, 14, 280-5.
414. Pickup K, Gavin A, Jones H B, Karlsson E, Page C, Ratcliffe K, Sarda S, Schulz-Utermoehl T & Wilson I 2012. The hepatic reductase null mouse as a model for exploring hepatic conjugation of xenobiotics: application to the metabolism of diclofenac. *Xenobiotica*, 42, 195-205.
415. Pickup K, Wills J, Rodrigues A, Jones H B, Page C, Martin S, Sarda S & Wilson I 2014. The metabolic fate of [14C]-fenclozic acid in the hepatic reductase null (HRN) mouse. *Xenobiotica*, 44, 164-73.
416. Pillai V C & Mehvar R 2011. Inhibition of NADPH-cytochrome P450 reductase by tannic acid in rat liver microsomes and primary hepatocytes: methodological artifacts and application to ischemia-reperfusion injury. *J Pharm Sci*, 100, 3495-505.
417. Pirmohamed M, Fitzgerald R, French N & Pushpakom S. 2017. FUTURE Initiative (Online). Available: <https://www.liverpool.ac.uk/health-and-life-sciences/future-initiative/home/> (Accessed 02 October 2017).
418. Pirmohamed M, James S, Meakin S, Green C, Scott A K, Walley T J, Farrar K, Park B K & Breckenridge A M 2004. Adverse drug reactions as cause of admission to hospital: prospective analysis of 18 820 patients. *Bmj*, 329, 15-9.
419. Pitt J J 2009. Principles and Applications of Liquid Chromatography-Mass Spectrometry in Clinical Biochemistry. *The Clinical Biochemist Reviews*, 30, 19-34.
420. Porter T D 2012. New insights into the role of cytochrome P450 reductase (POR) in microsomal redox biology. *Acta Pharmaceutica Sinica B*, 2, 102-106.
421. Postmus I, Trompet S, Deshmukh H A, Barnes M R, Li X, Warren H R, Chasman D I, Zhou K, Arsenault B J, Donnelly L A, Wiggins K L, Avery C L, Griffin P, Feng Q, Taylor K D, Li G, Evans D S, Smith A V, De Keyser C E, Johnson A D, De Craen A J, Stott D J, Buckley B M, Ford I, Westendorp R G, Eline Slagboom P, Sattar N, Munroe P B, Sever P, Poulter N, Stanton A, Shields D C, O'brien E, Shaw-Hawkins S, Ida Chen Y D, Nickerson D A, Smith J D, Pierre Dube M, Matthijs Boekholdt S, Kees Hovingh G, Kastelein J J, Mckeigue P M, Betteridge J, Neil A, Durrington P N, Doney A, Carr F, Morris A, McCarthy M I, Groop L, Ahlqvist E, Bis J C, Rice K, Smith N L, Lumley T, Whitsel E A, Sturmer T, Boerwinkle E, Ngwa J S, O'donnell C J, Vasan R S, Wei W Q, Wilke R A, Liu C T, Sun F, Guo X, Heckbert S R, Post W, Sotoodehnia N, Arnold A M, Stafford J M, Ding J, Herrington D M, Kritchevsky S B, Eiriksdottir G, Launer L J, Harris T B, Chu A Y, Giulianini F, Macfadyen J G, Barratt B J, Nyberg F, Stricker B H, Uitterlinden A G, Hofman A, Rivadeneira F, Emilsson V, Franco O H, Ridker P M, Gudnason V, Liu Y, Denny J C, Ballantyne C M,

- Rotter J I, Adrienne Cupples L, Psaty B M, Palmer C N, Tardif J C, Colhoun H M, Hitman G, *et al.* 2014. Pharmacogenetic meta-analysis of genome-wide association studies of LDL cholesterol response to statins. *Nat Commun*, 5, 5068.
422. Postmus I, Verschuren J J, De Craen A J, Slagboom P E, Westendorp R G, Jukema J W & Trompet S 2012. Pharmacogenetics of statins: achievements, whole-genome analyses and future perspectives. *Pharmacogenomics*, 13, 831-40.
423. Pourfarzam M & Zadhoush F 2013. Newborn Screening for inherited metabolic disorders; news and views. *Journal of Research in Medical Sciences : The Official Journal of Isfahan University of Medical Sciences*, 18, 801-808.
424. Prasad P P, Stypinski D, Vyas K H & Gonasun L 2004. Lack of Interaction between Modified-Release Fluvastatin and Amlodipine in Healthy Subjects. *Clin Drug Investig*, 24, 323-31.
425. Protasi F, Takekura H, Wang Y, Chen S R, Meissner G, Allen P D & Franzini-Armstrong C 2000. RYR1 and RYR3 have different roles in the assembly of calcium release units of skeletal muscle. *Biophys J*, 79, 2494-508.
426. Prueksaritanont T, Gorham L M, Ma B, Liu L, Yu X, Zhao J J, Slaughter D E, Arison B H & Vyas K P 1997. In vitro metabolism of simvastatin in humans [SBT]identification of metabolizing enzymes and effect of the drug on hepatic P450s. *Drug Metab Dispos*, 25, 1191-9.
427. Prueksaritanont T, Ma B & Yu N 2003. The human hepatic metabolism of simvastatin hydroxy acid is mediated primarily by CYP3A, and not CYP2D6. *Br J Clin Pharmacol*, 56, 120-4.
428. Prueksaritanont T, Subramanian R, Fang X, Ma B, Qiu Y, Lin J H, Pearson P G & Baillie T A 2002. Glucuronidation of statins in animals and humans: a novel mechanism of statin lactonization. *Drug Metab Dispos*, 30, 505-12.
429. Pruim R J, Welch R P, Sanna S, Teslovich T M, Chines P S, Gliedt T P, Boehnke M, Abecasis G R & Willer C J 2010. LocusZoom: regional visualization of genome-wide association scan results. *Bioinformatics*, 26, 2336-7.
430. Puccetti L, Ciani F & Auteri A 2010. Genetic involvement in statins induced myopathy. Preliminary data from an observational case-control study. *Atherosclerosis*, 211, 28-9.
431. Purcell S, Neale B, Todd-Brown K, Thomas L, Ferreira M A, Bender D, Maller J, Sklar P, De Bakker P I, Daly M J & Sham P C 2007. PLINK: a tool set for whole-genome association and population-based linkage analyses. *Am J Hum Genet*, 81, 559-75.
432. Quintilesims. 2015. IMS Health Forecasts Global Drug Spending to Increase 30 Percent by 2020, to \$1.4 Trillion, As Medicine Use Gap Narrows (Online). Available: <http://www.imshealth.com/en/about-us/news/ims-health-forecasts-global-drug-spending-to-increase-30-percent-by-2020> (Accessed 15 February 2017).
433. Quinzii C M & Hirano M 2011. Primary and secondary CoQ(10) deficiencies in humans. *Biofactors (Oxford, England)*, 37, 361-365.
434. R Core Team. 2017. R: a language and environment for statistical computing, (Online). Available: <https://www.R-project.org> (Accessed 03 July 2017).
435. Radulovic L L, Cilla D D, Posvar E L, Sedman A J & Whitfield L R 1995. Effect of food on the bioavailability of atorvastatin, an HMG-CoA reductase inhibitor. *J Clin Pharmacol*, 35, 990-4.
436. Rafieian-Kopaei M, Setorki M, Doudi M, Baradaran A & Nasri H 2014. Atherosclerosis: Process, Indicators, Risk Factors and New Hopes. *International Journal of Preventive Medicine*, 5, 927-946.
437. Ragia G, Kolovou V, Tavridou A, Elens L, Tselepis A D, Elisaf M, Van Schaik R H, Kolovou G & Manolopoulos V G 2014. Lack of association of the p450 oxidoreductase \*28 single nucleotide polymorphism with the lipid-lowering effect of statins in hypercholesterolemic patients. *Mol Diagn Ther*, 18, 323-31.
438. Rahavendran S V, Vekich S, Skor H, Batugo M, Nguyen L, Shetty B & Shen Z 2012. Discovery pharmacokinetic studies in mice using serial microsampling, dried blood spots and microbore LC-MS/MS. *Bioanalysis*, 4, 1077-95.
439. Raju S B, Varghese K & Madhu K 2013. Management of statin intolerance. *Indian J Endocrinol Metab*, 17, 977-82.
440. Rash J A, Campbell D J, Tonelli M & Campbell T S 2016. A systematic review of interventions to improve adherence to statin medication: What do we know about what works? *Prev Med*, 90, 155-69.
441. Rasmussen J N, Chong A & Alter D A 2007. Relationship between adherence to evidence-based pharmacotherapy and long-term mortality after acute myocardial infarction. *Jama*, 297, 177-86.
442. Rhoda Lee C, Sharp J & Baxter K. 2012. Drug interactions: Cytochrome P450 isoenzymes not the only interaction mechanism (Online). Available: <http://www.pharmaceutical-journal.com/learning/learning-article/drug-interactions-cytochrome-p450-isoenzymes-not-the-only-interaction-mechanism/11098984.article> (Accessed 12 July 2016).
443. Riccioni G & Sblendorio V 2012. Atherosclerosis: from biology to pharmacological treatment. *Journal of Geriatric Cardiology : JGC*, 9, 305-317.
444. Riddick D S, Ding X, Wolf C R, Porter T D, Pandey A V, Zhang Q Y, Gu J, Finn R D, Ronseaux S, Mclaughlin L A, Henderson C J, Zou L & Fluck C E 2013. NADPH-cytochrome P450 oxidoreductase: roles in physiology, pharmacology, and toxicology. *Drug Metab Dispos*, 41, 12-23.

445. Ridker P M, Everett B M, Thuren T, Macfadyen J G, Chang W H, Ballantyne C, Fonseca F, Nicolau J, Koenig W, Anker S D, Kastelein J J P, Cornel J H, Pais P, Pella D, Genest J, Cifkova R, Lorenzatti A, Forster T, Kobalava Z, Vida-Simiti L, Flather M, Shimokawa H, Ogawa H, Dellborg M, Rossi P R F, Troquay R P T, Libby P & Glynn R J 2017. Antiinflammatory Therapy with Canakinumab for Atherosclerotic Disease. *New England Journal of Medicine*.
446. Riedmaier S. 2011. Pharmacogenetic Determinants of Atorvastatin Metabolism and Response (Dissertation) (Online). Available: [https://publikationen.uni-tuebingen.de/xmlui/bitstream/handle/10900/49571/pdf/2011\\_Dissertation\\_Stephan\\_Riedmaier.pdf?sequence=1](https://publikationen.uni-tuebingen.de/xmlui/bitstream/handle/10900/49571/pdf/2011_Dissertation_Stephan_Riedmaier.pdf?sequence=1) (Accessed 7 July 2016).
447. Riedmaier S, Klein K, Hofmann U, Keskitalo J E, Neuvonen P J, Schwab M, Niemi M & Zanger U M 2010. UDP-glucuronosyltransferase (UGT) polymorphisms affect atorvastatin lactonization in vitro and in vivo. *Clin Pharmacol Ther*, 87, 65-73.
448. Riedmaier S, Klein K, Winter S, Hofmann U, Schwab M & Zanger U M 2011. Paraoxonase (PON1 and PON3) Polymorphisms: Impact on Liver Expression and Atorvastatin-Lactone Hydrolysis. *Front Pharmacol*, 2, 41.
449. Robinson R, Carpenter D, Shaw M A, Halsall J & Hopkins P 2006. Mutations in RYR1 in malignant hyperthermia and central core disease. *Hum Mutat*, 27, 977-89.
450. Roden D M, Johnson J A, Kimmel S E, Krauss R M, Medina M W, Shuldiner A & Wilke R A 2011. Cardiovascular pharmacogenomics. *Circ Res*, 109, 807-20.
451. Rogers J D, Zhao J, Liu L, Amin R D, Gagliano K D, Porras A G, Blum R A, Wilson M F, Stepanavage M & Vega J M 1999. Grapefruit juice has minimal effects on plasma concentrations of lovastatin-derived 3-hydroxy-3-methylglutaryl coenzyme A reductase inhibitors. *Clin Pharmacol Ther*, 66, 358-66.
452. Romaine S P R, Tomaszewski M, Condorelli G & Samani N J 2015. MicroRNAs in cardiovascular disease: an introduction for clinicians. *Heart*.
453. Rosenson R S. 2017. Statins: Actions, side effects, and administration (Online). UpToDate. Available: <https://www.uptodate.com/contents/statins-actions-side-effects-and-administration> (Accessed 15 March 2018).
454. Roten L, Schoenenberger R A, Krahenbuhl S & Schlienger R G 2004. Rhabdomyolysis in association with simvastatin and amiodarone. *Ann Pharmacother*, 38, 978-81.
455. Roth M, Obaidat A & Hagenbuch B 2012. OATPs, OATs and OCTs: the organic anion and cation transporters of the SLCO and SLC22A gene superfamilies. *Br J Pharmacol*, 165, 1260-87.
456. Ruano G, Thompson P D, Windemuth A, Seip R L, Dande A, Sorokin A, Kocherla M, Smith A, Holford T R & Wu A H 2007. Physiogenomic association of statin-related myalgia to serotonin receptors. *Muscle Nerve*, 36, 329-35.
457. Ruano G, Thompson P D, Windemuth A, Smith A, Kocherla M, Holford T R, Seip R & Wu A H 2005. Physiogenomic analysis links serum creatine kinase activities during statin therapy to vascular smooth muscle homeostasis. *Pharmacogenomics*, 6, 865-72.
458. Ruano G, Windemuth A, Wu A H, Kane J P, Malloy M J, Pullinger C R, Kocherla M, Bogaard K, Gordon B R, Holford T R, Gupta A, Seip R L & Thompson P D 2011. Mechanisms of statin-induced myalgia assessed by physiogenomic associations. *Atherosclerosis*, 218, 451-6.
459. Rublee D A, Chen S Y, Mardekian J, Wu N, Rao P & Boulanger L 2012. Evaluation of cardiovascular morbidity associated with adherence to atorvastatin therapy. *Am J Ther*, 19, 24-32.
460. Rudakova E V, Boltneva N P & Makhaeva G F 2011. Comparative analysis of esterase activities of human, mouse, and rat blood. *Bull Exp Biol Med*, 152, 73-5.
461. Ruth K S, Campbell P J, Chew S, Lim E M, Hadlow N, Stuckey B G, Brown S J & Feenstra B 2016. Genome-wide association study with 1000 genomes imputation identifies signals for nine sex hormone-related phenotypes. 24, 284-90.
462. Rutstein S E, Hosseinipour M C, Kamwendo D, Soko A, Mkandawire M, Biddle A K, Miller W C, Weinberger M, Wheeler S B, Sarr A, Gupta S, Chimbwandira F, Mwenda R, Kamiza S, Hoffman I & Mataya R 2015. Dried blood spots for viral load monitoring in Malawi: feasible and effective. *PLoS One*, 10, e0124748.
463. Rxlist. 2016. Livalo (pitavastatin) (Online). Available: <http://www.rxlist.com/livalo-drug/clinical-pharmacology.htm> (Accessed 7 July 2016).
464. Sabatine M S, Giugliano R P, Keech A C, Honarpour N, Wiviott S D, Murphy S A, Kuder J F, Wang H, Liu T, Wasserman S M, Sever P S & Pedersen T R 2017. Evolocumab and Clinical Outcomes in Patients with Cardiovascular Disease. *New England Journal of Medicine*, 376, 1713-1722.
465. Sakamoto K, Honda T, Yokoya S, Waguri S & Kimura J 2007. Rab-small GTPases are involved in fluvastatin and pravastatin-induced vacuolation in rat skeletal myofibers. *Faseb j*, 21, 4087-94.
466. Saliba W R & Elias M 2005. Severe myopathy induced by the co-administration of simvastatin and itraconazole. *Eur J Intern Med*, 16, 305.
467. Samuelsson L B, Hall M H, Mclean S, Porter J H, Berkman L, Marino M, Sembajwe G, Mcdade T W & Buxton O M 2015. Validation of Biomarkers of CVD Risk from Dried Blood Spots in Community-Based Research: Methodologies and Study-Specific Serum Equivalencies. *Biodemography Soc Biol*, 61, 285-97.

468. Santos P C, Gagliardi A C, Miname M H, Chacra A P, Santos R D, Krieger J E & Pereira A C 2012. SLCO1B1 haplotypes are not associated with atorvastatin-induced myalgia in Brazilian patients with familial hypercholesterolemia. *Eur J Clin Pharmacol*, 68, 273-9.
469. Sathasivam S & Lecky B 2008. Statin induced myopathy. *Bmj*, 337, a2286.
470. Schirris T J, Renkema G H, Ritschel T, Voermans N C, Bilos A, Van Engelen B G, Brandt U, Koopman W J, Beyrath J D, Rodenburg R J, Willems P H, Smeitink J A & Russel F G 2015a. Statin-Induced Myopathy Is Associated with Mitochondrial Complex III Inhibition. *Cell Metab*, 22, 399-407.
471. Schirris T J, Ritschel T, Bilos A, Smeitink J A & Russel F G 2015b. Statin Lactonization by Uridine 5'-Diphospho-glucuronosyltransferases (UGTs). *Mol Pharm*, 12, 4048-55.
472. Schmitt C, Kuhn B, Zhang X, Kivitz A J & Grange S 2011. Disease-drug-drug interaction involving tocilizumab and simvastatin in patients with rheumatoid arthritis. *Clin Pharmacol Ther*, 89, 735-40.
473. Schneck D W, Birmingham B K, Zalikowski J A, Mitchell P D, Wang Y, Martin P D, Lasseter K C, Brown C D, Windass A S & Raza A 2004. The effect of gemfibrozil on the pharmacokinetics of rosuvastatin. *Clin Pharmacol Ther*, 75, 455-63.
474. Scripture C D & Pieper J A 2001. Clinical pharmacokinetics of fluvastatin. *Clin Pharmacokinet*, 40, 263-81.
475. Seifalian A M, Chidambaram V, Rolles K & Davidson B R 1998. In vivo demonstration of impaired microcirculation in steatotic human liver grafts. *Liver Transpl Surg*, 4, 71-7.
476. Seifalian A M, Piasecki C, Agarwal A & Davidson B R 1999. The effect of graded steatosis on flow in the hepatic parenchymal microcirculation. *Transplantation*, 68, 780-4.
477. Serebruany V, Cherala G, Williams C, Surigin S, Booze C, Kuliczowski W & Atar D 2009. Association of platelet responsiveness with clopidogrel metabolism: role of compliance in the assessment of "resistance". *Am Heart J*, 158, 925-32.
478. Shah Y, Iqbal Z, Ahmad L, Khuda F, Khan A, Khan A, Khan M I & Ismail 2016. Effect of Omeprazole on the Pharmacokinetics of Rosuvastatin in Healthy Male Volunteers. *Am J Ther*, 23, e1514-e1523.
479. Shanmugam S, Ryu J K, Yoo S D, Choi H G & Woo J S 2011. Evaluation of Pharmacokinetics of Simvastatin and Its Pharmacologically Active Metabolite from Controlled-Release Tablets of Simvastatin in Rodent and Canine Animal Models. *Biomolecules & Therapeutics*, 19, 248-54.
480. Shen A L, O'leary K A & Kasper C B 2002. Association of multiple developmental defects and embryonic lethality with loss of microsomal NADPH-cytochrome P450 oxidoreductase. *J Biol Chem*, 277, 6536-41.
481. Shimada T, Yamazaki H, Mimura M, Wakamiya N, Ueng Y F, Guengerich F P & Inui Y 1996. Characterization of microsomal cytochrome P450 enzymes involved in the oxidation of xenobiotic chemicals in human fetal liver and adult lungs. *Drug Metab Dispos*, 24, 515-22.
482. Shin J, Pauly D F, Pacanowski M A, Langae T, Frye R F & Johnson J A 2011. Effect of cytochrome P450 3A5 genotype on atorvastatin pharmacokinetics and its interaction with clarithromycin. *Pharmacotherapy*, 31, 942-50.
483. Shirasaka Y, Sager J E, Lutz J D, Davis C & Isoherranen N 2013. Inhibition of CYP2C19 and CYP3A4 by omeprazole metabolites and their contribution to drug-drug interactions. *Drug Metab Dispos*, 41, 1414-24.
484. Siddiqui M K, Maroteau C, Veluchamy A, Tornio A, Tavendale R, Carr F, Abelega N U, Carr D, Bloch K, Hallberg P, Yue Q Y, Pearson E R, Colhoun H M, Morris A D, Dow E, George J, Pirmohamed M, Ridker P M, Doney A S F, Alfirevic A, Wadelius M, Maitland-Van Der Zee A H, Chasman D I & Palmer C N A 2017. A common missense variant of LILRB5 is associated with statin intolerance and myalgia. *Eur Heart J*.
485. Siedlik P H, Olson S C, Yang B B & Stern R H 1999. Erythromycin coadministration increases plasma atorvastatin concentrations. *J Clin Pharmacol*, 39, 501-4.
486. Sim S C, Edwards R J, Boobis A R & Ingelman-Sundberg M 2005. CYP3A7 protein expression is high in a fraction of adult human livers and partially associated with the CYP3A7\*1C allele. *Pharmacogenet Genomics*, 15, 625-31.
487. Simons L A, Levis G & Simons J 1996. Apparent discontinuation rates in patients prescribed lipid-lowering drugs. *Med J Aust*, 164, 208-11.
488. Simonson S G, Martin P D, Mitchell P, Schneck D W, Lasseter K C & Warwick M J 2003. Pharmacokinetics and pharmacodynamics of rosuvastatin in subjects with hepatic impairment. *Eur J Clin Pharmacol*, 58, 669-75.
489. Sing C F, Stengård J H & Kardia S L R 2003. Genes, Environment, and Cardiovascular Disease. *Arteriosclerosis, Thrombosis, and Vascular Biology*, 23, 1190.
490. Sipe B E, Jones R J & Bokhart G H 2003. Rhabdomyolysis causing AV blockade due to possible atorvastatin, esomeprazole, and clarithromycin interaction. *Ann Pharmacother*, 37, 808-11.
491. Sirvent P, Bordenave S, Vermaelen M, Roels B, Vassort G, Mercier J, Raynaud E & Lacampagne A 2005. Simvastatin induces impairment in skeletal muscle while heart is protected. *Biochem Biophys Res Commun*, 338, 1426-34.
492. Skeoch S & Bruce I N 2015. Atherosclerosis in rheumatoid arthritis: is it all about inflammation? *Nat Rev Rheumatol*, 11, 390-400.

493. Skottheim I B, Gedde-Dahl A, Hejazifar S, Hoel K & Asberg A 2008. Statin induced myotoxicity: the lactone forms are more potent than the acid forms in human skeletal muscle cells in vitro. *Eur J Pharm Sci*, 33, 317-25.
494. Slepneva I A, Sergeeva S V & Khramtsov V V 1995. Reversible inhibition of NADPH-cytochrome P450 reductase by alpha-lipoic acid. *Biochem Biophys Res Commun*, 214, 1246-53.
495. Slitt A L, Allen K, Morrone J, Aleksunes L M, Chen C, Maher J M, Manautou J E, Cherrington N J & Klaassen C D 2007. Regulation of transporter expression in mouse liver, kidney, and intestine during extrahepatic cholestasis. *Biochim Biophys Acta*, 1768, 637-47.
496. Smit P W, Sollis K A, Fiscus S, Ford N, Vitoria M, Essajee S, Barnett D, Cheng B, Crowe S M, Denny T, Landay A, Stevens W, Habiyambere V, Perriens J H & Peeling R W 2014. Systematic Review of the Use of Dried Blood Spots for Monitoring HIV Viral Load and for Early Infant Diagnosis. *PLoS ONE*, 9, e86461.
497. Smith H T, Jokubaitis L A, Troendle A J, Hwang D S & Robinson W T 1993. Pharmacokinetics of fluvastatin and specific drug interactions. *Am J Hypertens*, 6, 375s-382s.
498. Smith M E B, Lee N J, Haney E & Carson S. 2009. Drug Class Review: HMG-CoA Reductase Inhibitors (Statins) and Fixed-dose Combination Products Containing a Statin: Final Report Update 5 (Online). Oregon Health & Science University. Available: [http://www.ncbi.nlm.nih.gov/books/NBK47273/pdf/Bookshelf\\_NBK47273.pdf](http://www.ncbi.nlm.nih.gov/books/NBK47273/pdf/Bookshelf_NBK47273.pdf).
499. Spear B B, Heath-Chiozzi M & Huff J 2001. Clinical application of pharmacogenetics. *Trends Mol Med*, 7, 201-4.
500. Spence J D, Munoz C E, Hendricks L, Latchinian L & Khouri H E 1995. Pharmacokinetics of the combination of fluvastatin and gemfibrozil. *Am J Cardiol*, 76, 80a-83a.
501. Statista. 2016. Global spending on medicines from 2010 to 2020 (in billion U.S. dollars) (Online). Available: <https://www.statista.com/statistics/280572/medicine-spending-worldwide/> (Accessed 9 November 2016).
502. Stevens J C, Hines R N, Gu C, Koukouritaki S B, Manro J R, Tandler P J & Zaya M J 2003. Developmental expression of the major human hepatic CYP3A enzymes. *J Pharmacol Exp Ther*, 307, 573-82.
503. Stewart A 2013. SLCO1B1 Polymorphisms and Statin-Induced Myopathy. *PLoS Curr*, 5.
504. Stone N J, Robinson J G, Lichtenstein A H, Bairey Merz C N, Blum C B, Eckel R H, Goldberg A C, Gordon D, Levy D, Lloyd-Jones D M, McBride P, Schwartz J S, Shero S T, Smith S C, Jr., Watson K & Wilson P W 2014. 2013 ACC/AHA guideline on the treatment of blood cholesterol to reduce atherosclerotic cardiovascular risk in adults: a report of the American College of Cardiology/American Heart Association Task Force on Practice Guidelines. *J Am Coll Cardiol*, 63, 2889-934.
505. Stormo C, Bogsrud M P, Hermann M, Asberg A, Piehler A P, Retterstol K & Kringen M K 2013. UGT1A1\*28 is associated with decreased systemic exposure of atorvastatin lactone. *Mol Diagn Ther*, 17, 233-7.
506. Stroes E S, Thompson P D, Corsini A, Vladutiu G D, Raal F J, Ray K K, Roden M, Stein E, Tokgozoglul, Nordestgaard B G, Bruckert E, De Backer G, Krauss R M, Laufs U, Santos R D, Hegele R A, Hovingh G K, Leiter L A, Mach F, Marz W, Newman C B, Wiklund O, Jacobson T A, Catapano A L, Chapman M J & Ginsberg H N 2015. Statin-associated muscle symptoms: impact on statin therapy-European Atherosclerosis Society Consensus Panel Statement on Assessment, Aetiology and Management. *Eur Heart J*, 36, 1012-1022.
507. Svarstad B L, Chewning B A, Sleath B L & Claesson C 1999. The Brief Medication Questionnaire: a tool for screening patient adherence and barriers to adherence. *Patient Educ Couns*, 37, 113-24.
508. Taitel M, Jiang J, Rudkin K, Ewing S & Duncan I 2012. The impact of pharmacist face-to-face counseling to improve medication adherence among patients initiating statin therapy. *Patient Prefer Adherence*, 6, 323-9.
509. Tan S L, Li Z, Zhang W, Song G B, Liu L M, Peng J, Liu Z Q, Fan L, Meng X G, Wang L S, Chen Y, Zhou X M & Zhou H H 2013. Cytochrome P450 oxidoreductase genetic polymorphisms A503V and rs2868177 do not significantly affect warfarin stable dosage in Han-Chinese patients with mechanical heart valve replacement. *Eur J Clin Pharmacol*, 69, 1769-75.
510. Tavafi M 2013. Complexity of diabetic nephropathy pathogenesis and design of investigations. *J Renal Inj Prev*, 2, 59-62.
511. Taylor B A, Lorson L, White C M & Thompson P D 2015. A Randomized Trial of Coenzyme Q10 in Patients with Confirmed Statin Myopathy. *Atherosclerosis*, 238, 329-335.
512. Taylor F, Huffman M D, Macedo A F, Moore T H M, Burke M, Davey Smith G, Ward K & Ebrahim S 2013. Statins for the primary prevention of cardiovascular disease. *Cochrane Database of Systematic Reviews*.
513. Tee M K, Huang N, Damm I & Miller W L 2011. Transcriptional Regulation of the Human P450 Oxidoreductase Gene: Hormonal Regulation and Influence of Promoter Polymorphisms. *Molecular Endocrinology*, 25, 715-731.
514. The 1000 Genomes Project Consortium 2012. An integrated map of genetic variation from 1,092 human genomes. *Nature*, 491, 56-65.
515. The Cardiogramplus4d Consortium 2013. Large-scale association analysis identifies new risk loci for coronary artery disease. *Nature genetics*, 45, 25-33.

516. The Gtex Consortium 2013. The Genotype-Tissue Expression (GTEx) project. *Nature genetics*, 45, 580-585.
517. Thompson P D, Zmuda J M, Domalik L J, Zimet R J, Staggers J & Guyton J R 1997. Lovastatin increases exercise-induced skeletal muscle injury. *Metabolism*, 46, 1206-10.
518. Timmerman P, White S, Globig S, Ludtke S, Brunet L & Smeraglia J 2011. EBF recommendation on the validation of bioanalytical methods for dried blood spots. *Bioanalysis*, 3, 1567-75.
519. Tobert J A & Newman C B 2016. The nocebo effect in the context of statin intolerance. *J Clin Lipidol*, 10, 739-747.
520. Tomalik-Scharte D, Maiter D, Kirchheiner J, Ivison H E, Fuhr U & Arlt W 2010. Impaired hepatic drug and steroid metabolism in congenital adrenal hyperplasia due to P450 oxidoreductase deficiency. *Eur J Endocrinol*, 163, 919-24.
521. Tornio A, Vakkilainen J, Neuvonen M, Backman J T, Neuvonen P J & Niemi M 2015. SLCO1B1 polymorphism markedly affects the pharmacokinetics of lovastatin acid. *Pharmacogenet Genomics*.
522. Trenk D, Kristensen S D, Hochholzer W & Neumann F J 2013. High on-treatment platelet reactivity and P2Y12 antagonists in clinical trials. *Thromb Haemost*, 109, 834-45.
523. Tsamandouras N, Dickinson G, Guo Y, Hall S, Rostami-Hodjegan A, Galetin A & Aarons L 2014. Identification of the effect of multiple polymorphisms on the pharmacokinetics of simvastatin and simvastatin acid using a population-modeling approach. *Clin Pharmacol Ther*, 96, 90-100.
524. Tuppin P, Neumann A, Danchin N, De Peretti C, Weill A, Ricordeau P & Allemand H 2010. Evidence-based pharmacotherapy after myocardial infarction in France: adherence-associated factors and relationship with 30-month mortality and rehospitalization. *Arch Cardiovasc Dis*, 103, 363-75.
525. Turner R M, Park B K & Pirmohamed M 2015. Parsing interindividual drug variability: an emerging role for systems pharmacology. *Wiley Interdiscip Rev Syst Biol Med*, 7, 221-41.
526. Turner R M & Pirmohamed M 2014. Cardiovascular pharmacogenomics: expectations and practical benefits. *Clin Pharmacol Ther*, 95, 281-93.
527. Turner R M, Yin P, Hanson A, Fitzgerald R, Morris A P, Stables R H, Jorgensen A L & Pirmohamed M 2016. Investigating the prevalence, predictors and prognosis of suboptimal statin use early after a non-ST elevation acute coronary syndrome. *Journal of Clinical Lipidology*.
528. Turner R M, Yin P, Hanson A, Fitzgerald R, Morris A P, Stables R H, Jorgensen A L & Pirmohamed M 2017. Investigating the prevalence, predictors, and prognosis of suboptimal statin use early after a non-ST elevation acute coronary syndrome. *J Clin Lipidol*, 11, 204-214.
529. Turner S D 2014. qqman: an R package for visualizing GWAS results using Q-Q and manhattan plots. *bioRxiv*.
530. Twaddle S, Marshall M & Michael N. 2012. Programme Budgeting - Testing the Approach in Scotland (Online). Available: <http://www.gov.scot/Resource/0039/00391293.pdf> (Accessed 04 May 2016).
531. Ueda P, Lung T W-C, Clarke P & Danaei G 2017. Application of the 2014 NICE cholesterol guidelines in the English population: a cross-sectional analysis. *British Journal of General Practice*.
532. Umezawa H, Lee X P, Arima Y, Hasegawa C, Izawa H, Kumazawa T & Sato K 2008. Simultaneous determination of beta-blockers in human plasma using liquid chromatography-tandem mass spectrometry. *Biomed Chromatogr*, 22, 702-11.
533. Van Der Wouden C H, Cambon-Thomsen A, Cecchin E, Cheung K C, Davila-Fajardo C L, Deneer V H, Dolzan V, Ingelman-Sundberg M, Jonsson S, Karlsson M O, Kriek M, Mitropoulou C, Patrinos G P, Pirmohamed M, Samwald M, Schaeffeler E, Schwab M, Steinberger D, Stingl J, Sunder-Plassmann G, Toffoli G, Turner R M, Van Rhenen M H, Swen J J & Guchelaar H J 2017. Implementing Pharmacogenomics in Europe: Design and Implementation Strategy of the Ubiquitous Pharmacogenomics Consortium. *Clin Pharmacol Ther*, 101, 341-358.
534. Van Haandel L, Gibson K T, Leeder J S & Wagner J B 2016. Quantification of pravastatin acid, lactone and isomers in human plasma by UHPLC-MS/MS and its application to a pediatric pharmacokinetic study. *J Chromatogr B Analyt Technol Biomed Life Sci*, 1012-1013, 169-77.
535. Van Waterschoot R a B, Van Herwaarden A E, Lagas J S, Sparidans R W, Wagenaar E, Van Der Kruijssen C M M, Goldstein J A, Zeldin D C, Beijnen J H & Schinkel A H 2008. Midazolam metabolism in Cytochrome P450 3A knockout mice can be attributed to upregulated CYP2C enzymes. *Molecular pharmacology*, 73, 1029-1036.
536. Vickers S, Duncan C A, Chen I W, Rosegay A & Duggan D E 1990. Metabolic disposition studies on simvastatin, a cholesterol-lowering prodrug. *Drug Metab Dispos*, 18, 138-45.
537. Viktil K K, Blix H S, Eek A K, Davies M N, Moger T A & Reikvam A 2012. How are drug regimen changes during hospitalisation handled after discharge: a cohort study. *BMJ Open*, 2.
538. Vildhede A, Karlgren M, Svedberg E K, Wisniewski J R, Lai Y, Noren A & Artursson P 2014. Hepatic uptake of atorvastatin: influence of variability in transporter expression on uptake clearance and drug-drug interactions. *Drug Metab Dispos*, 42, 1210-8.
539. Vladutiu G D, Isackson P J, Kaufman K, Harley J B, Cobb B, Christopher-Stine L & Wortmann R L 2011. Genetic risk for malignant hyperthermia in non-anesthesia-induced myopathies. *Mol Genet Metab*, 104, 167-73.

540. Vladutiu G D, Simmons Z, Isackson P J, Tarnopolsky M, Peltier W L, Barboi A C, Sripathi N, Wortmann R L & Phillips P S 2006. Genetic risk factors associated with lipid-lowering drug-induced myopathies. *Muscle Nerve*, 34, 153-62.
541. Voora D, Shah S H, Spasojevic I, Ali S, Reed C R, Salisbury B A & Ginsburg G S 2009. The SLCO1B1\*5 genetic variant is associated with statin-induced side effects. *J Am Coll Cardiol*, 54, 1609-16.
542. Vrablik M, Zlatohlavek L, Stulc T, Adamkova V, Prusikova M, Schwarzova L, Hubacek J A & Ceska R 2014. Statin-associated myopathy: from genetic predisposition to clinical management. *Physiol Res*, 63 Suppl 3, S327-34.
543. Vree T B, Dammers E, Ulc I, Horkovics-Kovats S, Ryska M & Merckx I 2003. Differences between lovastatin and simvastatin hydrolysis in healthy male and female volunteers: gut hydrolysis of lovastatin is twice that of simvastatin. *ScientificWorldJournal*, 3, 1332-43.
544. Vu D H, Bolhuis M S, Koster R A, Greijdanus B, De Lange W C, Van Altena R, Brouwers J R, Uges D R & Alffenaar J W 2012. Dried blood spot analysis for therapeutic drug monitoring of linezolid in patients with multidrug-resistant tuberculosis. *Antimicrob Agents Chemother*, 56, 5758-63.
545. Wachtel M S & Yang S 2014. Odds of death after glioblastoma diagnosis in the United States by chemotherapeutic era. *Cancer Med*, 3, 660-6.
546. Wagner B K, Gilbert T J, Hanai J-I, Imamura S, Bodycombe N E, Bon R S, Waldmann H, Clemons P A, Sukhatme V P & Mootha V K 2011. A small-molecule screening strategy to identify suppressors of statin myopathy. *ACS chemical biology*, 6, 900-904.
547. Wagner B K, Kitami T, Gilbert T J, Peck D, Ramanathan A, Schreiber S L, Golub T R & Mootha V K 2008. Large-scale chemical dissection of mitochondrial function. *Nat Biotechnol*, 26, 343-51.
548. Wagner M, Tonoli D, Varesio E & Hopfgartner G 2016. The use of mass spectrometry to analyze dried blood spots. *Mass Spectrom Rev*, 35, 361-438.
549. Wang D, Guo Y, Wrighton S A, Cooke G E & Sadee W 2011. Intronic polymorphism in CYP3A4 affects hepatic expression and response to statin drugs. *Pharmacogenomics J*, 11, 274-86.
550. Wang D & Sadee W 2016. CYP3A4 intronic SNP rs35599367 (CYP3A4\*22) alters RNA splicing. *Pharmacogenet Genomics*, 26, 40-3.
551. Wang J, Luzum J A, Phelps M A & Kitzmiller J P 2015. Liquid chromatography-tandem mass spectrometry assay for the simultaneous quantification of simvastatin, lovastatin, atorvastatin, and their major metabolites in human plasma. *J Chromatogr B Analyt Technol Biomed Life Sci*, 983-984, 18-25.
552. Wang S L, Han J F, He X Y, Wang X R & Hong J Y 2007. Genetic variation of human cytochrome p450 reductase as a potential biomarker for mitomycin C-induced cytotoxicity. *Drug Metab Dispos*, 35, 176-9.
553. Wang X J, Chamberlain M, Vassieva O, Henderson C J & Wolf C R 2005. Relationship between hepatic phenotype and changes in gene expression in cytochrome P450 reductase (POR) null mice. *Biochem J*, 388, 857-67.
554. Ward L D & Kellis M 2016. HaploReg v4: systematic mining of putative causal variants, cell types, regulators and target genes for human complex traits and disease. *Nucleic Acids Research*, 44, D877-D881.
555. Watanabe K, Varesio E & Hopfgartner G 2014. Parallel ultra high pressure liquid chromatography-mass spectrometry for the quantification of HIV protease inhibitors using dried spot sample collection format. *J Chromatogr B Analyt Technol Biomed Life Sci*, 965, 244-53.
556. Waters D, Schwartz G G & Olsson A G 2001. The Myocardial Ischemia Reduction with Acute Cholesterol Lowering (MIRACL) trial: a new frontier for statins? *Curr Control Trials Cardiovasc Med*, 2, 111-114.
557. Wei L, Fahey T & Macdonald T M 2008. Adherence to statin or aspirin or both in patients with established cardiovascular disease: exploring healthy behaviour vs. drug effects and 10-year follow-up of outcome. *Br J Clin Pharmacol*, 66, 110-6.
558. Wei L, Wang J, Thompson P, Wong S, Struthers A D & Macdonald T M 2002. Adherence to statin treatment and readmission of patients after myocardial infarction: a six year follow up study. *Heart*, 88, 229-33.
559. Wei M Y, Ito M K, Cohen J D, Brinton E A & Jacobson T A 2013. Predictors of statin adherence, switching, and discontinuation in the USAGE survey: understanding the use of statins in America and gaps in patient education. *J Clin Lipidol*, 7, 472-83.
560. Westlind-Johnsson A, Malmbeo S, Johansson A, Otter C, Andersson T B, Johansson I, Edwards R J, Boobis A R & Ingelman-Sundberg M 2003. Comparative analysis of CYP3A expression in human liver suggests only a minor role for CYP3A5 in drug metabolism. *Drug Metab Dispos*, 31, 755-61.
561. Westra H-J, Peters M J, Esko T, Yaghootkar H, Schurmann C, Kettunen J, Christiansen M W, Fairfax B P, Schramm K, Powell J E, Zhernakova A, Zhernakova D V, Veldink J H, Van Den Berg L H, Karjalainen J, Withoff S, Uitterlinden A G, Hofman A, Rivadeneira F, T Hoen P a C, Reinmaa E, Fischer K, Nelis M, Milani L, Melzer D, Ferrucci L, Singleton A B, Hernandez D G, Nalls M A, Homuth G, Nauck M, Radke D, Volker U, Perola M, Salomaa V, Brody J, Suchy-Dicey A, Gharib S A, Enquobahrie D A, Lumley T, Montgomery G W, Makino S, Prokisch H, Herder C, Roden M, Grallert H, Meitinger T, Strauch K, Li Y, Jansen R C, Visscher P M, Knight J C, Psaty B M, Ripatti S, Teumer A, Frayling T M, Metspalu A, Van

- Meurs J B J & Franke L 2013. Systematic identification of trans eQTLs as putative drivers of known disease associations. *Nat Genet*, 45, 1238-1243.
562. Whitfield L R, Porcari A R, Alvey C, Abel R, Bullen W & Hartman D 2011. Effect of gemfibrozil and fenofibrate on the pharmacokinetics of atorvastatin. *J Clin Pharmacol*, 51, 378-88.
563. Wickremesinhe E R & Perkins E J 2015. Using Dried Blood Spot Sampling to Improve Data Quality and Reduce Animal Use in Mouse Pharmacokinetic Studies. *Journal of the American Association for Laboratory Animal Science : JAALAS*, 54, 139-144.
564. Wienkers L C & Heath T G 2005. Predicting in vivo drug interactions from in vitro drug discovery data. *Nat Rev Drug Discov*, 4, 825-33.
565. Wiggins B S, Saseen J J, Page R L, 2nd, Reed B N, Sneed K, Kostis J B, Lanfear D, Virani S & Morris P B 2016. Recommendations for Management of Clinically Significant Drug-Drug Interactions With Statins and Select Agents Used in Patients With Cardiovascular Disease: A Scientific Statement From the American Heart Association. *Circulation*.
566. Wilhelm A J, Den Burger J C & Swart E L 2014. Therapeutic drug monitoring by dried blood spot: progress to date and future directions. *Clin Pharmacokinet*, 53, 961-73.
567. Wilke R A, Moore J H & Burmester J K 2005. Relative impact of CYP3A genotype and concomitant medication on the severity of atorvastatin-induced muscle damage. *Pharmacogenet Genomics*, 15, 415-21.
568. Williams J A, Ring B J, Cantrell V E, Jones D R, Eckstein J, Ruterbories K, Hamman M A, Hall S D & Wrighton S A 2002. Comparative metabolic capabilities of CYP3A4, CYP3A5, and CYP3A7. *Drug Metab Dispos*, 30, 883-91.
569. Wiviott S D, Antman E M, Gibson C M, Montalescot G, Riesmeyer J, Weerakkody G, Winters K J, Warmke J W, McCabe C H & Braunwald E 2006. Evaluation of prasugrel compared with clopidogrel in patients with acute coronary syndromes: design and rationale for the TRial to assess Improvement in Therapeutic Outcomes by optimizing platelet Inhibition with prasugrel Thrombolysis In Myocardial Infarction 38 (TRITON-TIMI 38). *Am Heart J*, 152, 627-35.
570. World Health Organisation. 1972. WHO technical report no. 498. International drug monitoring: the role of national centres (Online). Available: <http://www.who-umc.org/graphics/24756.pdf> (Accessed 9 November 2016).
571. World Health Organisation. 2014a. Global status report on noncommunicable diseases 2014 (Online). Available: [http://apps.who.int/iris/bitstream/10665/148114/1/9789241564854\\_eng.pdf?ua=1](http://apps.who.int/iris/bitstream/10665/148114/1/9789241564854_eng.pdf?ua=1) (Accessed 04 May 2016).
572. World Health Organisation. 2014b. The top 10 causes of death (Online). Available: <http://www.who.int/mediacentre/factsheets/fs310/en/> (Accessed 04 May 2016).
573. World Health Organisation. 2016. The top 10 causes of death (Online). Available: <http://www.who.int/mediacentre/factsheets/fs310/en/index2.html> (Accessed 12 July 2017).
574. Xu X, Liu Y, Li K, Wang P, Xu L, Yang Z & Yang X 2016. Intensive atorvastatin improves endothelial function and decreases ADP-induced platelet aggregation in patients with STEMI undergoing primary PCI: A single-center randomized controlled trial. *Int J Cardiol*, 222, 467-72.
575. Yamazaki H, Nakano M, Imai Y, Ueng Y F, Guengerich F P & Shimada T 1996. Roles of cytochrome b5 in the oxidation of testosterone and nifedipine by recombinant cytochrome P450 3A4 and by human liver microsomes. *Arch Biochem Biophys*, 325, 174-82.
576. Yang A Y, Sun L, Musson D G & Zhao J J 2005. Application of a novel ultra-low elution volume 96-well solid-phase extraction method to the LC/MS/MS determination of simvastatin and simvastatin acid in human plasma. *J Pharm Biomed Anal*, 38, 521-7.
577. Yang W, Xu H, Song Y, Wang X, Ren X, Zhao D, Cai Y, Zhang S, Huang J, Zhang L R, Zhang T & Zuo M 2014. Pharmacokinetics of simvastatin lactone and its active metabolite simvastatin hydroxy acid in healthy Chinese male and female volunteers. *Int J Clin Pharmacol Ther*, 52, 151-8.
578. Yao L, Qiu L X, Yu L, Yang Z, Yu X J, Zhong Y & Yu L 2010. The association between TA-repeat polymorphism in the promoter region of UGT1A1 and breast cancer risk: a meta-analysis. *Breast Cancer Res Treat*, 122, 879-82.
579. Yates A, Akanni W, Amode M R, Barrell D, Billis K, Carvalho-Silva D, Cummins C, Clapham P, Fitzgerald S, Gil L, Girón C G, Gordon L, Hourlier T, Hunt S E, Janacek S H, Johnson N, Juettemann T, Keenan S, Lavidas I, Martin F J, Maurel T, McLaren W, Murphy D N, Nag R, Nuhn M, Parker A, Patricio M, Pignatelli M, Rahtz M, Riat H S, Sheppard D, Taylor K, Thormann A, Vullo A, Wilder S P, Zadissa A, Birney E, Harrow J, Muffato M, Perry E, Ruffier M, Spudich G, Trevanion S J, Cunningham F, Aken B L, Zerbino D R & Flicek P 2016. Ensembl 2016. *Nucleic Acids Research*, 44, D710-D716.
580. Yin O Q, Chang Q, Tomlinson B & Chow M S 2004. The effect of CYP2D6 genotype on the pharmacokinetics of lovastatin in Chinese subjects. *Clinical Pharmacology & Therapeutics*, 75, P18-P18.
581. Yin O Q, Mak V W, Hu M, Fok B S, Chow M S & Tomlinson B 2012. Impact of CYP2D6 polymorphisms on the pharmacokinetics of lovastatin in Chinese subjects. *Eur J Clin Pharmacol*, 68, 943-9.
582. Yin P, Jorgensen A, Morris A, Turner R M, Fitzgerald R, Stables R H, Hanson A & Pirmohamed M 2016. SNP-Treatment Interactions of Cardiovascular Medications and Risk of Acute Coronary Syndrome

- Recurrence, at The 2016 Annual Meeting of the International Genetic Epidemiology Society. *Genet. Epidemiol*, 40, 609-674.
583. Ziaontz C. 2016. Real Statistics Using Excel (Online). Available: <http://www.real-statistics.com/> (Accessed 26 April 2016).
584. Zanger U M & Schwab M 2013. Cytochrome P450 enzymes in drug metabolism: Regulation of gene expression, enzyme activities, and impact of genetic variation. *Pharmacology & Therapeutics*, 138, 103-141.
585. Zeharia A, Shaag A, Houtkooper R H, Hindi T, De Lonlay P, Erez G, Hubert L, Saada A, De Keyzer Y, Eshel G, Vaz F M, Pines O & Elpeleg O 2008. Mutations in LPIN1 cause recurrent acute myoglobinuria in childhood. *Am J Hum Genet*, 83, 489-94.
586. Zeng W T, Xu Q & Li C H 2016. Influence of genetic polymorphisms in cytochrome P450 oxidoreductase on the variability in stable warfarin maintenance dose in Han Chinese.
587. Zhang L. 2009. Drug interactions: what do we know about non-cyp drug metabolizing enzymes and transporters? (Online). Available: <https://www.fda.gov/downloads/Drugs/.../UCM206103.pdf> (Accessed 21 August 2017).
588. Zhang L. 2010. Transporter-mediated drug-drug interactions (DDIs) (Online). FDA. Available: <https://www.fda.gov/downloads/Drugs/DevelopmentApprovalProcess/DevelopmentResources/DrugInteractionsLabeling/UCM207267.pdf> (Accessed 18 July 2017).
589. Zhang W, Deng S, Chen X P, Zhou G, Xie H T, He F Y, Cao D, Li Y J & Zhou H H 2008. Pharmacokinetics of rosuvastatin when coadministered with rifampicin in healthy males: a randomized, single-blind, placebo-controlled, crossover study. *Clin Ther*, 30, 1283-9.
590. Zhang X, Li L, Ding X & Kaminsky L S 2011. Identification of cytochrome P450 oxidoreductase gene variants that are significantly associated with the interindividual variations in warfarin maintenance dose. *Drug Metab Dispos*, 39, 1433-9.
591. Zhang Y, Huo M, Zhou J & Xie S 2010. PKSolver: An add-in program for pharmacokinetic and pharmacodynamic data analysis in Microsoft Excel. *Comput Methods Programs Biomed*, 99, 306-14.
592. Zhou Q, Chen Q X, Ruan Z R, Yuan H, Xu H M & Zeng S 2013a. CYP2C9\*3(1075A > C), ABCB1 and SLCO1B1 genetic polymorphisms and gender are determinants of inter-subject variability in pitavastatin pharmacokinetics. *Pharmazie*, 68, 187-94.
593. Zhou Q, Ruan Z R, Jiang B, Yuan H & Zeng S 2013b. Simvastatin pharmacokinetics in healthy Chinese subjects and its relations with CYP2C9, CYP3A5, ABCB1, ABCG2 and SLCO1B1 polymorphisms. *Pharmazie*, 68, 124-8.
594. Zhou Q, Ruan Z R, Yuan H, Xu D H & Zeng S 2013c. ABCB1 gene polymorphisms, ABCB1 haplotypes and ABCG2 c.421c > A are determinants of inter-subject variability in rosuvastatin pharmacokinetics. *Pharmazie*, 68, 129-34.
595. Zhou S, Chan E, Li X & Huang M 2005. Clinical outcomes and management of mechanism-based inhibition of cytochrome P450 3A4. *Ther Clin Risk Manag*, 1, 3-13.
596. Zhou Y, Wang S N, Li H, Zha W, Wang X, Liu Y, Sun J, Peng Q, Li S, Chen Y & Jin L 2014. Association of UGT1A1 variants and hyperbilirubinemia in breast-fed full-term Chinese infants. *PLoS One*, 9, e104251.
597. Zhu Y, Ding X, Fang C & Zhang Q-Y 2014. Regulation of Intestinal Cytochrome P450 Expression by Hepatic Cytochrome P450: Possible Involvement of Fibroblast Growth Factor 15 and Impact on Systemic Drug Exposure. *Molecular Pharmacology*, 85, 139-147.
598. Zuccaro P, Mombelli G, Calabresi L, Baldassarre D, Palmi I & Sirtori C R 2007. Tolerability of statins is not linked to CYP450 polymorphisms, but reduced CYP2D6 metabolism improves cholestaemic response to simvastatin and fluvastatin. *Pharmacol Res*, 55, 310-7.